

# World Journal of *Gastroenterology*

*World J Gastroenterol* 2017 December 14; 23(46): 8109-8262





## Editorial Board

2014-2017

The *World Journal of Gastroenterology* Editorial Board consists of 1375 members, representing a team of worldwide experts in gastroenterology and hepatology. They are from 68 countries, including Algeria (2), Argentina (7), Australia (31), Austria (9), Belgium (11), Brazil (20), Brunei Darussalam (1), Bulgaria (2), Cambodia (1), Canada (25), Chile (4), China (165), Croatia (2), Cuba (1), Czech (6), Denmark (2), Egypt (9), Estonia (2), Finland (6), France (20), Germany (58), Greece (31), Guatemala (1), Hungary (14), Iceland (1), India (33), Indonesia (2), Iran (10), Ireland (9), Israel (18), Italy (194), Japan (149), Jordan (1), Kuwait (1), Lebanon (7), Lithuania (1), Malaysia (1), Mexico (11), Morocco (1), Netherlands (5), New Zealand (4), Nigeria (3), Norway (6), Pakistan (6), Poland (12), Portugal (8), Puerto Rico (1), Qatar (1), Romania (10), Russia (3), Saudi Arabia (2), Singapore (7), Slovenia (2), South Africa (1), South Korea (69), Spain (51), Sri Lanka (1), Sudan (1), Sweden (12), Switzerland (5), Thailand (7), Trinidad and Tobago (1), Tunisia (2), Turkey (55), United Kingdom (49), United States (180), Venezuela (1), and Vietnam (1).

### EDITORS-IN-CHIEF

Stephen C Strom, *Stockholm*  
Andrzej S Tarnawski, *Long Beach*  
Damian Garcia-Olmo, *Madrid*

### ASSOCIATE EDITORS

Yung-Jue Bang, *Seoul*  
Vincent Di Martino, *Besancon*  
Daniel T Farkas, *Bronx*  
Roberto J Firpi, *Gainesville*  
Maria Gazouli, *Athens*  
Chung-Feng Huang, *Kaohsiung*  
Namir Katkhouda, *Los Angeles*  
Anna Kramvis, *Johannesburg*  
Wolfgang Kruis, *Cologne*  
Peter L Lakatos, *Budapest*  
Han Chu Lee, *Seoul*  
Christine McDonald, *Cleveland*  
Nahum Mendez-Sanchez, *Mexico City*  
George K Michalopoulos, *Pittsburgh*  
Suk Woo Nam, *Seoul*  
Shu-You Peng, *Hangzhou*  
Daniel von Renteln, *Montreal*  
Angelo Sangiovanni, *Milan*  
Hildegard M Schuller, *Knoxville*  
Dong-Wan Seo, *Seoul*  
Adrian John Stanley, *Glasgow*  
Jurgen Stein, *Frankfurt*  
Bei-Cheng Sun, *Nanjing*  
Yoshio Yamaoka, *Yufu*

### GUEST EDITORIAL BOARD MEMBERS

Jia-Ming Chang, *Taipei*  
Jane CJ Chao, *Taipei*

Kuen-Feng Chen, *Taipei*  
Tai-An Chiang, *Tainan*  
Yi-You Chiou, *Taipei*  
Seng-Kee Chuah, *Kaohsiung*  
Wan-Long Chuang, *Kaohsiung*  
How-Ran Guo, *Tainan*  
Ming-Chih Hou, *Taipei*  
Po-Shiuan Hsieh, *Taipei*  
Ching-Chuan Hsieh, *Chiayi county*  
Jun-Te Hsu, *Taoyuan*  
Chung-Ping Hsu, *Taichung*  
Chien-Ching Hung, *Taipei*  
Chao-Hung Hung, *Kaohsiung*  
Chen-Guo Ker, *Kaohsiung*  
Yung-Chih Lai, *Taipei*  
Teng-Yu Lee, *Taichung City*  
Wei-Jei Lee, *Taoyuan*  
Jin-Ching Lee, *Kaohsiung*  
Jen-Kou Lin, *Taipei*  
Ya-Wen Lin, *Taipei*  
Hui-kang Liu, *Taipei*  
Min-Hsiung Pan, *Taipei*  
Bor-Shyang Sheu, *Tainan*  
Hon-Yi Shi, *Kaohsiung*  
Fung-Chang Sung, *Taichung*  
Dar-In Tai, *Taipei*  
Jung-Fa Tsai, *Kaohsiung*  
Yao-Chou Tsai, *New Taipei City*  
Chih-Chi Wang, *Kaohsiung*  
Liang-Shun Wang, *New Taipei City*  
Hsiu-Po Wang, *Taipei*  
Jaw-Yuan Wang, *Kaohsiung*  
Yuan-Huang Wang, *Taipei*  
Yuan-Chuen Wang, *Taichung*

Deng-Chyang Wu, *Kaohsiung*  
Shun-Fa Yang, *Taichung*  
Hsu-Heng Yen, *Changhua*

### MEMBERS OF THE EDITORIAL BOARD



#### Algeria

Saadi Berkane, *Algiers*  
Samir Rouabhia, *Batna*



#### Argentina

N Tolosa de Talamoni, *Córdoba*  
Eduardo de Santibanes, *Buenos Aires*  
Bernardo Frider, *Capital Federal*  
Guillermo Mazzolini, *Pilar*  
Carlos Jose Pirola, *Buenos Aires*  
Bernabé Matías Quesada, *Buenos Aires*  
María Fernanda Troncoso, *Buenos Aires*



#### Australia

Golo Ahlenstiel, *Westmead*  
Minoti V Apte, *Sydney*  
Jacqueline S Barrett, *Melbourne*  
Michael Beard, *Adelaide*  
Filip Braet, *Sydney*  
Guy D Eslick, *Sydney*  
Christine Feinle-Bisset, *Adelaide*  
Mark D Gorrell, *Sydney*  
Michael Horowitz, *Adelaide*



Gordon Stanley Howarth, *Roseworthy*  
 Seungha Kang, *Brisbane*  
 Alfred King Lam, *Gold Coast*  
 Ian C Lawrance, *Perth/Fremantle*  
 Barbara Anne Leggett, *Brisbane*  
 Daniel A Lemberg, *Sydney*  
 Rupert W Leong, *Sydney*  
 Finlay A Macrae, *Victoria*  
 Vance Matthews, *Melbourne*  
 David L Morris, *Sydney*  
 Reme Mountifield, *Bedford Park*  
 Hans J Netter, *Melbourne*  
 Nam Q Nguyen, *Adelaide*  
 Liang Qiao, *Westmead*  
 Rajvinder Singh, *Adelaide*  
 Ross Cyril Smith, *St Leonards*  
 Kevin J Spring, *Sydney*  
 Debbie Trinder, *Fremantle*  
 Daniel R van Langenberg, *Box Hill*  
 David Ian Watson, *Adelaide*  
 Desmond Yip, *Garran*  
 Li Zhang, *Sydney*



#### **Austria**

Felix Aigner, *Innsbruck*  
 Gabriela A Berlakovich, *Vienna*  
 Herwig R Cerwenka, *Graz*  
 Peter Ferenci, *Wien*  
 Alfred Gangl, *Vienna*  
 Kurt Lenz, *Linz*  
 Markus Peck-Radosavljevic, *Vienna*  
 Markus Raderer, *Vienna*  
 Stefan Riss, *Vienna*



#### **Belgium**

Michael George Adler, *Brussels*  
 Benedicte Y De Winter, *Antwerp*  
 Mark De Ridder, *Jette*  
 Olivier Detry, *Liege*  
 Denis Dufrane Dufrane, *Brussels*  
 Sven M Francque, *Edegem*  
 Nikos Kotzampassakis, *Liège*  
 Geert KMM Robaey, *Genk*  
 Xavier Sagaert, *Leuven*  
 Peter Starkel, *Brussels*  
 Eddie Wisse, *Keerbergen*



#### **Brazil**

SMP Balzan, *Santa Cruz do Sul*  
 JLF Caboclo, *Sao Jose do Rio Preto*  
 Fábio Guilherme Campos, *Sao Paulo*  
 Claudia RL Cardoso, *Rio de Janeiro*  
 Roberto J Carvalho-Filho, *Sao Paulo*  
 Carla Daltro, *Salvador*  
 José Sebastiao dos Santos, *Ribeirão Preto*  
 Eduardo LR Mello, *Rio de Janeiro*  
 Stihela Maria Murad-Regadas, *Fortaleza*  
 Claudia PMS Oliveira, *Sao Paulo*  
 Júlio C Pereira-Lima, *Porto Alegre*  
 Marcos V Perini, *Sao Paulo*  
 Vietla Satyanarayana Rao, *Fortaleza*

Raquel Rocha, *Salvador*  
 AC Simoes e Silva, *Belo Horizonte*  
 Mauricio F Silva, *Porto Alegre*  
 Aytan Miranda Sipahi, *Sao Paulo*  
 Rosa Leonôra Salerno Soares, *Niterói*  
 Cristiane Valle Tovo, *Porto Alegre*  
 Eduardo Garcia Vilela, *Belo Horizonte*



#### **Brunei Darussalam**

Vui Heng Chong, *Bandar Seri Begawan*



#### **Bulgaria**

Tanya Kirilova Kadiyska, *Sofia*  
 Mihaela Petrova, *Sofia*



#### **Cambodia**

Francois Rouet, *Phnom Penh*



#### **Canada**

Brian Bressler, *Vancouver*  
 Frank J Burczynski, *Winnipeg*  
 Wangxue Chen, *Ottawa*  
 Francesco Crea, *Vancouver*  
 Jane A Foster, *Hamilton*  
 Hugh J Freeman, *Vancouver*  
 Shahrokh M Ghobadloo, *Ottawa*  
 Yuewen Gong, *Winnipeg*  
 Philip H Gordon, *Quebec*  
 Rakesh Kumar, *Edmonton*  
 Wolfgang A Kunze, *Hamilton*  
 Patrick Labonte, *Laval*  
 Zhikang Peng, *Winnipeg*  
 Jayadev Raju, *Ottawa*  
 Maitreyi Raman, *Calgary*  
 Giada Sebastiani, *Montreal*  
 Maida J Sewitch, *Montreal*  
 Eldon A Shaffer, *Alberta*  
 Christopher W Teshima, *Edmonton*  
 Jean Sévigny, *Québec*  
 Pingchang Yang, *Hamilton*  
 Pingchang Yang, *Hamilton*  
 Eric M Yoshida, *Vancouver*  
 Bin Zheng, *Edmonton*



#### **Chile**

Marcelo A Beltran, *La Serena*  
 Flavio Nervi, *Santiago*  
 Adolfo Parra-Blanco, *Santiago*  
 Alejandro Soza, *Santiago*



#### **China**

Zhao-Xiang Bian, *Hong Kong*  
 San-Jun Cai, *Shanghai*  
 Guang-Wen Cao, *Shanghai*  
 Long Chen, *Nanjing*  
 Ru-Fu Chen, *Guangzhou*  
 George G Chen, *Hong Kong*

Li-Bo Chen, *Wuhan*  
 Jia-Xu Chen, *Beijing*  
 Hong-Song Chen, *Beijing*  
 Lin Chen, *Beijing*  
 Yang-Chao Chen, *Hong Kong*  
 Zhen Chen, *Shanghai*  
 Ying-Sheng Cheng, *Shanghai*  
 Kent-Man Chu, *Hong Kong*  
 Zhi-Jun Dai, *Xi'an*  
 Jing-Yu Deng, *Tianjin*  
 Yi-Qi Du, *Shanghai*  
 Zhi Du, *Tianjin*  
 Hani El-Nezami, *Hong Kong*  
 Bao-Ying Fei, *Hangzhou*  
 Chang-Ming Gao, *Nanjing*  
 Jian-Ping Gong, *Chongqing*  
 Zuo-Jiong Gong, *Wuhan*  
 Jing-Shan Gong, *Shenzhen*  
 Guo-Li Gu, *Beijing*  
 Yong-Song Guan, *Chengdu*  
 Mao-Lin Guo, *Luoyang*  
 Jun-Ming Guo, *Ningbo*  
 Yan-Mei Guo, *Shanghai*  
 Xiao-Zhong Guo, *Shenyang*  
 Guo-Hong Han, *Xi'an*  
 Ming-Liang He, *Hong Kong*  
 Peng Hou, *Xi'an*  
 Zhao-Hui Huang, *Wuxi*  
 Feng Ji, *Hangzhou*  
 Simon Law, *Hong Kong*  
 Yan-Chang Lei, *Hangzhou*  
 Yu-Yuan Li, *Guangzhou*  
 Meng-Sen Li, *Haikou*  
 Shu-De Li, *Shanghai*  
 Zong-Fang Li, *Xi'an*  
 Qing-Quan Li, *Shanghai*  
 Kang Li, *Lasa*  
 Han Liang, *Tianjin*  
 Xing'e Liu, *Hangzhou*  
 Zheng-Wen Liu, *Xi'an*  
 Xiao-Fang Liu, *Yantai*  
 Bin Liu, *Tianjin*  
 Quan-Da Liu, *Beijing*  
 Hai-Feng Liu, *Beijing*  
 Fei Liu, *Shanghai*  
 Ai-Guo Lu, *Shanghai*  
 He-Sheng Luo, *Wuhan*  
 Xiao-Peng Ma, *Shanghai*  
 Yong Meng, *Shantou*  
 Ke-Jun Nan, *Xi'an*  
 Siew Chien Ng, *Hong Kong*  
 Simon SM Ng, *Hong Kong*  
 Zhao-Shan Niu, *Qingdao*  
 Di Qu, *Shanghai*  
 Ju-Wei Mu, *Beijing*  
 Rui-Hua Shi, *Nanjing*  
 Bao-Min Shi, *Shanghai*  
 Xiao-Dong Sun, *Hangzhou*  
 Si-Yu Sun, *Shenyang*  
 Guang-Hong Tan, *Haikou*  
 Wen-Fu Tang, *Chengdu*  
 Anthony YB Teoh, *Hong Kong*  
 Wei-Dong Tong, *Chongqing*  
 Eric Tse, *Hong Kong*  
 Hong Tu, *Shanghai*

Rong Tu, *Haikou*  
 Jian-She Wang, *Shanghai*  
 Kai Wang, *Jinan*  
 Xiao-Ping Wang, *Xianyang*  
 Xiu-Yan Wang, *Shanghai*  
 Dao-Rong Wang, *Yangzhou*  
 De-Sheng Wang, *Xi'an*  
 Chun-You Wang, *Wuhan*  
 Ge Wang, *Chongqing*  
 Xi-Shan Wang, *Harbin*  
 Wei-hong Wang, *Beijing*  
 Zhen-Ning Wang, *Shenyang*  
 Wai Man Raymond Wong, *Hong Kong*  
 Chun-Ming Wong, *Hong Kong*  
 Jian Wu, *Shanghai*  
 Sheng-Li Wu, *Xi'an*  
 Wu-Jun Wu, *Xi'an*  
 Qing Xia, *Chengdu*  
 Yan Xin, *Shenyang*  
 Dong-Ping Xu, *Beijing*  
 Jian-Min Xu, *Shanghai*  
 Wei Xu, *Changchun*  
 Ming Yan, *Jinan*  
 Xin-Min Yan, *Kunming*  
 Yi-Qun Yan, *Shanghai*  
 Feng Yang, *Shanghai*  
 Yong-Ping Yang, *Beijing*  
 He-Rui Yao, *Guangzhou*  
 Thomas Yau, *Hong Kong*  
 Winnie Yeo, *Hong Kong*  
 Jing You, *Kunming*  
 Jian-Qing Yu, *Wuhan*  
 Ying-Yan Yu, *Shanghai*  
 Wei-Zheng Yang, *Chengdu*  
 Zong-Ming Zhang, *Beijing*  
 Dian-Liang Zhang, *Qingdao*  
 Ya-Ping Zhang, *Shijiazhuang*  
 You-Cheng Zhang, *Lanzhou*  
 Jian-Zhong Zhang, *Beijing*  
 Ji-Yuan Zhang, *Beijing*  
 Hai-Tao Zhao, *Beijing*  
 Jian Zhao, *Shanghai*  
 Jian-Hong Zhong, *Nanning*  
 Ying-Qiang Zhong, *Guangzhou*  
 Ping-Hong Zhou, *Shanghai*  
 Yan-Ming Zhou, *Xiamen*  
 Tong Zhou, *Nanchong*  
 Li-Ming Zhou, *Chengdu*  
 Guo-Xiong Zhou, *Nantong*  
 Feng-Shang Zhu, *Shanghai*  
 Jiang-Fan Zhu, *Shanghai*  
 Zhao-Hui Zhu, *Beijing*



#### **Croatia**

Tajana Filipec Kanizaj, *Zagreb*  
 Mario Tadic, *Zagreb*



#### **Cuba**

Damian Casadesus, *Havana*



#### **Czech**

Jan Bures, *Hradec Kralove*  
 Marcela Kopacova, *Hradec Kralove*

Otto Kucera, *Hradec Kralove*  
 Marek Minarik, *Prague*  
 Pavel Soucek, *Prague*  
 Miroslav Zavoral, *Prague*



#### **Denmark**

Vibeke Andersen, *Odense*  
 E Michael Danielsen, *Copenhagen*



#### **Egypt**

Mohamed MM Abdel-Latif, *Assiut*  
 Hussein Atta, *Cairo*  
 Ashraf Elbahrawy, *Cairo*  
 Mortada Hassan El-Shabrawi, *Cairo*  
 Mona El Said El-Raziky, *Cairo*  
 Elrashdy M Redwan, *New Borg Alrab*  
 Zeinab Nabil Ahmed Said, *Cairo*  
 Ragaa HM Salama, *Assiut*  
 Maha Maher Shehata, *Mansoura*



#### **Estonia**

Margus Lember, *Tartu*  
 Tamara Vorobjova, *Tartu*



#### **Finland**

Marko Kalliomäki, *Turku*  
 Thomas Kietzmann, *Oulu*  
 Kaija-Leena Kolho, *Helsinki*  
 Eija Korkeila, *Turku*  
 Heikki Makisalo, *Helsinki*  
 Tanja Pessi, *Tampere*



#### **France**

Armando Abergel Clermont, *Ferrand*  
 Elie K Chouillard, *Polssy*  
 Pierre Cordelier, *Toulouse*  
 Pascal P Crenn, *Garches*  
 Catherine Daniel, *Lille*  
 Fanny Daniel, *Paris*  
 Cedric Dray, *Toulouse*  
 Benoit Foligne, *Lille*  
 Jean-Noel Freund, *Strasbourg*  
 Hervé Guillou, *Toulouse*  
 Nathalie Janel, *Paris*  
 Majid Khatib, *Bordeaux*  
 Jacques Marescaux, *Strasbourg*  
 Jean-Claude Marie, *Paris*  
 Driffa Moussata, *Pierre Benite*  
 Hang Nguyen, *Clermont-Ferrand*  
 Hugo Perazzo, *Paris*  
 Alain L Servin, *Chatenay-Malabry*  
 Chang Xian Zhang, *Lyon*



#### **Germany**

Stavros A Antoniou, *Monchengladbach*  
 Erwin Biecker, *Siegburg*  
 Hubert E Blum, *Freiburg*

Thomas Bock, *Berlin*  
 Katja Breitkopf-Heinlein, *Mannheim*  
 Elke Cario, *Essen*  
 Güralp Onur Ceyhan, *Munich*  
 Angel Cid-Arregui, *Heidelberg*  
 Michael Clemens Roggendorf, *München*  
 Christoph F Dietrich, *Bad Mergentheim*  
 Valentin Fuhrmann, *Hamburg*  
 Nikolaus Gassler, *Aachen*  
 Andreas Geier, *Wuerzburg*  
 Markus Gerhard, *Munich*  
 Anton Gillissen, *Muenster*  
 Thorsten Oliver Goetze, *Offenbach*  
 Daniel Nils Gotthardt, *Heidelberg*  
 Robert Grützmann, *Dresden*  
 Thilo Hackert, *Heidelberg*  
 Claus Hellerbrand, *Regensburg*  
 Harald Peter Hoensch, *Darmstadt*  
 Jens Hoeppner, *Freiburg*  
 Richard Hummel, *Muenster*  
 Jakob Robert Izbicki, *Hamburg*  
 Gernot Maximilian Kaiser, *Essen*  
 Matthias Kapischke, *Hamburg*  
 Michael Keese, *Frankfurt*  
 Andrej Khandoga, *Munich*  
 Jorg Kleeff, *Munich*  
 Alfred Koenigsrainer, *Tuebingen*  
 Peter Christopher Konturek, *Saalfeld*  
 Michael Linnebacher, *Rostock*  
 Stefan Maier, *Kaufbeuren*  
 Oliver Mann, *Hamburg*  
 Marc E Martignoni, *Munic*  
 Thomas Minor, *Bonn*  
 Oliver Moeschler, *Osnabrueck*  
 Jonas Mudter, *Eutin*  
 Sebastian Mueller, *Heidelberg*  
 Matthias Ocker, *Berlin*  
 Andreas Ommer, *Essen*  
 Albrecht Piiper, *Frankfurt*  
 Esther Raskopf, *Bonn*  
 Christoph Reichel, *Bad Brückenau*  
 Elke Roeb, *Giessen*  
 Udo Rolle, *Frankfurt*  
 Karl-Herbert Schafer, *Zweibrücken*  
 Peter Schemmer, *Heidelberg*  
 Andreas G Schreyer, *Regensburg*  
 Manuel A Silva, *Penzberg*  
 Georgios C Sotiropoulos, *Essen*  
 Ulrike S Stein, *Berlin*  
 Dirk Uhlmann, *Leipzig*  
 Michael Weiss, *Halle*  
 Hong-Lei Weng, *Mannheim*  
 Karsten Wursthorn, *Hamburg*



#### **Greece**

Alexandra Alexopoulou, *Athens*  
 Nikolaos Antonakopoulos, *Athens*  
 Stelios F Assimakopoulos, *Patras*  
 Grigoris Chatzimavroudis, *Thessaloniki*  
 Evangelos Cholongitas, *Thessaloniki*  
 Gregory Christodoulidis, *Larisa*  
 George N Dalekos, *Larisa*  
 Urania Georgopoulou, *Athens*  
 Eleni Gigi, *Thessaloniki*



Stavros Gourgiotis, *Athens*  
 Leontios J Hadjileontiadis, *Thessaloniki*  
 Thomas Hyphantis, *Ioannina*  
 Ioannis Kanellos, *Thessaloniki*  
 Stylianos Karatapanis, *Rhodes*  
 Michael Koutsilieris, *Athens*  
 Spiros D Ladas, *Athens*  
 Theodoros K Liakakos, *Athens*  
 Emanuel K Manesis, *Athens*  
 Spiliot Manolakopoulos, *Athens*  
 Gerassimos John Mantzaris, *Athens*  
 Athanasios D Marinis, *Piraeus*  
 Nikolaos Ioannis Nikiteas, *Athens*  
 Konstantinos X Papamichael, *Athens*  
 George Sgourakis, *Athens*  
 Konstantinos C Thomopoulos, *Patras*  
 Konstantinos Triantafyllou, *Athens*  
 Christos Triantos, *Patras*  
 Georgios Zacharakis, *Athens*  
 Petros Zazos, *Alexandroupolis*  
 Demosthenes E Ziogas, *Ioannina*



#### **Guatemala**

Carlos Maria Parellada, *Guatemala*



#### **Hungary**

Mihaly Boros, *Szeged*  
 Tamás Decsi, *Pécs*  
 Gyula Farkas, *Szeged*  
 Andrea Furka, *Debrecen*  
 Y vette Mandi, *Szeged*  
 Peter L Lakatos, *Budapest*  
 Pal Miheller, *Budapest*  
 Tamás Molnar, *Szeged*  
 Attila Olah, *Gyor*  
 Maria Papp, *Debrecen*  
 Ferenc Sipos, *Budapest*  
 Miklós Tanyi, *Debrecen*  
 Tibor Wittmann, *Szeged*



#### **Iceland**

Tryggvi Bjorn Stefánsson, *Reykjavík*



#### **India**

Brij B Agarwal, *New Delhi*  
 Deepak N Amarapurkar, *Mumbai*  
 Shams ul Bari, *Srinagar*  
 Sriparna Basu, *Varanasi*  
 Runu Chakravarty, *Kolkata*  
 Devendra C Desai, *Mumbai*  
 Nutan D Desai, *Mumbai*  
 Suneela Sunil Dhaneshwar, *Pune*  
 Radha K Dhiman, *Chandigarh*  
 Pankaj Garg, *Mohali*  
 Uday C Ghoshal, *Lucknow*  
 Kalpesh Jani, *Vadodara*  
 Premashis Kar, *New Delhi*  
 Jyotdeep Kaur, *Chandigarh*  
 Rakesh Kochhar, *Chandigarh*  
 Pradyumna K Mishra, *Mumbai*

Asish K Mukhopadhyay, *Kolkata*  
 Imtiyaz Murtaza, *Srinagar*  
 P Nagarajan, *New Delhi*  
 Samiran Nundy, *Delhi*  
 Gopal Pande, *Hyderabad*  
 Benjamin Perakath, *Vellore*  
 Arun Prasad, *New Delhi*  
 D Nageshwar Reddy, *Hyderabad*  
 Lekha Saha, *Chandigarh*  
 Sundeep Singh Saluja, *New Delhi*  
 Mahesh Prakash Sharma, *New Delhi*  
 Sadiq Saleem Sikora, *Bangalore*  
 Sarman Singh, *New Delhi*  
 Rajeev Sinha, *Jhansi*  
 Rupjyoti Talukdar, *Hyderabad*  
 Rakesh Kumar Tandon, *New Delhi*  
 Narayanan Thirumoorthy, *Coimbatore*



#### **Indonesia**

David Handoyo Muljono, *Jakarta*  
 Andi Utama, *Jakarta*



#### **Iran**

Arezo Aghakhani, *Tehran*  
 Seyed Mohsen Dehghani, *Shiraz*  
 Ahad Eshraghian, *Shiraz*  
 Hossein Khedmat, *Tehran*  
 Sadegh Massarrat, *Tehran*  
 Marjan Mohammadi, *Tehran*  
 Roja Rahimi, *Tehran*  
 Farzaneh Sabahi, *Tehran*  
 Majid Sadeghizadeh, *Tehran*  
 Farideh Siavoshi, *Tehran*



#### **Ireland**

Gary Alan Bass, *Dublin*  
 David J Brayden, *Dublin*  
 Ronan A Cahill, *Dublin*  
 Glen A Doherty, *Dublin*  
 Liam J Fanning, *Cork*  
 Barry Philip McMahon, *Dublin*  
 RossMcManus, *Dublin*  
 Dervla O'Malley, *Cork*  
 Sinead M Smith, *Dublin*



#### **Israel**

Dan Carter, *Ramat Gan*  
 Jorge-Shmuel Delgado, *Metar*  
 Eli Magen, *Ashdod*  
 Nitsan Maharshak, *Tel Aviv*  
 Shaul Mordechai, *Beer Sheva*  
 Menachem Moshkowitz, *Tel Aviv*  
 William Bahij Nseir, *Nazareth*  
 Shimon Reif, *Jerusalem*  
 Ram Reifen, *Rehovot*  
 Ariella Bar-Gil Shitrit, *Jerusalem*  
 Noam Shussman, *Jerusalem*  
 Igor Sukhotnik, *Haifa*  
 Nir Wasserberg, *Petach Tikva*  
 Jacob Yahav, *Rehovot*

Doron Levi Zamir, *Gedera*  
 Shira Zelber-Sagi, *Haifa*  
 Romy Zemel, *Petach-Tikva*



#### **Italy**

Ludovico Abenavoli, *Catanzaro*  
 Luigi Elio Adinolfi, *Naples*  
 Carlo Virginio Agostoni, *Milan*  
 Anna Alisi, *Rome*  
 Piero Luigi Almasio, *Palermo*  
 Donato Francesco Altomare, *Bari*  
 Amedeo Amedei, *Florence*  
 Pietro Andreone, *Bologna*  
 Imerio Angriman, *Padova*  
 Vito Annese, *Florence*  
 Paolo Aurello, *Rome*  
 Salvatore Auricchio, *Naples*  
 Gian Luca Baiocchi, *Brescia*  
 Gianpaolo Balzano, *Milan*  
 Antonio Basoli, *Rome*  
 Gabrio Bassotti, *San Sisto*  
 Mauro Bernardi, *Bologna*  
 Alberto Biondi, *Rome*  
 Ennio Biscaldi, *Genova*  
 Massimo Bolognesi, *Padua*  
 Luigi Bonavina, *Milano*  
 Aldo Bove, *Chieti*  
 Raffaele Bruno, *Pavia*  
 Luigi Bruscianno, *Napoli*  
 Giuseppe Cabibbo, *Palermo*  
 Carlo Calabrese, *Bologna*  
 Daniele Calistri, *Meldola*  
 Vincenza Calvaruso, *Palermo*  
 Lorenzo Camellini, *Reggio Emilia*  
 Marco Candela, *Bologna*  
 Raffaele Capasso, *Naples*  
 Lucia Carulli, *Modena*  
 Renato David Caviglia, *Rome*  
 Luigina Cellini, *Chieti*  
 Giuseppe Chiarioni, *Verona*  
 Claudio Chiesa, *Rome*  
 Michele Cicala, *Roma*  
 Rachele Ciccocioppo, *Pavia*  
 Sandro Contini, *Parma*  
 Gaetano Corso, *Foggia*  
 Renato Costi, *Parma*  
 Alessandro Cucchetti, *Bologna*  
 Rosario Cuomo, *Napoli*  
 Giuseppe Currò, *Messina*  
 Paola De Nardi, *Milano*  
 Giovanni D De Palma, *Naples*  
 Raffaele De Palma, *Napoli*  
 Giuseppina De Petro, *Brescia*  
 Valli De Re, *Aviano*  
 Paolo De Simone, *Pisa*  
 Giuliana Decorti, *Trieste*  
 Emanuele Miraglia del Giudice, *Napoli*  
 Isidoro Di Carlo, *Catania*  
 Matteo Nicola Dario Di Minno, *Naples*  
 Massimo Donadelli, *Verona*  
 Mirko D'Onofrio, *Verona*  
 Maria Pina Dore, *Sassari*  
 Luca Elli, *Milano*  
 Massimiliano Fabozzi, *Aosta*  
 Massimo Falconi, *Ancona*

Ezio Falletto, *Turin*  
 Silvia Fargion, *Milan*  
 Matteo Fassan, *Verona*  
 Gianfranco Delle Fave, *Roma*  
 Alessandro Federico, *Naples*  
 Francesco Feo, *Sassari*  
 Davide Festi, *Bologna*  
 Natale Figura, *Siena*  
 Vincenzo Formica, *Rome*  
 Mirella Fraquelli, *Milan*  
 Marzio Frazzoni, *Modena*  
 Walter Fries, *Messina*  
 Gennaro Galizia, *Naples*  
 Andrea Galli, *Florence*  
 Matteo Garcovich, *Rome*  
 Eugenio Gaudio, *Rome*  
 Paola Ghiorzo, *Genoa*  
 Edoardo G Giannini, *Genova*  
 Luca Gianotti, *Monza*  
 Maria Cecilia Giron, *Padova*  
 Alberto Grassi, *Rimini*  
 Gabriele Grassi, *Trieste*  
 Francesco Greco, *Bergamo*  
 Luigi Greco, *Naples*  
 Antonio Grieco, *Rome*  
 Fabio Grizzi, *Rozzano*  
 Laurino Grossi, *Pescara*  
 Simone Guglielmetti, *Milan*  
 Tiberiu Hershcovici, *Jerusalem*  
 Calogero Iacono, *Verona*  
 Enzo Ierardi, *Bari*  
 Amedeo Indriolo, *Bergamo*  
 Raffaele Iorio, *Naples*  
 Paola Iovino, *Salerno*  
 Angelo A Izzo, *Naples*  
 Loretta Kondili, *Rome*  
 Filippo La Torre, *Rome*  
 Giuseppe La Torre, *Rome*  
 Giovanni Latella, *L'Aquila*  
 Salvatore Leonardi, *Catania*  
 Massimo Libra, *Catania*  
 Anna Licata, *Palermo*  
 Carmela Loguercio, *Naples*  
 Amedeo Lonardo, *Modena*  
 Carmelo Luigiano, *Catania*  
 Francesco Luzzo, *Catanzaro*  
 Giovanni Maconi, *Milano*  
 Antonio Macrì, *Messina*  
 Mariano Malaguarnera, *Catania*  
 Francesco Manguso, *Napoli*  
 Tommaso Maria Manzia, *Rome*  
 Daniele Marrelli, *Siena*  
 Gabriele Masselli, *Rome*  
 Sara Massironi, *Milan*  
 Giuseppe Mazzarella, *Avellino*  
 Michele Milella, *Rome*  
 Giovanni Milito, *Rome*  
 Antonella d'Arminio Monforte, *Milan*  
 Fabrizio Montecucco, *Genoa*  
 Giovanni Monteleone, *Rome*  
 Mario Morino, *Torino*  
 Vincenzo La Mura, *Milan*  
 Gerardo Nardone, *Naples*  
 Riccardo Nascimbeni, *Brescia*  
 Gabriella Nesi, *Florence*  
 Giuseppe Nigri, *Rome*

Erica Novo, *Turin*  
 Veronica Ojetti, *Rome*  
 Michele Orditura, *Naples*  
 Fabio Pace, *Seriate*  
 Lucia Pacifico, *Rome*  
 Omero Alessandro Paoluzi, *Rome*  
 Valerio Pazienza, *San Giovanni Rotondo*  
 Rinaldo Pellicano, *Turin*  
 Adriano M Pellicelli, *Rome*  
 Nadia Peparini, *Ciampino*  
 Mario Pescatori, *Rome*  
 Antonio Picardi, *Rome*  
 Alberto Pilotto, *Padova*  
 Alberto Piperno, *Monza*  
 Anna Chiara Piscaglia, *Rome*  
 Maurizio Pompili, *Rome*  
 Francesca Romana Ponziani, *Rome*  
 Cosimo Prantero, *Rome*  
 Girolamo Ranieri, *Bari*  
 Carlo Ratto, *Tome*  
 Barbara Renga, *Perugia*  
 Alessandro Repici, *Rozzano*  
 Maria Elena Riccioni, *Rome*  
 Lucia Ricci-Vitiani, *Rome*  
 Luciana Rigoli, *Messina*  
 Mario Rizzetto, *Torino*  
 Ballarin Roberto, *Modena*  
 Roberto G Romanelli, *Florence*  
 Claudio Romano, *Messina*  
 Luca Roncucci, *Modena*  
 Cesare Ruffolo, *Treviso*  
 Lucia Sacchetti, *Napoli*  
 Rodolfo Sacco, *Pisa*  
 Lapo Sali, *Florence*  
 Romina Salpini, *Rome*  
 Giulio Aniello, *Santoro Treviso*  
 Armando Santoro, *Rozzano*  
 Edoardo Savarino, *Padua*  
 Marco Senzolo, *Padua*  
 Annalucia Serafino, *Rome*  
 Giuseppe S Sica, *Rome*  
 Pierpaolo Sileri, *Rome*  
 Cosimo Sperti, *Padua*  
 Vincenzo Stanghellini, *Bologna*  
 Cristina Stasi, *Florence*  
 Gabriele Stocco, *Trieste*  
 Roberto Tarquini, *Florence*  
 Mario Testini, *Bari*  
 Guido Torzilli, *Milan*  
 Guido Alberto Massimo, *Tiberio Brescia*  
 Giuseppe Toffoli, *Aviano*  
 Alberto Tommasini, *Trieste*  
 Francesco Tonelli, *Florence*  
 Cesare Tosetti Porretta, *Terme*  
 Lucio Trevisani, *Cona*  
 Guglielmo M Trovato, *Catania*  
 Mariapia Vairetti, *Pavia*  
 Luca Vittorio Valenti, *Milano*  
 Mariateresa T Ventura, *Bari*  
 Giuseppe Verlato, *Verona*  
 Marco Vivarelli, *Ancona*  
 Giovanni Li Volti, *Catania*  
 Giuseppe Zanotti, *Padua*  
 Vincenzo Zara, *Lecce*  
 Gianguglielmo Zehender, *Milan*  
 Anna Linda Zignego, *Florence*  
 Rocco Antonio Zoccali, *Messina*

Angelo Zullo, *Rome*



## Japan

Yasushi Adachi, *Sapporo*  
 Takafumi Ando, *Nagoya*  
 Masahiro Arai, *Tokyo*  
 Makoto Arai, *Chiba*  
 Takaaki Arigami, *Kagoshima*  
 Itaru Endo, *Yokohama*  
 Munechika Enjoji, *Fukuoka*  
 Shunji Fujimori, *Tokyo*  
 Yasuhiro Fujino, *Akashi*  
 Toshiyoshi Fujiwara, *Okayama*  
 Yosuke Fukunaga, *Tokyo*  
 Toshio Fukusato, *Tokyo*  
 Takahisa Furuta, *Hamamatsu*  
 Osamu Handa, *Kyoto*  
 Naoki Hashimoto, *Osaka*  
 Yoichi Hiasa, *Toon*  
 Masatsugu Hiraki, *Saga*  
 Satoshi Hirano, *Sapporo*  
 Keiji Hirata, *Fukuoka*  
 Toru Hiyama, *Higashihiroshima*  
 Akira Hokama, *Nishihara*  
 Shu Hoteya, *Tokyo*  
 Masao Ichinose, *Wakayama*  
 Tatsuya Ide, *Kurume*  
 Masahiro Iizuka, *Akita*  
 Toshiro Iizuka, *Tokyo*  
 Kenichi Ikejima, *Tokyo*  
 Tetsuya Ikemoto, *Tokushima*  
 Hiroyuki Imaeda, *Saitama*  
 Atsushi Imagawa, *Kan-onji*  
 Hiroo Imazu, *Tokyo*  
 Shuji Isaji, *Tsu*  
 Toru Ishikawa, *Niigata*  
 Toshiyuki Ishiwata, *Tokyo*  
 Soichi Itaba, *Kitakyushu*  
 Yoshiaki Iwasaki, *Okayama*  
 Tatehiro Kagawa, *Isehara*  
 Satoru Kakizaki, *Maebashi*  
 Naomi Kakushima, *Shizuoka*  
 Terumi Kamisawa, *Tokyo*  
 Akihide Kamiya, *Isehara*  
 Osamu Kanauchi, *Tokyo*  
 Tatsuo Kanda, *Chiba*  
 Shin Kariya, *Okayama*  
 Shigeyuki Kawa, *Matsumoto*  
 Takumi Kawaguchi, *Kurume*  
 Takashi Kawai, *Tokyo*  
 Soo Ryang Kim, *Kobe*  
 Shinsuke Kiriya, *Gunma*  
 Tsuneo Kitamura, *Urayasu*  
 Masayuki Kitano, *Osakasayama*  
 Hiroto Kobayashi, *Tokyo*  
 Hironori Koga, *Kurume*  
 Takashi Kojima, *Sapporo*  
 Satoshi Kokura, *Kyoto*  
 Shuhei Komatsu, *Kyoto*  
 Tadashi Kondo, *Tokyo*  
 Yasuteru Kondo, *Sendai*  
 Yasuhiro Kuramitsu, *Yamaguchi*  
 Yukinori Kurokawa, *Osaka*  
 Shin Maeda, *Yokohama*  
 Koutarou Maeda, *Toyoake*



Hitoshi Maruyama, *Chiba*  
 Atsushi Masamune, *Sendai*  
 Hiroyuki Matsubayashi, *Suntogun*  
 Akihisa Matsuda, *Inzai*  
 Hirofumi Matsui, *Tsukuba*  
 Akira Matsumori, *Kyoto*  
 Yoichi Matsuo, *Nagoya*  
 Y Matsuzaki, *Ami*  
 Toshihiro Mitaka, *Sapporo*  
 Kouichi Miura, *Akita*  
 Shinichi Miyagawa, *Matumoto*  
 Eiji Miyoshi, *Suita*  
 Toru Mizuguchi, *Sapporo*  
 Nobumasa Mizuno, *Nagoya*  
 Zenichi Morise, *Nagoya*  
 Tomohiko Moriyama, *Fukuoka*  
 Kunihiko Murase, *Tusima*  
 Michihiro Mutoh, *Tsukiji*  
 Akihito Nagahara, *Tokyo*  
 Hikaru Nagahara, *Tokyo*  
 Hidenari Nagai, *Tokyo*  
 Koichi Nagata, *Shimotsuke-shi*  
 Masaki Nagaya, *Kawasaki*  
 Hisato Nakajima, *Nishi-Shinbashi*  
 Toshifusa Nakajima, *Tokyo*  
 Hiroshi Nakano, *Kawasaki*  
 Hiroshi Nakase, *Kyoto*  
 Toshiyuki Nakayama, *Nagasaki*  
 Takahiro Nakazawa, *Nagoya*  
 Shoji Natsugoe, *Kagoshima City*  
 Tsutomu Nishida, *Suita*  
 Shuji Nomoto, *Naogya*  
 Sachiyo Nomura, *Tokyo*  
 Takeshi Ogura, *Takatsukishi*  
 Nobuhiro Ohkohchi, *Tsukuba*  
 Toshifumi Ohkusa, *Kashiwa*  
 Hirohide Ohnishi, *Akita*  
 Teruo Okano, *Tokyo*  
 Satoshi Osawa, *Hamamatsu*  
 Motoyuki Otsuka, *Tokyo*  
 Michitaka Ozaki, *Sapporo*  
 Satoru Saito, *Yokohama*  
 Naoaki Sakata, *Sendai*  
 Ken Sato, *Maebashi*  
 Toshiro Sato, *Tokyo*  
 Tomoyuki Shibata, *Toyoake*  
 Tomohiko Shimatani, *Kure*  
 Yukihiro Shimizu, *Nanto*  
 Tadashi Shimoyama, *Hirosaki*  
 Masayuki Sho, *Nara*  
 Ikuo Shoji, *Kobe*  
 Atsushi Sofuni, *Tokyo*  
 Takeshi Suda, *Niigata*  
 M Sugimoto, *Hamamatsu*  
 Ken Sugimoto, *Hamamatsu*  
 Haruhiko Sugimura, *Hamamatsu*  
 Shoichiro Sumi, *Kyoto*  
 Hidekazu Suzuki, *Tokyo*  
 Masahiro Tajika, *Nagoya*  
 Hitoshi Takagi, *Takasaki*  
 Toru Takahashi, *Niigata*  
 Yoshihisa Takahashi, *Tokyo*  
 Shinsuke Takeno, *Fukuoka*  
 Akihiro Tamori, *Osaka*  
 Kyosuke Tanaka, *Tsu*  
 Shinji Tanaka, *Hiroshima*

Atsushi Tanaka, *Tokyo*  
 Yasuhito Tanaka, *Nagoya*  
 Shinji Tanaka, *Tokyo*  
 Minoru Tomizawa, *Yotsukaido City*  
 Kyoko Tsukiyama-Kohara, *Kagoshima*  
 Takuya Watanabe, *Niigata*  
 Kazuhiro Watanabe, *Sendai*  
 Satoshi Yamagiwa, *Niigata*  
 Takayuki Yamamoto, *Yokkaichi*  
 Hiroshi Yamamoto, *Otsu*  
 Kosho Yamanouchi, *Nagasaki*  
 Ichiro Yasuda, *Gifu*  
 Yutaka Yata, *Maebashi-city*  
 Shin-ichi Yokota, *Sapporo*  
 Norimasa Yoshida, *Kyoto*  
 Hiroshi Yoshida, *Tama-City*  
 Hitoshi Yoshiji, *Kashihara*  
 Kazuhiko Yoshimatsu, *Tokyo*  
 Kentaro Yoshioka, *Toyoake*  
 Nobuhiro Zaima, *Nara*



#### **Jordan**

Khaled Ali Jadallah, *Irbid*



#### **Kuwait**

Islam Khan, *Kuwait*



#### **Lebanon**

Bassam N Abboud, *Beirut*  
 Kassem A Barada, *Beirut*  
 Marwan Ghosn, *Beirut*  
 Iyad A Issa, *Beirut*  
 Fadi H Mourad, *Beirut*  
 AIA Sharara, *Beirut*  
 Rita Slim, *Beirut*



#### **Lithuania**

Antanas Mickevicius, *Kaunas*



#### **Malaysia**

Huck Joo Tan, *Petaling Jaya*



#### **Mexico**

Richard A Awad, *Mexico City*  
 Carlos R Camara-Lemarroy, *Monterrey*  
 Norberto C Chavez-Tapia, *Mexico City*  
 Wolfgang Gaertner, *Mexico City*  
 Diego Garcia-Compean, *Monterrey*  
 Arturo Panduro, *Guadalajara*  
 OT Teramoto-Matsubara, *Mexico City*  
 Felix Tellez-Avila, *Mexico City*  
 Omar Vergara-Fernandez, *Mexico City*  
 Saúl Villa-Trevino, *Cuidad de México*



#### **Morocco**

Samir Ahboucha, *Khouribga*



#### **Netherlands**

Robert J de Knegt, *Rotterdam*  
 Tom Johannes Gerardus Gevers, *Nijmegen*  
 Menno Hoekstra, *Leiden*  
 BW Marcel Spanier, *Arnhem*  
 Karel van Erpecum, *Utrecht*



#### **New Zealand**

Leo K Cheng, *Auckland*  
 Andrew Stewart Day, *Christchurch*  
 Jonathan Barnes Koea, *Auckland*  
 Max Petrov, *Auckland*



#### **Nigeria**

Olufunmilayo Adenike Lesi, *Lagos*  
 Jesse Abiodun Otegbayo, *Ibadan*  
 Stella Ifeanyi Smith, *Lagos*



#### **Norway**

Trond Berg, *Oslo*  
 Trond Arnulf Buanes, *Krokkleiva*  
 Thomas de Lange, *Rud*  
 Magdy El-Salhy, *Stord*  
 Rasmus Goll, *Tromso*  
 Dag Arne Lihaug Hoff, *Aalesund*



#### **Pakistan**

Zaigham Abbas, *Karachi*  
 Usman A Ashfaq, *Faisalabad*  
 Muhammad Adnan Bawany, *Hyderabad*  
 Muhammad Idrees, *Lahore*  
 Saeed Sadiq Hamid, *Karachi*  
 Yasir Waheed, *Islamabad*



#### **Poland**

Thomas Brzozowski, *Cracow*  
 Magdalena Chmiela, *Lodz*  
 Krzysztof Jonderko, *Sosnowiec*  
 Anna Kasicka-Jonderko, *Sosnowiec*  
 Michal Kukla, *Katowice*  
 Tomasz Hubert Mach, *Krakow*  
 Agata Mulak, *Wroclaw*  
 Danuta Owczarek, *Kraków*  
 Piotr Socha, *Warsaw*  
 Piotr Stalke, *Gdansk*  
 Julian Teodor Swierczynski, *Gdansk*  
 Anna M Zawilak-Pawlik, *Wroclaw*



#### **Portugal**

Marie Isabelle Cremers, *Setubal*  
 Ceu Figueiredo, *Porto*  
 Ana Isabel Lopes, *Lisbon*  
 M Paula Macedo, *Lisboa*  
 Ricardo Marcos, *Porto*  
 Rui T Marinho, *Lisboa*  
 Guida Portela-Gomes, *Estoril*

Filipa F Vale, *Lisbon*



**Puerto Rico**

Caroline B Appleyard, *Ponce*



**Qatar**

Abdulbari Bener, *Doha*



**Romania**

Mihai Ciocirlan, *Bucharest*

Dan Lucian Dumitrascu, *Cluj-Napoca*

Carmen Fierbinteanu-Braticevici, *Bucharest*

Romeo G Mihaila, *Sibiu*

Lucian Negreanu, *Bucharest*

Adrian Saftoiu, *Craiova*

Andrada Seicean, *Cluj-Napoca*

Ioan Sporea, *Timisoara*

Letitia Adela Maria Streba, *Craiova*

Anca Trifan, *Iasi*



**Russia**

Victor Pasechnikov, *Stavropol*

Vasiliy Ivanovich Reshetnyak, *Moscow*

Vitaly Skoropad, *Obninsk*



**Saudi Arabia**

Abdul-Wahed N Meshikhes, *Dammam*

M Ezzedien Rabie, *Khamis Mushait*



**Singapore**

Brian KP Goh, *Singapore*

Richie Soong, *Singapore*

Ker-Kan Tan, *Singapore*

Kok-Yang Tan, *Singapore*

Yee-Joo Tan, *Singapore*

Mark Wong, *Singapore*

Hong Ping Xia, *Singapore*



**Slovenia**

Matjaz Homan, *Ljubljana*

Martina Perse, *Ljubljana*



**South Korea**

Sang Hoon Ahn, *Seoul*

Seung Hyuk Baik, *Seoul*

Soon Koo Baik, *Wonju*

Soo-Cheon Chae, *Iksan*

Byung-Ho Choe, *Daegu*

Suck Chei Choi, *Iksan*

Hoon Jai Chun, *Seoul*

Yeun-Jun Chung, *Seoul*

Young-Hwa Chung, *Seoul*

Ki-Baik Hahm, *Seongnam*

Sang Young Han, *Busan*

Seok Joo Han, *Seoul*

Seung-Heon Hong, *Iksan*

Jin-Hyeok Hwang, *Seoungnam*

Jeong Won Jang, *Seoul*

Jin-Young Jang, *Seoul*

Dae-Won Jun, *Seoul*

Young Do Jung, *Kwangju*

Gyeong Hoon Kang, *Seoul*

Sung-Bum Kang, *Seoul*

Koo Jeong Kang, *Daegu*

Ki Mun Kang, *Jinju*

Chang Moo Kang, *Seodaemun-gu*

Gwang Ha Kim, *Busan*

Sang Soo Kim, *Goyang-si*

Jin Cheon Kim, *Seoul*

Tae Il Kim, *Seoul*

Jin Hong Kim, *Suwon*

Kyung Mo Kim, *Seoul*

Kyongmin Kim, *Suwon*

Hyung-Ho Kim, *Seongnam*

Seoung Hoon Kim, *Goyang*

Sang Il Kim, *Seoul*

Hyun-Soo Kim, *Wonju*

Jung Mogg Kim, *Seoul*

Dong Yi Kim, *Gwangju*

Kyun-Hwan Kim, *Seoul*

Jong-Han Kim, *Ansan*

Sang Wun Kim, *Seoul*

Ja-Lok Ku, *Seoul*

Kyu Taek Lee, *Seoul*

Hae-Wan Lee, *Chuncheon*

Inchul Lee, *Seoul*

Jung Eun Lee, *Seoul*

Sang Chul Lee, *Daejeon*

Song Woo Lee, *Ansan-si*

Hyuk-Joon Lee, *Seoul*

Seong-Wook Lee, *Yongin*

Kil Yeon Lee, *Seoul*

Jong-Inn Lee, *Seoul*

Kyung A Lee, *Seoul*

Jong-Baeck Lim, *Seoul*

Eun-Yi Moon, *Seoul*

SH Noh, *Seoul*

Seung Woon Paik, *Seoul*

Won Sang Park, *Seoul*

Sung-Joo Park, *Iksan*

Kyung Sik Park, *Daegu*

Se Hoon Park, *Seoul*

Yoonkyung Park, *Gwangju*

Seung-Wan Ryu, *Daegu*

Il Han Song, *Cheonan*

Myeong Jun Song, *Daejeon*

Yun Kyoung Yim, *Daejeon*

Dae-Yeul Yu, *Daejeon*



**Spain**

Mariam Aguas, *Valencia*

Raul J Andrade, *Málaga*

Antonio Arroyo, *Elche*

Josep M Bordas, *Barcelona*

Lisardo Boscá, *Madrid*

Ricardo Robles Campos, *Murcia*

Jordi Camps, *Reus*

Carlos Cervera, *Barcelona*

Alfonso Clemente, *Granada*

Pilar Codoner-Franch, *Valencia*

Fernando J Corrales, *Pamplona*

Fermin Sánchez de Medina, *Granada*

Alberto Herreros de Tejada, *Majadahonda*

Enrique de-Madaria, *Alicante*

JE Dominguez-Munoz, *Santiago de Compostela*

Vicente Felipo, *Valencia*

CM Fernandez-Rodriguez, *Madrid*

Carmen Frontela-Saseta, *Murcia*

Julio Galvez, *Granada*

Maria Teresa García, *Vigo*

MI Garcia-Fernandez, *Málaga*

Emilio Gonzalez-Reimers, *La Laguna*

Marcel Jimenez, *Bellaterra*

Angel Lanas, *Zaragoza*

Juan Ramón Larrubia, *Guadalajara*

Antonio Lopez-Sanroman, *Madrid*

Vicente Lorenzo-Zuniga, *Badalona*

Alfredo J Lucendo, *Tomelloso*

Vicenta Soledad Martinez-Zorzano, *Vigo*

José Manuel Martin-Villa, *Madrid*

Julio Mayol, *Madrid*

Manuel Morales-Ruiz, *Barcelona*

Alfredo Moreno-Egea, *Murcia*

Albert Pares, *Barcelona*

Maria Pellise, *Barcelona*

José Perea, *Madrid*

Miguel Angel Plaza, *Zaragoza*

María J Pozo, *Cáceres*

Enrique Quintero, *La Laguna*

Jose M Ramia, *Madrid*

Francisco Rodriguez-Frias, *Barcelona*

Silvia Ruiz-Gaspa, *Barcelona*

Xavier Serra-Aracil, *Barcelona*

Vincent Soriano, *Madrid*

Javier Suarez, *Pamplona*

Carlos Taxonera, *Madrid*

M Isabel Torres, *Jaén*

Manuel Vazquez-Carrera, *Barcelona*

Benito Velayos, *Valladolid*

Silvia Vidal, *Barcelona*



**Sri Lanka**

Arjuna Priyadarsin De Silva, *Colombo*



**Sudan**

Ishag Adam, *Khartoum*



**Sweden**

Roland G Andersson, *Lund*

Bergthor Björnsson, *Linköping*

Johan Christopher Bohr, *Örebro*

Mauro D'Amato, *Stockholm*

Thomas Franzen, *Norrköping*

Evangelos Kalaitzakis, *Lund*

Riadh Sadik, *Gothenburg*

Per Anders Sandstrom, *Linköping*

Ervin Toth, *Malmö*

Konstantinos Tsimogiannis, *Vasteras*

Apostolos V Tsolakis, *Uppsala*



**Switzerland**

Gieri Cathomas, *Liestal*  
Jean Louis Frossard, *Geneve*  
Christian Toso, *Geneva*  
Stephan Robert Vavricks, *Zurich*  
Dominique Velin, *Lausanne*

**Thailand**

Thawatchai Akaraviputh, *Bangkok*  
P Yoysungnoen Chintana, *Pathumthani*  
Veerapol Kukongviriyapan, *Muang*  
Vijitra Leardkamolkarn, *Bangkok*  
Varut Lohsiriwat, *Bangkok*  
Somchai Pinlaor, *Khaon Kaen*  
D Wattanasirichaigoon, *Bangkok*

**Trinidad and Tobago**

B Shivananda Nayak, *Mount Hope*

**Tunisia**

Ibtissem Ghedira, *Sousse*  
Lilia Zouiten-Mekki, *Tunis*

**Turkey**

Inci Alican, *Istanbul*  
Mustafa Altindis, *Sakarya*  
Mutay Aslan, *Antalya*  
Oktar Asoglu, *Istanbul*  
Yasemin Hatice Balaban, *Istanbul*  
Metin Basaranoglu, *Ankara*  
Yusuf Bayraktar, *Ankara*  
Süleyman Bayram, *Adiyaman*  
Ahmet Bilici, *Istanbul*  
Ahmet Sedat Boyacioglu, *Ankara*  
Züleyha Akkan Cetinkaya, *Kocaeli*  
Cavit Col, *Bolu*  
Yasar Colak, *Istanbul*  
Cagatay Erden Daphan, *Kirikkale*  
Mehmet Demir, *Hatay*  
Ahmet Merih Dobrucali, *Istanbul*  
Gülüm Ozlem Elpek, *Antalya*  
Ayse Basak Engin, *Ankara*  
Eren Ersoy, *Ankara*  
Osman Ersoy, *Ankara*  
Yusuf Ziya Erzin, *Istanbul*  
Mukaddes Esrefoglu, *Istanbul*  
Levent Filik, *Ankara*  
Ozgur Harmanaci, *Ankara*  
Koray Hekimoglu, *Ankara*  
Abdurrahman Kadayifci, *Gaziantep*  
Cem Kalayci, *Istanbul*  
Selin Kapan, *Istanbul*  
Huseyin Kayadibi, *Adana*  
Sabahattin Kaymakoglu, *Istanbul*  
Metin Kement, *Istanbul*  
Mevlut Kurt, *Bolu*  
Resat Ozaras, *Istanbul*  
Elvan Ozbek, *Adapazari*

Cengiz Ozcan, *Mersin*  
Hasan Ozen, *Ankara*  
Halil Ozguc, *Bursa*  
Mehmet Ozturk, *Izmir*  
Orhan V Ozkan, *Sakarya*  
Semra Paydas, *Adana*  
Ozlem Durmaz Suoglu, *Istanbul*  
Ilker Tasci, *Ankara*  
Müge Tecder-ünal, *Ankara*  
Mesut Tez, *Ankara*  
Serdar Topaloglu, *Trabzon*  
Murat Toruner, *Ankara*  
Gokhan Tumgor, *Adana*  
Oguz Uskudar, *Adana*  
Mehmet Yalniz, *Elazig*  
Mehmet Yaman, *Elazig*  
Veli Yazisiz, *Antalya*  
Yusuf Yilmaz, *Istanbul*  
Ozlem Yilmaz, *Izmir*  
Oya Yucel, *Istanbul*  
Ilhami Yuksel, *Ankara*

**United Kingdom**

Nadeem Ahmad Afzal, *Southampton*  
Navneet K Ahluwalia, *Stockport*  
Yeng S Ang, *Lancashire*  
Ramesh P Arasaradnam, *Coventry*  
Ian Leonard Phillip Beales, *Norwich*  
John Beynon, *Swansea*  
Barbara Braden, *Oxford*  
Simon Bramhall, *Birmingham*  
Geoffrey Burnstock, *London*  
Ian Chau, *Sutton*  
Thean Soon Chew, *London*  
Helen G Coleman, *Belfast*  
Anil Dhawan, *London*  
Sunil Dolwani, *Cardiff*  
Piers Gatenby, *London*  
Anil T George, *London*  
Pasquale Giordano, *London*  
Paul Henderson, *Edinburgh*  
Georgina Louise Hold, *Aberdeen*  
Stefan Hubscher, *Birmingham*  
Robin D Hughes, *London*  
Nusrat Husain, *Manchester*  
Matt W Johnson, *Luton*  
Konrad Koss, *Macclesfield*  
Anastasios Koulaouzidis, *Edinburgh*  
Simon Lal, *Salford*  
John S Leeds, *Aberdeen*  
JK K Limdi, *Manchester*  
Hongxiang Liu, *Cambridge*  
Michael Joseph McGarvey, *London*  
Michael Anthony Mendall, *London*  
Alexander H Mirnezami, *Southampton*  
J Bernadette Moore, *Guildford*  
Claudio Nicoletti, *Norwich*  
Savvas Papagrigoriadis, *London*  
Sylvia LF Pender, *Southampton*  
David Mark Pritchard, *Liverpool*  
James A Ross, *Edinburgh*  
Kamran Rostami, *Worcester*  
Xiong Z Ruan, *London*  
Frank I Tovey, *London*  
Dhiraj Tripathi, *Birmingham*

Vamsi R Velchuru, *Great Yarmouth*  
Nicholas T Ventham, *Edinburgh*  
Diego Vergani, *London*  
Jack Westwood Winter, *Glasgow*  
Terence Wong, *London*  
Ling Yang, *Oxford*

**United States**

Daniel E Abbott, *Cincinnati*  
Ghassan K Abou-Alfa, *New York*  
Julian Abrams, *New York*  
David William Adelson, *Los Angeles*  
Jonathan Steven Alexander, *Shreveport*  
Tauseef Ali, *Oklahoma City*  
Mohamed R Ali, *Sacramento*  
Rajagopal N Aravalli, *Minneapolis*  
Hassan Ashktorab, *Washington*  
Shashi Bala, *Worcester*  
Charles F Barish, *Raleigh*  
P Patrick Basu, *New York*  
Robert L Bell, *Berkeley Heights*  
David Bentrem, *Chicago*  
Henry J Binder, *New Haven*  
Joshua Bleier, *Philadelphia*  
Wojciech Blonski, *Johnson City*  
Kenneth Boorum, *Corvallis*  
Brian Boulay, *Chicago*  
Carla W Brady, *Durham*  
Kyle E Brown, *Iowa City*  
Adeel A Butt, *Pittsburgh*  
Weibiao Cao, *Providence*  
Andrea Castillo, *Cheney*  
Fernando J Castro, *Weston*  
Adam S Cheifetz, *Boston*  
Xiaoxin Luke Chen, *Durham*  
Ramsey Cheung, *Palo Alto*  
Parimal Chowdhury, *Little Rock*  
Edward John Ciccio, *New York*  
Dahn L Clemens, *Omaha*  
Yingzi Cong, *Galveston*  
Laura Iris Cosen-Binker, *Boston*  
Joseph John Cullen, *Iowa*  
Mark J Czaja, *Bronx*  
Mariana D Dabeva, *Bronx*  
Christopher James Damman, *Seattle*  
Isabelle G De Plaen, *Chicago*  
Punita Dhawan, *Nashville*  
Hui Dong, *La Jolla*  
Wael El-Rifai, *Nashville*  
Sukru H Emre, *New Haven*  
Paul Feuerstadt, *Hamden*  
Josef E Fischer, *Boston*  
Laurie N Fishman, *Boston*  
Joseph Che Forbi, *Atlanta*  
Temitope Foster, *Atlanta*  
Amy E Foxx-Orenstein, *Scottsdale*  
Daniel E Freedberg, *New York*  
Shai Friedland, *Palo Alto*  
Virgilio George, *Indianapolis*  
Ajay Goel, *Dallas*  
Oliver Grundmann, *Gainesville*  
Stefano Guandalini, *Chicago*  
Chakshu Gupta, *St. Joseph*  
Grigoriy E Gurvits, *New York*

Xiaonan Han, *Cincinnati*  
 Mohamed Hassan, *Jackson*  
 Martin Hauer-Jensen, *Little Rock*  
 Koichi Hayano, *Boston*  
 Yingli Hee, *Atlanta*  
 Samuel B Ho, *San Diego*  
 Jason Ken Hou, *Houston*  
 Lifang Hou, *Chicago*  
 K-Qin Hu, *Orange*  
 Jamal A Ibdah, *Columbia*  
 Robert Thomas Jensen, *Bethesda*  
 Huanguang "Charlie" Jia, *Gainesville*  
 Rome Jutabha, *Los Angeles*  
 Andreas M Kaiser, *Los Angeles*  
 Avinash Kambadakone, *Boston*  
 David Edward Kaplan, *Philadelphia*  
 Randeep Kashyap, *Rochester*  
 Rashmi Kaul, *Tulsa*  
 Ali Keshavarzian, *Chicago*  
 Amir Maqbul Khan, *Marshall*  
 Nabeel Hasan Khan, *New Orleans*  
 Sahil Khanna, *Rochester*  
 Kusum K Kharbanda, *Omaha*  
 Hyun Sik Kim, *Pittsburgh*  
 Joseph Kim, *Duarte*  
 Jae S Kim, *Gainesville*  
 Miran Kim, *Providence*  
 Timothy R Koch, *Washington*  
 Burton I Korelitz, *New York*  
 Betsy Kren, *Minneapolis*  
 Shiu-Ming Kuo, *Buffalo*  
 Michelle Lai, *Boston*  
 Andreas Larentzakis, *Boston*  
 Edward Wolfgang Lee, *Los Angeles*  
 Daniel A Leffler, *Boston*  
 Michael Leitman, *New York*  
 Suthat Liangpunsakul, *Indianapolis*  
 Joseph K Lim, *New Haven*  
 Elaine Y Lin, *Bronx*  
 Henry C Lin, *Albuquerque*  
 Rohit Loomba, *La Jolla*  
 James David Luketich, *Pittsburgh*

Li Ma, *Stanford*  
 Mohammad F Madhoun, *Oklahoma City*  
 Thomas C Mahl, *Buffalo*  
 Ashish Malhotra, *Bettendorf*  
 Pranoti Mandrekar, *Worcester*  
 John Marks, *Wynnewood*  
 Wendy M Mars, *Pittsburgh*  
 Julien Vahe Matricon, *San Antonio*  
 Craig J McClain, *Louisville*  
 Tamir Miloh, *Phoenix*  
 Ayse Leyla Mindikoglu, *Baltimore*  
 Huanbiao Mo, *Denton*  
 Klaus Monkemuller, *Birmingham*  
 John Morton, *Stanford*  
 Adnan Muhammad, *Tampa*  
 Michael J Nowicki, *Jackson*  
 Patrick I Okolo, *Baltimore*  
 Giusepp Orlando, *Winston Salem*  
 Natalia A Osona, *Omaha*  
 Virendra N Pandey, *Newark*  
 Mansour A Parsi, *Cleveland*  
 Michael F Picco, *Jacksonville*  
 Daniel S Pratt, *Boston*  
 Xiaofa Qin, *Newark*  
 Janardan K Reddy, *Chicago*  
 Victor E Reyes, *Galveston*  
 Jon Marc Rhoads, *Houston*  
 Giulia Roda, *New York*  
 Jean-Francois Armand Rossignol, *Tampa*  
 Paul A Rufo, *Boston*  
 Madhusudana Girija Sanal, *New York*  
 Miguel Saps, *Chicago*  
 Sushil Sarna, *Galveston*  
 Ann O Scheimann, *Baltimore*  
 Bernd Schnabl, *La Jolla*  
 Matthew J Schuchert, *Pittsburgh*  
 Ekihiro Seki, *La Jolla*  
 Chanjuan Shi, *Nashville*  
 David Quan Shih, *Los Angeles*  
 Shadab A Siddiqi, *Orlando*  
 William B Silverman, *Iowa City*  
 Shashideep Singhal, *New York*

Bronislaw L Slomiany, *Newark*  
 Steven F Solga, *Bethlehem*  
 Byoung-Joon Song, *Bethesda*  
 Dario Sorrentino, *Roanoke*  
 Scott R Steele, *Fort Lewis*  
 Branko Stefanovic, *Tallahassee*  
 Arun Swaminath, *New York*  
 Kazuaki Takabe, *Richmond*  
 Naoki Tanaka, *Bethesda*  
 Hans Ludger Tillmann, *Durham*  
 George Triadafilopoulos, *Stanford*  
 John Richardson Thompson, *Nashville*  
 Andrew Ukleja, *Weston*  
 Miranda AL van Tilburg, *Chapel Hill*  
 Gilberto Vaughan, *Atlanta*  
 Vijayakumar Velu, *Atlanta*  
 Gebhard Wagener, *New York*  
 Kasper Saonun Wang, *Los Angeles*  
 Xiangbing Wang, *New Brunswick*  
 Daoyan Wei, *Houston*  
 Theodore H Welling, *Ann Arbor*  
 C Mel Wilcox, *Birmingham*  
 Jacqueline Lee Wolf, *Boston*  
 Laura Ann Woollett, *Cincinnati*  
 Harry Hua-Xiang Xia, *East Hanover*  
 Wen Xie, *Pittsburgh*  
 Guang Yu Yang, *Chicago*  
 Michele T Yip-Schneider, *Indianapolis*  
 Sam Zakhari, *Bethesda*  
 Kezhong Zhang, *Detroit*  
 Huiping Zhou, *Richmond*  
 Xiao-Jian Zhou, *Cambridge*  
 Richard Zubarik, *Burlington*



**Venezuela**

Miguel Angel Chiurillo, *Barquisimeto*



**Vietnam**

Van Bang Nguyen, *Hanoi*



**REVIEW**

- 8109** Relation of the IGF/IGF1R system to autophagy in colitis and colorectal cancer

*Sipos F, Székely H, Kis ID, Tulassay Z, Múzes G*

**MINIREVIEWS**

- 8120** Retreatment of patients with treatment failure of directacting antivirals: Focus on hepatitis C virus genotype 1b

*Kanda T, Nirei K, Matsumoto N, Higuchi T, Nakamura H, Yamagami H, Matsuoka S, Moriyama M*

**ORIGINAL ARTICLE****Basic Study**

- 8128** Structural shift of gut microbiota during chemo-preventive effects of epigallocatechin gallate on colorectal carcinogenesis in mice

*Wang X, Ye T, Chen WJ, Lv Y, Hao Z, Chen J, Zhao JY, Wang HP, Cai YK*

- 8140** miR-192-5p regulates lipid synthesis in non-alcoholic fatty liver disease through SCD-1

*Liu XL, Cao HX, Wang BC, Xin FZ, Zhang RN, Zhou D, Yang RY, Zhao ZH, Pan Q, Fan JG*

- 8152** *In vivo* hepatic differentiation potential of human umbilical cord-derived mesenchymal stem cells: Therapeutic effect on liver fibrosis/cirrhosis

*Zhang GZ, Sun HC, Zheng LB, Guo JB, Zhang XL*

- 8169** Pharmacokinetics and pharmacodynamics of Shengjiang decoction in rats with acute pancreatitis for protecting against multiple organ injury

*Zhu L, Li JY, Zhang YM, Kang HX, Chen H, Su H, Li J, Tang WF*

**Retrospective Cohort Study**

- 8182** Prevalence of- and risk factors for work disability in Dutch patients with inflammatory bowel disease

*Spekhorst LM, Oldenburg B, van Bodegraven AA, de Jong DJ, Imhann F, van der Meulen-de Jong AE, Pierik MJ, van der Woude JC, Dijkstra G, D'Haens G, Löwenberg M, Weersma RK, Festen EAM; PARELSNOER Institute and the Dutch Initiative on Crohn and Coliti*

**Retrospective Study**

- 8193** Endoscopic ultrasound staging for early esophageal cancer: Are we denying patients neoadjuvant chemo-radiation?

*Luu C, Amaral M, Klapman J, Harris C, Almhanna K, Hoffe S, Frakes J, Pimiento JM, Fontaine JP*

- 8200 Early gastric cancer frequently has high expression of KK-LC-1, a cancer-testis antigen

*Futawatari N, Fukuyama T, Yamamura R, Shida A, Takahashi Y, Nishi Y, Ichiki Y, Kobayashi N, Yamazaki H, Watanabe M*

- 8207 Diagnostic classification of endosonography for differentiating colorectal ulcerative diseases: A new statistical method

*Qiu EQ, Guo W, Cheng TM, Yao YL, Zhu W, Liu SD, Zhi FC*

### Clinical Trial Study

- 8217 Characteristics of fecal microbial communities in patients with non-anastomotic biliary strictures after liver transplantation

*Zhang J, Ren FG, Liu P, Zhang HK, Zhu HY, Feng Z, Zhang XF, Wang B, Liu XM, Zhang XG, Wu RQ, Lv Y*

### Observational Study

- 8227 Balloon dilatation for treatment of hepatic venous outflow obstruction following pediatric liver transplantation

*Zhang ZY, Jin L, Chen G, Su TH, Zhu ZJ, Sun LY, Wang ZC, Xiao GW*

### Prospective Study

- 8235 Efficacy of noninvasive evaluations in monitoring inflammatory bowel disease activity: A prospective study in China

*Chen JM, Liu T, Gao S, Tong XD, Deng FH, Nie B*

### CASE REPORT

- 8248 Are liver nested stromal epithelial tumors always low aggressive?

*Meletani T, Cantini L, Lanese A, Nicolini D, Cimadamore A, Agostini A, Ricci G, Antognoli S, Mandolesi A, Guido M, Alaggio R, Giuseppetti GM, Scarpelli M, Vivarelli M, Berardi R*

- 8256 Combined thoracoscopic and endoscopic surgery for a large esophageal schwannoma

*Onodera Y, Nakano T, Takeyama D, Maruyama S, Taniyama Y, Sakurai T, Heishi T, Sato C, Kumagai T, Kamei T*

### LETTER TO THE EDITOR

- 8261 Extended pelvic side wall excision for locally advanced rectal cancers

*Shaikh IA, Jenkins JT*

ABOUT COVER

Editorial board member of *World Journal of Gastroenterology*, Antonio Macri, MD, Associate Professor, Department of Human Pathology, University of Messina, Messina 98125, Italy

AIMS AND SCOPE

*World Journal of Gastroenterology* (*World J Gastroenterol*, *WJG*, print ISSN 1007-9327, online ISSN 2219-2840, DOI: 10.3748) is a peer-reviewed open access journal. *WJG* was established on October 1, 1995. It is published weekly on the 7<sup>th</sup>, 14<sup>th</sup>, 21<sup>st</sup>, and 28<sup>th</sup> each month. The *WJG* Editorial Board consists of 1375 experts in gastroenterology and hepatology from 68 countries.

The primary task of *WJG* is to rapidly publish high-quality original articles, reviews, and commentaries in the fields of gastroenterology, hepatology, gastrointestinal endoscopy, gastrointestinal surgery, hepatobiliary surgery, gastrointestinal oncology, gastrointestinal radiation oncology, gastrointestinal imaging, gastrointestinal interventional therapy, gastrointestinal infectious diseases, gastrointestinal pharmacology, gastrointestinal pathophysiology, gastrointestinal pathology, evidence-based medicine in gastroenterology, pancreatology, gastrointestinal laboratory medicine, gastrointestinal molecular biology, gastrointestinal immunology, gastrointestinal microbiology, gastrointestinal genetics, gastrointestinal translational medicine, gastrointestinal diagnostics, and gastrointestinal therapeutics. *WJG* is dedicated to become an influential and prestigious journal in gastroenterology and hepatology, to promote the development of above disciplines, and to improve the diagnostic and therapeutic skill and expertise of clinicians.

INDEXING/ABSTRACTING

*World Journal of Gastroenterology* (*WJG*) is now indexed in Current Contents<sup>®</sup>/Clinical Medicine, Science Citation Index Expanded (also known as SciSearch<sup>®</sup>), Journal Citation Reports<sup>®</sup>, Index Medicus, MEDLINE, PubMed, PubMed Central and Directory of Open Access Journals. The 2017 edition of Journal Citation Reports<sup>®</sup> cites the 2016 impact factor for *WJG* as 3.365 (5-year impact factor: 3.176), ranking *WJG* as 29<sup>th</sup> among 79 journals in gastroenterology and hepatology (quartile in category Q2).

FLYLEAF

I-IX Editorial Board

EDITORS FOR  
THIS ISSUE

Responsible Assistant Editor: *Xiang Li*  
Responsible Electronic Editor: *Yu-Jie Ma*  
Proofing Editor-in-Chief: *Lian-Sheng Ma*

Responsible Science Editor: *Ze-Mao Gong*  
Proofing Editorial Office Director: *Jin-Lei Wang*

NAME OF JOURNAL  
*World Journal of Gastroenterology*

ISSN  
ISSN 1007-9327 (print)  
ISSN 2219-2840 (online)

LAUNCH DATE  
October 1, 1995

FREQUENCY  
Weekly

EDITORS-IN-CHIEF  
**Damian Garcia-Olmo, MD, PhD, Doctor, Professor, Surgeon**, Department of Surgery, Universidad Autonoma de Madrid; Department of General Surgery, Fundacion Jimenez Diaz University Hospital, Madrid 28040, Spain

**Stephen C Strom, PhD, Professor**, Department of Laboratory Medicine, Division of Pathology, Karolinska Institutet, Stockholm 141-86, Sweden

**Andrzej S Tarnawski, MD, PhD, DSc (Med), Professor of Medicine, Chief Gastroenterology**, VA Long Beach Health Care System, University of California, Irvine, CA, 5901 E. Seventh Str., Long Beach,

CA 90822, United States

EDITORIAL BOARD MEMBERS  
All editorial board members resources online at <http://www.wjgnet.com/1007-9327/editorialboard.htm>

EDITORIAL OFFICE  
Jin-Lei Wang, Director  
Ze-Mao Gong, Vice Director  
*World Journal of Gastroenterology*  
Baishideng Publishing Group Inc  
7901 Stoneridge Drive, Suite 501,  
Pleasanton, CA 94588, USA  
Telephone: +1-925-2238242  
Fax: +1-925-2238243  
E-mail: [editorialoffice@wjgnet.com](mailto:editorialoffice@wjgnet.com)  
Help Desk: <http://www.f6publishing.com/helpdesk>  
<http://www.wjgnet.com>

PUBLISHER  
Baishideng Publishing Group Inc  
7901 Stoneridge Drive, Suite 501,  
Pleasanton, CA 94588, USA  
Telephone: +1-925-2238242  
Fax: +1-925-2238243  
E-mail: [bpgoffice@wjgnet.com](mailto:bpgoffice@wjgnet.com)  
Help Desk: <http://www.f6publishing.com/helpdesk>  
<http://www.wjgnet.com>

PUBLICATION DATE  
December 14, 2017

COPYRIGHT  
© 2017 Baishideng Publishing Group Inc. Articles published by this Open-Access journal are distributed under the terms of the Creative Commons Attribution Non-commercial License, which permits use, distribution, and reproduction in any medium, provided the original work is properly cited, the use is non commercial and is otherwise in compliance with the license.

SPECIAL STATEMENT  
All articles published in journals owned by the Baishideng Publishing Group (BPG) represent the views and opinions of their authors, and not the views, opinions or policies of the BPG, except where otherwise explicitly indicated.

INSTRUCTIONS TO AUTHORS  
Full instructions are available online at <http://www.wjgnet.com/bpg/gerinfo/204>

ONLINE SUBMISSION  
<http://www.f6publishing.com>



## Relation of the IGF/IGF1R system to autophagy in colitis and colorectal cancer

Ferenc Sipos, Hajnal Székely, Imre Dániel Kis, Zsolt Tulassay, Györgyi Múzes

Ferenc Sipos, Hajnal Székely, Györgyi Múzes, 2<sup>nd</sup> Department of Internal Medicine, Semmelweis University, Budapest 1088, Hungary

Imre Dániel Kis, Faculty of Medicine, Semmelweis University, Budapest 1088, Hungary

Zsolt Tulassay, Molecular Medicine Research Group, Hungarian Academy of Sciences, Budapest 1088, Hungary

ORCID number: Ferenc Sipos (0000-0002-2767-7746); Hajnal Székely (0000-0001-7024-6944); Imre Dániel Kis (0000-0001-5012-7083); Zsolt Tulassay (0000-0003-2452-6640); Györgyi Múzes (0000-0002-9099-0372).

**Author contributions:** Sipos F, Székely H and Múzes G substantially contributed to the writing, editing and revision of the manuscript, and approved the final version of the article to be published; Sipos F and Székely H contributed equally to the writing of the manuscript; Kis ID contributed in revising the paper and figure editing; Tulassay Z revised the final version of the manuscript.

**Supported by** the Hungarian Scientific Research Fund (No. OTKA-K111743) to Tulassay Z. The funders had no role in data collection, decision to publish, or preparation of the manuscript.

**Conflict-of-interest statement:** No conflict of interest.

**Open-Access:** This article is an open-access article which was selected by an in-house editor and fully peer-reviewed by external reviewers. It is distributed in accordance with the Creative Commons Attribution Non Commercial (CC BY-NC 4.0) license, which permits others to distribute, remix, adapt, build upon this work non-commercially, and license their derivative works on different terms, provided the original work is properly cited and the use is non-commercial. See: <http://creativecommons.org/licenses/by-nc/4.0/>

**Manuscript source:** Invited manuscript

**Correspondence to:** Ferens Sipos, MD, PhD, Assistant Professor, Immunology and Medicine, 2<sup>nd</sup> Department of Internal Medicine, Semmelweis University, Szentkirályi street 46, Budapest 1088, Hungary. [dr.siposf@gmail.com](mailto:dr.siposf@gmail.com)

Telephone: +36-1-266926-55622

Fax: +36-1-266926-55622

Received: October 27, 2017

Peer-review started: October 28, 2017

First decision: November 21, 2017

Revised: November 28, 2017

Accepted: December 4, 2017

Article in press: December 4, 2017

Published online: December 14, 2017

### Abstract

Metabolic syndrome (MetS), as a chronic inflammatory disorder has a potential role in the development of inflammatory and cancerous complications of the colonic tissue. The interaction of DNA damage and inflammation is affected by the insulin-like growth factor 1 receptor (IGF1R) signaling pathway. The IGF1R pathway has been reported to regulate autophagy, as well, but sometimes through a bidirectional context. Targeting the IGF1R-autophagy crosstalk could represent a promising strategy for the development of new antiinflammatory and anticancer therapies, and may help for subjects suffering from MetS who are at increased risk of colorectal cancer. However, therapeutic responses to targeted therapies are often shortlived, since a signaling crosstalk of IGF1R with other receptor tyrosine kinases or autophagy exists, leading to acquired cellular resistance to therapy. From a pharmacological point of view, it is attractive to speculate that synergistic benefits could be achieved by inhibition of one of the key effectors of the IGF1R pathway, in parallel with the pharmacological stimulation of the autophagy machinery, but cautiousness is also required, because pharmacologic IGF1R modulation can initiate additional, sometimes unfavorable biologic effects.

**Key words:** Insulin-like growth factor; IGF1R; Autophagy; Colitis; Colorectal cancer; Metabolic syndrome

© The Author(s) 2017. Published by Baishideng Publishing Group Inc. All rights reserved.

**Core tip:** Targeting the insulin-like growth factor 1 receptor (IGF1R)-autophagy crosstalk could represent a promising strategy for the development of new antiinflammatory and anticancer therapies, and may help for subjects suffering from metabolic syndrome who are at increased risk of colorectal cancer. However, cautiousness is also required, because pharmacologic IGF1R modulation can initiate additional, sometimes unfavorable biologic effects.

Sipos F, Székely H, Kis ID, Tulassay Z, Múzes G. Relation of the IGF/IGF1R system to autophagy in colitis and colorectal cancer. *World J Gastroenterol* 2017; 23(46): 8109-8119 Available from: URL: <http://www.wjgnet.com/1007-9327/full/v23/i46/8109.htm> DOI: <http://dx.doi.org/10.3748/wjg.v23.i46.8109>

## INTRODUCTION

Nowadays, metabolic syndrome (MetS) has being viewed as a chronic inflammatory disorder<sup>[1]</sup>. Although numerous molecular mechanisms still have to be clearly defined, the role of pro-inflammatory cytokines, reactive oxygen species and free fatty acid intermediaries have been suggested as key factors in modulating specific intracellular signaling pathways that appear to regulate insulin sensitivity<sup>[2]</sup>. In order to expand our understanding of MetS, it is important to link their potential role in the development of complications.

In mild, longstanding colonic inflammation, the expression of epithelial insulin-like growth factor 1 receptor (IGF1R) is elevated both on mRNA and protein levels<sup>[3]</sup>. This may allow epithelial cells bearing inflammation-associated genetic defects to pathologically survive and proliferate. In acute murine colitis, however, insulin-like growth factor 1 (IGF1)-primed macrophages were found to suppress immune inflammation in the intestine by producing interleukin-10<sup>[4]</sup>. Regarding colonic inflammation, the biologic role of the IGF1/IGF1R axis seems to be controversial.

Under inflammatory circumstances, immune and epithelial cells release reactive oxygen and nitrogen species, resulting in DNA damage<sup>[5]</sup>. The crosstalk between DNA damage and inflammation has a role in cancer development, therefore chronic inflammation represents a hallmark phenomenon of tumorigenesis<sup>[6]</sup>. The prevalence of MetS is increasing in parallel with growing incidence of cancerous diseases worldwide. Previous studies have reported that MetS is associated with the development of several types of tumors including colorectal cancer (CRC)<sup>[7-9]</sup>. The elevated risk of CRC in MetS patients<sup>[8]</sup> indicates that the consequence of MetS in cancer is an important issue

needs to be resolved.

The binding of insulin to cell surface receptors like insulin receptor and IGF1R on cancer cells results in cell proliferation and survival<sup>[10]</sup>. Elevated serum insulin levels modify the IGF-IGF1R axis involved in cancer development and progression<sup>[11]</sup>. Based on these results, antiinflammatory and anti-cancer strategies blocking the aberrant activation of IGF1R are therapeutically relevant.

Autophagy is a fundamental eukaryotic cellular homeostatic process and integral component of the immune system influencing inflammation and immunity<sup>[12]</sup>. Regarding colorectal carcinogenesis it has a dual-faced role. The down-regulation of autophagy-associated genes promotes colorectal cancer development and invasion<sup>[13,14]</sup>, while induction of autophagy redounds the proliferative arrest of human colon cancer cell lines<sup>[15,16]</sup>. Autophagy is considered to be a crucial approach of killing apoptosis-resistant tumor cells<sup>[17-19]</sup>. The insulin/IGF1/PI3K-Akt-mTOR (mammalian target of rapamycin) pathway has been reported to regulate autophagy through the insulin receptor<sup>[20,21]</sup>. Moreover, the autophagic lysosomal pathway can be suppressed by the activation of IGF1R-signaling<sup>[22,23]</sup>. Thus, targeting the IGF1R-autophagy crosstalk could represent a promising strategy for the development of new antiinflammatory and anticancer therapies, and may help for subjects suffering from MetS who are at increased risk of colorectal cancer.

## THE INSULIN/IGF/IGFR SYSTEM

The first identified member of the insulin/IGF family was insulin. Determination of the protein's structure, functions, mode of action, role in glucose metabolism, and its implication in the etiology of diabetes mellitus resulted in the concession of three Nobel Prizes; in 1923 for the discovery of its capacity to treat diabetes (by Frederick Banting and J. J. Macleod); in 1958 for studies regarding the protein structure and sequence (by Frederick Sanger); and, in 1963 for the first determination of the three-dimensional structure (by Dorothy Hodgkin).

The existence of the IGFs was first proposed by Salmon and Daughaday (in 1957)<sup>[24]</sup>, based on studies indicating that growth hormone-mediated stimulation of sulfate incorporation into the cartilage is mediated through a serum factor. This factor was originally termed "sulfation factor", then "somatomedin". The term "insulin-like" was later used, based on the partial structural homology with insulin and stimulation of glucose uptake into fat- and muscle cells<sup>[25]</sup>.

IGF1 and IGF2 are growth factors with both mitogenic and metabolic functions, having a role in the growth, differentiation and survival of numerous cell types and tissues. IGFs are unique among growth factors, since they can act as systemically (like hormones), as locally (like autocrine/paracrine factors)<sup>[26]</sup>.

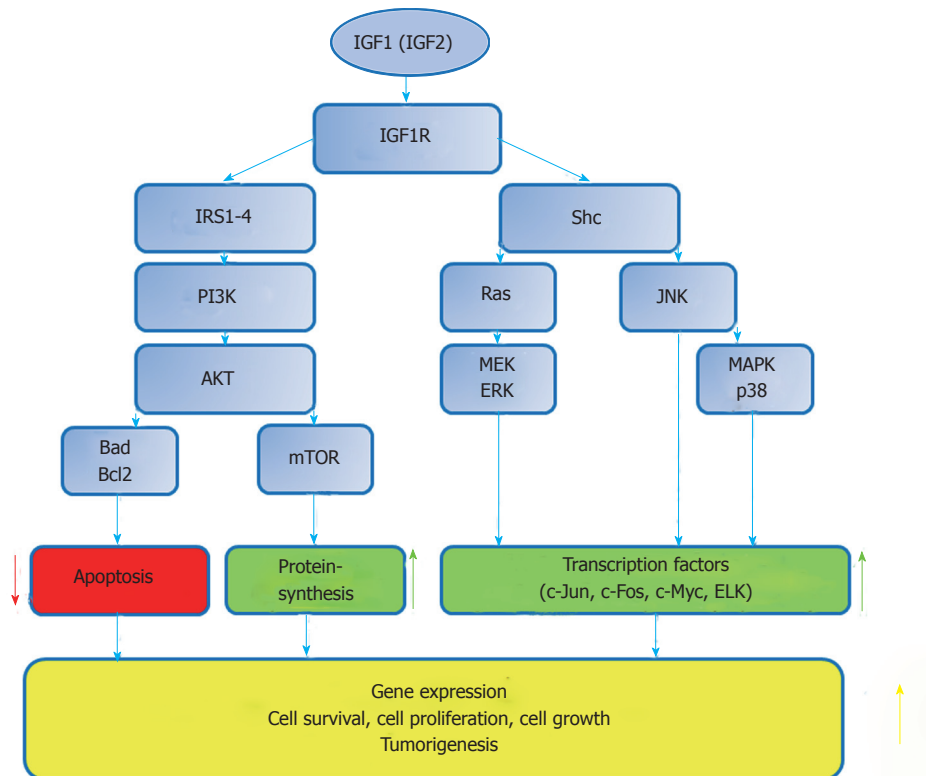


**Figure 1 The IGF/IGF1R axis: schematic representation of the composition and function.** Signaling of the IGF/IGF1R axis is mediated by IRS and Shc. PI3K-AKT activation is the predominant downstream event, but the Ras/MEK/ERK and JNK/MAPK pathways can also be activated. IGF: Insulin-like growth factor; IGF1R: Insulin-like growth factor receptor 1; IRS: Insulin receptor substrate; PI3K: Phosphatidylinositol-3-kinase; AKT: Serine/threonine kinase, named protein kinase B (PKB); mTOR: Mammalian target of rapamycin; Bad: Bcl-2-associated death promoter; Bcl2: B-cell lymphoma 2; Shc: Adaptor protein; Ras: GTPase protein; JNK: c-Jun N-terminal kinase; MEK: Mitogen-activated protein kinase kinase; ERK: Extracellular regulated kinase; MAPK: Mitogen-activated protein kinase; ELK: ETS domain-containing protein.

The metabolic functions of the insulin/IGF axis are well known, since insulin is a key regulator controlling cellular glucose-, amino-, and fatty-acid uptake, as well as glycogen-, lipid-, and protein synthesis, and other related metabolic processes<sup>[26]</sup>.

IGFs also display multiple functions. They are expressed ubiquitously, although in different amounts and ratios in a variety of tissues and cells, exerting auto-, para- and endocrine biological effects. They act mainly as growth hormones, regulating the growth of human cells and tissues, as well as influencing their lifespan. They have a substantial effect on maintaining tissue homeostasis and a differentiated phenotype in normal tissue, are involved in angiogenesis, cell adhesion, migration and wound healing<sup>[27]</sup>.

This network, along with a complex crosstalk with other signaling pathways has also a role in determining the balance between apoptosis and cell survival. The antiapoptotic and pro-survival effects are of major importance in the development and progression of some cancer types<sup>[28]</sup>. The variety of cellular responses to the insulin/IGF signal depend on the availability of growth factors, the ratios of the receptors and signalling molecules, the cell and tissue types as well as tissue microenvironment<sup>[28]</sup> (Figure 1).

Insulin receptors (IR) exist in IR-A, IR-B and IRR isoforms, while IGF receptors include IGF1R and IGF2R<sup>[29]</sup>. IGF1R, IR and IRR are composed of an

extracellular ligand-binding domain and an intracellular protein kinase domain. Their structural similarity permits the formation of heterodimer receptors, formed by subunits of different receptor proteins. Heterodimers are spontaneously formed and represent the most abundant receptor subtype in many tissues. These receptors bind insulin and IGF ligands with different affinities, depending on their subunit composition. Ranking from high to low and very low affinity, IGF1R binds IGF1, IGF2 and insulin; IGF2R binds IGF2 and other ligands, such as mannose-6-phosphate, IGF1; IR binds insulin, IGF2 and IGF1. IR-A possesses higher IGF2 affinity than IR-B. IRR is an orphan receptor with unknown ligand binding; it participates primarily in signal transduction<sup>[29,30]</sup>.

IGFs and IRs constitute a complex interacting receptor network. Depending on the availability of IGF/insulin ligands and the ratios of these receptors, IGFs can activate IR and, conversely, insulin activates IGF1R<sup>[28]</sup>.

The endocrine actions of IGFs are regulated by the IGF-binding protein (IGFBP) system by modulating the amount of bioavailable IGFs in a positive or negative manner. The IGFBPs produced locally act as autocrine/paracrine regulators of IGF actions. IGFBPs may also fix IGFs in the extracellular matrices for future actions. Some IGFBPs act also by a mechanism independent of IGFs<sup>[26]</sup>.



Binding of IGFs by inhibitory IGFBPs results in altered IGF actions, thus preventing the interaction of IGFs with the specific IGF receptors (until released) and protecting them from proteases within the circulation. Due to the significantly greater affinity of IGFBPs for IGFs as compared to the affinity of IGFs to their receptors only few IGF binds to receptors in the presence of an equimolar concentration of receptor and binding protein. In this regard the excess presence of IGFBPs in various tissues is an additional factor. By limiting the complex functions of the IGFs, it may be hypothesised that IGFBPs may to certain extent act as tumor suppressors<sup>[26,31]</sup>.

Nevertheless, IGFBPs may promote IGF signalling. IGFBPs stabilise and allow slow release of IGFs for receptor interactions, thereby preventing receptor downregulation by high IGF exposure, and thusly promoting a prolonged and constant receptor activation<sup>[28]</sup>.

IGFBP proteases presented in the circulation, as well may release IGFBP-bound ligands by degrading IGFBP into a form with a considerably lower affinity for IGFs compared with that of intact IGFBP. The amount of these proteases may be modified under certain physiological and pathological conditions, and their activity depends on the activators and inhibitors of proteases<sup>[26]</sup>.

## CONNECTION OF THE IGF/IGF1R SYSTEM WITH AUTOPHAGY

Autophagy, an evolutionarily highly conserved process of cellular self-digestion<sup>[32]</sup> is intensely implicated in the regulation of various functions, such as cell development, differentiation, survival, or senescence<sup>[33]</sup>. Additionally, it influences inflammation along with the innate and adaptive immunity<sup>[34]</sup>. Autophagy involves several sequential steps, including autophagosome nucleation, elongation, lipidation, and degradation, which are controlled by autophagy-related genes (Atgs)<sup>[32]</sup>. Intact basal autophagy serves constantly and constitutively as a critical adaptive and surveillance mechanism in maintaining cellular homeostasis<sup>[35]</sup>. However, to preserve cell viability autophagy is inducible in response to different cellular metabolic stress conditions, and, in case of protein aggregation and accumulation of misfolded proteins, when structural remodeling is warranted<sup>[36]</sup>.

Defective autophagy has been ultimately related to several chronic inflammatory diseases including inflammatory bowel disease (IBD), or malignancies<sup>[35-38]</sup>. Regarding tumorigenesis, a Janus-faced role of autophagy has been proposed. It may be critical for cancer cell survival and progression, in particular under stressful situations, however, it may also elicit tumor death signaling pathways. The pro-survival or pro-death function of autophagy is context-dependent, and influenced by several intra- and extracellular factors, like

involved tissues, surrounding microenvironment, genetic background, or stages of tumor development<sup>[37,39]</sup>.

The connection of the IGF1/IGF1R system to the autophagy machinery is rather complicated. Insulin receptor substrate 1 (IRS1), an adaptor of IGF1R has a crucial role in the signal transduction of IGF1R. Tyrosine phosphorylation of IGF1R induces the binding of IRS1 to IGF1R, and phosphorylation of tyrosine residues in IRS1. This allows IRS1 to activate the PI3K pathway<sup>[40]</sup>. The PI3K-Akt-mTOR pathway has been documented to regulate autophagy *via* the insulin receptor<sup>[20]</sup>. In addition, IGF1R-mediated cell survival under hypoxia depends on enhanced autophagy caused by the suppression of the PI3K-Akt-mTOR signaling pathway<sup>[21]</sup>. The autophagic lysosomal pathway can also be suppressed by the activation of IGF1R-signaling<sup>[22,23]</sup>.

In a recent study<sup>[41]</sup>, it has been shown that fragments of IGF1R are localized separately from full-length IGF1R, colocalizing with LC-3 II, and activate the ubiquitously expressed Shc A adapter protein in dense organelles. The IGF1R fragments and Shc A have been found to be phosphorylated, indicating that after activation both the IGF1R and a key adapter protein are sequestered in autophagic vacuoles for degradation. Shc adapter protein transmits IGF1/IGF1R signaling *via* the mitogen activated protein kinase (MAPK) pathway, resulting finally in cell proliferation. Upon cathepsin inhibition autophagy seems to be involved in downregulation of IGF1-mediated cell proliferation<sup>[41]</sup>.

The nicotinamide adenine dinucleotide (NAD<sup>+</sup>)-dependent protein deacetylase sirtuin 1 (SIRT1; silent mating type information regulation 2 homolog 1) has emerged as a significant target for epigenetic therapeutics of colon cancer since its increased expression is closely related to cancer progression. Additionally, SIRT1 represses p53 function *via* deacetylation, and so, promotes tumor growth<sup>[42]</sup>. IGF1R signaling can be improved by adipokines through SIRT1<sup>[43]</sup>. Moreover, SIRT1 overexpression stimulates epithelial wound healing *via* the downregulation of the IGFBP3 protein, the activation of the IGF1R/Akt pathway, and the posttranslational modification of p53 expression<sup>[44]</sup>. It has also been demonstrated that IGF1 and IGF1R expression levels can be negatively regulated by SIRT1 upon modulation of the AKT and ERK1/2 phosphorylation<sup>[45]</sup>. In turn, in human cancer cells aberrant cytoplasmic localization and protein stability of SIRT1 has been found to be regulated by the PI3K/IGF1R signaling<sup>[46]</sup>. SIRT1 can directly interact with and deacetylate several Atg proteins, including Atg5, Atg7, and Atg8, leading to the activation of these proteins<sup>[47,48]</sup>. By decreasing genetic stability and DNA mismatch repair, impaired SIRT1 and autophagy signaling pathway could increase the risk of genetic mutations and carcinogenesis. Further, the dysregulation of mTOR and AMP activated kinase (PRKA) pathways could remodel cell metabolism during the growth and metastasis of cancer cells.

**Table 1** Modulation of the IGF1R-autophagy crosstalk may induce controversial therapeutic effects

Inducing effects/therapeutic agents	Corresponding cellular actions/processes		Final outcome
Resveratrol	mTOR inhibition ↑ IGF1R inhibition ↑ SIRT1 activation ↓	Autophagy induction ↑	IGF1-induced fibrosis ↓
Targeted inhibition of IGF1	IGF1/IGF1R signaling ↓	Altered autophagy machinery	Amelioration of colitis
Modifying IGF1 stability	IGF1/IGF1R signaling ↓	Altered autophagy machinery	Amelioration of colitis
Chronic inflammation	IGF/IGF1R signaling ↑	Altered autophagy machinery; Survival and proliferation of cells bearing genetic errors ↑	Pro-tumor effect ↑
Chronic inflammation + small molecule RTK inhibitors	IGF/IGF1R signaling ↓	Survival and proliferation of cells bearing genetic errors ↓	Pro-tumor effect ↓
Targeted inhibition of IGF1R	IGF1R signaling ↓	Cell-protective autophagy ↑	Efficacy of IGF1R targeting ↓
Targeted inhibition of IGF1R + Autophagy disrupting agents	IGF1R signaling ↓	Cell-protective autophagy ↓	Efficacy of IGF1R targeting ↑
BCAA	IGF1R activation ↓	Insulin-induced cell proliferation ↓	Anti-tumor effect ↑
IGF1R/EGFR inhibition + Increasing miR216b level + autophagy blocking	IGF1R activation ↓	Cell-protective autophagy ↓	Anti-tumor effect ↑

mTOR: Mammalian target of rapamycin; IGF/1R: Insulin-like growth factor/receptor-1; SIRT: Sirtuin; RTK: Receptor tyrosine kinase; BCAA: Branched chain amino acid; EGFR: Epidermal growth factor receptor.

Moreover, these pathways may couple metabolic and epigenetic alterations that are essential to tumorigenic transformation<sup>[49]</sup>. Therefore, the modulation of the IGF1R/SIRT1/autophagy system is of great therapeutic interest in colon cancer.

The neural-specific deletion of sirtuin 6 (SIRT6) has been found to attenuate IGF1 level<sup>[50]</sup>. This finding may connect SIRT6 to IGF1 signaling, a conserved pathway with the ability to affect lifespan, metabolism, neurodegeneration, or cancer<sup>[51,52]</sup>. Recent evidences propose that autophagy may be associated with increased activation of SIRT6, because transcriptional factors like nuclear factor  $\kappa$  light chain enhancer of activated B cells (NF- $\kappa$ B), and activator protein 1 (AP-1), whose activity is negatively regulated by SIRT6, are shown to be positive regulators of autophagy<sup>[53,54]</sup>. These findings suggest that pharmacologic modulation of IGF1/SIRT6 might have a therapeutic value, as well.

The stress-induced protein TRB3 is a member of mammalian Tribbles homologs, which contain a Ser/thr protein kinase-like domain, but lack the ATP binding pocket and catalytic residues<sup>[55]</sup>. TRB3 coordinates crucial cellular processes, such as lipid and glucose metabolism, apoptosis, cell differentiation, and stress response<sup>[55]</sup>. In several human tumors and cancer cells metabolic stress conditions, including insulin/IGF1 enhance the expression of TRB3. In cancer cells TRB3 depletion protects against the tumor-promoting actions of insulin/IGF1. TRB3 interacts with p62, and interferes with the p62 cargo function, hence it results in p62 accumulation and p62-mediated autophagy dysfunction<sup>[56]</sup>. The interaction between TRB3 and sequestosome-1 (SQSTM1) has been found to be essential to mediate the insulin/IGF1-related (metabolic stress-promoted) tumorigenesis by suppressing autophagic and proteasomal degradation<sup>[57]</sup>.

## THERAPEUTIC ASPECTS OF THE IGF/IGF1R AND AUTOPHAGY INTERACTIONS IN COLONIC INFLAMMATION

Metabolic disorders display a strong inflammatory basis, and vice versa, inflammation is deeply associated with metabolic alterations<sup>[58,59]</sup>. At molecular level, metabolically-driven and immune-mediated disorders induce cellular stress responses<sup>[60]</sup>, and, further, in several chronic diseases increased levels of pro-inflammatory cytokines, dysregulated autophagy, as well as alterations in the intestinal microbiome can be detected<sup>[61-63]</sup>.

Intestinal epithelial cells (IECs) maintain homeostasis by creating an interface between the gut microbiota and the immune system. IECs directly sense enteric luminal bacteria, collaborate with intraepithelial lymphocytes and immune cells of the lamina propria<sup>[64]</sup>. Evidences suggest that the IGF/IGFR system plays a fundamental role in the gastrointestinal tract<sup>[65]</sup>. IBD patients often exhibit metabolic changes concomitantly with the altered adipokine levels and increased inflammatory parameters<sup>[66,67]</sup>. Relative insulin resistance (*i.e.* increased insulin levels with normal blood glucose levels) and changes of lipid metabolism are common phenomena in IBD<sup>[67]</sup>. Moreover, in IBD patients hyperinsulinemia was proved as an independent protective factor for a 6-month-maintenance of remission<sup>[68]</sup>. In mild and moderately active ulcerative colitis epithelial IGF1R expression was found to be elevated as compared to severely inflamed or normal mucosa<sup>[3]</sup>. In Crohn's disease, elevated IGF1R expression was observed in submucosal fibroblast-like cells, subserosal adipocytes, and hypertrophic nervous plexi<sup>[69]</sup>. Intestinal fibrosis in form of fibrotic strictures is a well described complication of

longstanding Crohn's disease. IGF1 stimulates collagen I synthesis in intestinal fibroblasts *via* the IGF1/IGF1R/ERK1/2 pathway<sup>[70]</sup>. These may suggest a role for IGF1R in the maintenance of chronic inflammation and stricture formation in IBD.

It has recently been found that IGF1-induced collagen I expression of intestinal fibroblasts can be repressed by resveratrol either *via* activating SIRT1 or inhibiting the activation of IGF1R<sup>[70]</sup>. In SW620 cells, mTOR has also been proposed as a novel direct target of resveratrol action. In addition, mTOR inhibition is necessary for autophagy induction. Inhibition of mTOR by resveratrol was found to be independent of AMPK, SIRT1, PDE, and PI3K<sup>[71]</sup>, raising a putative role of the IGF/IGF1R system while mediating this inhibitory effect.

Inflammation-associated catabolic states, including sepsis and cancer are characterized by accelerated proteolysis. Among the signaling pathways that could mediate proteolysis induced by acute inflammation, like in IBD, the transcription factor forkhead box O induced by glucocorticoids and inhibited by IGF1, is likely to play a key role. Lipopolysaccharide can stimulate the expression of several components of the autophagy. This induction is associated with a rapid increase of circulating levels of TNF $\alpha$  together with an activation of NF- $\kappa$ B followed by a decrease in circulating and tissue levels of IGF1<sup>[72]</sup>. In murine model of colitis, serum IGF1 level was found to be reduced in ileitis<sup>[73]</sup>. This reduction may be due to post-growth hormone receptor effects of IL-6 on IGF1 stability<sup>[74]</sup>. Furthermore, granulocyte-monocyte colony stimulating factor neutralization *via* STAT5 suppression and the deficiency of the CARD15 gene, an autophagy-activating sensor may also be involved in that phenomenon<sup>[73]</sup>. Therefore, targeted inhibition of IGF1 either by restoring tissue and circulating IGF1 levels, or modifying IGF1 stability all could have possible therapeutic potentials in IBD, partly due to alteration of the autophagy process (Table 1).

## THERAPEUTIC ASPECTS OF THE IGF/IGF1R AND AUTOPHAGY INTERACTIONS IN COLORECTAL CANCER

Although combinations of surgery, radiotherapy and chemotherapy are used generally, innovative strategies are needed to improve the therapeutic outcome of CRC patients, especially with advanced stages of the disease. In the last decade new hypotheses have been considered on the mechanisms implicated in the early steps of CRC. Mainly, it has been postulated that mucosal inflammation, and epithelial injury can be considered as important determinants. Indeed, tissue injury caused by infectious, mechanical, or chemical agents may elicit a chronic immune response leading to cell proliferation, regeneration, and altered autophagy. When the immune response fails to resolve

injury, the inflammatory milieu rich in cytokines, growth factors (including IGFs/IGFRs), and reactive oxygen species participates in making an attempt to repair, resulting finally in accumulation of genetic errors and a sustained inappropriate proliferation. Numerous evidence supports the contribution of inflammatory responses in the subsequent development of CRC<sup>[75]</sup>. The development of targeted therapies that block selectively molecular pathways driving CRC is in the focus of current research. Small molecule inhibitors specific for receptor tyrosine kinases (including IGFRs) have so far demonstrated promising effects<sup>[76,77]</sup>.

IGFRs, expressed physiologically in the mucosal and muscular layers of the colon<sup>[78]</sup>, are definitely overexpressed by colon cancer cells<sup>[79]</sup>. Abnormal activation of the IGF/IGF1R axis is a key element in MetS-related cancer development, since it affects the expression and function of many proteins being involved in regulation of autophagy and apoptosis, and is also involved in cancer cell survival, resistance to apoptosis, and cell-cycle progression<sup>[80]</sup>.

The biologic function of autophagy in CRC is rather controversial. Indeed, the down-regulated expression of Atgs are associated with colorectal tumorigenesis<sup>[13,14]</sup>, however, the induction of autophagy contributes to proliferative arrest of human colon cancer cells<sup>[15,16]</sup>. It has also been suggested that cytotoxic agents, including chemotherapeutics, induce autophagy in cancer cells<sup>[22,81]</sup>.

In general, treatment with anti-IGF1R monoclonal antibodies seems to be relatively well-tolerated; the main detected side effects include hyperglycemia, fatigue, and thrombocytopenia. Its beneficial clinical activities have been observed in a broad range of different tumor, including CRC<sup>[82]</sup>; nonetheless, in groups of unselected cancer patients clinical studies with pharmacological agents targeting the IGF pathway have so far demonstrated modest efficacy regarding the outcome. The complexity of the IGF/IGFR pathway may in part account for this failure. Similar to IGF1R interaction with IGF1, binding of IGF2 to IGF1R or IR-A can also stimulate IGF signaling. The situation is further complicated if cells contain hybrid heterodimeric receptors consisting of IGF1R and IR subunits, which can act as a major transducer of IGF signaling<sup>[83]</sup>. In case of triple negative breast cancer cells, IGF1R inhibition on the one part induces cell-protective autophagy, which may to some degree rescue cells from other actions of the same receptorial inhibition, like proliferation suppression and apoptosis, and thereby weakens the efficacy of IGF1R-targeting agents. However, autophagy-disrupting agents can enhance the effect of IGF1R inhibitors<sup>[84]</sup>, which may constitute a potential therapeutic strategy for cancers, including CRC (Figure 2).

By defining a cut-off for IGF2 overexpression based on differential expression between colorectal tumors and normal tissue samples, an attractive patient selection biomarker for IGF pathway inhibitors were



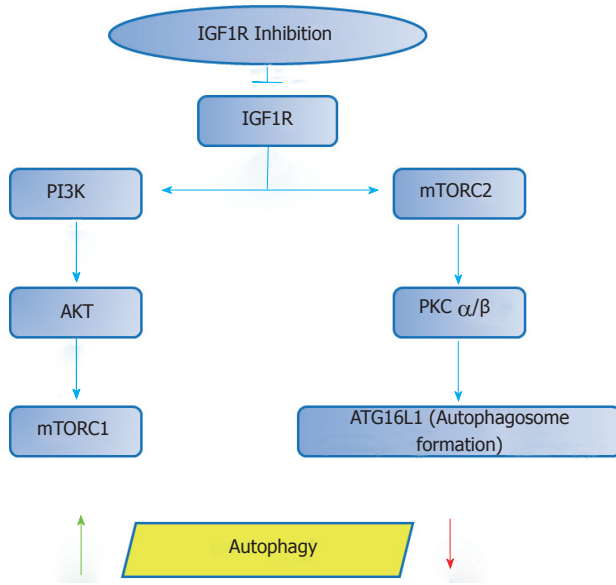


**Figure 2 Controversial therapeutic effects of IGF1R inhibition.** In case of IGF1R inhibition the simultaneously induced cell-protective autophagy could promote cell proliferation and suppress apoptosis, thus *via* autophagy antagonize its own original actions on cells. If IGF1R inhibition is combined with autophagy disruptive agents autophagy can be blocked, hence cancer cell proliferation will be suppressed and apoptosis enhanced. IGF1R: Insulin-like growth factor receptor 1.

found<sup>[85]</sup>. Additionally, combined targeting of IGF/VEGF and autophagy systems may further improve clinical outcomes<sup>[86]</sup>.

*In vivo* studies have reported that branched chain amino acid (BCAA) supplementation inhibits the activation of IGF1R<sup>[87-89]</sup>. BCAA has been found to enhance LC3-II and beclin 1 expressions, indicating its putative autophagy inductive effect. Moreover, BCAA also decreases the insulin-induced proliferation of HCT-116 colon cancer cells by inhibiting IGF1R and inducing autophagy<sup>[90]</sup>. These results suggest that an active intervention using BCAA might serve as a novel therapeutic approach for insulin-related CRC.

In case of cathepsin inhibition, higher levels of activated Shc and reduction of activated MAPK can be found in epithelial-derived cells. The activated Shc trapped in autophagic vesicles is not able to activate downstream cytosolic proteins including MAPK. Further activation of MAPK by IGF-1 is also diminished. Cathepsin inhibition in cancer cells leads to accumulation of Shc proteins in autophagolysosomes and impairs MAPK signaling, identifying a novel mechanism by which protease inhibitors can block cell proliferation, and lead to tumor cell death<sup>[41]</sup>.

Therapeutic responses to targeted therapies are often shortlived as tumor cells acquire resistance pathways. The IGF1R system plays a critical role in the regulation of cell growth and malignant transformation *via* the MAPK and PI3K/Akt pathways. Interactions of IGF1R with other receptor tyrosine kinases have been reported, and a signaling crosstalk of IGF1R/EGFR was also observed<sup>[77]</sup>. The use of monoclonal antibodies

for EGFR blockade is a well-established strategy in CRC treatment. Nevertheless, the loss of EGFR signaling in CRC cells can be compensated simply *via* activation of alternative signaling pathways, controlled in part by IGF1R<sup>[91]</sup>. Moreover, studies indicate that the mechanism of resistance to anti-EGFR antibodies biochemically involves as the Ras/Raf/Mek/Erk, as the PI3K/Akt/mTOR pathways. In addition, recent data suggest that failure of anti-EGFR therapies is accompanied by inhibition of EGFR internalization, ubiquitination, degradation and prolonged down-regulation<sup>[92,93]</sup>.

Cetuximab, a monoclonal antibody blocking EGFR has been used for CRC treatment, but some CRCs failed to respond to anti-EGFR therapy. Anti-EGFR therapy, *in vitro*, has been found to activate dose-dependently Beclin-1 when HT29 and SW480 CRC cell lines were used. Moreover, microRNA (miR)-216b level was significantly downregulated in anti-EGFR-treated CRC cells<sup>[94]</sup>. According to these data, anti-EGFR antibodies may decrease miR-216b level in CRC cells, with the subsequent upregulation of Beclin-1 that increases cancer cell autophagy in order to antagonize anti-EGFR-induced cell death.

One can speculate, that in CRC the outcome of combined anti-receptor tyrosine kinase therapies could be optimized by strategies that inhibit IGF1R/EGFR<sup>[95]</sup>, increase miR-216b level, or block cell autophagy simultaneously.

## CONTROVERSIAL EFFECTS OF IGF1R SIGNALING ON AUTOPHAGY

The possibility of targeting the IGF1R with several actions involved in carcinogenesis suggests that it may represent a potential therapeutic option. Even so, cautiousness is required, since pharmacologic modulation of the IGF1R can initiate additional biologic effects. According to recent data, IGF1R inhibition may lead to a decrease in mTORC2 function, which, in turn, reduces the activity of protein kinase C (PKC) alpha and beta, and thus, influences the autophagosome formation by modulating the cytoskeleton and the rate of endocytosis<sup>[96]</sup>. Therefore, *via* IGF1R inhibition the process of autophagy could be affected bi-directionally (Figure 3).

From a pharmacological point of view, however, it is attractive to speculate that synergistic benefits could be achieved by inhibition of one of the key effectors of the IGF1R pathway, in parallel with the pharmacological stimulation of the autophagy machinery. Additionally, data also suggest that there may be benefits in using dual mTORC1/2 catalytic inhibitors for longer periods, as these may result in autophagy inhibition, which may decrease viability of at least some types of cancers<sup>[97-99]</sup>.

The crosstalk between cell cycle progression and autophagy is not fully understood. According to earlier

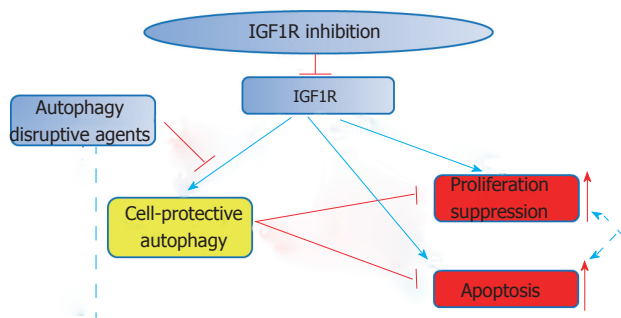


**Figure 3** Proposed model for the bi-directional IGF1R signaling-dependent modulation of the autophagic pathway. IGF1R targeting *via* suppression of the "canonical" PI3K/Akt/mTORC1 pathway stimulates the autophagy process. However, it can also result in a reduced formation of autophagosomal precursors at the plasma membrane. IGF1R depletion inhibits mTORC2, which reduces the activity of protein kinase C alpha and beta. This finally negatively impacts autophagosome precursor formation. IGF1R: Insulin-like growth factor receptor 1; PI3K: Phosphatidylinositol-3-kinase; AKT: Serine/threonine kinase, named protein kinase B (PKB); mTORC1/2: Mammalian target of rapamycin complex 1/2; PKC: Protein kinase C; ATG16L1: Autophagy-related protein 16-1.

results, cells undergoing mitosis are more resistant to autophagy stimuli like mTOR inhibition<sup>[100]</sup>. The active ingredient of a gum resin from *Boswellia serrata*, 3-acetyl-11-keto- $\beta$ -boswellic acid (AKBA), has recently gained attention as a chemopreventive compound due to its ability to target key oncogenic proteins<sup>[101, 102]</sup>. AKBA has been shown to inhibit the growth of CRC cells partly by its ability to regulate cell epigenetic machinery<sup>[103]</sup>. Using a potent natural AKBA analog (BA145) robust autophagy was detected in pancreatic cancer cells in a time and dose dependent manner<sup>[104]</sup>. The BA145-triggered autophagy resulted in G2/M arrest of cell cycle along with inhibited cell growth. Induction of autophagy was associated with the BA145-mediated inhibition of mTOR, which, in turn led to feedback activation of Akt *via* IGF1R/PI3K signaling. This feedback activation of Akt, however, lessened the BA145-triggered autophagy and its related effects on cell cycle arrest and cell death, thus indicating the decreased effectiveness of a single target-based cancer therapy.

## CONCLUSION

In summary, recent data suggest that inhibition of IGF/IGF1R system along with manipulation of the autophagy process could play an important role in suppressing insulin-related inflammatory and cancerous disorders of the colon. On the other hand, wariness is required, as well, since single or combined pharmacologic modulation of the IGF1R - autophagy machinery can initiate further, sometimes undesirable pathobiologic outcomes.

## REFERENCES

- 1 Lopez-Candales A, Hernández Burgos PM, Hernandez-Suarez DF, Harris D. Linking Chronic Inflammation with Cardiovascular

- Disease: From Normal Aging to the Metabolic Syndrome. *J Nat Sci* 2017; **3**: Pii: e341 [PMID: 28670620]
- 2 Bastard JP, Maachi M, Lagathu C, Kim MJ, Caron M, Vidal H, Capeau J, Feve B. Recent advances in the relationship between obesity, inflammation, and insulin resistance. *Eur Cytokine Netw* 2006; **17**: 4-12 [PMID: 16613757]
- 3 Sipos F, Galamb O, Herszényi L, Molnár B, Solymosi N, Zágóni T, Berczi L, Tulassay Z. Elevated insulin-like growth factor 1 receptor, hepatocyte growth factor receptor and telomerase protein expression in mild ulcerative colitis. *Scand J Gastroenterol* 2008; **43**: 289-298 [PMID: 18938767 DOI: 10.1080/00365520701714434]
- 4 Ge RT, Mo LH, Wu R, Liu JQ, Zhang HP, Liu Z, Liu Z, Yang PC. Insulin-like growth factor-1 endues monocytes with immune suppressive ability to inhibit inflammation in the intestine. *Sci Rep* 2015; **5**: 7735 [PMID: 25588622 DOI: 10.1038/srep07735]
- 5 Kawanishi S, Ohnishi S, Ma N, Hiraku Y, Murata M. Crosstalk between DNA Damage and Inflammation in the Multiple Steps of Carcinogenesis. *Int J Mol Sci* 2017; **18**: Pii: E1808 [PMID: 28825631 DOI: 10.3390/ijms18081808]
- 6 Hanahan D, Weinberg RA. Hallmarks of cancer: the next generation. *Cell* 2011; **144**: 646-674 [PMID: 21376230 DOI: 10.1016/j.cell.2011.02.013]
- 7 Calle EE, Kaaks R. Overweight, obesity and cancer: epidemiological evidence and proposed mechanisms. *Nat Rev Cancer* 2004; **4**: 579-591 [PMID: 15286738 DOI: 10.1038/nrc1408]
- 8 Giovannucci E, Michaud D. The role of obesity and related metabolic disturbances in cancers of the colon, prostate, and pancreas. *Gastroenterology* 2007; **132**: 2208-2225 [PMID: 17498513 DOI: 10.1053/j.gastro.2007.03.050]
- 9 Frezza EE, Wachtel MS, Chiriva-Internati M. Influence of obesity on the risk of developing colon cancer. *Gut* 2006; **55**: 285-291 [PMID: 16239255 DOI: 10.1136/gut.2005.073163]
- 10 Hagiwara A, Nishiyama M, Ishizaki S. Branched-chain amino acids prevent insulin-induced hepatic tumor cell proliferation by inducing apoptosis through mTORC1 and mTORC2-dependent mechanisms. *J Cell Physiol* 2012; **227**: 2097-2105 [PMID: 21769869 DOI: 10.1002/jcp.22941]
- 11 Durai R, Yang W, Gupta S, Seifalian AM, Winslet MC. The role of the insulin-like growth factor system in colorectal cancer: review of current knowledge. *Int J Colorectal Dis* 2005; **20**: 203-220 [PMID: 15650828 DOI: 10.1007/s00384-004-0675-4]
- 12 Múzes G, Constantinovits M, Fűri I, Tulassay Z, Sipos F. Interaction of autophagy and Toll-like receptors: a regulatory cross-talk—even in cancer cells? *Curr Drug Targets* 2014; **15**: 743-752 [PMID: 24852605 DOI: 10.2174/1389450115666140522120427]
- 13 Mariño G, Salvador-Montoliu N, Fueyo A, Knecht E, Mizushima N, López-Otín C. Tissue-specific autophagy alterations and increased tumorigenesis in mice deficient in Atg4C/autophagin-3. *J Biol Chem* 2007; **282**: 18573-18583 [PMID: 17442669 DOI: 10.1074/jbc.M701194200]
- 14 Cho DH, Jo YK, Kim SC, Park IJ, Kim JC. Down-regulated expression of ATG5 in colorectal cancer. *Anticancer Res* 2012; **32**: 4091-4096 [PMID: 22993366]
- 15 Xie CM, Chan WY, Yu S, Zhao J, Cheng CH. Bufalin induces autophagy-mediated cell death in human colon cancer cells through reactive oxygen species generation and JNK activation. *Free Radic Biol Med* 2011; **51**: 1365-1375 [PMID: 21763418 DOI: 10.1016/j.freeradbiomed.2011.06.016]
- 16 Huang S, Sinicrope FA. Celecoxib-induced apoptosis is enhanced by ABT-737 and by inhibition of autophagy in human colorectal cancer cells. *Autophagy* 2010; **6**: 256-269 [PMID: 20104024 DOI: 10.4161/auto.6.2.11124]
- 17 Pal S, Salunke-Gawalib S, Konkimallaa VB. Induction of Autophagic Cell Death in Apoptosis-resistant Pancreatic Cancer Cells using Benzo[ $\alpha$ ]phenoxazines Derivatives, 10-methylbenzo[ $\alpha$ ]phenoxazine-5-one and benzo[ $\alpha$ ]phenoxazine-5-one. *Anticancer Agents Med Chem* 2017; **17**: 115-125 [PMID: 27349450]

- 18 **Hu T**, Wang L, Zhang L, Lu L, Shen J, Chan RL, Li M, Wu WK, To KK, Cho CH. Sensitivity of apoptosis-resistant colon cancer cells to tanshinones is mediated by autophagic cell death and p53-independent cytotoxicity. *Phytomedicine* 2015; **22**: 536-544 [PMID: 25981919 DOI: 10.1016/j.phymed.2015.03.010]
- 19 **Chitikova ZV**, Gordeev SA, Bykova TV, Zubova SG, Pospelov VA, Pospelova TV. Sustained activation of DNA damage response in irradiated apoptosis-resistant cells induces reversible senescence associated with mTOR downregulation and expression of stem cell markers. *Cell Cycle* 2014; **13**: 1424-1439 [PMID: 24626185 DOI: 10.4161/cc.28402]
- 20 **Lum JJ**, Bauer DE, Kong M, Harris MH, Li C, Lindsten T, Thompson CB. Growth factor regulation of autophagy and cell survival in the absence of apoptosis. *Cell* 2005; **120**: 237-248 [PMID: 15680329 DOI: 10.1016/j.cell.2004.11.046]
- 21 **Liu Q**, Guan JZ, Sun Y, Le Z, Zhang P, Yu D, Liu Y. Insulin-like growth factor I receptor-mediated cell survival in hypoxia depends on the promotion of autophagy via suppression of the PI3K/Akt/mTOR signaling pathway. *Mol Med Rep* 2017; **15**: 2136-2142 [PMID: 28260056 DOI: 10.3892/mmr.2017.6265]
- 22 **Degtyarev M**, De Mazière A, Orr C, Lin J, Lee BB, Tien JY, Prior WW, van Dijk S, Wu H, Gray DC, Davis DP, Stern HM, Murray LJ, Hoeflich KP, Klumperman J, Friedman LS, Lin K. Akt inhibition promotes autophagy and sensitizes PTEN-null tumors to lysosomotropic agents. *J Cell Biol* 2008; **183**: 101-116 [PMID: 18838554 DOI: 10.1083/jcb.200801099]
- 23 **Arico S**, Petiot A, Bauvy C, Dubbelhuis PF, Meijer AJ, Codogno P, Ogier-Denis E. The tumor suppressor PTEN positively regulates macroautophagy by inhibiting the phosphatidylinositol 3-kinase/protein kinase B pathway. *J Biol Chem* 2001; **276**: 35243-35246 [PMID: 11477064 DOI: 10.1074/jbc.C100319200]
- 24 **SALMON WD Jr**, DAUGHADAY WH. A hormonally controlled serum factor which stimulates sulfate incorporation by cartilage in vitro. *J Lab Clin Med* 1957; **49**: 825-836 [PMID: 13429201]
- 25 **Brahmkhatri VP**, Prasanna C, Atreya HS. Insulin-like growth factor system in cancer: novel targeted therapies. *Biomed Res Int* 2015; **2015**: 538019 [PMID: 25866791 DOI: 10.1155/2015/538019]
- 26 **Mohan S**, Baylink DJ. IGF-binding proteins are multifunctional and act via IGF-dependent and -independent mechanisms. *J Endocrinol* 2002; **175**: 19-31 [PMID: 12379487 DOI: 10.1677/joe.0.1750019]
- 27 **Iams WT**, Lovly CM. Molecular Pathways: Clinical Applications and Future Direction of Insulin-like Growth Factor-1 Receptor Pathway Blockade. *Clin Cancer Res* 2015; **21**: 4270-4277 [PMID: 26429980 DOI: 10.1158/1078-0432.CCR-14-2518]
- 28 **Massoner P**, Ladurner-Rennau M, Eder IE, Klocker H. Insulin-like growth factors and insulin control a multifunctional signalling network of significant importance in cancer. *Br J Cancer* 2010; **103**: 1479-1484 [PMID: 20924377 DOI: 10.1038/sj.bjc.6605932]
- 29 **Pandini G**, Frasca F, Mineo R, Sciacca L, Vigneri R, Belfiore A. Insulin/insulin-like growth factor I hybrid receptors have different biological characteristics depending on the insulin receptor isoform involved. *J Biol Chem* 2002; **277**: 39684-39695 [PMID: 12138094 DOI: 10.1074/jbc.M202766200]
- 30 **Belfiore A**, Frasca F, Pandini G, Sciacca L, Vigneri R. Insulin receptor isoforms and insulin receptor/insulin-like growth factor receptor hybrids in physiology and disease. *Endocr Rev* 2009; **30**: 586-623 [PMID: 19752219 DOI: 10.1210/er.2008-0047]
- 31 **Kasprzak A**, Kwasniewski W, Adamek A, Gozdzińska-Jozefiak A. Insulin-like growth factor (IGF) axis in cancerogenesis. *Mutat Res Rev Mutat Res* 2017; **772**: 78-104 [PMID: 28528692 DOI: 10.1016/j.mrrev.2016.08.007]
- 32 **Yang Z**, Klionsky DJ. Eaten alive: a history of macroautophagy. *Nat Cell Biol* 2010; **12**: 814-822 [PMID: 20811353 DOI: 10.1038/ncb0910-814]
- 33 **Levine B**, Klionsky DJ. Development by self-digestion: molecular mechanisms and biological functions of autophagy. *Dev Cell* 2004; **6**: 463-477 [PMID: 15068787 DOI: 10.1016/S1534-5807(04)00099-1]
- 34 **Levine B**, Deretic V. Unveiling the roles of autophagy in innate and adaptive immunity. *Nat Rev Immunol* 2007; **7**: 767-777 [PMID: 17767194 DOI: 10.1038/nri2161]
- 35 **Mizushima N**, Levine B, Cuervo AM, Klionsky DJ. Autophagy fights disease through cellular self-digestion. *Nature* 2008; **451**: 1069-1075 [PMID: 18305538 DOI: 10.1038/nature06639]
- 36 **Levine B**, Kroemer G. Autophagy in the pathogenesis of disease. *Cell* 2008; **132**: 27-42 [PMID: 18191218 DOI: 10.1016/j.cell.2007.12.018]
- 37 **Levine B**. Cell biology: autophagy and cancer. *Nature* 2007; **446**: 745-747 [PMID: 17429391 DOI: 10.1038/446745a]
- 38 **Cadwell K**, Patel KK, Komatsu M, Virgin HW 4th, Stappenbeck TS. A common role for Atg16L1, Atg5 and Atg7 in small intestinal Paneth cells and Crohn disease. *Autophagy* 2009; **5**: 250-252 [PMID: 19139628 DOI: 10.4161/auto.5.2.7560]
- 39 **Dalby KN**, Tekedereli I, Lopez-Berestein G, Ozpolat B. Targeting the prodeath and prosurvival functions of autophagy as novel therapeutic strategies in cancer. *Autophagy* 2010; **6**: 322-329 [PMID: 20224296 DOI: 10.4161/auto.6.3.11625]
- 40 **Kawaguchi T**, Nagao Y, Matsuoka H, Ide T, Sata M. Branched-chain amino acid-enriched supplementation improves insulin resistance in patients with chronic liver disease. *Int J Mol Med* 2008; **22**: 105-112 [PMID: 18575782 DOI: 10.3892/ijmm.22.1.105]
- 41 **Soori M**, Lu G, Mason RW. Cathepsin Inhibition Prevents Autophagic Protein Turnover and Downregulates Insulin Growth Factor-1 Receptor-Mediated Signaling in Neuroblastoma. *J Pharmacol Exp Ther* 2016; **356**: 375-386 [PMID: 26660229 DOI: 10.1124/jpet.115.229229]
- 42 **Ghosh A**, Sengupta A, Seerapu GPK, Nakhi A, Shivaji Ramarao EVV, Bung N, Bulusu G, Pal M, Haldar D. A novel SIRT1 inhibitor, 4bb induces apoptosis in HCT116 human colon carcinoma cells partially by activating p53. *Biochem Biophys Res Commun* 2017; **488**: 562-569 [PMID: 28526414 DOI: 10.1016/j.bbrc.2017.05.089]
- 43 **Reverchon M**, Rame C, Bunel A, Chen W, Froment P, Dupont J. VISOATIN (NAMPT) Improves In Vitro IGF1-Induced Steroidogenesis and IGF1 Receptor Signaling Through SIRT1 in Bovine Granulosa Cells. *Biol Reprod* 2016; **94**: 54 [PMID: 26792944 DOI: 10.1095/biolreprod.115.134650]
- 44 **Wang Y**, Zhao X, Shi D, Chen P, Yu Y, Yang L, Xie L. Overexpression of SIRT1 promotes high glucose-attenuated corneal epithelial wound healing via p53 regulation of the IGFBP3/IGF-1R/AKT pathway. *Invest Ophthalmol Vis Sci* 2013; **54**: 3806-3814 [PMID: 23661372 DOI: 10.1167/iovs.13-12091]
- 45 **Sansone L**, Reali V, Pellegrini L, Villanova L, Aventaggiato M, Marfe G, Rosa R, Nebbioso M, Tafani M, Fini M, Russo MA, Pucci B. SIRT1 silencing confers neuroprotection through IGF-1 pathway activation. *J Cell Physiol* 2013; **228**: 1754-1761 [PMID: 23359486 DOI: 10.1002/jcp.24334]
- 46 **Byles V**, Chmielewski LK, Wang J, Zhu L, Forman LW, Faller DV, Dai Y. Aberrant cytoplasm localization and protein stability of SIRT1 is regulated by PI3K/IGF-1R signaling in human cancer cells. *Int J Biol Sci* 2010; **6**: 599-612 [PMID: 20941378 DOI: 10.7150/ijbs.6.599]
- 47 **Lee IH**, Cao L, Mostoslavsky R, Lombard DB, Liu J, Bruns NE, Tsokos M, Alt FW, Finkel T. A role for the NAD-dependent deacetylase Sirt1 in the regulation of autophagy. *Proc Natl Acad Sci USA* 2008; **105**: 3374-3379 [PMID: 18296641 DOI: 10.1073/pnas.0712145105]
- 48 **Pillai VB**, Sundaresan NR, Gupta MP. Regulation of Akt signaling by sirtuins: its implication in cardiac hypertrophy and aging. *Circ Res* 2014; **114**: 368-378 [PMID: 24436432 DOI: 10.1161/CIRCRESAHA.113.300536]
- 49 **Yang J**, Nishihara R, Zhang X, Ogino S, Qian ZR. Energy sensing pathways: Bridging type 2 diabetes and colorectal cancer? *J Diabetes Complications* 2017; **31**: 1228-1236 [PMID: 28465145 DOI: 10.1016/j.jdiacomp.2017.04.012]
- 50 **Schwer B**, Schumacher B, Lombard DB, Xiao C, Kurtev MV, Gao J, Schneider JI, Chai H, Bronson RT, Tsai LH, Deng CX, Alt FW.



- Neural sirtuin 6 (Sirt6) ablation attenuates somatic growth and causes obesity. *Proc Natl Acad Sci USA* 2010; **107**: 21790-21794 [PMID: 21098266 DOI: 10.1073/pnas.1016306107]
- 51 **Kenyon CJ.** The genetics of ageing. *Nature* 2010; **464**: 504-512 [PMID: 20336132 DOI: 10.1038/nature08980]
- 52 **Bartke A,** Brown-Borg H. Life extension in the dwarf mouse. *Curr Top Dev Biol* 2004; **63**: 189-225 [PMID: 15536017 DOI: 10.1016/S0070-2153(04)63006-7]
- 53 **Xiao G.** Autophagy and NF-kappaB: fight for fate. *Cytokine Growth Factor Rev* 2007; **18**: 233-243 [PMID: 17485237 DOI: 10.1016/j.cytogfr.2007.04.006]
- 54 **Guo Y,** Chang C, Huang R, Liu B, Bao L, Liu W. API is essential for generation of autophagosomes from the trans-Golgi network. *J Cell Sci* 2012; **125**: 1706-1715 [PMID: 22328508 DOI: 10.1242/jcs.093203]
- 55 **Schwarzer R,** Dames S, Tondera D, Klippel A, Kaufmann J. TRB3 is a PI 3-kinase dependent indicator for nutrient starvation. *Cell Signal* 2006; **18**: 899-909 [PMID: 16129579 DOI: 10.1016/j.cellsig.2005.08.002]
- 56 **Hua F,** Li K, Yu JJ, Lv XX, Yan J, Zhang XW, Sun W, Lin H, Shang S, Wang F, Cui B, Mu R, Huang B, Jiang JD, Hu ZW. TRB3 links insulin/IGF to tumour promotion by interacting with p62 and impeding autophagic/proteasomal degradations. *Nat Commun* 2015; **6**: 7951 [PMID: 26268733 DOI: 10.1038/ncomms8951]
- 57 **Hua F,** Li K, Yu JJ, Hu ZW. The TRIB3-SQSTM1 interaction mediates metabolic stress-promoted tumorigenesis and progression via suppressing autophagic and proteasomal degradation. *Autophagy* 2015; **11**: 1929-1931 [PMID: 26301314 DOI: 10.1080/15548627.2015.1084458]
- 58 **Hotamisligil GS.** Inflammation and metabolic disorders. *Nature* 2006; **444**: 860-867 [PMID: 17167474 DOI: 10.1038/nature05485]
- 59 **Zietek T,** Rath E. Inflammation Meets Metabolic Disease: Gut Feeling Mediated by GLP-1. *Front Immunol* 2016; **7**: 154 [PMID: 27148273 DOI: 10.3389/fimmu.2016.00154]
- 60 **Rath E,** Haller D. Inflammation and cellular stress: a mechanistic link between immune-mediated and metabolically driven pathologies. *Eur J Nutr* 2011; **50**: 219-233 [PMID: 21547407 DOI: 10.1007/s00394-011-0197-0]
- 61 **Brestoff JR,** Artis D. Immune regulation of metabolic homeostasis in health and disease. *Cell* 2015; **161**: 146-160 [PMID: 25815992 DOI: 10.1016/j.cell.2015.02.022]
- 62 **Monkkonen T,** Debnath J. Inflammatory signaling cascades and autophagy in cancer. *Autophagy* 2017; **1-9** [PMID: 28813180 DOI: 10.1080/15548627.2017.1345412]
- 63 **Öyri SF,** Müzes G, Sipos F. Dysbiotic gut microbiome: A key element of Crohn's disease. *Comp Immunol Microbiol Infect Dis* 2015; **43**: 36-49 [PMID: 26616659 DOI: 10.1016/j.cimid.2015.10.005]
- 64 **Clavel T,** Haller D. Bacteria- and host-derived mechanisms to control intestinal epithelial cell homeostasis: implications for chronic inflammation. *Inflamm Bowel Dis* 2007; **13**: 1153-1164 [PMID: 17476679 DOI: 10.1002/ibd.20174]
- 65 **Kuemmerle JF.** Insulin-like growth factors in the gastrointestinal tract and liver. *Endocrinol Metab Clin North Am* 2012; **41**: 409-423, vii [PMID: 22682638 DOI: 10.1016/j.ecl.2012.04.018]
- 66 **Korkmaz H,** Sahin F, Ipekci SH, Temel T, Kebapcilar L. Increased pulse wave velocity and relationship with inflammation, insulin, and insulin resistance in inflammatory bowel disease. *Eur J Gastroenterol Hepatol* 2014; **26**: 725-732 [PMID: 24901818 DOI: 10.1097/MEG.000000000000104]
- 67 **Karrasch T,** Obermeier F, Straub RH. Systemic metabolic signaling in acute and chronic gastrointestinal inflammation of inflammatory bowel diseases. *Horm Metab Res* 2014; **46**: 445-451 [PMID: 24799023 DOI: 10.1055/s-0034-1374587]
- 68 **Valentini L,** Wirth EK, Schweizer U, Hengstermann S, Schaper L, Koernicke T, Dietz E, Norman K, Buning C, Winklhofer-Roob BM, Lochs H, Ockenga J. Circulating adipokines and the protective effects of hyperinsulinemia in inflammatory bowel disease. *Nutrition* 2009; **25**: 172-181 [PMID: 18849144 DOI: 10.1016/j.nut.2008.07.020]
- 69 **El Yafi F,** Winkler R, Delvenne P, Boussif N, Belaiche J, Louis E. Altered expression of type I insulin-like growth factor receptor in Crohn's disease. *Clin Exp Immunol* 2005; **139**: 526-533 [PMID: 15730399 DOI: 10.1111/j.1365-2249.2004.02724.x]
- 70 **Li P,** Liang ML, Zhu Y, Gong YY, Wang Y, Heng D, Lin L. Resveratrol inhibits collagen I synthesis by suppressing IGF-1R activation in intestinal fibroblasts. *World J Gastroenterol* 2014; **20**: 4648-4661 [PMID: 24782617 DOI: 10.3748/wjg.v20.i16.4648]
- 71 **Park D,** Jeong H, Lee MN, Koh A, Kwon O, Yang YR, Noh J, Suh PG, Park H, Ryu SH. Resveratrol induces autophagy by directly inhibiting mTOR through ATP competition. *Sci Rep* 2016; **6**: 21772 [PMID: 26902888 DOI: 10.1038/srep21772]
- 72 **Schakman O,** Dehoux M, Bouchuati S, Delaere S, Laue P, Decroly N, Shoelson SE, Thissen JP. Role of IGF-I and the TNF $\alpha$ /NF- $\kappa$ B pathway in the induction of muscle atrogenes by acute inflammation. *Am J Physiol Endocrinol Metab* 2012; **303**: E729-E739 [PMID: 22739109 DOI: 10.1152/ajpendo.00060.2012]
- 73 **D'Mello S,** Trauernicht A, Ryan A, Bonkowski E, Willson T, Trapnell BC, Frank SJ, Kugasathan S, Denson LA. Innate dysfunction promotes linear growth failure in pediatric Crohn's disease and growth hormone resistance in murine ileitis. *Inflamm Bowel Dis* 2012; **18**: 236-245 [PMID: 21337672 DOI: 10.1002/ibd.21689]
- 74 **De Benedetti F,** Meazza C, Oliveri M, Pignatti P, Vivarelli M, Alonzi T, Fattori E, Garrone S, Barreca A, Martini A. Effect of IL-6 on IGF binding protein-3: a study in IL-6 transgenic mice and in patients with systemic juvenile idiopathic arthritis. *Endocrinology* 2001; **142**: 4818-4826 [PMID: 11606449 DOI: 10.1210/endo.142.11.8511]
- 75 **Mariani F,** Sena P, Roncucci L. Inflammatory pathways in the early steps of colorectal cancer development. *World J Gastroenterol* 2014; **20**: 9716-9731 [PMID: 25110410 DOI: 10.3748/wjg.v20.i29.9716]
- 76 **Hopfner M,** Sutter AP, Huether A, Baradari V, Scherubl H. Tyrosine kinase of insulin-like growth factor receptor as target for novel treatment and prevention strategies of colorectal cancer. *World J Gastroenterol* 2006; **12**: 5635-5643 [PMID: 17007015 DOI: 10.3748/wjg.v12.i35.5635]
- 77 **Kaulfuss S,** Burfeind P, Gaedcke J, Scharf JG. Dual silencing of insulin-like growth factor-I receptor and epidermal growth factor receptor in colorectal cancer cells is associated with decreased proliferation and enhanced apoptosis. *Mol Cancer Ther* 2009; **8**: 821-833 [PMID: 19372555 DOI: 10.1158/1535-7163.MCT-09-0058]
- 78 **Alemán JO,** Eusebi LH, Ricciardiello L, Patidar K, Sanyal AJ, Holt PR. Mechanisms of obesity-induced gastrointestinal neoplasia. *Gastroenterology* 2014; **146**: 357-373 [PMID: 24315827 DOI: 10.1053/j.gastro.2013.11.051]
- 79 **Ouban A,** Muraca P, Yeatman T, Coppola D. Expression and distribution of insulin-like growth factor-1 receptor in human carcinomas. *Hum Pathol* 2003; **34**: 803-808 [PMID: 14506643 DOI: 10.1016/S0046-8177(03)00291-0]
- 80 **Chang CK,** Ulrich CM. Hyperinsulinaemia and hyperglycaemia: possible risk factors of colorectal cancer among diabetic patients. *Diabetologia* 2003; **46**: 595-607 [PMID: 12764580 DOI: 10.1007/s00125-003-1109-5]
- 81 **Tran TT,** Medline A, Bruce WR. Insulin promotion of colon tumors in rats. *Cancer Epidemiol Biomarkers Prev* 1996; **5**: 1013-1015 [PMID: 8959325]
- 82 **Chu E.** The IGF-1R pathway as a therapeutic target. *Oncology (Williston Park)* 2011; **25**: 538-539, 543 [PMID: 21717909]
- 83 **Pandini G,** Vigneri R, Costantino A, Frasca F, Ippolito A, Fujita-Yamaguchi Y, Siddle K, Goldfine ID, Belfiore A. Insulin and insulin-like growth factor-I (IGF-I) receptor overexpression in breast cancers leads to insulin/IGF-I hybrid receptor overexpression: evidence for a second mechanism of IGF-I signaling. *Clin Cancer Res* 1999; **5**: 1935-1944 [PMID: 10430101]
- 84 **Wu W,** Ma J, Shao N, Shi Y, Liu R, Li W, Lin Y, Wang S. Co-Targeting IGF-1R and Autophagy Enhances the Effects of Cell Growth Suppression and Apoptosis Induced by the IGF-1R

- Inhibitor NVP-AEW541 in Triple-Negative Breast Cancer Cells. *PLoS One* 2017; **12**: e0169229 [PMID: 28046018 DOI: 10.1371/journal.pone.0169229]
- 85 **Sanderson MP**, Hofmann MH, Garin-Chesa P, Schweifer N, Wernitznig A, Fischer S, Jeschko A, Meyer R, Moll J, Pecina T, Arnhof H, Weyer-Czernilofsky U, Zahn SK, Adolf GR, Kraut N. The IGF1R/INSR Inhibitor BI 885578 Selectively Inhibits Growth of IGF2-Overexpressing Colorectal Cancer Tumors and Potentiates the Efficacy of Anti-VEGF Therapy. *Mol Cancer Ther* 2017; **16**: 2223-2233 [PMID: 28729397 DOI: 10.1158/1535-7163.MCT-17-0336]
  - 86 **Stanton MJ**, Dutta S, Polavaram NS, Roy S, Muders MH, Datta K. Angiogenic growth factor axis in autophagy regulation. *Autophagy* 2013; **9**: 789-790 [PMID: 23388383 DOI: 10.4161/auto.23783]
  - 87 **Shimizu M**, Shirakami Y, Iwasa J, Shiraki M, Yasuda Y, Hata K, Hirose Y, Tsurumi H, Tanaka T, Moriwaki H. Supplementation with branched-chain amino acids inhibits azoxymethane-induced colonic preneoplastic lesions in male C57BL/KsJ-db/db mice. *Clin Cancer Res* 2009; **15**: 3068-3075 [PMID: 19366832 DOI: 10.1158/1078-0432.CCR-08-2093]
  - 88 **Iwasa J**, Shimizu M, Shiraki M, Shirakami Y, Sakai H, Terakura Y, Takai K, Tsurumi H, Tanaka T, Moriwaki H. Dietary supplementation with branched-chain amino acids suppresses diethylnitrosamine-induced liver tumorigenesis in obese and diabetic C57BL/KsJ-db/db mice. *Cancer Sci* 2010; **101**: 460-467 [PMID: 19906067 DOI: 10.1111/j.1349-7006.2009.01402.x]
  - 89 **Yoshiji H**, Noguchi R, Kitade M, Kaji K, Ikenaka Y, Namisaki T, Yoshii J, Yanase K, Yamazaki M, Tsujimoto T, Akahane T, Kawarata H, Uemura M, Fukui H. Branched-chain amino acids suppress insulin-resistance-based hepatocarcinogenesis in obese diabetic rats. *J Gastroenterol* 2009; **44**: 483-491 [PMID: 19319465 DOI: 10.1007/s00535-009-0031-0]
  - 90 **Wubetu GY**, Utsunomiya T, Ishikawa D, Ikemoto T, Yamada S, Morine Y, Iwahashi S, Saito Y, Arakawa Y, Imura S, Arimochi H, Shimada M. Branched chain amino acid suppressed insulin-initiated proliferation of human cancer cells through induction of autophagy. *Anticancer Res* 2014; **34**: 4789-4796 [PMID: 25202059]
  - 91 **Ekyalongo RC**, Mukohara T, Kataoka Y, Funakoshi Y, Tomioka H, Kiyota N, Fujiwara Y, Minami H. Mechanisms of acquired resistance to insulin-like growth factor 1 receptor inhibitor in MCF-7 breast cancer cell line. *Invest New Drugs* 2013; **31**: 293-303 [PMID: 22828916 DOI: 10.1007/s10637-012-9855-1]
  - 92 **Feng Y**, Gao S, Gao Y, Wang X, Chen Z. Anti-EGFR antibody sensitizes colorectal cancer stem-like cells to Fluorouracil-induced apoptosis by affecting autophagy. *Oncotarget* 2016; **7**: 81402-81409 [PMID: 27833077 DOI: 10.18632/oncotarget.13233]
  - 93 **Koustas E**, Karamouzis MV, Mihailidou C, Schizas D, Papavassiliou AG. Co-targeting of EGFR and autophagy signaling is an emerging treatment strategy in metastatic colorectal cancer. *Cancer Lett* 2017; **396**: 94-102 [PMID: 28323034 DOI: 10.1016/j.canlet.2017.03.023]
  - 94 **Chen Z**, Gao S, Wang D, Song D, Feng Y. Colorectal cancer cells are resistant to anti-EGFR monoclonal antibody through adapted autophagy. *Am J Transl Res* 2016; **8**: 1190-1196 [PMID: 27158405]
  - 95 **Oberthür R**, Seemann H, Gehrig J, Rave-Fränk M, Bremmer F, Halpape R, Conradi LC, Scharf JG, Burfeind P, Kaulfuß S. Simultaneous inhibition of IGF1R and EGFR enhances the efficacy of standard treatment for colorectal cancer by the impairment of DNA repair and the induction of cell death. *Cancer Lett* 2017; **407**: 93-105 [PMID: 28823963 DOI: 10.1016/j.canlet.2017.08.009]
  - 96 **Renna M**, Bento CF, Fleming A, Menzies FM, Siddiqi FH, Ravikumar B, Puri C, Garcia-Arencibia M, Sadiq O, Corrochano S, Carter S, Brown SD, Acevedo-Arozena A, Rubinsztein DC. IGF-1 receptor antagonism inhibits autophagy. *Hum Mol Genet* 2013; **22**: 4528-4544 [PMID: 23804751 DOI: 10.1093/hmg/ddt300]
  - 97 **Rubinsztein DC**, Codogno P, Levine B. Autophagy modulation as a potential therapeutic target for diverse diseases. *Nat Rev Drug Discov* 2012; **11**: 709-730 [PMID: 22935804 DOI: 10.1038/nrd3802]
  - 98 **Wang RC**, Wei Y, An Z, Zou Z, Xiao G, Bhagat G, White M, Reichelt J, Levine B. Akt-mediated regulation of autophagy and tumorigenesis through Beclin 1 phosphorylation. *Science* 2012; **338**: 956-959 [PMID: 23112296 DOI: 10.1126/science.1225967]
  - 99 **Choi AM**, Ryter SW, Levine B. Autophagy in human health and disease. *N Engl J Med* 2013; **368**: 651-662 [PMID: 23406030 DOI: 10.1056/NEJMr1205406]
  - 100 **Eskelinen EL**, Prescott AR, Cooper J, Brachmann SM, Wang L, Tang X, Backer JM, Lucocq JM. Inhibition of autophagy in mitotic animal cells. *Traffic* 2002; **3**: 878-893 [PMID: 12453151 DOI: 10.1034/j.1600-0854.2002.31204.x]
  - 101 **Liu JJ**, Nilsson A, Oredsson S, Badmaev V, Zhao WZ, Duan RD. Boswellic acids trigger apoptosis via a pathway dependent on caspase-8 activation but independent on Fas/Fas ligand interaction in colon cancer HT-29 cells. *Carcinogenesis* 2002; **23**: 2087-2093 [PMID: 12507932 DOI: 10.1093/carcin/23.12.2087]
  - 102 **Liu JJ**, Huang B, Hooi SC. Acetyl-keto-beta-boswellic acid inhibits cellular proliferation through a p21-dependent pathway in colon cancer cells. *Br J Pharmacol* 2006; **148**: 1099-1107 [PMID: 16783403 DOI: 10.1038/sj.bjp.0706817]
  - 103 **Takahashi M**, Sung B, Shen Y, Hur K, Link A, Boland CR, Aggarwal BB, Goel A. Boswellic acid exerts antitumor effects in colorectal cancer cells by modulating expression of the let-7 and miR-200 microRNA family. *Carcinogenesis* 2012; **33**: 2441-2449 [PMID: 22983985 DOI: 10.1093/carcin/bgs286]
  - 104 **Pathania AS**, Guru SK, Kumar S, Kumar A, Ahmad M, Bhushan S, Sharma PR, Mahajan P, Shah BA, Sharma S, Nargotra A, Vishwakarma R, Korkaya H, Malik F. Interplay between cell cycle and autophagy induced by boswellic acid analog. *Sci Rep* 2016; **6**: 33146 [PMID: 27680387 DOI: 10.1038/srep33146]

P- Reviewer: Zhong ZH S- Editor: Chen K L- Editor: A  
E- Editor: Ma YJ



## Retreatment of patients with treatment failure of direct-acting antivirals: Focus on hepatitis C virus genotype 1b

Tatsuo Kanda, Kazushige Nirei, Naoki Matsumoto, Teruhisa Higuchi, Hitomi Nakamura, Hiroaki Yamagami, Shunichi Matsuoka, Mitsuhiro Moriyama

Tatsuo Kanda, Kazushige Nirei, Naoki Matsumoto, Teruhisa Higuchi, Hitomi Nakamura, Hiroaki Yamagami, Shunichi Matsuoka, Mitsuhiro Moriyama, Division of Gastroenterology and Hepatology, Department of Internal Medicine, Nihon University School of Medicine, Itabashi-ku, Tokyo 173-8610, Japan

ORCID number: Tatsuo Kanda (0000-0002-9565-4669); Kazushige Nirei (0000-0003-3926-5076); Naoki Matsumoto (0000-0002-9982-6130); Teruhisa Higuchi (0000-0003-4104-4213); Hitomi Nakamura (0000-0001-7748-5833); Hiroaki Yamagami (0000-0003-0174-7811); Shunichi Matsuoka (0000-0002-3221-7939); Mitsuhiro Moriyama (0000-0002-4617-508x).

**Author contributions:** These authors contributed to all aspects of this paper.

**Supported by** AMED; and JSPS KAKENHI, No. 17K09404.

**Conflict-of-interest statement:** Kanda T received research grants from AbbVie, MSD, Chugai Pharma and Sysmex. These company played no role in this study. Other authors declare no conflict of interest related to this publication.

**Open-Access:** This article is an open-access article which was selected by an in-house editor and fully peer-reviewed by external reviewers. It is distributed in accordance with the Creative Commons Attribution Non Commercial (CC BY-NC 4.0) license, which permits others to distribute, remix, adapt, build upon this work non-commercially, and license their derivative works on different terms, provided the original work is properly cited and the use is non-commercial. See: <http://creativecommons.org/licenses/by-nc/4.0/>

**Manuscript source:** Invited manuscript

**Correspondence to:** Tatsuo Kanda, MD, PhD, Associate Professor, Division of Gastroenterology and Hepatology, Department of Internal Medicine, Nihon University School of Medicine, 30-1 Oyaguchi-Kamicho, Itabashi-ku, Tokyo 173-8610, Japan. [kandat-cib@umin.ac.jp](mailto:kandat-cib@umin.ac.jp)  
Telephone: +81-3-39728111  
Fax: +81-3-39568496

Received: October 13, 2017

Peer-review started: October 13, 2017

First decision: October 30, 2017

Revised: November 10, 2017

Accepted: November 28, 2017

Article in press: November 28, 2017

Published online: December 14, 2017

### Abstract

The recent development of direct-acting antiviral agents (DAAs) against hepatitis C virus (HCV) infection could lead to higher sustained virological response (SVR) rates, with shorter treatment durations and fewer adverse events compared with regimens that include interferon. However, a relatively small proportion of patients cannot achieve SVR in the first treatment, including DAAs with or without peginterferon and/or ribavirin. Although retreatment with a combination of DAAs should be conducted for these patients, it is more difficult to achieve SVR when retreating these patients because of resistance-associated substitutions (RASs) or treatment-emergent substitutions. In Japan, HCV genotype 1b (GT1b) is founded in 70% of HCV-infected individuals. In this minireview, we summarize the retreatment regimens and their SVR rates for HCV GT1b. It is important to avoid drugs that target the regions targeted by initial drugs, but next-generation combinations of DAAs, such as sofosbuvir/velpatasvir/voxilaprevir for 12 wk or glecaprevir/pibrentasvir for 12 wk, are proposed to be potential solution for the HCV GT1b-infected patients with treatment failure, mainly on a basis of targeting distinctive regions. Clinicians should follow the new information and resources for DAAs and select the proper combination of DAAs for the retreatment of HCV GT1b-infected patients with treatment failure.

**Key words:** Direct-acting antiviral agent; Genotype 1b;



Hepatitis C virus; Resistance-associated substitutions

© **The Author(s) 2017.** Published by Baishideng Publishing Group Inc. All rights reserved.

**Core tip:** In this minireview, we focused on the retreatment of patients with treatment failure of direct-acting antiviral agents against hepatitis C virus genotype 1b (HCV GT1b) infection. We summarized the retreatment regimens for patients with failure of peginterferon and ribavirin plus HCV NS3/4A inhibitors and for those with failure of HCV NS5A inhibitors. We also demonstrated the resistance-associated substitutions of HCV NS5B nucleos(t)ide inhibitors. Attention should be paid when selecting both the initial treatment and retreat regimens to completely eradicate HCV infection.

Kanda T, Nirei K, Matsumoto N, Higuchi T, Nakamura H, Yamagami H, Matsuoka S, Moriyama M. Retreatment of patients with treatment failure of direct-acting antivirals: Focus on hepatitis C virus genotype 1b. *World J Gastroenterol* 2017; 23(46): 8120-8127 Available from: URL: <http://www.wjgnet.com/1007-9327/full/v23/i46/8120.htm> DOI: <http://dx.doi.org/10.3748/wjg.v23.i46.8120>

## INTRODUCTION

In the interferon era, the eradication of the hepatitis C virus (HCV) has had beneficial effects, such as the regression of liver fibrosis, hepatic decompensation, and the reduction of hepatocellular carcinoma (HCC) in HCV-infected individuals<sup>[1]</sup>. Based on these results, in the direct-acting antiviral agents (DAAs) era, it also seems important to eradicate HCV to improve the prognosis of HCV-infected individuals.

Interferon acts on the target cells, such as hepatocytes and/or lymphocytes through the interferon receptors on their surface and induces interferon-stimulated genes (ISGs) and antiviral effects<sup>[2]</sup>. Almost all human cells have interferon receptors on their surfaces, and the use of interferon exhibits numerous adverse events. However, because interferon acts in a HCV-nonspecific manner, interferon can eradicate mutant viruses in most cases (Figure 1). The achievement of sustained virological response at week 24 after the end of treatment (SVR24) was strongly affected by single-nucleotide polymorphisms (SNPs) near the interleukin-28 B (IL28B)/interferon lambda 3-coding region in patients who were treated with peginterferon plus ribavirin, with or without DAAs<sup>[3-6]</sup>.

HCV genome encodes at least 10 proteins: core, E1, E2, p7, NS2, NS3, NS4A, NS4B, NS5A and NS5B<sup>[7]</sup>. In current DAA treatment for patients infected with HCV, viral proteins targeted by HCV DAAs are HCV NS3/4A, NS5A and/or NS5B. A combination of HCV NS3/4A protease inhibitors, HCV NS5A inhibitors and/

or HCV NS5B polymerase inhibitors, with or without ribavirin, are currently available for the treatment of HCV-infected patients, according to their HCV genotypes (GTs)<sup>[7]</sup>. Until the appearance of HCV pan-genotypic DAA regimens, most of treatments had been HCV GT-specific regimens. Representative HCV pan-genotypic drugs are shown in Table 1.

The daily oral administration of DAAs does not require injection therapy. Interferon-free treatment acts directly on HCV in a HCV RNA genome-specific manner and has fewer adverse events than interferon treatment does (Figure 1)<sup>[8-10]</sup>. In interferon-era or interferon-free-era, respectively, SVR24 and SVR12 have been defined as SVR because DAA combination regimens have stronger effects. However, resistance-associated substitutions (RASs) in the HCV RNA genome at baseline reduce the efficacy of some DAA combination regimens<sup>[11-13]</sup>. It is well known that RASs in HCV genomes with treatment failure have significantly negative effects on the efficacy of retreatment with DAAs<sup>[14-16]</sup>. Ultra-deep sequencing has been used for the research purpose, but direct-sequencing method is applicable for the screening detection of RASs in daily clinical practice. When using DAA combinations, attention should be paid to the RASs and the drug-drug interactions.

Naturally occurring HCV variants depend on different geographic areas and they have some impacts on the context of current HCV therapy. Because of the high-prevalent infection of HCV GT1b in Japanese chronic hepatitis C patients, retreatment regimens of HCV GT1b is intensively discussed.

## RE-TREATMENT OF PATIENTS INFECTED WITH HCV GT1B WITH FAILURE OF PEGINTERFERON AND RIBAVIRIN PLUS HCV NS3/4A INHIBITORS

Using a combination of peginterferon and ribavirin plus protease inhibitors has led to approximately 70% SVR rates in HCV GT1b-infected patients<sup>[6,17-22]</sup>. This combination including second generation protease inhibitors has fewer adverse events than do regimens including telaprevir or boceprevir, and it has similar SVR rates<sup>[6,22-25]</sup>.

Among HCV GT1-infected Japanese patients, 98%-99% of these patients are infected with HCV GT1b<sup>[26]</sup>. D168N mutations were observed in only 1.1% (1/88) of HCV GT1b NS3/4A inhibitor-treatment-naïve patients<sup>[27]</sup>. In Japan, resistance mutations at the HCV NS3/4A regions are not always measured before treatment with a combination of peginterferon and ribavirin plus HCV NS3/4A protease inhibitors. During and after the use of HCV NS3/4A inhibitors, treatment failure occurs in HCV GT1a patients more often than it occurs in HCV GT1b patients. We have previously summarized the resistance mutations associated with



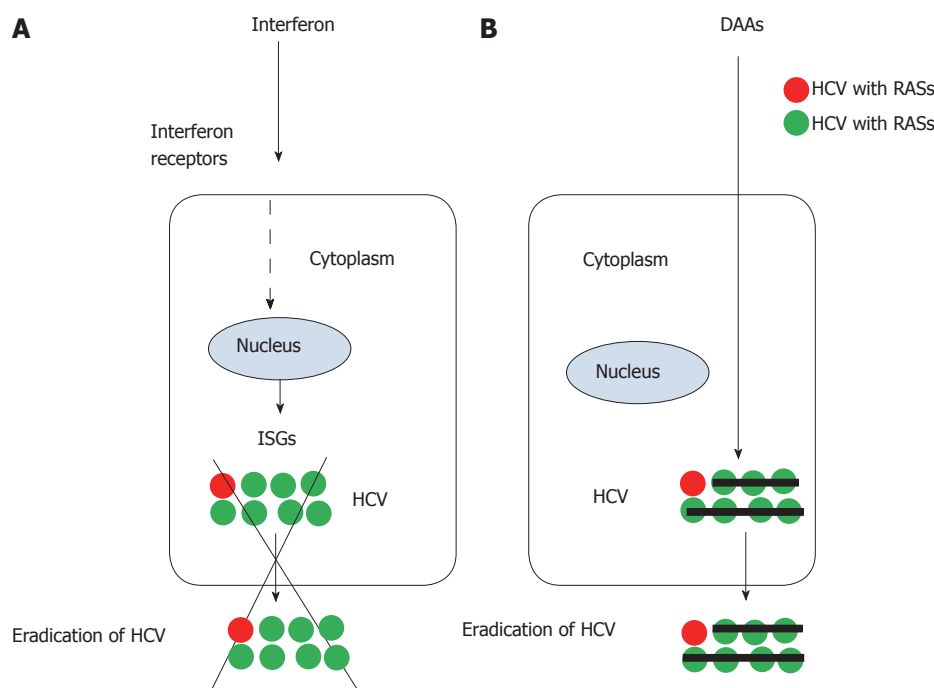


**Figure 1** Eradication of hepatitis C virus by interferon and direct-acting antiviral agents against hepatitis C virus. A: Interferon. Interferon induces interferon-stimulated genes (ISGs) transcription after binding its receptors and antiviral proteins. ISGs eradicate hepatitis C virus (HCV) with or without resistance associated substitutions (RASs) although interleukin-28B (IL28B) genotypes have an effect on its treatment results. B: direct-acting antiviral agents (DAAs) easily eradicate HCV without RASs because DAAs work in HCV sequence-specific manner. In some cases, it is difficult for DAAs to eradicate HCV with RASs.

**Table 1** Representative direct-acting antivirals, their targets and hepatitis C virus genotypes

Target regions	DAAs	HCV GTs
NS3/4A	Glecaprevir	Pan-GTs
	Grazoprevir	1, 4
	Asunaprevir	1b
	Paritaprevir	1, 2a, 4
	Simeprevir	1, 4
	Telaprevir	1, 2
	Boceprevir	1
NS5A	Pibrentasvir	Pan-GTs
	Velpatasvir	Pan-GTs
	Elbasvir	Pan-GTs
	Daclatasvir	Pan-GTs
	Ledipasvir	1, 4, 5
	Ombitasvir	1, 4
NS5B	Sofosbuvir [nucleos(t)ide inhibitor]	Pan-GTs
	Dasabuvir [non-nucleos(t)ide inhibitor]	1

DAAs: Direct-acting antivirals; HCV GTs: Hepatitis C virus genotypes.

resistance to HCV NS3/4A protease inhibitors<sup>[27]</sup>.

The American Association for the Study of Liver Diseases (AASLD)<sup>[28-31]</sup> has recommended a daily fixed-dose combination of sofosbuvir (400 mg)/HCV NS5A inhibitor velpatasvir (100 mg) for 12 wk, or a daily fixed-dose combination of HCV NS3/4A inhibitor glecaprevir (300 mg)/HCV NS5A inhibitor pibrentasvir (120 mg) for 12 wk, for the retreatment against HCV NS3/4A protease inhibitor with peginterferon and ribavirin-experienced, HCV GT1-patients with or without cirrhosis. They also recommended a daily

fixed-dose combination of HCV NS5A inhibitor elbasvir (50 mg)/HCV NS3/4A inhibitor grazoprevir (100 mg) for 12 wk or a daily fixed-dose combination of HCV NS5A inhibitor ledipasvir (90 mg)/HCV NS5B polymerase inhibitor sofosbuvir (400 mg) for 12 wk in the retreatment for HCV GT1b patients with or without cirrhosis, respectively<sup>[28,29]</sup>.

For HCV GT1 and non-cirrhotic/cirrhotic patients who were previously treated with peginterferon and ribavirin plus HCV NS3/4A protease inhibitors, a daily fixed-dose combination of ledipasvir (90 mg)/sofosbuvir (400 mg) with or without ribavirin for 12 and 24 wk led to SVR rates of 96.2% (50/52)/85.7% (12/14) or 100% (51/51)/84.6% (11/13) and 97.2% (35/36)/100% (14/14) or 100% (38/38)/100% (13/13), respectively<sup>[29]</sup>. In the retreatment of previous users of peginterferon plus ribavirin with HCV NS3/4A inhibitors, ledipasvir plus sofosbuvir should be selected as a first-line treatment<sup>[1,6,28]</sup>. We reported that 100% SVR rates (25/25) were achieved by 12 wk of combination treatment with ledipasvir plus sofosbuvir in patients previously treated with peginterferon plus ribavirin with various HCV NS3/4A inhibitors<sup>[6]</sup>. It may be important to avoid drugs that target the regions targeted by initial drugs.

For HCV GT1 and cirrhotic patients who were previously treated with peginterferon and ribavirin plus DAAs, a daily fixed-dose combination of sofosbuvir (400 mg)/velpatasvir (100 mg) for 12 wk led to 100% (48/48) SVR rates [100% (37/37) and 100% (11/11) in GT1a and GT1b patients, respectively]<sup>[30]</sup>. Among

**Table 2** Resistance-associated substitutions or treatment-emergent substitutions of hepatitis C virus NS5B nucleos(t)ide inhibitors

Domains of HCV NS5B polymerase <sup>[45]</sup>	HCV genotypes (GTs)			Ref.
	GT1	GT1a	GT1b	
Fingers domain (AA1-188, 226-287)		C14R		[40]
		D61G		[40]
			T77T/A	[41]
	S96T			[42]
	N142T		N142S	[40,42]
	L159F			[40-44]
		E237G		[40]
Palm domain (AA188-226, 287-371)	S282T	S282R		[40-42]
	M289I/L			[42,44]
		L314P		[40]
			C316R	[41]
	L320F	L320I/V		[40-42]
	V321A	V321I		[40,42,43]
		T344I		[40]
Thumb domain (AA371-530)		F415Y		[43]
			E440G, E/G	[42]
		S470G		[40]

β-hairpin, AA443-453; C-term linker, AA530-565<sup>[44]</sup>. HCV: Hepatitis C virus.

**Table 3** Retreatment regimens for patients with hepatitis C virus infection for whom the initial combination of direct-acting antivirals has failed

Patients	APASL (2016) <sup>[1]</sup>	AASLD (2017) <sup>[28]</sup>
GT1		
Peginterferon and ribavirin plus HCV NS3/4A inhibitors-failure non-cirrhotic patients	Sofosbuvir/ledipasvir 12 wk	Sofosbuvir/ledipasvir 12 wk Sofosbuvir/velpatasvir 12 wk Glecaprevir/pibrentasvir 12 wk
Peginterferon and ribavirin plus HCV NS3/4A inhibitors-failure compensated cirrhotic patients	Sofosbuvir/ledipasvir 12 wk	Sofosbuvir/velpatasvir 12 wk Glecaprevir/pibrentasvir 12 wk (For GT1b) Elbasvir/grazoprevir 12 wk
HCV NS5A inhibitors-failure non-cirrhotic patients	Wait	Sofosbuvir/velpatasvir/voxilaprevir 12 wk
HCV NS5A inhibitors-failure compensated cirrhotic patients	RAS check	Sofosbuvir/velpatasvir/voxilaprevir 12 wk
Non-NS5A inhibitor/ sofosbuvir-failure non-cirrhotic patients	N/A	Glecaprevir/pibrentasvir 12 wk (For GT1a) Sofosbuvir/velpatasvir/voxilaprevir 12 wk (For GT1b) Sofosbuvir/velpatasvir 12 wk
Non-NS5A inhibitor/ sofosbuvir-failure compensated cirrhotic patients	N/A	Glecaprevir/pibrentasvir 12 wk (For GT1a) Sofosbuvir/velpatasvir/voxilaprevir 12 wk (For GT1b) Sofosbuvir/velpatasvir 12 wk
GT2		
Sofosbuvir/ribavirin-failure patients	N/A	Sofosbuvir/velpatasvir 12 wk Glecaprevir/pibrentasvir 12 wk
GT3		
DAA (including NS5A inhibitors) - failure patients	N/A	Sofosbuvir/velpatasvir/voxilaprevir 12 wk (For NS5A inhibitor-failure) weight-based ribavirin is recommended
GT4		
DAA (including NS5A inhibitors) - failure patients	N/A	Sofosbuvir/velpatasvir/voxilaprevir 12 wk
GT5/GT6		
DAA (including NS5A inhibitors) - failure patients	N/A	Sofosbuvir/velpatasvir/voxilaprevir 12 wk

DAAs: Direct-acting antivirals; HCV GTs: Hepatitis C virus genotypes; RAS: Resistance-associated variants; N/A: Not available.

those previously treated with HCV NS3/4A protease inhibitor-based therapy without HCV NS5A inhibitor exposure who were retreated with the daily fixed-dose combination of glecaprevir (300 mg)/pibrentasvir (120 mg) administered as three 100 mg/40 mg fixed-dose combination pills for 12 wk, the SVR12 rates were

92% (23/25)<sup>[31]</sup>. These next-generation combinations of DAAs are proposed to be potential solution for the HCV GT1b-infected patients with treatment failure, mainly on a basis of targeting distinctive regions.

The use of daclatasvir plus asunaprevir for HCV GT1b was ineffective for patients with pre-existent HCV

NS5A RASs or simeprevir failure, regardless of fibrosis status<sup>[32]</sup>. If possible, retreatment without HCV NS3/4A inhibitors should be selected for HCV GT1b-infected patients with treatment failure of peginterferon and ribavirin plus HCV NS3/4A inhibitors<sup>[6,33]</sup>.

## RETREATMENT OF PATIENTS INFECTED WITH HCV GT1B WITH FAILURE OF HCV NS5A INHIBITORS

HCV NS5A inhibitors, such as daclatasvir and ledipasvir, in combination with other DAAs against other regions of HCV, with or without peginterferon/ribavirin, could efficiently inhibit HCV replication, according to HCV GTs<sup>[34]</sup>. We have also reported the summary of resistance mutations associated with resistance to HCV NS5A inhibitors<sup>[34]</sup>.

In Japan, daclatasvir plus HCV NS3/4A protease inhibitor asunaprevir was introduced for the treatment of chronic HCV GT1b infection in 2013<sup>[35]</sup>. Treatment with daclatasvir and asunaprevir after screening for HCV NS5A RASs is a relatively safe and effective treatment for HCV GT1b patients in Japan<sup>[36,37]</sup>. However, 85.3% (29/34) of the patients with virologic failure had RASs to both daclatasvir (predominantly HCV NS5A-L31M/V-Y93H) and asunaprevir (predominantly NS3-D168 variants) detected at failure<sup>[35]</sup>. Japanese clinicians used the combination regimens of ledipasvir plus sofosbuvir for 12 wk in daclatasvir/asunaprevir-failure patients, resulting in only 64%-70% SVR rates<sup>[14,15,38]</sup>.

The prevalence of HCV NS5A RASs was significantly higher in daclatasvir/asunaprevir-failure patients at amino acid positions 24, 28, 30, 31, 32 and 93 than it was in daclatasvir/asunaprevir-treatment naïve patients<sup>[38]</sup>. The presence of HCV NS5A RAS at positions 31, 32, 92, and 93 significantly attenuated the efficacy of retreatment with ledipasvir plus sofosbuvir. Of importance, HCV NS5A RASs at these positions have a negative impact on the achievement of SVR.

Recently, more effective regimens for treatment-experienced patients with HCV NS5A inhibitors have appeared<sup>[28]</sup>, although it was recommended that treatment-experienced patients with HCV NS5A inhibitors should check their RASs or wait before further treatment<sup>[1]</sup>. AASLD guidelines recommend the daily fixed-dose combination of sofosbuvir (400 mg)/velpatasvir (100 mg)/HCV NS3/4A protease inhibitor voxilaprevir (100 mg) for GT1 patients with or without cirrhosis<sup>[28]</sup> (See also next sections<sup>[39]</sup>).

## HCV NS5B POLYMERASE INHIBITORS-RASs IN PATIENTS INFECTED WITH HCV GT1B

There are two types of HCV NS5B polymerase in-

hibitors: nucleos(t)ide inhibitors and non-nucleoside inhibitors. Treatment regimens including sofosbuvir, which is a nucleoside analogue, achieved higher SVR rates. RASs associated with the use of sofosbuvir are shown in Table 2<sup>[40-44]</sup>. Although RASs are distributed in all domains of the HCV NS5B polymerase structure<sup>[45]</sup>, the S282 is located at the fingers domain near the palm domain, and the C316 and V321 are both located at the palm domain<sup>[41,45]</sup>. Of note, ribavirin associated RASs T390I and F415Y are both located in the thumb domain of HCV NS5B polymerase<sup>[42]</sup>. It has been reported that RASs of non-nucleoside inhibitors are the following: C316N/Y, M414I/V/T, L419M/S, R422K, M423A/I/T/B, C445F, Y448H, Y452H, I482L, A486I/T, V494A, P495A/T, V499A, P496S, G554S, S556G and D559G, which are all located at the palm and thumb domains of HCV NS5B polymerase structure<sup>[42]</sup>.

When treatment failure was observed in case where the first-generation HCV NS5A inhibitor plus nucleoside inhibitor such as sofosbuvir with or without ribavirin had been selected as an initial DAA treatment for HCV GT1 patients, HCV genome sequences often had HCV NS5A RASs. It has been reported in POLARIS-1 and POLARIS-4 studies that treatment with sofosbuvir/velpatasvir/voxilaprevir for 12 wk could lead to 96% (253/263) and 98% (178/182) SVR rates, respectively, in HCV GTs1-6 patients who were previously treated with DAAs<sup>[39]</sup>. In POLARIS-1 and POLARIS-4 studies, respectively, SVR rates of 97% (146/150) and 97% (76/78), respectively, were achieved in HCV GT1-patients, by sofosbuvir/velpatasvir/voxilaprevir for 12 wk<sup>[39]</sup>; 96% (97/101) and 98% (53/54) in HCV GT1a-patients; and 100% (45/45) and 96% (23/24) in HCV GT1b-patients<sup>[39]</sup>. Twelve weeks of treatment with a fixed-dose combination of sofosbuvir/velpatasvir/voxilaprevir was effective and well tolerated among patients with GT1 infection for whom a DAA-based regimen had previously failed<sup>[39,46]</sup>.

## CONCLUSION

Sergi *et al.*<sup>[47]</sup> reviewed that there was the association between HCV GT1b and fulminant liver failure, although HCV is a rare cause of fulminant hepatitis in Japan<sup>[48]</sup>. Of their two HCV RNA-positive cases with evidence of HBV infection, one case had a real coinfection showing simultaneous detection of HBV DNA in serum and liver, while the other patient was a chronic HBV carrier, seropositive for HBsAg and anti-HBc IgG but negative for anti-HBc IgM and HBV DNA in liver tissue<sup>[47]</sup>. It has been reported that hepatitis B reactivation during or after the treatment of DAA for chronic hepatitis C<sup>[49]</sup>. Similar SVR rates seem to be achieved with DAAs in HCV/HBV co-infected patients<sup>[50,51]</sup>. However, nucleos(t)ide analogues for HBV should be added to DAA therapy for HCV when serum HBV DNA levels are elevated<sup>[1]</sup>.

There is no doubt that new, more effective combinations of DAAs have appeared and will continue

to appear in the retreatment of patients who have experienced treatment failure of DAAs. Clinicians should pay careful attention when selecting the initial treatment and retreatment regimens to completely eradicate HCV infection (Table 3).

## REFERENCES

- 1 **Omata M**, Kanda T, Wei L, Yu ML, Chuang WL, Ibrahim A, Lesmana CR, Sollano J, Kumar M, Jindal A, Sharma BC, Hamid SS, Dokmeci AK, Mamun-AI-Mahtab, McCaughan GW, Wasim J, Crawford DH, Kao JH, Yokosuka O, Lau GK, Sarin SK. APASL consensus statements and recommendation on treatment of hepatitis C. *Hepatol Int* 2016; **10**: 702-726 [PMID: 27130427 DOI: 10.1007/s12072-016-9717-6]
- 2 **Sasaki R**, Kanda T, Nakamoto S, Haga Y, Nakamura M, Yasui S, Jiang X, Wu S, Arai M, Yokosuka O. Natural interferon-beta treatment for patients with chronic hepatitis C in Japan. *World J Hepatol* 2015; **7**: 1125-1132 [PMID: 26052401 DOI: 10.4254/wjh.v7.i8.1125]
- 3 **Ge D**, Fellay J, Thompson AJ, Simon JS, Shianna KV, Urban TJ, Heinzen EL, Qiu P, Bertelsen AH, Muir AJ, Sulkowski M, McHutchison JG, Goldstein DB. Genetic variation in IL28B predicts hepatitis C treatment-induced viral clearance. *Nature* 2009; **461**: 399-401 [PMID: 19684573 DOI: 10.1038/nature08309]
- 4 **Suppiah V**, Moldovan M, Ahlenstiel G, Berg T, Weltman M, Abate ML, Bassendine M, Spengler U, Dore GJ, Powell E, Riordan S, Sheridan D, Smedile A, Fragomeli V, Müller T, Bahlo M, Stewart GJ, Booth DR, George J. IL28B is associated with response to chronic hepatitis C interferon-alpha and ribavirin therapy. *Nat Genet* 2009; **41**: 1100-1104 [PMID: 19749758 DOI: 10.1038/ng.447]
- 5 **Tanaka Y**, Nishida N, Sugiyama M, Kurosaki M, Matsuura K, Sakamoto N, Nakagawa M, Korenaga M, Hino K, Hige S, Ito Y, Mita E, Tanaka E, Mochida S, Murawaki Y, Honda M, Sakai A, Hiasa Y, Nishiguchi S, Koike A, Sakaida I, Imamura M, Ito K, Yano K, Masaki N, Sugauchi F, Izumi N, Tokunaga K, Mizokami M. Genome-wide association of IL28B with response to pegylated interferon-alpha and ribavirin therapy for chronic hepatitis C. *Nat Genet* 2009; **41**: 1105-1109 [PMID: 19749757 DOI: 10.1038/ng.449]
- 6 **Kanda T**, Nakamoto S, Sasaki R, Nakamura M, Yasui S, Haga Y, Ogasawara S, Tawada A, Arai M, Mikami S, Imazeki F, Yokosuka O. Sustained Virologic Response at 24 Weeks after the End of Treatment Is a Better Predictor for Treatment Outcome in Real-World HCV-Infected Patients Treated by HCV NS3/4A Protease Inhibitors with Peginterferon plus Ribavirin. *Int J Med Sci* 2016; **13**: 310-315 [PMID: 27076789 DOI: 10.7150/ijms.14953]
- 7 **Kanda T**, Imazeki F, Yokosuka O. New antiviral therapies for chronic hepatitis C. *Hepatol Int* 2010; **4**: 548-561 [PMID: 21063477 DOI: 10.1007/s12072-010-9193-3]
- 8 **Gane EJ**, Roberts SK, Stedman CA, Angus PW, Ritchie B, Elston R, Ipe D, Morcos PN, Baher L, Najera I, Chu T, Lopatin U, Berrey MM, Bradford W, Laughlin M, Shulman NS, Smith PF. Oral combination therapy with a nucleoside polymerase inhibitor (RG7128) and danoprevir for chronic hepatitis C genotype 1 infection (INFORM-1): a randomised, double-blind, placebo-controlled, dose-escalation trial. *Lancet* 2010; **376**: 1467-1475 [PMID: 20951424 DOI: 10.1016/S0140-6736(10)61384-0]
- 9 **Lawitz E**, Poordad FF, Pang PS, Hyland RH, Ding X, Mo H, Symonds WT, McHutchison JG, Membreno FE. Sofosbuvir and ledipasvir fixed-dose combination with and without ribavirin in treatment-naïve and previously treated patients with genotype 1 hepatitis C virus infection (LONESTAR): an open-label, randomised, phase 2 trial. *Lancet* 2014; **383**: 515-523 [PMID: 24209977 DOI: 10.1016/S0140-6736(13)62121-2]
- 10 **Sulkowski M**, Hezode C, Gerstoft J, Vierling JM, Mallolas J, Pol S, Kugelmas M, Murillo A, Weis N, Nahass R, Shibolet O, Serfaty L, Bourliere M, DeJesus E, Zuckerman E, Dutko F, Shaughnessy M, Hwang P, Howe AY, Wahl J, Robertson M, Barr E, Haber B. Efficacy and safety of 8 weeks versus 12 weeks of treatment with grazoprevir (MK-5172) and elbasvir (MK-8742) with or without ribavirin in patients with hepatitis C virus genotype 1 mono-infection and HIV/hepatitis C virus co-infection (C-WORTHY): a randomised, open-label phase 2 trial. *Lancet* 2015; **385**: 1087-1097 [PMID: 25467560 DOI: 10.1016/S0140-6736(14)61793-1]
- 11 **Lok AS**, Gardiner DF, Lawitz E, Martorell C, Everson GT, Ghalib R, Reindollar R, Rustgi V, McPhee F, Wind-Rotolo M, Persson A, Zhu K, Dimitrova DI, Eley T, Guo T, Grasele DM, Pasquinelli C. Preliminary study of two antiviral agents for hepatitis C genotype 1. *N Engl J Med* 2012; **366**: 216-224 [PMID: 22256805 DOI: 10.1056/NEJMoa1104430]
- 12 **Karino Y**, Toyota J, Ikeda K, Suzuki F, Chayama K, Kawakami Y, Ishikawa H, Watanabe H, Hernandez D, Yu F, McPhee F, Kumada H. Characterization of virologic escape in hepatitis C virus genotype 1b patients treated with the direct-acting antivirals daclatasvir and asunaprevir. *J Hepatol* 2013; **58**: 646-654 [PMID: 23178977 DOI: 10.1016/j.jhep.2012.11.012]
- 13 **Kumada H**, Chayama K, Rodrigues L Jr, Suzuki F, Ikeda K, Toyoda H, Sato K, Karino Y, Matsuzaki Y, Kioka K, Setze C, Pilot-Matias T, Patwardhan M, Vilchez RA, Burroughs M, Redman R. Randomized phase 3 trial of ombitasvir/paritaprevir/ritonavir for hepatitis C virus genotype 1b-infected Japanese patients with or without cirrhosis. *Hepatology* 2015; **62**: 1037-1046 [PMID: 26147154 DOI: 10.1002/hep.27972]
- 14 **Akuta N**, Sezaki H, Suzuki F, Fujiyama S, Kawamura Y, Hosaka T, Kobayashi M, Kobayashi M, Saitoh S, Suzuki Y, Arase Y, Ikeda K, Kumada H. Ledipasvir plus sofosbuvir as salvage therapy for HCV genotype 1 failures to prior NS5A inhibitors regimens. *J Med Virol* 2017; **89**: 1248-1254 [PMID: 28079269 DOI: 10.1002/jmv.24767]
- 15 **Iio E**, Shimada N, Takaguchi K, Senoh T, Eguchi Y, Atsukawa M, Tsubota A, Abe H, Kato K, Kusakabe A, Miyaki T, Matsuura K, Matsunami K, Shinkai N, Fujiwara K, Nojiri S, Tanaka Y. Clinical evaluation of sofosbuvir/ledipasvir in patients with chronic hepatitis C genotype 1 with and without prior daclatasvir/asunaprevir therapy. *Hepatol Res* 2017; **47**: 1308-1316 [PMID: 28332272 DOI: 10.1111/hepr.12898]
- 16 **Kawakami Y**, Ochi H, Hayes CN, Imamura M, Tsuge M, Nakahara T, Katamura Y, Kohno H, Kohno H, Tsuji K, Takaki S, Mori N, Honda Y, Arataki K, Takahashi S, Kira S, Tamura T, Masuda K, Nakamura T, Kikkawa M, Chayama K. Efficacy and safety of ledipasvir/sofosbuvir with ribavirin in chronic hepatitis C patients who failed daclatasvir/asunaprevir therapy: pilot study. *J Gastroenterol* 2017; Epub ahead of print [PMID: 28815329 DOI: 10.1007/s00535-017-1380-8]
- 17 **Poordad F**, McCone J Jr, Bacon BR, Bruno S, Manns MP, Sulkowski MS, Jacobson IM, Reddy KR, Goodman ZD, Boparai N, DiNubile MJ, Sniukiene V, Brass CA, Albrecht JK, Bronowicki JP; SPRINT-2 Investigators. Boceprevir for untreated chronic HCV genotype 1 infection. *N Engl J Med* 2011; **364**: 1195-1206 [PMID: 21449783 DOI: 10.1056/NEJMoa1010494]
- 18 **Bacon BR**, Gordon SC, Lawitz E, Marcellin P, Vierling JM, Zeuzem S, Poordad F, Goodman ZD, Sings HL, Boparai N, Burroughs M, Brass CA, Albrecht JK, Esteban R; HCV RESPOND-2 Investigators. Boceprevir for previously treated chronic HCV genotype 1 infection. *N Engl J Med* 2011; **364**: 1207-1217 [PMID: 21449784 DOI: 10.1056/NEJMoa1009482]
- 19 **McHutchison JG**, Manns MP, Muir AJ, Terrault NA, Jacobson IM, Afdhal NH, Heathcote EJ, Zeuzem S, Reesink HW, Garg J, Bsharat M, George S, Kauffman RS, Adda N, Di Bisceglie AM; PROVE3 Study Team. Telaprevir for previously treated chronic HCV infection. *N Engl J Med* 2010; **362**: 1292-1303 [PMID: 20375406 DOI: 10.1056/NEJMoa0908014]
- 20 **Jacobson IM**, McHutchison JG, Dusheiko G, Di Bisceglie AM, Reddy KR, Bzowej NH, Marcellin P, Muir AJ, Ferenci P, Flisiak R, George J, Rizzetto M, Shouval D, Sola R, Terg RA, Yoshida EM, Adda N, Bengtsson L, Sankoh AJ, Kieffer TL, George S, Kauffman RS, Zeuzem S; ADVANCE Study Team. Telaprevir for



- previously untreated chronic hepatitis C virus infection. *N Engl J Med* 2011; **364**: 2405-2416 [PMID: 21696307 DOI: 10.1056/NEJMoa1012912]
- 21 **Zeuzem S**, Andreone P, Pol S, Lawitz E, Diago M, Roberts S, Focaccia R, Younossi Z, Foster GR, Horban A, Ferenci P, Nevens F, Müllhaupt B, Pockros P, Terg R, Shouval D, van Hoek B, Weiland O, Van Heeswijk R, De Meyer S, Luo D, Boogaerts G, Polo R, Picchio G, Beumont M; REALIZE Study Team. Telaprevir for retreatment of HCV infection. *N Engl J Med* 2011; **364**: 2417-2428 [PMID: 21696308 DOI: 10.1056/NEJMoa1013086]
  - 22 **Kanda T**, Yokosuka O, Omata M. Faldaprevir for the treatment of hepatitis C. *Int J Mol Sci* 2015; **16**: 4985-4996 [PMID: 25749475 DOI: 10.3390/ijms16034985]
  - 23 **Manns M**, Marcellin P, Poordad F, de Araujo ES, Buti M, Horsmans Y, Janczewska E, Villamil F, Scott J, Peeters M, Lenz O, Ouwerkerk-Mahadevan S, De La Rosa G, Kalmeijer R, Sinha R, Beumont-Mauviel M. Simeprevir with pegylated interferon alfa 2a or 2b plus ribavirin in treatment-naïve patients with chronic hepatitis C virus genotype 1 infection (QUEST-2): a randomised, double-blind, placebo-controlled phase 3 trial. *Lancet* 2014; **384**: 414-426 [PMID: 24907224 DOI: 10.1016/S0140-6736(14)60538-9]
  - 24 **Jacobson IM**, Dore GJ, Foster GR, Fried MW, Radu M, Rafalsky VV, Moroz L, Craxi A, Peeters M, Lenz O, Ouwerkerk-Mahadevan S, De La Rosa G, Kalmeijer R, Scott J, Sinha R, Beumont-Mauviel M. Simeprevir with pegylated interferon alfa 2a plus ribavirin in treatment-naïve patients with chronic hepatitis C virus genotype 1 infection (QUEST-1): a phase 3, randomised, double-blind, placebo-controlled trial. *Lancet* 2014; **384**: 403-413 [PMID: 24907225 DOI: 10.1016/S0140-6736(14)60494-3]
  - 25 **Kanda T**, Nakamoto S, Wu S, Yokosuka O. New treatments for genotype 1 chronic hepatitis C - focus on simeprevir. *Ther Clin Risk Manag* 2014; **10**: 387-394 [PMID: 24920913 DOI: 10.2147/TCRM.S50170]
  - 26 **Wu S**, Kanda T, Nakamoto S, Jiang X, Miyamura T, Nakatani SM, Ono SK, Takahashi-Nakaguchi A, Gono T, Yokosuka O. Prevalence of hepatitis C virus subgenotypes 1a and 1b in Japanese patients: ultra-deep sequencing analysis of HCV NS5B genotype-specific region. *PLoS One* 2013; **8**: e73615 [PMID: 24069214 DOI: 10.1371/journal.pone.0073615]
  - 27 **Wu S**, Kanda T, Nakamoto S, Imazeki F, Yokosuka O. Hepatitis C virus protease inhibitor-resistance mutations: our experience and review. *World J Gastroenterol* 2013; **19**: 8940-8948 [PMID: 24379619 DOI: 10.3748/wjg.v19.i47.8940]
  - 28 AASLD HCV Guidance: Recommendations for Testing, Managing, and Treating Hepatitis C. Available from: URL: <http://www.hcvguidelines.org> accessed on 2017/10/02
  - 29 **Afdhal N**, Reddy KR, Nelson DR, Lawitz E, Gordon SC, Schiff E, Nahass R, Ghalib R, Gitlin N, Herring R, Lalezari J, Younes ZH, Pockros PJ, Di Bisceglie AM, Arora S, Subramanian GM, Zhu Y, Dvory-Sobol H, Yang JC, Pang PS, Symonds WT, McHutchison JG, Muir AJ, Sulkowski M, Kwo P; ION-2 Investigators. Ledipasvir and sofosbuvir for previously treated HCV genotype 1 infection. *N Engl J Med* 2014; **370**: 1483-1493 [PMID: 24725238 DOI: 10.1056/NEJMoa1316366]
  - 30 **Feld JJ**, Jacobson IM, Hézode C, Asselah T, Ruane PJ, Gruener N, Abergel A, Mangia A, Lai CL, Chan HL, Mazzotta F, Moreno C, Yoshida E, Shafran SD, Towner WJ, Tran TT, McNally J, Osinusi A, Svarovskaia E, Zhu Y, Brainard DM, McHutchison JG, Agarwal K, Zeuzem S; ASTRAL-1 Investigators. Sofosbuvir and Velpatasvir for HCV Genotype 1, 2, 4, 5, and 6 Infection. *N Engl J Med* 2015; **373**: 2599-2607 [PMID: 26571066 DOI: 10.1056/NEJMoa1512610]
  - 31 **Poordad F**, Felizarta F, Asatryan A, Sulkowski MS, Reindollar RW, Landis CS, Gordon SC, Flamm SL, Fried MW, Bernstein DE, Lin CW, Liu R, Lovell SS, Ng TI, Kort J, Mensa FJ. Glecaprevir and pibrentasvir for 12 weeks for hepatitis C virus genotype 1 infection and prior direct-acting antiviral treatment. *Hepatology* 2017; **66**: 389-397 [PMID: 28128852 DOI: 10.1002/hep.29081]
  - 32 **Ogawa E**, Furusyo N, Yamashita N, Kawano A, Takahashi K, Dohmen K, Nakamuta M, Satoh T, Nomura H, Azuma K, Koyanagi T, Kotoh K, Shimoda S, Kajiwaru E, Hayashi J; Kyushu University Liver Disease Study(KULDS) Group. Effectiveness and safety of daclatasvir plus asunaprevir for patients with hepatitis C virus genotype 1b aged 75 years and over with or without cirrhosis. *Hepatol Res* 2017; **47**: E120-E131 [PMID: 27142311 DOI: 10.1111/hepr.12738]
  - 33 **Bourlière M**, Bronowicki JP, de Ledinghen V, Hézode C, Zoulim F, Mathurin P, Tran A, Larrey DG, Ratzin V, Alric L, Hyland RH, Jiang D, Doehle B, Pang PS, Symonds WT, Subramanian GM, McHutchison JG, Marcellin P, Habersetzer F, Guyader D, Grangé JD, Loustaud-Ratti V, Serfaty L, Metivier S, Leroy V, Abergel A, Pol S. Ledipasvir-sofosbuvir with or without ribavirin to treat patients with HCV genotype 1 infection and cirrhosis non-responsive to previous protease-inhibitor therapy: a randomised, double-blind, phase 2 trial (SIRIUS). *Lancet Infect Dis* 2015; **15**: 397-404 [PMID: 25773757 DOI: 10.1016/S1473-3099(15)70050-2]
  - 34 **Nakamoto S**, Kanda T, Wu S, Shirasawa H, Yokosuka O. Hepatitis C virus NS5A inhibitors and drug resistance mutations. *World J Gastroenterol* 2014; **20**: 2902-2912 [PMID: 24659881 DOI: 10.3748/wjg.v20.i11.2902]
  - 35 **Kumada H**, Suzuki Y, Ikeda K, Toyota J, Karino Y, Chayama K, Kawakami Y, Ido A, Yamamoto K, Takaguchi K, Izumi N, Koike K, Takehara T, Kawada N, Sata M, Miyagoshi H, Eley T, McPhee F, Damokosh A, Ishikawa H, Hughes E. Daclatasvir plus asunaprevir for chronic HCV genotype 1b infection. *Hepatology* 2014; **59**: 2083-2091 [PMID: 24604476 DOI: 10.1002/hep.27113]
  - 36 **Kanda T**, Yasui S, Nakamura M, Suzuki E, Arai M, Haga Y, Sasaki R, Wu S, Nakamoto S, Imazeki F, Yokosuka O. Daclatasvir plus Asunaprevir Treatment for Real-World HCV Genotype 1-Infected Patients in Japan. *Int J Med Sci* 2016; **13**: 418-423 [PMID: 27279790 DOI: 10.7150/ijms.15519]
  - 37 **Hirotsu Y**, Kanda T, Matsumura H, Moriyama M, Yokosuka O, Omata M. HCV NS5A resistance-associated variants in a group of real-world Japanese patients chronically infected with HCV genotype 1b. *Hepatol Int* 2015; **9**: 424-430 [PMID: 25791176 DOI: 10.1007/s12072-015-9624-2]
  - 38 **Kurosaki M**, Itakura J, Higuchi M, Yasui Y, Tamaki N, Tsuchiya K, Izumi N. Real world experience of re-treatment by ledipasvir/sofosbuvir for patients who failed previous daclatasvir plus asunaprevir therapy: interim analysis from large scale nationwide study. *Hepatology* 2017; **66** Suppl 1: 579A [DOI: 10.1002/hep.29501]
  - 39 **Bourlière M**, Gordon SC, Flamm SL, Cooper CL, Ramji A, Tong M, Ravendhran N, Vierling JM, Tran TT, Pianko S, Bansal MB, de Ledinghen V, Hyland RH, Stamm LM, Dvory-Sobol H, Svarovskaia E, Zhang J, Huang KC, Subramanian GM, Brainard DM, McHutchison JG, Verna EC, Buggisch P, Landis CS, Younes ZH, Curry MP, Strasser SI, Schiff ER, Reddy KR, Manns MP, Kowdley KV, Zeuzem S; POLARIS-1 and POLARIS-4 Investigators. Sofosbuvir, Velpatasvir, and Voxilaprevir for Previously Treated HCV Infection. *N Engl J Med* 2017; **376**: 2134-2146 [PMID: 28564569 DOI: 10.1056/NEJMoa1613512]
  - 40 **Wyles D**, Dvory-Sobol H, Svarovskaia ES, Doehle BP, Martin R, Afdhal NH, Kowdley KV, Lawitz E, Brainard DM, Miller MD, Mo H, Gane EJ. Post-treatment resistance analysis of hepatitis C virus from phase II and III clinical trials of ledipasvir/sofosbuvir. *J Hepatol* 2017; **66**: 703-710 [PMID: 27923693 DOI: 10.1016/j.jhep.2016.11.022]
  - 41 **Donaldson EF**, Harrington PR, O'Rear JJ, Naeger LK. Clinical evidence and bioinformatics characterization of potential hepatitis C virus resistance pathways for sofosbuvir. *Hepatology* 2015; **61**: 56-65 [PMID: 25123381 DOI: 10.1002/hep.27375]
  - 42 **Sarrazin C**, Dvory-Sobol H, Svarovskaia ES, Doehle BP, Pang PS, Chuang SM, Ma J, Ding X, Afdhal NH, Kowdley KV, Gane EJ, Lawitz E, Brainard DM, McHutchison JG, Miller MD, Mo H. Prevalence of Resistance-Associated Substitutions in HCV NS5A, NS5B, or NS3 and Outcomes of Treatment With Ledipasvir and Sofosbuvir. *Gastroenterology* 2016; **151**: 501-512.e1 [PMID:

- 27296509 DOI: 10.1053/j.gastro.2016.06.002]
- 43 **Kowdley KV**, Gordon SC, Reddy KR, Rossaro L, Bernstein DE, Lawitz E, Shiffman ML, Schiff E, Ghalib R, Ryan M, Rustgi V, Chojkier M, Herring R, Di Bisceglie AM, Pockros PJ, Subramanian GM, An D, Svarovskaia E, Hyland RH, Pang PS, Symonds WT, McHutchison JG, Muir AJ, Pound D, Fried MW; ION-3 Investigators. Ledipasvir and sofosbuvir for 8 or 12 weeks for chronic HCV without cirrhosis. *N Engl J Med* 2014; **370**: 1879-1888 [PMID: 24720702 DOI: 10.1056/NEJMoa1402355]
  - 44 **Svarovskaia ES**, Dvory-Sobol H, Parkin N, Hebner C, Gontcharova V, Martin R, Ouyang W, Han B, Xu S, Ku K, Chiu S, Gane E, Jacobson IM, Nelson DR, Lawitz E, Wyles DL, Bekele N, Brainard D, Symonds WT, McHutchison JG, Miller MD, Mo H. Infrequent development of resistance in genotype 1-6 hepatitis C virus-infected subjects treated with sofosbuvir in phase 2 and 3 clinical trials. *Clin Infect Dis* 2014; **59**: 1666-1674 [PMID: 25266287 DOI: 10.1093/cid/ciu697]
  - 45 **Mosley RT**, Edwards TE, Murakami E, Lam AM, Grice RL, Du J, Sofia MJ, Furman PA, Otto MJ. Structure of hepatitis C virus polymerase in complex with primer-template RNA. *J Virol* 2012; **86**: 6503-6511 [PMID: 22496223 DOI: 10.1128/JVI.00386-12]
  - 46 **Lawitz E**, Poordad F, Wells J, Hyland RH, Yang Y, Dvory-Sobol H, Stamm LM, Brainard DM, McHutchison JG, Landaverde C, Gutierrez J. Sofosbuvir-velpatasvir-voxilaprevir with or without ribavirin in direct-acting antiviral-experienced patients with genotype 1 hepatitis C virus. *Hepatology* 2017; **65**: 1803-1809 [PMID: 28220512 DOI: 10.1002/hep.29130]
  - 47 **Sergi C**, Jundt K, Seipp S, Goeser T, Theilmann L, Otto G, Otto HF, Hofmann WJ. The distribution of HBV, HCV and HGV among livers with fulminant hepatic failure of different aetiology. *J Hepatol* 1998; **29**: 861-871 [PMID: 9875631 DOI: 10.1016/S0168-8278(98)80112-8]
  - 48 **Kanda T**, Yokosuka O, Imazeki F, Saisho H. Acute hepatitis C virus infection, 1986-2001: a rare cause of fulminant hepatitis in Chiba, Japan. *Hepatogastroenterology* 2004; **51**: 556-558 [PMID: 15086201]
  - 49 **Holmes JA**, Yu ML, Chung RT. Hepatitis B reactivation during or after direct acting antiviral therapy - implication for susceptible individuals. *Expert Opin Drug Saf* 2017; **16**: 651-672 [PMID: 28471314 DOI: 10.1080/14740338.2017.1325869]
  - 50 **Wang C**, Ji D, Chen J, Shao Q, Li B, Liu J, Wu V, Wong A, Wang Y, Zhang X, Lu L, Wong C, Tsang S, Zhang Z, Sun J, Hou J, Chen G, Lau G. Hepatitis due to Reactivation of Hepatitis B Virus in Endemic Areas Among Patients With Hepatitis C Treated With Direct-acting Antiviral Agents. *Clin Gastroenterol Hepatol* 2017; **15**: 132-136 [PMID: 27392759 DOI: 10.1016/j.cgh.2016.06.023]
  - 51 **Chen G**, Wang C, Chen J, Ji D, Wang Y, Wu V, Karlberg J, Lau G. Hepatitis B reactivation in hepatitis B and C coinfectd patients treated with antiviral agents: A systematic review and meta-analysis. *Hepatology* 2017; **66**: 13-26 [PMID: 28195337 DOI: 10.1002/hep.29109]

**P- Reviewer:** Pan Q, Said ZAN, Sergi CM, Tamori A, Yoshioka K

**S- Editor:** Ma YJ **L- Editor:** A **E- Editor:** Ma YJ



## Basic Study

**Structural shift of gut microbiota during chemo-preventive effects of epigallocatechin gallate on colorectal carcinogenesis in mice**

Xin Wang, Tao Ye, Wen-Jie Chen, You Lv, Zong Hao, Jun Chen, Jia-Ying Zhao, Hui-Peng Wang, Yuan-Kun Cai

Xin Wang, Tao Ye, Wen-Jie Chen, You Lv, Zong Hao, Jun Chen, Jia-Ying Zhao, Hui-Peng Wang, Yuan-Kun Cai, Department of General Surgery, The 5<sup>th</sup> People's Hospital of Shanghai, Fudan University, Shanghai 200240, China

**Author contributions:** All authors contributed to the manuscript; Wang HP and Cai YK contributed equally to the article.

**Supported by** Natural Science Foundation of Minhang District of Shanghai, No. 2012MHZ001.

**Conflict-of-interest statement:** The authors declare that there is no conflict of interest regarding the publication of this paper.

**Open-Access:** This article is an open-access article which was selected by an in-house editor and fully peer-reviewed by external reviewers. It is distributed in accordance with the Creative Commons Attribution Non Commercial (CC BY-NC 4.0) license, which permits others to distribute, remix, adapt, build upon this work non-commercially, and license their derivative works on different terms, provided the original work is properly cited and the use is non-commercial. See: <http://creativecommons.org/licenses/by-nc/4.0/>

**Manuscript source:** Unsolicited manuscript

**Correspondence to:** Yuan-Kun Cai, MSc, Associate Professor, Chief Doctor, Surgeon of General Surgery, Department of General Surgery, The 5<sup>th</sup> People's Hospital of Shanghai, Fudan University, 801 Heqing Road, Shanghai 200240, China. [yunkun@medmail.com.cn](mailto:yunkun@medmail.com.cn)  
Telephone: +86-18918168583  
Fax: +86-21-64307611

**Received:** February 23, 2017

**Peer-review started:** February 24, 2017

**First decision:** April 28, 2017

**Revised:** September 15, 2017

**Accepted:** November 2, 2017

**Article in press:** November 2, 2017

**Published online:** December 14, 2017

**Abstract****AIM**

To investigate the effect of epigallocatechin gallate (EGCG) on structural changes of gut microbiota in colorectal carcinogenesis.

**METHODS**

An azoxymethane (AOM)/dextran sodium sulfate (DSS)-induced colitis mouse model was established. Forty-two female FVB/N mice were randomly divided into the following three groups: group 1 (10 mice, negative control) was treated with vehicle, group 2 (16 mice, positive control) was treated with AOM plus vehicle, and group 3 (16 mice, EG) was treated with AOM plus EGCG. For aberrant crypt foci (ACF) evaluation, the colons were rapidly took out after sacrifice, rinsed with saline, opened longitudinally, laid flat on a polystyrene board, and fixed with 10% buffered formaldehyde solution before being stained with 0.2% methylene blue in saline. For tumor evaluation, the colon was macroscopically inspected and photographed, then the total number of tumors was enumerated and tumor size measured. For histological examination, the fixed tissues were paraffin-embedded and sectioned at 5 mm thickness. Microbial genomic DNA was extracted from fecal and intestinal content samples using a commercial kit. The V4 hypervariable regions of 16S rRNA were PCR-amplified with the barcoded fusion primers. Using the best hit classification option, the sequences from each sample were aligned to the RDP 16S rRNA training set to classify the taxonomic abundance in QIIME. Statistical analyses were then performed.

**RESULTS**

Treatment of mice with 1% EGCG caused a significant decrease in the mean number of ACF per mouse, when compared with the model mice treated with

AOM/DSS ( $5.38 \pm 4.24$  vs  $13.13 \pm 3.02$ ,  $P < 0.01$ ). Compared with the positive control group, 1% EGCG treatment dependently decreased tumor load per mouse by 85% ( $33.96 \pm 6.10$  vs  $2.96 \pm 2.86$ , respectively,  $P < 0.01$ ). All revealed that EGCG could inhibit colon carcinogenesis by decreasing the number of precancerous lesions as well as solid tumors, with reduced tumor load and delayed histological progression of CRC. During the cancerization, the diversity of gut microbiota increased, potential carcinogenic bacteria such as *Bacteroides* were enriched, and the abundance of butyrate-producing bacteria (*Clostridiaceae*, *Ruminococcus*, etc.) decreased continuously. In contrast, the structure of gut microbiota was relatively stable during the intervention of EGCG on colon carcinogenesis. Enrichment of probiotics (*Bifidobacterium*, *Lactobacillus*, etc.) might be a potential mechanism for EGCG's effects on tumor suppression. Via bioinformatics analysis, principal coordinate analysis and cluster analysis of the tumor formation process, we found that the diversity of gut microbiota increased in the tumor model group while that in the EGCG interfered group (EG) remained relatively stable.

## CONCLUSION

Gut microbiota imbalance might be a potential mechanism for the prevention of malignant transformation by EGCG, which is significant for diagnosis, treatment, prognosis evaluation, and prevention of colorectal cancer.

**Key words:** Epigallocatechin gallate; Gut microbiota; Colorectal cancer; High throughput sequencing; Chemoprevention; Animal experiment

© The Author(s) 2017. Published by Baishideng Publishing Group Inc. All rights reserved.

**Core tip:** Our study revealed the protective effect of epigallocatechin gallate (EGCG) on colorectal carcinogenesis and structural changes of intestinal flora in an animal model of colorectal cancer. EGCG was detected for its roles through azoxymethane/dextran sulfate sodium induced tumor (aberrant crypt foci) formation. The microbial population was compared among groups at different developmental stages by pyrosequencing of V4 regions of 16S rRNA genes. Results suggested that intestinal flora imbalance might be a potential mechanism for the prevention of malignant transformation by the green tea extract EGCG, which is significant for the diagnosis, treatment, prognosis evaluation, and prevention of colorectal cancer.

Wang X, Ye T, Chen WJ, Lv Y, Hao Z, Chen J, Zhao JY, Wang HP, Cai YK. Structural shift of gut microbiota during chemopreventive effects of epigallocatechin gallate on colorectal carcinogenesis in mice. *World J Gastroenterol* 2017; 23(46): 8128-8139 Available from: URL: <http://www.wjgnet.com/1007-9327/full/v23/i46/8128.htm> DOI: <http://dx.doi.org/10.3748/wjg.v23.i46.8128>

## INTRODUCTION

There are approximately 1.2 million people diagnosed with colorectal cancer (colon cancer) every year, and it is the third most common cancer in the human population. There is a fairly high incidence of colon cancer in developed countries<sup>[1]</sup>. The human body contains about 1000 kinds of bacteria, approximately  $10^{14}$  in total, most of which are distributed in the large intestine. The total number of microbial genes is at least 150 times that of human genes<sup>[2]</sup>, and both together are termed the human metagenome. Now it is considered that the gut microbiota plays an important role in the construction of the biological barrier, which helps with nutrient absorption, energy metabolism, and immune regulation<sup>[3]</sup>. Meanwhile, more and more evidence indicates that imbalance of gut microbiota plays an important role in gastrointestinal, metabolic, liver, and autoimmune diseases<sup>[4-6]</sup>. Previous studies found that similar to some tumor related microorganisms (such as *Helicobacter pylori*, *human papilloma virus*, and *hepatitis B virus*, etc.), many bacteria (such as toxigenic fragile bacteroides, *Enterococcus faecalis*, and *Streptococcus spp.*) may be toxic enough to cause colorectal cancer<sup>[7]</sup>. In addition, based on the study of fecal bacterial culture in patient and control populations, it was found that there were differences between the two groups<sup>[8]</sup>. With the development of molecular biology techniques, especially the next generation high throughput sequencing, detection of the complex structure of gut microbiota becomes feasible. A large number of reports have confirmed the role of bacterial flora in the pathogenesis of colorectal cancer, outlining the structure of gut microbiota in patients with colorectal cancer<sup>[9-12]</sup>. Previous studies in our group also found that there was a reduction in the abundance of colonic mucosal flora in patients with colorectal cancer, and the increase of *Bacteroides* may be related to the occurrence of colorectal cancer<sup>[13]</sup>. The mechanisms by which bacteria cause colon cancer may include: inducing chronic inflammation of the intestine, producing carcinogenic metabolites, forming carcinogenic biofilms, etc<sup>[14]</sup>. Although the relationship between gut microbiota and the occurrence of colorectal cancer and its accurate mechanism remain unclear, it can be speculated that the regulation with gut microbiota as a target is a potential breakthrough point for the prevention and treatment of colorectal cancer<sup>[15]</sup>. Based on this theoretical basis, therapeutic means for the intervention of gut microbiota such as supplementation with probiotics and prebiotics, fecal bacteria transplantation, and even weight loss surgery have become research focuses<sup>[16-17]</sup>.

The biological availability of epigallocatechin gallate (EGCG) is low, and its elimination half-time in blood is only 2.0-3.5 h. Most EGCG is fermented by bacteria in the large intestine, and discharged with stool. The large intestine is the main metabolic site for EGCG and is also the most active portion of the body for the interaction with bacteria. Importantly, when compared to smaller bacteria density in the proximal



small intestine, the incidence of colorectal cancer is significantly higher<sup>[18]</sup>. Therefore, the interaction of EGCG with gut microbiota is very likely to affect the occurrence and development of colorectal cancer.

In this study, gut microbiota was considered a target for disease prevention and treatment, which will further broaden our understanding of the effects of drugs and diet on the body's health by regulating gut microbiota in humans and animals.

## MATERIALS AND METHODS

### *Animals, reagents, and diets*

Six-week-old female FVB/N mice (18–22 g) were purchased from Laboratory Animal Center of Shanghai East China Normal University (SCXK2011-0031) and were quarantined for 7 d before the experiment. All animals were housed in individual plastic cages (with 4 or 5 mice/cage) and maintained under controlled conditions of humidity (44% ± 5%), light (12 h light/dark cycles), and temperature (22 ± 2 °C). They had free access to drinking water and a pelleted basal diet. Azoxymethane (AOM, A5486-25 mg), a colonic carcinogen, EGCG (E4268-100MG), and dextran sodium sulfate (DSS, 42867-5G) for the induction of colitis were purchased from Sigma-Aldrich (St. Louis, MO, United States).

### *AOM/DSS-induced model of colitis*

All animal experiments were performed in compliance with the Institutional Animal Care and Use Committee of the East China Normal University. Forty-two female FVB/N mice were randomly divided into the following three groups (Figure 1): group 1 (10 mice, negative control) was treated with vehicle; group 2 (16 mice, positive control) was treated with AOM plus vehicle; group 3 (16 mice, EG) was treated with AOM plus EGCG. AOM (30 mg/kg, total dose) was administered intraperitoneally (IP), at single doses of 10 mg/kg body weight, on the first days of week 1, week 4, and week 7. One day after each injection, the mice received 2.5% (v/v) DSS in drinking water for 3 consecutive days. One percent (v/v) of EGCG was given by gavage in group 3 throughout the experiment.

### *Sample collection*

Half of all animals were sacrificed by asphyxiation with CO<sub>2</sub> 8 wk after the first AOM injection. A significant number of aberrant crypt foci (ACF) were observed at this time. The remaining animals were sacrificed at week 13 of the experiment. The gut tissue samples of all animals were collected for further investigation. Stool samples were collected at regular intervals and snap frozen in liquid nitrogen during the course of the study. The stool samples were then transferred to -80 °C until DNA extraction was performed.

### *ACF and tumor evaluation*

For ACF evaluation, the colons were rapidly took out

after sacrifice, rinsed with saline, opened longitudinally, laid flat on a polystyrene board, and fixed with 10% buffered formaldehyde solution before being stained with 0.2% methylene blue in saline. After measurement of the length (from the ileocecal junction to the anal verge), the colon specimens were cut into two parts: the distal part (5 cm from the anus) and the proximal part (the remainder of the colon). Specimens were examined using a light microscope at × 20 magnification. Only foci with four or more crypts were evaluated since they indicate early neoplastic occurrence. ACF were distinguished from their surrounding normal crypts by greater size, larger and elongated luminal opening, thicker lining, and compression of the surrounding epithelium. The total number of ACF throughout the colon was scored.

For tumor evaluation, the colon was macroscopically inspected and photographed, then the total number of tumors was enumerated and tumor size measured. Tumor load was the accumulation of diameter (average of three diameter measurements). For histological examination, colon tumors were separately excised and fixed in 10% neutral phosphate-buffered formalin.

### *Histological examination*

For histological examination, the fixed tissues were paraffin-embedded and sectioned at 5 mm thickness. Sections were H&E stained and then microscopically examined by two independent researchers in a blind fashion. Microscopic observations were graded according to the morphological criteria.

### *Gut microbe 16S rRNA sequencing*

Microbial genomic DNA was extracted from fecal and intestinal content samples using the TIANGEN DNA stool mini kit (TIANGEN, cat#DP328) following the manufacturer's guidelines. The V4 hypervariable regions of 16S rRNA were PCR-amplified with the barcoded fusion primers. The PCR condition was as follows: initial denaturation at 94 °C for 5 min; denaturation at 94 °C for 30 s, annealing at 50 °C for 30 s, and extension at 72 °C for 30 s, repeated for 25 cycles; and final extension at 72 °C for 7 min. PCR products were extracted using a QIAGEN quick Gel Extraction Kit (QIAGEN). Then a sequencing library for each sample was constructed with the Illumina TruSeq DNA Sample Preparation Kit. For each sample, Barcoded V4 PCR amplicons were sequenced with Illumina Miseq platform. 16S rRNA amplification and sequencing services were provided by Personal Biotechnology Co.Ltd. (Shanghai, China). Sequence reads were eliminated if they contained ambiguous bases, if average paired score was lower than 25, if homopolymer run exceeded 6, if there were mismatches in the primers, or if sequence length was shorter than 100 bp. Sequences that overlapped the region between R1 and R2, longer than 10 bp without any mismatches, were assembled according to their overlap sequence. This step was ensured to remove chimeras. The sequence

**Table 1 Comparison of mouse weight (13<sup>th</sup> week)**

Group	Treatment	<i>n</i>	Weight (g) (mean ± SD)
1	Control (BD)	5	32.60 ± 1.81
2	AOM/DSS (MO)	5	28.63 ± 1.60 <sup>1</sup>
3	AOM/DSS + 1% EGCG (EG)	8	30.95 ± 1.38 <sup>2,3</sup>

<sup>1</sup>Significantly different from group 1 ( $P = 0.006$ ); <sup>2</sup>No significant difference from group 1 ( $P = 0.088$ ); <sup>3</sup>No significant difference from group 2 ( $P = 0.18$ ). AOM: Azoxymethane. EGCG: Epigallocatechin gallate; DSS: Dextran sodium sulfate.

reads which could not be assembled were discarded. Barcode and sequencing primers were trimmed from sequence reads. Trimmed and assembled sequences were uploaded to QIIME for further analysis (This part of the study was assisted by Personal bioBiological Technology Company).

### Taxonomic classification and statistical analysis

Using the best hit classification option, the sequences from each sample were aligned to the RDP 16S rRNA training set to classify the taxonomic abundance in QIIME<sup>[19]</sup>. Delineation of operational taxonomic units (OTUs) was conducted with UCLUST function in QIIME at a 97% cutoff<sup>[20]</sup>. Richness estimators (Ace, chao) and diversity estimators (Shannon index) were calculated with mothur software package<sup>[21-23]</sup>. We also conducted the UniFrac distance metrics analysis using OTUs from each sample, and performed the principal co-ordinates analysis and NMDS results in terms of the matrix of distance (This part of the study was assisted by Personal bioBiological Technology Company).

### Other statistical analyses

Statistical analyses were performed using SPSS version 20.0 and Graph prism 5.0. Results are expressed as mean ± SE of the mean for normally distributed data. Inter-group comparisons for body weights were performed using one-way ANOVA with correction for multiple comparisons by Tukey's post hoc test;  $P < 0.05$  was considered statistically different. Inter-group comparisons of ACF counts and tumor measurements were assessed with the  $2 \times 2$  factorial designs;  $P < 0.05$  was regarded as statistically significant for each main effect and interaction.

## RESULTS

### General observations

As shown in Figure 2, all mice had a steady body weight gain and the administration of AOM/DSS and 1% EGCG did not affect the growth of the mice during the first eight weeks in all groups measured at different time points. Also, we observed a significant body weight loss or toxicity in mice administered AOM/DSS only; however, no significant body weight loss was observed in mice treated with 1% EGCG after AOM/DSS. Table 1 compares the differences in the mean

weights of the three groups at the time of sacrificing. In groups 1 and 2, all mice survived to the end of the experiment and two mice died in group 3, from asphyxia caused by gavage and intestinal obstruction. During the entire period of the experiment, there were no signs of toxicity or otherwise adverse conditions suggesting adverse effects caused by administration of EGCG.

### EGCG reduces experimental colitis and inhibits the formation of ACF

In the current study, we used the well-established protocol of the mouse colorectal carcinogenesis model system and chose ACF as the end point because it is considered to be pre-neoplastic lesions and is regarded as a useful biomarker. Half of mice in each group were harvested for ACF evaluation at 8 wk. Table 2 shows the length of the large intestine as well as the number of ACF in both distal (5 cm from the anus) and proximal (the remainder of the colon) parts among the three groups. Mice fed a basal diet ( $n = 5$ ) showed no evidence of ACF formation in the colonic mucosa. All AOM/DSS treated mice ( $n = 8$ ,  $r = 100\%$  incidence) developed ACF, whereas those treated with 1% EGCG ( $n = 8$ ,  $r = 75\%$  incidence) were found to have significantly fewer ACF. Almost all ACF were observed in the distal colon. In group 3, treatment of mice with 1% EGCG caused a significant decrease in the mean number of ACF per mouse, when compared with the model mice treated with AOM/DSS ( $5.38 \pm 4.24$  vs  $13.13 \pm 3.02$ ,  $P < 0.01$ ). These results indicate that 1% EGCG significantly inhibited ACF formation induced by AOM/DSS in FVB mice.

### EGCG attenuates AOM/DSS-induced colorectal carcinogenesis

Starting from 10 wk after treatment, mice in the model group showed apparent diarrhea and rectal bleeding. The presence and development of inflammation manifested clearly. In the EG group, suppression of experimental colitis by EGCG was not only evident during AOM/DSS treatment, but also obvious after the cessation of DSS administration (*i.e.*, week 10), suggesting that EGCG significantly promoted recovery from colitis. Unfortunately, a mouse treated by AOM/DSS died in the 12<sup>th</sup> week of colonic obstruction and cachexia. As a result, we decided to euthanize the remainder of mice in the 13<sup>th</sup> week in order to keep the mouse life cycle in concordance.

At necropsy, macroscopically, nodular, polypoid, or caterpillar-like tumors were observed in the entire colons of mice. Neither benign adenomas nor metastatic invasion of the colonic tumors to the liver, peritoneum, or regional lymph nodes were observed. Tumors mostly occurred in the distal colon. Figure 3C summarizes the total number of tumors per mouse and compares the mean number as well as tumor load between the MO and EG groups. Mice fed a basal diet showed no evidence of tumor formation at 13 wk. For AOM/DSS

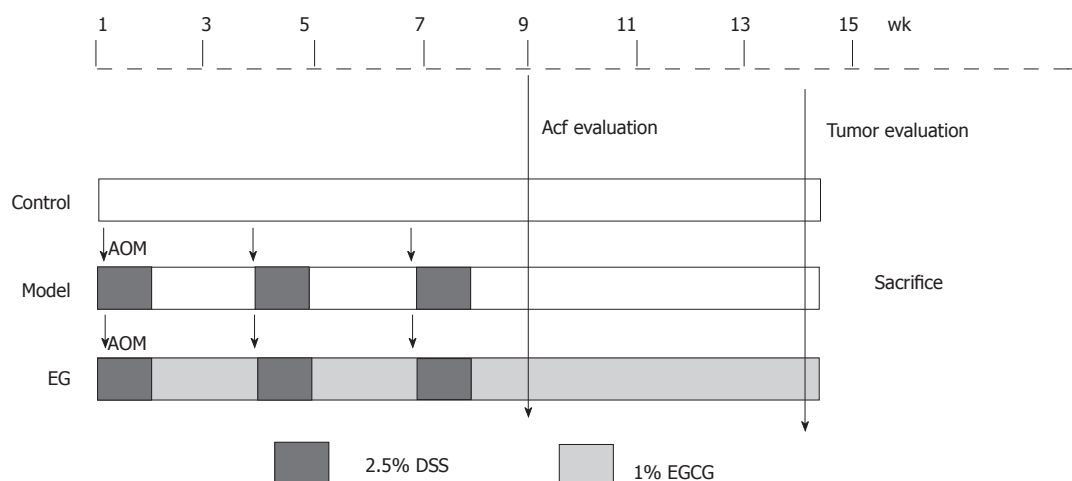


**Figure 1 Experimental protocol.** Experimental FVB/N mice were divided into three groups, i.e., control group, model group, and epigallocatechin gallate treatment group. Animals in the model and EG groups initially received a single intraperitoneal injection of azoxymethane (AOM: 10 mg/kg). After the AOM administration, mice in the model and EG groups received 2.5% dextran sodium sulfate (DSS) in drinking water for 3 consecutive days. Mice in the EG group also received oral 1% EGCG 20 mg/kg per day for 13 wk. AOM: Azoxymethane; EGCG: Epigallocatechin gallate.

**Table 2 Effects of epigallocatechin gallate on azoxymethane-induced aberrant crypt foci in FVB mice (8<sup>th</sup> week): distribution of aberrant crypt foci along the large bowel and comparison of aberrant crypt foci in different parts**

Group	Treatment	n	Length (cm)	Rate (%)	Number of ACF		
					Proximal	Distal	Entire
1	Control	5	9.73 ± 0.76	/	/	/	/
2	AOM/DSS (MO)	8	8.27 ± 0.37	100	1.13 ± 1.36	12.50 ± 3.67	13.13 ± 3.02
3	AOM/DSS + 1% EGCG	8	8.68 ± 0.47 <sup>1</sup>	75	0.63 ± 0.87	4.75 ± 3.70 <sup>2</sup>	5.38 ± 4.24 <sup>2</sup>

<sup>1</sup>Different from group 2 ( $P < 0.05$ ); <sup>2</sup>Significantly different from group 2 ( $P < 0.01$ ). AOM: Azoxymethane; DSS: Dextran sodium sulfate; EGCG: Epigallocatechin gallate; ACF: Aberrant crypt foci.

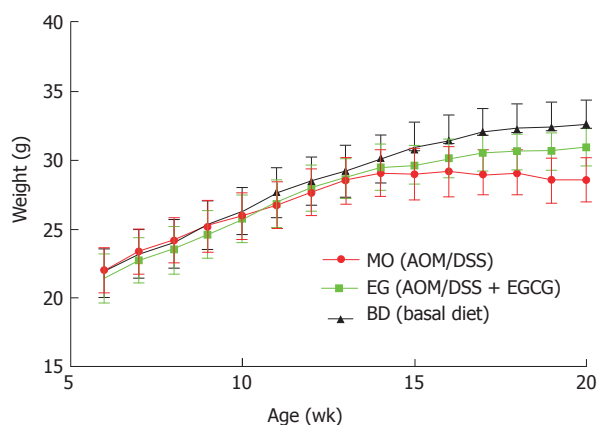


**Figure 2 Body weight gain of azoxymethane/dextran sulfate sodium-treated female FVB/N mice.**

treated mice, colonic adenocarcinomas developed in all mice (5/5, 100%) 13 wk after the first injection of AOM, while the incidence in group 3 was 62.5% (5/8). The number of malignant colonic tumors per mice was  $8.2 \pm 2.2$  and  $1.4 \pm 1.3$  for the AOM/DSS and EGCG treatment groups, respectively ( $P < 0.01$ ). In addition, compared with the positive control group, 1% EGCG treatment decreased tumor load per mouse by 85% ( $33.96 \pm 6.10$  vs  $2.96 \pm 2.86$ , respectively,

$P < 0.01$ ) as showed in Figure 3C. Likewise, Figure 3D is a representative macroscopic morphologic depiction of the distal colon for the model and EG groups. Obvious tumorigenesis was observed in the model group. However, in the EGCG treatment group, the tumor number and size were significantly fewer and relatively small, respectively. This result suggests that the inhibition of colorectal tumor development by EGCG was due to not only a reduction in the number of but also the size of tumors. Figure 3 (A and B) shows representative H&E staining of histological sections of the three groups. In colonic tissue from the model animals, multifocal adenomatous lesions were observed without invasion into the submucosa; there was mild inflammation with cryptitis, and mild degree of loss of goblet cells, fibrosis, and apoptotic changes. For the EGCG treatment group, the mucosa revealed tightly packed glands with a normal number of goblet cells while crypt architecture remained normal. Compared to the model, the histological sections of the EGCG treatment group are more similar to those of the control group.

#### Characteristics of V4 pyrosequencing

Table 3 shows the range of valid and trimmed sequences of different groups of mice. In this study,



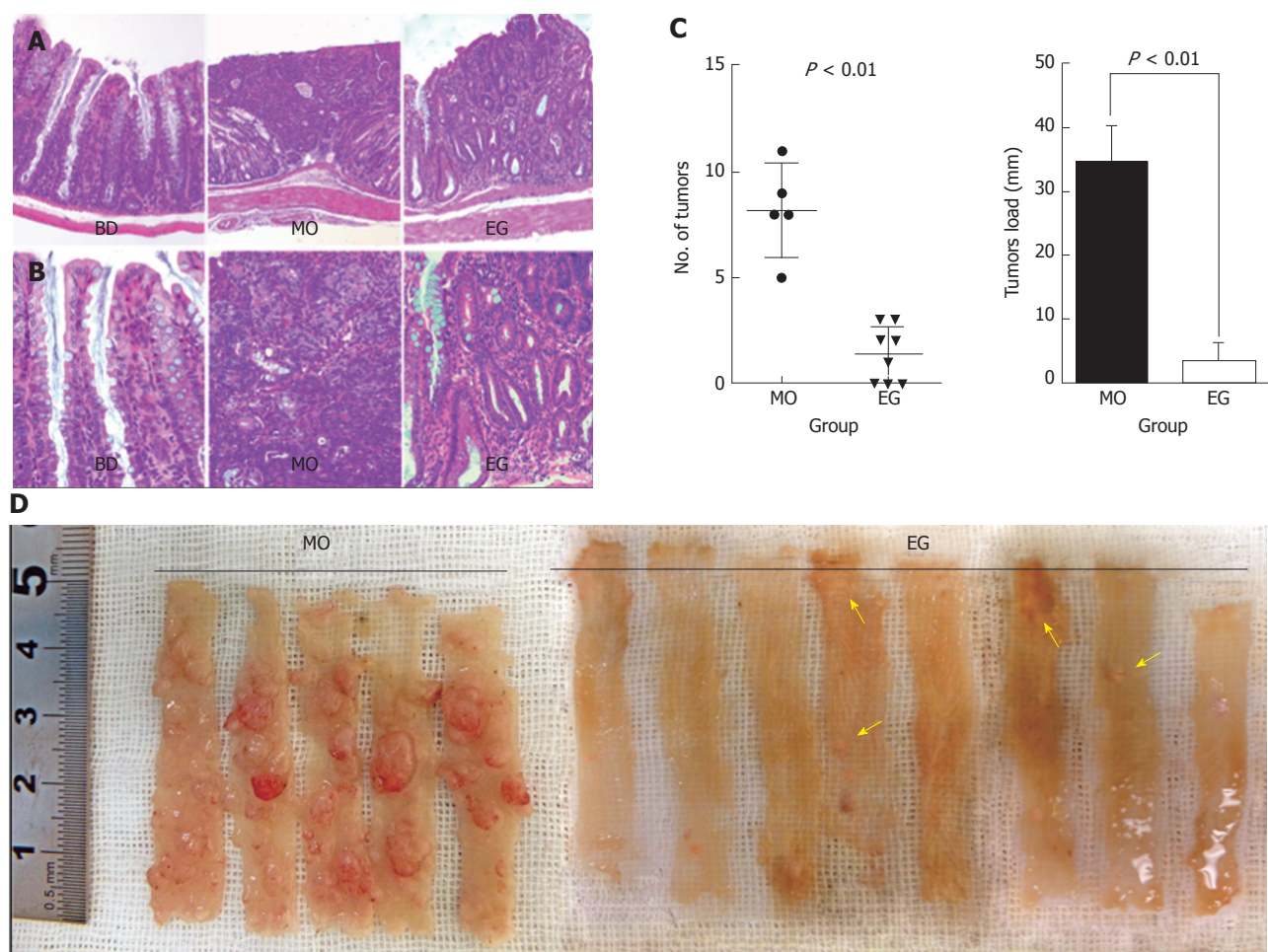


**Figure 3** Chemo-preventive effect of epigallocatechin gallate on colorectal carcinogenesis in azoxymethane/dextran sulfate sodium-treated mice. A and B: Representative hematoxylin and eosin stained histological sections of the control, model, and EG groups. A:  $\times 10$ ; B:  $\times 40$ ; C: Number of colon tumors and tumor load were reduced very significantly in the epigallocatechin gallate (EGCG) group compared to the model group ( $P < 0.01$  and  $P < 0.001$ , respectively); D: Representative macroscopic morphology of colon tumors in the model and EG groups. Arrows indicate the azoxymethane/dextran sodium sulfate-induced tumors.

**Table 3** Statistics of valid sequences and trimmed sequences in different group

Group	Valid sequences (mean)	Trimmed sequences (mean)
BD Group	75116-49662 (615022)	65936-45406 (54162)
MO Group	82804-25360 (56551)	73924-22895 (50842)
EG Group	79506-40705 (65124)	74876-36795 (59693)

OTUs were defined as sharing 97% sequence identity using furthest neighbor method (<http://www.mothur.org/wiki/Cluster>). The total number of OTUs at 97% similarity level was 41923, with an average of 2096 OTUs per sample. The value of Good's coverage for each group was over 93%, indicating that the 16S rRNA sequences identified in the groups represent the majority of bacteria present in the study samples.

Whereas we did not observe the plateau of the refraction curve with the current sequencing, the Shannon diversity estimates of all samples had already reached stable values at this sequencing depth, which suggests that, although identification of

new phylotypes would be expected from additional sequencing, the range of diversity within the samples had been captured.

As Figure 4 shows, we examined the estimators of community richness (Chao and Ace indexes) and diversity and evenness (Shannon and Simpson indexes) in MO and EG samples during the 8<sup>th</sup> week. Statistically significant differences were seen in the Shannon and Simpson indexes between the MO group and control group (4.10 vs 3.23,  $P = 0.022$ ), while no significance was seen between the EG group and control group (2.81 vs 3.23,  $P = 0.230$ ) (Figure 4A). The Simpson indexes between the MO and control groups (0.04 vs 0.10,  $P = 0.022$ ) had no significant differences, while significant differences were seen between the MO and EG groups (0.04 vs 0.17,  $P = 0.009$ ) (Figure 4B).

During the 11<sup>st</sup> week (T2), the Shannon index in the MO group became higher than that in the BD group (3.88 vs 3.23,  $P = 0.003$ ), but no significant difference between the BD and EG groups was noted (3.23 vs 3.94,  $P = 0.058$ , Figure 4C). The same result



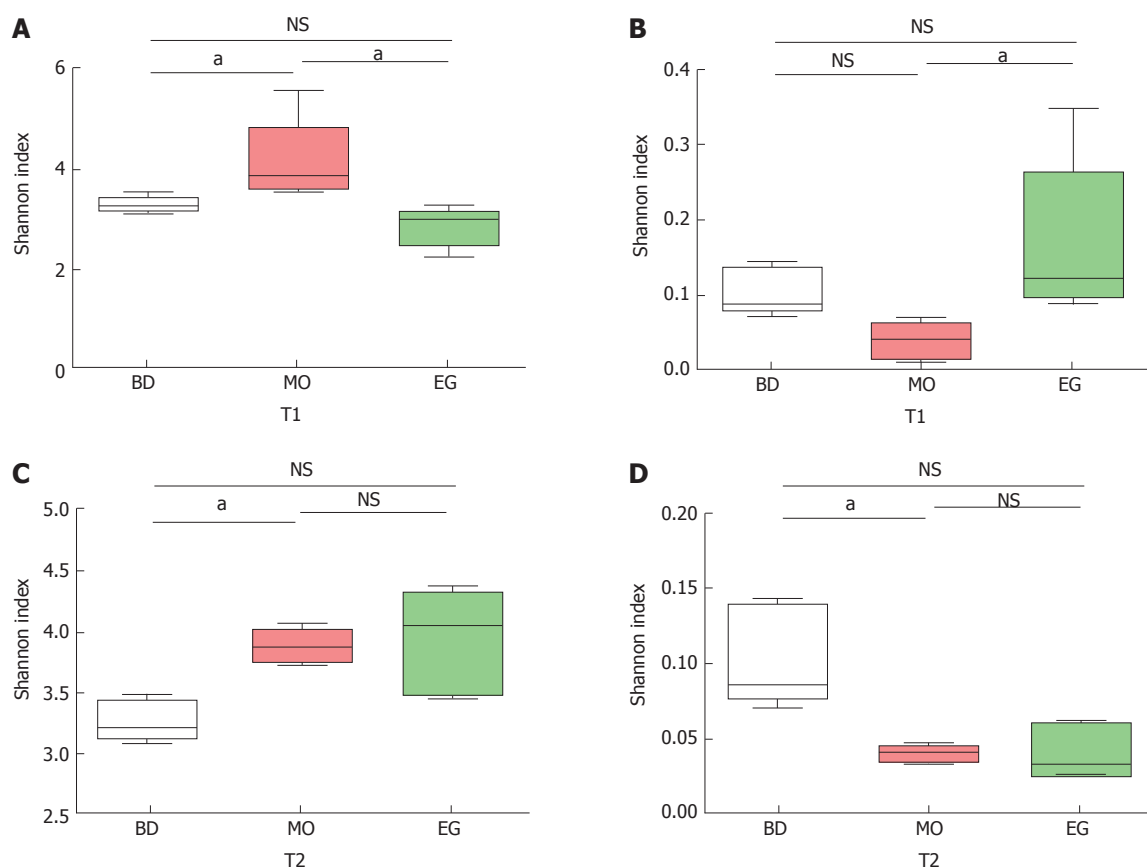


Figure 4 Comparative analysis of alpha diversity at T1 and T2 at the 8<sup>th</sup> and 13<sup>th</sup> week. <sup>a</sup> $P < 0.05$ .

can be noted for Simpson index (Figure 4D).

#### Potentially cancer-causing bacteria and probiotics

In this study, 339 genera were annotated; we only compared the abundant differences of 16 species among groups. As Figure 5 shows at the 8th week, the abundance of *Bacteroides* as well as *Anaerotruncus* in the MO group was significantly higher than that in the BD group and EG group, but *Clostridiaceae* which can produce butyrate, and *Ruminococcus* in the MO group were significantly reduced. Butyrate is recognized to alleviate intestinal inflammation. The enrichment of *Fusobacterium* was previously reported in colorectal cancer tissue but was not reproduced in our study. As the recognized probiotics, *Bifidobacterium* and *Lactobacillus* were increased in the EG group.

The abundance of other important butyrate-producing strains such as *Lachnospiraceae* and *Faecalibacterium* were not significantly decreased in the MO group. In addition, we found that *Ochrobactrum*, *Veillonella*, and *Desulfococcus* had significantly lower abundance in the MO group. In addition, common intestinal opportunistic pathogens, such as *Enterobacteriaceae*, *Streptococcus*, and *Prevotella*, were not found to be enriched in the MO group.

Specifically, at week 11, the abundance of *Lactobacilli* in the EG group was significantly higher than that in the BD group and the MO group ( $P^1 = 0.028$ ,

$P^2 = 0.049$ ). The difference of *Bifidobacterium* was not significant among the three groups (Figure 6).

## DISCUSSION

Sporadic reports suggested that EGCG may inhibit proliferation of intestinal pathogenic bacteria (such as *Clostridium perfringens*, *Clostridium difficile*, and *Bacteroides*) *in vitro*, but EGCG is less inhibitory to or even stimulatory to probiotic bacteria (such as *Bacillus bifidus* and *Lactobacillus*). Animal and human experiments also confirmed that EGCG may affect the growth and floral structure of specific intestinal specific bacteria, and participates in the regulation of the body's energy metabolism<sup>[24,25]</sup>. The role of gut microbiota as an intermediate link for EGCG's impact on colorectal cancer occurrence and development is still unclear.

EGCG acts as a means of chemical prevention of colorectal cancer, and gut microbiota is very likely to be one of its targets. Its impact on overall floral structure or specific bacteria may be related to the inhibition of colorectal cancer.

In this study, we used a mouse model of colorectal cancer (chemically induced) and intragastrically administered the mice with EGCG to inhibit colorectal cancer. At the same time, to further explore the mechanism of EGCG in the prevention of colorectal

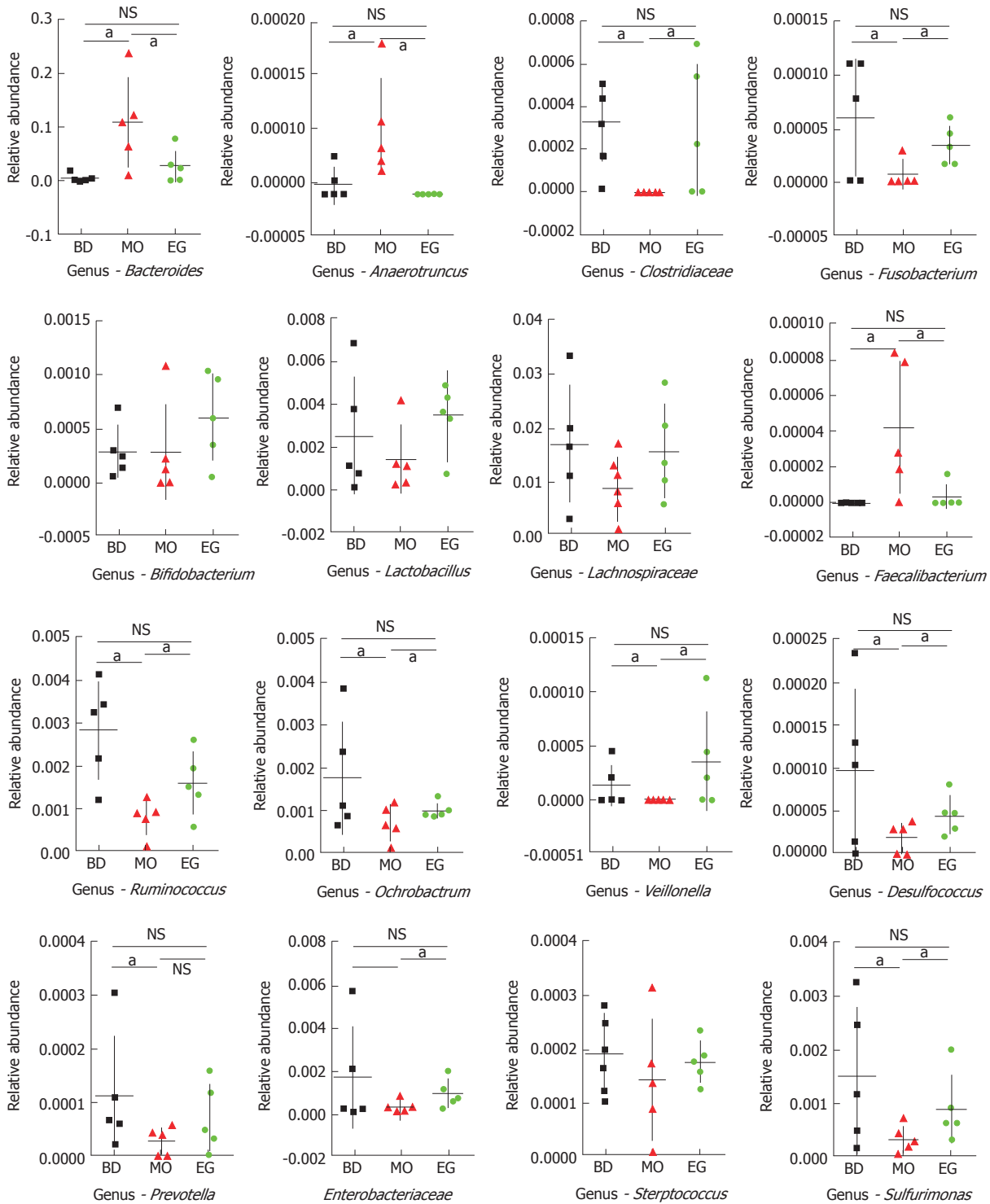


Figure 5 Statistical analysis for 16 genera (families) at T1 ( $P < 0.05$ , NS means no significant differences).

cancer, we collected the fresh feces of mice during the interference of tumor formation. *Via* bacterial 16S cDNA high throughput sequencing in combination with bioinformatics, we analyzed changes in the structure of gut microbiota in mice, and flora differences among the groups, to uncover the role of bacterial flora in the EGCG-mediated inhibition of carcinogenesis.

The development of colorectal cancer is generally known to take at least 3 years (progressing from

normal mucosa, to adenoma, and finally to adenocarcinoma) and to include three phases, *i.e.*, initial mutation, cancer promotion, and progression. The main purpose for the study of chemical prevention is preventive treatment of disease. ACF are a commonly acknowledged precancerous lesion of humans and rodents and is convenient for *in vitro* recognition after methylene blue staining. ACF often show proliferative lesions with poor differentiation, and enhanced gland

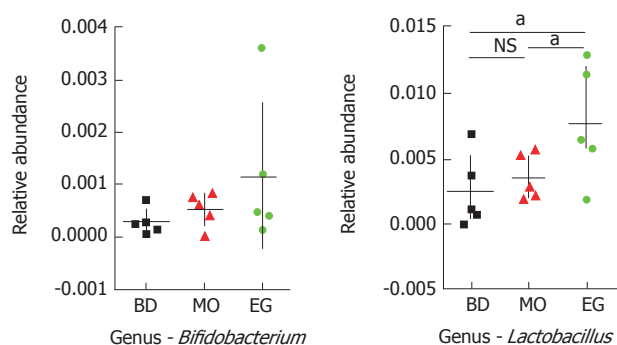


Figure 6 Statistical analysis for *Lactobacilli* and *Bifidobacterium* (family) at T2 (\* $P < 0.05$ , NS means no significant differences).

cell division and proliferation. At the molecular level, mutations of the *APC* and *ras* genes are common. At the end of the eighth week in this experiment, the results showed that EGCG could effectively reduce the number of precancerous lesions of colorectal cancer. ACF in the distal intestine of the interfering group were reduced by 59%, indicating that EGCG may play a preventive role in the early stages (mutation and cancer promoting stages) of colorectal cancer. In the past, Xiao *et al.*<sup>[26]</sup> interfered the AOM induced tumor formation process in rats with a high fat diet *via* green tea polyphenols (65% of the components were EGCG). That study also showed reduced ACF numbers, in particular the larger highly atypical hyperplastic ACF types. Similar results were confirmed in mice<sup>[27]</sup>. To determine the effect of EGCG on colorectal cancer formation, in another study, tumor formation in *APC*<sup>min/+</sup> was interfered by 0.08% and 0.16% of EGCG. Tumor numbers were decreased by 37% and 47%, respectively. In our study, however, at the end of the 13<sup>th</sup> week after intervention, tumor number in the interfered group was reduced by 82.9% as compared to the control group, and tumor load was reduced by 91.3%, both indicating that the inhibitory effect of EGCG on tumor formation was more obvious than in the past. The possible reason is that the concentration of EGCG in our study was 1%, much higher than those used in previous studies. On the other hand, this also suggested that EGCG plays a preventive role in colorectal cancer occurrence in a dose-dependent manner.

We conducted further studies to uncover the effect of green tea extract EGCG on the gut microbiota of mice, using macro-genomics in combination with bioinformatics analysis. Considering the complexity of gut microbiota, this study was designed with the following research objectives in mind: (1) to preliminarily understand the compositions of the gut microbiota in mice at the 8<sup>th</sup> week (precancerous stage) and the 11<sup>th</sup> week (progressive stage) of colorectal cancer; (2) to preliminarily understand the change in gut microbiota during the process of colorectal cancer progression in mice as compared to healthy mice, and to clarify the effects of EGCG intervention on this change; and (3)

through statistical analysis and bioinformatics, to try to find specific bacteria that can distinguish the structure of each group of bacteria, *i.e.*, the specific bacterial target of EGCG intervention.

With the aid of the 454 sequencing platform for the detection of 16S rDNA V3 region or V3/V4 region<sup>[10]</sup>, we analyzed the structure of gut microbiota in mice by amplification of the V4 region in this study, which was good for identification. The sequencing results were under strict quality control. The distribution map, dilution curve, and abundance curve of the sequences acquired all confirmed that the sequencing results could well reflect the structure of the gut microbiota in mice.

It is worthwhile to note that in 2011, Kostic *et al.*<sup>[11]</sup>, Castellarin *et al.*<sup>[12]</sup>, and Marchesi *et al.*<sup>[28]</sup> simultaneously found that there were gut microbiota disorders at varying degrees in colorectal cancer patients, using sequencing techniques, and the *Fusobacterium* was enriched in cancer tissues as compared to the healthy tissues. Meanwhile, it was also found that the abundance of *Fusobacterium* was directly proportional to the rate of lymph node metastasis. It is noticeable from the above reports that despite the increasing concern about the relationship between colorectal cancer and bacteria and that exciting results were obtained by relevant studies, the studies focused mainly on the structure of gut microbiota or specific bacteria during colorectal cancer progression (especially during the middle and late stages), which was only a snapshot of the big picture. Little is known about the dynamic changes of the gut microbiota in the process of tumor formation, especially for the status of gut microbiota during the early stage of disease progression, which indeed is a key time point for chemical prevention.

At the same time, it will be informative for the elucidation of flora changes as a direct cause of colorectal cancer formation, or flora changes as a direct result of colorectal cancer occurrence and/or progression. In this study, we examined and compared the composition of gut microbiota in mice with precancerous lesions and in mice during tumor progression. This was helpful for further understanding the roles of different species of bacteria in carcinogenesis, cancer promotion, and tumor suppression, and therefore the potential EGCG target bacteria could be explored. In fact, during the precancerous stage, there were anomalies seen in gut microbiota structures in the mice of the MO group, mainly manifesting as enrichment of *Bacteroides* and *Anaerotruncus* and reduced abundance of *Clostridiaceae*, *Ruminococcus*, *Ochrobactrum*, *Veillonella alcalescens*, *Desulfococcus*, *etc.* The enrichment of *Bacteroides* in the MO group was consistent with our previous study on mucosal flora in patients with colorectal cancer<sup>[15]</sup>. The relationship between *Anaerotruncus* and colon cancer occurrence is still unclear. Previous studies have suggested that *Bacteroides* and its lower species could promote the occurrence and development of colorectal cancer by inducing chronic inflammation,

producing tumor-promoting metabolites, or changing the expression of host mucosal glycosylation. Among them, toxigenic fragile bacteroides is representative and was considered a pathogenic bacterium of colorectal cancer, initially because it was found to be able to produce the toxins of toxigenic fragile bacteroides (bacteroides fragilis toxin, BFT). BFT can rapidly change the structure and function of intestinal mucosal epithelial cells (decomposition of tumor suppression protein and E-cadherin), enhancing the intranuclear expression of Wnt/B adhesion protein signaling pathway, and therefore inducing continuous proliferation of colon adenocarcinoma cells and the expression of oncogene MYC. Besides, BFT may induce inflammatory responses by inducing expression of cytokines in intestinal mucosal epithelia cells through the NF- $\kappa$ B signaling pathway. Notably, increased expression of NF- $\kappa$ B signaling pathway could also promote the carcinogenesis of mucosal epithelium. In animal experiments, continuous colonization of toxigenic fragile bacteroides into APC<sup>min/+</sup> mice could greatly promote the incidence of adenomas<sup>[29]</sup>. Sears *et al.*<sup>[30]</sup> suggested that this type of bacterium might induce mucosal immune defense changes to promote tumor development through direct secretion of endotoxin or indirect changes of gut microbiota, and might supplant probiotics to further expand inflammatory responses, promoting occurrence of multiple pathogenic bacteria and ultimately promoting tumor progression.

Furthermore, it was found in this study that in the precancerous stage, the *Clostridiaceae* and bacteria of the *Ruminococcus* maintained their low abundances in the tumor model group, but not in the intervention group. The *Clostridiaceae* includes multiple important butyrate producing bacteria, such as *Eubacterium rectale* and *Roseburia intestinalis*. This type of bacterium was reported to be reduced in the intestinal tract of patients with colorectal cancer, obese patients, and patients with a high fat diet. Similarly, *Ruminococcus* is also butyrate producing bacteria, and they can effectively decompose and ferment the cellulose and polysaccharide in foods into short chain fatty acids, such as butyrate. Butyrate in the intestinal tract may provide the intestinal mucosa with energy, promoting sodium and potassium absorption. More importantly, it can reduce intestinal inflammation, protect the intestinal mucosal barrier, and even inhibit the growth of colon cancer cells<sup>[31,32]</sup>. A study by Jahns *et al.*<sup>[33]</sup> on human colorectal cancer tissues showed that butyrate could inhibit COX2 gene expression in nodal tissues and the activities of related proteins; *in vitro* studies also found that butyrate might activate caspase 3 and caspase 9 to induce apoptosis of colorectal cancer cells, upregulate pro-apoptotic gene BAK expression, and activate mitochondrial pathways to induce cell apoptosis and the like.

The gut microbiota of mice in the same tumor model group was different. The structure of the gut microbiota

of mice interfered with green tea extract EGCG basically remained relatively stable, and bioinformatics analysis showed that the structure of the flora in these mice was similar to that of healthy mice, with no obvious fluctuations in the number of bacteria. Instead, probiotics such as *Lactobacillus* and *Bifidobacterium* were increased in the EG group, and the relative abundance of the former was significantly increased after long-term EGCG intervention. Probiotics are defined by WHO/FAO as "live bacteria that can promote body health if taken in a proper amount". In recent years, some studies have showed that probiotics may have certain antagonistic effects on tumors. For example, *Lactobacillus* may significantly reduce the incidence of mouse sarcoma, colorectal cancer, and bladder cancer. Its main mechanisms may include optimization of the combined gut microbiota to inhibit the growth of carcinogenic bacteria; production of anti-tumor active substances; and stimulation and enhancement of the host immune system to prevent chronic inflammation.

It could be inferred accordingly that EGCG plays a role in cancer inhibition by maintaining the stability of gut microbiota, inhibiting the proliferation of potential pathogenic bacteria, and promoting the enrichment of probiotics. However, gut microbiota is influenced by many factors, such as diet and region, for its role in health promotion. Further study is certainly required to uncover the causal relationship(s) between gut microbiota and colorectal cancer, the interaction between bacteria and the host, as well as the interaction between EGCG and bacteria.

## COMMENTS

### Background

Studies have shown that gut microbiota plays a certain role in the occurrence and development of cancer. Inhibition of colorectal carcinogenesis by green tea, especially epigallocatechin gallate (EGCG), has been extensively investigated, but studies on microbial flora are much fewer. The interaction of EGCG with gut microbiota is very likely to affect the occurrence and development of colorectal cancer and the research of EGCG is needed. To further confirm the protective effect of EGCG on colorectal carcinogenesis and observe structural changes of gut microbiota involved during this process, an animal model of colorectal cancer was established.

### Research frontiers

A large number of reports have confirmed the role of bacterial flora in the pathogenesis of colorectal cancer, outlining the structure of gut microbiota in patients with colorectal cancer. Previous studies found that there was a reduction in the abundance of colonic mucosal flora in patients with colorectal cancer, and the increase of *Bacteroides* may be related to the occurrence of colorectal cancer. The biological availability of EGCG in the current study is low. Most EGCG is fermented by bacteria in the large intestine, and discharged with stool. The large intestine is the main metabolic site for EGCG and is also the most active portion of the body for the interaction with bacteria.

### Innovations and breakthroughs

The authors used a mouse model of colorectal cancer and intragastrically administered the mice with EGCG to inhibit colorectal cancer. Via bacterial 16s cDNA high throughput sequencing in combination with bioinformatics, we analyzed changes in the structure of gut microbiota of mice, and flora



differences among the groups, to uncover the role of bacterial flora in the EGCG-mediated inhibition of carcinogenesis. We conducted further studies to uncover the effect of green tea extract EGCG on the gut microbiota of mice, using macro-genomics in combination with bioinformatics analysis.

## Applications

EGCG plays a role in cancer inhibition by maintaining the stability of gut microbiota, inhibiting the proliferation of potential pathogenic bacteria, and promoting the enrichment of probiotics. Gut microbiota imbalance might be a potential mechanism for the prevention of malignant transformation by the green tea extract EGCG, which is significant for the diagnosis, treatment, prognosis evaluation, and prevention of colorectal cancer.

## Terminology

EGCG is extracted from the green tea. Most EGCG is fermented by bacteria in the large intestine, and discharged with stool. The large intestine is the main metabolic site for EGCG and is also the most active portion of the body for the interaction with bacteria.

## Peer-review

In general, this manuscript provides the useful information about the relationship between epigallocatechin gallate and colorectal cancer. However, there are also some problems and flaws in presentation. Authors did not describe the mechanism of how EGCG suppressed colorectal cancer. In Discussion part, there is little consideration on the obtained data in this experiment, and authors should increase the consideration of the obtained data in this experiment.

## ACKNOWLEDGMENTS

The authors would like to thank Personal bioBiological Technology Company (Shanghai, China) for the contributions to this research as well as Dr. Ma Xueyun from the East China Normal University for technical support of animal experiments.

## REFERENCES

- Brenner H, Kloor M, Pox CP. Colorectal cancer. *Lancet* 2014; **383**: 1490-1502 [PMID: 24225001 DOI: 10.1016/S0140-6736(13)61649-9]
- Qin J, Li R, Raes J, Arumugam M, Burgdorf KS, Manichanh C, Nielsen T, Pons N, Levenez F, Yamada T, Mende DR, Li J, Xu J, Li S, Li D, Cao J, Wang B, Liang H, Zheng H, Xie Y, Tap J, Lepage P, Bertalan M, Batto JM, Hansen T, Le Paslier D, Linneberg A, Nielsen HB, Pelletier E, Renault P, Sicheritz-Ponten T, Turner K, Zhu H, Yu C, Li S, Jian M, Zhou Y, Li Y, Zhang X, Li S, Qin N, Yang H, Wang J, Brunak S, Doré J, Guarner F, Kristiansen K, Pedersen O, Parkhill J, Weissenbach J; MetaHIT Consortium, Bork P, Ehrlich SD, Wang J. A human gut microbial gene catalogue established by metagenomic sequencing. *Nature* 2010; **464**: 59-65 [PMID: 20203603 DOI: 10.1038/nature08821]
- Tremaroli V, Bäckhed F. Functional interactions between the gut microbiota and host metabolism. *Nature* 2012; **489**: 242-249 [PMID: 22972297 DOI: 10.1038/nature11552]
- Qin N, Yang F, Li A, Prifti E, Chen Y, Shao L, Guo J, Le Chatelier E, Yao J, Wu L, Zhou J, Ni S, Liu L, Pons N, Batto JM, Kennedy SP, Leonard P, Yuan C, Ding W, Chen Y, Hu X, Zheng B, Qian G, Xu W, Ehrlich SD, Zheng S, Li L. Alterations of the human gut microbiome in liver cirrhosis. *Nature* 2014; **513**: 59-64 [PMID: 25079328 DOI: 10.1038/nature13568]
- Shen J, Obin MS, Zhao L. The gut microbiota, obesity and insulin resistance. *Mol Aspects Med* 2013; **34**: 39-58 [PMID: 23159341 DOI: 10.1016/j.mam.2012.11.001]
- Wang M, Karlsson C, Olsson C, Adlerberth I, Wold AE, Strachan DP, Martricardi PM, Aberg N, Perkin MR, Tripodi S, Coates AR, Hesselmar B, Saalman R, Molin G, Ahrné S. Reduced diversity in the early fecal microbiota of infants with atopic eczema. *J Allergy Clin Immunol* 2008; **121**: 129-134 [PMID: 18028995 DOI: 10.1016/j.jaci.2007.09.011]
- Sears CL, Garrett WS. Microbes, microbiota, and colon cancer. *Cell Host Microbe* 2014; **15**: 317-328 [PMID: 24629338 DOI: 10.1016/j.chom.2014.02.007]
- O'Keefe SJ, Chung D, Mahmoud N, Sepulveda AR, Manafe M, Arch J, Adada H, van der Merwe T. Why do African Americans get more colon cancer than Native Africans? *J Nutr* 2007; **137**: 175S-182S [PMID: 17182822]
- Ahn J, Sinha R, Pei Z, Dominianni C, Wu J, Shi J, Goedert JJ, Hayes RB, Yang L. Human gut microbiome and risk for colorectal cancer. *J Natl Cancer Inst* 2013; **105**: 1907-1911 [PMID: 24316595 DOI: 10.1093/jnci/djt300]
- Wang T, Cai G, Qiu Y, Fei N, Zhang M, Pang X, Jia W, Cai S, Zhao L. Structural segregation of gut microbiota between colorectal cancer patients and healthy volunteers. *ISME J* 2012; **6**: 320-329 [PMID: 21850056 DOI: 10.1038/ismej.2011.109]
- Kostic AD, Gevers D, Pedamallu CS, Michaud M, Duke F, Earl AM, Ojesina AI, Jung J, Bass AJ, Taberner J, Baselga J, Liu C, Shivdasani RA, Ogino S, Birren BW, Huttenhower C, Garrett WS, Meyerson M. Genomic analysis identifies association of *Fusobacterium* with colorectal carcinoma. *Genome Res* 2012; **22**: 292-298 [PMID: 22009990 DOI: 10.1101/gr.126573.111]
- Castellarin M, Warren RL, Freeman JD, Dreolini L, Krzywinski M, Strauss J, Barnes R, Watson P, Allen-Vercos E, Moore RA, Holt RA. *Fusobacterium nucleatum* infection is prevalent in human colorectal carcinoma. *Genome Res* 2012; **22**: 299-306 [PMID: 22009989 DOI: 10.1101/gr.126516.111]
- Huipeng W, Lifeng G, Chuang G, Jiaying Z, Yuankun C. The differences in colonic mucosal microbiota between normal individual and colon cancer patients by polymerase chain reaction-denaturing gradient gel electrophoresis. *J Clin Gastroenterol* 2014; **48**: 138-144 [PMID: 24162169 DOI: 10.1097/MCG.0b013e3182a26719]
- Dejea CM, Wick EC, Hechenbleikner EM, White JR, Mark Welch JL, Rossetti BJ, Peterson SN, Snesrud EC, Borisy GG, Lazarev M, Stein E, Vadivelu J, Roslani AC, Malik AA, Wanyiri JW, Goh KL, Thevambiga I, Fu K, Wan F, Llosa N, Housseau F, Romans K, Wu X, McAllister FM, Wu S, Vogelstein B, Kinzler KW, Pardoll DM, Sears CL. Microbiota organization is a distinct feature of proximal colorectal cancers. *Proc Natl Acad Sci USA* 2014; **111**: 18321-18326 [PMID: 25489084 DOI: 10.1073/pnas.1406199111]
- Jia W, Li H, Zhao L, Nicholson JK. Gut microbiota: a potential new territory for drug targeting. *Nat Rev Drug Discov* 2008; **7**: 123-129 [PMID: 18239669 DOI: 10.1038/nrd2505]
- Liou AP, Paziuk M, Luevano JM Jr, Machineni S, Turnbaugh PJ, Kaplan LM. Conserved shifts in the gut microbiota due to gastric bypass reduce host weight and adiposity. *Sci Transl Med* 2013; **5**: 178ra41 [PMID: 23536013 DOI: 10.1126/scitranslmed.3005687]
- Borody TJ, Brandt LJ, Paramsothy S. Therapeutic faecal microbiota transplantation: current status and future developments. *Curr Opin Gastroenterol* 2014; **30**: 97-105 [PMID: 24257037 DOI: 10.1097/MOG.0000000000000027]
- Proctor LM. The Human Microbiome Project in 2011 and beyond. *Cell Host Microbe* 2011; **10**: 287-291 [PMID: 22018227 DOI: 10.1016/j.chom.2011.10.001]
- Caporaso JG, Kuczynski J, Stombaugh J, Bittinger K, Bushman FD, Costello EK, Fierer N, Peña AG, Goodrich JK, Gordon JI, Huttley GA, Kelley ST, Knights D, Koenig JE, Ley RE, Lozupone CA, McDonald D, Muegge BD, Pirrung M, Reeder J, Sevinsky JR, Turnbaugh PJ, Walters WA, Widmann J, Yatsunenko T, Zaneveld J, Knight R. QIIME allows analysis of high-throughput community sequencing data. *Nat Methods* 2010; **7**: 335-336 [PMID: 20383131 DOI: 10.1038/nmeth.f.303]
- Edgar RC, Haas BJ, Clemente JC, Quince C, Knight R. UCHIME improves sensitivity and speed of chimera detection. *Bioinformatics* 2011; **27**: 2194-2200 [PMID: 21700674 DOI: 10.1093/bioinformatics/btr381]
- Pitta DW, Pinchak E, Dowd SE, Osterstock J, Gontcharova V, Youn E, Dorton K, Yoon I, Min BR, Fulford JD, Wickersham TA,

- Malinowski DP. Rumen bacterial diversity dynamics associated with changing from bermudagrass hay to grazed winter wheat diets. *Microb Ecol* 2010; **59**: 511-522 [PMID: 20037795 DOI: 10.1007/s00248-009-9609-6]
- 22 **Shannon CE**. The mathematical theory of communication. 1963. *MD Comput* 1997; **14**: 306-317 [PMID: 9230594]
- 23 **Mahaffee WF**, Klopper JW. Temporal Changes in the Bacterial Communities of Soil, Rhizosphere, and Endorhiza Associated with Field-Grown Cucumber (*Cucumis sativus* L.) *Microb Ecol* 1997; **34**: 210-223 [PMID: 9337416 DOI: 10.1007/s002489900050]
- 24 **Unno T**, Sakuma M, Mitsuhashi S. Effect of dietary supplementation of (-)-epigallocatechin gallate on gut microbiota and biomarkers of colonic fermentation in rats. *J Nutr Sci Vitaminol* (Tokyo) 2014; **60**: 213-219 [PMID: 25078378 DOI: 10.3177/jnsv.60.213]
- 25 **Axling U**, Olsson C, Xu J, Fernandez C, Larsson S, Ström K, Ahrné S, Holm C, Molin G, Berger K. Green tea powder and *Lactobacillus plantarum* affect gut microbiota, lipid metabolism and inflammation in high-fat fed C57BL/6J mice. *Nutr Metab* (Lond) 2012; **9**: 105 [PMID: 23181558 DOI: 10.1186/1743-7075-9-105]
- 26 **Xiao H**, Hao X, Simi B, Ju J, Jiang H, Reddy BS, Yang CS. Green tea polyphenols inhibit colorectal aberrant crypt foci (ACF) formation and prevent oncogenic changes in dysplastic ACF in azoxymethane-treated F344 rats. *Carcinogenesis* 2008; **29**: 113-119 [PMID: 17893236 DOI: 10.1093/carcin/bgm204]
- 27 **Shimizu M**, Shirakami Y, Sakai H, Adachi S, Hata K, Hirose Y, Tsurumi H, Tanaka T, Moriwaki H. (-)-Epigallocatechin gallate suppresses azoxymethane-induced colonic premalignant lesions in male C57BL/KsJ-db/db mice. *Cancer Prev Res* (Phila) 2008; **1**: 298-304 [PMID: 19138973 DOI: 10.1158/1940-6207.CAPR-08-0045]
- 28 **Marchesi JR**, Dutilh BE, Hall N, Peters WH, Roelofs R, Boleij A, Tjalsma H. Towards the human colorectal cancer microbiome. *PLoS One* 2011; **6**: e20447 [PMID: 21647227 DOI: 10.1371/journal.pone.0020447]
- 29 **Wu S**, Rhee KJ, Albesiano E, Rabizadeh S, Wu X, Yen HR, Huso DL, Brancati FL, Wick E, McAllister F, Housseau F, Pardoll DM, Sears CL. A human colonic commensal promotes colon tumorigenesis via activation of T helper type 17 T cell responses. *Nat Med* 2009; **15**: 1016-1022 [PMID: 19701202 DOI: 10.1038/nm.2015]
- 30 **Sears CL**, Pardoll DM. Perspective: alpha-bugs, their microbial partners, and the link to colon cancer. *J Infect Dis* 2011; **203**: 306-311 [PMID: 21208921 DOI: 10.1093/jinfdis/jiq061]
- 31 **Hamer HM**, Jonkers D, Venema K, Vanhoutvin S, Troost FJ, Brummer RJ. Review article: the role of butyrate on colonic function. *Aliment Pharmacol Ther* 2008; **27**: 104-119 [PMID: 17973645 DOI: 10.1111/j.1365-2036.2007.03562.x]
- 32 **Bultman SJ**. Molecular pathways: gene-environment interactions regulating dietary fiber induction of proliferation and apoptosis via butyrate for cancer prevention. *Clin Cancer Res* 2014; **20**: 799-803 [PMID: 24270685 DOI: 10.1158/1078-0432.CCR-13-2483]
- 33 **Jahns F**, Wilhelm A, Jablonowski N, Mothes H, Radeva M, Wölfert A, Greulich KO, Gleit M. Butyrate suppresses mRNA increase of osteopontin and cyclooxygenase-2 in human colon tumor tissue. *Carcinogenesis* 2011; **32**: 913-920 [PMID: 21459756 DOI: 10.1093/carcin/bgr061]

**P- Reviewer:** Hosomi R **S- Editor:** Qi Y **L- Editor:** Wang TQ  
**E- Editor:** Ma YJ



## Basic Study

# miR-192-5p regulates lipid synthesis in non-alcoholic fatty liver disease through SCD-1

Xiao-Lin Liu, Hai-Xia Cao, Bao-Can Wang, Feng-Zhi Xin, Rui-Nan Zhang, Da Zhou, Rui-Xu Yang, Ze-Hua Zhao, Qin Pan, Jian-Gao Fan

Xiao-Lin Liu, Hai-Xia Cao, Bao-Can Wang, Feng-Zhi Xin, Rui-Nan Zhang, Da Zhou, Rui-Xu Yang, Ze-Hua Zhao, Qin Pan and Jian-Gao Fan, Center for Fatty Liver, Department of Gastroenterology, Xinhua Hospital Affiliated to Shanghai Jiao Tong University School of Medicine, Shanghai 200092, China

ORCID number: Xiao-Lin Liu (0000-0003-4560-7589); Hai-Xia Cao (0000-0002-8265-9460); Bao-Can Wang (0000-0002-6288-8100); Feng-Zhi Xin (0000-0001-9674-0481); Rui-Nan Zhang (0000-0001-9049-3010); Da Zhou (0000-0001-8838-1351); Rui-Xu Yang (0000-0001-9384-6408); Ze-Hua Zhao (0000-0002-3708-8881); Qin Pan (0000-0001-5855-4952); Jian-Gao Fan (0000-0001-7443-5056).

**Author contributions:** Fan JG, Cao HX and Liu XL conceived and designed the study; Liu XL, Xin FZ, Zhang RN, Zhou D, Yang RX and Zhao ZH performed the experiments; Wang BC and Pan Q analyzed the data; Fan JG, Cao HX and Liu XL wrote the paper; Liu XL, Cao HX and Fan JG contributed equally to this work.

**Supported by** National Key R&D Program of China No. 2017YFC0908900; National Key Basic Research Project, No. 2012CB517501; and National Natural Science Foundation of China, No. 81470840 and No. 81600464.

**Institutional review board statement:** The study was reviewed and approved by the Ethics Committee of Xinhua Hospital Affiliated to Shanghai Jiaotong University School of Medicine.

**Institutional animal care and use committee statement:** All procedures involving animals were reviewed and approved by the Institutional Animal Care and Use Committee of SHRM (SHRM-IACUC-001).

**Conflict-of-interest statement:** The authors declare that there is no conflict of interest related to this study.

**Open-Access:** This article is an open-access article which was selected by an in-house editor and fully peer-reviewed by external reviewers. It is distributed in accordance with the Creative Commons Attribution Non Commercial (CC BY-NC 4.0) license, which permits others to distribute, remix, adapt, build upon this

work non-commercially, and license their derivative works on different terms, provided the original work is properly cited and the use is non-commercial. See: <http://creativecommons.org/licenses/by-nc/4.0/>

**Manuscript source:** Unsolicited manuscript

**Correspondence to:** Jian-Gao Fan, PhD, Professor, Center for Fatty Liver, Department of Gastroenterology, Xinhua Hospital Affiliated to Shanghai Jiao Tong University School of Medicine, 1665 Kong Jiang Road, Shanghai 200092, China. [fanjiangao@xinhua.com.cn](mailto:fanjiangao@xinhua.com.cn)  
Telephone: +86-21-25077340

**Received:** August 24, 2017  
**Peer-review started:** August 25, 2017  
**First decision:** October 11, 2017  
**Revised:** October 16, 2017  
**Accepted:** October 27, 2017  
**Article in press:** October 27, 2017  
**Published online:** December 14, 2017

## Abstract

### AIM

To evaluate the levels of miR-192-5p in non-alcoholic fatty liver disease (NAFLD) models and demonstrate the role of miR-192-5p in lipid accumulation.

### METHODS

Thirty Sprague Dawley rats were randomly divided into three groups, which were given a standard diet, a high-fat diet (HFD), and an HFD with injection of liraglutide. At the end of 16 weeks, hepatic miR-192-5p and stearoyl-CoA desaturase 1 (SCD-1) levels were measured. MiR-192-5p mimic and inhibitor and SCD-1 siRNA were transfected into Huh7 cells exposed to palmitic acid (PA). Lipid accumulation was evaluated by oil red O staining and triglyceride assays. Direct

interaction was validated by dual-luciferase reporter gene assays.

### RESULTS

The HFD rats showed a 0.46-fold decrease and a 3.5-fold increase in hepatic miR-192-5p and SCD-1 protein levels compared with controls, respectively, which could be reversed after disease remission by liraglutide injection ( $P < 0.01$ ). The Huh7 cells exposed to PA also showed down-regulation and up-regulation of miR-192-5p and SCD-1 protein levels, respectively ( $P < 0.01$ ). Transfection with miR-192-5p mimic and inhibitor in Huh7 cells induced dramatic repression and promotion of SCD-1 protein levels, respectively ( $P < 0.01$ ). Luciferase activity was suppressed and enhanced by miR-192-5p mimic and inhibitor, respectively, in wild-type SCD-1 ( $P < 0.01$ ) but not in mutant SCD-1. MiR-192-5p overexpression reduced lipid accumulation significantly in PA-treated Huh7 cells, and SCD-1 siRNA transfection abrogated the lipid deposition aggravated by miR-192-5p inhibitor ( $P < 0.01$ ).

### CONCLUSION

This study demonstrates that miR-192-5p has a negative regulatory role in lipid synthesis, which is mediated through its direct regulation of SCD-1.

**Key words:** miR-192-5p; Stearoyl-CoA desaturase 1; High fat diet; Lipid synthesis; Non-alcoholic fatty liver disease

© The Author(s) 2017. Published by Baishideng Publishing Group Inc. All rights reserved.

**Core tip:** Hepatic miR-192-5p levels decreased in non-alcoholic steatohepatitis rat models fed a high-fat diet and the decrease could be reversed after disease remission by liraglutide therapy. miR-192-5p showed a direct interaction with stearoyl-CoA desaturase 1 (SCD-1). miR-192-5p overexpression significantly alleviated lipid accumulation in Huh7 cells exposed to PA, and SCD-1 siRNA abrogated the lipid deposition aggravated by miR-192-5p inhibitor. Our study provides evidence that miR-192-5p participates in lipid synthesis in non-alcoholic fatty liver disease (NAFLD) through SCD-1 and suggests that the overexpression of miR-192-5p may represent a promising treatment for NAFLD.

Liu XL, Cao HX, Wang BC, Xin FZ, Zhang RN, Zhou D, Yang RY, Zhao ZH, Pan Q, Fan JG. miR-192-5p regulates lipid synthesis in non-alcoholic fatty liver disease through SCD-1. *World J Gastroenterol* 2017; 23(46): 8140-8151 Available from: URL: <http://www.wjgnet.com/1007-9327/full/v23/i46/8140.htm> DOI: <http://dx.doi.org/10.3748/wjg.v23.i46.8140>

## INTRODUCTION

With the prevalence of obesity and metabolic syndrome, non-alcoholic fatty liver disease (NAFLD) has become the most common chronic liver disease worldwide, including China<sup>[1]</sup>. Based on the “multiple hit” theory of NAFLD pathogenesis, lipid accumulation initiates simple hepatic steatosis and subsequently triggers multiple insults, ultimately inducing non-alcoholic steatohepatitis (NASH), cirrhosis, and even hepatocellular carcinoma in predisposed individuals<sup>[2,3]</sup>. Briefly, high levels of lipid metabolites, such as free fatty acids, could cause mitochondrial dysfunction, endoplasmic reticulum stress, and consequent activation of inflammatory responses<sup>[4,5]</sup>. In addition to the classical factors involved in the progression of NAFLD, epigenetic mechanisms are gradually identified as important regulators in the pathogenesis of this disease. The most thoroughly studied markers for epigenetic alterations in NAFLD are DNA methylation and the actions of microRNAs<sup>[6-8]</sup>. MicroRNAs are non-coding RNAs composed of 18 to 25 nucleotides, and they play important roles in regulating a wide spectrum of biological processes, including fatty acid metabolism<sup>[9,10]</sup>. Serum miR-192-5p levels have been reported to differentiate control livers, simple hepatic steatosis, and NASH in clinical studies<sup>[11]</sup>. Similarly, our previous research in NAFLD patients also found that serum miR-192-5p levels showed good correlations with hepatic steatosis and inflammatory activity<sup>[12]</sup>. Although miR-192-5p is abundant in the liver, early studies mainly focused on its regulatory role in cell growth, apoptosis, and tumor metastasis<sup>[13,14]</sup>, little is known about its role in lipid metabolism.

Stearoyl-CoA desaturase 1 (SCD-1) plays an important role in the biosynthesis of monounsaturated fatty acids and serves as a key regulatory enzyme in the last stage of hepatic *de novo* lipogenesis (DNL). Increased DNL has been confirmed in NAFLD patients compared with controls<sup>[15]</sup>. Enhanced hepatic SCD-1 activity promotes the accumulation of hepatic lipids, especially triglyceride (TG), and consequently leads to the progression of NAFLD<sup>[16]</sup>. Recent research has suggested that the expression of SCD-1 may be regulated through SREBP-1c-dependent and SREBP-1c-independent pathways<sup>[17]</sup>, but whether SCD-1 can be regulated by microRNAs in NAFLD has not been fully studied.

To address the above questions, we conducted this study in high-fat diet (HFD)-fed rats and palmitic acid (PA)-treated Huh7 cells. The hepatic and hepatocellular levels of miR-192-5p in NAFLD were evaluated both *in vivo* and *in vitro*. Overexpression and knockdown of miR-192-5p were performed in Huh7 cells to determine the regulatory effects of miR-192-5p in lipid



accumulation, and luciferase reporter assays were used to confirm the direct interaction between miR-192-5p and SCD-1. Collectively, we attempted to illustrate the role of miR-192-5p in hepatic lipid metabolism in NAFLD.

## MATERIALS AND METHODS

### *Animals and treatment*

The animal experiment was designed to minimize pain or discomfort to the animals. A total of 30 male Sprague-Dawley rats (6-wk-old) were purchased from the Shanghai Experimental Animal Center of the Chinese Academy of Sciences (Shanghai, China) and were housed under controlled conditions of temperature ( $24^{\circ}\text{C} \pm 2^{\circ}\text{C}$ ), humidity ( $50\% \pm 5\%$ ), and a light/dark cycle (12 h) with free access to food and water. After acclimation for one week on a standard diet, they were randomized into three groups (10 rats/group). The control group received a standard diet; the HFD group was fed an HFD (88% standard diet, 10% lard, and 2% cholesterol); and the therapy group was fed an HFD and received intraperitoneal injections of liraglutide (Sigma, St. Louis, United States; 0.6 mg/kg in saline solution) for the last 8 wk. This experiment followed the National Research Council's Guide for the Care and Use of Laboratory Animals and was approved by the Institutional Animal Care and Use Committee of SHRM (SHRM-IACUC-001).

### *Sample collection and measurement*

At the end of 16 wk, the rats were euthanized after an overnight fast. Parts of the rat livers were fixed in 4% paraformaldehyde overnight and embedded in paraffin for histological assessments with hematoxylin-eosin (H&E) staining. The remaining portions were snap frozen in liquid nitrogen and stored at  $-80^{\circ}\text{C}$  for oil red O staining and other analyses. The hepatic TG levels of the rats were measured with an assay kit (Nanjing Jiancheng Bioengineering Institute, Nanjing, China) according to the manufacturer's instructions.

### *Cell culture*

The Huh7 cell line was obtained from American Type Culture Collection (ATCC; Manassas, VA, United States) and cultured in Dulbecco's modified eagle medium (DMEM) supplemented with 10% fetal bovine serum (FBS; Gibco, CA, United States) under an atmosphere of 5%  $\text{CO}_2$  at  $37^{\circ}\text{C}$ . PA powder (Sigma, St. Louis, United States) was dissolved in Milli-Q water supplemented with 1% fatty acid-free BSA (Sigma, St. Louis, United States) at  $70^{\circ}\text{C}$  and filtrated through a  $0.22\text{-}\mu\text{m}$  filter to yield a 5 mmol/L stock solution of PA. The working PA solution was added to the cells at 0.3 mmol/L and 0.5 mmol/L.

### *Cell viability detection*

We performed cell viability measurements using

the Cell Counting Kit-8 (CCK-8; Dojindo Molecular Technologies, Kumamoto, Japan) according to the manufacturer's instructions. Huh7 cells were plated onto a 96-well plate and 0, 0.3, and 0.5 mmol/L of PA in culture medium was added for 8, 16, and 24 h of incubation. The absorbance of the CCK-8 was read at 450 nm, and the values were normalized to those of the control group.

### *Oil red O staining and intracellular TG assay*

For oil red O staining, the cell culture plate was washed twice with phosphate-buffered saline and fixed in 10% neutral formalin. Oil red O (Sigma, St. Louis, United States) was dissolved in isopropanol as a stock solution and was diluted 3:2 with ddH<sub>2</sub>O to be added to the plate for 15 min, followed by washing in 60% isopropanol. Then, the plate was counterstained with hematoxylin after rinsing in distilled water. The intracellular TG levels in Huh7 cells were measured using a TG assay kit (Applygen Technologies Inc., Beijing, China) according to the manufacturer's instructions. Cellular TG levels were normalized to their protein contents.

### *MiRNA and small interfering RNA (siRNA) transfection*

Huh7 cells were transfected with 50 nmol/L miR-192-5p mimic (Cat. No: miR10000222; Ribobio, Guangzhou, China), 200 nmol/L miR-192-5p inhibitor (Cat. No: miR20000222; Ribobio, Guangzhou, China), 50 nmol/L SCD-1 siRNA (Cat. No: stB0007776A; Ribobio, Guangzhou, China), and their respective negative control (NC; Ribobio, Guangzhou, China) according to the manufacturer's instructions with Lipofectamine 2000 (Invitrogen, Carlsbad, United States) and Opti-MEM medium (Gibco, CA, United States). The medium was replaced with DMEM with 10% FBS after transfection for 6 h. Experiments were performed 24 h after transfection.

### *Luciferase reporter assay*

The sequence of the wild type (WT) or mutant (Mut) seed region of SCD-1 was cloned into a psiCHECK-2 luciferase vector (Promega, Madison, WI, United States) between XhoI and NotI sites. After being plated onto a 96-well plate, 293T cells were transfected with 0.16  $\mu\text{g}$  of a SCD-1 3' untranslated region (UTR) vector (WT and Mut) and the empty vector as well as 50 nmol/L miR-192-5p mimic, 200 nmol/L inhibitor, and their respective NC. The culture medium was changed to complete DMEM after 6 h. Luciferase activity was measured using the Promega Dual-Luciferase system 48 h after transfection, and the relative luciferase activity was calculated as Renilla luciferase to Firefly luciferase.

### *Quantitative real-time polymerase chain reaction*

Total RNA enriched with miRNA was isolated and extracted from frozen liver tissue and Huh7 cells

**Table 1** Biochemical parameters of animal models

Parameter	Group		
	Control ( <i>n</i> = 10)	HFD ( <i>n</i> = 10)	Liraglutide ( <i>n</i> = 10)
ALT, in U/L	37.4 ± 1.9	114.3 ± 26.7 <sup>a</sup>	34.3 ± 3.1 <sup>c</sup>
AST, in U/L	92.1 ± 5.6	160.1 ± 16.8 <sup>a</sup>	90.2 ± 5.5 <sup>c</sup>
HDL, in mmol/L	0.33 ± 0.01	0.25 ± 0.01 <sup>a</sup>	0.24 ± 0.01 <sup>a</sup>
LDL, in mmol/L	0.14 ± 0.01	0.42 ± 0.04 <sup>a</sup>	0.53 ± 0.07 <sup>a</sup>

Data are expressed as mean ± SEM. <sup>a</sup>*P* < 0.05 *vs* the control group; <sup>c</sup>*P* < 0.05 *vs* the HFD group. ALT: Alanine transaminase; AST: Aspartate transaminase; HDL: High density lipoprotein; LDL: Low density lipoprotein.

using TRIzol (Invitrogen, Carlsbad, CA, United States). RNA samples were analyzed on a NanoDrop 1000 spectrophotometer (Nano-drop Technologies, Wilmington, DE, United States) to assess its yield and purity. As previously described, complementary DNA for mRNA was synthesized using the PrimeScript RT Reagent Kit (Takara, Shiga, Japan) and SYBR Premix Ex Taq (Cat. No: RR420A; Takara, Shiga, Japan) was used for quantitative real-time polymerase chain reaction (qRT-PCR). In the reverse-transcription reactions of miRNA, poly A modification and first-strand cDNA synthesis were performed with 500 ng of total RNA each reaction using the Mir-X miRNA First-Strand Synthesis Kit (Cat. No: 638313; Takara, Shiga, Japan) according to the manufacturer's instructions. Subsequent qPCR was performed in a total reaction volume of 20 µL containing 2 µL of diluted (1:10) cDNA using SYBR Premix Ex Taq II (Cat. No: RR820A; Takara, Shiga, Japan) according to the manufacturer's instructions. Dissociation curve analysis was performed at the end of cycling program to control PCR specificity. The mRNA and miRNA abundance was normalized to that of 18 s and U6, and relative gene expression was analyzed based on the 2<sup>-ΔΔCt</sup> method. Sequences of primers used were: SCD-1: 5'-GGATGCTCGTGCCAGTG-3', 5'-ACTCAGTGCCAGGTTAGAAG-3'; 18s: 5'-AAGTTTCAGCACATCCTGCGAGTA-3', 5'-TTGGTG A GGTCAATGTCTGCTTTC-3'; miR-192-5p: 5'-CT GACCTATGAATTGACAGCC-3'; and U6: 5'-AGA GAA GAT TAGCATGGCCCCTG-3'.

#### Western blot analysis

Protein samples of 30 µg were analyzed by 10% sodium dodecyl sulfate-polyacrylamide gel electrophoresis and then transferred to nitrocellulose membranes. The membranes were blocked with 5% skim milk in TBST for 2 h at room temperature and then incubated with mouse monoclonal antibody against SCD-1 (Abcam, Cambridge, United Kingdom) and mouse monoclonal tubulin antibody (Beyotime, Shanghai, China) overnight at 4 °C. Then, these membranes were washed and incubated at room temperature with an anti-mouse secondary antibody (Beyotime, Shanghai, China) for 1 h. Immune complexes were detected using a Western

chemiluminescent HRP substrate (Millipore Corporation, Billerica, MA, United States).

#### Statistical analysis

The data are expressed as the mean ± SEM. A statistical comparison was made using a two-tailed Student *t*-test between two groups and a one-way analysis of variance test followed by Student-Newman-Kuels analyses among multiple groups. Differences were considered significant at *P* < 0.05. All analyses were performed using GraphPad Prism 6.0 software (San Diego, CA, United States). The statistical methods used in this study were reviewed by Guang-Yu Chen from Clinical Epidemiology Center, Shanghai Jiao Tong University.

## RESULTS

#### miR-192-5p and SCD-1 levels in the liver of rat models

At the end of the 16<sup>th</sup> week, all the rats in the HFD group developed NASH with significant hepatic macro-vesicular steatosis, ballooning degeneration, and lobular inflammation. The mean body weight of the HFD rats (661.7 ± 15.8 g) was higher than that of the controls (566.7 ± 8.1 g, *P* < 0.01), and they also had increased hepatic TG levels (335 ± 9 mol/g) compared with the control group (101 ± 10 µmol/g, *P* < 0.01). The injection of liraglutide in HFD rats alleviated hepatic steatosis and reduced body weight (533.1 ± 7.4 g) and hepatic TG levels (241 ± 14 µmol/g) significantly (*P* < 0.01, Figure 1A-C). The analysis of serum biochemical parameters in animal models showed that the HFD rats had higher alanine transaminase (ALT), aspartate transaminase (AST), and low density lipoprotein (LDL) levels, and lower high density lipoprotein (HDL) levels compared with the control group (*P* < 0.05). The liraglutide group showed a significant decrease of ALT and AST compared with the HFD group (*P* < 0.05), but there was no statistical difference in serum LDL or HDL levels (Table 1). The qRT-PCR results showed that HFD rats had decreased hepatic miR-192-5p levels (0.46-fold) compared with the controls and that liraglutide therapy could abrogate the reduction of miR-192-5p in HFD rat livers (*P* < 0.01; Figure 1D). In addition to decreased hepatic miR-192-5p levels, the protein expression of hepatic SCD-1 was markedly elevated (3.5-fold) in rats fed an HFD, and liraglutide therapy could reduce hepatic SCD-1 levels in HFD rats (*P* < 0.01; Figure 1E).

#### Palmitate induces the down-regulation of miR-192-5p in vitro

According to the results of the CCK-8 test, 0.5 mmol/L PA induced cell death as early as 8 h, but 0.3 mmol/L PA showed no significant cytotoxic effects until 16 h (Figure 2A). To induce lipid accumulation without cytotoxicity *in vitro*, we chose to expose Huh7 cells to 0.3 mmol/L PA for 8 h. The TG levels in Huh7 cells

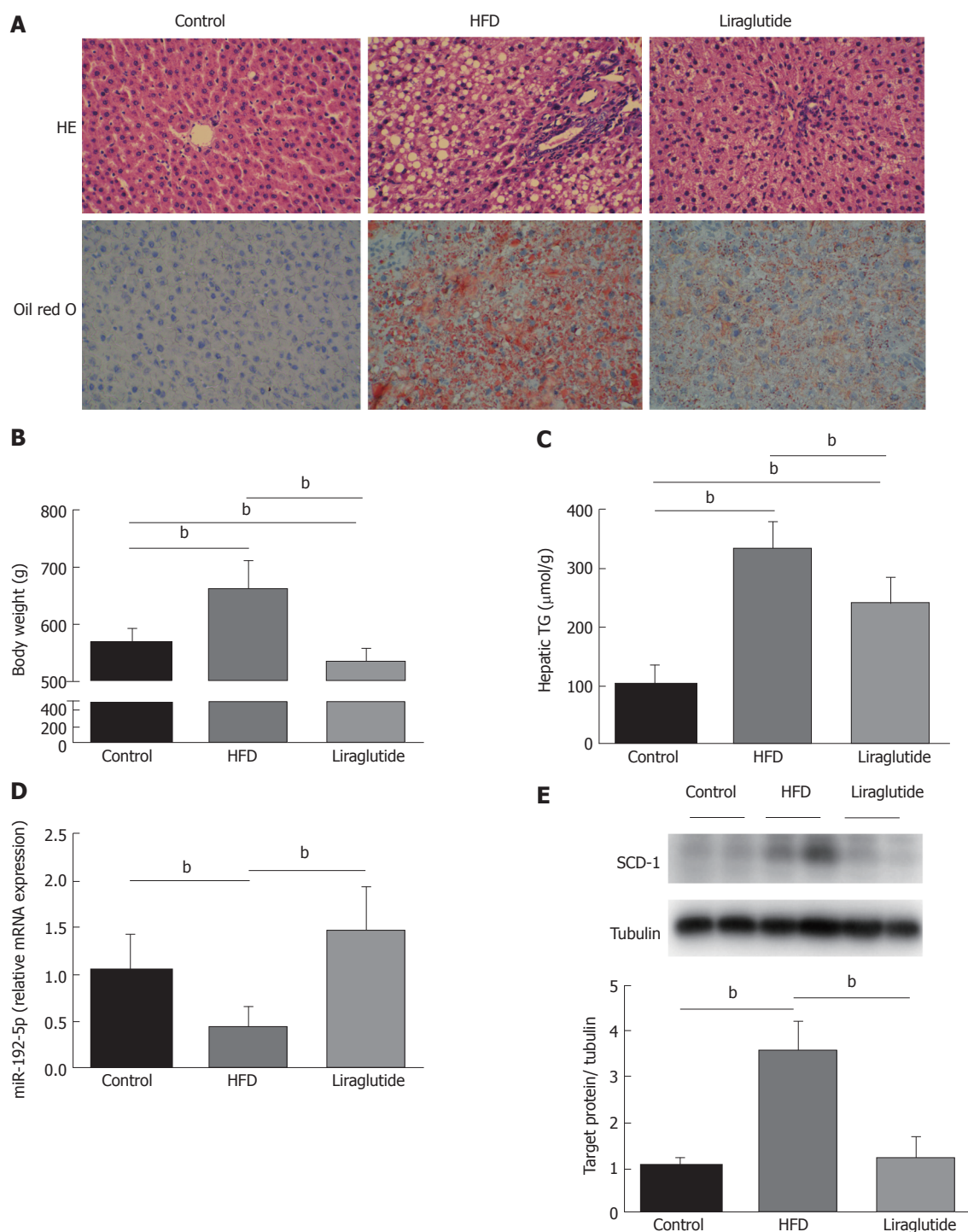


**Figure 1** Hepatic miR-192-5p and SCD-1 levels in rat models. H&E staining of livers (A), body weight (B), hepatic TG levels (C), hepatic miR-192-5p levels (D), and SCD-1 protein levels (E) in rats fed an HFD and treated with liraglutide. The data are expressed as the mean  $\pm$  SEM ( $n = 10$  rats/group), <sup>b</sup> $P < 0.01$ .

increased to approximately 45  $\mu\text{mol/g}$  after exposure to 0.3 mmol/L PA for 8 h (Figure 2B), and the oil red O staining showed obvious lipid droplets in the cells (Figure 2C). Similar to HFD rat livers, the miR-192-5p levels in PA-treated Huh7 cells showed significant downregulation (55%,  $P < 0.01$ ) compared to the controls (Figure 2D). However, the SCD-1 protein levels showed a 2.64-fold increase in PA-treated Huh7

cells ( $P < 0.01$ ; Figure 2E).

### SCD-1 is a direct target of miR-192-5p

Based on the results from the TargetScan, miRanda, and PicTar databases, there are hundreds of predicted targets for miR-192-5p. Among these, SCD-1 is the one that participates in lipid metabolism and increase dramatically in NAFLD. Therefore, we performed dual

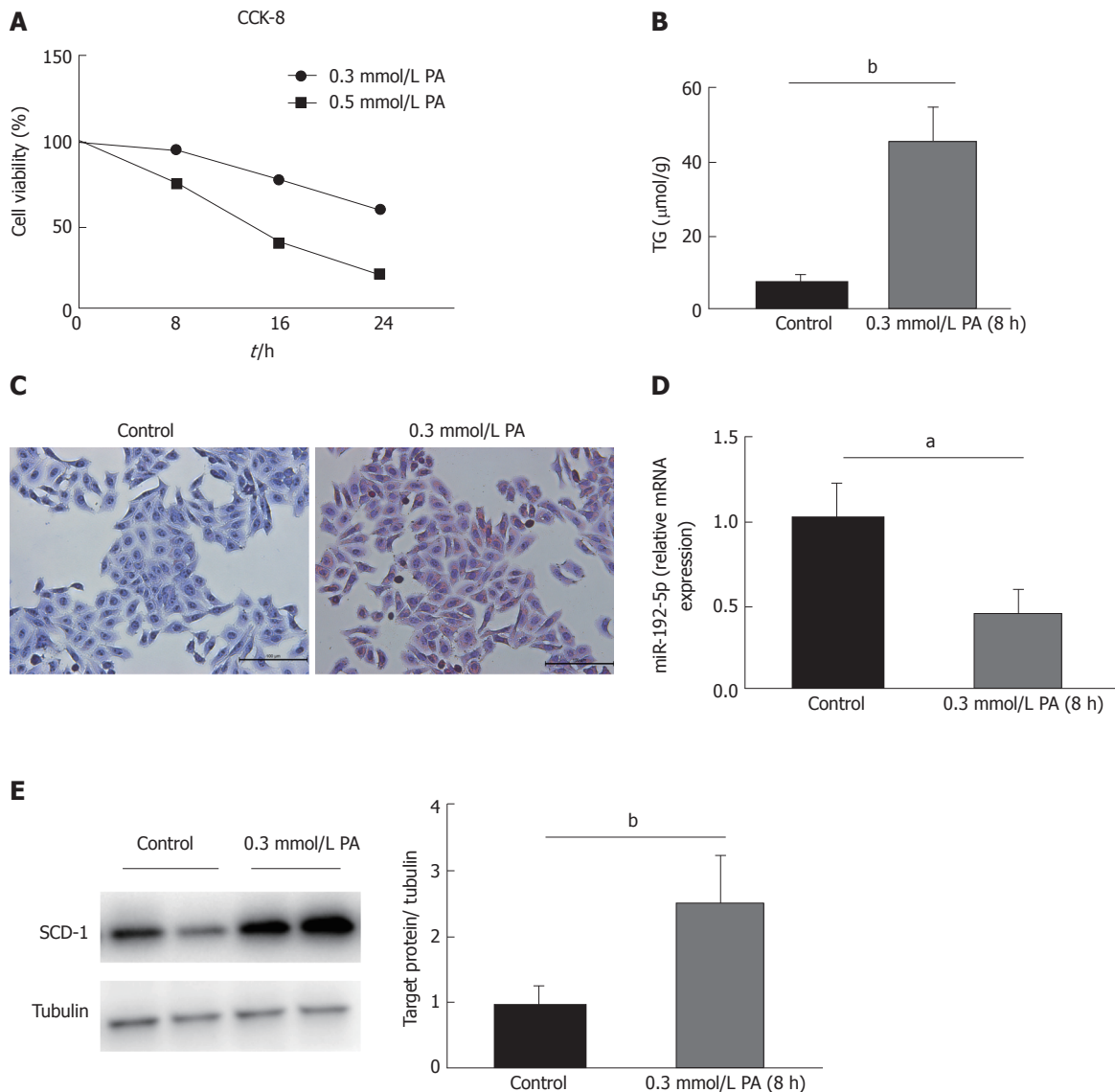


**Figure 2** PA induces a decrease in miR-192-5p and an increase in SCD-1 in Huh7 cells. A: The cytotoxic effects of PA on Huh7 cells by the CCK-8 test; B: Cellular TG levels; C: Oil red O staining; D: MiR-192-5p levels; and E: SCD-1 protein levels in Huh7 cells treated with PA. The data are expressed as the mean  $\pm$  SEM,  $^aP < 0.01$ .

luciferase reporter gene assays to validate the direct interaction between miR-192-5p and SCD-1. The binding sites of miR-192-5p with 3' UTR of SCD-1 are shown in Figure 3A, and the miR-192-5p seed sequence was deleted in mutant SCD-1. The luciferase activity in WT SCD-1 3' UTR was suppressed to 60% by miR-192-5p mimic and showed a 1.25-fold increase by miR-192-5p inhibitor compared with their respective negative controls ( $P < 0.01$ ). However, these repressive and stimulatory effects could be abrogated by the mutation of the SCD-1 3' UTR (Figure 3B), suggesting the direct interaction between miR-192-5p and the 3' UTR of SCD-1 mRNA. At the same time, we measured the mRNA levels of SCD-1 in Huh7 cells when transfected with miR-192-5p mimic and inhibitor, but neither of them showed significant differences compared with their respective negative control (Figure 3C). Fortunately, we found an obvious reduction in

SCD-1 protein levels in Huh7 cells transfected with miR-192-5p mimic and an induction of these levels when transfected with miR-192-5p inhibitor compared with their separate negative control ( $P < 0.01$ ; Figure 3D).

#### miR-192-5p alleviates lipid accumulation by interacting with SCD-1

To evaluate the function of miR-192-5p in lipid metabolism, we transfected Huh7 cells with mimic NC and miR-192-5p mimic and cultured them in 0.3 mM PA medium. From oil red O staining, we found that the overexpression of miR-192-5p could alleviate lipid accumulation in Huh7 cells after exposure to PA for 8 hours (Figure 4A). As expected, Huh7 cells transfected with miR-192-5p mimic resulted in a significant reduction (23%) in cellular TG levels compared with mimic NC after PA exposure ( $P < 0.01$ ; Figure 4B).



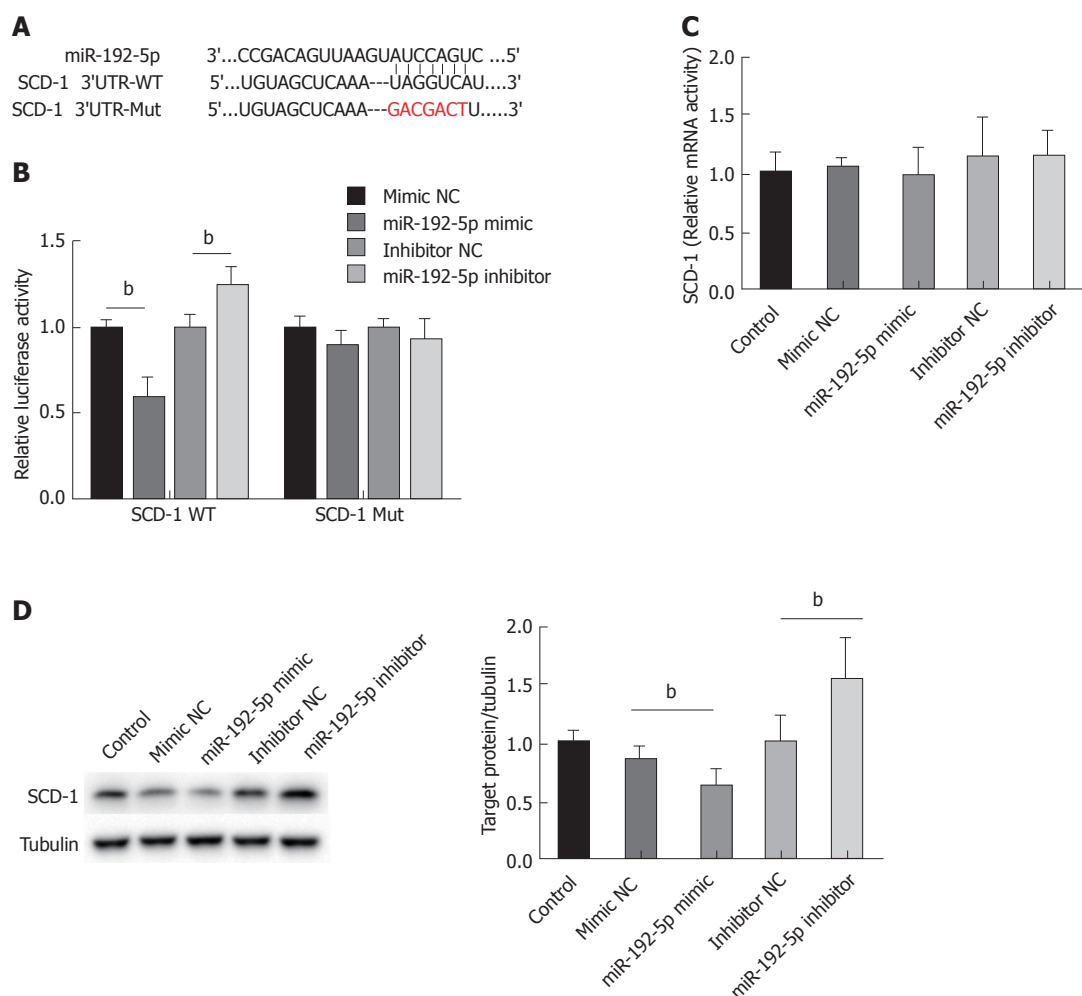


**Figure 3 SCD-1 is a direct target of miR-192-5p.** A: The binding sites of miR-192-5p with the 3' UTR of SCD-1; B: The dual luciferase activity in the wild type and mutant SCD-1 3' UTRs in 293T cells treated with miR-192-5p mimic and inhibitor, respectively. The mRNA (C) and protein levels (D) of SCD-1 in Huh7 cells transfected with miR-192-5p mimic and inhibitor. The data are expressed as the mean  $\pm$  SEM, <sup>b</sup> $P < 0.01$ .

We further explored the regulatory effect of miR-192-5p on SCD-1 expression in PA-treated Huh7 cells. The protein levels of SCD-1 were enriched significantly after PA exposure, and the increase could be blocked by the transfection of miR-192-5p mimic (Figure 4C).

#### SCD-1 mediates the promoting effect of the miR-192-5p inhibitor on lipid accumulation

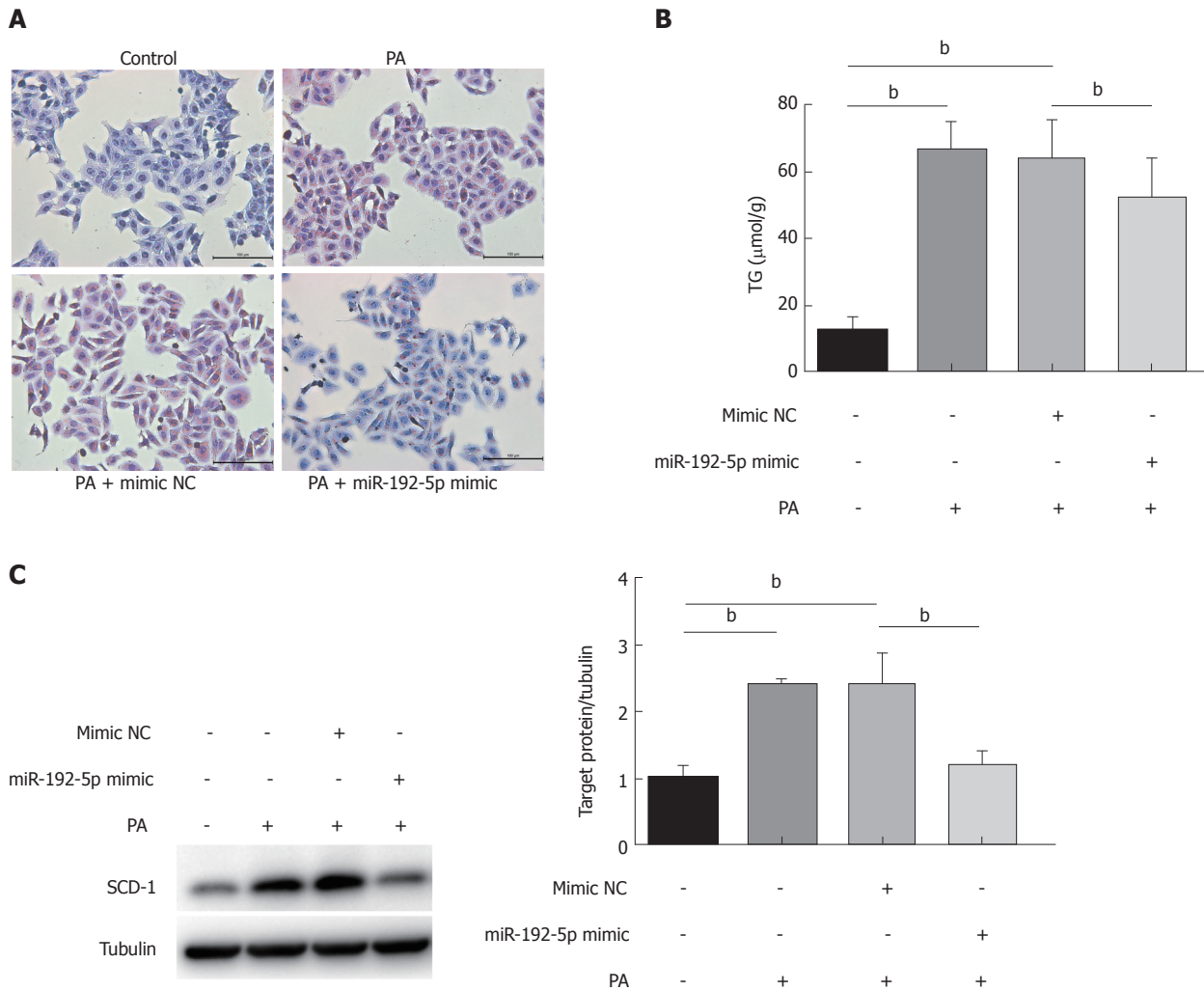
To further investigate whether the regulation of lipid metabolism by miR-192-5p is mediated by SCD-1, we applied SCD-1 siRNA to perform the functional remedial experiment. As expected, the miR-192-5p inhibitor significantly increased the protein levels of SCD-1 in PA-treated Huh7 cells compared with its negative control, and the concomitant SCD-1 siRNA transfection could abrogate the elevated SCD-1 protein levels (Figure 5A). The inhibition of miR-192-5p could aggravate lipid accumulation in PA-treated Huh7 cells, but this could be reversed by SCD-1 knockdown (Figure 5B). Similarly, cellular TG increased after the inhibition of miR-192-5p compared with its negative control, and this promoting effect could be blocked by the transfection of SCD-1

siRNA ( $P < 0.01$ ; Figure 5C).

## DISCUSSION

In the current study, we demonstrated that miR-192-5p decreased in NAFLD both *in vivo* and *in vitro* and the decrease could be reversed after disease remission by liraglutide therapy in animal models. Meanwhile, we confirmed that miR-192-5p had a negative regulatory role in lipid synthesis, which was mediated through its regulation of lipogenic gene SCD-1.

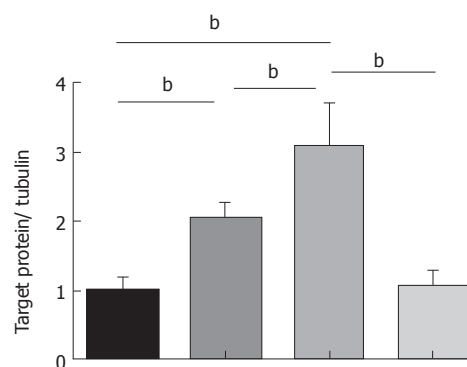
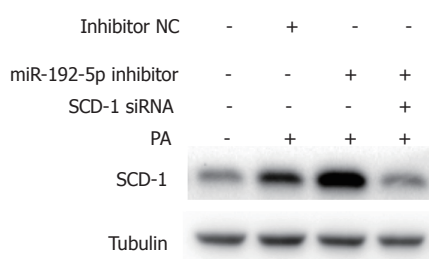
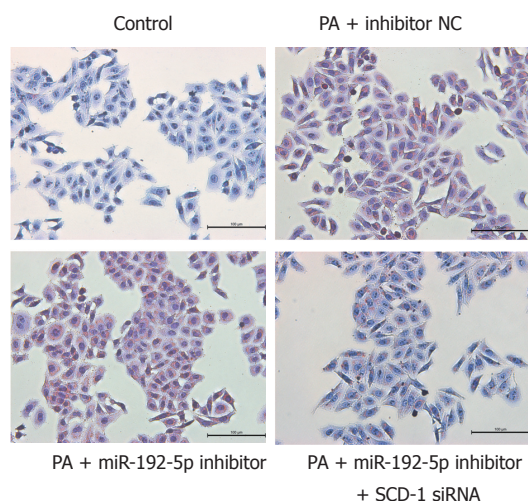
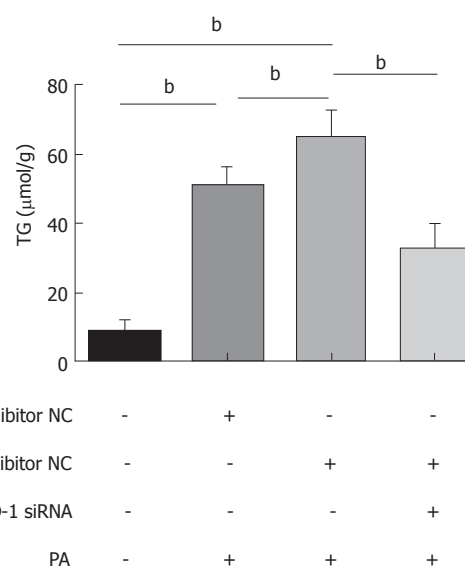
Because of the abundance of miR-192-5p in the liver, many researchers have focused on miR-192-5p as a serum biomarker of liver injury. For example, serum levels of miR-192-5p have been found to increase in patients with various liver diseases, such as drug-induced liver injury<sup>[18]</sup>, chronic hepatitis B<sup>[19]</sup>, hepatocellular carcinoma<sup>[20,21]</sup>, and NAFLD<sup>[11,22]</sup>. Serum miR-122 and miR-192 levels have been reported to differentiate control livers, simple hepatic steatosis, and NASH in clinical studies<sup>[11]</sup>. Similarly, our previous research in NAFLD patients also found that miR-122,



**Figure 4** MiR-192-5p alleviates lipid accumulation in PA-treated Huh7 cells. Oil red O staining (A), cellular TG levels (B), and SCD-1 protein levels (C) in Huh7 cells transfected with miR-192-5p mimic and its negative control followed by exposure to PA. The data are expressed as the mean  $\pm$  SEM, <sup>b</sup> $P < 0.01$ .

miR-192, and miR-34a showed good correlations with hepatic steatosis and inflammatory activity<sup>[12]</sup>. Among the three microRNAs, miR-122 is the most studied in NAFLD and can regulate numerous genes involved in lipid metabolism, such as sterol regulatory element binding protein (SREBP), acetyl coenzyme A carboxylase 2 (ACC2), and 3-hydroxy-3-methylglutaryl coenzyme A reductase (HMGCR)<sup>[23,24]</sup>. Similarly, miR-34a is characterized as a regulator of peroxisome proliferator-activated receptor  $\alpha$  (PPAR- $\alpha$ ) and its downstream genes and it induces lipid accumulation in a hepatocyte nuclear factor 4 $\alpha$  (HNF-4 $\alpha$ )-dependent way<sup>[25,26]</sup>. However, the regulatory role of miR-192-5p in NAFLD remains unknown. In our *in vivo* and *in vitro* models of NAFLD, miR-192-5p decreased in livers with steatosis and in cells with lipid accumulation. Because liraglutide is a well-known therapeutic option for weight loss and NAFLD<sup>[27]</sup>, the injection of liraglutide in HFD rats significantly alleviated the steatosis and hepatic TG levels, accompanied by the induction of hepatic miR-192-5p levels. These results may indicate that miR-192-5p has a negative correlation with hepatic lipid accumulation.

Originally, miR-192-5p was identified as an oncogene in some cancers and shows a negative correlation with the liver metastatic potential of colon cancer cells<sup>[28]</sup>. The expression of miR-192-5p is regulated partly by transforming growth factor  $\beta$ 1 (TGF $\beta$ 1) and hepatocyte nuclear factor 4 $\alpha$  (HNF4 $\alpha$ )<sup>[29,30]</sup>. A study by Roy *et al* shows that hepatic miR-192-5p can protect against acute liver injury induced by oxidative stress through the mediation of target gene Zeb2, which is a principal transcriptional regulator in cell survival<sup>[13]</sup>. Furthermore, docosahexaenoic acid can up-regulate miR-192 levels in enterocyte-like Caco-2 cells, and miR-192 shows a repressive effect on the expression of genes involved in lipid metabolism, such as insulin-like growth factor 1 (IGF1), fatty acid binding protein 3 (FABP3), and very low-density lipoprotein receptor (VLDLR)<sup>[31]</sup>. Recently, miR-192-5p was reported to play a role in bisphenol A-triggered NAFLD by regulating SREBF1<sup>[32]</sup>. In our NASH animal models fed an HFD and in the Huh7 cells treated with saturated fatty acid PA, which are the most recognized models for this disease, we demonstrated that the hepatic and cellular levels of miR-192-5p decreased significantly and that

**A****B****C**

**Figure 5** SCD-1 knockdown alleviates the promoting effect of the miR-192-5p inhibitor on lipid accumulation. The protein level of SCD-1 (A), Oil red O staining (B), and cellular TG levels (C) in Huh7 cells transfected with miR-192-5p inhibitor and SCD-1 siRNA followed by exposure to PA. The data are expressed as the mean  $\pm$  SEM, <sup>b</sup> $P < 0.01$ .

the overexpression of miR-192-5p could alleviate lipid accumulation in Huh7 cells. These results suggested that, in addition to its role in cell death and apoptosis, miR-192-5p could participate in lipid metabolism in NAFLD.

In the livers of NAFLD patients, fat accumulates because of an imbalance between lipid deposition and removal, which is driven by the hepatic synthesis of TG and DNL, especially in conditions of insulin resistance<sup>[16,33]</sup>. The contribution of DNL to hepatic TG synthesis and oxidative stress is significant, so inhibitors of DNL, such as Aramchol, are important NAFLD treatments for reducing hepatic fat accumulation<sup>[34,35]</sup>. SREBP-1c is reported to be the predominant regulator of DNL in the liver and activates key lipogenic genes such as SCD-1<sup>[17]</sup>. Meanwhile, hepatic SCD-1 can also

induce hepatic steatosis independent of upstream regulation by SREBP-1c<sup>[36]</sup>. SCD-1 is an enzyme that catalyzes the desaturation of fatty acyl-CoA substrates and participates in the biosynthesis of monounsaturated fatty acids, which constitute the primary components of TG<sup>[37]</sup>. Increased SCD-1 activity accelerates the last stage of TG synthesis and stimulates lipid accumulation<sup>[38]</sup>, but repressed SCD-1 expression up-regulates the components in the insulin-signaling pathway<sup>[39]</sup> and reduces obesity in HFD-fed animal models<sup>[40]</sup>. Our present study showed an increase in hepatic SCD-1 levels in rats fed an HFD, and treatment with liraglutide could decrease its levels dramatically.

In addition to regulation by upstream transcription factors, SCD-1 may be repressed through a mi-

croRNA-mediated mechanism. Recent studies have demonstrated the roles of miR-125b and miR-29a in the regulation of SCD-1<sup>[41,42]</sup>. In our study, we found that a region of the SCD 3' UTR completely matched a seed sequence (5'-UGACCUA-3') at the binding site of miR-192-5p, demonstrating a direct interaction between miR-192-5p and SCD-1. The knockdown and overexpression of miR-192-5p in Huh7 cells showed significant promotion and inhibition effects, respectively, on the protein expression of SCD-1, but no effects were observed on the mRNA levels of this gene. This result suggested that miR-192-5p could regulate the SCD-1 expression at the post-transcriptional level. Since the mRNA targets are only partially complementary to microRNAs in animals, microRNA-induced silencing complexes can mediate post-transcriptional silencing in the absence of mRNA degradation<sup>[43]</sup>. In addition, the functional remedial experiment showed that the transfection with SCD-1 siRNA could significantly abrogate the lipid accumulation induced by miR-192-5p inhibitor, indicating that miR-192-5p regulated lipid metabolism at least partly through an interaction with SCD-1.

The potential limitation of our study is that the specific regulatory role of miR-192-5p in NAFLD has not been thoroughly validated *in vivo*. Although one study demonstrated that the overexpression of miR-192-5p could abrogate bisphenol A-induced hepatic steatosis and lipid accumulation in C57BL/6 mice, whether miR-192-5p can alleviate hepatic steatosis in NAFLD patients remains uncertain. Therefore, hepatic miR-192-5p levels and the treatment effect of miR-192-5p need to be validated in clinical practice. It may be difficult to acquire enough participants due to the invasive method required for the retrieval of liver samples from NAFLD patients, but it would be of practical implications if clinical experiments support our claims going forward. In addition, as the therapy with liraglutide in NAFLD is accompanied by the upregulation of hepatic miR-192-5p levels, the rationale between liraglutide and hepatic miR-192-5p is also an open question.

In conclusion, we demonstrated that hepatic miR-192-5p levels decreased in NASH rat models fed an HFD and that this decrease could be reversed after disease remission by liraglutide therapy. We first confirmed that miR-192-5p had a direct regulatory effect on lipogenic gene SCD-1 and that this mediated the negative regulatory effect of miR-192-5p in lipid synthesis in NAFLD. These data complement the regulators involved in the progression of NAFLD and help us better understand the role of epigenetic factors in this disease. Meanwhile, our study suggests that the overexpression of miR-192-5p may reflect a

promising treatment strategy for NAFLD, which calls for more validated data in the future.

## ARTICLE HIGHLIGHTS

### Research background

Based on the "multiple hit" theory of non-alcoholic fatty liver disease (NAFLD) pathogenesis, lipid accumulation initiates simple hepatic steatosis and subsequently triggers multiple insults, ultimately inducing non-alcoholic steatohepatitis, cirrhosis, and even hepatocellular carcinoma. In addition to the classical factors involved in the progression of NAFLD, microRNAs, which represent epigenetic alterations, have been identified as important post-transcriptional regulators in the pathogenesis of this disease.

### Research motivation

Due to the abundance of miR-192-5p in the liver, many researchers have focused on miR-192-5p as a serum biomarker of liver injury, such as drug-induced liver injury, chronic hepatitis B, hepatocellular carcinoma, and NAFLD. Because microRNAs are important regulators in a wide spectrum of biological processes and metabolic homeostasis, the role of microRNAs in NAFLD pathogenesis is of particular interest. Our previous research in NAFLD patients found that serum miR-192-5p levels could differentiate different stages of NAFLD and showed good correlations with hepatic steatosis and inflammatory activity, but little is known about its regulatory role in lipid metabolism.

### Research objectives

We aimed to evaluate the hepatic levels of miR-192-5p in rat models of NAFLD, and figure out the role of miR-192-5p in lipid metabolism. After the present study, we have identified the lipogenic gene SCD-1 as a target gene of miR-192-5p, confirming the negative regulatory effect of miR-192-5p in lipid synthesis in NAFLD. These realized objectives give us a better understanding about the functional mechanism of miR-192-5p in NAFLD and provide a new insight in the miRNA-intervention treatment strategy for this disease.

### Research methods

We conducted this study in HFD-fed rats and palmitic acid-treated Huh7 cells. The hepatic and hepatocellular levels of miR-192-5p in NAFLD were evaluated using quantitative real-time polymerase chain reaction both *in vivo* and *in vitro*. The SCD-1 protein levels were examined by Western blot analysis. Oil red O staining and TG assay were used to detect the lipid accumulation in rat livers and hepatocytes. Overexpression and knockdown of miR-192-5p were performed in Huh7 cells with miR-192-5p mimic and inhibitor. Luciferase reporter assays confirmed the direct interaction between miR-192-5p and SCD-1.

### Research results

In the current study, we found that miR-192-5p decreased in NAFLD both *in vivo* and *in vitro* and the decrease could be reversed after disease remission by liraglutide therapy in animal models. Meanwhile, we confirmed that miR-192-5p had a negative regulatory role in lipid synthesis, which was mediated through its regulation on lipogenic gene SCD-1. However, the specific regulatory role of miR-192-5p in NAFLD patients remains unclear, which needs to be validated in clinical studies.

### Research conclusions

The authors demonstrated that miR-192-5p decreased in NAFLD conditions both *in vivo* and *in vitro*, which could provide more evidence for the clinical use of circulating miR-192-5p as a biomarker in NAFLD. We first confirmed that miR-192-5p showed direct regulation on lipogenic gene SCD-1 and that this could mediate the negative regulatory effect of miR-192-5p in lipid synthesis in NAFLD. These data complement the regulators involved in the progression of NAFLD and help us better understand the role of epigenetic factors in this



disease. Meanwhile, the study suggests that the overexpression of miR-192-5p may reflect a promising treatment strategy for NAFLD, which calls for more validated data in the future.

### Research perspectives

This study suggests that the miRNA intervention may be a promising treatment strategy for NAFLD. The future study might focus on the specific regulatory role of miR-192-5p in NAFLD *in vivo*, and the therapeutic effect of miR-192-5p needs to be validated in clinical practice. It would be of practical implications if clinical experiments support our claims going forward.

## REFERENCES

- Fan JG, Kim SU, Wong VW. New trends on obesity and NAFLD in Asia. *J Hepatol* 2017; **67**: 862-873 [PMID: 28642059 DOI: 10.1016/j.jhep.2017.06.003]
- Farrell GC, Larter CZ. Nonalcoholic fatty liver disease: from steatosis to cirrhosis. *Hepatology* 2006; **43**: S99-S112 [PMID: 16447287 DOI: 10.1002/hep.20973]
- Wong VW, Wong GL, Choi PC, Chan AW, Li MK, Chan HY, Chim AM, Yu J, Sung JJ, Chan HL. Disease progression of non-alcoholic fatty liver disease: a prospective study with paired liver biopsies at 3 years. *Gut* 2010; **59**: 969-974 [PMID: 20581244 DOI: 10.1136/gut.2009.205088]
- Buzzetti E, Pinzani M, Tsochatzis EA. The multiple-hit pathogenesis of non-alcoholic fatty liver disease (NAFLD). *Metabolism* 2016; **65**: 1038-1048 [PMID: 26823198 DOI: 10.1016/j.metabol.2015.12.012]
- Sookoian S, Rosselli MS, Gemma C, Burgueño AL, Fernández Gianotti T, Castaño GO, Pirola CJ. Epigenetic regulation of insulin resistance in nonalcoholic fatty liver disease: impact of liver methylation of the peroxisome proliferator-activated receptor  $\gamma$  coactivator 1 $\alpha$  promoter. *Hepatology* 2010; **52**: 1992-2000 [PMID: 20890895 DOI: 10.1002/hep.23927]
- Liu XL, Cao HX, Fan JG. MicroRNAs as biomarkers and regulators of nonalcoholic fatty liver disease. *J Dig Dis* 2016; **17**: 708-715 [PMID: 27628945 DOI: 10.1111/1751-2980.12408]
- Sun C, Fan JG, Qiao L. Potential epigenetic mechanism in non-alcoholic fatty liver disease. *Int J Mol Sci* 2015; **16**: 5161-5179 [PMID: 25751727 DOI: 10.3390/ijms16035161]
- Pirola CJ, Gianotti TF, Burgueño AL, Rey-Funes M, Loidl CF, Mallardi P, Martino JS, Castaño GO, Sookoian S. Epigenetic modification of liver mitochondrial DNA is associated with histological severity of nonalcoholic fatty liver disease. *Gut* 2013; **62**: 1356-1363 [PMID: 22879518 DOI: 10.1136/gutjnl-2012-302962]
- Bartel DP. MicroRNAs: genomics, biogenesis, mechanism, and function. *Cell* 2004; **116**: 281-297 [PMID: 14744438 DOI: 10.1016/S0092-8674(04)00045-5]
- Rottiers V, Näär AM. MicroRNAs in metabolism and metabolic disorders. *Nat Rev Mol Cell Biol* 2012; **13**: 239-250 [PMID: 22436747 DOI: 10.1038/nrm3313]
- Pirola CJ, Fernández Gianotti T, Castaño GO, Mallardi P, San Martino J, Mora Gonzalez Lopez Ledesma M, Flichman D, Mirshahi F, Sanyal AJ, Sookoian S. Circulating microRNA signature in non-alcoholic fatty liver disease: from serum non-coding RNAs to liver histology and disease pathogenesis. *Gut* 2015; **64**: 800-812 [PMID: 24973316 DOI: 10.1136/gutjnl-2014-306996]
- Liu XL, Pan Q, Zhang RN, Shen F, Yan SY, Sun C, Xu ZJ, Chen YW, Fan JG. Disease-specific miR-34a as diagnostic marker of non-alcoholic steatohepatitis in a Chinese population. *World J Gastroenterol* 2016; **22**: 9844-9852 [PMID: 27956809 DOI: 10.3748/wjg.v22.i44.9844]
- Roy S, Benz F, Alder J, Bantel H, Janssen J, Vucur M, Gautheron J, Schneider A, Schüller F, Loosen S, Luedde M, Koch A, Tacke F, Luedde T, Trautwein C, Roderburg C. Down-regulation of miR-192-5p protects from oxidative stress-induced acute liver injury. *Clin Sci (Lond)* 2016; **130**: 1197-1207 [PMID: 27129188 DOI: 10.1042/CS20160216]
- Lian J, Jing Y, Dong Q, Huan L, Chen D, Bao C, Wang Q, Zhao F, Li J, Yao M, Qin L, Liang L, He X. miR-192, a prognostic indicator, targets the SLC39A6/SNAIL pathway to reduce tumor metastasis in human hepatocellular carcinoma. *Oncotarget* 2016; **7**: 2672-2683 [PMID: 26684241 DOI: 10.18632/oncotarget.6603]
- Lambert JE, Ramos-Roman MA, Browning JD, Parks EJ. Increased de novo lipogenesis is a distinct characteristic of individuals with nonalcoholic fatty liver disease. *Gastroenterology* 2014; **146**: 726-735 [PMID: 24316260 DOI: 10.1053/j.gastro.2013.11.049]
- Saponaro C, Gaggini M, Carli F, Gastaldelli A. The Subtle Balance between Lipolysis and Lipogenesis: A Critical Point in Metabolic Homeostasis. *Nutrients* 2015; **7**: 9453-9474 [PMID: 26580649 DOI: 10.3390/nu7115475]
- Miyazaki M, Dobrzyn A, Man WC, Chu K, Sampath H, Kim HJ, Ntambi JM. Stearoyl-CoA desaturase 1 gene expression is necessary for fructose-mediated induction of lipogenic gene expression by sterol regulatory element-binding protein-1c-dependent and -independent mechanisms. *J Biol Chem* 2004; **279**: 25164-25171 [PMID: 15066988 DOI: 10.1074/jbc.M402781200]
- Krauskopf J, Caiment F, Claessen SM, Johnson KJ, Warner RL, Schomaker SJ, Burt DA, Aubrecht J, Kleinjans JC. Application of high-throughput sequencing to circulating microRNAs reveals novel biomarkers for drug-induced liver injury. *Toxicol Sci* 2015; **143**: 268-276 [PMID: 25359176 DOI: 10.1093/toxsci/kfu232]
- Brunetto MR, Cavallone D, Oliveri F, Moriconi F, Colombatto P, Coco B, Ciccorossi P, Rastelli C, Romagnoli V, Cherubini B, Teilmann MW, Blondal T, Bonino F. A serum microRNA signature is associated with the immune control of chronic hepatitis B virus infection. *PLoS One* 2014; **9**: e110782 [PMID: 25350115 DOI: 10.1371/journal.pone.0110782]
- Zhu HT, Liu RB, Liang YY, Hasan AME, Wang HY, Shao Q, Zhang ZC, Wang J, He CY, Wang F, Shao JY. Serum microRNA profiles as diagnostic biomarkers for HBV-positive hepatocellular carcinoma. *Liver Int* 2017; **37**: 888-896 [PMID: 28061012 DOI: 10.1111/liv.13356]
- Wen Y, Han J, Chen J, Dong J, Xia Y, Liu J, Jiang Y, Dai J, Lu J, Jin G, Han J, Wei Q, Shen H, Sun B, Hu Z. Plasma miRNAs as early biomarkers for detecting hepatocellular carcinoma. *Int J Cancer* 2015; **137**: 1679-1690 [PMID: 25845839 DOI: 10.1002/ijc.29544]
- Becker PP, Rau M, Schmitt J, Malsch C, Hammer C, Bantel H, Mühlhaupt B, Geier A. Performance of Serum microRNAs -122, -192 and -21 as Biomarkers in Patients with Non-Alcoholic Steatohepatitis. *PLoS One* 2015; **10**: e0142661 [PMID: 26565986 DOI: 10.1371/journal.pone.0142661]
- Castoldi M, Vujic Spasic M, Altamura S, Elmén J, Lindow M, Kiss J, Stolte J, Sparla R, D'Alessandro LA, Klingmüller U, Fleming RE, Longerich T, Gröne HJ, Benes V, Kauppinen S, Hentze MW, Muckenthaler MU. The liver-specific microRNA miR-122 controls systemic iron homeostasis in mice. *J Clin Invest* 2011; **121**: 1386-1396 [PMID: 21364282 DOI: 10.1172/JCI44883]
- Esau C, Davis S, Murray SF, Yu XX, Pandey SK, Pear M, Watts L, Booten SL, Graham M, McKay R, Subramaniam A, Propp S, Lollo BA, Freier S, Bennett CF, Bhanot S, Monia BP. miR-122 regulation of lipid metabolism revealed by in vivo antisense targeting. *Cell Metab* 2006; **3**: 87-98 [PMID: 16459310 DOI: 10.1016/j.cmet.2006.01.005]
- Ding J, Li M, Wan X, Jin X, Chen S, Yu C, Li Y. Effect of miR-34a in regulating steatosis by targeting PPAR $\alpha$  expression in nonalcoholic fatty liver disease. *Sci Rep* 2015; **5**: 13729 [PMID: 26330104 DOI: 10.1038/srep13729]
- Xu Y, Zalzal M, Xu J, Li Y, Yin L, Zhang Y. A metabolic stress-inducible miR-34a-HNF4 $\alpha$  pathway regulates lipid and lipoprotein metabolism. *Nat Commun* 2015; **6**: 7466 [PMID: 26100857 DOI: 10.1038/ncomms8466]
- Armstrong MJ, Gaunt P, Aithal GP, Barton D, Hull D, Parker R, Hazlehurst JM, Guo K, ; LEAN trial team, Abouda G, Aldersley MA, Stocken D, Gough SC, Tomlinson JW, Brown RM, Hübscher

- SG, Newsome PN. Liraglutide safety and efficacy in patients with non-alcoholic steatohepatitis (LEAN): a multicentre, double-blind, randomised, placebo-controlled phase 2 study. *Lancet* 2016; **387**: 679-690 [PMID: 26608256 DOI: 10.1016/S0140-6736(15)00803-X]
- 28 **Geng L**, Chaudhuri A, Talmon G, Wisecarver JL, Are C, Brattain M, Wang J. MicroRNA-192 suppresses liver metastasis of colon cancer. *Oncogene* 2014; **33**: 5332-5340 [PMID: 24213572 DOI: 10.1038/onc.2013.478]
- 29 **Lu H**, Lei X, Liu J, Klaassen C. Regulation of hepatic microRNA expression by hepatocyte nuclear factor 4 alpha. *World J Hepatol* 2017; **9**: 191-208 [PMID: 28217257 DOI: 10.4254/wjh.v9.i4.191]
- 30 **Jenkins RH**, Martin J, Phillips AO, Bowen T, Fraser DJ. Transforming growth factor  $\beta$ 1 represses proximal tubular cell microRNA-192 expression through decreased hepatocyte nuclear factor DNA binding. *Biochem J* 2012; **443**: 407-416 [PMID: 22264233 DOI: 10.1042/BJ20111861]
- 31 **Gil-Zamorano J**, Martin R, Daimiel L, Richardson K, Giordano E, Nicod N, García-Carrasco B, Soares SM, Iglesias-Gutiérrez E, Lasunción MA, Sala-Vila A, Ros E, Ordovás JM, Visioli F, Dávalos A. Docosahexaenoic acid modulates the enterocyte Caco-2 cell expression of microRNAs involved in lipid metabolism. *J Nutr* 2014; **144**: 575-585 [PMID: 24623846 DOI: 10.3945/jn.113.189050]
- 32 **Lin Y**, Ding D, Huang Q, Liu Q, Lu H, Lu Y, Chi Y, Sun X, Ye G, Zhu H, Wei J, Dong S. Downregulation of miR-192 causes hepatic steatosis and lipid accumulation by inducing SREBF1: Novel mechanism for bisphenol A-triggered non-alcoholic fatty liver disease. *Biochim Biophys Acta* 2017; **1862**: 869-882 [PMID: 28483554 DOI: 10.1016/j.bbailip.2017.05.001]
- 33 **Marchesini G**, Petta S, Dalle Grave R. Diet, weight loss, and liver health in nonalcoholic fatty liver disease: Pathophysiology, evidence, and practice. *Hepatology* 2016; **63**: 2032-2043 [PMID: 26663351 DOI: 10.1002/hep.28392]
- 34 **Rotman Y**, Sanyal AJ. Current and upcoming pharmacotherapy for non-alcoholic fatty liver disease. *Gut* 2017; **66**: 180-190 [PMID: 27646933 DOI: 10.1136/gutjnl-2016-312431]
- 35 **Bechmann LP**, Hannivoort RA, Gerken G, Hotamisligil GS, Trauner M, Canbay A. The interaction of hepatic lipid and glucose metabolism in liver diseases. *J Hepatol* 2012; **56**: 952-964 [PMID: 22173168 DOI: 10.1016/j.jhep.2011.08.025]
- 36 **Liu L**, Wang S, Yao L, Li JX, Ma P, Jiang LR, Ke DZ, Pan YQ, Wang JW. Long-term fructose consumption prolongs hepatic stearyl-CoA desaturase 1 activity independent of upstream regulation in rats. *Biochem Biophys Res Commun* 2016; **479**: 643-648 [PMID: 27697525 DOI: 10.1016/j.bbrc.2016.09.160]
- 37 **Paton CM**, Ntambi JM. Biochemical and physiological function of stearyl-CoA desaturase. *Am J Physiol Endocrinol Metab* 2009; **297**: E28-E37 [PMID: 19066317 DOI: 10.1152/ajpendo.90897.2008]
- 38 **Flowers MT**, Ntambi JM. Role of stearyl-coenzyme A desaturase in regulating lipid metabolism. *Curr Opin Lipidol* 2008; **19**: 248-256 [PMID: 18460915 DOI: 10.1097/MOL.0b013e3282f9b54d]
- 39 **Hyun CK**, Kim ED, Flowers MT, Liu X, Kim E, Strable M, Ntambi JM. Adipose-specific deletion of stearyl-CoA desaturase 1 up-regulates the glucose transporter GLUT1 in adipose tissue. *Biochem Biophys Res Commun* 2010; **399**: 480-486 [PMID: 20655875 DOI: 10.1016/j.bbrc.2010.07.072]
- 40 **Miyazaki M**, Sampath H, Liu X, Flowers MT, Chu K, Dobrzyn A, Ntambi JM. Stearyl-CoA desaturase-1 deficiency attenuates obesity and insulin resistance in leptin-resistant obese mice. *Biochem Biophys Res Commun* 2009; **380**: 818-822 [PMID: 19338759 DOI: 10.1016/j.bbrc.2009.01.183]
- 41 **Cheng X**, Xi QY, Wei S, Wu D, Ye RS, Chen T, Qi QE, Jiang QY, Wang SB, Wang LN, Zhu XT, Zhang YL. Critical role of miR-125b in lipogenesis by targeting stearyl-CoA desaturase-1 (SCD-1). *J Anim Sci* 2016; **94**: 65-76 [PMID: 26812313 DOI: 10.2527/jas.2015-9456]
- 42 **Qiang J**, Tao YF, He J, Sun YL, Xu P. miR-29a modulates SCD expression and is regulated in response to a saturated fatty acid diet in juvenile genetically improved farmed tilapia (*Oreochromis niloticus*). *J Exp Biol* 2017; **220**: 1481-1489 [PMID: 28167804 DOI: 10.1242/jeb.151506]
- 43 **Jonas S**, Izaurralde E. Towards a molecular understanding of microRNA-mediated gene silencing. *Nat Rev Genet* 2015; **16**: 421-433 [PMID: 26077373 DOI: 10.1038/nrg3965]

**P- Reviewer:** Gallego-Duran R, Pirola CJ **S- Editor:** Qi Y **L- Editor:** Wang TQ **E- Editor:** Ma YJ



## Basic Study

***In vivo* hepatic differentiation potential of human umbilical cord-derived mesenchymal stem cells: Therapeutic effect on liver fibrosis/cirrhosis**

Guo-Zun Zhang, Hui-Cong Sun, Li-Bo Zheng, Jin-Bo Guo, Xiao-Lan Zhang

Guo-Zun Zhang, Hui-Cong Sun, Li-Bo Zheng, Jin-Bo Guo, Xiao-Lan Zhang, Department of Gastroenterology, The Second Hospital of Hebei Medical University, Shijiazhuang 050000, Hebei Province, China

Guo-Zun Zhang, First Department of Gastroenterology, Cangzhou Central Hospital, Cangzhou 061001, Hebei Province, China

Hui-Cong Sun, Department of Internal Medicine, Ningbo Women and Children's Hospital, Ningbo 315012, Zhejiang Province, China

**Author contributions:** Zhang GZ and Sun HC substantially contributed to the conception and design of the study and the acquisition, analysis and interpretation of the data; all authors drafted the article, made critical revisions related to the intellectual content of the manuscript, and approved the final version of the article to be published; Zhang GZ and Sun HC contributed equally to this manuscript.

**Institutional review board statement:** The study was reviewed and approved by the Hebei Medical University Institutional Review Board.

**Institutional animal care and use committee statement:** All procedures involving animals were reviewed and approved by the Institutional Animal Care and Use Committee of the Experimental Animal Center of Hebei Medical University (No. 911102).

**Conflict-of-interest statement:** We declare that there are no conflicts of interest to disclose.

**Data sharing statement:** Technical appendix, statistical code, and data set available from the corresponding author at [xiaolanzh@126.com](mailto:xiaolanzh@126.com). Participants gave informed consent for data sharing.

**Open-Access:** This article is an open-access article which was selected by an in-house editor and fully peer-reviewed by external reviewers. It is distributed in accordance with the Creative Commons Attribution Non Commercial (CC BY-NC 4.0) license,

which permits others to distribute, remix, adapt, build upon this work non-commercially, and license their derivative works on different terms, provided the original work is properly cited and the use is non-commercial. See: <http://creativecommons.org/licenses/by-nc/4.0/>

**Manuscript source:** Unsolicited manuscript

**Correspondence to:** Xiao-Lan Zhang, MD, PhD, Professor, Department of Gastroenterology, The Second Hospital of Hebei Medical University, 215 West Heping Road, Shijiazhuang 050000, Hebei Province, China. [xiaolanzh@hb2h.com](mailto:xiaolanzh@hb2h.com)  
**Telephone:** +86-311-66007370

**Received:** March 27, 2017

**Peer-review started:** March 29, 2017

**First decision:** May 3, 2017

**Revised:** May 29, 2017

**Accepted:** August 9, 2017

**Article in press:** August 9, 2017

**Published online:** December 14, 2017

**Abstract****AIM**

To investigate the hepatic differentiation potential of human umbilical cord-derived mesenchymal stem cells (hUC-MSCs) and to evaluate their therapeutic effect on liver fibrosis/cirrhosis.

**METHODS**

A CCl<sub>4</sub>-induced liver fibrotic/cirrhotic rat model was used to assess the effect of hUC-MSCs. Histopathology was assessed by hematoxylin and eosin (H&E), Masson trichrome and Sirius red staining. The liver biochemical profile was measured using a Beckman Coulter analyzer. Expression analysis was performed using immunofluorescent staining, immunohistochemistry, Western blot, and real-time PCR.

## RESULTS

We demonstrated that the infused hUC-MSCs could differentiate into hepatocytes *in vivo*. Functionally, the transplantation of hUC-MSCs to CCl<sub>4</sub>-treated rats improved liver transaminases and synthetic function, reduced liver histopathology and reversed hepatobiliary fibrosis. The reversal of hepatobiliary fibrosis was likely due to the reduced activation state of hepatic stellate cells, decreased collagen deposition, and enhanced extracellular matrix remodeling *via* the up-regulation of MMP-13 and down-regulation of TIMP-1.

## CONCLUSION

Transplanted hUC-MSCs could differentiate into functional hepatocytes that improved both the biochemical and histopathologic changes in a CCl<sub>4</sub>-induced rat liver fibrosis model. hUC-MSCs may offer therapeutic opportunities for treating hepatobiliary diseases, including cirrhosis.

**Key words:** Liver fibrosis/cirrhosis; Mesenchymal stem cells; Collagen metabolism; Hepatocyte; Differentiation

© The Author(s) 2017. Published by Baishideng Publishing Group Inc. All rights reserved.

**Core tip:** Transplanted human umbilical cord-derived mesenchymal stem cells (hUC-MSCs) could differentiate into hepatocytes *in vivo*, thereby reducing the activation state of hepatic stellate cells, decreasing collagen deposition, and enhancing extracellular matrix remodeling in liver cirrhosis. hUC-MSCs play an important role in treating liver fibrosis and cirrhosis.

Zhang GZ, Sun HC, Zheng LB, Guo JB, Zhang XL. *In vivo* hepatic differentiation potential of human umbilical cord-derived mesenchymal stem cells: Therapeutic effect on liver fibrosis/cirrhosis. *World J Gastroenterol* 2017; 23(46): 8152-8168 Available from: URL: <http://www.wjgnet.com/1007-9327/full/v23/i46/8152.htm> DOI: <http://dx.doi.org/10.3748/wjg.v23.i46.8152>

## INTRODUCTION

Chronic liver inflammation is a major driving force for extracellular matrix (ECM) accumulation and can lead to liver cirrhosis with resultant complications such as portal hypertension and hepatocellular carcinoma<sup>[1,2]</sup>. The economic burden of cirrhosis is significant with the cost for treatment in 2008 ranging from \$14 million to \$2 billion in the United States, depending on the disease etiology<sup>[3]</sup>. This burden is expected to rise over the next 20 years. Given that cirrhosis is a worldwide problem that is associated with substantial socioeconomic burden, effective therapeutic strategies would be impactful.

Liver transplantation is an effective method for treating end-stage liver disease, but donor scarcity and

immunological rejection limit its clinical application<sup>[4]</sup>. This has led to the search for alternative sources of hepatocytes, including cell-based therapy using mesenchymal stem cells (MSCs). MSCs are multipotent stromal cells that can differentiate into a variety of cell types. MSCs, including bone marrow-derived MSCs (BM-MSCs), have been demonstrated to reduce the generation of ECM and collagen deposition, thereby ameliorating liver fibrosis and cirrhosis<sup>[5,6]</sup>. In addition, BM-MSCs can differentiate into functional hepatocytes to repair damaged liver tissue, improving liver fibrosis and cirrhosis<sup>[7]</sup>.

Among various MSCs types, human umbilical cord-derived MSCs (hUC-MSCs) may be best as an alternative for hepatocyte transplantation, because of their ease of extraction, low risk of viral transmission, low immunogenicity and immunosuppressive effects. To better understand the mechanism and therapeutic potential of hUC-MSCs, we developed a CCl<sub>4</sub>-induced rat liver fibrosis/cirrhosis model. We described the dynamic differentiation process of hUC-MSCs into functional hepatocytes *in vivo* and showed that transplanted hUC-MSCs can improve biochemical and histological abnormalities in this model. Our data suggest that hUC-MSCs may be an attractive, alternative therapeutic for treating liver disease, including cirrhosis.

## MATERIALS AND METHODS

### MSC isolation and culture

The umbilical cord was cut into 1-mm<sup>3</sup> pieces and filtered through a 1.5-mm mesh. Filtered umbilical cord pieces were seeded in DMEM/F12 complete medium. Fresh medium was replaced every 3 to 4 d, and non-adherent cells were discarded. When the observed cells reached 80% confluency, hUC-MSCs were separated by trypsin digestion, cultured, and identified by Alliances Bioscience Co., Ltd.

### Animal models

One hundred and twenty adult male Wistar rats, weighing 350-450 g, were obtained from the Experimental Animal Center of Hebei Medical University. The research was conducted in accordance with the internationally accepted principles for laboratory animal use and care, as found in the US guidelines (NIH publication #85-23, revised in 1985). The experiment was performed in compliance with the national ethical guidelines for the care and use of laboratory animals (Certificate No. 911102).

Rat models of liver fibrosis and cirrhosis were established by hypodermic injection of CCl<sub>4</sub> mixed with olive oil at a concentration of 40% (2 mL/kg) every Monday and Thursday. Rats injected with saline served as a control group. In the fibrosis group, after the sixth injection of CCl<sub>4</sub>, 5 × 10<sup>6</sup> hUC-MSCs were injected into the rats *via* the tail vein. Rats continued to be treated



with CCl<sub>4</sub>. After 1, 2, or 4 wk of hUC-MSCs infusion, rats were sacrificed to assess the related index of liver fibrosis. In the cirrhosis group, rats were treated with CCl<sub>4</sub> for up to 6 wk, and  $5 \times 10^6$  hUC-MSCs were injected into the rats *via* the tail vein. Rats continued to be treated with CCl<sub>4</sub>. After 2, 4, or 8 wk, rats were sacrificed to determine the related indicators. In the control group, the same volumes of saline were injected into the rats *via* the tail vein.

#### Serum parameter determination

Alanine aminotransferase (ALT), aspartate aminotransferase (AST), albumin (ALB), total bilirubin (TBIL) and direct bilirubin (DBIL) were evaluated in the samples of serum obtained at the end of the experiment. All tests were completed using the BECKMAN COULTER CX9 automatic biochemical analyzer.

#### Histopathology

Liver specimens were fixed for 12–24 h in 4% phosphate-buffered paraformaldehyde (Huarui Scientific and Technological Co.) and then embedded in paraffin for light microscopy examination. Tissue sections (3 µm thick) were stained with hematoxylin and eosin (H&E) for morphological evaluation and Masson trichrome (MT) to assess the degree of fibrosis.

#### Immunofluorescence

Immunofluorescent studies were performed on 3-µm paraffin-embedded liver sections. Briefly, the sections were fixed with 4% phosphate-buffered paraformaldehyde and washed with 0.1% TritonX-100 TBS (TBSTx). Five percent bovine serum albumin (BSA) in TBSTx was used as a sealed liquid and then the specimens were incubated overnight at 4 °C with mouse monoclonal anti-human specific albumin (ALB) antibody (1:100; BETHYL) and mouse monoclonal anti-human specific  $\alpha$ -fetoprotein (AFP) antibody (1:100; Thermo Scientific, Inc., United States). After the sections were washed, the Cy3-labeled goat anti-mouse IgG secondary antibody or FITC-labeled goat anti-rabbit (1:400 dilution) (Beyotime Institute of Biotechnology, Shanghai, China) was added and the sections were incubated at 37 °C for 1 h. DAPI (4', 6-diamidino-2-phenylindole) was used for nuclear staining. The negative control samples were processed under the same conditions, except that 5% BSA in TBSTx was used in place of the primary antibody. The ALB and AFP positive expression levels were measured using a Motic Med 6.0 digital video image analysis system (Motic China Group Co., Ltd., Xiamen, China) and expressed as optical density values.

#### Immunohistochemistry

Immunohistochemistry studies were performed on 3-µm paraffin-embedded liver sections. The sections were fixed with 4% phosphate-buffered

paraformaldehyde and washed with PBS. Five percent BSA in TBSTx was used as a sealed liquid, and the specimens were then incubated overnight at 4 °C with the primary antibody mouse monoclonal anti-human specific CK18 antibody (1:200; Thermo Scientific, Inc.), mouse monoclonal anti-human specific CK19 antibody (1:200; Thermo Scientific, Inc.), mouse monoclonal anti-human specific vimentin antibody (1:200; Santa Cruz Biotechnology, Inc., Santa Cruz, CA, United States), mouse monoclonal anti-human specific E-cadherin antibody (1:200; Santa Cruz Biotechnology, Inc.), mouse monoclonal anti-human specific  $\alpha$ -catenin antibody (1:200; Santa Cruz Biotechnology, Inc.), rabbit monoclonal anti- $\alpha$ -SMA antibody (1:200; Santa Cruz Biotechnology, Inc.), goat polyclonal anti-collagen I antibody (1:100; Santa Cruz Biotechnology, Inc.), mouse polyclonal anti-collagen III antibody (1:200; Santa Cruz Biotechnology, Inc.), rabbit polyclonal anti-MMP-13 antibody (1:200; Boasens, Beijing, China), and rabbit polyclonal anti-TIMP-1 antibody (1:200; Santa Cruz Biotechnology, Inc.). After incubation with peroxidase-conjugated secondary antibody, signals were visualized with a diaminobenzidine peroxidase substrate kit (Vector Laboratories). The negative control samples were processed under the same conditions, except that 5% BSA in TBSTx was used in place of the primary antibody. The expression levels were measured using a Motic Med 6.0 digital video image analysis system (Motic China Group Co., Ltd.) and expressed as optical density values.

#### Western blot analysis

Primary antibodies included mouse anti-CK18, CK19, ALB, and AFP monoclonal antibodies (1:500); mouse anti-vimentin, E-cadherin, and  $\alpha$ -catenin antibodies (1:200); goat anti-collagen I polyclonal antibody (1:100); mouse anti-collagen III polyclonal antibody (1:500); rabbit anti-MMP-13 and TIMP-1 polyclonal antibody (1:200) and rabbit anti- $\beta$ -actin monoclonal antibody (1:200). Western blot was performed as previously described<sup>[8]</sup>.

#### Real-time fluorescent quantitative PCR

Total RNA was extracted with TRIzol reagent (Invitrogen, United States) according to the manufacturer's instructions. cDNA was generated using 2 µg of total RNA as described<sup>[9]</sup>.

Primer Express 5.0 was used to design the following primers: ALB forward primer, 5'-GCT TGA ATG TGC TGA TGA CAG G-3' and reverse primer, 5'-TGG GAT TTT TCC AAC AGA GGT T-3'; AFP forward primer, 5'-AAG TGA AGA GGG AAG ACA TAA C-3' and reverse primer, 5'-AGA AGA ATT GTA GGT GCA TAC A-3'; CK18 forward primer, 5'-TAA TCT TGG TGA TGC CTT GGA C-3' and reverse primer, 5'-CCT CAG AAC TTT GGT GTC ATT G-3'; CK19 forward primer, 5'-GCC ACT ACT ACA CGA CCA TCC A-3' and reverse primer, 5'-AGA GCC

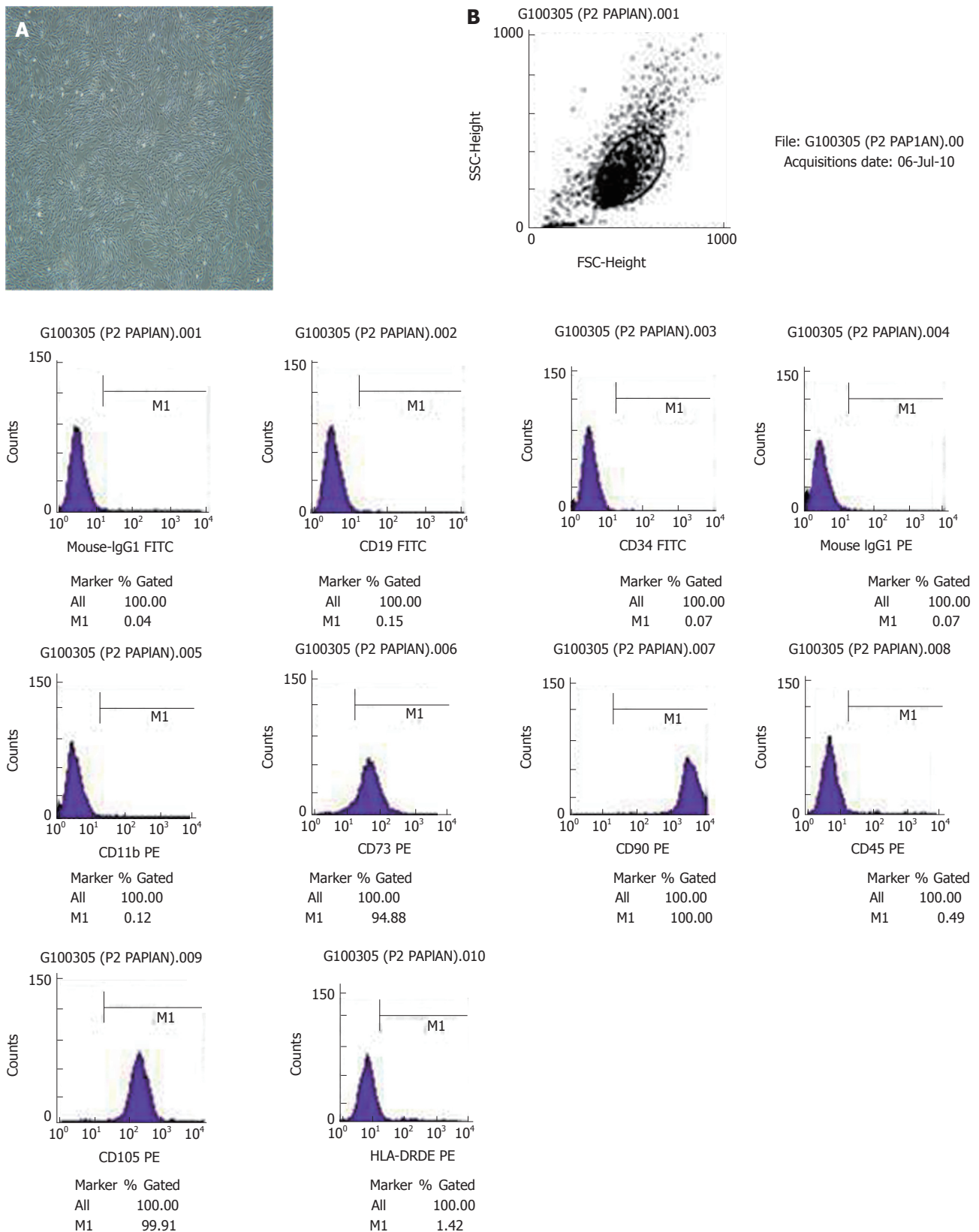


**Figure 1 Morphology of umbilical cord-derived mesenchymal stem cells and immunophenotype analysis using FACS.** A: The morphology of umbilical cord-derived mesenchymal stem cells (UC-MSCs) ( $\times 100$ ); B: Immunophenotype analysis using FACS. The 3rd passage hUC-MSCs are shown, and the adherent cells displayed a fibroblastic morphology. Immunophenotype analysis using FACS showed that hUC-MSCs were positive for the human MSC-specific markers CD90, CD105 and CD73 but were negative for CD34, CD19, CD11b, HLA-DR and CD45.

TGT TCC GTC TCA AAC T-3'; vimentin forward primer, 5'-ATG TTG ACA ATG CGT CTC TGG CTC CA-3' and

reverse primer, 5'-ATT TCC TCT TCG TGG AGT TTC T-3'; N-cadherin forward primer, 5'-CAG CCT CCA ACT GGT

ATC TTC A-3' and reverse primer, 5'-ATC TAC TGC ATG TGC CC TCA AA-3'; E-cadherin forward primer, 5'-CCA GGA GGT CTT TAA GGG GTC T-3' and reverse primer, 5'-GCT GAGG ATG GTG TAA GCG ATG-3';  $\alpha$ -catenin forward primer, 5'-GCA AAG AAT GGA AAT GAG AAA G-3' and reverse primer, 5'-AAT AAC CTG AGG ACA GAG GGC T-3'; collagen I forward primer, 5'-GTG CGA TGG GGT GCT ATG-3' and reverse primer, 5'-TCT GCG TCT GGT GAT ACA TAT TC-3'; collagen III forward primer, 5'-ACC TGC TCC TGT CAT TCC-3' and reverse primer, 5'- CCT CCG ACT CCA GAC TTG-3'; MMP-13 forward primer, 5'-CCA CCT TCT TGT TGA GTT G-3' and reverse primer, 5'-AAG AGT CAC AGG ATG GTA GTA TG-3'; TIMP-1 forward primer, 5'-CGC TGG TAT AAG GTG GTC TC-3' and reverse primer, 5'-CGC TGG TAT AAG GTG GTC TC-3'; and GAPDH forward primer, 5'-GGC AAG TTC AAC GGC ACA G-3' and reverse primer, 5'-CGC CAG TAG ACT CCA CGA CAT -3'. Real-time fluorescent quantitative PCR was performed on an ABI Prism 7700 real-time fluorescent quantitative PCR thermal cycler (Applied Biosystems, Foster City, CA, United States), and the expression of the above genes was normalized to that of GAPDH.

### Statistical analysis

Data are presented as the mean  $\pm$  SD and analyzed using SPSS18.0 software. The performed statistical analyses included one-way ANOVA, the LSD test and Pearson's correlation analysis.  $P < 0.05$  was considered statistically significant.

## RESULTS

### Characterization of hUC-MSCs *in vitro* and *in vivo*

We isolated hUC-MSCs that exhibited fibroblast-like morphology from the umbilical cord (Figure 1A). Flow cytometry showed that hUC-MSCs expressed high levels of MSCs-specific markers CD90, CD105 and CD73 but no or low levels of CD34, CD19, CD11b, HLA-DR and CD45 (Figure 1B). We next transplanted hUC-MSCs into rats and assessed their potential to differentiate into hepatocytes. We detected ALB, AFP, CK18 and CK19 from human origin, but the rat-derived ALB, AFP, CK18 and CK19 were not detected. Therefore, the differentiated hepatocytes of rats had no effect on the results. Prior to transplantation, there was no positive expression of human ALB, AFP, CK18 or CK19. After transplantation, we detected the expression of the above markers.

Immunofluorescence and immunohistochemistry showed that compared to the saline/CCl<sub>4</sub> groups, the positive expression of the above markers showed different patterns in the MSCs/CCl<sub>4</sub> fibrotic and cirrhotic groups. The expression of ALB, AFP, CK18 and CK19 was weakly positive and faint in spots at 1 or 2 wk, respectively, in the MSCs/CCl<sub>4</sub> fibrotic and cirrhotic groups. However, at 2, 4, or 8 wk after hUC-MSC infusion, with an extension of the transplantation time,

the positive expression of ALB, AFP, CK18 and CK19 was gradually increased, in addition to the decreased expression of the AFP and CK19 in the MSCs/CCl<sub>4</sub> cirrhotic group at 8 wk after hUC-MSC infusion.

The mRNA levels of ALB and CK18 were not significantly different between 2 wk and 1 wk in the MSCs/CCl<sub>4</sub> fibrotic groups, while the expression of ALB and CK18 mRNAs was significantly increased at 4 wk compared to 2 wk ( $P < 0.01$ ). With the extension of the transplantation time, the expression levels of AFP and CK19 mRNAs were significantly elevated ( $P < 0.01$ ). In the cirrhotic MSCs/CCl<sub>4</sub> groups, the expression levels of AFP and CK19 mRNAs were significantly elevated at 4 wks compared to 2 wk ( $P < 0.01$ ). However, the expression levels of AFP and CK19 mRNAs were significantly decreased at 8 wk compared to 4 wk ( $P < 0.01$ ); as the time of hUC-MSC transplantation was extended, the expression levels of ALB and hCK18 increased, and the relative protein quantitation was consistent with the above results (Figure 2).

### *hUC-MSCs differentiate into hepatocyte-like cells through the mesenchymal-to-epithelial transition in vivo*

Next, we analyzed the levels of human vimentin (a mesenchymal marker) and human E-cadherin and  $\alpha$ -catenin (epithelial markers) by immunohistochemistry, Western blot and real-time PCR. To determine whether hUC-MSCs experienced the mesenchymal-to-epithelial transition (MET) during hepatocyte differentiation *in vivo*, the expression levels of vimentin, E-cadherin and  $\alpha$ -catenin were detected. After 1 or 2 wk of hUC-MSC transplantation, in the fibrotic and cirrhotic MSCs/CCl<sub>4</sub> groups, many positive cells for vimentin were expressed in the portal vein and portal area. As the time of hUC-MSC transplantation extended, the expression of vimentin was significantly decreased in both the fibrotic and cirrhotic MSCs/CCl<sub>4</sub> groups. At 8 wk after hUC-MSC transplantation, a low level of vimentin was expressed. There was no expression before hUC-MSC transplantation. The relative expression levels of protein and mRNA were consistent with the above results ( $P < 0.01$ ).

In the fibrotic MSCs/CCl<sub>4</sub> groups, at 1 wk after hUC-MSC transplantation, low levels of E-cadherin and  $\alpha$ -catenin expression were detected by immunohistochemistry, which gradually increased with the extension of hUC-MSC transplantation. In the cirrhotic MSCs/CCl<sub>4</sub> groups, at 2 wk after hUC-MSC transplantation, low E-cadherin and  $\alpha$ -catenin levels were seen. The E-cadherin and  $\alpha$ -catenin expressions levels were significantly increased at 4 wk after hUC-MSCs transplantation compared to 2 wk in the fibrotic and cirrhotic MSCs/CCl<sub>4</sub> groups. By contrast, the levels of the above indicators decreased significantly at 8 wk compared to 4 wk after hUC-MSC transplantation. The relative protein and mRNA expression levels were



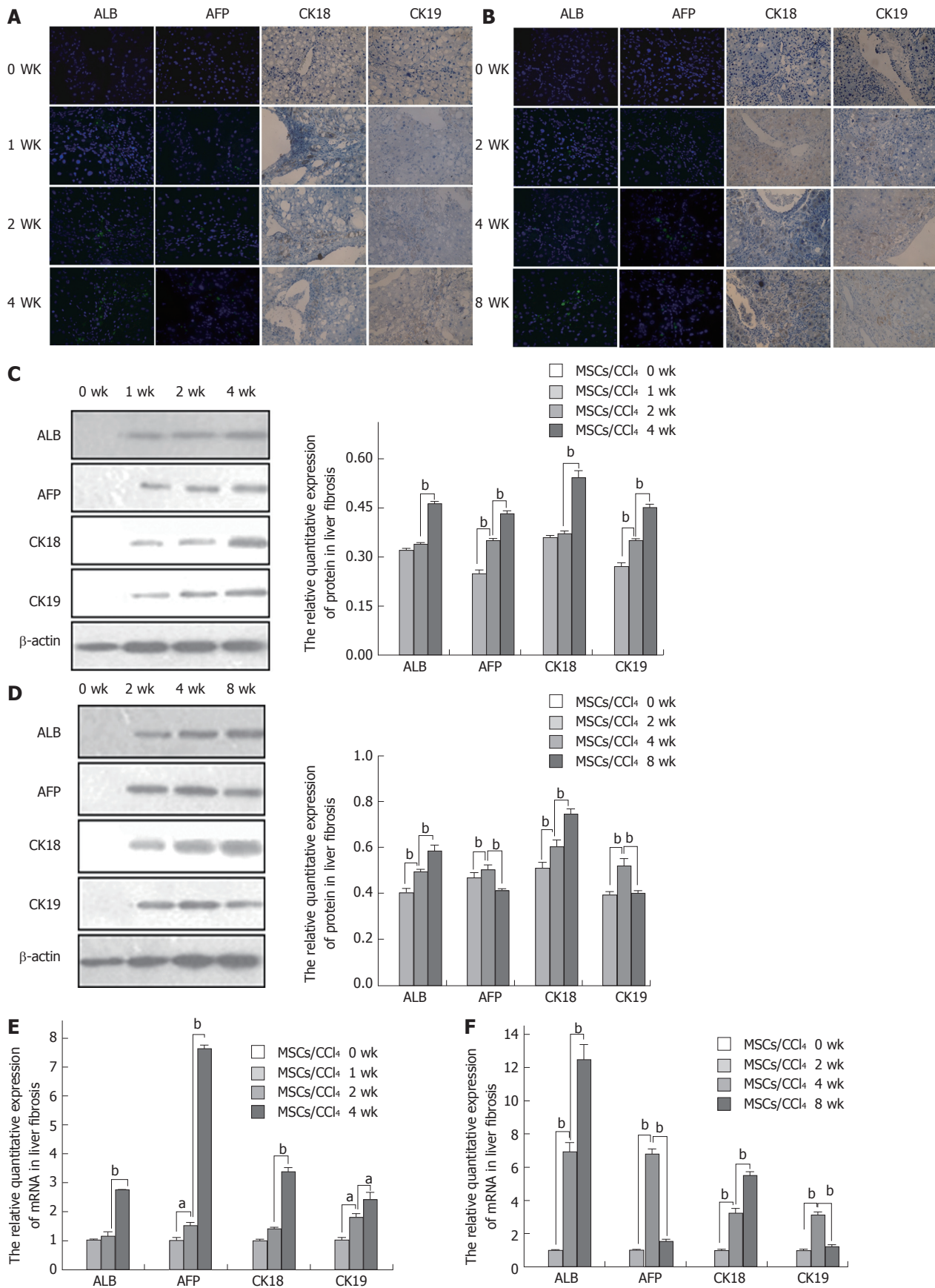


**Figure 2** Expression of human hepatic markers in rat liver tissues. A, C, and E: Immunohistochemical, Western blot, and real-time PCR analysis of human albumin (ALB), α-fetoprotein (AFP), CK18, and CK19 in rat fibrotic livers at 0, 1, 2, and 4 wk after human umbilical cord-derived mesenchymal stem cell (hUC-MSC) transplantation, respectively; B, D, and F: Immunohistochemical, Western blot, and real-time PCR analysis of human ALB, AFP, CK18, or CK19 in rat cirrhotic livers at 0, 2, 4, and 8 wk after hUC-MSC transplantation, respectively, <sup>a</sup>*P* < 0.05; <sup>b</sup>*P* < 0.01.



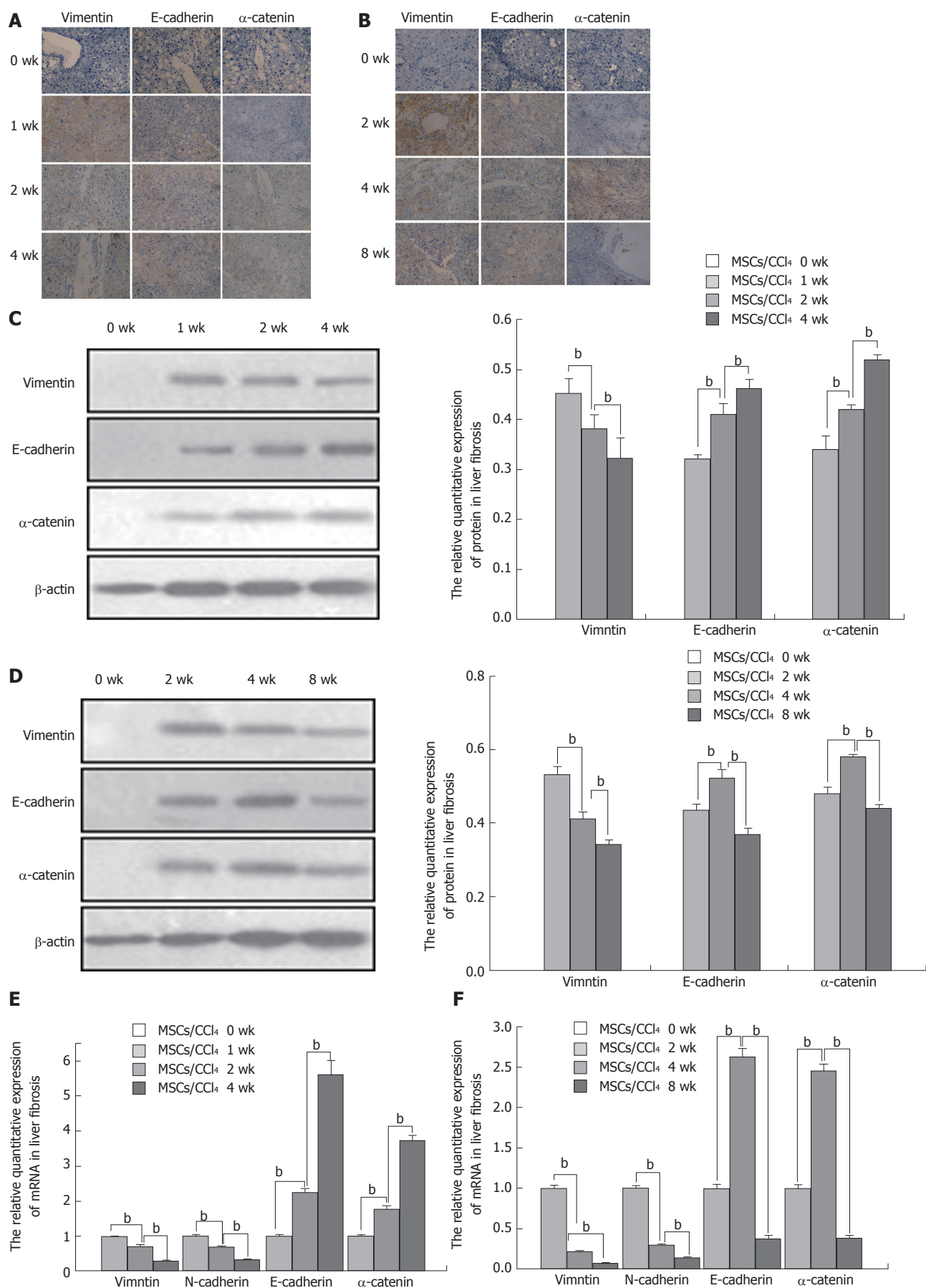


**Figure 3** Expression of human vimentin, a mesenchymal marker, and human E-cadherin and  $\alpha$ -catenin, epithelial markers, in rat liver tissues. A, C, and E: Immunohistochemical, Western blot, and real-time PCR analysis of human vimentin, E-cadherin and  $\alpha$ -catenin in rat fibrotic livers at 0, 1, 2, and 4 wk after human umbilical cord-derived mesenchymal stem cell (hUC-MSC) transplantation, respectively; B, D, and F: Immunohistochemical, Western blot, and real-time PCR analysis of human vimentin, E-cadherin and  $\alpha$ -catenin in rat cirrhotic livers at 0, 2, 4, and 8 wk after hUC-MSC transplantation, respectively,  $^bP < 0.01$ .

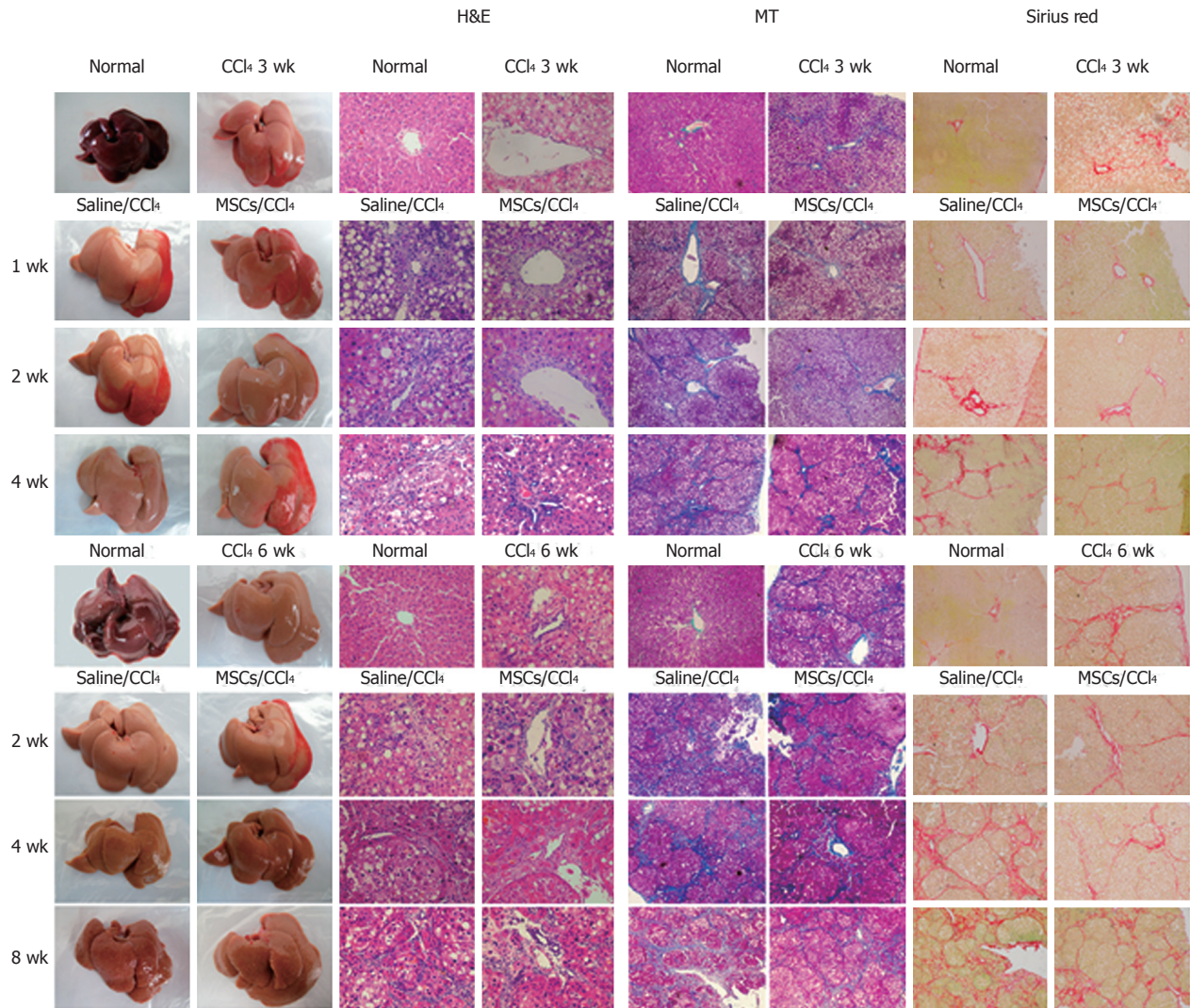


**Figure 4** Representative photographs of the fresh livers, hematoxylin and eosin staining (H&E staining), Masson's trichrome staining (MT staining) and sirius red staining in rat fibrotic or cirrhotic hepatic tissues. Liver sections were stained with hematoxylin and eosin (H&E,  $\times 400$ ), Masson's trichrome (MT,  $\times 100$ ) and Sirius red ( $\times 100$ ) or representative photographs of the fresh livers without fixation were used to evaluate histopathological changes for liver tissues in control conditions; with CCl<sub>4</sub> for 3 wk; or with 1, 2, and 4 wk in fibrotic rat tissues; with CCl<sub>4</sub> for 6 wk; or with 2, 4, and 8 wk in cirrhotic rat tissues after human umbilical cord-derived mesenchymal stem cell (hUC-MSC) or saline injection into rats.

**Table 1** Impact of mesenchymal stem cells on liver function indexes in each group ( $n = 10$ , mean  $\pm$  SD)

Group		ALT(U/L)	AST(U/L)	ALB(g/L)	TBIL ( $\mu$ mol/L)	DBIL ( $\mu$ mol/L)
Liver fibrosis groups	Saline/CCl <sub>4</sub> 1 wk	141.00 $\pm$ 16.33	150.76 $\pm$ 15.13	29.99 $\pm$ 1.53	0.97 $\pm$ 0.15	0.70 $\pm$ 0.02
	MSCs/CCl <sub>4</sub> 1 wk	130.32 $\pm$ 15.35	142.32 $\pm$ 14.24	32.17 $\pm$ 2.25	0.93 $\pm$ 0.08	0.60 $\pm$ 0.04
	Saline/CCl <sub>4</sub> 2 wk	152.35 $\pm$ 14.56	172.22 $\pm$ 19.34	24.54 $\pm$ 1.21	1.51 $\pm$ 0.21	0.90 $\pm$ 0.07
	MSCs/CCl <sub>4</sub> 2 wk	132.88 $\pm$ 13.23 <sup>a</sup>	146.23 $\pm$ 13.23 <sup>a</sup>	26.60 $\pm$ 2.34	1.33 $\pm$ 0.25	0.70 $\pm$ 0.05
	Saline/CCl <sub>4</sub> 4 wk	239.24 $\pm$ 26.32	262.34 $\pm$ 28.12	28.12 $\pm$ 2.13	2.10 $\pm$ 0.23	1.10 $\pm$ 0.17
	MSCs/CCl <sub>4</sub> 4 wk	192.32 $\pm$ 21.24 <sup>b</sup>	204.52 $\pm$ 23.24 <sup>b</sup>	21.12 $\pm$ 1.94 <sup>b</sup>	1.57 $\pm$ 0.15 <sup>b</sup>	0.50 $\pm$ 0.03 <sup>b</sup>
Liver cirrhosis groups	Saline/CCl <sub>4</sub> 2 wk	334.36 $\pm$ 37.48	375.24 $\pm$ 41.26	26.55 $\pm$ 1.51	2.27 $\pm$ 0.15	1.32 $\pm$ 0.12
	MSCs/CCl <sub>4</sub> 2 wk	204.31 $\pm$ 22.52 <sup>c</sup>	289.13 $\pm$ 32.22 <sup>c</sup>	19.62 $\pm$ 1.54	1.90 $\pm$ 0.14 <sup>c</sup>	0.80 $\pm$ 0.09 <sup>c</sup>
	Saline/CCl <sub>4</sub> 4 wk	353.35 $\pm$ 38.76	406.24 $\pm$ 44.31	22.69 $\pm$ 2.72	3.34 $\pm$ 0.76	2.07 $\pm$ 0.15
	MSCs/CCl <sub>4</sub> 4 wk	214.11 $\pm$ 23.24 <sup>d</sup>	292.24 $\pm$ 32.32 <sup>d</sup>	20.36 $\pm$ 1.53 <sup>d</sup>	2.06 $\pm$ 0.14 <sup>d</sup>	1.10 $\pm$ 0.13 <sup>d</sup>
	Saline/CCl <sub>4</sub> 8 wk	391.22 $\pm$ 43.57	418.63 $\pm$ 45.71	19.31 $\pm$ 1.52	4.82 $\pm$ 0.52	3.74 $\pm$ 0.25
	MSCs/CCl <sub>4</sub> 8 wk	247.31 $\pm$ 27.36 <sup>e</sup>	307.22 $\pm$ 34.36 <sup>e</sup>	23.70 $\pm$ 7.72 <sup>e</sup>	3.32 $\pm$ 0.31 <sup>e</sup>	2.13 $\pm$ 0.15 <sup>e</sup>

<sup>a</sup> $P < 0.05$  vs Saline/CCl<sub>4</sub> 2 wk, <sup>b</sup> $P < 0.05$  vs Saline/CCl<sub>4</sub> 4 wk (in the liver fibrosis groups); <sup>c</sup> $P < 0.05$  vs Saline/CCl<sub>4</sub> 2 wk, <sup>d</sup> $P < 0.01$  vs Saline/CCl<sub>4</sub> 4 wk, and <sup>e</sup> $P < 0.01$  vs Saline/CCl<sub>4</sub> 8 wk (in the liver cirrhosis groups). ALT: Alanine aminotransferase; AST: Aspartate aminotransferase; ALB: Albumin; TBIL: Total bilirubin; DBIL: Direct bilirubin.



**Table 2** Inflammation scores in each group ( $n = 10$ , mean  $\pm$  SD)

	Liver fibrosis groups			Liver cirrhosis groups		
	1 wk	2 wk	4 wk	2 wk	4 wk	8 wk
Saline/CCl <sub>4</sub>	1.63 $\pm$ 0.05	1.95 $\pm$ 0.06	2.67 $\pm$ 0.08	3.09 $\pm$ 0.07	3.61 $\pm$ 0.09	4.12 $\pm$ 0.11
MSCs/CCl <sub>4</sub>	1.25 $\pm$ 0.04	1.45 $\pm$ 0.05 <sup>a</sup>	1.75 $\pm$ 0.07 <sup>b</sup>	2.15 $\pm$ 0.06 <sup>c</sup>	2.28 $\pm$ 0.07 <sup>d</sup>	3.06 $\pm$ 0.08 <sup>d</sup>

<sup>a</sup> $P < 0.05$  vs Saline/CCl<sub>4</sub> 2 wk, <sup>b</sup> $P < 0.05$  vs Saline/CCl<sub>4</sub> 4 wk (in the liver fibrosis groups); <sup>c</sup> $P < 0.05$  vs Saline/CCl<sub>4</sub> 2 wk, <sup>d</sup> $P < 0.01$  vs Saline/CCl<sub>4</sub> 4 wk, (in the liver cirrhosis groups).

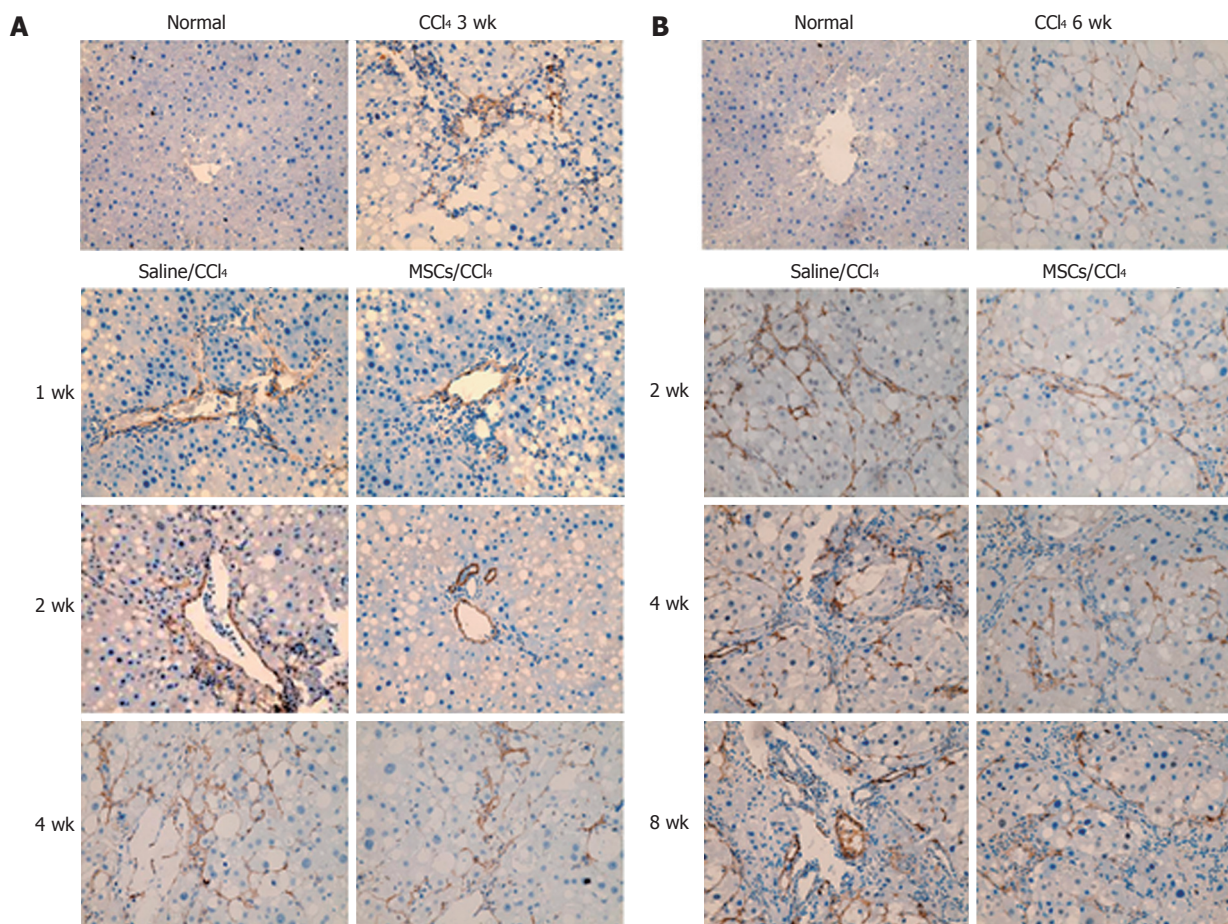


**Figure 5** Immunohistochemical staining for  $\alpha$ -smooth muscle actin in hepatic fibrosis and cirrhosis groups ( $\times 400$ ). A: Immunohistochemical staining for  $\alpha$ -smooth muscle actin ( $\alpha$ -SMA) in hepatic fibrosis groups; B: Immunohistochemical staining for  $\alpha$ -SMA in hepatic cirrhosis groups. In normal rat liver,  $\alpha$ -SMA was occasionally detected in vascular smooth muscle cells, and the expression level was low, revealing few activated hepatic stellate cells (HSCs). After CCl<sub>4</sub> administration, the  $\alpha$ -SMA spread to the portal area, showing more activated HSCs. The expression of  $\alpha$ -SMA in liver tissues increased significantly in the saline infusion group compared with the normal group. Compared with the saline infusion groups, they significantly decreased in the MSC transplantation groups.

consistent with these results ( $P < 0.01$ ; Figure 3).

#### **hUC-MSCs improve the biochemical indexes in the CCl<sub>4</sub>-induced hepatic injury model**

CCl<sub>4</sub>-induced hepatic injury in rats has been used as a model system to study liver damage and fibrosis, and we used this model to assess the therapeutic effect of hUC-MSCs. The hUC-MSCs were transplanted into a CCl<sub>4</sub>-induced liver fibrotic/cirrhotic rat model, and we observed a significant reduction in the serum levels of ALT and AST at 2 and 4 wk in the fibrotic MSCs/CCl<sub>4</sub>

groups and at 2, 4, and 8 wk in the cirrhotic MSCs/CCl<sub>4</sub> groups ( $P < 0.05$ ). In addition, the serum level of ALB was gradually reduced with further CCl<sub>4</sub> induction in the fibrotic and cirrhotic saline/CCl<sub>4</sub> groups, whereas after the transplantation of hUC-MSCs, the serum levels of ALB were markedly increased at 4 wk in the fibrotic MSCs/CCl<sub>4</sub> groups and at 4 and 8 wk in the cirrhotic MSCs/CCl<sub>4</sub> groups ( $P < 0.05$ ). Compared with the saline/CCl<sub>4</sub> groups, the serum levels of TBIL and DBIL greatly dropped at 4 wk in the fibrotic MSCs/CCl<sub>4</sub> groups and at 2, 4, and 8 wk in the cirrhotic MSCs/CCl<sub>4</sub>

groups ( $P < 0.05$ ; Table 1). The inflammation score in rat liver fibrosis and cirrhosis induced by CCl<sub>4</sub> in each group are listed in Table 2.

#### ***hUC-MSCs reverse the CCl<sub>4</sub>-induced liver histopathological changes***

Transplantation of hUC-MSCs improved the gross liver morphology by reducing the surface coarseness, reducing the liver turgor, and improving the liver perfusion (Figure 4, right panels).

Histologic examination of the CCl<sub>4</sub>-treated liver revealed swelling of the hepatocytes, fatty degeneration, necrosis and regeneration, particularly with continued CCl<sub>4</sub> administration (Figure 4). These alterations were reduced after the infusion of hUC-MSCs.

To determine the extent of the collagen deposition, MT and Sirius red staining were performed. By 3 wk after CCl<sub>4</sub> injection, liver fibrosis was observed (Figure 4), as evidenced by fiber extension, large fibrous septa formation, pseudo lobe separation and collagen accumulation in the periportal region. These alterations were remarkably reduced after infusion of hUC-MSCs (Figure 4). Together, our data show that transplanted hUC-MSCs can reverse established liver histopathology induced by CCl<sub>4</sub>.

#### ***hUC-MSCs inhibit the activation of HSCs and reduce collagen deposition***

To study the possible impact of hUC-MSCs on HSC activation and collagen deposition, immunohistochemistry was performed to detect the  $\alpha$ -SMA and collagen I and III expression. With the progression of liver fibrosis, positive  $\alpha$ -SMA, collagen I and collagen III cells in the rat liver tissue gradually increased, mainly in the portal area, fibrous septa and hyperplasia of bile duct cells. Compared with the saline/CCl<sub>4</sub> group, the positive expression of  $\alpha$ -SMA and collagen I and III in the MSCs/CCl<sub>4</sub> group was reduced, although they gradually increased as the time of transplantation extended. In addition, hUC-MSCs significantly reduced the protein and mRNA expression of collagen I and III in the fibrotic and cirrhotic groups ( $P < 0.05$ ), except in the first week after hUC-MSC transplantation in these groups (Figures 5 and 6).

#### ***hUC-MSCs reduce the collagen deposition by up-regulating MMP-13 expression and down-regulating TIMP-1 expression***

To detect the mechanism by which hUC-MSCs reduce collagen deposition, immunohistochemical analysis for MMP-13 and TIMP-1, which are mainly expressed in the cells of portal area and the central vein area, was performed in the liver tissues of fibrotic and cirrhotic rats. With the extension of the CCl<sub>4</sub> induction time, MMP-13 and TIMP-1 gradually increased in both the saline/CCl<sub>4</sub> groups and MSCs/CCl<sub>4</sub> groups. After the same CCl<sub>4</sub> injection, the MMP-13 in the MSCs/CCl<sub>4</sub> groups significantly increased compared with the

saline/CCl<sub>4</sub> groups. However, in the MSCs/CCl<sub>4</sub> groups, the expression of TIMP-1 decreased compared with the saline/CCl<sub>4</sub> groups. Western blot and real-time PCR were further applied, which showed that hUC-MSCs significantly lowered the collagen deposition by increasing MMP-13 expression ( $P < 0.05$ ) and decreasing TIMP-1 ( $P < 0.05$ ) expression, except in the first week after the transplantation of hUC-MSCs in the fibrotic MSCs/CCl<sub>4</sub> groups (Figure 7).

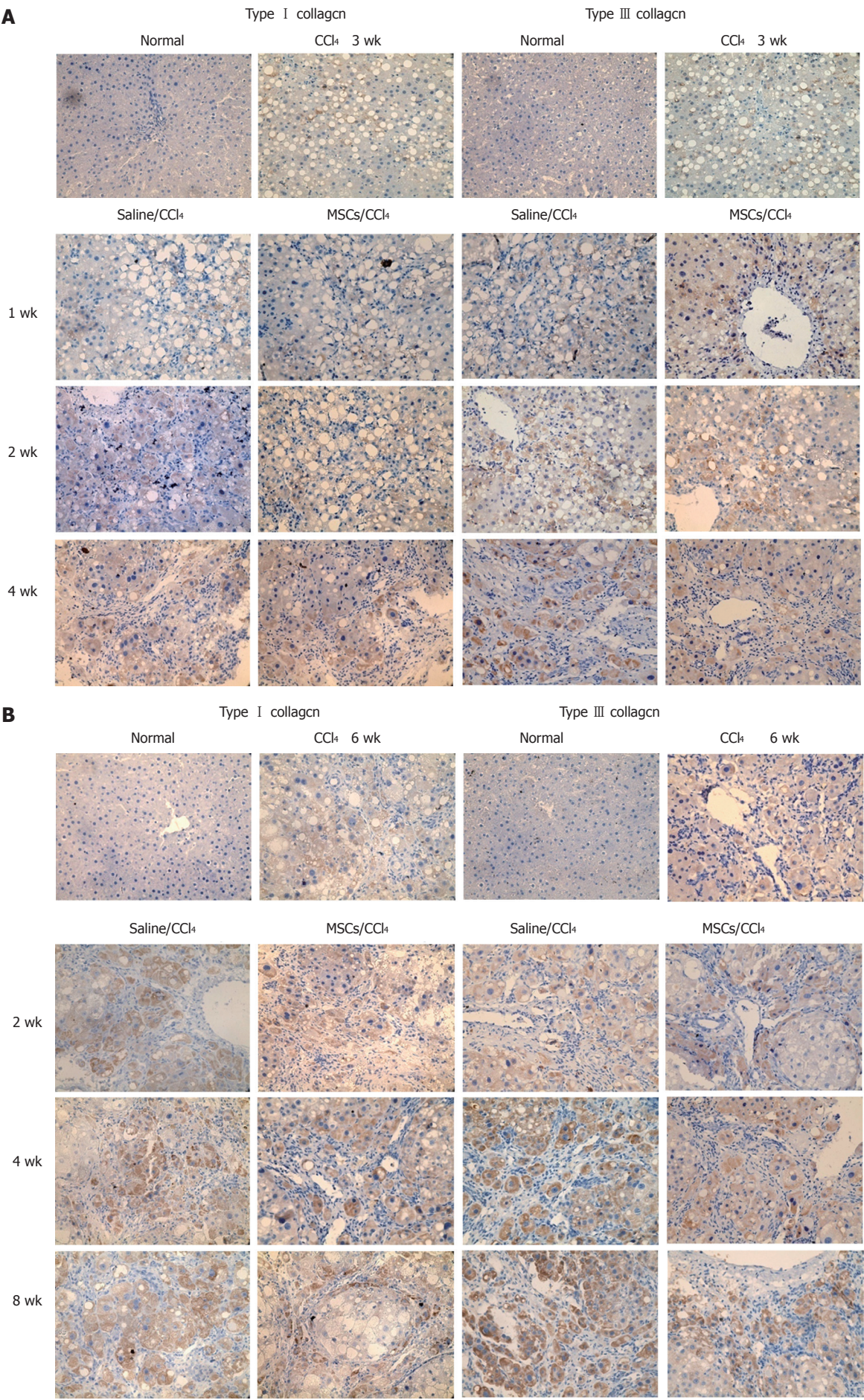
## **DISCUSSION**

At present, liver cirrhosis and other chronic liver diseases seriously affect human health, and liver transplantation is an effective treatment. However, many of its side effects limit its clinical applications. Stem cell-based therapy is of potential value in tissue and organ replacement and regeneration. Among various types of MSCs, hUC-MSCs are optimal with many advantages, such as easy extraction, low risk of viral transmission, low immunogenicity and immunosuppressive effects<sup>[10,11]</sup>.

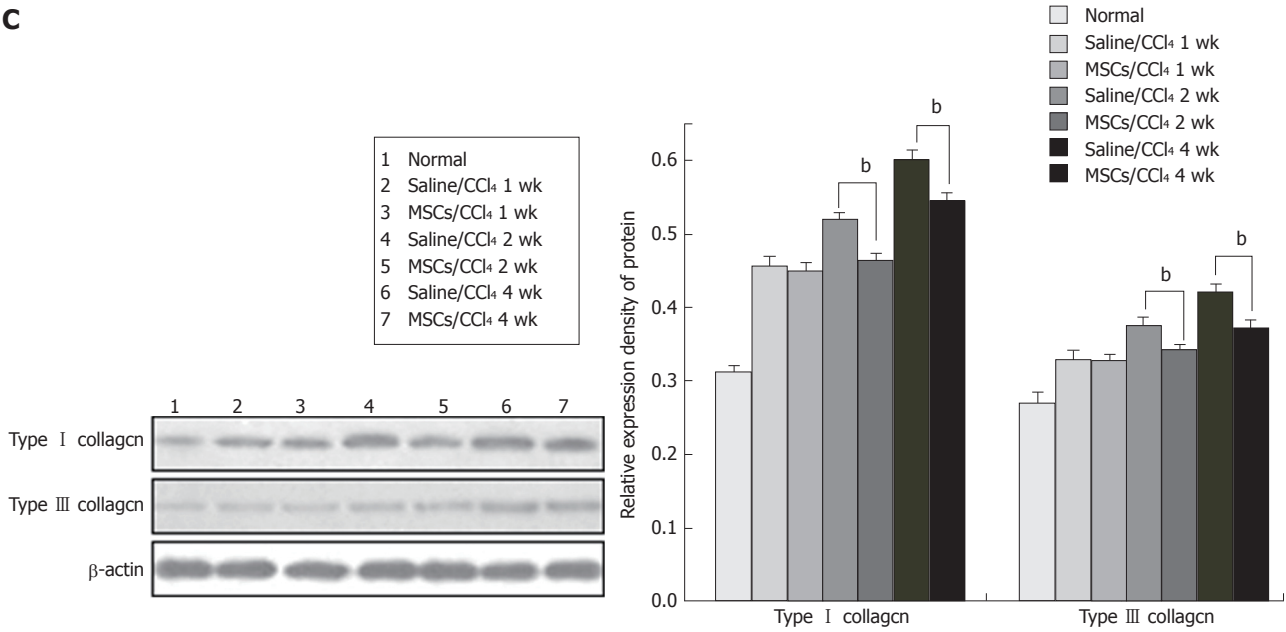
Hepatocytes undergo damage in case of liver cirrhosis. In addition, under the given conditions, MSCs can differentiate into bone, nerve cells, hepatocytes and many other cell types<sup>[12-16]</sup>. Human MSCs differentiated into hepatocyte-like cells *in vitro*<sup>[17]</sup>. Can MSCs differentiate into hepatocyte-like cells to replace damaged hepatocytes that play a role *in vivo*? Piryaei *et al.*<sup>[18]</sup> found that BM-MSCs could differentiate into hepatocyte-like cells in the liver fibrotic mice *in vivo*. Another study also confirmed that MSCs infused into the CCl<sub>4</sub>-induced liver fibrotic rats could differentiate into hepatocyte-like cells<sup>[19]</sup>. Human MSCs labelled with CM-Di I well integrated into the injured liver tissue in CCl<sub>4</sub>-induced cirrhotic rats<sup>[20]</sup>. Our study showed that the expression of human ALB, AFP, CK18 and CK19 was detected in liver tissue of the fibrotic and cirrhotic rats after hUC-MSC transplantation. Human ALB and CK18 were weakly detected after 1 wk of hUC-MSC transplantation, and they were increased in a time-dependent manner. Interestingly, the human AFP and CK19 expression levels first increased and then decreased with the extension of the transplantation time. These results suggest that transplanted hUC-MSCs could migrate into the injured liver in CCl<sub>4</sub>-induced fibrosis and cirrhosis, where they could differentiate into hepatocyte-like cells. Few hUC-MSCs differentiated into hepatocyte-like cells within 1 wk after hUC-MSC transplantation. hUC-MSCs first differentiated into immature hepatocytes and later became mature, which was a dynamic differentiation process.

Yamamoto *et al.*<sup>[21]</sup> induced adipose tissue-derived MSCs (AT-MSCs) to differentiate into AT-MSC-derived hepatocytes (AT-MSC-Hepas) *in vitro*. AT-MSC-Hepas had epithelial cell-like morphology. However, undifferentiated AT-MSCs had a fibroblast-like shape,

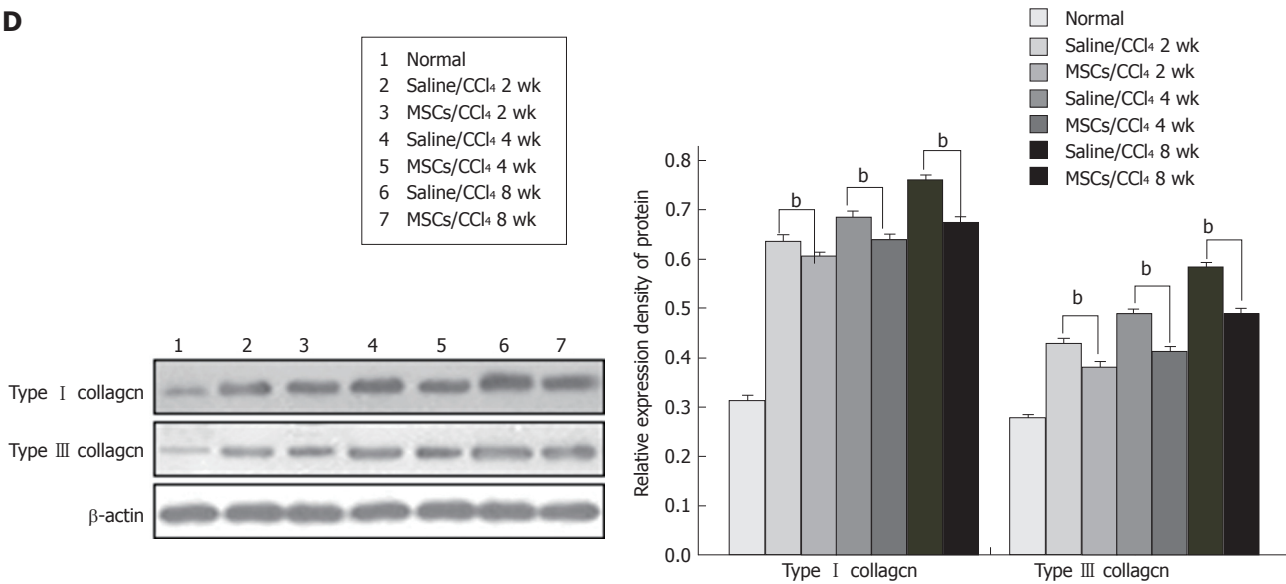




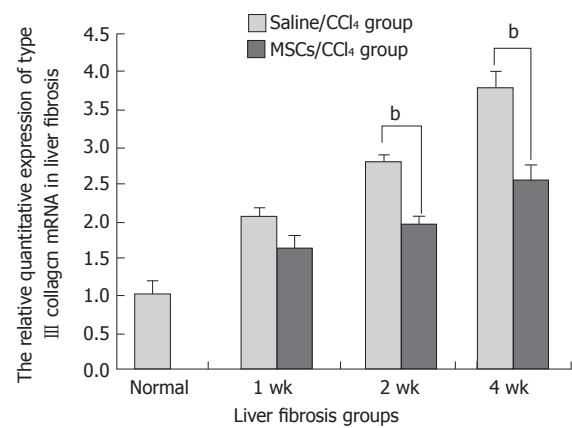
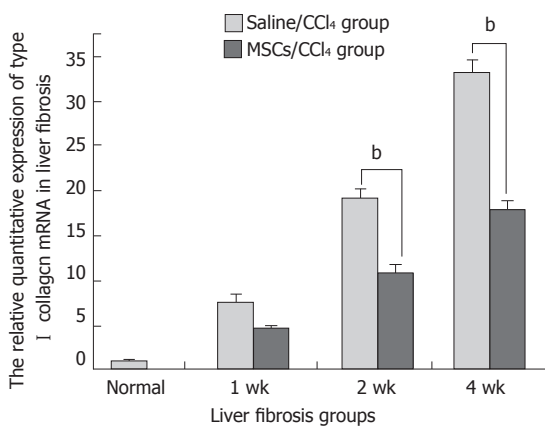
**C**



**D**



**E**





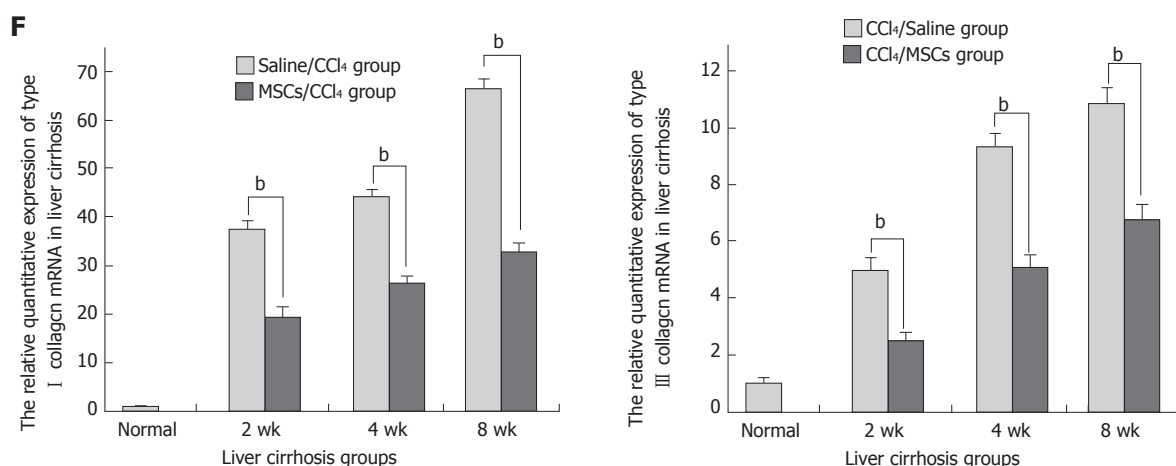


**Figure 6** Changes of collagen I and III in the liver fibrosis and cirrhosis groups. A, C, and E: Immunohistochemical, Western blot, and real-time PCR analysis of collagen I and III in fibrotic livers, respectively, in normal rats, rats at 3 wk after CCl<sub>4</sub> treatment, and rats at 1, 2, or 4 wk after human umbilical cord-derived mesenchymal stem cells (hUC-MSCs) transplantation; B, D, and F: Immunohistochemical, Western blot, and real-time PCR analysis of collagen I and III in cirrhotic livers, respectively, in normal rats; rats at 6 wk after CCl<sub>4</sub> treatment; and rats at 2, 4, or 8 wk after hUC-MSC transplantation.

indicating that during hepatic differentiation, the cell morphology changed markedly from fibroblast cell-like to epithelial cell-like. Meanwhile, microarray analysis showed that Twist and Snail, which induced the epithelial-to-mesenchymal transition, were down-regulated in the hepatic differentiation process. In addition, the expression levels of E-cadherin and  $\alpha$ -catenin, genes expressed in epithelial cells, were up-regulated in MSC-derived hepatocytes. In contrast, the expression of vimentin and N-cadherin, genes expressed in interstitial cells, was down-regulated after differentiation. Tsai *et al.*<sup>[22]</sup> reported that the phosphorylation of a factor of liver mesenchymal epithelial conversion was up-regulated in rats with HMSC transplantation. In summary, these data support the hypothesis that MET occurs during the hepatic differentiation of MSCs.

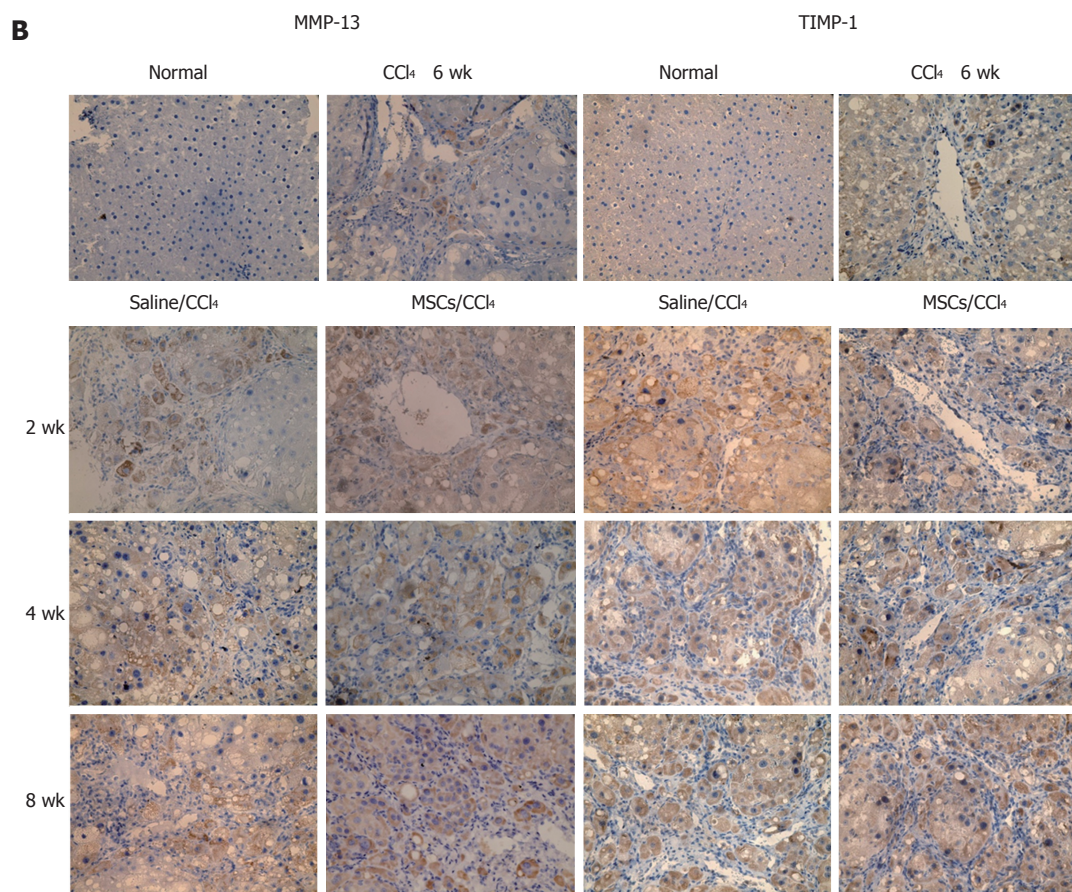
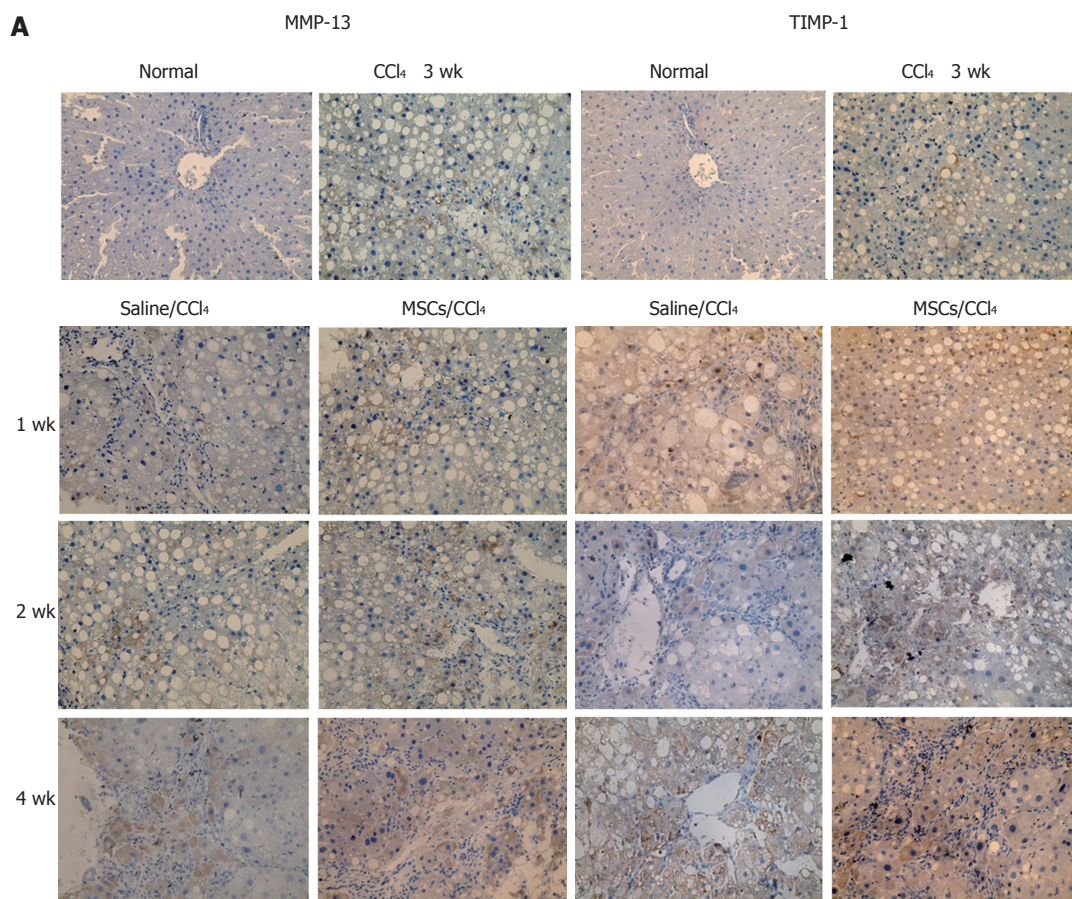
We previously confirmed that hUC-MSCs could differentiate into functional hepatocytes in liver fibrosis and cirrhosis in rats. Do hUC-MSCs undergo the MET during this differentiation? A recent study speculated that MET might be one of the mechanisms for lung hMSCs to treat chronic lung diseases<sup>[23]</sup>. Our study confirmed that vimentin and N-cadherin expression was gradually reduced in both fibrotic and cirrhotic rats with the extension of hUC-MSC transplantation. However, E-cadherin and  $\alpha$ -catenin expression first increased and then decreased, indicating that hUC-MSCs did not directly differentiate into functional hepatocytes; instead, they first differentiated into epithelial cell-like cells and then differentiated into hepatocyte-like cells. During this differentiation process, epithelial cell-like cells were in the intermediate stage.

BM-MSCs and hepatocytes transplanted into CCl<sub>4</sub>-

induced liver fibrotic rats were evaluated after co-culture for 14 d; then, after 1, 3, or 4 wk, rats were sacrificed. The results showed that hepatic fibrosis was markedly improved, indicating the therapeutic effect of BM-MSCs on liver fibrosis<sup>[24]</sup>. In liver cirrhosis, activated HSCs are the main source of the ECM, with collagen I and III as the main ingredients. A recent study has demonstrated that human MSCs implanted into CCl<sub>4</sub>-induced liver cirrhotic rats inhibited the expression of collagen I and  $\alpha$ -SMA, improving liver cirrhosis<sup>[25]</sup>. Our results showed that hUC-MSC infusion significantly reduced the deposition of collagen I and III, except in the first week after hUC-MSCs transplantation, indicating that hUC-MSCs had a therapeutic effect at a late stage rather than immediately at onset.

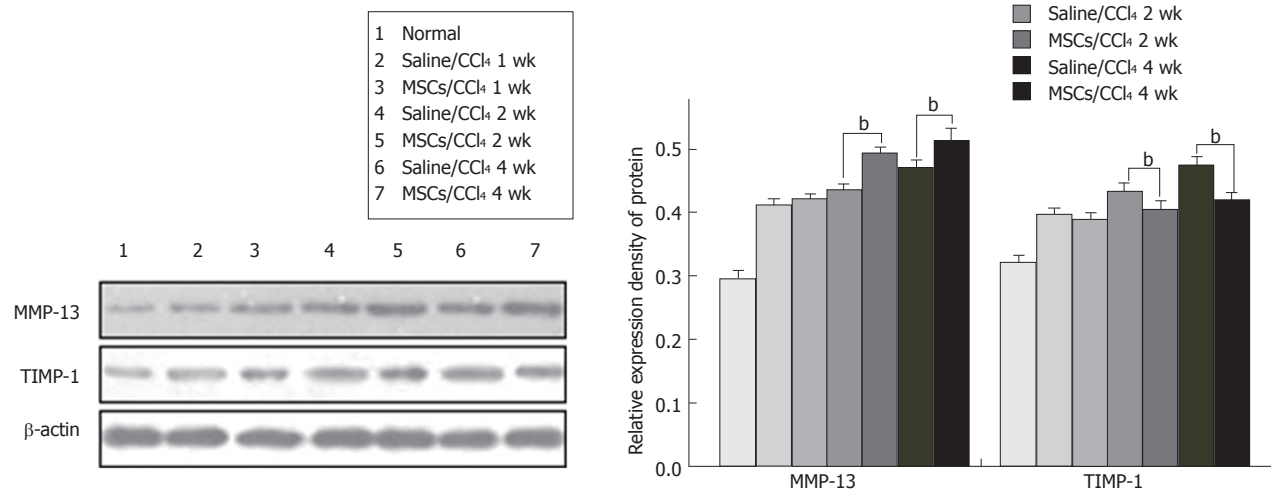
Under normal conditions, the collagenase mainly maintains collagen balance. MMP-13, a rodent interstitial metal collagenase, plays a major role in the balance of the contents of collagen I and III, which can be inhibited by TIMP-1. How do the MSCs participate in collagen metabolism? In this study, hUC-MSC transplantation degraded collagen deposition and clearly improved liver fibrosis with the up-regulation of MMP-13 expression and reduction of TIMP-1 expression. As indicated by immunohistochemical staining, Western blot and real-time PCR, MSCs reduced the collagen deposition by up-regulating MMP expression and down-regulating TIMP expression.

These data support that hUC-MSCs have the potential for hepatic differentiation *in vivo* and hUC-MSC transplantation could exert a protective effect against liver fibrosis/cirrhosis, suggesting that these cells may provide a new approach for cell therapy in liver diseases. The exact mechanisms by which hUC-MSCs repair liver injury and undergo hepatic di-

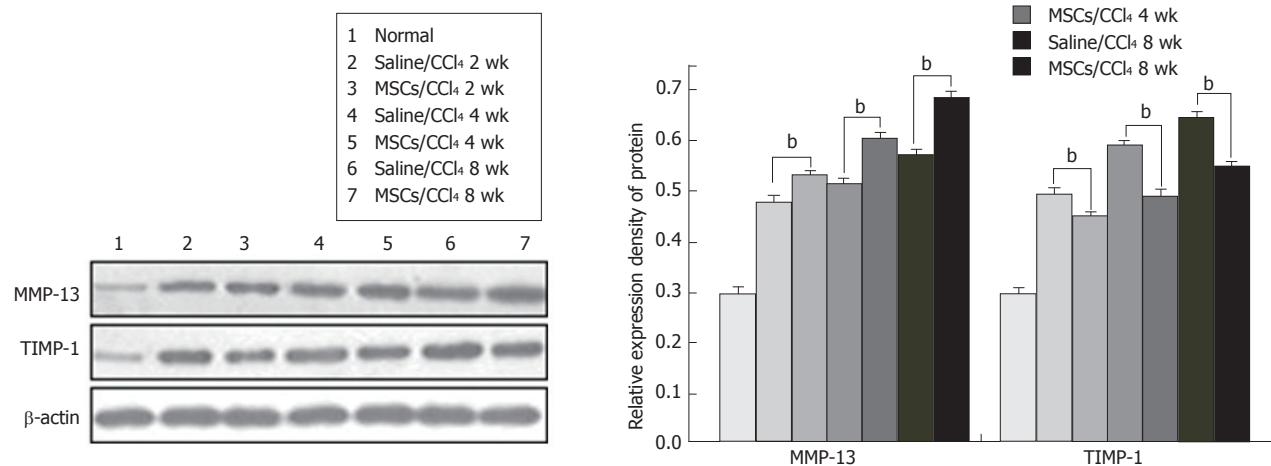




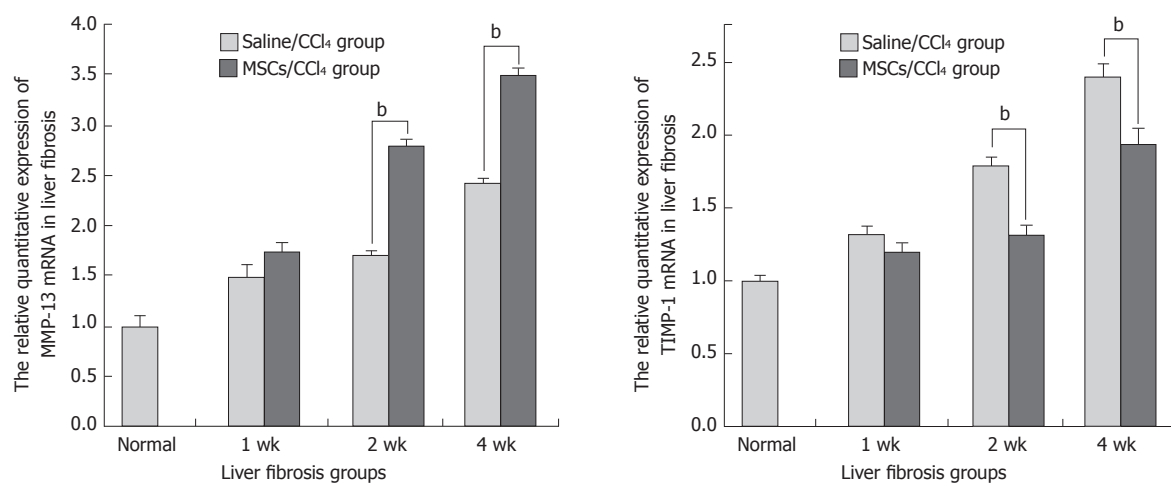
**C**



**D**



**E**



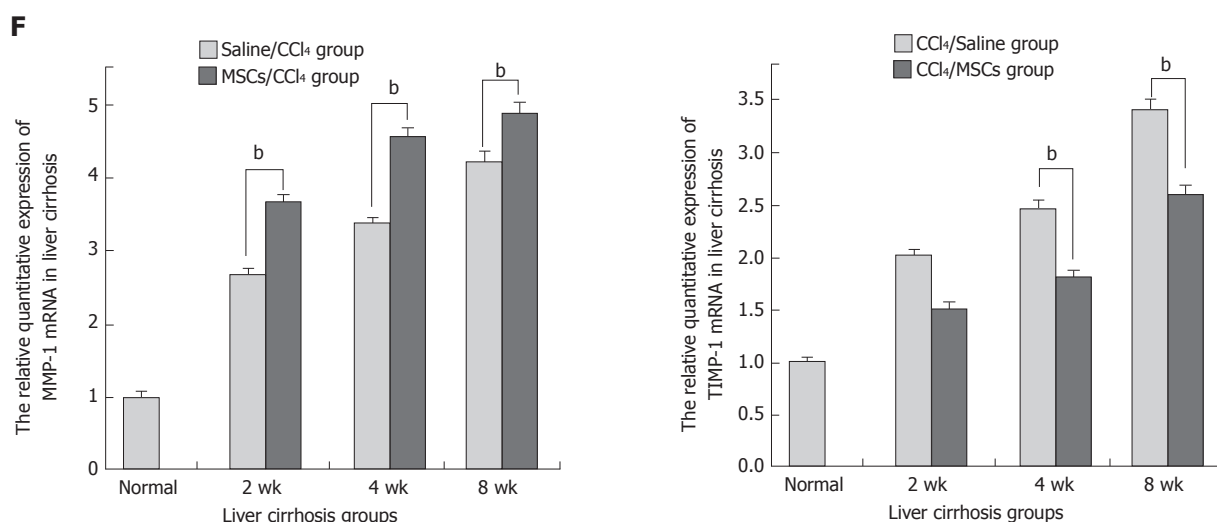


**Figure 7** Expression of MMP-13 and TIMP-1 in the liver fibrosis or cirrhosis groups. A, C, and E: Immunohistochemical, Western blot, and real-time PCR analysis of MMP-13 and TIMP-1 in rat fibrotic livers, respectively, in normal rats; rats at 3 wk after CCl<sub>4</sub> treatment; and rats at 1, 2, or 4 wk after human umbilical cord-derived mesenchymal stem cell (hUC-MSC) transplantation; B, D, and F: Immunohistochemical, Western blot, and real-time PCR analysis of MMP-13 and TIMP-1 in rat cirrhotic livers, respectively, in normal rats; rats at 6 wk after CCl<sub>4</sub> treatment; and rats at 2, 4, or 8 wk after hUC-MSC transplantation.

fferentiation remain to be elucidated in future studies.

## COMMENTS

### Background

Chronic liver inflammation is a major driving force for extracellular matrix accumulation, leading to liver cirrhosis with complications. Liver transplantation is an effective method for treating end-stage liver disease, but donor scarcity and immunological rejection limit its clinical application. This has led to the search for alternative sources of hepatocytes, including cell-based therapy using mesenchymal stem cells (MSCs). MSCs have been demonstrated to improve liver disease.

### Research frontiers

Among the various MSCs types, human umbilical cord-derived mesenchymal stem cells (hUC-MSCs) may be optimal as an alternative for hepatocyte transplantation, because of ease of extraction, low risk of viral transmission, low immunogenicity and immunosuppressive effects. The authors used a CCl<sub>4</sub>-induced rat liver fibrosis/cirrhosis model to better understand the mechanism and therapeutic potential of hUC-MSCs.

### Innovations and breakthroughs

This is the first study to evaluate the *in vivo* hepatic differentiation potential of human umbilical cord-derived MSCs and their therapeutic effect on liver fibrosis.

### Applications

Transplanted hUC-MSCs could differentiate into functional hepatocytes that improved both biochemical and histopathologic changes in a CCl<sub>4</sub>-induced rat liver fibrosis model. hUC-MSCs may offer therapeutic opportunities in the treatment of hepatobiliary diseases, including cirrhosis.

### Terminology

The mesenchymal-to-epithelial transition is a crucial physiologic event that converts motile mesenchymal cells to polarized epithelial cells, favoring the epithelial regeneration. hUC-MSCs differentiated into hepatocyte-like cells via the mesenchymal-to-epithelial transition *in vivo*.

### Peer-review

Good research on cord stem cells in the treatment of liver disease. Change all typos saying "collagen I and III TO collagen I and III".

## ACKNOWLEDGMENTS

We thank Alliances Bioscience Co., Ltd. for providing hUC-MSCs and the ENT laboratory, The First Hospital of Hebei Medical University for providing laboratory equipment on immunofluorescence and real-time PCR.

## REFERENCES

- 1 **Afdhal NH**, Manning D. Diagnosis of liver fibrosis in 2008 and beyond. *Gastroenterol Clin Biol* 2008; **32**: 88-90 [PMID: 18973851 DOI: 10.1016/S0399-8320(08)73998-8]
- 2 **Mormone E**, Lu Y, Ge X, Fiel MI, Nieto N. Fibromodulin, an oxidative stress-sensitive proteoglycan, regulates the fibrogenic response to liver injury in mice. *Gastroenterology* 2012; **142**: 612-621.e5 [PMID: 22138190 DOI: 10.1053/j.gastro.2011.11.029]
- 3 **Neff GW**, Duncan CW, Schiff ER. The current economic burden of cirrhosis. *Gastroenterol Hepatol* (N Y) 2011; **7**: 661-671 [PMID: 22298959]
- 4 **Baertschiger RM**, Serre-Beinier V, Morel P, Bosco D, Peyrou M, Clément S, Sgroi A, Kaelin A, Buhler LH, Gonelle-Gispert C. Fibrogenic potential of human multipotent mesenchymal stromal cells in injured liver. *PLoS One* 2009; **4**: e6657 [PMID: 19684854 DOI: 10.1371/journal.pone.0006657]
- 5 **Oyagi S**, Hirose M, Kojima M, Okuyama M, Kawase M, Nakamura T, Ohgushi H, Yagi K. Therapeutic effect of transplanting HGF-treated bone marrow mesenchymal cells into CCl<sub>4</sub>-injured rats. *J Hepatol* 2006; **44**: 742-748 [PMID: 16469408 DOI: 10.1016/j.jhep.2005.10.026]
- 6 **Zhao DC**, Lei JX, Chen R, Yu WH, Zhang XM, Li SN, Xiang P. Bone marrow-derived mesenchymal stem cells protect against experimental liver fibrosis in rats. *World J Gastroenterol* 2005; **11**: 3431-3440 [PMID: 15948250 DOI: 10.3748/wjg.v11.i22.3431]
- 7 **Ju S**, Teng GJ, Lu H, Jin J, Zhang Y, Zhang A, Ni Y. *In vivo* differentiation of magnetically labeled mesenchymal stem cells into hepatocytes for cell therapy to repair damaged liver. *Invest Radiol* 2010; **45**: 625-633 [PMID: 20808237 DOI: 10.1097/RLI.0b013e3181ed55f4]
- 8 **Hao LS**, Zhang XL, An JY, Karlin J, Tian XP, Dun ZN, Xie SR, Chen S. PTEN expression is down-regulated in liver tissues of rats with hepatic fibrosis induced by biliary stenosis. *APMIS* 2009; **117**: 681-691 [PMID: 19703128 DOI: 10.1111/j.1600-0463.2009.02515.x]

- 9 **Zheng L**, Chen X, Guo J, Sun H, Liu L, Shih DQ, Zhang X. Differential expression of PTEN in hepatic tissue and hepatic stellate cells during rat liver fibrosis and its reversal. *Int J Mol Med* 2012; **30**: 1424-1430 [PMID: 23041795 DOI: 10.3892/ijmm.2012.1151]
- 10 **Chen MY**, Lie PC, Li ZL, Wei X. Endothelial differentiation of Wharton's jelly-derived mesenchymal stem cells in comparison with bone marrow-derived mesenchymal stem cells. *Exp Hematol* 2009; **37**: 629-640 [PMID: 19375653 DOI: 10.1016/j.exphem.2009.02.003]
- 11 **Zhao Q**, Ren H, Li X, Chen Z, Zhang X, Gong W, Liu Y, Pang T, Han ZC. Differentiation of human umbilical cord mesenchymal stromal cells into low immunogenic hepatocyte-like cells. *Cytotherapy* 2009; **11**: 414-426 [PMID: 19513901 DOI: 10.1080/14653240902849754]
- 12 **Gregory CA**, Prockop DJ, Spees JL. Non-hematopoietic bone marrow stem cells: molecular control of expansion and differentiation. *Exp Cell Res* 2005; **306**: 330-335 [PMID: 15925588 DOI: 10.1016/j.yexcr.2005.03.018]
- 13 **La Rocca G**, Anzalone R, Corrao S, Magno F, Loria T, Lo Iacono M, Di Stefano A, Giannuzzi P, Marasà L, Cappello F, Zummo G, Farina F. Isolation and characterization of Oct-4+/HLA-G+ mesenchymal stem cells from human umbilical cord matrix: differentiation potential and detection of new markers. *Histochem Cell Biol* 2009; **131**: 267-282 [PMID: 18836737 DOI: 10.1007/s00418-008-0519-3]
- 14 **Yang XF**, He X, He J, Zhang LH, Su XJ, Dong ZY, Xu YJ, Li Y, Li YL. High efficient isolation and systematic identification of human adipose-derived mesenchymal stem cells. *J Biomed Sci* 2011; **18**: 59 [PMID: 21854621 DOI: 10.1186/1423-0127-18-59]
- 15 **Thanabalasundaram G**, Arumalla N, Tailor HD, Khan WS. Regulation of differentiation of mesenchymal stem cells into musculoskeletal cells. *Curr Stem Cell Res Ther* 2012; **7**: 95-102 [PMID: 22023628 DOI: 10.2174/157488812799218974]
- 16 **Satija NK**, Singh VK, Verma YK, Gupta P, Sharma S, Afrin F, Sharma M, Sharma P, Tripathi RP, Gurudutta GU. Mesenchymal stem cell-based therapy: a new paradigm in regenerative medicine. *J Cell Mol Med* 2009; **13**: 4385-4402 [PMID: 19602034 DOI: 10.1111/j.1582-4934.2009.00857.x]
- 17 **Hong SH**, Gang EJ, Jeong JA, Ahn C, Hwang SH, Yang IH, Park HK, Han H, Kim H. In vitro differentiation of human umbilical cord blood-derived mesenchymal stem cells into hepatocyte-like cells. *Biochem Biophys Res Commun* 2005; **330**: 1153-1161 [PMID: 15823564 DOI: 10.1016/j.bbrc.2005.03.086]
- 18 **Piryaei A**, Valojerdi MR, Shahsavani M, Baharvand H. Differentiation of bone marrow-derived mesenchymal stem cells into hepatocyte-like cells on nanofibers and their transplantation into a carbon tetrachloride-induced liver fibrosis model. *Stem Cell Rev* 2011; **7**: 103-118 [PMID: 20182823 DOI: 10.1007/s12015-010-9126-5]
- 19 **Pan Q**, Fouraschen SM, Kaya FS, Verstegen MM, Pescatori M, Stubbs AP, van Ijcken W, van der Sloot A, Smits R, Kwekkeboom J, Metselaar HJ, Kazemier G, de Jonge J, Tilanus HW, Wagemaker G, Janssen HL, van der Laan LJ. Mobilization of hepatic mesenchymal stem cells from human liver grafts. *Liver Transpl* 2011; **17**: 596-609 [PMID: 21506248 DOI: 10.1002/lt.22260]
- 20 **Jung KH**, Shin HP, Lee S, Lim YJ, Hwang SH, Han H, Park HK, Chung JH, Yim SV. Effect of human umbilical cord blood-derived mesenchymal stem cells in a cirrhotic rat model. *Liver Int* 2009; **29**: 898-909 [PMID: 19422480 DOI: 10.1111/j.1478-3231.2009.02031.x]
- 21 **Yamamoto Y**, Banas A, Murata S, Ishikawa M, Lim CR, Teratani T, Hatada I, Matsubara K, Kato T, Ochiya T. A comparative analysis of the transcriptome and signal pathways in hepatic differentiation of human adipose mesenchymal stem cells. *FEBS J* 2008; **275**: 1260-1273 [PMID: 18318837 DOI: 10.1111/j.1742-4658.2008.06287.x]
- 22 **Tsai PC**, Fu TW, Chen YM, Ko TL, Chen TH, Shih YH, Hung SC, Fu YS. The therapeutic potential of human umbilical mesenchymal stem cells from Wharton's jelly in the treatment of rat liver fibrosis. *Liver Transpl* 2009; **15**: 484-495 [PMID: 19399744 DOI: 10.1002/lt.21715]
- 23 **Ricciardi M**, Malpeli G, Bifari F, Bassi G, Pacelli L, Nwabo Kamdje AH, Chilosi M, Krampera M. Comparison of epithelial differentiation and immune regulatory properties of mesenchymal stromal cells derived from human lung and bone marrow. *PLoS One* 2012; **7**: e35639 [PMID: 22567106 DOI: 10.1371/journal.pone.0035639]
- 24 **Li TZ**, Kim JH, Cho HH, Lee HS, Kim KS, Lee SW, Suh H. Therapeutic potential of bone-marrow-derived mesenchymal stem cells differentiated with growth-factor-free coculture method in liver-injured rats. *Tissue Eng Part A* 2010; **16**: 2649-2659 [PMID: 20367252 DOI: 10.1089/ten.TEA.2009.0814]
- 25 **Jung KH**, Shin HP, Lee S, Lim YJ, Hwang SH, Han H, Park HK, Chung JH, Yim SV. Effect of human umbilical cord blood-derived mesenchymal stem cells in a cirrhotic rat model. *Liver Int* 2009; **29**: 898-909 [PMID: 19422480 DOI: 10.1111/j.1478-3231.2009.02031.x]

**P- Reviewer:** Julie NL, Sun BC **S- Editor:** Qi Y **L- Editor:** Wang TQ **E- Editor:** Ma YJ



## Basic Study

**Pharmacokinetics and pharmacodynamics of Shengjiang decoction in rats with acute pancreatitis for protecting against multiple organ injury**

Lv Zhu, Jun-Yi Li, Yu-Mei Zhang, Hong-Xin Kang, Huan Chen, Hang Su, Juan Li, Wen-Fu Tang

Lv Zhu, Yu-Mei Zhang, Hong-Xin Kang, Huan Chen, Hang Su, Juan Li, Wen-Fu Tang, Sichuan Provincial Pancreatitis Center, Department of Integrative Medicine, West China Hospital, Sichuan University, Chengdu 610041, Sichuan Province, China

Jun-Yi Li, Department of Traditional Chinese Medicine, Wuhan Union Hospital, Wuhan 430000, Hubei Province, China

ORCID number: Lv Zhu (0000-0002-4302-3339); Jun-Yi Li (0000-0003-2599-2889); Yu-Mei Zhang (0000-0001-9802-776X); Hong-Xin Kang (0000-0001-8212-0134); Huan Chen (0000-0002-4763-6730); Hang Su (0000-0003-2468-557X); Juan Li (0000-0002-5775-9355); Wen-Fu Tang (0000-0001-9294-6634).

**Author contributions:** Zhu L and Li JY contributed equally to this work; Tang WF designed the research; Zhu L, Li JY, Zhang YM, Kang HX and Chen H performed the study; Su H and Li J analyzed the data; Zhu L and Li JY wrote the paper; Tang WF was responsible for the critical revision of the paper.

**Supported by the National Natural Science Foundation of China,** No. 81603519, No. 81573857, and No. 81374042.

**Institutional review board statement:** The study was approved by the Animal Ethics Committee of the Animal Facility of West China Hospital (Chengdu, China).

**Institutional animal care and use committee statement:** All procedure involving animals were reviewed and approved by the Animal Ethics Committee of the Animal Facility of the West China Hospital (protocol number: 2017052A, Chengdu, China), and performed according to the Guide for the Care and Use of Laboratory Animals of Sichuan University.

**Conflict-of-interest statement:** The authors declare that they have no conflicts of interest to this work.

**Data sharing statement:** No additional data are available.

**Open-Access:** This article is an open-access article which was

selected by an in-house editor and fully peer-reviewed by external reviewers. It is distributed in accordance with the Creative Commons Attribution Non Commercial (CC BY-NC 4.0) license, which permits others to distribute, remix, adapt, build upon this work non-commercially, and license their derivative works on different terms, provided the original work is properly cited and the use is non-commercial. See: <http://creativecommons.org/licenses/by-nc/4.0/>

**Manuscript source:** Unsolicited manuscript

**Correspondence to:** Wen-Fu Tang, PhD, Professor, Sichuan Provincial Pancreatitis Center, Department of Integrative Medicine, West China Hospital, Sichuan University, No. 37, Guoxue Alley, Chengdu 610041, Sichuan Province, China. [tangwf@scu.edu.cn](mailto:tangwf@scu.edu.cn)  
**Telephone:** +86-28-85423546  
**Fax:** +86-28-85423373

**Received:** September 19, 2017

**Peer-review started:** September 20, 2017

**First decision:** October 10, 2017

**Revised:** October 24, 2017

**Accepted:** November 14, 2017

**Article in press:** November 14, 2017

**Published online:** December 14, 2017

**Abstract****AIM**

To explore the pharmacokinetics and pharmacodynamics of Shengjiang decoction (SJD) in rats with acute pancreatitis (AP) for protecting against multiple organ injury.

**METHODS**

An AP model was established by retrograde perfusion of 3.5% sodium taurocholate into the biliopancreatic



duct, and a control group (CG) received 0.9% sodium chloride instead. Twelve male Sprague-Dawley rats were randomly divided into a CG treated with SJD (CG + SJD) and a model group treated with SJD (MG + SJD), both of which were orally administered with SJD (5 g/kg) 2 h after surgery. Blood samples were collected *via* the tail vein at 10, 20, and 40 min and 1, 2, 3, 4, 6, 8, and 12 h after a single dose of SJD to detect its main components using high-performance liquid chromatography-tandem mass spectrometry. The pharmacokinetic parameters were compared. In the pharmacodynamic experiment, 18 male Sprague-Dawley rats were randomly divided into a CG, an AP model group (MG), and an SJD treated AP group (SJDG). Serum amylase, lipase, and inflammatory cytokines were measured, and heart, lung, liver, spleen, pancreas, kidney, and intestine tissues were collected for pathological examination.

## RESULTS

The MG + SJD displayed significantly shorter mean residence time (MRT) and higher clearance (CL) for emodin and aloe-emodin; significantly shorter time of maximum concentration and  $T_{1/2}$  and a lower area under curve (AUC) for aloe-emodin; a significantly higher AUC and lower CL for rhein; and longer MRT and lower CL for chrysophanol than the CG + SJD. In the pharmacodynamic experiment, the amylase, interleukin (IL)-6, IL-10, and tumor necrosis factor (TNF)- $\alpha$  levels in the MG were higher than those in the CG ( $P < 0.05$ ). After the herbal decoction treatment, the SJDG had higher IL-10 and lower TNF- $\alpha$  levels than the MG ( $P < 0.05$ ). The MG had the highest pathological scores, and the pathological scores of the lung, pancreas, kidney, and intestine in the SJDG were significantly lower than those in the MG ( $P < 0.05$ ).

## CONCLUSION

AP may have varying effects on the pharmacokinetics of the major SJD components in rats. SJD might alleviate pathological injuries of the lung, pancreas, kidney, and intestine in rats with AP *via* regulating pro- and anti-inflammatory responses, which might guide the clinical application of SJD for AP treatment.

**Key words:** Pancreatic distribution; Pharmacodynamics; Shengjiang decoction; Pharmacokinetics; Acute pancreatitis

© **The Author(s) 2017.** Published by Baishideng Publishing Group Inc. All rights reserved.

**Core tip:** Shengjiang decoction (SJD) has been identified to be effective in treating acute pancreatitis (AP) in both *in vivo* and *in vitro* tests. We report the metabolic processes of major components of SJD *in vivo* and the pharmacodynamic mechanism of SJD in relieving AP. This study demonstrated that AP may have varying effects on the pharmacokinetics of the major SJD components in rats. Rhein and bisdemethoxycurcumin

may be potential active components for the treatment of AP based on the hypothesis of tissue pharmacology of herbal recipe. SJD may attenuate AP by regulating inflammatory responses to protect against multiple organ injury.

Zhu L, Li JY, Zhang YM, Kang HX, Chen H, Su H, Li J, Tang WF. Pharmacokinetics and pharmacodynamics of Shengjiang decoction in rats with acute pancreatitis for protecting against multiple organ injury. *World J Gastroenterol* 2017; 23(46): 8169-8181 Available from: URL: <http://www.wjgnet.com/1007-9327/full/v23/i46/8169.htm> DOI: <http://dx.doi.org/10.3748/wjg.v23.i46.8169>

## INTRODUCTION

Acute pancreatitis (AP) is an acute inflammatory disorder of the pancreas and the surrounding tissues caused by pancreatic digestive enzymes due to various aetiological factors<sup>[1]</sup>. The overall mortality of AP is currently approximately 2%<sup>[2]</sup>, but it approaches 30%-56% among patients with severe acute pancreatitis (SAP), which is characterized by persistent systemic inflammatory response syndrome (SIRS) and persistent organ failure<sup>[3-5]</sup>. Mortality associated with AP has decreased over time due to the widespread application of Chinese medicines, including traditional Chinese decoctions and acupuncture<sup>[6-9]</sup>.

Shengjiang decoction (SJD), a classical traditional Chinese herbal formula, was recorded in *Shanghan Wenyi Tiaobian* by Li-Shan Yang, a well-known heat disease specialist in the Qing Dynasty. Composed of *Rhei Radix et Rhizoma* B. (rhubarb root and rhizome), *Curcumae Longae Rhizoma* L. (turmeric), *Bombyx Batryticatus* L. (stiff silkworm), and *Cicadae Periostracum* F. (cicada slough), SJD has been a prestigious prescription for the treatment of various heat diseases or syndromes for hundreds of years. *Rhei Radix et Rhizoma* B. is recorded in *Shennong's Classic of Materia Medica* and is reported to expel pathogens by purgation, clearing heat-fire, and removing stasis. It has also been declared to be effective in reducing injuries of the gastrointestinal tract, lung, and liver induced by sepsis *via* reducing oxidative stress and inflammation, ameliorating microcirculatory disturbances, and maintaining the immune balance<sup>[10,11]</sup>. *Curcumae Longae Rhizoma* L. promotes Qi and activates blood circulation. Moreover, curcumin, demethoxycurcumin, and bide-methoxycurcumin, which are extracted from *Curcumae Longae Rhizoma* L., have been shown to regulate anti-inflammatory responses and prevent systemic complications in AP associated with cytokine damage<sup>[12,13]</sup>. Both *Bombyx Batryticatus* L. and *Cicadae Periostracum* F. dispel wind and have an anti-inflammatory effect.

Notably, an increasing number of clinical and experimental studies have reported that SJD is effective for the treatment of AP, especially in individuals with fever or severe infections, which could be differentiated as heat syndrome. SJD, in combination with conventional Western medicine, markedly reduced the APACHE II score, multiple organ dysfunction syndrome (MODS) severity score, and intra-abdominal pressure in patients with SIRS/MODS compared to Western medical treatment alone<sup>[14]</sup>. SJD can significantly reduce the inflammatory response and improve the clinical symptoms and prognosis<sup>[15]</sup> in early sepsis patients<sup>[16]</sup>. Moreover, it also plays a protective role against gastric mucosal damage by weakening aggressive factors and strengthening protective factors<sup>[17]</sup> in SIRS *via* regulation of pro- and anti-inflammatory responses<sup>[18]</sup>. SJD can also protect against nonalcoholic fatty liver disease associated with metabolic syndrome<sup>[19]</sup>. Our previous study has demonstrated that SJD ameliorates inflammation of the systemic microenvironment, reduces apoptosis of pancreatic acinar cells, and promotes repair of the pancreas in rats with AP<sup>[20]</sup>.

Indisputably, SJD is an effective prescription for the treatment of AP, but the exact active components are not clear. Little is known about the *in vivo* metabolic process of SJD. Full elucidation of the pharmacokinetic and pharmacodynamic mechanisms of SJD associated with the amelioration of AP is urgently needed. Therefore, this study aimed to explore the pharmacokinetics, pharmacodynamics, and pancreatic distribution of the main components of SJD in rats with AP to provide pharmacokinetic and pharmacodynamic evidence for its clinical application for the treatment of AP.

## MATERIALS AND METHODS

### Animals

Male clean-grade, healthy Sprague-Dawley rats (body weight:  $300 \pm 20$  g; age:  $75 \pm 5$  d) were used in the study [Certification No. 0000589-SCXK (Chuan) 2013-24]. The rats were housed, fed, and handled according to the University Guidelines and Animal Ethics Committee Guidelines of the Animal Facility of the West China Hospital (protocol number: 2017052A, Chengdu, China). Animals were maintained in air-conditioned animal quarters under the following conditions: temperature,  $22 \pm 2$  °C; relative humidity,  $65\% \pm 10\%$ ; free access to water; and fed laboratory rodent chow (Chengdu, China). The animal were acclimatized to the facilities for one week and fasted for 12 h prior to the experiment.

### Preparation of SJD

Spray dried particles of SJD ingredients including *Rhei Radix et Rhizoma* B. (batch No. 16110150), *Curcuma Longae Rhizoma* L. (batch No. 16080008 ),

*Bombyx Batryticatus* L. (batch No. 16100147), and *Cicadae Periostracum* F. (batch No. 16080020) were all purchased from the Affiliated Hospital of Chengdu University of Traditional Chinese Medicine (Chengdu, China) and authenticated by Professor WM Wang (Department of Herbal Pharmacy, West China Hospital, Sichuan University, China) according to the Chinese Pharmacopoeia (The Pharmacopoeia Commission of PRC, 2010). Voucher specimens were deposited at our laboratory. The spray dried particles were mixed and reconstituted with sterile distilled water (proportions: 4:3:2:1; concentration: 0.5 g/mL).

### High-performance liquid chromatography-tandem mass spectrometry (HPLC-MS/MS) and fingerprint analysis

The components of SJD were determined by HPLC, with an ultimate XB-C18 column (5  $\mu$ m, 50 mm  $\times$  4.6 mm) with methanol-water (92:8, v/v) at a flow rate of 0.5 mL/min with the column temperature set at 40 °C. The liquid chromatography mass spectrometry (LC/MS) system was operated under the multiple reaction monitoring mode using electrospray ionization in the negative ion mode. The ion pairs were emodin 269.0  $\rightarrow$  241.2 (m/z), aloe-emodin 269.0  $\rightarrow$  239.9 (m/z), rhein 283.2  $\rightarrow$  238.8 (m/z), chrysophanol 253.2  $\rightarrow$  224.7 (m/z), curcumin 366.6  $\rightarrow$  216.9 (m/z), demethoxycurcumin 336.7  $\rightarrow$  216.9 (m/z), bide-methoxycurcumin 306.7  $\rightarrow$  186.8 (m/z), and inner standard ibuprofen 205.1  $\rightarrow$  160.9 (m/z).

### Animal models and treatment with SJD

In the pharmacokinetic experiment, male Sprague-Dawley rats were randomly divided into a control group (CG) that received SJD (CG + SJD) ( $n = 6$ ) and a model group that received SJD (MG + SJD) ( $n = 6$ ). The AP model was established by retrograde perfusion of 3.5% sodium taurocholate (Sigma, St. Louis, MO, United States) into the biliopancreatic duct (1 mL/kg body weight) at a rate of 6 mL/h with a micro-infusion pump after intraperitoneal injection with 10% chloral hydrate (3 mL/kg body weight) for anesthesia, while the CG received 0.9% sodium chloride instead of sodium taurocholate. Both groups were orally administered with SJD (5 g/kg) 2 h after the operation.

In the pharmacodynamic experiment, male Sprague-Dawley rats were randomly divided into a CG ( $n = 6$ ), an AP model group (MG) ( $n = 6$ ), and an SJD treated AP group (SJDG) ( $n = 6$ ). Model induction was identical to the procedure used in the pharmacokinetic experiment, and the SJDG was orally administered with SJD (5 g/kg) 2 h after the operation.

### Collection and measurement of serum and tissue samples

In the pharmacokinetic experiment, after administration of a single dose of SJD, a 0.5 mL blood sample was collected *via* the tail vein at 10, 20, and 40 min

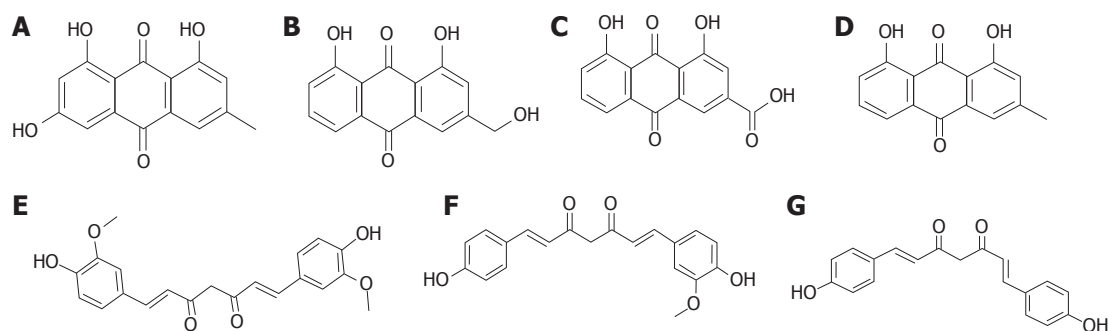


**Figure 1** Chemical structure of the major components of Shengjiang decoction detected in the serum and pancreas. A: Emodin; B: Aloe-emodin; C: Rhein; D: Chrysophanol; E: Curcumin; F: Demethoxycurcumin; G: Bisdemethoxycurcumin.

and 1, 2, 3, 4, 6, 8, and 12 h. After centrifugation at 3000 r/min for 7 min, the serum samples were stored at  $-80^{\circ}\text{C}$  for detection by HPLC-MS/MS. The rats were sacrificed 12 h after administration of SJD; pancreatic tissue samples were homogenized and the supernatants were obtained after centrifugation at 3000 r/min for 7 min and stored at  $-80^{\circ}\text{C}$  for detection.

In the pharmacodynamic experiment, the rats were sacrificed 12 h after administration of SJD. Blood samples (5 mL) were collected to obtain serum samples to measure amylase and lipase, using an Automatic Biochemical Analyzer (AU5400, SIEMENS, Munich, Germany), and to measure interleukin (IL)-6, IL-10, and tumor necrosis factor (TNF)- $\alpha$  levels using a Milliplex MAP Rat Cytokine/Chemokine magnetic bead immunoassay kit (Millipore Corporation, Billerica, MA, United States). Heart, lung, liver, spleen, pancreas, kidney, and intestine tissue samples were collected for pathological examination.

#### Data collection and analysis

The concentrations of the main components of SJD in serum were measured by HPLC-MS/MS. Analyst 1.4.2 software for HPLC-MS/MS was used for data collection, peak integration, and calibration. The concentrations of the quality control and unknown samples were measured by interpolation from the calibration curves. Drug and statistics software programmed by the Chinese Pharmacological Society (DAS 2.0) was used to process the serum concentration data and for compartment model fitting; then, all pharmacokinetic parameters were determined. The following pharmacokinetic parameters were calculated: maximum concentration, time of maximum concentration ( $T_{\text{max}}$ ), area under the curve (AUC) (0-t), half-life ( $T_{1/2}$ ), mean residence time (MRT), and clearance (CL).

All statistical analyses were performed with PEMS3.1 statistical software for windows. Quantitative data are expressed as the mean  $\pm$  standard deviation when normally distributed. Comparisons of the pharmacokinetic parameters between the CG + SJD and MG + SJD were performed by Student's *t*-test.

One-way repeated-measures ANOVA followed by multiple pair-wise comparisons using the Student-Newman-Keuls test was used to detect differences among the CG, MG, and SJDG. The level of statistical significance was set at  $P < 0.05$ .

## RESULTS

### Components of SJD detected in the serum and pancreas of the rats

In the study, seven components, emodin, aloe-emodin, rhein, chrysophanol, curcumin, demethoxycurcumin, and bisdemethoxycurcumin, were detected in the serum and pancreas in the CG + SJD and the MG + SJD by HPLC-MS/MS. The structural formula and HPLC chromatogram of each component are shown in Figures 1 and 2, respectively.

### Pharmacokinetics of major components of SJD

Both emodin and aloe-emodin displayed significantly shorter MRT and higher CL in the MG + SJD than in the CG + SJD ( $P < 0.05$ , Table 1), while aloe-emodin had significantly shorter  $T_{\text{max}}$  and  $T_{1/2}$  and a lower AUC in the MG + SJD ( $P < 0.05$ , Table 1). The AUC of rhein was significantly higher and the CL was lower in the MG + SJD than in the CG + SJD ( $P < 0.05$ , Table 1). The MRT of chrysophanol was longer and the CL of chrysophanol was lower in the MG + SJD than in the CG + SJD ( $P < 0.05$ , Table 1). The pharmacokinetic parameters of curcumin, demethoxycurcumin, and bisdemethoxycurcumin were not significantly different between the two groups ( $P > 0.05$ , Table 1).

According to the estimated concentration-time curve (Figure 3) and the pharmacokinetic values in Table 1, the concentration of emodin absorbed into the rat serum was similar between the two groups. However, the serum concentration of rhein was considerably higher in the MG + SJD during the first 12 h, which was in sharp contrast to curcumin and bisdemethoxycurcumin, which displayed lower serum concentrations in the MG + SJD than in the CG + SJD during the first 12 h. Both aloe-emodin and demethoxycurcumin showed a greater increase in

**Table 1** Pharmacokinetic parameters of the seven components of Shengjiang decoction

Component	Group	T <sub>max</sub> (h)	T <sub>1/2</sub> (h)	MRT (0-t) (h)	CL (L/h/kg)	C <sub>max</sub> (μg/L)	AUC (0-t) (μg/L/h)
Emodin	CG + SJD	0.56 ± 0.27	0.85 ± 1.09	4.13 ± 0.41	396 ± 147	16.23 ± 4.11	44.78 ± 18.87
	MG + SJD	0.50 ± 0.28	0.26 ± 0.12	3.08 ± 0.48 <sup>a</sup>	619 ± 193 <sup>a</sup>	16.47 ± 7.35	34.34 ± 14.78
ALEM	CG + SJD	3.89 ± 2.12	4.15 ± 2.08	4.77 ± 0.40	261 ± 97	17.88 ± 5.90	80.61 ± 23.75
	MG + SJD	0.83 ± 0.62 <sup>a</sup>	0.46 ± 0.49 <sup>a</sup>	3.18 ± 0.45 <sup>a</sup>	564 ± 209 <sup>a</sup>	13.77 ± 3.00	38.51 ± 16.63 <sup>a</sup>
Rhein	CG + SJD	0.44 ± 0.18	0.71 ± 0.65	2.32 ± 0.40	3.07 ± 0.39	4388 ± 957	6136.71 ± 816.0
	MG + SJD	0.39 ± 0.14	0.82 ± 0.57	2.19 ± 0.21	2.41 ± 0.35 <sup>a</sup>	5206 ± 1703	8025.27 ± 1074.26 <sup>a</sup>
CHRY	CG + SJD	0.50 ± 0.19	1.02 ± 1.63	2.93 ± 0.57	411 ± 118	22.46 ± 7.78	39.12 ± 5.9
	MG + SJD	0.56 ± 0.27	0.96 ± 0.66	4.04 ± 0.63 <sup>a</sup>	271 ± 76 <sup>a</sup>	17.44 ± 3.71	58.90 ± 23.74
Curcumin	CG + SJD	0.44 ± 0.18	0.71 ± 0.27	4.60 ± 1.26	15957 ± 8161	0.93 ± 1.42	1.01 ± 0.86
	MG + SJD	0.52 ± 0.08	0.69 ± 0.43	5.38 ± 0.71	25172 ± 11861	0.18 ± 0.04	0.56 ± 0.23
DEME	CG + SJD	0.89 ± 0.27	0.60 ± 0.49	4.90 ± 0.58	1518 ± 944	2.08 ± 0.37	10.62 ± 3.41
	MG + SJD	0.50 ± 0.19	0.36 ± 0.45	5.83 ± 0.91	1064 ± 717	1.99 ± 0.91	8.60 ± 1.90
BISD	CG + SJD	0.50 ± 0.28	3.18 ± 0.30	4.44 ± 0.46	4117 ± 677	1.03 ± 0.27	3.97 ± 0.52
	MG + SJD	0.61 ± 0.55	2.99 ± 0.14	3.93 ± 1.34	5159 ± 1829	0.83 ± 0.09	3.28 ± 0.47

<sup>a</sup>*P* < 0.05 vs CG + SJD. ALEM: Aloe-emodin; CHRY: Chrysophanol; DEME: Demethoxycurcumin; BISD: Bisdemethoxycurcumin; C<sub>max</sub>: Maximum concentration; T<sub>max</sub>: Time of maximum concentration; MRT: Mean residence time.

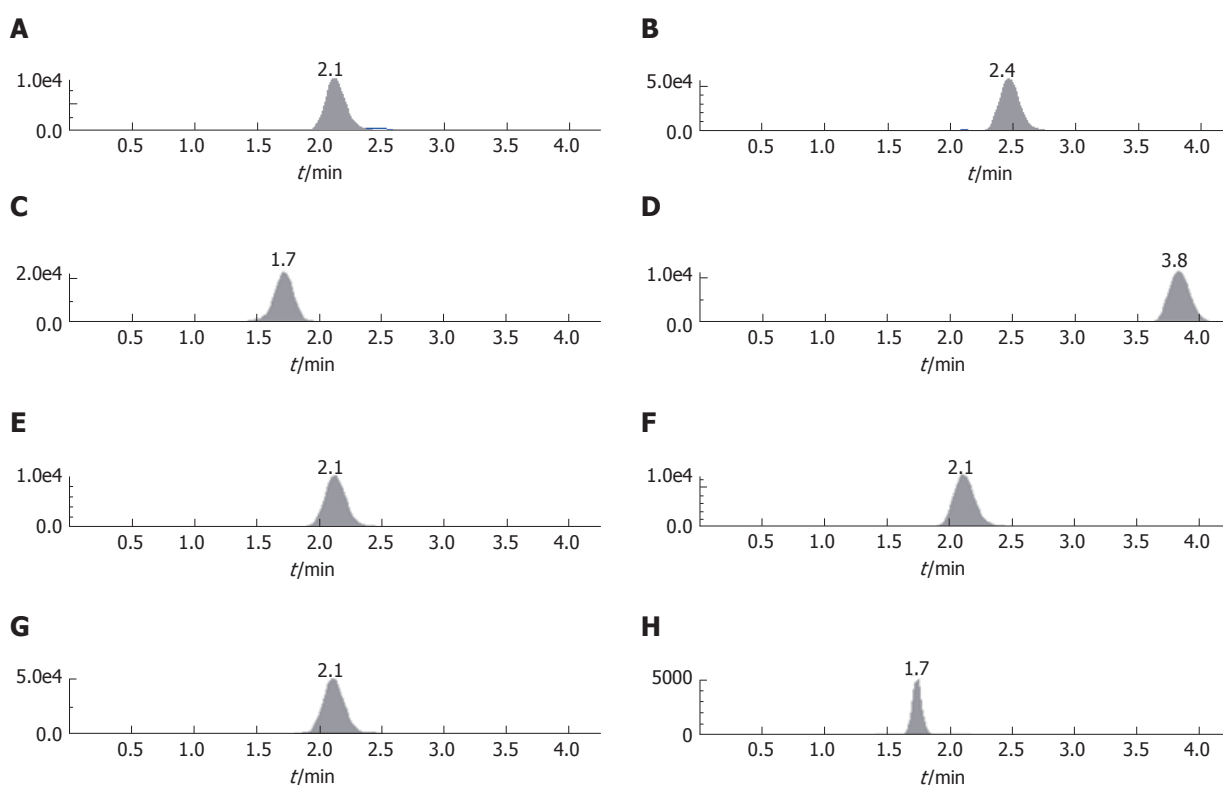


**Figure 2** HPLC chromatograms of the major components of Shengjiang decoction detected in the serum and pancreas. A: Emodin; B: Aloe-emodin; C: Rhein; D: Chrysophanol; E: Curcumin; F: Demethoxycurcumin; G: Bisdemethoxycurcumin; H: Internal standard (I.S.).

serum concentrations during the early phase in the MG + SJD than in the CG + SJD, which was opposite to the trend of chrysophanol.

#### Pancreatic distribution of major components of SJD

Regarding the distribution in the pancreas, although the concentration of rhein in the MG + SJD was significantly lower than that in the CG + SJD (*P* < 0.05, Table 2), it was notable among all components. Bisdemethoxycurcumin showed a drastically

higher pancreatic distribution in the MG + SJD (*P* < 0.05, Table 2). No significant difference was observed between the two groups for the remaining components.

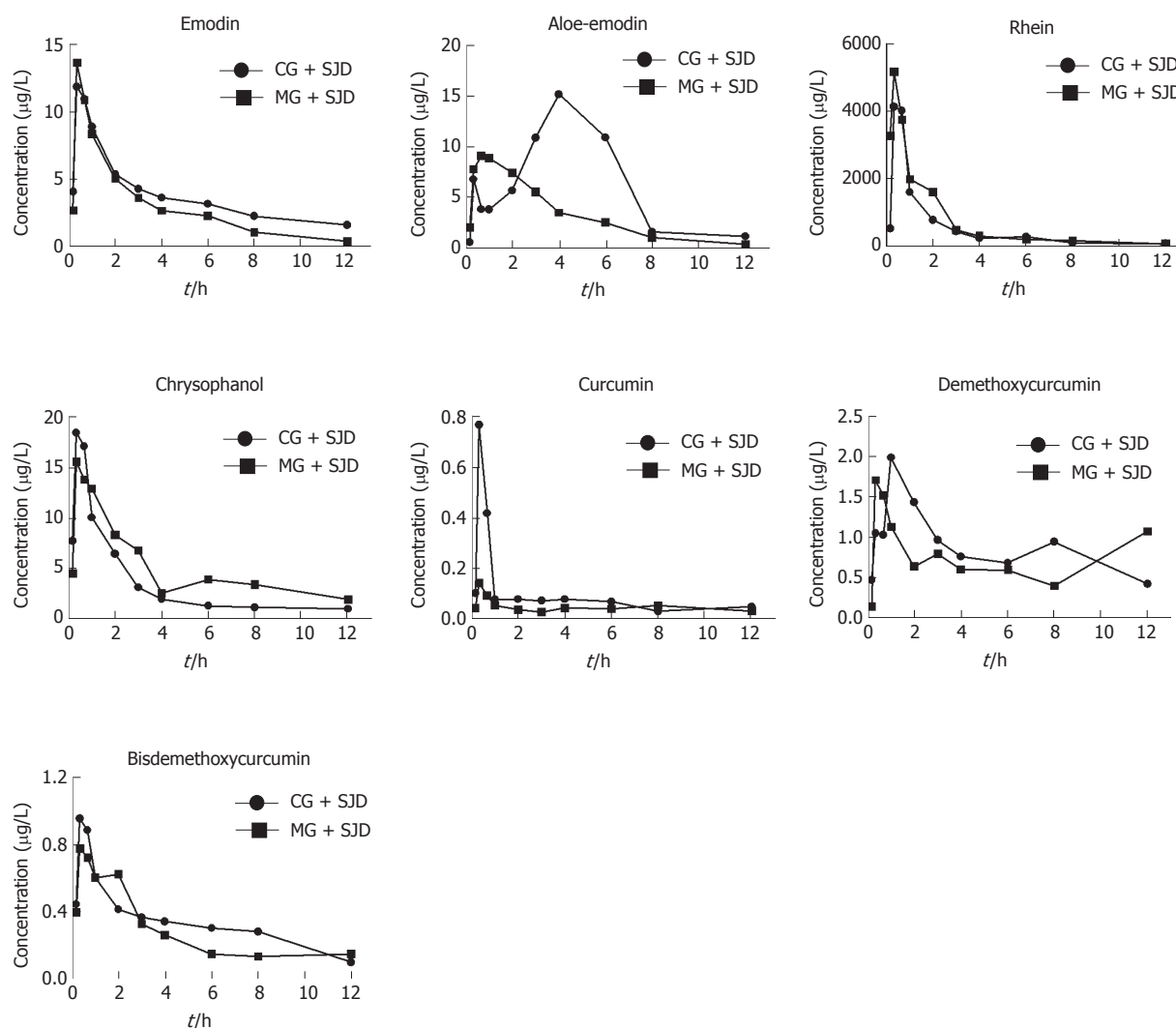
#### SJD regulates the inflammatory response in rats with AP

The serum amylase level was higher in the MG than in the CG (*P* < 0.05, Figure 4), which showed that the AP model was established successfully, while the lipase level in the two groups showed no significant



**Table 2** Component concentrations of Shengjiang decoction in the pancreas (ng/mL) (*n* = 6)

Group	Emodin	ALEM	Rhein	CHRY	Curcumin	DEME	BISD
CG + SJD	0.79 ± 0.38	0.29 ± 0.15	96.52 ± 31.35	0.54 ± 0.37	4.64 ± 2.74	0.22 ± 0.12	0.14 ± 0.03
MG + SJD	1.08 ± 0.30	0.26 ± 0.10	31.41 ± 13.27 <sup>a</sup>	0.58 ± 0.22	6.08 ± 2.77	0.20 ± 0.05	0.59 ± 0.22 <sup>a</sup>

<sup>a</sup>*P* < 0.05 *vs* CG + SJD. ALEM: Aloe-emodin; CHRY: Chrysophanol; DEME: Demethoxycurcumin; BISD: Bisdemethoxycurcumin.**Figure 3** Estimated concentration-time curves of seven components in the two groups. Twelve male Sprague-Dawley rats were randomly divided into a control group treated with SJD (CG + SJD) and a model group treated with SJD (MG + SJD), both of which were orally administered with SJD (5 g/kg) 2 h after surgery. Blood samples were collected *via* the tail vein at 10, 20, and 40 min and 1, 2, 3, 4, 6, 8, and 12 h after a single dose of SJD to detect its main components.

difference. The IL-6, IL-10, and TNF- $\alpha$  levels in the MG were significantly higher than those in the CG (*P* < 0.05, Figure 5). Compared to the MG, the SJDG exhibited a significantly higher IL-10 level and a lower TNF- $\alpha$  level (*P* < 0.05, Figure 5).

#### **SJD ameliorates multiple organ injury in rats with AP**

The CG showed no significant signs of edema, hemorrhage, inflammatory cell infiltration, or necrosis in the heart, lung, liver, spleen, pancreas, kidney, and intestine tissues. However, the MG exhibited a characteristic feature of pancreatitis. Pancreatic

tissues showed interstitial congestion, edema, inflammatory cell infiltration, focal or confluent necrosis and hemorrhage. The pathological images indicated obvious edema in the alveolar space and lung interstitium, broadened alveolar wall, inflammatory cell infiltration, telangiectasia, congestion, focal or flake hemorrhage and necrosis. The kidney samples exhibited edema and inflammatory cell infiltration in the renal interstitium, blurry boundaries in renal tubule epithelial cells, and stenosis or atresia in the lumens. The intestinal mucosa showed inflammatory cell infiltration in various mucosal layers, broadened intervillous lacunae,

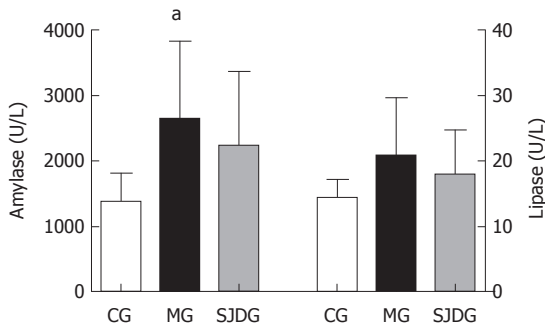


**Figure 4** Amylase and lipase concentrations of the control group, model group, and Shengjiang decoction group. Rats were randomly divided into a control group (CG), an AP model group (MG), and an SJD treated AP group (SJDG) ( $n = 6$  per group). The rats were sacrificed 12 h after administration of SJD. Blood samples were collected to obtain serum samples to measure amylase and lipase. Data are expressed as mean  $\pm$  SD. <sup>a</sup> $P < 0.05$  vs CG.

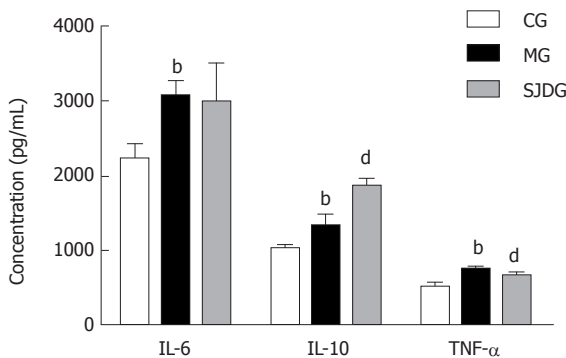


**Figure 5** Serum concentrations of IL-6, IL-10, and TNF- $\alpha$  in the control group, model group, and Shengjiang decoction group. Rats were randomly divided into a control group (CG), an AP model group (MG), and an SJD treated AP group (SJDG) ( $n = 6$  per group). The rats were sacrificed 12 h after administration of SJD. Blood samples were collected to obtain serum samples to measure IL-6, IL-10, and TNF- $\alpha$ . Data are expressed as mean  $\pm$  SD. <sup>b</sup> $P < 0.01$  vs CG; <sup>d</sup> $P < 0.01$  vs MG.

decreased beaker cells, and atrophic mucosa. Organic damage was also found in the heart, liver, and spleen of rats in the MG.

The MG had higher pathological scores than the CG for each organ tested ( $P < 0.05$ , Figure 6). After treatment with SJD, the pathological scores of the lung, pancreas, kidney, and intestine in the SJDG were significantly lower than those in the MG ( $P < 0.05$ , Figure 6). The pathological images of the seven organs are shown in Figure 7.

## DISCUSSION

We performed pharmacokinetic research to study the effect of AP on the metabolic processes of SJD *in vivo* and found that AP had varying effects on the pharmacokinetics of different components of SJD. In addition to the pharmacodynamic study, we further assessed the therapeutic properties and mechanisms of SJD involved in attenuating AP through

the regulation of inflammatory responses to protect against multiple organ injury.

Our previous study has established a quantitative method to determine 10 major components from Chinese Herbal Dachengqi Decoction (DCQD) simultaneously in rats and dogs<sup>[21,22]</sup>. Using the established method of HPLC-MS/MS, the main absorbed components including emodin, aloë-emodin, rhein, chrysophanol, curcumin, demethoxycurcumin, and bisdemethoxycurcumin in rats after administration of SJD were detected. The study confirmed that the seven major components of SJD could be absorbed into rat serum and pancreas through oral administration.

The pharmacokinetic parameters showed that AP had varying effects on different components of SJD. This study indicated that AP could promote the pharmacokinetic processes of emodin and aloë-emodin in rats, which is consistent with our previous studies<sup>[23,24]</sup>, thus demonstrating that AP could lower the blood concentration and accelerate the process of elimination of aloë-emodin.

However, the clearly higher AUC and lower CL values of rhein in the MG + SJD indicate that rhein could be better absorbed in rats with AP. This finding is in sharp contrast with the results regarding rhein from the DCQD study, which presented a lower AUC and higher pancreatic distribution in the AP group<sup>[23]</sup>. One possible explanation may be that concentrations of absorbed components may be associated with the effects of the Chinese herbal formula and the complex interactions among different components<sup>[25,26]</sup>. Interestingly, although the concentration of rhein in the pancreas in the MG + SJD was lower than that in the CG + SJD, it was highest among other components in the pancreas (Table 2). This is consistent with the results of the DQCD study, which provides evidence that rhein may be the potential active component of pancreas-targeted treatment in rats with AP<sup>[27-29]</sup>.

Furthermore, this study found that AP could slow the pharmacokinetic process of chrysophanol. In addition, AP had almost no influence on the pharmacokinetics of curcumin, demethoxycurcumin, and bisdemethoxycurcumin. Nevertheless, due to its higher concentration in the pancreas than in the CG + SJD, bisdemethoxycurcumin may be another potential active component of SJD for the treatment of AP.

Other studies have also revealed the effectiveness of rhein and bisdemethoxycurcumin in anti-inflammation in AP. Liu *et al.*<sup>[30]</sup> demonstrated that rhein glucoside, rhein isomer methylation, and emodin glucuronide conjugation were the main anti-AP components in Da-Huang-Fu-Zi-Tang. It has been reported that rhein attenuates inflammation *via* inhibition of NF- $\kappa$ B and NALP3 inflammasome pathways *in vivo* and *in vitro*<sup>[31]</sup>. In order to reach sufficient therapeutic accumulation in the pancreas to inhibit both the local and systemic complications with AP, the inflammatory

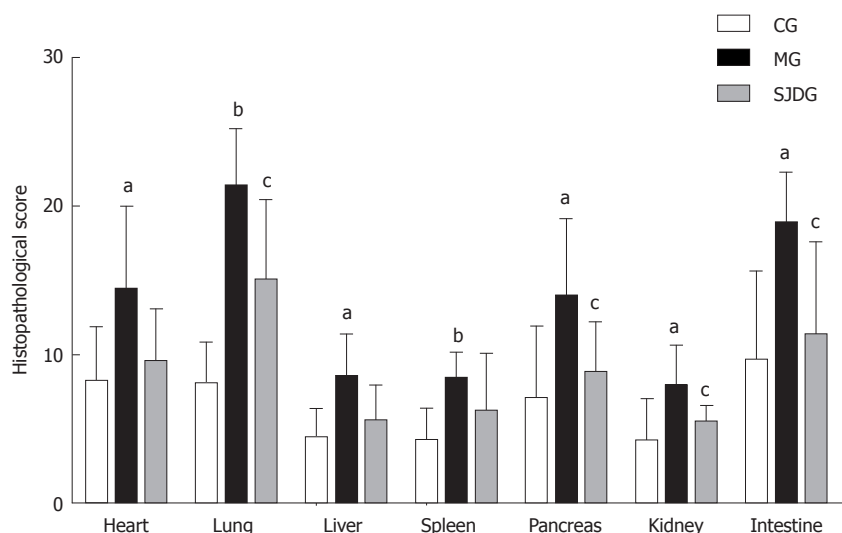


**Figure 6** Pathological scores of multiple organs in the control group, model group, and Shengjiang decoction group. Rats were randomly divided into a control group (CG), an AP model group (MG), and an SJD treated AP group (SJDG) ( $n = 6$  per group). The rats were sacrificed 12 h after administration of SJD. Tissue samples were collected for pathological examination. Data are expressed as mean  $\pm$  SD. <sup>a</sup> $P < 0.05$  vs CG; <sup>b</sup> $P < 0.01$  vs CG; <sup>c</sup> $P < 0.05$  vs MG; <sup>d</sup> $P < 0.01$  vs MG.

compound rhein has been tailored as dual pancreas- and lung-targeting therapy mediated by a phenolic propanediamine moiety<sup>[32]</sup>.

Bisdemethoxycurcumin has been demonstrated to exhibit anti-oxidative and anti-inflammatory activities such as inhibiting NO production and COX-2 and iNOS expression and suppressing LPS-induced I $\kappa$ B- $\alpha$  phosphorylation<sup>[33,34]</sup>, promote apoptosis through a GRP78-dependent pathway and mitochondrial dysfunctions, and potentiate the antitumor effect of gemcitabine in human pancreatic cancer cells<sup>[35]</sup>.

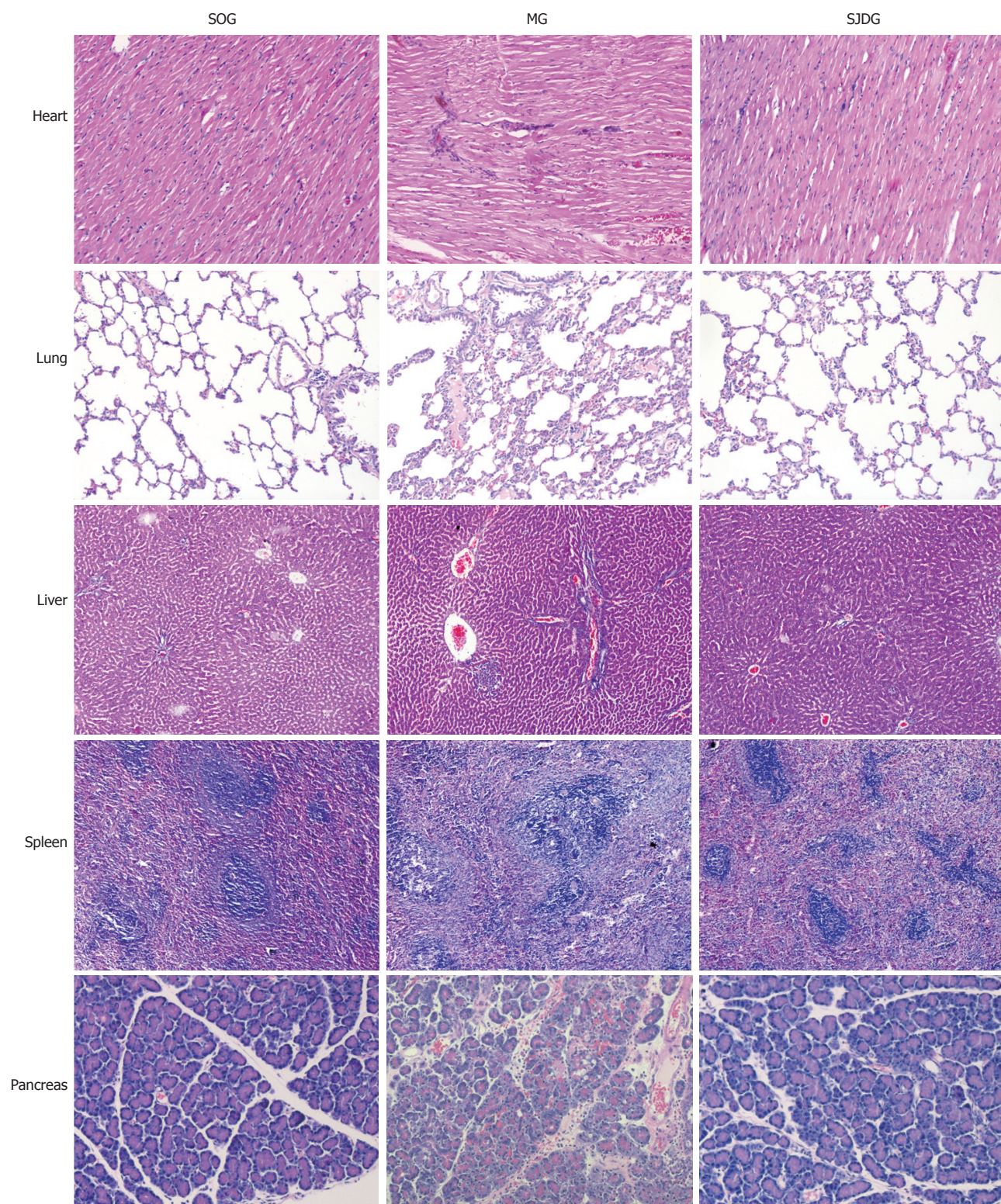
Cytokines play major roles in the pathogenesis of AP, including underlying systemic inflammatory responses, tissue damage, and organ dysfunction. Due to the release of pancreatin and activation of mononuclear macrophages, the excess neutrophilic leukocytes may produce or release substantial inflammatory mediators that form a network to cause inflammatory “cascade effects”, which manifest clinically as SIRS<sup>[36]</sup> in AP. When SIRS is persistent, there is an increased risk of developing multiple organ failure<sup>[37]</sup>. TNF- $\alpha$ , an early onset pro-inflammatory cytokine, directly injures the cells of multiple organs, causes ischemia, hemorrhage, necrosis, inflammation, and edema, and even triggers the synthesis of a wide range of other pro-inflammatory mediators such as IL-6 and IL-1<sup>[38]</sup>. IL-6, which produces extensive pro-inflammatory effects that cause tissue damage, has been identified as an early biomarker of severe organ failure and mortality<sup>[39,40]</sup>. Moreover, IL-6 may induce the release of TNF- $\alpha$  in a positive feedback pattern, leading to a vicious cycle<sup>[41]</sup>. Notably, the elevated IL-10 level, which may inhibit and reduce the synthesis and release of pro-inflammatory cytokines and colony

stimulating factor, signifies a pro-inflammatory state in SAP that is associated with an early anti-inflammatory response<sup>[42]</sup>. In this study, the MG showed higher TNF- $\alpha$ , IL-6, and IL-10 levels than the CG, indicating that AP could result in an inflammatory imbalance at the very beginning of the disease.

The imbalance of inflammatory mediators in circulation and target tissues may aggravate the progression of AP<sup>[43]</sup>. Moreover, the time courses of serum pro-inflammatory cytokine levels and anti-inflammatory cytokine levels differ, resulting in immune dysregulation, which leads to multisystem organ failure, mortality, and secondary infection<sup>[44]</sup>. Thus, varying degrees of pathological injuries in the heart, lung, liver, spleen, pancreas, kidney, and intestine were observed microscopically, which implies that SAP exhibits systemic involvement.

These pathological injuries may also explain the differences in pharmacokinetics between the CG + SJD and MG + SJD. Hypoperfusion of organs is common during shock and peripheral circulatory failure in SAP. When gastrointestinal disorders such as gastrointestinal mucosa ischemia and enteroplegia are present, they will have a detrimental impact on the absorption of the decoction<sup>[45]</sup>. Undermined by the initial local inflammatory reaction and microcirculation disturbance, the distortion of the blood-pancreas barrier may accelerate or inhibit the absorption of certain components into the pancreas<sup>[46]</sup>. Additionally, the initiation of organ failure in the hepatic and renal systems (such as the decreased serum albumin concentration and glomerular filtration rate), where most drugs are metabolized and eliminated, may also contribute to the changes in the pharmacokinetic







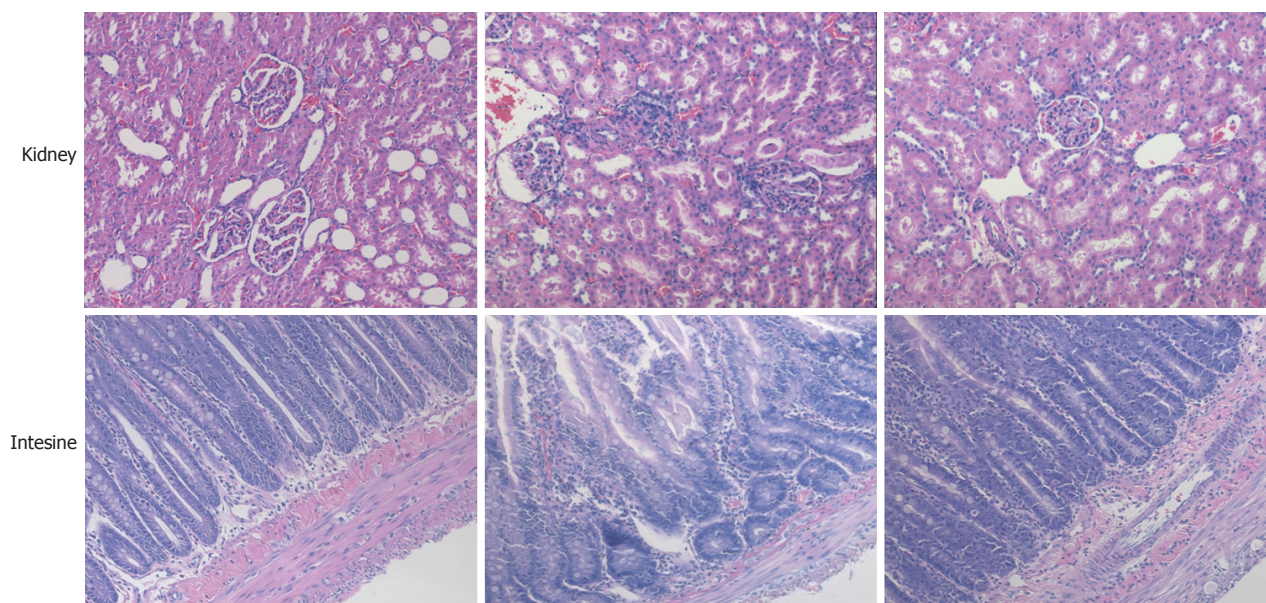


**Figure 7** Pathological images of multiple organs from the control group, model group, and Shengjiang decoction group. Pathological images of the heart (HE, × 200), lung (HE, × 200), liver (HE, × 100), spleen (HE, × 100), pancreas (HE, × 200), kidney (HE, × 200), and intestine (HE, × 100) in the CG, MG, and SJDG. CG: Control group; MG: AP model group; SJDG: SJD treated AP group.

parameters of SJD in rats with AP<sup>[47,48]</sup>. Moreover, other factors that may influence the pharmacokinetics of different components of Chinese herb prescriptions are associated with physical and chemical properties of the components, including the molecular size, lipid solubility, charge, and protein binding rate as well as methods of application<sup>[49]</sup>.

Notably, after treatment with SJD, the SJDG displayed a lower TNF- $\alpha$  level and a higher IL-10 level than the MG, indicating that SJD could regulate the balance of pro- and anti-inflammatory responses in AP. By decreasing pro-inflammatory cytokines and elevating anti-inflammatory cytokines, SJD could reduce inflammatory reactions, thus ameliorating the severity of AP induced by inflammatory responses. Moreover, SJD was effective in relieving injuries of the lung, kidney, intestine, and pancreas, which provided basic evidence of the effectiveness of SJD for its clinical application in the treatment of AP.

Apart from the pharmacokinetic and pharmacodynamic parameters as well as the distribution of the major components of SJD, the distribution of the effective components to other target tissues should be tested to provide more systematic and comprehensive evidence for the Chinese decoction, thus allowing more effective clinical application. Furthermore, the specific molecular mechanism of how the potential active components alleviate the disease needs to be investigated to optimize herbal formulations and therapies.

In conclusion, AP may have varying effects on the pharmacokinetics of the major components of SJD in rats. AP could accelerate the pharmacokinetic process

of emodin and aloe-emodin and slow that of rhein and chrysophanol. Rhein and bisdemethoxycurcumin may be potential active components for the treatment of AP. SJD may attenuate AP by regulating inflammatory responses to protect against multiple organ injury.

## ARTICLE HIGHLIGHTS

### Research background

Acute pancreatitis (AP) is one of the most common gastrointestinal disorders associated with a mortality rate up to 30%-56% among severe cases with systemic inflammatory response syndrome. Shengjiang decoction (SJD) is an effective prescription for the treatment of AP, but the exact active components are not clear. Little is known about the *in vivo* metabolic process of SJD. Therefore, full elucidation of the pharmacokinetic and pharmacodynamic mechanisms of SJD associated with the amelioration of AP is urgently needed.

### Research motivation

This study aimed to explore the pharmacokinetics, pharmacodynamics, and pancreatic distribution of the main components of SJD in rats with AP to provide pharmacokinetic and pharmacodynamic evidence for its clinical application for the treatment of AP in the future.

### Research objectives

This study aimed to explore the pharmacokinetics and pharmacodynamics of SJD in rats with AP for protecting against multiple organ injury.

### Research methods

The AP model was established by retrograde perfusion of 3.5% sodium taurocholate into the biliopancreatic duct, which was widely accepted and used in the induction of AP in rats.

The concentrations of the main components of SJD in serum were measured by HPLC-MS/MS, which is a simple, rapid, accurate, and sensitive way to detect the components in serum and tissues of SJD. Analyst 1.4.2 software for HPLC-MS/MS was used for data collection.

All statistical analyses were performed with PEMS3.1 statistical software

for windows. Quantitative data are expressed as the mean  $\pm$  standard deviation when normally distributed. Comparisons of the pharmacokinetic parameters were performed by Student's *t*-test. One-way repeated-measures ANOVA followed by multiple pair-wise comparisons using the Student-Newman-Keuls test was used to detect differences of the pharmacodynamic parameters.

## Research results

In the pharmacokinetic experiment, the MG + SJD displayed significantly shorter mean residence time (MRT) and higher clearance (CL) for emodin and aloe-emodin; significantly shorter *T*<sub>max</sub> and *T*<sub>1/2</sub> and a lower area under curve (AUC) for aloe-emodin; an apparently higher AUC and lower CL for rhein; and longer MRT and lower CL for chrysophanol than the CG + SJD. In the pharmacodynamic experiment, the amylase, IL-6, IL-10, and TNF- $\alpha$  levels in MG were higher than those in the CG ( $P < 0.05$ ). After the herbal decoction treatment, the SJDG had higher IL-10 and lower TNF- $\alpha$  levels than the MG ( $P < 0.05$ ). The MG had the highest pathological scores, and the pathological scores of the lung, pancreas, kidney, and intestine in the SJDG were significantly lower than those in the MG ( $P < 0.05$ ). The results revealed metabolic process of the major components of SJD absorbed in serum and pancreas as well as the possible mechanism of SJD in alleviating AP.

What remains to be solved is that the distribution of the effective components to other target tissues to provide more systematic and comprehensive evidence for the clinical application of Chinese decoction. Furthermore, the specific molecular mechanism of how the potential active components alleviate the disease needs to be investigated to optimize herbal formulations and therapies.

## Research conclusions

In the study, we found that AP may have varying effects on the pharmacokinetics of the major SJD components in rats, rhein and bisdemethoxycurcumin may be potential active components for the treatment of AP, and SJD might alleviate pathological injuries of the lung, pancreas, kidney, and intestine in rats with AP via regulating pro- and anti-inflammatory responses. The conclusions are based on our previous theory of 'tissue pharmacology of recipe', and are in accordance with the clinical and experiment results available that SJD is an effective way to alleviate AP.

We report the metabolic processes of major components of SJD *in vivo* and the pharmacodynamic mechanism of SJD in relieving AP. The study indicated that diseased condition of the body as well as formula composition may have certain effect on the metabolic process of different components in decoctions. As AP involves systemic inflammatory responses, based on the findings above, the mechanism for SJD to attenuate AP may be through the regulation of inflammatory responses to protect against multiple organ injury.

## Research perspectives

As we have found the potential components of SJD in alleviating AP, further investigation about the interaction of these components is urgently needed to provide evidence for optimizing and simplifying the formula. Moreover, more in-depth studies about the molecular mechanism of SJD in alleviating AP should be explored to have a deeper and more comprehensive understanding of SJD in treating AP.

## REFERENCES

- 1 Ince AT, Baysal B. Pathophysiology, classification and available guidelines of acute pancreatitis. *Turk J Gastroenterol* 2014; **25**: 351-357 [PMID: 25254514 DOI: 10.5152/tjg.2014.13005]
- 2 Yadav D, Lowenfels AB. The epidemiology of pancreatitis and pancreatic cancer. *Gastroenterology* 2013; **144**: 1252-1261 [PMID: 23622135 DOI: 10.1053/j.gastro.2013.01.068]
- 3 Yadav D, Lowenfels AB. Trends in the epidemiology of the first attack of acute pancreatitis: a systematic review. *Pancreas* 2006; **33**: 323-330 [PMID: 17079934 DOI: 10.1097/01.mpa.0000236733.31617.52]
- 4 Forsmark CE, Vege SS, Wilcox CM. Acute Pancreatitis. *N Engl J Med* 2016; **375**: 1972-1981 [PMID: 27959604 DOI: 10.1056/NEJMr1505202]
- 5 Dellinger EP, Forsmark CE, Layer P, Lévy P, Maravi-Poma E, Petrov MS, Shimosegawa T, Siriwardena AK, Uomo G, Whitcomb DC, Windsor JA; Pancreatitis Across Nations Clinical Research and Education Alliance (PANCREA). Determinant-based classification of acute pancreatitis severity: an international multidisciplinary consultation. *Ann Surg* 2012; **256**: 875-880 [PMID: 22735715 DOI: 10.1097/SLA.0b013e318256f778]
- 6 Chen W, Yang X, Huang L, Xue P, Wan M, Guo J, Zhu L, Jin T, Huang Z, Chen G, Tang W, Xia Q. Qing-Yi decoction in participants with severe acute pancreatitis: a randomized controlled trial. *Chin Med* 2015; **10**: 11 [PMID: 26029248 DOI: 10.1186/s13020-015-0039-8]
- 7 Ji CH, Tang CW, Feng WM, Bao Y, Yao LQ. A Chinese Herbal Decoction, Huoxue Qingyi Decoction, Promotes Rehabilitation of Patients with Severe Acute Pancreatitis: A Retrospective Study. *Evid Based Complement Alternat Med* 2016; **2016**: 3456510 [PMID: 27110265 DOI: 10.1155/2016/3456510]
- 8 Zhu SF, Guo H, Zhang RR, Zhang Y, Li J, Zhao XL, Chen TR, Wan MH, Chen GY, Tang WF. Effect of electroacupuncture on the inflammatory response in patients with acute pancreatitis: an exploratory study. *Acupunct Med* 2015; **33**: 115-120 [PMID: 25520280 DOI: 10.1136/acupmed-2014-010646]
- 9 Wan MH, Yao J, Li J, Xia Q, Zhu L, Tang WF. The effectiveness of purgation and electroacupuncture in extrahepatic bile duct stone complicated with acute biliary pancreatitis: management of biliary stone pancreatitis through traditional Chinese medicine. *Pancreas* 2011; **40**: 483-484 [PMID: 21412122 DOI: 10.1097/MPA.0b013e318205e52f]
- 10 Lai F, Zhang Y, Xie DP, Mai ST, Weng YN, Du JD, Wu GP, Zheng JX, Han Y. A Systematic Review of Rhubarb (a Traditional Chinese Medicine) Used for the Treatment of Experimental Sepsis. *Evid Based Complement Alternat Med* 2015; **2015**: 131283 [PMID: 26339264 DOI: 10.1155/2015/131283]
- 11 Zhang L, Chen J, Jiang D, Zhang P. Adjuvant treatment with crude rhubarb for patients with systemic inflammation reaction syndrome/sepsis: a meta-analysis of randomized controlled trials. *J Crit Care* 2015; **30**: 282-289 [PMID: 25617260 DOI: 10.1016/j.jcrc.2014.11.008]
- 12 Gulcubuk A, Altunatmaz K, Sonmez K, Haktanir-Yatkin D, Uzun H, Gurel A, Aydin S. Effects of curcumin on tumour necrosis factor-alpha and interleukin-6 in the late phase of experimental acute pancreatitis. *J Vet Med A Physiol Pathol Clin Med* 2006; **53**: 49-54 [PMID: 16411910 DOI: 10.1111/j.1439-0442.2006.00786.x]
- 13 Sandur SK, Pandey MK, Sung B, Ahn KS, Murakami A, Sethi G, Limtrakul P, Badmaev V, Aggarwal BB. Curcumin, demethoxycurcumin, bisdemethoxycurcumin, tetrahydrocurcumin and turmerones differentially regulate anti-inflammatory and anti-proliferative responses through a ROS-independent mechanism. *Carcinogenesis* 2007; **28**: 1765-1773 [PMID: 17522064 DOI: 10.1093/carcin/bgm123]
- 14 Sun K. Shengjiangsan combined with routine therapy for effect on severity score and serological nutrition indicators of patients with SIRS/MODS. Shandong University of TCM 2013
- 15 Gu WY, Zhao L, Qian FH, Wu Y, Cao DF. Treatment of Acute Pancreatitis with Shengjiang Powder. *Jilin Zhongyiyao* 2013; **33**: 1232-1234
- 16 Gao B, Li R, Zhu L, Zhang W, Qian Y. Study of Shengjiangsan on Major Chinese Medicine Clinical Symptoms in Patients with Early Sepsis. *Liaoning Zhongyiyao Daxue Xuebao* 2009; **11**: 100-102 [DOI: 10.13194/j.jlunivtcm.2009.12.102.gaob.048]
- 17 Niu D, Hou F. Effects of Shengjiang powder on contents of 6-keto-PGF-1 $\alpha$ , TXB2, TNF- $\alpha$  and EGF in rats with acute gastric mucosal damage. *Wujing Yixue* 2005; **16**: 417-419
- 18 Qian YM, Zhu L, Gao B. Effect of serum IL-2, IL-4 and IL-6 intervention in patients with systemic inflammatory response syndrome. *Zhongwai Yiliao* 2008; **10**: 34-35 [DOI: 10.16662/j.cnki.1674-0742.2008.10.007]



- 19 **Han JH**, Su HS. Clinical effect of Modified Decoction Combined with metformin in the treatment of nonalcoholic fatty liver disease with metabolic syndrome. *Shanxi Zhongyi* 2013; 989-991
- 20 **Li J**, Tang WF. Effect of Sheng-jiang-san in regulating obesity-mediated systemic inflammatory microenvironment and mitigating multiple organ injury in obese rats with acute pancreatitis. Proceedings of The Twelfth National Conference of Chinese traditional and Western medicine experimental medical Specialized Committee. 2015: 41-42
- 21 **Liu YL**, Zhao XL, Li J, Wan MH, Chen GY, Chen WW, Tang WF. Effect of acute pancreatitis on the pharmacokinetics of Chinese herbal micron Liuhe Pill ointment in rats. *Chin J Integr Med* 2015; **21**: 922-927 [PMID: 26138330 DOI: 10.1007/s11655-015-2080-y]
- 22 **Yu Q**, Xiang J, Tang W, Liang M, Qin Y, Nan F. Simultaneous determination of the 10 major components of Da-Cheng-Qi decoction in dog plasma by liquid chromatography tandem mass spectrometry. *J Chromatogr B Analyt Technol Biomed Life Sci* 2009; **877**: 2025-2031 [PMID: 19523886 DOI: 10.1016/j.jchromb.2009.05.030]
- 23 **Tang WF**, Yu Q, Xiang J. Effect of AP on the pharmacokinetics of Dachengqi Decoction in rats. The twentieth National Conference on digestive system diseases of Chinese traditional and Western Medicine and Compilation of papers on the progress in diagnosis and treatment of digestive diseases. 2008: 178
- 24 **Gong HL**, Tang WF, Yu Q, Xiang J, Xia Q, Chen GY, Huang X, Liang MZ. Effect of severe acute pancreatitis on pharmacokinetics of Da-Cheng-Qi Decoction components. *World J Gastroenterol* 2009; **15**: 5992-5999 [PMID: 20014465 DOI: 10.3748/wjg.15.5992]
- 25 **Gong HL**, Tang WF, Wang J, Chen GY, Huang X. Effect of formula compatibility on the pharmacokinetics of components from Dachengqi Decoction [See Text] in rats. *Chin J Integr Med* 2012; **18**: 708-713 [PMID: 22936325 DOI: 10.1007/s11655-012-1205-9]
- 26 **Zhang W**, Di LQ, Li JS, Shan JJ, Kang A, Qian S, Chen LT. The effects of Glycyrrhizae uralensis and its major bioactive components on pharmacokinetics of daphnetin in Cortex daphnes in rats. *J Ethnopharmacol* 2014; **154**: 584-592 [PMID: 24704595 DOI: 10.1016/j.jep.2014.03.047]
- 27 **Li JY**, Zhu L, Xiang J, Zhao JL, Li J, Guo H. Targeted tissue distribution of Da-Cheng-Qi decoction in rat with acute *Zhongguo Shiyan Fangyixue Zazhi* 2016; **22**: 40-45
- 28 **Zhao J**, Tang W, Wang J, Xiang J, Gong H, Chen G. Pharmacokinetic and pharmacodynamic studies of four major phytochemical components of Da-Cheng-Qi decoction to treat acute pancreatitis. *J Pharmacol Sci* 2013; **122**: 118-127 [PMID: 23739595]
- 29 **Zhao XL**, Xiang J, Wan MH, Yu Q, Chen WW, Chen GY, Tang WF. Effect of acute pancreatitis on the pharmacokinetics of Chinese herbal ointment Liu-He-Dan in anaesthetized rats. *J Ethnopharmacol* 2013; **145**: 94-99 [PMID: 23127650 DOI: 10.1016/j.jep.2012.10.036]
- 30 **Liu X**, Wang XL, Wu L, Li H, Qin KM, Cai H, Pei K, Liu T, Cai BC. Investigation on the spectrum-effect relationships of Da-Huang-Fu-Zi-Tang in rats by UHPLC-ESI-Q-TOF-MS method. *J Ethnopharmacol* 2014; **154**: 606-612 [PMID: 24768806 DOI: 10.1016/j.jep.2014.04.027]
- 31 **Ge H**, Tang H, Liang Y, Wu J, Yang Q, Zeng L, Ma Z. Rhein attenuates inflammation through inhibition of NF- $\kappa$ B and NALP3 inflammasome in vivo and in vitro. *Drug Des Devel Ther* 2017; **11**: 1663-1671 [PMID: 28652704 DOI: 10.2147/DDDT.S133069]
- 32 **Li J**, Zhang J, Fu Y, Sun X, Gong T, Jiang J, Zhang Z. Dual pancreas- and lung-targeting therapy for local and systemic complications of acute pancreatitis mediated by a phenolic propanediamine moiety. *J Control Release* 2015; **212**: 19-29 [PMID: 26071629 DOI: 10.1016/j.jconrel.2015.06.011]
- 33 **Guo LY**, Cai XF, Lee JJ, Kang SS, Shin EM, Zhou HY, Jung JW, Kim YS. Comparison of suppressive effects of demethoxycurcumin and bisdemethoxycurcumin on expressions of inflammatory mediators in vitro and in vivo. *Arch Pharm Res* 2008; **31**: 490-496 [PMID: 18449507 DOI: 10.1007/s12272-001-1183-8]
- 34 **Kim AN**, Jeon WK, Lee JJ, Kim BC. Up-regulation of heme oxygenase-1 expression through CaMKII-ERK1/2-Nrf2 signaling mediates the anti-inflammatory effect of bisdemethoxycurcumin in LPS-stimulated macrophages. *Free Radic Biol Med* 2010; **49**: 323-331 [PMID: 20430097 DOI: 10.1016/j.freeradbiomed.2010.04.015]
- 35 **Yang HP**, Fan SJ, An Y, Wang X, Pan Y, Xiaokaiti Y, Duan JH, Li X, Tie L, Ye M, Li XJ. Bisdemethoxycurcumin exerts pro-apoptotic effects in human pancreatic adenocarcinoma cells through mitochondrial dysfunction and a GRP78-dependent pathway. *Oncotarget* 2016; **7**: 83641-83656 [PMID: 27845899 DOI: 10.18632/oncotarget.13272]
- 36 **Mansfield C**. Pathophysiology of acute pancreatitis: Potential application from experimental models and human medicine to dogs. *J Vet Intern Med* 2012; **26**: 875-887 [PMID: 22676262 DOI: 10.1111/j.1939-1676.2012.00949.x]
- 37 **Singh VK**, Wu BU, Bollen TL, Repas K, Maurer R, Mortelet KJ, Banks PA. Early systemic inflammatory response syndrome is associated with severe acute pancreatitis. *Clin Gastroenterol Hepatol* 2009; **7**: 1247-1251 [PMID: 19686869 DOI: 10.1016/j.cgh.2009.08.012]
- 38 **Akinosoglou K**, Gogos C. Immune-modulating therapy in acute pancreatitis: fact or fiction. *World J Gastroenterol* 2014; **20**: 15200-15215 [PMID: 25386069 DOI: 10.3748/wjg.v20.i41.15200]
- 39 **Phillip V**, Steiner JM, Algül H. Early phase of acute pancreatitis: Assessment and management. *World J Gastrointest Pathophysiol* 2014; **5**: 158-168 [PMID: 25133018 DOI: 10.4291/wjgp.v5.i3.158]
- 40 **Sathyanarayan G**, Garg PK, Prasad H, Tandon RK. Elevated level of interleukin-6 predicts organ failure and severe disease in patients with acute pancreatitis. *J Gastroenterol Hepatol* 2007; **22**: 550-554 [PMID: 17376050 DOI: 10.1111/j.1440-1746.2006.04752.x]
- 41 **Han T**, Li X, Cai D, Zhong Y, Chen LG, Geng S, Yin S. Effect of glutamine on apoptosis of intestinal epithelial cells of severe acute pancreatitis rats receiving nutritional support in different ways. *Int J Clin Exp Pathol* 2013; **6**: 503-509 [PMID: 23412711]
- 42 **Laveda R**, Martinez J, Munoz C, Penalva JC, Saez J, Belda G, Navarro S, Feu F, Mas A, Palazon JM, Sanchez-Paya J, Such J, Perez-Mateo M. Different profile of cytokine synthesis according to the severity of acute pancreatitis. *World J Gastroenterol* 2005; **11**: 5309-5313 [PMID: 16149137 DOI: 10.3748/wjg.v11.i34.5309]
- 43 **Vasseur P**, Devaure I, Sellier J, Delwail A, Chagneau-Derode C, Chazier F, Tougeron D, Tasu JP, Rabeony H, Lecron JC, Silvain C. High plasma levels of the pro-inflammatory cytokine IL-22 and the anti-inflammatory cytokines IL-10 and IL-1ra in acute pancreatitis. *Pancreatol* 2014; **14**: 465-469 [PMID: 25240697 DOI: 10.1016/j.pan.2014.08.005]
- 44 **Shen Y**, Deng X, Xu N, Li Y, Miao B, Cui N. Relationship between the degree of severe acute pancreatitis and patient immunity. *Surg Today* 2015; **45**: 1009-1017 [PMID: 25410475 DOI: 10.1007/s00595-014-1083-1]
- 45 **Landahl P**, Ansari D, Andersson R. Severe Acute Pancreatitis: Gut Barrier Failure, Systemic Inflammatory Response, Acute Lung Injury, and the Role of the Mesenteric Lymph. *Surg Infect (Larchmt)* 2015; **16**: 651-656 [PMID: 26237406 DOI: 10.1089/sur.2015.034]
- 46 **Tomkötter L**, Erbes J, Trepte C, Hinsch A, Dupree A, Bockhorn M, Mann O, Izbicki JR, Bachmann K. The Effects of Pancreatic Microcirculatory Disturbances on Histopathologic Tissue Damage and the Outcome in Severe Acute Pancreatitis. *Pancreas* 2016; **45**: 248-253 [PMID: 26646271 DOI: 10.1097/MPA.0000000000000440]
- 47 **Petejova N**, Martinek A. Acute kidney injury following acute pancreatitis: A review. *Biomed Pap Med Fac Univ Palacky Olomouc Czech Repub* 2013; **157**: 105-113 [PMID: 23774848 DOI: 10.5507/bp.2013.048]
- 48 **Ou ZB**, Miao CM, Ye MX, Xing DP, He K, Li PZ, Zhu RT, Gong JP. Investigation for role of tissue factor and blood coagulation



system in severe acute pancreatitis and associated liver injury. *Biomed Pharmacother* 2017; **85**: 380-388 [PMID: 27923687 DOI: 10.1016/j.biopha.2016.11.039]

49 **Xu H**, Jiang J, Xia ZL, Wang ML. Permeability of cefpiramide through blood- pancreatic barrier in the mice with sever acute pancreatitis. *Zhongguo Yaowu Jingjie* 2014; **11**: 645-648

**P- Reviewer:** Chiu KW, Dambrasukas Z, Liao KF **S- Editor:** Chen K  
**L- Editor:** Wang TQ **E- Editor:** Huang Y



## Retrospective Cohort Study

# Prevalence of- and risk factors for work disability in Dutch patients with inflammatory bowel disease

Lieke M Spekhorst, Bas Oldenburg, Ad A van Bodegraven, Dirk J de Jong, Floris Imhann, Andrea E van der Meulen-de Jong, Marieke J Pierik, Janneke C van der Woude, Gerard Dijkstra, Geert D'Haens, Mark Löwenberg, Rinse K Weersma, Eleonora AM Festen; Parelsnoer Institute and the Dutch Initiative on Crohn and Colitis

Lieke M Spekhorst, Floris Imhann, Eleonora AM Festen, Gerard Dijkstra, Rinse K Weersma, Department of Gastroenterology and Hepatology, University of Groningen and University Medical Centre Groningen, Groningen, 9700 RB Groningen, the Netherlands

Lieke M Spekhorst, Floris Imhann, Eleonora AM Festen, Department of Genetics, University of Groningen and University Medical Centre Groningen, Groningen, 9700 RB Groningen, the Netherlands

Bas Oldenburg, Department of Gastroenterology and Hepatology, University Medical Center Utrecht, Utrecht, 3584 CX Utrecht, the Netherlands

Ad A van Bodegraven, Department of Gastroenterology and Hepatology, VU University Medical Center, Amsterdam, 1081 HV Amsterdam, the Netherlands

Dirk J de Jong, Department of Gastroenterology and Hepatology, University Medical Center St. Radboud, Nijmegen, 6525 GA Nijmegen, the Netherlands

Andrea E van der Meulen-de Jong, Department of Gastroenterology and Hepatology, Leiden University Medical Center, Leiden, 2333 ZA Leiden, the Netherlands

Marieke J Pierik, Department of Gastroenterology and Hepatology, University Medical Center Maastricht, Maastricht, 6229 HX Maastricht, the Netherlands

Janneke C van der Woude, Department of Gastroenterology and Hepatology, Erasmus Medical Center, the Netherlands, Rotterdam, 3015 CE Rotterdam, the Netherlands

Geert D'Haens, Mark Löwenberg, Department of Gastroenterology and Hepatology, Amsterdam Medical Center, Amsterdam, 1105 AZ Amsterdam-Zuidoost, the Netherlands

ORCID number: Lieke M Spekhorst (0000-0002-9313-76

41); Bas Oldenburg (0000-0002-3962-6831); Ad A van Bodegraven (0000-0003-2636-303X); Dirk J de Jong (0000-0003-3659-8449); Floris Imhann (0000-0001-5278-903X); Andrea E van der Meulen-de Jong (0000-0001-9353-5431); Marieke J Pierik (0000-0001-6981-6516); Janneke C van der Woude (0000-0003-3875-6957); Gerard Dijkstra (0000-0003-4563-7462); Geert D'Haens (0000-0003-2784-4046); Mark Löwenberg (0000-0002-4975-9945); Rinse K Weersma (0000-0001-7928-7371); Eleonora AM Festen (0000-0002-3255-6930).

**Author contributions:** The Parelsnoer Institute, founded by the Dutch Federation of University Medical Centers, provided the research infrastructure; Oldenburg B, van Bodegraven AA, de Jong DJ, van der Meulen-de Jong AE, Pierik MJ, van der Woude JC, Dijkstra G, Imhann F, Festen EAM and Weersma RK enrolled the IBD patients, collected the patient data and performed a critical revision of the manuscript; Weersma RK, Spekhorst LM and Festen EAM designed the study, Spekhorst LM interpreted the data, performed the statistical analysis and drafted the manuscript; all authors approved the final manuscript.

**Supported by the Netherlands Organisation for Scientific Research, VIDI grant No. 016.136.308 to Weersma RK; Career Development grant of the Dutch Digestive Foundation, No. CDG 14-04 to Festen EAM.**

**Institutional review board statement:** This nationwide Parelsnoer Institute project is part of and funded by the Netherlands Federation of University Medical Centers and has received initial funding from the Dutch Government (from 2007-2011). The Parelsnoer Institute currently facilitates the uniform nationwide collection of information on and biomaterials of thirteen other diseases.

**Informed consent statement:** All patients included in this study gave informed consent prior to study inclusion.

**Conflict-of-interest statement:** All authors have no conflict of interest related to the manuscript.

**Data sharing statement:** Festen EAM is accepting full responsibility for the conduct of the study. This author has had access to the data and had control of the decision to publish.

**Open-Access:** This article is an open-access article which was selected by an in-house editor and fully peer-reviewed by external reviewers. It is distributed in accordance with the Creative Commons Attribution Non Commercial (CC BY-NC 4.0) license, which permits others to distribute, remix, adapt, build upon this work non-commercially, and license their derivative works on different terms, provided the original work is properly cited and the use is non-commercial. See: <http://creativecommons.org/licenses/by-nc/4.0/>

**Manuscript source:** Unsolicited manuscript

**Correspondence to:** Eleonora AM Festen, MD, PhD, Department of Gastroenterology and Hepatology, University of Groningen and University Medical Centre Groningen, Hanzeplein 1, Groningen, 9700 RB Groningen, the Netherlands. [e.a.m.festen@umcg.nl](mailto:e.a.m.festen@umcg.nl)  
Telephone: +31-503-610426  
Fax: +31-503-619306

Received: June 28, 2017

Peer-review started: June 28, 2017

First decision: July 27, 2017

Revised: August 26, 2017

Accepted: September 13, 2017

Article in press: September 13, 2017

Published online: December 14, 2017

## Abstract

### AIM

To determine the prevalence of work disability in inflammatory bowel disease (IBD), and to assess risk factors associated with work disability.

### METHODS

For this retrospective cohort study, we retrieved clinical data from the Dutch IBD Biobank on July 2014, containing electronic patient records of 3388 IBD patients treated in the eight University Medical Centers in the Netherlands. Prevalence of work disability was assessed in 2794 IBD patients and compared with the general Dutch population. Multivariate analyses were performed for work disability (sick leave, partial and full disability) and long-term full work disability (> 80% work disability for > 2 years).

### RESULTS

Prevalence of work disability was higher in Crohn's disease (CD) (29%) and ulcerative colitis (UC) (19%) patients compared to the general Dutch population (7%). In all IBD patients, female sex, a lower education level, and extra-intestinal manifestations, were associated with work disability. In CD patients, an age > 40 years at diagnosis, disease duration > 15 years,

smoking, surgical interventions, and anti-TNF $\alpha$  use were associated with work disability. In UC patients, an age > 55 years, and immunomodulator use were associated with work disability. In CD patients, a lower education level (OR = 1.62, 95%CI: 1.02-2.58), and in UC patients, disease complications (OR = 3.39, 95%CI: 1.09-10.58) were associated with long-term full work disability.

### CONCLUSION

The prevalence of work disability in IBD patients is higher than in the general Dutch population. Early assessment of risk factors for work disability is necessary, as work disability is substantial among IBD patients.

**Key words:** Inflammatory bowel disease; Crohn's disease; Ulcerative colitis; Work disability; Health care costs

© The Author(s) 2017. Published by Baishideng Publishing Group Inc. All rights reserved.

**Core tip:** Our study shows that a lower education is patients with Crohn's disease, and disease complications (osteopenia, thromboembolic event) in patients with ulcerative colitis are associated with long-term full work disability (> 80% work disability for > 2 years). This highlights the need for early assessment of risk factors for work disability, as work disability is substantial among inflammatory bowel disease patients and associated with high societal health care costs.

Spekhorst LM, Oldenburg B, van Bodegraven AA, de Jong DJ, Imhann F, van der Meulen-de Jong AE, Pierik MJ, van der Woude JC, Dijkstra G, D'Haens G, Löwenberg M, Weersma RK, Festen EAM; Parelinoer Institute and the Dutch Initiative on Crohn and Colitis. Prevalence of- and risk factors for work disability in Dutch patients with inflammatory bowel disease. *World J Gastroenterol* 2017; 23(46): 8182-8192 Available from: URL: <http://www.wjgnet.com/1007-9327/full/v23/i46/8182.htm> DOI: <http://dx.doi.org/10.3748/wjg.v23.i46.8182>

## INTRODUCTION

Inflammatory bowel disease (IBD), consisting of Crohn's disease (CD) and ulcerative colitis (UC) is a heterogeneous/multifaceted disease. Patients suffer from symptoms like diarrhoea, abdominal pain, fatigue, and weight loss. The disease course is unpredictable, complicated by flares, need for chronic medication use and need for surgery. This leads to increasing intestinal damage with a high disease burden in many patients with IBD<sup>[1]</sup>. It has been established that, depending on disease activity, patients with IBD experience a lower



**Table 1** Definition of used parelsnoer information model items

Diagnosis of IBD	
Crohn's disease	Diagnosis of IBD was defined by clinical symptoms of the disease and confirmed by endoscopy, radiology or histology. If differentiation between CD and UC was not possible, patient were classified as Inflammatory Bowel Disease Unclassified (IBD-U). In the case that a pathologist was not able to differentiate between CD or UC following colectomy, the patient was classified as Inflammatory Bowel Disease Indeterminate (IBD-I).
Ulcerative colitis	
IBD-unclassified	
IBD-Indeterminate	
Family history of IBD	Family history of IBD was registered up to 3 <sup>rd</sup> degree relatives
Smoking status	Smoking status at diagnosis was documented. Patients were classified as never smokers, current smokers or former smokers
Education level	Patients were classified in two groups; low education (Lower general education; Lower vocational education; General secondary education; Vocational secondary education; Did not finish primary school) and high education (Pre-university secondary education; Vocational post-secondary education; University)
Disease behavior	Disease behavior is reported if it occurred at any point in the disease course up to baseline.
Fistulising disease	Fistulising disease is confirmed by physical examination, radiological or endoscopy assessment.
Strictureing disease	A stricture had to be symptomatic.
Penetrating disease	An anal stenosis had to be symptomatic and confirmed by physical examination.
Prescribed medication	Penetrating disease is defined as an intestinal abscess or intestinal perforation due to disease activity.
Anti-tumor necrosis factor alpha	Prescribed medication included anti-tumor necrosis factor alpha (TNF-alpha) agents (infliximab, adalimumab or certolizumab). Data on medication use was available for the entire disease course; medication use was therefore defined as medication 'ever used'
Immunomodulators	immunomodulators (mercaptopurine, azathioprine, thioguanine or methotrexate). Data on medication use was available for the entire disease course; medication use was therefore defined as medication 'ever used'
IBD-related surgical interventions	IBD-related surgical interventions included small bowel resection, ileocecal resection, colon resection, resection other, strictureplasty, ileostomy/colostomy, surgery for abscesses or fistula, stoma and pouch
Extra-intestinal manifestations	
Skin manifestations	Skin manifestations unrelated to the use of IBD medication such as pyoderma gangrenosum, erythema nodosum, hidradenitis suppurativa, psoriasis or palmoplantar psoriasiform pustulosis, and metastatic CD.
Musculoskeletal manifestations	Arthritis was defined as red and swollen joints, dactylitis, reactive arthritis and gout.
	Arthropathy was defined as painful joints, without any swelling or redness, with an inflammatory pattern: pain at night or at rest (e.g., sacroiliitis, ankylosing spondylitis, enthesitis, and inflammatory back pain).
Ocular manifestations	Ocular manifestations included uveitis and episcleritis.
Complications	
Osteopenia	Osteopenia was defined as a bone mineral density T-score lower than -1.
Thromboembolic event	A thromboembolic event was confirmed by additional tests (radiology, endoscopy or histology).

IBD: Inflammatory bowel disease; CD: Crohn's disease; UC: Ulcerative colitis.

quality of life<sup>[2,3]</sup>. IBD generally makes its debut during the second or third decade of life. Therefore, patients with IBD can encounter major problems during their economically productive life, which can lead to work disability, sometimes at young age. Work disability in patients with IBD is associated with a further decrease in quality of life, and high societal costs, especially if work disability is long-term and arises at a young age<sup>[4,5]</sup>. Preventing work disability is therefore an important goal in IBD management.

Work disability rates have been reported before, but reported rates are heterogeneous, ranging between 5% and 33% depending on sample size, methodology, and study population<sup>[6-12]</sup>. Several clinical factors have been suggested to play a role in work disability, such as female sex, age, disease duration, disease severity, and surgical interventions<sup>[10-16]</sup>. However, in most study designs, risk factors for any form of work disability are the focus of interest, neglecting risk factors associated specifically with long-term full work disability (> 80% work disability for > 2 years).

Therefore, our aims were: (1) to assess the prevalence of work disability in patients with IBD and to compare this with the general Dutch population; and (2) to identify risk factors for work disability, especially risk factors for long-term full work disability.

## MATERIALS AND METHODS

### Study design and study population

For this study, we used data from the Dutch IBD Biobank, which is part of the Parelsnoer Institute ([www.parelsnoer.org](http://www.parelsnoer.org)). Since 2007, every patient with IBD that is treated in one of the eight Dutch University Medical Centers (UMCs) is invited to participate. The data is collected prospectively and patients with IBD are being enrolled continuously. Clinical data is retrieved from medical records by using a standardized information model containing 225 IBD related items. Items used for this study are; demographic items, diagnosis, smoking status, employment status, disease location, disease behaviour, education level,

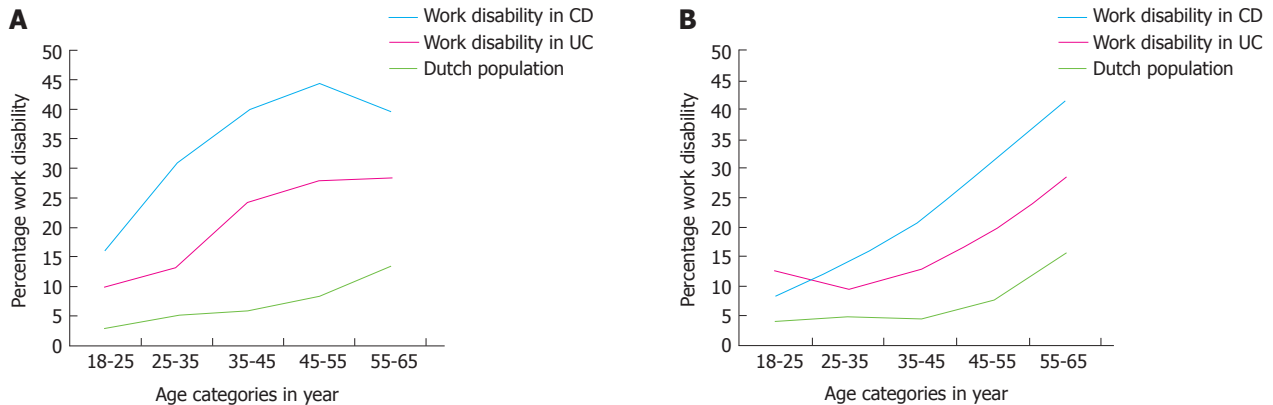


**Figure 1 Percentage of work disability per age category in females and males.** Comparing work disability rates in patients with CD and patients with UC with the general Dutch population. A: Work disability in females; B: Work disability in males. CD: Crohn's disease; UC: Ulcerative colitis.

surgery-related items, medication use, extra-intestinal manifestations and complications. Definitions of these items can be found in Table 1. At the moment of data freeze (the 17<sup>th</sup> of July 2014), the Dutch IBD Biobank contained 3388 patients with IBD. For this study, patients for whom employment status was missing were excluded. We only included adult patients with IBD within working age, and thus excluded patients over the age of 65 years.

#### Definition of work disability

Patients were asked about their employment status at inclusion, which was defined using the following categories; (1) working full time (80%-100%, or working 30 h or more a week); (2) working part time (< 80%, or working less than 30 h a week); (3) partial work disability (35%-80% work disability for > 2 years); (4) full work disability (> 80% work disability for > 2 years); (5) sick leave (work disability for < 2 years); (6) retired; and (7) "Other".

A Dutch law ("Wet werk en inkomen naar arbeidsvermogen" or WIA) prescribes that from the moment Dutch citizens are disabled to work they are entitled to receive a maximum of 170% of their wages during a period of 104 mo (generally 100% for 52 wk, followed by 70% for 52 wk). If after 104 mo the person is still on sick leave the same law prescribes whether patients receive a disability pension. There are two types of disability pension; partial disability (35%-80% work disability) and full disability (more than 80% work disability). A specialized physician determines the percentage of work disability based on questionnaires and physical examination.

Due to the nature of our data we could not distinguish whether work disability was solely attributable to IBD or whether there was an additional cause.

To compare the currently reported work disability rates with the general Dutch population we retrieved information from Statistics Netherlands (CBS), a national institute gathering statistical information about the Dutch population, including employment rates<sup>[17,18]</sup>.

Employment rates were collected for 2014 and matched for sex and age.

#### Statistical analysis

In all analyses, patients with UC were grouped with patients with IBD-Unclassified (IBD-U) and IBD-Indeterminate (IBD-I). Dichotomous variables were compared using the Pearson  $\chi^2$  test. Continuous variables were compared using the Mann-Whitney-*U* test. The Student *t*-test was used to compare overall work disability in our cohort to the general Dutch population. The variable "age" represented the age at inclusion at which employment status was assessed. To assess clinical predictors of work disability in patients with IBD, we categorized the variable employment status into two groups; employed (both full time and part time) and disabled for work (including partial disability, full disability and sick leave). Retirement and "other" were left out of the final analyses after we determined that "other" was unlikely to contain undeclared differential work disability, such as pregnancy leave. We performed a multivariate analysis with employment status as outcome and included demographic and clinical items that had a  $P < 0.10$  in the univariate analysis for employment status. Analyses were repeated in patients with CD and patients with UC, separately. To assess risk factors for long-term full work disability, patients with full disability were compared to patients with partial disability. Statistical analyses were performed with Stata Software V.13.1<sup>[19]</sup>.

## RESULTS

#### Patient population and demographic characteristics

A total of 2794 patients with IBD were within working age and were included in the analysis; 1740 patients with CD and 1054 patients with UC. Demographic and clinical characteristics are depicted in Table 2. In our cohort, more patients with CD were female compared to patients with UC (63% vs 53%,  $P < 0.01$ ). Age at diagnosis was lower in patients with CD compared

**Table 2** Demographic and clinical characteristics in patients with Crohn's disease and ulcerative colitis *n* (%)

	CD	UC	<i>P</i> value
<i>n</i>	1740	1054	
Sex (female)	1103 (63)	561 (53)	< 0.01
Median age, yr, (IQR 25-75)	39.9 (30-51)	43.4 (33-53)	< 0.01
Median age diagnosis, yr, (IQR 25-75)	24.1 (19-32)	29.0 (22-39)	< 0.01
Median age disease duration, yr, (IQR 25-75)	11.7 (6-21)	10.3 (5-18)	< 0.01
Family history of IBD <sup>1</sup>	518 (30)	266 (25)	0.01
Appendectomy <sup>1</sup>	266 (15)	70 (7)	< 0.01
Smoking	1620 (100)	984 (100)	
Yes	439 (27)	117 (12)	< 0.01
Disease location			
L1: ileal disease <sup>2</sup>	324 (22)		
L2: colon disease <sup>2</sup>	450 (31)		
L3: ileocolon disease <sup>2</sup>	696 (47)		
L4: upper GI disease <sup>1</sup>	156 (9)		
P: peri-anal disease <sup>1</sup>	485 (28)		
E1: proctitis <sup>3</sup>		77 (8)	
E2: left-sided colitis <sup>3</sup>		315 (34)	
E3: extensive colitis <sup>3</sup>		541 (58)	
Disease behavior CD			
Fistulising disease <sup>1</sup>	289 (17)		
Penetrating disease <sup>1</sup>	232 (13)		
Stricturing disease <sup>1</sup>	445 (26)		
Education	1708 (100)	1036 (100)	
Low	932 (55)	517 (50)	0.02
Employment status			
Full-time	607 (35)	440 (42)	< 0.01
Part-time	359 (21)	224 (21)	
Partially disabled to work	129 (7)	54 (5)	
Fully disabled to work	342 (20)	124 (12)	
Sick leave	77 (4)	36 (3)	
Retired	22 (1.3)	21 (2)	
Other	204 (12)	155 (15)	

<sup>1</sup>Missing values were scored as non-present; <sup>2</sup>These percentages are calculated for 1470 patients with CD; <sup>3</sup>These percentages are calculated for 993 patients with UC. CD: Crohn's disease; UC: Ulcerative colitis.

to patients with UC (24 years old vs 29 years old,  $P < 0.01$ ). The prevalence of a family history positive for IBD (30% vs 25%,  $P = 0.01$ ) as well as the appendectomy rate (15% vs 7%,  $P < 0.01$ ) were higher in patients with CD. Patients with CD were more often smokers than patients with UC (27% vs 12%,  $P < 0.01$ ). According to the Montreal classification, most patients with CD had ileocolonic disease [47% (L3)], whereas most patients with UC had an extensive colitis [58% (E3)] (Table 2).

#### **Employment status in patients with IBD compared to the general Dutch population**

Figure 1 shows the percentages of work disability in patients with CD, patients with UC and the general Dutch population per age category in females (Figure 1A) and males (Figure 1B). Overall, work disability was significantly higher in IBD patients compared to the general Dutch population, independent of sex ( $P < 0.05$ ).

#### **Clinical risk factors of (long-term full) work disability in patients with CD**

Table 3 depicts the (clinical) risk factors that were

significantly associated with work disability in CD (548 patients with CD were fully disabled and 966 patients with CD were employed). In the multivariate model, female sex (OR = 2.03, 95%CI: 1.53-2.69), an age > 40 years at diagnosis (OR = 3.69, 95%CI: 1.83-7.42), a disease duration > 15 years (OR = 1.67, 95%CI: 1.15-2.43), a lower education level (OR = 2.02, 95%CI: 1.55-2.64), smoking (OR = 1.45, 95%CI: 1.09-1.92), surgical interventions (OR = 1.48, 95%CI: 1.10-2.00), anti-Tumor necrosis factor alpha (TNF $\alpha$ ) use (OR = 1.86, 95%CI: 1.43-2.43), and extra-intestinal manifestations (OR = 1.36, 95%CI: 1.05-1.77) were all associated with an increased odds ratio for work disability in CD.

In the second analysis, partial disability was compared to long-term full work disability for CD. In the multivariate model, an age > 55 years (OR = 3.06, 95%CI: 1.54-6.07), and a lower education level (OR = 1.62, 95%CI: 1.02-2.58) were associated with long-term full work disability in CD (Table 4).

#### **Clinical risk factors of (long-term full) work disability in patients with UC**

In Table 5, (clinical) risk factors that were significantly associated with work disability in UC (214 patients



**Table 3** Univariate and multivariate regression analyses of work disability in patients with Crohn's disease *n* (%)

	Work disability	Employed	Unadj. OR (95%CI)	Adj. OR (95%CI)
<i>n</i>	548 (100)	966 (100)		
Sex (female)	397 (72)	556 (58)	1.94 (1.55-2.43)	2.03 (1.53-2.69)
Age, yr				
< 40	215 (39)	537 (55)	1.00	1.00
40-55	220 (40)	335 (35)	1.64 (1.30-2.07)	0.94 (0.65-1.35)
> 55	113 (21)	94 (10)	3.00 (2.19-4.12)	1.63 (0.95-2.77)
Age at diagnosis, yr				
A1: diagnosis ≤ 16	47 (9)	156 (16)	1.00	1.00
A2: diagnosis 17-40	413 (75)	719 (75)	1.91 (1.35-2.70)	2.02 (1.30-3.13)
A3: diagnosis > 40	88 (16)	91 (9)	3.21 (2.07-4.98)	3.69 (1.83-7.42)
Disease duration, yr				
≤ 15	285 (52)	618 (64)	1.00	1.00
> 15	263 (48)	348 (36)	1.64 (1.32-2.03)	1.67 (1.15-2.43)
Education	537 (100)	950 (100)		
Low	366 (68)	446 (47)	2.42 (1.94-3.02)	2.02 (1.55-2.64)
Smoking	508 (100)	904 (100)		
Yes	180 (35)	203 (22)	1.90 (1.49-2.41)	1.45 (1.09-1.92)
Disease location				
L1: ileal disease <sup>1</sup>	88 (19)	184 (23)	1.00	1.00
L2: colon disease <sup>1</sup>	138 (30)	263 (33)	1.10 (0.79-1.52)	1.10 (0.75-1.61)
L3: ileocolon disease <sup>1</sup>	237 (51)	359 (44)	1.38 (1.02-1.87)	1.29 (0.91-1.83)
L4: upper GI disease <sup>2</sup>	52 (9)	82 (8)	1.13 (0.79-1.63)	-
P: peri-anal disease <sup>2</sup>	170 (31)	256 (26)	1.25 (0.99-1.57)	1.03 (0.77-1.37)
Disease behavior CD				
Fistulising disease <sup>2</sup>	95 (17)	156 (16)	1.09 (0.82-1.44)	-
Stricturing disease <sup>2</sup>	145 (26)	248 (26)	1.04 (0.82-1.32)	-
Penetrating disease <sup>2</sup>	72 (13)	128 (13)	0.99 (0.73-1.35)	-
Pouch <sup>2</sup>	12 (2)	17 (1.8)	1.25 (0.59-2.64)	-
Stoma <sup>2</sup>	96 (18)	108 (11)	1.69 (1.25-2.27)	1.15 (0.78-1.69)
Surgery <sup>2</sup>	288 (53)	406 (42)	1.53 (1.24-1.89)	1.48 (1.10-2.00)
Medication	537 (100)	949 (100)		
Anti-TNFα	309 (58)	435 (46)	1.60 (1.29-1.98)	1.86 (1.43-2.43)
Immunomodulators	395 (74)	698 (74)	1.00 (0.79-1.27)	-
Extra-intestinal manifestations <sup>2</sup>	229 (42)	294 (30)	1.64 (1.32-2.04)	1.36 (1.05-1.77)
PSC <sup>2</sup>	7 (1.3)	14 (1.5)	0.88 (0.35-2.19)	-
Complications <sup>2</sup>	155 (28)	223 (23)	1.31 (1.04-1.67)	1.18 (0.88-1.59)

<sup>1</sup>These percentages are calculated for 463 patients with CD that were disabled for work and 806 patients with CD that were employed; <sup>2</sup>Missing values were scored as non-present. CD: Crohn's disease; Unadj: Unadjusted; TNFα: Tumor necrosis factor alpha; PSC: Primary sclerosing cholangitis.

with UC were fully disabled and 664 patients with UC were employed) have been shown. In the multivariate model, female sex (OR = 1.76, 95%CI: 1.23-2.53), an age > 55 years (OR = 2.93, 95%CI: 1.68-5.14), a lower education level (OR = 2.59, 95%CI: 1.81-3.70), immunomodulator use (OR = 1.58, 95%CI: 1.09-2.28), and extra-intestinal manifestations (OR = 2.13, 95%CI: 1.47-3.09) were all associated with an increased odds ratio for work disability in UC.

In the second analysis, partial disability was compared to long-term full work disability for UC. In the multivariate model, an age > 55 years (OR = 3.49, 95%CI: 1.23-9.92), and complications (OR = 3.39, 95%CI: 1.09-10.58) were associated with long-term full work disability in UC (Table 6).

## DISCUSSION

In this nationwide clinical database and biobank study we assessed work disability rates in patients with IBD. We found higher rates of work disability in patients

with IBD compared to the general Dutch population. Furthermore, in patients with IBD female sex, a lower education level, and extra-intestinal manifestations were significantly associated with work disability. In patients with CD, an age > 40 years at diagnosis, disease duration > 15 years, smoking, surgical interventions, and anti-TNFα use were significantly associated with higher work disability. In patients with UC, an age > 55 years, and immunomodulator use were significantly associated with higher work disability. In patients with CD a lower education level was associated with long-term full work disability, whereas in patients with UC disease complications were associated with long-term full work disability.

### High work disability rates in patients with IBD

In patients with IBD, the overall proportion of work disability was 29% in CD, and 19% in UC. These work disability rates were higher than those in the age-adjusted general Dutch population (7%). Suffering from (severe) IBD may in itself be explanatory for this

**Table 4** Univariate and multivariate regression analyses of full and partial work disability in patients with Crohn's disease *n* (%)

	Full disability	Partial disability	Unadj. OR (95%CI)	Adj. OR (95%CI)
<i>n</i>	342 (100)	129 (100)		
Sex (female)	251 (73)	100 (78)	0.80 (0.50-1.29)	-
Age				
< 40 yr	110 (32)	54 (42)	1.00	1.00
40-55 yr	137 (40)	61 (47)	1.10 (0.71-1.72)	1.05 (0.65-1.70)
> 55 yr	95 (28)	14 (11)	3.33 (1.74-6.37)	3.06 (1.54-6.07)
Age at diagnosis				
A1: diagnosis ≤ 16 yr	28 (8)	13 (10)	1.00	-
A2: diagnosis 17-40 yr	256 (75)	103 (80)	1.15 (0.58-2.32)	
A3: diagnosis > 40 yr	58 (17)	13 (10)	2.07 (0.85-5.05)	
Disease duration				
≤ 15 yr	151 (44)	65 (50)	1.00	-
> 15 yr	191 (56)	64 (50)	1.28 (0.86-1.93)	
Education	332 (100)	128 (100)		
Low	236 (71)	73 (57)	1.85 (1.21-2.83)	1.62 (1.02-2.58)
Smoking	323 (100)	115 (100)		
Yes	125 (39)	33 (29)	1.57 (0.99-2.49)	1.53 (0.93-2.50)
Disease location				
L1: ileal disease <sup>1</sup>	56 (19)	21 (19)	1.00	-
L2: colon disease <sup>1</sup>	80 (28)	38 (35)	0.79 (0.42-1.49)	
L3: ileocolon disease <sup>1</sup>	155 (53)	50 (46)	1.16 (0.64-2.11)	
L4: upper GI disease <sup>2</sup>	38 (11)	8 (6)	1.89 (0.86-4.17)	-
P: peri-anal disease <sup>2</sup>	109 (32)	45 (35)	0.87 (0.57-1.34)	-
Disease behavior CD				
Fistulising disease <sup>2</sup>	64 (19)	23 (18)	1.06 (0.63-1.80)	-
Stricturing disease <sup>2</sup>	92 (27)	33 (26)	1.07 (0.67-1.70)	-
Penetrating disease <sup>2</sup>	47 (14)	19 (15)	0.92 (0.52-1.64)	-
Pouch <sup>2</sup>	6 (1.8)	4 (3)	0.56 (0.15-2.01)	-
Stoma <sup>2</sup>	69 (20)	20 (16)	1.38 (0.80-2.38)	-
Surgery <sup>2</sup>	192 (56)	64 (50)	1.30 (0.87-1.95)	-
Medication	335 (100)	125 (100)		
Anti-TNFα	193 (58)	68 (54)	1.14 (0.75-1.72)	-
Immunomodulators	249 (74)	87 (70)	1.26 (0.80-1.99)	-
Extra-intestinal manifestations <sup>2</sup>	152 (44)	50 (39)	1.26 (0.84-1.91)	-
PSC <sup>2</sup>	2 (0.6)	4 (3)	0.18 (0.03-1.02)	0.19 (0.03-1.10)
Complications <sup>2</sup>	106 (31)	34 (26)	1.25 (0.80-1.98)	-

<sup>1</sup>These percentages are calculated for 291 patients with CD that were fully disabled and 109 patients with CD that were partially disabled; <sup>2</sup>Missing values were scored as non-present. CD: Crohn's disease; Unadj: Unadjusted; TNFα: Tumor necrosis factor alpha; PSC: Primary sclerosing cholangitis.

higher percentage. Furthermore, all patients in the Dutch IBD Biobank were treated in tertiary referral centers with a severe disease course signature: 47% ileocolonic disease (L3 Montreal CD) and 58% extensive colitis (E3 Montreal UC). Indeed, disease in remission was associated with increased employment in CD<sup>[5]</sup> whereas disease severity was a predictor of work disability in IBD<sup>[16]</sup>.

Criteria for disability pension differ between countries due to political and socioeconomic factors. Comparison of work disability rates between different countries is therefore difficult. In addition, differences in selection criteria, study methodology, sample size, and definitions of work disability result in highly variable disability rates reported (from 5% to 33%)<sup>[6-14]</sup>. In two comparable Dutch IBD-population studies it has been concluded by the authors that disability rates in CD and in UC were higher compared to the general Dutch population, which is in line with the current results. However, work disability rates of 33% in CD, 24% in UC, and 11% in the control population were reported in the first study that was conducted in 2002<sup>[8]</sup>, which is higher than the

disability rates we found. This may be due to changes in the welfare system since 2002, when patients got a disability pension after one year of sick leave, instead of after two years as it is now. Disability rates in a second, more recent Dutch study, by van der Valk *et al.*<sup>[10]</sup>, were more in line with our findings but lower (18% in CD, 10% in UC, and 7% in the control population). Although there seems to be a wide range in work disability rates in IBD, it may be concluded that the rate of work disability is substantial among patients with IBD.

### Clinical risk factor for work disability

Female sex<sup>[10,11,13,15,16]</sup>, an age > 40 years at diagnosis<sup>[11,13]</sup>, older age at inclusion<sup>[10,12,13,15,16]</sup>, a lower education level<sup>[10,13]</sup>, extra-intestinal manifestations<sup>[10,12,16]</sup>, a disease duration > 15 years<sup>[12,15,16]</sup>, surgical interventions<sup>[11-13]</sup>, and immunomodulator use<sup>[16]</sup> have been reported to be associated with work disability in patients with IBD.

In UC, an age > 55 years was associated with work disability, which might not be directly disease related. Indeed, it has been reported that disability

**Table 5** Univariate and multivariate regression analyses of work disability in patients with ulcerative colitis *n* (%)

	Work disability	Employed	Unadj. OR (95%CI)	Adj. OR (95%CI)
<i>n</i>	214 (100)	664 (100)		
Sex (female)	124 (58)	333 (50)	1.37 (1.00-1.87)	1.76 (1.23-2.53)
Age				
< 40 yr	58 (27)	287 (43)	1.00	1.00
40-55 yr	94 (44)	277 (42)	1.68 (1.16-2.42)	1.52 (0.97-2.40)
> 55 yr	62 (29)	100 (15)	3.07 (2.01-4.69)	2.93 (1.68-5.14)
Age at diagnosis				
A1: diagnosis ≤ 16 yr	18 (8)	64 (10)	1.00	1.00
A2: diagnosis 17-40 yr	124 (58)	474 (71)	0.93 (0.53-1.63)	1.06 (0.55-2.04)
A3: diagnosis > 40 yr	72 (34)	126 (19)	2.03 (1.12-3.69)	1.99 (0.92-4.28)
Disease duration				
≤ 15 yr	129 (60)	439 (66)	1.00	-
> 15 yr	85 (40)	225 (34)	1.29 (0.94-1.77)	-
Education				
Low	144 (69)	282 (43)	2.98 (2.14-4.16)	2.59 (1.81-3.70)
Smoking				
Yes	30 (15)	71 (11)	1.32 (0.83-2.09)	-
Disease location				
E1: proctitis <sup>1</sup>	14 (7)	54 (9)	1.00	-
E2: left-sided colitis <sup>1</sup>	54 (27)	215 (37)	0.97 (0.50-1.87)	-
E3: extensive colitis <sup>1</sup>	130 (66)	317 (54)	1.58 (0.85-2.95)	-
Pouch <sup>2</sup>	37 (17)	54 (8)	2.36 (1.50-3.71)	1.72 (0.81-3.65)
Stoma <sup>2</sup>	35 (16)	54 (8)	2.21 (1.40-3.49)	1.13 (0.54-2.38)
Surgery <sup>2</sup>	60 (28)	97 (15)	2.28 (1.58-3.29)	1.68 (0.75-3.75)
Medication				
Anti-TNFα	53 (25)	120 (18)	1.48 (1.02-2.14)	1.33 (0.86-2.06)
Immunomodulators	139 (66)	350 (54)	1.65 (1.19-2.28)	1.58 (1.09-2.28)
Extra-intestinal manifestations <sup>2</sup>	78 (36)	130 (20)	2.36 (1.68-3.30)	2.13 (1.47-3.09)
PSC <sup>2</sup>	8 (4)	21 (3)	1.19 (0.52-2.73)	-
Complications <sup>2</sup>	37 (17)	89 (13)	1.35 (0.89-2.05)	-

<sup>1</sup>These percentages are calculated for 198 patients with UC that were disabled for work and 586 patients with UC that were employed; <sup>2</sup>Missing values were scored as non-present. UC: Ulcerative colitis; Unadj: Unadjusted; Adj: Adjusted; TNFα: Tumor necrosis factor alpha; PSC: Primary sclerosing cholangitis.

pensions were not caused by UC but often by other age-related comorbidities<sup>[11,12]</sup>. On the other hand, in CD it has been found that patients with CD receive their disability pension because of IBD or other IBD related comorbidity<sup>[11]</sup>, rather than other age related comorbidities.

Surgical interventions were a risk factor for work disability in patients with CD, but not in UC. As surgery is an indicator of severe disease these data seemed to corroborate the hypothesis that severity of disease predicts work disability. In line with this, higher work disability rates have been reported after colectomy in patients with UC<sup>[14]</sup>. A recent review has shown that surgical rates have declined since the introduction of biologicals, indicating a beneficial effect of treatment with biologicals on disease outcome<sup>[20]</sup>. Our study is not well suited to study this effect, since our most reliable clinical information has been collected after the introduction of biologicals. Other studies report no differences in disability between patients receiving anti-TNFα treatment or patient that underwent surgery<sup>[21,22]</sup>. At the moment, a clinical trial (LIRIC) assesses differences in outcome comparing anti-TNFα treatment with Ileocecal resection in patients with CD not responsive to prednisolone<sup>[23]</sup>.

While it has been established that anti-TNFα and/or immunomodulators are generally used to ma-

intain remission in patients with IBD, our study found an association between use of anti-TNFα use and (full) work disability. This could be due to selection bias, as all patients were treated in tertiary referral centers, with most of them having extensive disease involvement (Montreal classification; 47% L3 and 58% E3). Therefore, it is likely that patients receiving anti-TNFα and immunomodulator therapy are patients with more severe disease, receiving "rescue therapy" rather than "top-down therapy". Smoking was found to be a risk factor for work disability in CD, but not in UC. In this study, smoking status was scored at moment of inclusion, as it has been known that smoking can increase frequency and severity of flares in CD<sup>[24]</sup>, while it can ameliorate disease in UC<sup>[25]</sup>. It has been reported that smoking at diagnosis was associated with work disability in UC<sup>[13]</sup>, whereas others reported on an association between numbers of sick leave days and smoking at the onset of CD<sup>[16]</sup>, corroborating the current findings.

#### Clinical risk factor for long-term full work disability

We replicated most known, clinical risk factors for work disability and evaluated risk factors for long-term full work disability (> 80% work disability) comparing it to partial work disability (> 35% work disability). A lower education level was the only factor,



**Table 6** Univariate and multivariate regression analyses of full and partial work disability in patients with ulcerative colitis *n* (%)

	Full disability	Partial disability	Unadj. OR (95%CI)	Adj. OR (95%CI)
<i>n</i>	124 (100)	54 (100)		
Sex (female)	75 (60)	26 (48)	1.65 (0.87-3.14)	-
Age				
< 40 yr	25 (20)	15 (28)	1.00	1.00
40-55 yr	52 (42)	32 (59)	0.98 (0.45-2.12)	0.90 (0.40-2.03)
> 55 yr	47 (38)	7 (13)	4.03 (1.45-11.17)	3.49 (1.23-9.92)
Age at diagnosis				
A1: diagnosis ≤ 16 yr	7 (6)	5 (9)	1.00	-
A2: diagnosis 17-40 yr	70 (56)	34 (63)	1.47 (0.43-4.97)	
A3: diagnosis > 40 yr	47 (38)	15 (28)	2.24 (0.62-8.10)	
Disease duration				
≤ 15 yr	65 (52)	36 (67)	1.00	1.00
> 15 yr	59 (48)	18 (33)	1.82 (0.93-3.54)	1.78 (0.87-3.62)
Education	122 (100)	50 (100)		
Low	84 (69)	37 (74)	0.78 (0.37-1.63)	-
Smoking	121 (100)	52 (100)		
Yes	18 (15)	7 (13)	1.12 (0.44-2.88)	-
Disease location				
E1: proctitis <sup>1</sup>	9 (8)	4 (8)	1.00	-
E2: left-sided colitis <sup>1</sup>	39 (33)	9 (18)	1.93 (0.48-7.68)	-
E3: extensive colitis <sup>1</sup>	70 (59)	38 (74)	0.82 (0.24-2.84)	-
Pouch <sup>2</sup>	24 (19)	9 (17)	1.20 (0.52-2.79)	-
Stoma <sup>2</sup>	23 (19)	8 (15)	1.31 (0.54-3.15)	-
Surgery <sup>2</sup>	37 (30)	14 (26)	1.22 (0.59-2.50)	-
Medication	122 (100)	53 (100)		
Anti-TNFα	30 (25)	10 (19)	1.40 (0.63-3.13)	-
Immunomodulators	77 (63)	37 (70)	0.74 (0.37-1.48)	-
Extra-intestinal manifestations <sup>2</sup>	51 (41)	19 (35)	1.29 (0.66-2.50)	-
PSC <sup>2</sup>	3 (2)	4 (7)	0.31 (0.07-1.44)	-
Complications <sup>2</sup>	28 (23)	4 (7)	3.65 (1.21-10.97)	3.39 (1.09-10.58)

<sup>1</sup>These percentages are calculated for 118 patients with UC that were fully disabled and 51 patients with UC that were partially disabled; <sup>2</sup>Missing values were scored as non-present. UC: Ulcerative colitis; Unadj: Unadjusted; Adj: Adjusted; TNFα: Tumor necrosis factor alpha; PSC: Primary sclerosing cholangitis.

which remained statistically significantly associated with long-term full work disability in CD. In only a few studies, educational level has been taken into account showing conflicting results. A higher education level seemed to be associated to work disability and sick leave in patients with CD in previous studies<sup>[8,13]</sup>. On the other hand, a study by Vester-Andersen *et al.* reported no patients with CD with a higher education level that were receiving a disability pension<sup>[13]</sup>. Hence, the relationship between education level and work disability remains unclear, and more population specific studies are needed before hard conclusions can be drawn<sup>[26,27]</sup>.

Risk factors identified in this report should be interpreted with caution, as the confidence intervals were quite large and data were derived from third-line referral centres. Furthermore, due to the nature of our data we could not distinguish between work disability solely attributable to IBD, or work disability due to a different cause. However, the median age in our study was 40 years for CD patients and 43 years for UC patients, ages at which age-related comorbidities are generally low. Furthermore, we did not score how physically heavy the patients' jobs were, known to contribute to work disability. Moreover, the reason for work disability was unknown. It could have been

that sick leave (< 2 years), was caused by another reason than IBD, for example pregnancy leave or psychological health problems. When comparing our data from the Dutch social security system with the more widely used Work Productivity and Activity Impairment Questionnaire (WPAI), the main difference lies within the objectivity of the data from the Dutch social security system, since it is assessed by a physician as opposed to the more subjective WPAI, which is patient reported. A main disadvantage of the data from the Dutch social security system is that it makes no distinction between work disability due to IBD or due to a different cause. Furthermore, the WPAI assesses activity, not solely work related, on a weekly basis, providing more insight in the disease course.

The strength of our study is the extended disease and patient documentation by the clinician.

In conclusion, in this study we show a higher prevalence of work disability in IBD compared to the general Dutch population. Furthermore, we identified risk factors associated with work disability, with a lower level of education being a risk factor for long-term full work disability in CD, and disease complications being a risk factor for long-term full work disability in UC. In future studies web-based follow-up of Patient-Reported Outcome Measurements (PROMs) including

clinical disease activity scores, could be promising tool for detecting a decline in work activity due to disease activity.

## COMMENTS

### Background

Inflammatory bowel disease (IBD), consisting of Crohn's disease (CD) and ulcerative colitis (UC) is a heterogeneous/multifaceted disease. Patients suffer from symptoms like diarrhoea, abdominal pain, fatigue, and weight loss. IBD generally makes its debut during the second or third decade of life. Therefore, patients with IBD can encounter major problems during their economically productive life, which can lead to work disability, sometimes at young age. Preventing work disability is therefore an important goal in IBD management.

### Research frontiers

Work disability rates have been reported before, but reported rates are heterogeneous, ranging between 5% and 33% depending on sample size, methodology, and study population. However, in most study designs, risk factors for any form of work disability are the focus of interest, neglecting risk factors associated specifically with long-term full work disability (> 80% work disability for > 2 years). This study assesses the prevalence of work disability in patients with IBD and to compare this with the general Dutch population, and secondly this study tries to identify risk factors for work disability, especially risk factors for long-term full work disability.

### Innovations and breakthroughs

In patients with IBD, the overall proportion of work disability was 29% in CD, and 19% in UC. These work disability rates were higher than those in the age-adjusted general Dutch population (7%). Suffering from (severe) IBD may in itself be explanatory for this higher percentage. Furthermore, all patients in the Dutch IBD Biobank were treated in tertiary referral centers with a severe disease course signature: 47% ileocolonic disease (L3 Montreal CD) and 58% extensive colitis (E3 Montreal UC). The authors replicated most known, clinical risk factors (female sex, an age > 40 years at diagnosis, older age at inclusion, a lower education level, extra-intestinal manifestations, a disease duration > 15 years surgical interventions, and immunomodulator use) for work disability. A lower education level was the only factor, which remained statistically significantly associated with long-term full work disability in CD. In patients with UC disease complications were associated with long-term full work disability.

### Applications

This study shows that a lower education is patients with CD, and disease complications (osteopenia, thromboembolic event) in patients with UC are associated with long-term full work disability (> 80% work disability for > 2 years). This highlights the need for early assessment of risk factors for work disability, as work disability is substantial among IBD patients and associated with high societal health care costs and lower quality of life. In future studies web-based follow-up of Patient-Reported Outcome Measurements (PROMs) including clinical disease activity scores, could be a promising tool for detecting a decline in work activity due to disease activity.

### Terminology

To identify risk factors for work disability we categorized the variable employment status into two groups; employed (both full time and part time) versus disabled for work (including partial disability, full disability and sick leave). To evaluate risk factors for long-term full work disability, we compared risk factors for long-term full work disability (> 80% work disability) to risk factors for partial work disability (> 35% work disability).

### Peer-review

In this paper, the authors investigate the prevalence of and risk factors for partial and full work disability in Dutch patients with IBD. The manuscript is complete and well written, and it is expected to improve our knowledge of the health economics of IBD. This is a well-written paper exploring a rapidly evolving area of IBD research. The inherent limitations of this study are somewhat understandable and provide further direction to research in this important area.

## ACKNOWLEDGMENTS

We would like to thank all the IBD patients who participate in the Dutch IBD Biobank. This nationwide PSI project is part of and funded by the Netherlands Federation of University Medical Centers and has received initial funding from the Dutch Government (from 2007-2011). The PSI currently facilitates the uniform nationwide collection of information on and biomaterials of thirteen other diseases.

## REFERENCES

- 1 **Pariente B**, Cosnes J, Danese S, Sandborn WJ, Lewin M, Fletcher JG, Chowers Y, D'Haens G, Feagan BG, Hibi T, Hommes DW, Irvine EJ, Kamm MA, Loftus EV Jr, Louis E, Michetti P, Munkholm P, Oresland T, Panés J, Peyrin-Biroulet L, Reinisch W, Sands BE, Schoelmerich J, Schreiber S, Tilg H, Travis S, van Assche G, Vecchi M, Mary JY, Colombel JF, Lémann M. Development of the Crohn's disease digestive damage score, the Lémann score. *Inflamm Bowel Dis* 2011; **17**: 1415-1422 [PMID: 21560202 DOI: 10.1002/ibd.21506]
- 2 **Casellas F**, Arenas JJ, Baudet JS, Fábregas S, García N, Gelabert J, Medina C, Ochotorena I, Papo M, Rodrigo L, Malagelada JR. Impairment of health-related quality of life in patients with inflammatory bowel disease: a Spanish multicenter study. *Inflamm Bowel Dis* 2005; **11**: 488-496 [PMID: 15867589 DOI: 10.1097/01.MIB.0000159661.55028.56]
- 3 **Russel MG**, Pastoor CJ, Brandon S, Rijken J, Engels LG, van der Heijde DM, Stockbrügger RW. Validation of the Dutch translation of the Inflammatory Bowel Disease Questionnaire (IBDQ): a health-related quality of life questionnaire in inflammatory bowel disease. *Digestion* 1997; **58**: 282-288 [PMID: 9243124 DOI: 10.1159/000201455]
- 4 **Stark R**, König HH, Leidl R. Costs of inflammatory bowel disease in Germany. *Pharmacoeconomics* 2006; **24**: 797-814 [PMID: 16898849 DOI: 10.2165/00019053-200624080-00006]
- 5 **Lichtenstein GR**, Yan S, Bala M, Hanauer S. Remission in patients with Crohn's disease is associated with improvement in employment and quality of life and a decrease in hospitalizations and surgeries. *Am J Gastroenterol* 2004; **99**: 91-96 [PMID: 14687148 DOI: 10.1046/j.1572-0241.2003.04010.x]
- 6 **Feagan BG**, Bala M, Yan S, Olson A, Hanauer S. Unemployment and disability in patients with moderately to severely active Crohn's disease. *J Clin Gastroenterol* 2005; **39**: 390-395 [PMID: 15815207 DOI: 10.1097/01.mcg.0000159220.70290.41]
- 7 **Bernklev T**, Jahnsen J, Henriksen M, Lygren I, Aadland E, Sauar J, Schulz T, Stray N, Vatn M, Moum B. Relationship between sick leave, unemployment, disability, and health-related quality of life in patients with inflammatory bowel disease. *Inflamm Bowel Dis* 2006; **12**: 402-412 [PMID: 16670530 DOI: 10.1097/01.MIB.0000218762.61217.4a]
- 8 **Boonen A**, Dagnelie PC, Feleus A, Hesselink MA, Muris JW, Stockbrügger RW, Russel MG. The impact of inflammatory bowel disease on labor force participation: results of a population sampled case-control study. *Inflamm Bowel Dis* 2002; **8**: 382-389 [PMID: 12454613 DOI: 10.1097/00054725-200211000-00002]
- 9 **De Boer AG**, Bennebroek Evertsz F, Stokkers PC, Bockting CL, Sanderma R, Hommes DW, Sprangers MA, Frings-Dresen MH. Employment status, difficulties at work and quality of life in inflammatory bowel disease patients. *Eur J Gastroenterol Hepatol* 2016; **28**: 1130-1136 [PMID: 27340897 DOI: 10.1097/MEG.0000000000000685]
- 10 **van der Valk ME**, Mangen MJ, Leenders M, Dijkstra G, van Bodegraven AA, Fidder HH, de Jong DJ, Pierik M, van der Woude CJ, Romberg-Camps MJ, Clemens CH, Jansen JM, Mahmood N, van de Meeberg PC, van der Meulen-de Jong AE, Ponsioen CY, Bolwerk CJ, Vermeijden JR, Siersema PD, van Oijen MG, Oldenburg B, COIN study group; Dutch Initiative on Crohn and Colitis. Risk factors of work disability in patients

- with inflammatory bowel disease--a Dutch nationwide web-based survey: work disability in inflammatory bowel disease. *J Crohns Colitis* 2014; **8**: 590-597 [PMID: 24351733 DOI: 10.1016/j.crohns.2013.11.019]
- 11 **Høivik ML**, Moum B, Solberg IC, Henriksen M, Cvancarova M, Bernklev T; IBSEN Group. Work disability in inflammatory bowel disease patients 10 years after disease onset: results from the IBSEN Study. *Gut* 2013; **62**: 368-375 [PMID: 22717453 DOI: 10.1136/gutjnl-2012-302311]
  - 12 **Mandel MD**, Bálint A, Lovász BD, Gulácsi L, Strbák B, Golovics PA, Farkas K, Kürti Z, Szilágyi BK, Mohás A, Molnár T, Lakatos PL. Work disability and productivity loss in patients with inflammatory bowel diseases in Hungary in the era of biologics. *Eur J Health Econ* 2014; **15** Suppl 1: S121-S128 [PMID: 24832845 DOI: 10.1007/s10198-014-0603-7]
  - 13 **Vester-Andersen MK**, Prossberg MV, Vind I, Andersson M, Jess T, Bendtsen F. Low Risk of Unemployment, Sick Leave, and Work Disability Among Patients with Inflammatory Bowel Disease: A 7-year Follow-up Study of a Danish Inception Cohort. *Inflamm Bowel Dis* 2015; **21**: 2296-2303 [PMID: 26164663 DOI: 10.1097/MIB.0000000000000493]
  - 14 **Neovius M**, Arkema EV, Blomqvist P, Ekblom A, Smedby KE. Patients with ulcerative colitis miss more days of work than the general population, even following colectomy. *Gastroenterology* 2013; **144**: 536-543 [PMID: 23232295 DOI: 10.1053/j.gastro.2012.12.004]
  - 15 **Netjes JE**, Rijken M. Labor participation among patients with inflammatory bowel disease. *Inflamm Bowel Dis* 2013; **19**: 81-91 [PMID: 22374877 DOI: 10.1002/ibd.22921]
  - 16 **Siebert U**, Wurm J, Gothe RM, Arvandi M, Vavricka SR, von Känel R, Begré S, Sulz MC, Meyenberger C, Sagmeister M; Swiss IBD Cohort Study Group. Predictors of temporary and permanent work disability in patients with inflammatory bowel disease: results of the swiss inflammatory bowel disease cohort study. *Inflamm Bowel Dis* 2013; **19**: 847-855 [PMID: 23446333 DOI: 10.1097/MIB.0b013e31827f278e]
  - 17 CBS StatLine - Arbeidsongeschiktheidsuitkering per wet; kenmerken uitkeringsontvanger. [cited 2017 Feb 14]. Available from: URL: <http://statline.cbs.nl/Statweb/publication/?DM=SLNLP&A=80904NEDD1=0D2=1-2D3=1-5D4=0D5=0D6=4HDR=TSTB=G1,G2,G3,G4,G5VW=T>
  - 18 CBS StatLine - Arbeidsdeelname; kerncijfers. [cited 2017 Feb 14]. Available from: URL: <http://statline.cbs.nl/Statweb/publication/?DM=SLNLP&A=82309NEDD1=0D2=1-2D3=1,4-6,9D4=0D5=59HDR=G4STB=G1,G2,G3,TVW=T>
  - 19 Data Analysis and Statistical Software | Stata. [cited 2017 Feb 14]. Available from: URL: <http://www.stata.com/>
  - 20 **Olivera P**, Spinelli A, Gower-Rousseau C, Danese S, Peyrin-Biroulet L. Surgical rates in the era of biological therapy: up, down or unchanged? *Curr Opin Gastroenterol* 2017; **33**: 246-253 [PMID: 28463854 DOI: 10.1097/MOG.0000000000000361]
  - 21 **Meijs S**, Gardenbroek TJ, Sprangers MA, Bemelman WA, Buskens CJ, D'Haens GR, Löwenberg M. Health-related quality of life and disability in patients with ulcerative colitis and proctocolectomy with ileoanal pouch versus treatment with anti-TNF agents. *J Crohns Colitis* 2014; **8**: 686-692 [PMID: 24418659 DOI: 10.1016/j.crohns.2013.12.011]
  - 22 **van Gennep S**, Sahami S, Buskens CJ, van den Brink GR, Ponsioen CY, D'Hoore A, de Buck van Overstraeten A, van Assche G, Ferrante M, Vermeire S, Bemelman WA, D'Haens GR, Löwenberg M. Comparison of health-related quality of life and disability in ulcerative colitis patients following restorative proctocolectomy with ileal pouch-anal anastomosis versus anti-tumor necrosis factor therapy. *Eur J Gastroenterol Hepatol* 2017; **29**: 338-344 [PMID: 27902515 DOI: 10.1097/MEG.0000000000000798]
  - 23 LIRIC-trial [Internet]. 2016 [cited 2017 May 27] Available from: URL: <https://www.crohn-colitis.nl/wp-content/uploads/2016/09/LIRIC-trial.pdf>
  - 24 **Cosnes J**. Smoking, physical activity, nutrition and lifestyle: environmental factors and their impact on IBD. *Dig Dis* 2010; **28**: 411-417 [PMID: 20926865 DOI: 10.1159/000320395]
  - 25 **Bastida G**, Beltrán B. Ulcerative colitis in smokers, non-smokers and ex-smokers. *World J Gastroenterol* 2011; **17**: 2740-2747 [PMID: 21734782 DOI: 10.3748/wjg.v17.i22.2740]
  - 26 **Stjernman H**, Tysk C, Almer S, Ström M, Hjortswang H. Unfavourable outcome for women in a study of health-related quality of life, social factors and work disability in Crohn's disease. *Eur J Gastroenterol Hepatol* 2011; **23**: 671-679 [PMID: 21654323 DOI: 10.1097/MEG.0b013e328346f622]
  - 27 **Longobardi T**, Jacobs P, Bernstein CN. Work losses related to inflammatory bowel disease in the United States: results from the National Health Interview Survey. *Am J Gastroenterol* 2003; **98**: 1064-1072 [PMID: 12809829 DOI: 10.1111/j.1572-0241.2003.07285.x]

**P- Reviewer:** Ahluwalia NK, Annese V, Blonski W, Brzozowski T, Jadallah KA, Limdi JKK, Sergi CM, Lakatos PL  
**S- Editor:** Ma YJ **L- Editor:** A **E- Editor:** Ma YJ





## Retrospective Study

# Endoscopic ultrasound staging for early esophageal cancer: Are we denying patients neoadjuvant chemo-radiation?

Carrie Luu, Marisa Amaral, Jason Klapman, Cynthia Harris, Khaldoun Almhanna, Sarah Hoffe, Jessica Frakes, Jose M Pimiento, Jacques P Fontaine

Carrie Luu, Marisa Amaral, Jacques P Fontaine, Department of Thoracic Oncology, H. Lee Moffitt Cancer Center and Research Institute, Tampa, FL 33612, United States

Jason Klapman, Jose M Pimiento, Cynthia Harris, Khaldoun Almhanna, Department of Gastrointestinal Oncology, H. Lee Moffitt Cancer Center and Research Institute, Tampa, FL 33612, United States

Sarah Hoffe, Jessica Frakes, Department of Radiation Oncology, H. Lee Moffitt Cancer Center and Research Institute, Tampa, FL 33612, United States

**Author contributions:** Luu C provided the conception and design; Fontaine JP contributed to acquisition, analysis, or interpretation of data; all authors drafted, revised and finally approved of the manuscript.

**Institutional review board statement:** This study was reviewed and approved by the Institutional Review Board at Moffitt Cancer Center.

**Informed consent statement:** This is a retrospective study using de-identified clinical data that was obtained after approval from the institution's IRB. Since all information was anonymous and does not impact patients in any way, no patient consent was required.

**Conflict-of-interest statement:** We have no financial relationships to disclose.

**Data sharing statement:** No additional data are available

**Open-Access:** This article is an open-access article which was selected by an in-house editor and fully peer-reviewed by external reviewers. It is distributed in accordance with the Creative Commons Attribution Non Commercial (CC BY-NC 4.0) license, which permits others to distribute, remix, adapt, build upon this work non-commercially, and license their derivative works on different terms, provided the original work is properly cited and the use is non-commercial. See: <http://creativecommons.org/licenses/by-nc/4.0/>

[licenses/by-nc/4.0/](http://creativecommons.org/licenses/by-nc/4.0/)

**Manuscript source:** Unsolicited manuscript

**Correspondence to:** Jacques P Fontaine, MD, Associate Member, Department Thoracic Oncology, Moffitt Cancer Center, 12902 Magnolia Dr., Tampa, FL 33612, United States. [jacques.fontaine@moffitt.org](mailto:jacques.fontaine@moffitt.org)  
Telephone: +1-813-7453050  
Fax: +1-813-7453027

**Received:** January 23, 2017

**Peer-review started:** January 27, 2017

**First decision:** May 12, 2017

**Revised:** July 4, 2017

**Accepted:** August 2, 2017

**Article in press:** August 2, 2017

**Published online:** December 14, 2017

## Abstract

### AIM

To evaluate the accuracy of endoscopic ultrasound (EUS) in early esophageal cancer (EC) performed in a high-volume tertiary cancer center.

### METHODS

A retrospective review of patients undergoing esophagectomy was performed and patients with cT1N0 and cT2N0 esophageal cancer by EUS were evaluated. Patient demographics, tumor characteristics, and treatment were reviewed. EUS staging was compared to surgical pathology to determine accuracy of EUS. Descriptive statistics was used to describe the cohort. Student's *t* test and Fisher's exact test or  $\chi^2$  test was used to compare variables. Logistic regression analysis was used to determine if clinical variables such as

tumor location and tumor histology were associated with EUS accuracy.

## RESULTS

Between 2000 and 2015, 139 patients with clinical stage I or II A esophageal cancer undergoing esophagectomy were identified. There were 25 (18%) female and 114 (82%) male patients. The tumor location included the middle third of the esophagus in 11 (8%) and lower third and gastroesophageal junction in 128 (92%) patients. Ninety-three percent of patients had adenocarcinoma. Preoperative EUS matched the final surgical pathology in 73/139 patients for a concordance rate of 53%. Twenty-nine patients (21%) were under-staged by EUS; of those, 19 (14%) had unrecognized nodal disease. Positron emission tomography (PET) was used in addition to EUS for clinical staging in 62/139 patients. Occult nodal disease was only found in 4 of 62 patients (6%) in whom both EUS and PET were negative for nodal involvement.

## CONCLUSION

EUS is less accurate in early EC and endoscopic mucosal resection might be useful in certain settings. The addition of PET to EUS improves staging accuracy.

**Key words:** Esophageal cancer; Endoscopic ultrasound; Staging; Early esophageal cancer; Endoscopic mucosal resection

© The Author(s) 2017. Published by Baishideng Publishing Group Inc. All rights reserved.

**Core tip:** Endoscopic ultrasound (EUS) is an important and widely used staging modality in esophageal cancer. However, our study corroborates other reports that EUS is less accurate in early cancer. The use of positron emission tomography in this setting improves rates of accurate staging. Also, more liberal use of endoscopic mucosal resection will potentially improve staging in early esophageal cancer. Further evaluation of the under-staged group in this review is needed to determine if unrecognized nodal disease by preoperative staging workup in early stage esophageal cancer affects long-term survival or disease-free interval.

Luu C, Amaral M, Klapman J, Harris C, Almhanna K, Hoffe S, Frakes J, Pimiento JM, Fontaine JP. Endoscopic ultrasound staging for early esophageal cancer: Are we denying patients neoadjuvant chemo-radiation? *World J Gastroenterol* 2017; 23(46): 8193-8199 Available from: URL: <http://www.wjgnet.com/1007-9327/full/v23/i46/8193.htm> DOI: <http://dx.doi.org/10.3748/wjg.v23.i46.8193>

## INTRODUCTION

In the United States, an estimated 16910 cases

of esophageal cancer will be diagnosed each year and 15690 deaths are expected from the disease<sup>[1]</sup>. Approximately 50% of patients initially present with unresectable or metastatic disease<sup>[1]</sup>. Early stage disease carries a better prognosis with five-year overall survival (OS) ranging from 80%-93% in stage I disease after esophagectomy<sup>[2,3]</sup>. For locally advanced disease (T3N0 or TxN+), the addition of neoadjuvant therapy to surgical resection improves survival and is currently standard of care in the United States<sup>[4]</sup>. Management of T2N0 esophageal cancer is more controversial. In the randomized trial by van Hagen *et al*<sup>[5]</sup> which demonstrated a survival benefit to neoadjuvant therapy, T2N0 patients were included in the trial; however, Mariette *et al*<sup>[6]</sup> did not demonstrate a survival benefit for neoadjuvant chemoradiotherapy in stage I and II esophageal cancer.

Therefore, clinical staging is critical in determining optimal therapy for esophageal cancer. Modalities for clinical staging include computed tomography (CT), positron emission tomography (PET), and endoscopic ultrasound (EUS). Magnetic resonance imaging (MRI) is not generally used for staging at our institution though it may be useful in certain circumstances. In a systematic review of PET staging, the reported sensitivity and specificity for locoregional metastasis was 0.51 and 0.84, respectively<sup>[7]</sup>. Specificity for distant metastasis was higher at 0.97. EUS is another key component of clinical staging and is routine in evaluating locally advanced esophageal cancer<sup>[8]</sup>. When compared to various staging modalities, EUS is more accurate in assessing locoregional disease. In a meta-analysis of EUS studies by Puli *et al*<sup>[9]</sup>, the sensitivity and specificity of EUS for defining tumor depth was 80%-90% and more than 90%, respectively, with increased accuracy for more advanced T stage. In the same study, the pooled sensitivity of EUS for nodal staging was 84.7% and the specificity was 84.6%. The addition of fine needle aspiration (FNA) of equivocal lymph nodes increased the sensitivity and specificity of nodal staging to 96.7% and 95.5%, respectively<sup>[7]</sup>.

Despite its utility in locoregional staging, EUS is reported to be less accurate in early disease. A review of studies of EUS in early esophageal cancer reported a 65% tumor stage concordance between EUS and pathology<sup>[9]</sup>. It is especially challenging to differentiate between T2 tumors that invade the muscularis propria and T3 tumors, which invade the adventitia. The distinction is critically important, as it determines which patients should undergo upfront surgery and which would benefit from neoadjuvant therapy prior to curative resection. In addition, distinguishing between benign reactive lymph nodes and lymph node metastasis can be challenging, although FNA can improve accuracy. This study explores our institution's experience with early stage cT1N0 and cT2N0 esophageal cancer and evaluates variables which affect EUS staging. In this manner, we aim to elucidate

**Table 1 Clinicopathologic characteristics *n* (%)**

Characteristics	
Mean 64.9 yr (range 40-83)	
Gender	
Male	114 (82)
Female	25 (18)
Tumor location	
Middle 1/3 of esophagus	11 (8)
Lower 1/3 of esophagus and GEJ	128 (92)
Tumor histology	
Adenocarcinoma	129 (92.8)
Squamous cell carcinoma	10 (7.2)
Clinical stage	
T1N0	110 (79.1)
T2N0	29 (20.9)
Type of esophagectomy	
Three-field	2 (1.4)
Transhiatal	26 (18.7)
Ivor-Lewis	111 (79.9)
Adjuvant therapy	
Chemotherapy	6 (4.3)
Chemoradiation	3 (2.2)
None	130 (93.5)

factors which can improve staging and allow for optimal treatment of esophageal carcinoma.

## MATERIALS AND METHODS

A retrospective chart review was performed and patients who underwent esophagectomy for malignancy from 2000 to 2015 at a single institution were identified. Patients who were clinically staged as T1N0 (cT1N0) and T2N0 (cT2N0) were identified. Over this time period, there were also 70 patients with cT1a esophageal carcinoma who underwent endoscopic mucosal resection (EMR). These patients were not included into the study because complete pathologic staging, *i.e.*, nodal staging, would not be obtainable. Patient demographics, tumor characteristics, operative treatment and perioperative outcomes, surgical pathology, and long term outcomes were recorded.

Clinical staging was performed by EUS for all patients in addition to a combination of CT and PET imaging. The majority of patients (128/139) underwent EUS at our institution. EUS was performed by two gastroenterologists (Harris C and Klapman J) who have advanced training in EUS and have seven and 12 years of EUS experience, respectively. Each endoscopist performed an average of 150 EUS procedures a year. The radial echoendoscope was used by both endoscopists, but CH also adds the linear echoendoscope to evaluate the nodal mediastinal stations: 2R, 2L, 4R, 4L, 5, 6, 7, 8, and 9. Of note, the processor was updated within the last 3 years from an Aloka SSD-5000 (Aloka Co., Ltd., Tokyo, Japan) to an Aloka alpha 10 (Aloka Co., Ltd., Tokyo, Japan). Ultrasound-guided fine needle aspiration of lymph nodes was also performed during the procedure for equivocal or suspicious lymph nodes. EUS and other clinical

**Table 2 Comparison of clinical and pathologic staging for cT1N0 and cT2N0 sub-groups**

	Clinical stage		Pathologic stage		
	cT1N0	pTisN0	pT1N0	pT2-3N0	pN+
	110	22	67	9	12
	cT2N0	pTis-1N0	pT2N0	pT3N0	pN+
	29	15	6	1	7
Total	139	37	73	10	19

staging modalities were not repeated for patients who had completed the procedure at an outside facility.

After complete preoperative evaluation, all patients underwent esophagectomy without any neoadjuvant chemotherapy, radiation, or chemoradiation. Type of esophagectomy was determined by the judgment of the operating surgeon and included minimally invasive and open approaches. For Ivor-Lewis esophagectomies, thoracic lymphadenectomy was also performed to include mediastinal lymph node stations 7-9. Surgical specimens were staged by the tumor-node-metastasis (TNM) classification according to American Joint Committee on Cancer guidelines. Accuracy rates of EUS were determined by comparing EUS tumor depth and nodal staging to depth and nodal status on surgical pathology. Patients who were found to have more advanced disease on surgical pathology than suggested by preoperative work-up were referred to medical and radiation oncology for discussion of adjuvant therapy.

Statistical analysis was carried out by SPSS software version 23 (Chicago, IL, United States). Descriptive statistics was used to describe the cohort, with means and medians for continuous variables and frequencies and percentages for categorical variables. Student's *t* test and Fisher's exact test or  $\chi^2$  test was used to compare variables. Two-sided *P*-value was used with *P* < 0.05 considered statistically significant. Logistic regression analysis was used to determine if clinical variables such as tumor location and tumor histology were associated with EUS accuracy. Institutional review board approval was obtained prior to initiation of the study.

## RESULTS

Between 2000 and 2015, 139 patients with early stage esophageal carcinoma (cT1N0 and cT2N0) were identified. Patient demographics and tumor characteristics are outlined in Table 1. Briefly, there were 25 (18%) female and 114 (82%) male patients with tumors predominantly in the lower third of the esophagus and the gastroesophageal (GE) junction. Ninety-three percent of patients had adenocarcinoma and 7% had squamous cell carcinoma on final pathology. Clinical staging was as follows: 110 (79%) patients had cT1N0M0 and 29 (21%) patients had cT2N0M0 tumors. Type of surgical resection included three-field



esophagectomy (2/139), transhiatal esophagectomy (26/139), and Ivor-Lewis esophagectomy (111/139). Fifty-three (38%) procedures were by a minimally invasive approach (laparoscopic or robotic-assisted). The median lymph node count was 12 (range 1-63).

For the entire cohort, preoperative EUS staging matched the final surgical pathology in 73 of 139 patients for a concordance rate of 53% (Table 2). Thirty-seven patients (27%) were over-staged and 29 (19%) were under-staged. Of these, 10/139 (7%) were under-staged by tumor depth and 19/139 (14%) had nodal disease unrecognized pre-operatively (pN+) (Table 2). Of patients with cT1N0 disease who were clinically over-staged, 22 had carcinoma *in-situ* or Barrett's with high grade dysplasia on final surgical pathology. Of patients with nodal disease, 17/19 were pN1 and 2/19 were pN2. We could not ascertain from pathology reports whether microscopic or macroscopic nodal metastasis was present in these cases. By clinical stage, preoperative ultrasound was less reliable in identifying nodal disease for tumors with greater depth, though this was not statistically significant. EUS missed nodal disease for 12/110 (11%) of cT1 tumors and 7/29 (24%) of cT2 tumors ( $P = 0.075$ ).

Other factors which could influence ability of EUS to predict pathological staging were also analyzed. We examined the time period in which patients underwent EUS. Patients were divided by whether they underwent EUS between 2000 and 2010 or between 2011 and 2015. Of patients who underwent EUS in 2010 or earlier, 17/110 (16%) had unrecognized nodal disease compared to 2/29 (7%) of patients who had EUS performed in 2011 or later ( $P = 0.363$ ). In our series, PET was used for clinical staging in addition to EUS in 62 of the 139 patients. Of 62 patients that had both EUS and PET, only 4 (6%) had occult nodal involvement on surgical pathology compared to 15/77 (19%) of patients that did not undergo PET preoperatively ( $P = 0.028$ ).

Logistic regression was performed to evaluate whether tumor location, tumor histology, time period of EUS, and whether EUS was performed at our institution were associated with accurate staging by EUS. None of these variables were related to the ability of EUS to accurately stage patients ( $P > 0.05$ ). Factors such as tumor length, presence of Barrett's dysplasia, presence of strictures, and traversability of lesions were not evaluated in this study due to incomplete or missing data.

Of the cohort, 29 patients (21%) were under-staged. Nine patients underwent adjuvant therapy, with six undergoing chemotherapy and three undergoing chemoradiation. The remaining patients did not undergo adjuvant therapy. Median follow-up was 51 mo (range 1-186 mo). Median overall survival was 107 mo for the entire cohort.

## DISCUSSION

The current standard of care for early stage esophageal cancer includes EMR for T1aN0 disease and upfront surgery for T1bN0 and T2N0 disease. Trimodality therapy is the standard of care in patients with more advanced disease<sup>[10]</sup>. The staging of esophageal cancer, therefore, is important not only as a prognostic indicator, but also as a means by which we may determine the best therapeutic approach.

EUS is believed to offer improved sensitivity and specificity to the clinical staging process. However, in our cohort the concordance of EUS with pathological stage was lower than prior reports of EUS staging for esophageal cancer, though these studies included early and locally advanced disease. There is a degree of operator dependence with EUS, but this is an unlikely explanation. The accuracy of EUS for the evaluation of early stage esophageal cancer has been examined in multiple recent retrospective reviews and they demonstrate similar findings<sup>[11-14]</sup>. These studies identified the limited ability of EUS to accurately stage T1N0 and T2N0 disease. In their study, Young *et al*<sup>[9]</sup> cited a 56% concordance rate with EUS and surgical pathology in early esophageal cancer. These limitations may be related to the anatomy of the esophagus and its complex lymphatic system. Other cited factors which decrease EUS accuracy include tumor length, tumor location (specifically tumors at the gastroesophageal junction and cardia), and presence of Barrett's esophagus<sup>[8,10]</sup>.

Tumors may be under-staged by either underestimating the depth of invasion (T stage) or the presence of nodal involvement (N stage). In our series, EUS underestimated the depth of invasion in 10 (7%) patients without pathological lymph node involvement. In the study by van Hagen *et al*<sup>[5]</sup>, neoadjuvant treatment increases the rate of complete resection with negative margins. Despite this fact, all patients in this series were able to undergo complete surgical resection with negative margins. The more problematic issue is when clinical under-staging presents as unrecognized nodal involvement. This leads to unreliable prognostication and inappropriate treatment selection. The importance of this issue is demonstrated in the dismal 5-year survival rate for patients with lymph node metastasis<sup>[15]</sup>. Furthermore, several studies have established a survival advantage to neoadjuvant therapy before surgery in patients with lymph node involvement<sup>[16,17]</sup>. In our series, 19 of 139 (14%) patients had unrecognized nodal disease pre-operatively. Had their clinical staging been accurately assessed, neoadjuvant chemoradiation would have been recommended prior to proceeding with surgical resection. The role of adjuvant therapy in these patients is controversial and the delivery of

concurrent chemotherapy and or radiation therapy following surgical resection might be challenging due to concerns of decreased efficacy and poor tolerance<sup>[18,19]</sup>. In a randomized trial of preoperative vs postoperative chemotherapy for esophageal squamous cell carcinoma, five-year overall survival was 43% for the adjuvant chemotherapy group vs 55% for the neoadjuvant chemotherapy group<sup>[19]</sup>. In addition, rates of treatment after surgery may be lowered due to poor postoperative performance status or patient refusal, as seen in the present series in which only half of the patients who met criteria for adjuvant therapy received it.

Due to the potential for understaging and missed opportunities for neoadjuvant therapy, consideration for neoadjuvant therapy in T2 esophageal carcinoma has been examined, though controversy exists. As mentioned above, the rate of nodal metastasis in clinical T1 and T2 disease is not negligible. Bergeron *et al.* demonstrated that 15% of cT1a and 18% of cT1b tumors were under-staged by nodal status<sup>[14]</sup>. Keeping in mind the relationship between tumor depth and nodal status in esophageal cancer, tumors that penetrate the submucosal layer may be able to also invade the network of lymphatic channels that course the length of the esophagus<sup>[20]</sup>. In the evaluation of depth of tumor as a predictor of regional lymph node involvement by Rice *et al.*<sup>[20]</sup>, up to 40% of T2 lesions were identified to have lymph node involvement. In this series, 24% of cT2N0 patients had nodal involvement on surgical pathology. In the randomized trial by van Hagen *et al.*<sup>[5]</sup> that established a benefit for neoadjuvant chemoradiation, T2 patients were included in the study. Similarly, a propensity matched study of stage I and II patients demonstrated that stage I and II patients who underwent neoadjuvant chemotherapy had a 47.7% five-year OS rate compared to a 38.6% rate in patients who underwent upfront surgery ( $P = 0.016$ ). However, when upfront surgery vs neoadjuvant chemoradiation was evaluated in this population in a randomized trial, there were no survival differences ( $P = 0.94$ ) but increased postoperative mortality ( $P = 0.049$ )<sup>[5]</sup>.

Since 2009, our center has added the routine use of PET with EUS for staging early esophageal cancer. This has improved accuracy of staging, as confirmed in other series<sup>[21]</sup>. Of the 139 patients with clinical T1N0 or T2N0 esophageal cancer, 62 patients had a PET included as part of their clinical workup. Only four patients were found to have nodal disease on pathologic specimen when their EUS and PET imaging showed negative nodal involvement. Seventy-seven patients in this series did not undergo PET imaging as part of their clinical staging. Of that group, 15 patients (19%) were identified as having occult nodal disease. These findings suggest that the combination of both EUS and PET for staging of early esophageal cancer improves clinical accuracy. We cannot definitively predict that a PET would have

demonstrated hypermetabolic activity in those understaged lymph nodes, as many patients had low volume nodal disease with only one positive lymph node on final pathology. Interestingly, in a SEER study, the authors noted that EUS and/or CT-PET was associated with improved overall survival, probably due to the improvement in staging and receipt of therapies for patients undergoing these procedures<sup>[22]</sup>.

Although the consequences of clinically understaging may seem evident, over-staging by EUS also has important ramifications. Over-staging may lead to unnecessary surgical procedures. In clinical series, the mortality and morbidity rate of esophagectomy are 2%-6% and 50%-64%, respectively<sup>[23-25]</sup>. In this series, the 30-d mortality rate was 2.2%. Of 110 patients with cT1N0 tumors, 22 had carcinoma *in situ* (Tis) or Barrett's with high grade dysplasia (HGD) on final surgical pathology. These disease processes could have been treated with a less invasive endoscopic mucosal resection rather than esophagectomy. EMR has been proven to be an effective treatment option for patients with Tis and Barrett's with HGD, as long as deep radial and deep margins are free of tumor<sup>[26]</sup>. For this reason, our institution now utilizes EMR not only as a therapeutic tool when appropriate, but also as a diagnostic tool which can evaluate pathologically and more accurately the depth of invasion of the tumor.

The decreased accuracy of EUS in early stage disease is unlikely related to evolving technology or improved technique over time at our institution. In similar studies, retrospective data collected over a decade time span has proposed technology to be a limitation, contributing to possible EUS inaccuracy if obtained during the early 2000s<sup>[11]</sup>. This was evaluated in our review by grouping patients into two separate time periods. Endoscopes used for the majority of patients in this review ranged in frequencies from 5-10 MHz. Of note, the processor was updated within the last 3 years from a 5 MHz endoscope to a 10 MHz endoscope. No significant difference was identified between patients whose EUS was performed before or after 2010 with respect to unrecognized nodal disease by EUS.

This study has several important limitations. There are inherent biases due to the retrospective nature of this study. In addition, though it appears that the concordance rate of EUS with surgical pathology was low in this study, other published studies report similar numbers in the setting of early esophageal cancer. In addition, we did not include patients that underwent endoscopic mucosal resection, which likely would have improved our accuracy rates. The decision to exclude those patients was made because it would not be possible to figure out the true nodal status of those patients without undergoing surgery. Also, one of our study objectives was to demonstrate factors associated with inaccurate EUS, but due to the time span of the study many prior endoscopic reports were missing pertinent information such as length of

the tumor and presence of Barrett's esophagus. Our study had an overwhelming majority of patients with adenocarcinoma, which is more typical of Western populations. Though we could not ascertain from endoscopy reports exactly how many patients had Barrett's esophagus, we speculate that many of our patients diagnosed with carcinoma were undergoing surveillance for Barrett's esophagus. In addition, patients who had EUS at an outside institution were included, but the number was relatively small and likely did not impact the results of this study.

However, this study does bring to light the limitations of one of the more specific and sensitive tools in the staging of esophageal cancer. As suggested by the results of our study, the initial use of endoscopic mucosal resection may be an appropriate diagnostic and possible therapeutic technique for patients with cT1N0 disease. It is especially difficult to distinguish T1a disease from T1b disease by EUS and therefore EMR is even more important as a diagnostic tool. For patients who may be under-staged based solely on depth of invasion (T stage), which carries a 7% risk in our series, meticulous surgical technique with adequate radial resection margins mitigates potential incomplete resections. Also, the addition of PET reduces the rate of finding occult nodal disease in these patients with early disease. When staged with a combination of EUS and PET, the risk of occult nodal disease is only 4% in this group. Therefore, current treatment algorithms of clinical stage T1N0 and T2N0 esophageal cancer should be re-evaluated so that appropriate therapy is administered, without over- or under-treatment. Further evaluation of the under-staged group in this review is needed to determine if unrecognized nodal disease by preoperative staging workup in early stage esophageal cancer affects long-term survival or disease-free interval. As for patients with cT2N0 lesions based on both EUS and PET, a frank and detailed discussion must be undertaken regarding the risks and benefits of neoadjuvant therapy, as 18% of this group of patients will have clinically unrecognized nodal involvement. Further studies are required to elucidate various clinical and pathological risk factors for occult nodal involvement. Future developments in molecular profiling techniques would also aid the diagnosis and treatment of these patients.

## COMMENTS

### Background

Studies demonstrate the importance of neoadjuvant therapy in esophageal cancer. Accurate staging determines which patients should undergo neoadjuvant treatment and is vital to improved patient outcomes. Computed tomography, magnetic resonance imaging, positron emission tomography, and endoscopic ultrasound (EUS) are important modalities for staging in esophageal cancer. EUS is a widely used modality with high sensitivity and specificity, though studies suggest that it is less accurate in early disease.

### Research frontiers

EUS for esophageal cancer is standard practice. The distinction between

tumors that invade the muscularis propria from those that invade the adventitia is critically important as it determines which patient will require upfront surgery vs neoadjuvant treatment. However, reports suggest that EUS staging is less accurate in early esophageal cancer.

### Innovations and breakthroughs

This clinical study demonstrates that even in high volume cancer centers, improved staging is necessary. The addition of PET-CT leads to greater improvement in staging accuracy. Endoscopic mucosal resection is another useful diagnostic tool in the setting of early esophageal cancer.

### Applications

Based on the findings of this study, we recommend increased use of PET-CT and EMR in addition to EUS in the staging of early esophageal cancer. Continued advances in these modalities will lead to more accurate determination of staging and treatment strategies for patients with early esophageal cancer.

### Peer-review

The manuscript describes the experience from an oncologic center with EUS as the main tool, sometimes associated to PET-SCAN for the treatment of esophagus cancer.

## REFERENCES

- 1 What are the key statistics about cancer of the esophagus? 2016. Available from: URL: <http://www.cancer.org/cancer/esophaguscancer/detailedguide/esophagus-cancer-key-statistics>
- 2 Enzinger PC, Mayer RJ. Esophageal cancer. *N Engl J Med* 2003; **349**: 2241-2252 [PMID: 14657432 DOI: 10.1056/NEJMra035010]
- 3 Visbal AL, Allen MS, Miller DL, Deschamps C, Trastek VF, Pairero PC. Ivor Lewis esophagogastric resection for esophageal cancer. *Ann Thorac Surg* 2001; **71**: 1803-1808 [PMID: 11426751 DOI: 10.1016/S0003-4975(01)02601-7]
- 4 Low DE, Kunz S, Schembre D, Otero H, Malpass T, Hsi A, Song G, Hinke R, Kozarek RA. Esophagectomy--it's not just about mortality anymore: standardized perioperative clinical pathways improve outcomes in patients with esophageal cancer. *J Gastrointest Surg* 2007; **11**: 1395-1402; discussion 1402 [PMID: 17763917 DOI: 10.1007/s11605-007-0265-1]
- 5 van Hagen P, Hulshof MC, van Lanschot JJ, Steyerberg EW, van Berge Henegouwen MI, Wijnhoven BP, Richel DJ, Nieuwenhuijzen GA, Hospers GA, Bonenkamp JJ, Cuesta MA, Blaisse RJ, Busch OR, ten Kate FJ, Creemers GJ, Punt CJ, Plukker JT, Verheul HM, Spillenaar Bilgen EJ, van Dekken H, van der Sagen MJ, Rozema T, Biermann K, Beukema JC, Piet AH, van Rij CM, Reinders JG, Tilanus HW, van der Gaast A; CROSS Group. Preoperative chemoradiotherapy for esophageal or junctional cancer. *N Engl J Med* 2012; **366**: 2074-2084 [PMID: 22646630 DOI: 10.1056/NEJMoa1112088]
- 6 Mariette C, Dahan L, Mornex F, Maillard E, Thomas PA, Meunier B, Boige V, Pezet D, Robb WB, Le Brun-Ly V, Bosset JF, Mabrut JY, Triboulet JP, Bedenne L, Seitz JF. Surgery alone vs chemoradiotherapy followed by surgery for stage I and II esophageal cancer: final analysis of randomized controlled phase III trial FFCD 9901. *J Clin Oncol* 2014; **32**: 2416-2422 [PMID: 24982463 DOI: 10.1200/JCO.2013.53.6532]
- 7 van Westreenen HL, Westertep M, Bossuyt PM, Pruim J, Sloof GW, van Lanschot JJ, Groen H, Plukker JT. Systematic review of the staging performance of 18F-fluorodeoxyglucose positron emission tomography in esophageal cancer. *J Clin Oncol* 2004; **22**: 3805-3812 [PMID: 15365078 DOI: 10.1200/JCO.2004.01.083]
- 8 Puli SR, Reddy JB, Bechtold ML, Antillon D, Ibdah JA, Antillon MR. Staging accuracy of esophageal cancer by endoscopic ultrasound: a meta-analysis and systematic review. *World J Gastroenterol* 2008; **14**: 1479-1490 [PMID: 18330935 DOI: 10.3748/wjg.14.1479]
- 9 Young PE, Gentry AB, Acosta RD, Greenwald BD, Riddle M. Endoscopic ultrasound does not accurately stage early adenocarcinoma or high-grade dysplasia of the esophagus. *Clin*



- Gastroenterol Hepatol* 2010; **8**: 1037-1041 [PMID: 20831900 DOI: 10.1016/j.cgh.2010.08.020]
- 10 **Sjoquist KM**, Burmeister BH, Smithers BM, Zalcberg JR, Simes RJ, Barbour A, Gebiski V; Australasian Gastro-Intestinal Trials Group. Survival after neoadjuvant chemotherapy or chemoradiotherapy for resectable oesophageal carcinoma: an updated meta-analysis. *Lancet Oncol* 2011; **12**: 681-692 [PMID: 21684205 DOI: 10.1016/S1470-2045(11)70142-5]
  - 11 **Dhupar R**, Rice RD, Correa AM, Weston BR, Bhutani MS, Maru DM, Betancourt SL, Rice DC, Swisher SG, Hofstetter WL. Endoscopic Ultrasound Estimates for Tumor Depth at the Gastroesophageal Junction Are Inaccurate: Implications for the Liberal Use of Endoscopic Resection. *Ann Thorac Surg* 2015; **100**: 1812-1816 [PMID: 26233274 DOI: 10.1016/j.athoracsur.2015.05.038]
  - 12 **O'Farrell NJ**, Malik V, Donohoe CL, Johnston C, Muldoon C, Reynolds JV, O'Toole D. Appraisal of staging endoscopic ultrasonography in a modern high-volume esophageal program. *World J Surg* 2013; **37**: 1666-1672 [PMID: 23568244 DOI: 10.1007/s00268-013-2004-y]
  - 13 **Tekola BD**, Sauer BG, Wang AY, White GE, Shami VM. Accuracy of endoscopic ultrasound in the diagnosis of T2N0 esophageal cancer. *J Gastrointest Cancer* 2014; **45**: 342-346 [PMID: 24788081 DOI: 10.1007/s12029-014-9616-9]
  - 14 **Bergeron EJ**, Lin J, Chang AC, Orringer MB, Reddy RM. Endoscopic ultrasound is inadequate to determine which T1/T2 esophageal tumors are candidates for endoluminal therapies. *J Thorac Cardiovasc Surg* 2014; **147**: 765-771: Discussion 771-773 [PMID: 24314788 DOI: 10.1016/j.jtcvs.2013.10.003]
  - 15 **Cho JW**, Choi SC, Jang JY, Shin SK, Choi KD, Lee JH, Kim SG, Sung JK, Jeon SW, Choi IJ, Kim GH, Jee SR, Lee WS, Jung HY; Korean ESD Study Group. Lymph Node Metastases in Esophageal Carcinoma: An Endoscopist's View. *Clin Endosc* 2014; **47**: 523-529 [PMID: 25505718 DOI: 10.5946/ce.2014.47.6.523]
  - 16 **Urschel JD**, Vasani H, Blewett CJ. A meta-analysis of randomized controlled trials that compared neoadjuvant chemotherapy and surgery to surgery alone for resectable esophageal cancer. *Am J Surg* 2002; **183**: 274-279 [PMID: 11943125 DOI: 10.1016/S0002-9610(02)00795-X]
  - 17 **Campbell NP**, Villafior VM. Neoadjuvant treatment of esophageal cancer. *World J Gastroenterol* 2010; **16**: 3793-3803 [PMID: 20698042 DOI: 10.3748/wjg.v16.i30.3793]
  - 18 **Ando N**, Kato H, Igaki H, Shinoda M, Ozawa S, Shimizu H, Nakamura T, Yabusaki H, Aoyama N, Kurita A, Ikeda K, Kanda T, Tsujinaka T, Nakamura K, Fukuda H. A randomized trial comparing postoperative adjuvant chemotherapy with cisplatin and 5-fluorouracil vs preoperative chemotherapy for localized advanced squamous cell carcinoma of the thoracic esophagus (JCOG9907). *Ann Surg Oncol* 2012; **19**: 68-74 [PMID: 21879261 DOI: 10.1245/s10434-011-2049-9]
  - 19 **Pasquer A**, Gronnier C, Renaud F, Duhamel A, Théreaux J, Carrere N, Gagniere J, Meunier B, Collet D, Mariette C. Impact of Adjuvant Chemotherapy on Patients with Lymph Node-Positive Esophageal Cancer who are primarily Treated with Surgery. *Ann Surg Oncol* 2015; **22** Suppl 3: S1340-S1349 [PMID: 26065869 DOI: 10.1245/s10434-015-4658-1]
  - 20 **Rice TW**, Zuccaro G Jr, Adelstein DJ, Rybicki LA, Blackstone EH, Goldblum JR. Esophageal carcinoma: depth of tumor invasion is predictive of regional lymph node status. *Ann Thorac Surg* 1998; **65**: 787-792 [PMID: 9527214 DOI: 10.1016/S0003-4975(97)01387-8]
  - 21 **Varghese TK Jr**, Hofstetter WL, Rizk NP, Low DE, Darling GE, Watson TJ, Mitchell JD, Krasna MJ. The society of thoracic surgeons guidelines on the diagnosis and staging of patients with esophageal cancer. *Ann Thorac Surg* 2013; **96**: 346-356 [PMID: 23752201 DOI: 10.1016/j.athoracsur.2013.02.069]
  - 22 **Wani S**, Das A, Rastogi A, Drahos J, Ricker W, Parsons R, Bansal A, Yen R, Hosford L, Jankowski M, Sharma P, Cook MB. Endoscopic ultrasonography in esophageal cancer leads to improved survival rates: results from a population-based study. *Cancer* 2015; **121**: 194-201 [PMID: 25236485 DOI: 10.1002/cncr.29043]
  - 23 **Atkins BZ**, Shah AS, Hutcheson KA, Mangum JH, Pappas TN, Harpole DH Jr, D'Amico TA. Reducing hospital morbidity and mortality following esophagectomy. *Ann Thorac Surg* 2004; **78**: 1170-1176; discussion 1170-1176 [PMID: 15464465 DOI: 10.1016/j.athoracsur.2004.02.034]
  - 24 **Dhungel B**, Diggs BS, Hunter JG, Sheppard BC, Vetto JT, Dolan JP. Patient and peri-operative predictors of morbidity and mortality after esophagectomy: American College of Surgeons National Surgical Quality Improvement Program (ACS-NSQIP), 2005-2008. *J Gastrointest Surg* 2010; **14**: 1492-1501 [PMID: 20824375 DOI: 10.1007/s11605-010-1328-2]
  - 25 **Merritt RE**, Whyte RI, D'Arcy NT, Hoang CD, Shrager JB. Morbidity and mortality after esophagectomy following neoadjuvant chemoradiation. *Ann Thorac Surg* 2011; **92**: 2034-2040 [PMID: 21945223 DOI: 10.1016/j.athoracsur.2011.05.121]
  - 26 **Shah PM**, Gerdes H. Endoscopic options for early stage esophageal cancer. *J Gastrointest Oncol* 2015; **6**: 20-30 [PMID: 25642334 DOI: 10.3978/j.issn.2078-6891.2014.096]

P- Reviewer: Caboclo JLF, Chiba T S- Editor: Ma YJ L- Editor: A  
E- Editor: Ma YJ



## Retrospective Study

# Early gastric cancer frequently has high expression of KK-LC-1, a cancer-testis antigen

Nobue Futawatari, Takashi Fukuyama, Rui Yamamura, Akiko Shida, Yoshihito Takahashi, Yatsushi Nishi, Yoshinobu Ichiki, Noritada Kobayashi, Hitoshi Yamazaki, Masahiko Watanabe

Nobue Futawatari, Department of Surgery, Sagami National Hospital, Sagami, Kanagawa 252-0392, Japan

Takashi Fukuyama, Rui Yamamura, Noritada Kobayashi, Division of Biomedical Research, Kitasato University Medical Center, Kitamoto, Saitama 364-8501, Japan

Nobue Futawatari, Akiko Shida, Masahiko Watanabe, Department of Surgery, School of Medicine, Kitasato University, Sagami, Kanagawa 252-0374, Japan

Yoshihito Takahashi, Yatsushi Nishi, Department of Surgery, Kitasato University Medical Center, Kitamoto, Saitama 364-8501, Japan

Yoshinobu Ichiki, Second Department of Surgery, School of Medicine, University of Occupational and Environmental Health, Kitakyushu, Fukuoka 807-8555, Japan

Hitoshi Yamazaki, Department of Pathology, Kitasato University Medical Center, Kitamoto, Saitama 364-8501, Japan

ORCID number: Nobue Futawatari (0000-0001-5666-308X); Takashi Fukuyama (0000-0003-1772-3478); Rui Yamamura (0000-0003-3891-1929); Akiko Shida (0000-0002-7457-5160); Yoshihito Takahashi (0000-0001-9433-0403); Yatsushi Nishi (0000-0002-6605-092X); Yoshinobu Ichiki (0000-0002-1293-6952); Noritada Kobayashi (0000-0003-0321-6379); Hitoshi Yamazaki (0000-0001-9452-1445); Masahiko Watanabe (0000-0001-5801-7559).

**Author contributions:** Futawatari N and Fukuyama T contributed equally to this work; Futawatari N, Fukuyama T, Ichiki Y, Yamazaki H and Watanabe M designed the research; Futawatari N, Fukuyama T, Yamamura R, Shida A, Takahashi Y, Nishi Y, Kobayashi N and Yamazaki H performed the research; Futawatari N performed statistical analysis; Futawatari N, Fukuyama T and Watanabe M wrote the paper.

Supported by Grant-in-Aid for research by Kitasato University

Medical Center, No. H25-0006 and the JSPS, KAKENHI, No. 26670609 to Futawatari N, and the JSPS, KAKENHI, No. 21700510 and No. 17K16578, Takeda Science Foundation and Kitasato University Research Grant for Young Researchers to Fukuyama T.

**Institutional review board statement:** The study protocol was approved by the Human Ethics Review Committee of Kitasato University Medical Center, Japan.

**Conflict-of-interest statement:** There are no conflicts of interest to declare.

**Data sharing statement:** No additional data are available.

**Open-Access:** This article is an open-access article which was selected by an in-house editor and fully peer-reviewed by external reviewers. It is distributed in accordance with the Creative Commons Attribution Non Commercial (CC BY-NC 4.0) license, which permits others to distribute, remix, adapt, build upon this work non-commercially, and license their derivative works on different terms, provided the original work is properly cited and the use is non-commercial. See: <http://creativecommons.org/licenses/by-nc/4.0/>

**Manuscript source:** Unsolicited manuscript

**Correspondence to:** Takashi Fukuyama, PhD, Investigator, Division of Biomedical Research, 6-100 Arai, Kitamoto, Saitama 364-8501, Japan. [fukuyam@insti.kitasato-u.ac.jp](mailto:fukuyam@insti.kitasato-u.ac.jp)

**Telephone:** +81-48-5931236

**Fax:** +81-48-5931262

**Received:** October 5, 2017

**Peer-review started:** October 6, 2017

**First decision:** October 18, 2017

**Revised:** October 30, 2017

**Accepted:** November 14, 2017

**Article in press:** November 14, 2017

**Published online:** December 14, 2017

## Abstract

### AIM

To assess cancer-testis antigens (CTAs) expression in gastric cancer patients and examined their associations with clinicopathological factors.

### METHODS

Eighty-three gastric cancer patients were evaluated in this study. Gastric cancer specimens were evaluated for the gene expression of CTAs, Kitakyushu lung cancer antigen-1 (KK-LC-1), melanoma antigen (MAGE)-A1, MAGE-A3 and New York esophageal cancer-1 (NY-ESO-1), by reverse transcription PCR. Clinicopathological background information, such as gender, age, tumor size, macroscopic type, tumor histology, depth of invasion, lymph node metastasis, lymphatic invasion, venous invasion, and pathological stage, was obtained. Statistical comparisons between the expression of each CTA and each clinicopathological background were performed using the  $\chi^2$  test.

### RESULTS

The expression rates of KK-LC-1, MAGE-A1, MAGE-A3, and NY-ESO-1 were 79.5%, 32.5%, 39.8%, and 15.7%, respectively. In early stage gastric cancer specimens, the expression of KK-LC-1 was 79.4%, which is comparable to the 79.6% observed in advanced stage specimens. The expression of KK-LC-1 was not significantly associated with clinicopathological factors, while there were considerable differences in the expression rates of MAGE-A1 and MAGE-A3 with *vs* without lymphatic invasion (MAGE-A1, 39.3% *vs* 13.6%,  $P = 0.034$ ; MAGE-A3, 47.5% *vs* 18.2%,  $P = 0.022$ ) and/or vascular invasion (MAGE-A1, 41.5% *vs* 16.7%,  $P = 0.028$ ; MAGE-A3, 49.1% *vs* 23.3%,  $P = 0.035$ ) and, particularly, MAGE-A3, in patients with early *vs* advanced stage (36.5% *vs* 49.0%,  $P = 0.044$ ), respectively. Patients expressing MAGE-A3 and NY-ESO-1 were older than those not expressing MAGE-A3 and NY-ESO-1 (MAGE-A3,  $73.7 \pm 7.1$  *vs*  $67.4 \pm 12.3$ ,  $P = 0.009$ ; NY-ESO-1,  $75.5 \pm 7.2$  *vs*  $68.8 \pm 11.2$ ,  $P = 0.042$ ).

### CONCLUSION

The KK-LC-1 expression rate was high even in patients with stage I cancer, suggesting that KK-LC-1 is a useful biomarker for early diagnosis of gastric cancer.

**Key words:** Cancer-testis antigen; Kitakyushu lung cancer antigen-1; Melanoma antigen-A1; Melanoma antigen-A3; Gastric cancer; New York esophageal cancer-1; Clinicopathological factor; Early stage

© The Author(s) 2017. Published by Baishideng Publishing Group Inc. All rights reserved.

**Core tip:** The Kitakyushu lung cancer antigen-1 (KK-LC-1) is a relatively later cancer-testis antigen and has received interest because it was reported that KK-LC-1 is a predominant antigen for cancer immuno-

therapy. We found that the expression rate of KK-LC-1 in gastric cancer was 79.5%, which was higher than that of other cancer-testis antigens and the same as that in both early- and late-stage patients. KK-LC-1 is a potential biomarker for early detection of gastric cancer and identification of patients at high risk for gastric cancer. Furthermore, KK-LC-1 is a potential target for immunotherapy in gastric cancer.

Futawatari N, Fukuyama T, Yamamura R, Shida A, Takahashi Y, Nishi Y, Ichiki Y, Kobayashi N, Yamazaki H, Watanabe M. Early gastric cancer frequently has high expression of KK-LC-1, a cancer-testis antigen. *World J Gastroenterol* 2017; 23(46): 8200-8206 Available from: URL: <http://www.wjgnet.com/1007-9327/full/v23/i46/8200.htm> DOI: <http://dx.doi.org/10.3748/wjg.v23.i46.8200>

## INTRODUCTION

Gastric cancer is the third leading cause of cancer-related death worldwide, after lung and liver cancers<sup>[1]</sup>. Endoscopic therapy, surgical resection, and chemotherapy are established treatments for gastric cancer; however, the mortality rate of gastric cancer patients remains high and thus new treatment strategies must be developed.

Cancer-testis antigens (CTAs) are a group of tumor antigens expressed in a wide variety of cancer tissues but not in normal tissue except for testicular germ cells<sup>[2]</sup>. Because of their tumor specificity, CTAs are considered potential targets for new treatment strategies including immunotherapy<sup>[3,4]</sup>, and the expression of each CTA has potential significance for the prognosis of several types of cancer<sup>[5]</sup>. While studies have reported the expression patterns of CTAs in various cancer types, fewer studies have focused on those in gastric cancer<sup>[5-7]</sup>.

Kita-Kyushu lung cancer antigen-1 (KK-LC-1) was first identified in patients with lung cancer<sup>[8]</sup> and is a CTA recognized by cytotoxic T lymphocytes (CTL). When CTL against KK-LC-1 accumulate predominantly among tumor-infiltrating lymphocytes (TILs), adaptive immunotherapy using TILs leads to a good response<sup>[9]</sup>. The expression rate of KK-LC-1 in non-small cell cancer was reported to be 32.6%<sup>[10]</sup> and has also been reported in other types of cancer. In a study of triple-negative breast cancer, the expression rate of KK-LC-1 was reported to be 75%<sup>[11]</sup>. In our previous study of CTAs in gastric cancer, the expression rate of KK-LC-1 was shown to be as high as 81.6%, which was higher than the rates of other CTAs<sup>[6]</sup>. There are no reports of tumor-associated antigens being expressed as highly as KK-LC-1 in gastric cancer, indicating that KK-LC-1 is an ideal therapeutic target. In terms of diagnostic applications, tumor-associated antigens that are highly expressed in early stage cancers are considered



useful targets. Here, the expression patterns of CTAs including KK-LC-1 were assessed in gastric cancer patients and the usefulness of these CTAs for diagnosis and determining the appropriate treatment strategy were examined.

## MATERIALS AND METHODS

The study protocol was approved by the Human Ethics Review Committee of Kitasato University Medical Center, Japan, and signed informed consent was obtained from each patient prior to collecting the tissue samples used in this study.

### Patients

A total of 134 patients underwent surgical resection of gastric cancer at the Department of Surgery, Kitasato University Medical Center, Kitamoto, Japan between June 2011 and March 2014, and 83 specimens were successfully obtained from 52 male patients and 31 female patients. The mean age of the patients was 69.8 years (range, 30–86 years).

Clinicopathological findings were classified according to the Japanese Classification of Gastric Carcinoma (14<sup>th</sup> edition)<sup>[12]</sup>. In the present study, based on macroscopic data, tumor types 0, 1, and 2 were reclassified as localized tumors and 3, 4, and 5 as infiltrated tumors. Based on histological findings, papillary adenocarcinoma and tubular adenocarcinoma were reclassified as differentiated tumors, while poorly differentiated adenocarcinoma, signet ring cell adenocarcinoma, and mucinous carcinoma were classified as undifferentiated tumors. The relationships between CTAs and each of the nine clinicopathological factors (gender, age, tumor size, macroscopic type, tumor histology, depth, lymphatic invasion, and venous invasion) were assessed in this study.

### Tissue specimens

The tumor tissue samples obtained from the 83 patients with gastric cancer were immediately preserved in RNAlater® (Life Technologies, Carlsbad, CA, United States). The specimens were incubated at 4 °C overnight to allow for penetration of RNAlater and then stored at -80 °C until use.

### RNA isolation, cDNA synthesis, and PCR analysis of CTA expression

Total RNA was isolated from the tumor specimens using the BioRobot® EZ1™ and EZ1 RNA Tissue Mini Kits (48) (Qiagen, Hilden, Germany) according to the manufacturer's instructions and then converted to cDNA using oligo-p(dN)<sub>6</sub> random primers and Superscript™ II reverse transcriptase (Life Technologies).  $\beta$ -Actin was used as an internal standard to assess the quality of the isolated RNA in which the expression of the CTAs, including KK-LC-1, was evaluated. The expression levels of ACTB ( $\beta$ -actin),

MAGE-A1, MAGE-A3, and NY-ESO-1 were measured with TaqMan® Gene Expression Assays, ID numbers Hs99999903\_m1, Hs00607097\_m1, H200366532\_m1, and Hs00265824\_m1, respectively, using a 7900HT Fast Real-Time PCR system (Life Technologies). For cDNAs for which expression [represented by threshold cycle number (Ct)] of the ACTB gene yielded a Ct of < 28, the expression of KK-LC-1 was examined using endpoint reverse transcription PCR (RT-PCR) rather than a probe-based assay, as an appropriate probe for detecting KK-LC-1 mRNA has not been established. For RT-PCR of KK-LC-1, the oligonucleotides 5'-ATGAACCTTCTATTTACTCTAGCGAGC-3' and 5'-TTAGGTGGATTCCGGTGAGG-3' were used as specific primers, and annealing was performed at 67 °C for 40 cycles, yielding a 342-base pair product. The intensity of KK-LC-1 positive- or negative-amplicon was shown in Figure 1.

### Statistical analysis

Statistical comparisons between the expression levels of the four CTAs and between the nine clinicopathological factors were performed using the  $\chi^2$  test with the level of significance set at  $P < 0.05$ . All statistical analyses were conducted using EZR (Saitama Medical Centre, Jichi Medical University; Kanda, 2012)<sup>[13]</sup>.

## RESULTS

The expression rates of KK-LC-1, MAGE-A1, MAGE-A3, and NY-ESO-1 in gastric cancer were 79.5%, 32.5%, 39.8%, and 15.7%, respectively. Among them, KK-LC-1 had the highest expression rate (Table 1).

Table 2 shows the expression of CTAs that exhibited significant associations with any of the measured clinicopathological factors including age, sex, tumor size, macroscopic type, tumor histology, invasion depth, lymph node metastasis, lymphatic invasion, venous invasion, and disease stage. The expression rate of MAGE-A1 was significantly higher in patients with lymphatic and/or venous invasion than in those without ( $P = 0.034$  and  $0.028$ , respectively). The age of patients expressing MAGE-A3 was significantly higher than that of patients not expressing MAGE-A3 ( $P = 0.009$ ). The expression rate of MAGE-A3 was higher in patients with advanced stage ( $P = 0.044$ ), lymphatic ( $P = 0.022$ ), and/or venous ( $P = 0.035$ ) invasion than in those without. The age of patients expressing NY-ESO-1 was significantly higher than that of patients not expressing NY-ESO-1 ( $P = 0.042$ ).

Although KK-LC-1 was not significantly associated with any of the nine clinicopathological factors, the expression rate of KK-LC-1 (79.4%) in early stage samples was markedly higher than that of MAGE-A1 (23.5%), MAGE-A3 (26.5%), and NY-ESO-1 (8.8%) in early stage samples and was comparable to the KK-LC-1 expression rate in advanced stage cancer (79.6%; Figure 2A). In contrast, the expression rates of the

**Table 1** Cancer-testis antigen expression in 83 patients with gastric cancer

CTA	Positive	Negative	Proportion (%)
KK-LC-1	66	17	79.5
MAGE-A1	27	56	32.5
MAGE-A3	33	50	39.7
NY-ESO-1	13	70	15.7

CTA: Cancer-testis antigen; KK-LC-1: Kita-Kyushu lung cancer antigen-1; MAGE: Melanoma antigen; NY-ESO-1: New York esophageal cancer-1.

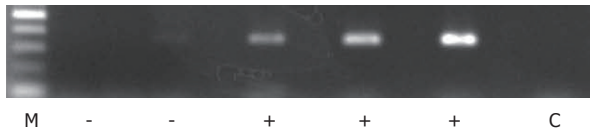


**Figure 1** Expression of Kita-Kyushu lung cancer antigen-1 in the gastric cancer tumors. The expression of KK-LC-1 was detected as a 342-bp band of the amplicon. The three specimens were assessed as KK-LC-1 positive (+) in this panel. The brightest band of top in lane M indicates 500 bp of 75 ng. M: 100 bp ladder; C: Negative control; -: KK-LC-1 negative; +: KK-LC-1 positive. KK-LC-1: Kita-Kyushu lung cancer antigen-1.

other CTAs were not comparable to those of KK-LC-1 in advanced stage samples (38.8% for MAGE-A1, 49.0% for MAGE-A3, and 16.0% for NY-ESO-1). The ratios of the expression rates in early/advanced stage (E/A ratio) were estimated for each CTA (Figure 2B) and higher ratios (closer to 1; *i.e.*, the CTA concerned was expressed at similar levels in early stage compared to advanced stage) were associated with CTAs that are more useful in early stage diagnosis and targeted immunotherapy. The E/A ratio of KK-LC-1 was the highest among them (KK-LC-1: 1.00, MAGE-A1: 0.61, MAGE-A3: 0.54, and NY-ESO-1: 0.43).

## DISCUSSION

In the present study, the potential associations between KK-LC-1 expression and various clinicopathological factors were examined. The usefulness of KK-LC-1 as a target for cancer immunotherapy and a biomarker for early diagnosis was also evaluated.

The expression rate of KK-LC-1 in the present study (79.5%) was shown to be markedly higher than those of other CTAs measured. We assessed KK-LC-1 expression as visibility of PCR amplicon, and have not experienced contamination of other sequences in the 342-bp of KK-LC-1 amplicon, then there would be few pseudo-positive cases. On the other hand, the specimens included much normal cells, such as normal stomach cells, fibroblasts and immune cells, the expression of KK-LC-1 would not detect even if tumor cells produced it. The specimens used in this study were not evaluated the rate of inclusion tumor cells, then the pseudo-negative specimens might be included.

The expression of KK-LC-1 has been assessed in various cancer types<sup>[10,11,14]</sup>. The basal form of breast cancer, also known as triple-negative breast cancer, exhibited high expression rates of KK-LC-1 compared with other CTAs; however, KK-LC-1 expression in whole breast cancer was low. In this study, high KK-LC-1 expression rates were detected in whole gastric cancer, where detecting KK-LC-1 in stomach tissue is considered more advantageous for mining tumors than in breast tissue.

The expression rates of other CTAs in gastric cancer have been reported in several studies: Wang *et al.*<sup>[15]</sup> reported the expression rates of MAGE-A1, MAGE-A3, and NY-ESO-1 as 23.8%, 41.6%, and 11.9%, respectively; Ogata *et al.*<sup>[5]</sup> reported the expression rate of MAGE-A1 to be 32.6%; and Mashino *et al.*<sup>[16]</sup> reported the expression rate of NY-ESO-1 as 7.8%. In our study, the expression rates of MAGE-A1, MAGE-A3, and NY-ESO-1 were 32.5%, 39.8%, and 15.7%, respectively, which agree with previously reported rates.

Assessing CTAs in relation to the clinicopathological factors in this study revealed that the expression of KK-LC-1 was not significantly associated with any of the measured clinicopathological factors, indicating that KK-LC-1 was highly expressed in gastric cancer patients regardless of the presence of lymph node metastasis, lymphatic invasion, or disease stage. This suggests that KK-LC-1 is a useful target for cancer immunotherapy, regardless of disease stage.

Regarding tumor-associated antigens including tumor markers and CTAs (shown in part in Figure 1), it is known that the detection rate in early stage cancer is lower than that in advanced stage cancer<sup>[17]</sup>. The expression rates of MAGE-A1 and MAGE-A3 were higher in patients with lymphatic and venous invasion than in those without. The ages of groups expressing MAGE-A3 or NY-ESO-1 were higher than those not expressing these genes. Examination of the influence of the disease stage revealed a significant difference in the expression rates of MAGE-A3 between disease stages (from stage I to stage IV). Ogata *et al.*<sup>[5]</sup> reported that MAGE-A1 expression is significantly associated with age, macroscopic type, and venous invasion, but not with disease stage, invasion depth, or lymph node metastasis. In another study, however, the expression rates of CTAs were reported to be higher in gastric cancer patients with advanced stages or in those with greater invasion depth<sup>[7]</sup>, which is inconsistent with the above findings.

Recently, a KK-LC-1 peptide restricted by HLA-B62 and HLA-A2 was discovered<sup>[8,10]</sup>. The frequencies of HLA-B62 and HLA-A2 expression among Japanese gastric cancer patients were reported to be 15% and 45%, respectively<sup>[18]</sup> and the frequency of patients expressing at least one of these two HLA proteins was approximated at 55%. Given that the expression rate

**Table 2** Correlation between CTAs and clinicopathological factors *n* (%)

Characteristics	The expression number of each CTA			
	KK-LC-1	MAGE-A1	MAGE-A3	NY-ESO-1
Age (yr) (mean ± SD)	<i>P</i> = 0.944	<i>P</i> = 0.104	<i>P</i> = 0.009	<i>P</i> = 0.042
Positive	69.8 ± 11.4 ( <i>n</i> = 66)	72.7 ± 7.9 ( <i>n</i> = 27)	73.7 ± 7.1 ( <i>n</i> = 33)	75.5 ± 7.2 ( <i>n</i> = 13)
Negative	70.1 ± 9.5 ( <i>n</i> = 17)	68.5 ± 12.0 ( <i>n</i> = 56)	67.4 ± 12.3 ( <i>n</i> = 50)	68.8 ± 11.2 ( <i>n</i> = 70)
Tumor size (mm) (mean ± SD)	<i>P</i> = 0.5202	<i>P</i> = 0.4752	<i>P</i> = 0.862	<i>P</i> = 0.831
Positive	59.9 ± 4.2 ( <i>n</i> = 65)	62.5 ± 6.6 ( <i>n</i> = 27)	57.9 ± 5.9 ( <i>n</i> = 33)	60.5 ± 9.5 ( <i>n</i> = 13)
Negative	53.8 ± 8.5 ( <i>n</i> = 16)	56.8 ± 4.6 ( <i>n</i> = 54)	59.2 ± 4.9 ( <i>n</i> = 48)	58.3 ± 4.1 ( <i>n</i> = 68)
Gender	<i>P</i> = 0.406	<i>P</i> = 1	<i>P</i> = 0.645	<i>P</i> = 0.758
Male ( <i>n</i> = 52)	43 (82.7)	17 (32.7)	22 (42.3)	9 (17.3)
Female ( <i>n</i> = 31)	23 (74.2)	10 (32.3)	11 (35.5)	4 (12.9)
Macroscopic type	<i>P</i> = 0.591	<i>P</i> = 1	<i>P</i> = 0.649	<i>P</i> = 1
Localized ( <i>n</i> = 49)	40 (81.6)	16 (32.7)	18 (36.7)	8 (16.3)
Infiltrated ( <i>n</i> = 34)	26 (76.5)	11 (32.4)	15 (44.1)	5 (14.7)
Histological type	<i>P</i> = 0.599	<i>P</i> = 0.246	<i>P</i> = 1	<i>P</i> = 1
Differentiated ( <i>n</i> = 44)	36 (81.8)	17 (38.6)	18 (40.9)	7 (15.9)
Undifferentiated ( <i>n</i> = 39)	30 (76.9)	10 (25.6)	15 (38.5)	6 (15.4)
Depth of invasion	<i>P</i> = 0.269	<i>P</i> = 0.089	<i>P</i> = 0.243	<i>P</i> = 0.761
T1 ( <i>n</i> = 30)	26 (86.7)	6 (20.0)	9 (30.0)	4 (13.3)
Intramucosal ( <i>n</i> = 11)	11 (100)	0 (0)	2 (18.2)	1 (9.1)
Submucosal 1 ( <i>n</i> = 5)	4 (80.0)	2 (40.0)	3 (60.0)	1 (20.0)
Submucosal 2 ( <i>n</i> = 14)	11 (78.6)	4 (28.6)	4 (28.6)	2 (14.3)
T2-T4 ( <i>n</i> = 53)	40 (75.5)	21 (39.6)	24 (45.3)	9 (17.0)
Lymph node metastasis	<i>P</i> = 1	<i>P</i> = 0.17	<i>P</i> = 0.823	<i>P</i> = 1
Negative ( <i>n</i> = 40)	32 (80.0)	10 (25.0)	15 (37.5)	6 (15.0)
Positive ( <i>n</i> = 43)	34 (79.1)	17 (39.5)	18 (41.9)	7 (16.3)
Lymphatic invasion	<i>P</i> = 1	<i>P</i> = 0.034	<i>P</i> = 0.022	<i>P</i> = 0.498
Negative ( <i>n</i> = 22)	18 (81.8)	3 (13.6)	4 (18.2)	2 (9.1)
Positive ( <i>n</i> = 61)	48 (78.7)	24 (39.3)	29 (47.5)	11 (18.0)
Venous invasion	<i>P</i> = 0.583	<i>P</i> = 0.028	<i>P</i> = 0.035	<i>P</i> = 0.121
Negative ( <i>n</i> = 30)	25 (83.3)	5 (16.7)	7 (23.3)	2 (6.7)
Positive ( <i>n</i> = 53)	41 (77.4)	22 (41.5)	26 (49.1)	11 (20.8)
Stage	<i>P</i> = 1	<i>P</i> = 0.162	<i>P</i> = 0.044	<i>P</i> = 0.222
Early (I) ( <i>n</i> = 34)	27 (79.4)	8 (23.5)	9 (26.5)	3 (8.8)
Advanced (II-IV) ( <i>n</i> = 49)	39 (79.6)	19 (38.8)	24 (49.0)	10 (20.4)
II ( <i>n</i> = 21)	16 (76.2)	7 (33.3)	11 (52.4)	3 (14.3)
III ( <i>n</i> = 15)	11 (73.3)	7 (46.7)	7 (46.7)	3 (20.0)
IV ( <i>n</i> = 13)	12 (92.3)	5 (38.5)	6 (46.2)	4 (30.8)

KK-LC-1: Kita-Kyushu lung cancer antigen-1; MAGE: Melanoma antigen; NY-ESO-1: New York esophageal cancer-1.

of KK-LC-1 in gastric cancer was found to be 79.5% in this study, approximately 44% of patients with gastric cancer are potential candidates for immunotherapy targeting KK-LC-1. By the same reasoning and using the peptide database of shared tumor-specific antigens from Cancer Immunity (<http://cancerimmunity.org/peptide/tumor-specific/>) as well as findings published by Ikeda *et al*<sup>[18]</sup>, the KK-LC-1 expression rates in patients considered potential candidates for immunotherapy targeting MAGE-A1 and MAGE-A3 were approximated at 27% and 38%, respectively. Although 10 epitope peptides of MAGE-A3 bind to HLA and are recognized by CTL, the covering rate of patients for MAGE-A3 immunotherapy would be lower than that of KK-LC-1 immunotherapy, as KK-LC-1 contains only two epitope peptides.

Fukuyama *et al*<sup>[19]</sup> further demonstrated that *Helicobacter pylori* infection induced the expression of murine MAGE-A3. After KK-LC-1, MAGE-A3 was the most highly expressed CTA among those tested in the present study. Notably, the 79.5% KK-LC-1 expression frequency is in accordance with the > 80% of patients

who had gastric cancer caused by *H. pylori* infection<sup>[20]</sup>. In the study by Fukuyama, the potential correlation between murine Kk-lc-1 and *H. pylori* infection could not be evaluated because there is no sequence in the murine genome comparable to the human KK-LC-1 gene sequence. Considering that KK-LC-1 is expressed in tumor tissues regardless of invasion depth and disease stage, it is possible that *H. pylori* induces CTA expression<sup>[21]</sup>.

Given that KK-LC-1 is tumor-specific and can be frequently detected even in early stages, the assessment of CTAs in gastric mucosa infected with *H. pylori* may be useful for identifying patients with a high risk of gastric cancer. Overall, immunotherapy targeting KK-LC-1 may represent a new treatment strategy for gastric cancer.

## ARTICLE HIGHLIGHTS

### Research background

One CTA's expression rate was high in gastric cancer. The expression rate of CTAs is commonly higher at advanced stages than early stage of cancers of

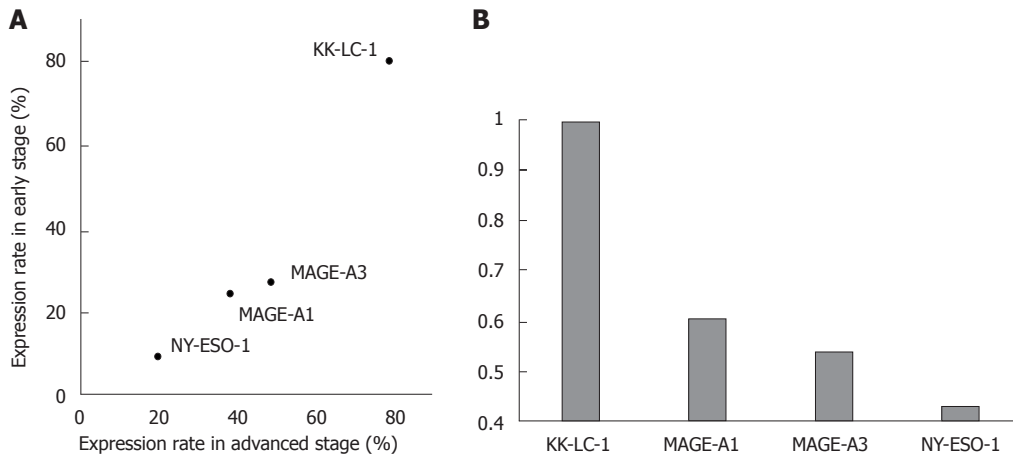


**Figure 2 Ratio of CTA expression between early and advanced stage gastric cancer.** These figures show a comparison of expression rates of each CTA between early and advanced stage. A: Distribution of expression rate of each CTA in early and advanced stages; B: Early/advanced stage expression ratios (E/A ratios) were used to evaluate whether the CTAs concerned were frequently expressed in early- as well as advanced-stage samples. (E/A ratio = expression rate of early stage/expression rate of advanced stage).

any organs. We hypothesized that KK-LC-1 expression rate would be higher in advanced stage than in early stage.

### Research motivation

One CTA was not analyzed the relation of clinicopathological factors and other CTAs were little known the relation of them. Now, tumor immunotherapy has been remarked because of PD-1 therapy, then CTAs, targets for immunotherapy, will be also remarked.

### Research objectives

We search the new approach of CTAs for therapy or diagnosis of cancer. For the objective, we performed their characteristics. Especially, the high-rate expressing CTAs should be mined and characterized for cancer therapy/diagnosis.

### Research methods

The process was very simple. We collected fresh tumor tissues of stomach resected from gastric cancer patients and evaluated the expression of four CTAs using RT-PCR method. Also we collected the clinicopathological background in their clinical records. We calculated the proportion of each CTA expression and evaluated the difference of clinicopathological background between the patients with expression of each CTA and without them. We performed statistical analysis of  $\chi^2$  test using EZR.

### Research results

The expression rate of KK-LC-1 in early stage was as high as in advanced stages. The expression rate of KK-LC-1 was about 80% high at any statement of clinicopathological background. And we supplied the knowledges about the correlation between expression of each CTA and clinicopathological background.

### Research conclusions

Our results of High-rate expression of KK-LC-1 not only in advanced stage but also in early stage indicated that it would be an attractive target for immunotherapy and early diagnosis in gastric cancer.

### Research perspectives

We need to evaluate that KK-LC-1 is correlate to infection of *H. pylori* in gastric cancer and that KK-LC-1 is detected at the less invasive methods than biopsy.

## ACKNOWLEDGMENTS

The authors thank Ms. Etsuko Terayama, and Ms. Maki

Kobayashi for providing technical assistance.

## REFERENCES

- 1 Stewart BW, Wild CP, editors. World Cancer Report 2014. Lyon, France: International Agency for Research on Cancer 2014
- 2 van der Bruggen P, Traversari C, Chomez P, Lurquin C, De Plaen E, Van den Eynde B, Knuth A, Boon T. A gene encoding an antigen recognized by cytolytic T lymphocytes on a human melanoma. *Science* 1991; **254**: 1643-1647 [PMID: 1840703]
- 3 Gjerstorff MF, Andersen MH, Ditzel HJ. Oncogenic cancer/testis antigens: prime candidates for immunotherapy. *Oncotarget* 2015; **6**: 15772-15787 [PMID: 26158218 DOI: 10.18632/oncotarget.4694]
- 4 Ghafouri-Fard S, Modarressi MH. Cancer-testis antigens: potential targets for cancer immunotherapy. *Arch Iran Med* 2009; **12**: 395-404 [PMID: 19566358]
- 5 Ogata K, Aihara R, Mochiki E, Ogawa A, Yanai M, Toyomasu Y, Ando H, Ohno T, Asao T, Kuwano H. Clinical significance of melanoma antigen-encoding gene-1 (MAGE-1) expression and its correlation with poor prognosis in differentiated advanced gastric cancer. *Ann Surg Oncol* 2011; **18**: 1195-1203 [PMID: 21042944 DOI: 10.1245/s10434-010-1399-z]
- 6 Shida A, Futawatari N, Fukuyama T, Ichiki Y, Takahashi Y, Nishi Y, Kobayashi N, Yamazaki H, Watanabe M. Frequent High Expression of Kita-Kyushu Lung Cancer Antigen-1 (KK-LC-1) in Gastric Cancer. *Anticancer Res* 2015; **35**: 3575-3579 [PMID: 26026129]
- 7 Honda T, Tamura G, Waki T, Kawata S, Terashima M, Nishizuka S, Motoyama T. Demethylation of MAGE promoters during gastric cancer progression. *Br J Cancer* 2004; **90**: 838-843 [PMID: 14970862 DOI: 10.1038/sj.bjc.6601600]
- 8 Fukuyama T, Hanagiri T, Takenoyama M, Ichiki Y, Mizukami M, So T, Sugaya M, So T, Sugio K, Yasumoto K. Identification of a new cancer/germline gene, KK-LC-1, encoding an antigen recognized by autologous CTL induced on human lung adenocarcinoma. *Cancer Res* 2006; **66**: 4922-4928 [PMID: 16651449 DOI: 10.1158/0008-5472.CAN-05-3840]
- 9 Stevanović S, Pasetto A, Helman SR, Gartner JJ, Prickett TD, Howie B, Robins HS, Robbins PF, Klebanoff CA, Rosenberg SA, Hinrichs CS. Landscape of immunogenic tumor antigens in successful immunotherapy of virally induced epithelial cancer. *Science* 2017; **356**: 200-205 [PMID: 28408606 DOI: 10.1126/science.aak9510]
- 10 Shigematsu Y, Hanagiri T, Shiota H, Kuroda K, Baba T, Mizukami M, So T, Ichiki Y, Yasuda M, So T, Takenoyama M, Yasumoto K.



- Clinical significance of cancer/testis antigens expression in patients with non-small cell lung cancer. *Lung Cancer* 2010; **68**: 105-110 [PMID: 19545928 DOI: 10.1016/j.lungcan.2009.05.010]
- 11 **Paret C**, Simon P, Vormbrock K, Bender C, Kölsch A, Breitzkreuz A, Yildiz Ö, Omokoko T, Hubich-Rau S, Hartmann C, Häcker S, Wagner M, Roldan DB, Selmi A, Türeci Ö, Sahin U. CXorf61 is a target for T cell based immunotherapy of triple-negative breast cancer. *Oncotarget* 2015; **6**: 25356-25367 [PMID: 26327325 DOI: 10.18632/oncotarget.4516]
  - 12 Japanese Gastric Cancer Association: Japanese Classification of Gastric Carcinoma: 3rd English edition. *Gastric Cancer* 2011; **14**: 101-112
  - 13 **Kanda Y**. Investigation of the freely available easy-to-use software 'EZR' for medical statistics. *Bone Marrow Transplant* 2013; **48**: 452-458 [PMID: 23208313 DOI: 10.1038/bmt.2012.244]
  - 14 **Yao J**, Caballero OL, Yung WK, Weinstein JN, Riggins GJ, Strausberg RL, Zhao Q. Tumor subtype-specific cancer-testis antigens as potential biomarkers and immunotherapeutic targets for cancers. *Cancer Immunol Res* 2014; **2**: 371-379 [PMID: 24764584 DOI: 10.1158/2326-6066.CIR-13-0088]
  - 15 **Wang Y**, Wu XJ, Zhao AL, Yuan YH, Chen YT, Jungbluth AA, Gnjjatic S, Santiago D, Ritter G, Chen WF, Old LJ, Ji JF. Cancer/testis antigen expression and autologous humoral immunity to NY-ESO-1 in gastric cancer. *Cancer Immun* 2004; **4**: 11 [PMID: 15516106]
  - 16 **Mashino K**, Sadanaga N, Tanaka F, Yamaguchi H, Nagashima H, Inoue H, Sugimachi K, Mori M. Expression of multiple cancer-testis antigen genes in gastrointestinal and breast carcinomas. *Br J Cancer* 2001; **85**: 713-720 [PMID: 11531257 DOI: 10.1054/bjoc.2001.1974]
  - 17 **Wang W**, Chen XL, Zhao SY, Xu YH, Zhang WH, Liu K, Chen XZ, Yang K, Zhang B, Chen ZX, Chen JP, Zhou ZG, Hu JK. Prognostic significance of preoperative serum CA125, CA19-9 and CEA in gastric carcinoma. *Oncotarget* 2016; **7**: 35423-35436 [PMID: 27097114 DOI: 10.18632/oncotarget.8770]
  - 18 **Ikeda N**, Kojima H, Nishikawa M, Hayashi K, Futagami T, Tsujino T, Kusunoki Y, Fujii N, Suegami S, Miyazaki Y, Middleton D, Tanaka H, Saji H. Determination of HLA-A, -C, -B, -DRB1 allele and haplotype frequency in Japanese population based on family study. *Tissue Antigens* 2015; **85**: 252-259 [PMID: 25789826 DOI: 10.1111/tan.12536]
  - 19 **Fukuyama T**, Yamazaki T, Fujita T, Uematsu T, Ichiki Y, Kaneko H, Suzuki T, Kobayashi N. Helicobacter pylori, a carcinogen, induces the expression of melanoma antigen-encoding gene (Mage)-A3, a cancer/testis antigen. *Tumour Biol* 2012; **33**: 1881-1887 [PMID: 22773374 DOI: 10.1007/s13277-012-0448-6]
  - 20 **Uemura N**, Okamoto S, Yamamoto S, Matsumura N, Yamaguchi S, Yamakido M, Taniyama K, Sasaki N, Schlemper RJ. Helicobacter pylori infection and the development of gastric cancer. *N Engl J Med* 2001; **345**: 784-789 [PMID: 11556297 DOI: 10.1056/NEJMoa001999]
  - 21 **Fukuyama T**, Futawatari N, Ichiki Y, Shida A, Yamazaki T, Nishi Y, Nonoguchi H, Takahashi Y, Yamazaki H, Kobayashi N. Correlation Between Expression of the Cancer/Testis Antigen KK-LC-1 and Helicobacter pylori Infection in Gastric Cancer. *In Vivo* 2017; **31**: 403-407 [PMID: 28438869]

**P- Reviewer:** Aoyagi K, Luo HS   **S- Editor:** Gong ZM   **L- Editor:** A  
**E- Editor:** Huang Y



## Retrospective Study

**Diagnostic classification of endosonography for differentiating colorectal ulcerative diseases: A new statistical method**

En-Qi Qiu, Wen Guo, Tian-Ming Cheng, Yong-Li Yao, Wei Zhu, Si-De Liu, Fa-Chao Zhi

En-Qi Qiu, Wen Guo, Tian-Ming Cheng, Yong-Li Yao, Wei Zhu, Si-De Liu, Fa-Chao Zhi, Department of Gastroenterology, Nanfang Hospital, Southern Medical University, Institute of Digestive Diseases of Guangdong Province, Guangdong Provincial Key Laboratory of Gastroenterology, Guangzhou 510515, Guangdong Province, China

ORCID number: En-Qi Qiu (0000-0002-9729-7941); Wen Guo (0000-0001-8130-9031); Tian-Ming Cheng (0000-0003-3588-4064); Yong-Li Yao (0000-0003-2903-1946); Wei Zhu (0000-0003-3604-8797); Si-De Liu (0000-0001-5589-2817); Fa-Chao Zhi (0000-0003-2213-896X).

**Author contributions:** Qiu EQ and Guo W designed the study; Qiu EQ collected the cases; Guo W and Cheng TM evaluated the endoscopic ultrasound images; Qiu EQ recorded and analyzed the data; Guo W, Yao YL and Zhu W interpreted the results of analysis; Qiu EQ wrote the paper; Guo W and Zhi FC revised the manuscript; Liu SD and Zhi FC approved the final version and coordinated all aspects of work.

**Institutional review board statement:** The study was reviewed and approved by the Institutional Review Board of Nanfang Hospital, Southern Medical University.

**Conflict-of-interest statement:** The authors declare that there is no conflict of interest related to this study.

**Open-Access:** This article is an open-access article which was selected by an in-house editor and fully peer-reviewed by external reviewers. It is distributed in accordance with the Creative Commons Attribution Non Commercial (CC BY-NC 4.0) license, which permits others to distribute, remix, adapt, build upon this work non-commercially, and license their derivative works on different terms, provided the original work is properly cited and the use is non-commercial. See: <http://creativecommons.org/licenses/by-nc/4.0/>

**Manuscript source:** Unsolicited manuscript

**Correspondence to:** Fa-Chao Zhi, MD, Professor, Department of Gastroenterology, Nanfang Hospital, Southern Medical University, Institute of Digestive Diseases of

Guangdong Province, Guangdong Provincial Key Laboratory of Gastroenterology, Dadao North No. 1838, Guangzhou 510515, Guangdong Province, China. [zhifc@smu.edu.cn](mailto:zhifc@smu.edu.cn)  
Telephone: +86-20-61641532  
Fax: +86-20-87280770

Received: September 10, 2017

Peer-review started: September 10, 2017

First decision: September 20, 2017

Revised: October 13, 2017

Accepted: November 7, 2017

Article in press: November 7, 2017

Published online: December 14, 2017

**Abstract****AIM**

To establish a classification method for differential diagnosis of colorectal ulcerative diseases, especially Crohn's disease (CD), primary intestinal lymphoma (PIL) and intestinal tuberculosis (ITB).

**METHODS**

We searched the in-patient medical record database for confirmed cases of CD, PIL and ITB from 2008 to 2015 at our center, collected data on endoscopic ultrasound (EUS) from randomly-chosen patients who formed the training set, conducted univariate logistic regression analysis to summarize EUS features of CD, PIL and ITB, and created a diagnostic classification method. All cases found to have colorectal ulcers using EUS were obtained from the endoscopy database and formed the test set. We then removed the cases which were easily diagnosed, and the remaining cases formed the perplexing test set. We re-diagnosed the cases in the three sets using the classification method, determined EUS diagnostic accuracies, and adjusted the classification accordingly. Finally, the re-diagnosing

and accuracy-calculating steps were repeated.

## RESULTS

In total, 272 CD, 60 PIL and 39 ITB cases were diagnosed from 2008 to 2015 based on the in-patient database, and 200 CD, 30 PIL and 20 ITB cases were randomly chosen to form the training set. The EUS features were summarized as follows: CD: Thickened submucosa with a slightly high echo level and visible layer; PIL: Absent layer and diffuse hypoechoic mass; and ITB: Thickened mucosa with a high or slightly high echo level and visible layer. The test set consisted of 77 CD, 30 PIL, 23 ITB and 140 cases of other diseases obtained from the endoscopy database. Seventy-four cases were excluded to form the perplexing test set. After adjustment of the classification, EUS diagnostic accuracies for CD, PIL and ITB were 83.6% (209/250), 97.2% (243/250) and 85.6% (214/250) in the training set, were 89.3% (241/270), 97.8% (264/270) and 84.1% (227/270) in the test set, and were 86.7% (170/196), 98.0% (192/196) and 85.2% (167/196) in the perplexing set, respectively.

## CONCLUSION

The EUS features of CD, PIL and ITB are different. The diagnostic classification method is reliable in the differential diagnosis of colorectal ulcerative diseases.

**Key words:** Endoscopic ultrasound; Ulcerative diseases; Crohn's disease; Primary intestinal lymphoma; Intestinal tuberculosis; Classification

© **The Author(s) 2017.** Published by Baishideng Publishing Group Inc. All rights reserved.

**Core tip:** A classification method was created for the differential diagnosis of Crohn's disease (CD), primary intestinal lymphoma (PIL) and intestinal tuberculosis (ITB) by endoscopic ultrasound (EUS), and yielded good results. The classification was designed based on univariate logistic regression analysis of EUS features of CD, PIL and ITB. This classification method is useful for diagnosing these three diseases in daily EUS practice.

Qiu EQ, Guo W, Cheng TM, Yao YL, Zhu W, Liu SD, Zhi FC. Diagnostic classification of endosonography for differentiating colorectal ulcerative diseases: A new statistical method. *World J Gastroenterol* 2017; 23(46): 8207-8216 Available from: URL: <http://www.wjgnet.com/1007-9327/full/v23/i46/8207.htm> DOI: <http://dx.doi.org/10.3748/wjg.v23.i46.8207>

## INTRODUCTION

Some gastrointestinal diseases, including Crohn's disease (CD), primary intestinal lymphoma (PIL) and intestinal tuberculosis (ITB), can lead to colorectal ulcers, are difficult to differentiate<sup>[1-4]</sup>, and usually require entirely different treatments. Their architecture

on resection histology can be easily distinguished at low magnification<sup>[5-7]</sup>. Endoscopic ultrasound (EUS) can demonstrate bowel wall structural changes<sup>[8-10]</sup> and identify lesions under the mucosa<sup>[11-14]</sup>, which are valuable signs in the above-mentioned diseases<sup>[15]</sup>. However, there are few reports available regarding the value of EUS in the differential diagnosis of these three diseases. We attempted to create an EUS diagnostic classification method for CD, PIL, ITB and other colorectal ulcerative diseases.

## MATERIALS AND METHODS

### Training set: Collection of EUS data

We searched our in-patient medical record database for patients who underwent EUS at our center from 2008 to 2015 and were confirmed to have CD, PIL or ITB, and found 272 cases of CD, 60 cases of PIL and 39 cases of ITB. We randomly chose 200 CD, 30 PIL and 20 ITB cases to form the training set, and summarized the EUS features. EUS images and written reports of these cases were obtained from the endoscopy database. The EUS data were recorded according to the following eight parameters: (1) Total bowel wall thickness (TWT, in mm); (2) Changes in layers (thickened, thinned or disappeared), including the mucosa (M), submucosa (SM), muscularis propria (MP) and serosa (S); (3) Echo level of lesions or changed layers, including Level 1 (echo level of normal SM), Level 2 (between Levels 1 and 3), Level 3 (echo level of liver), Level 4 (between Levels 3 and 5), Level 5 (echo level of normal MP), and Level 6 (echo level of fluid); (4) Echo homogeneity, including homogeneous and heterogeneous; in addition, an independent option of "diffuse lesion" was included; (5) Definition of layer borderlines, including clear, unclear and invisible; (6) Integrity of the S, including smooth, non-smooth and interrupted; (7) Special EUS bowel wall feature, including "cobblestone sign" (multiple thickened SM-like masses close to each other, with an intact M), vascular structures with a diameter > 2 mm in SM; and (8) Extra-luminal presentation, including nearby enlarged lymph nodes, abscesses, ascites, sinus and fistulae.

### Training set: Creation of a diagnostic classification method

All data on these parameters were analyzed using univariate logistic regression analysis to calculate the odds ratio (OR) of each option for each disease. The tendency scores for each disease for each option were then set according to the following rules: (1) The score was +1 if: a: the option was pathological, OR > 1 and  $P < 0.05$ ; or b:  $P \geq 0.05$ , but the proportion was > 50%; (2) The score was -1 if: a: OR < 1 and  $P < 0.05$ ; or b: OR was infinitesimal and  $P$  value was unavailable; and (3) The score was 0 when other situations were met.

**Table 1 Sex and age of all patients**

Total			Sex		Age, yr	
			Male	Female	Range	Mean
Diseases	CD	277 <sup>1</sup>	151	126	12-71	31.85
	PIL	60	37	23	18-73	43.76
	ITB	43 <sup>1</sup>	27	16	17-69	45.73

<sup>1</sup>Five CD and four ITB cases received treatment in the out-patient clinic, so were absent from the in-patient system. CD: Crohn's disease; ITB: Intestinal tuberculosis; PIL: Primary intestinal lymphoma.

The tendency scores formed the EUS diagnostic classification as follows: (1) All scores of each matched option were summed for each disease to obtain three tendency scores for CD, PIL and ITB, respectively; (2) When the parameters "layers changed" and "layer borders" both met the option "disappeared", only one point was added or subtracted; (3) The highest scoring disease was considered as the new EUS diagnosis; if the highest score was < 2 or was non-unique, the diagnosis was "other diseases"; and (4) When a sign unique to one disease (special sign) was detected, this disease was considered as the diagnosis directly, without including the score.

#### **Test set: Reassessment of EUS diagnoses**

We assessed the cases which formed the test set to evaluate the accuracy of EUS in differentiating colorectal ulcerative diseases. The search option "endoscopic findings" and key word "ulcer" were used to identify all cases of ulcers diagnosed by EUS at our center from 2008 to 2015. All EUS images of these cases were obtained from the endoscopy database. The EUS images (without written report) for each case were placed in the patient file, and then copied to two blinded researchers by another researcher.

The cases were deleted before being copied when they met the following conditions: (1) Appearance in the training set; (2) Having an obvious visible epithelial or subepithelial tumor in the images; and (3) Having images that did not provide enough information on the eight parameters mentioned above.

Two endosonographers re-evaluated the EUS images in each case and recorded the data according to the eight parameters. If the data for one case recorded by the two endosonographers were inconsistent, the difference was resolved through discussion. The new EUS diagnoses in the test set were then established using the classification method.

#### **Test set: Confirming actual diagnoses**

We consulted the clinical and out-patient databases, and the endoscopy database, to determine the final diagnosis of each case in the test set. Cases were excluded if the final diagnosis was not successfully obtained or the clinical data were incomplete. The diagnoses of all patients were confirmed by one of the

following four methods: Endoscopic biopsy pathology; Surgical pathology; Experimental treatment; or Other clinical methods (imaging modalities, special signs, laboratory examinations). Endoscopic biopsy specimens were obtained by forceps, endoscopic mucosal resection, endoscopic submucosal dissection and EUS-guided fine needle aspiration. Experimental treatment referred to: (1) CD: Infliximab, mesalazine or glucocorticoid treatment for at least 6 mo; (2) ITB: Quadruple anti-TB therapy for at least 2 mo; and (3) Other enteritis: Anti-infection (infective enteritis), immunosuppressant (autoimmune diseases) and tailored treatments (ischemic, drug and radiation enteritis). After the experimental treatment, final diagnoses were established if the symptoms were relieved, and colorectal ulcers were healed and did not reappear within 6 mo.

#### **All cases: Evaluation of EUS diagnostic accuracies**

The EUS and actual diagnoses in all cases were compared. The overall EUS diagnostic accuracy, sensitivity and specificity were calculated. We excluded the cases easily diagnosed in the test set and calculated the EUS diagnostic accuracy in the remaining cases (perplexing test set). Finally, the classification was adjusted and the diagnostic accuracies were recalculated. All processes are shown in Figure 1.

#### **Statistical analysis**

All data were analyzed using SPSS (Statistical Product and Service Solutions 13.0.0.246, International Business Machines Corporation, Armonk, NY, United States). Measurement data (age, TWT) are presented as the mean  $\pm$  SD. Multiple comparisons of groups were analyzed using the LSD-*t* test for TWT. Enumeration data (case number) are presented as a proportion, and comparisons of groups were analyzed using univariate logistic regression analysis.  $P < 0.05$  was considered statistically significant.

## **RESULTS**

#### **Patient data**

The data on sex and age obtained from all cases are shown in Table 1.

#### **EUS changes in TWT, stratification and echo level**

The data on mean TWT in the three diseases are shown in Table 2. TWT in the PIL group was greater than that in the other two groups ( $P < 0.05$ ). The case numbers and proportions of each option in each group are shown in Table 3.

#### **Special bowel wall signs and extra-luminal presentations**

The frequencies and proportions of special bowel wall signs and extra-luminal EUS images are shown in Table 4.



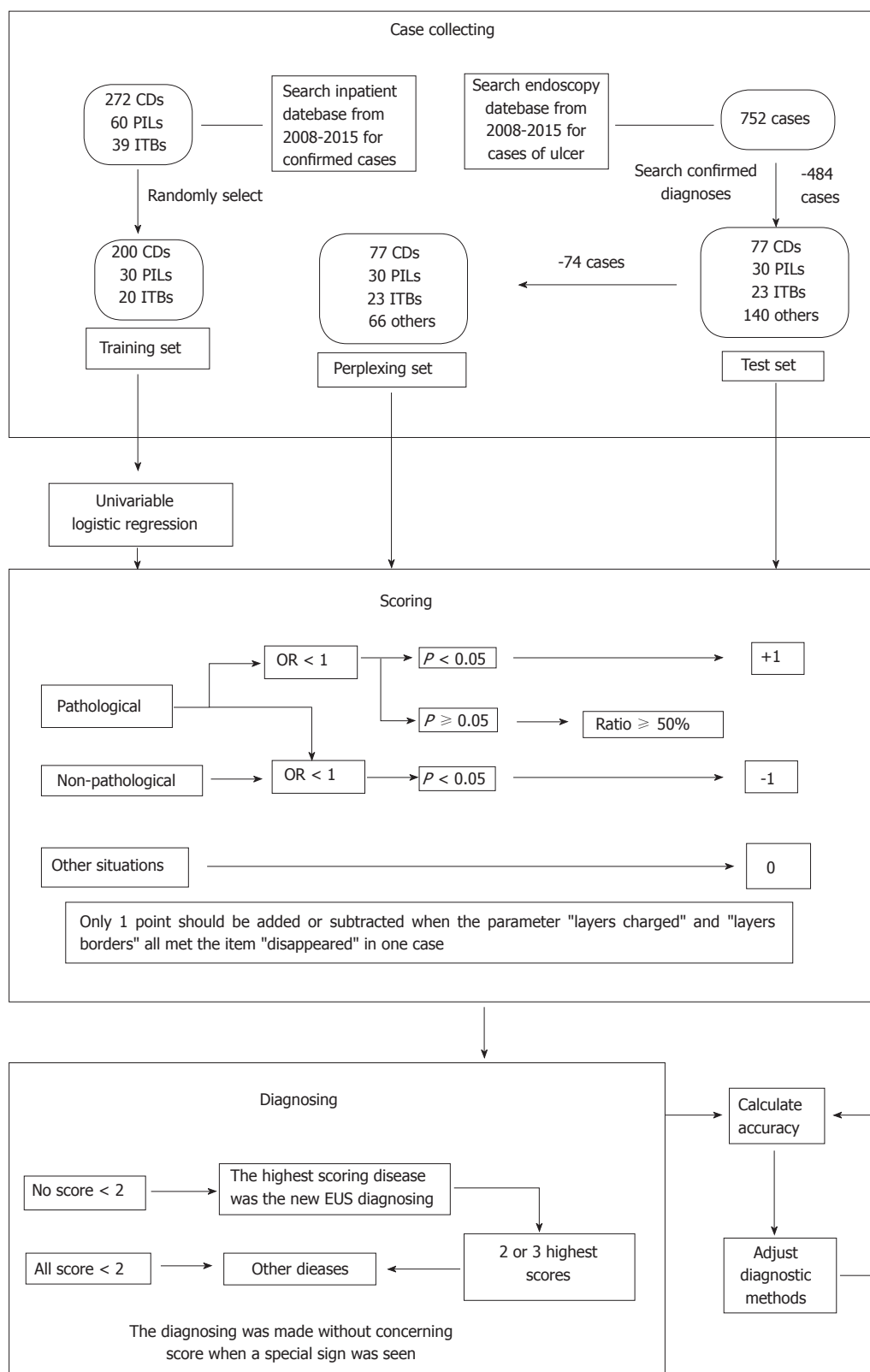


**Figure 1 Flowchart of the study.** The cases diagnosed with PIL previously were rediagnosed as cancer when the echo of the lesion was heterogeneous; cases were diagnosed with PIL when a diffuse echo was detected. CD: Crohn's disease; ITB: Intestinal tuberculosis; OR: Odds ratio; PIL: Primary intestinal lymphoma.

### EUS diagnostic classification

The ORs and *P* values from univariate logistic regression analysis, and the corresponding scores of each option set according to the above-mentioned rules, are listed

in Table 5. An option was not shown in the table if all *P* values were unavailable or were > 0.05. The options scoring +1 and -1 are summarized in Table 6. Classical EUS patterns of the three diseases are shown in

**Table 2** Comparison of the mean total wall thickness in Crohn's disease, primary intestinal lymphoma and intestinal tuberculosis

		TWT, mm		P value
		Range	Mean $\pm$ SD	
Diseases	CD	2.7-19.4	8.48 $\pm$ 2.90	(CD and PIL) < 0.001
	PIL	3.7-29.6	13.49 $\pm$ 6.38	(PIL and ITB) 0.002
	ITB	3.2-22.0	10.19 $\pm$ 6.14	(ITB and CD) 0.080
	F		23.389	
	P		< 0.001	

Data was analyzed by the LSD-*t* test. The difference was significant (*P* = 0.05). CD: Crohn's disease; ITB: Intestinal tuberculosis; PIL: Primary intestinal lymphoma; TWT: Total wall thickness.

Figures 2-4.

### Diagnostic accuracies in the training set

Using the classification method, we obtained the concordance between EUS and final diagnoses. The diagnostic accuracies for CD, PIL and ITB were 83.6% (209/250), 95.6% (239/250) and 91.2% (228/250), sensitivities were 79.5% (159/200), 73.3% (22/30) and 70.0% (14/20) and specificities were 100.0% (50/50), 98.6% (217/220) and 93.0% (214/230), respectively.

### Diagnostic accuracies in the test set

We collected EUS data on 752 cases from the endoscopy database, and 482 of these cases were excluded according to the exclusion criteria described in the Materials and Methods. The remaining 270 cases consisted of 77 CD, 30 PIL, 23 ITB and 140 patients with other diseases, including 30 cases of ulcers after endoscopic surgery, 29 cases of ulcerative colitis, 22 cases of colorectal cancer, 16 cases of nonspecific enteritis, 12 cases of infective colitis, 9 cases of radiation-induced bowel injury, 7 cases of ischemic enteritis, 6 cases of solitary ulcer, 3 cases of Behcet's disease, and 6 cases of multiple myeloma, abdominal-type allergic purpura, eosinophilic gastroenteritis, congenital megacolon, inflammatory granuloma after trauma, and indeterminate colitis, respectively. Using the classification methods, we yielded an accuracy for CD, PIL and ITB of 88.9% (240/270), 88.9% (240/270) and 83.7% (226/270), a sensitivity of 77.9% (60/77), 60.0% (18/30) and 78.3% (18/23), and a specificity of 93.2% (180/193), 92.5% (222/240) and 84.2% (208/247), respectively. After excluding a total of 74 cases of ulcers after surgery, infective and nonspecific colitis, radiation-induced bowel injury, and ischemic enteritis, we yielded accuracies for CD, PIL and ITB of 86.2% (169/196), 86.7% (170/196) and 84.7% (166/196), unchanged sensitivities, and specificities of 91.6% (109/119), 91.6% (152/166) and 85.5% (148/173), respectively.

### EUS diagnostic accuracies after adjusting the classification

The adjustments were as follows: (1) The cases

**Table 3** Common endoscopic ultrasound parameters of the bowel wall in Crohn's disease, primary intestinal lymphoma and intestinal tuberculosis *n* (%)

	CD	PIL	ITB
Thickened layers			
None	6 (3.0)	0 (0)	2 (10.0)
M	21 (10.5)	5 (16.7)	14 (70.0)
SM	160 (80.0)	2 (6.7)	0 (0)
M + SM	4 (2.0)	0 (0)	1 (5.0)
SM + MP	3 (1.5)	0 (0)	0 (0)
All	2 (1.0)	0 (0)	0 (0)
Layers disappeared <sup>1</sup>	4 (2.0)	23 (76.7)	3 (15.0)
Thinned layers			
SM	0 (0)	0 (0)	6 (30.0)
M/SM border			
Clear	85 (42.5)	3 (10.0)	8 (40.0)
Unclear	111 (55.5)	4 (13.3)	9 (45.0)
Invisible	4 (4.0)	23 (76.7)	3 (15.0)
SM/MP border			
Clear	157 (78.5)	3 (10.0)	12 (60.0)
Unclear	41 (21.5)	4 (13.3)	5 (25.0)
Invisible	2 (1.0)	23 (76.7)	3 (15.0)
Echo level of main lesion or changed layer			
1 (hyperechoic)	14 (7.0)	0 (0)	4 (20.0)
2	166 (83.0)	0 (0)	12 (60.0)
3 (medium)	3 (1.5)	3 (10.0)	1 (5.0)
4	11 (5.5)	5 (16.7)	1 (5.0)
5 (hypoechoic)	6 (3.0)	22 (73.3)	2 (10.0)
Echo homogeneity <sup>2</sup>			
Homogeneous	87 (43.5)	23 (76.7)	5 (25)
Heterogeneous	106 (53)	7 (23.3)	13 (65)
Diffuse lesion	3 (1.5)	26 (86.7)	0 (0)
Serosal integrity			
Smooth	185 (92.5)	14 (46.7)	15 (75)
Non-smooth	9 (4.5)	2 (6.6)	4 (20)
Interrupted	6 (3)	14 (46.7)	1 (5)

<sup>1</sup>Absent layers were included in the thickened layers because when the layers disappeared it was impossible to recognize the thickness change;

<sup>2</sup>Seven CD and two ITB cases were excluded because the thickness of the layers was too small and the echo homogeneity was difficult to determine. The options without matched cases are not given. CD: Crohn's disease; ITB: Intestinal tuberculosis; M: Mucosa; MP: Muscularis propria; PIL: Primary intestinal lymphoma; SM: Submucosa.

diagnosed as PIL previously were re-diagnosed as cancer (other diseases) when the echo of the lesion was heterogeneous; and (2) One case was diagnosed as PIL when a diffuse lesion echo was detected, without including any other factors. The accuracies increased after adjustment in the three sets. In the training set, the accuracy, sensitivity and specificity of PIL changed to 97.2% (243/250), 90.0% (27/30) and 98.2% (216/220), respectively, with no change in the CD and ITB groups. In the test set, the accuracies of CD, PIL and ITB improved to 89.3% (241/270), 97.8% (264/270) and 84.1% (227/270), sensitivities to 77.9% (60/77), 90.0% (27/30) and 78.3% (18/23), and specificities to 93.8% (181/193), 98.8% (237/240) and 84.6% (209/247), respectively. After excluding cases which were easily diagnosed, the accuracies of CD, PIL and ITB changed to 86.7% (170/196), 98.0% (192/196) and 85.2% (167/196), sensitivities were the same, and specificities changed to 92.4%

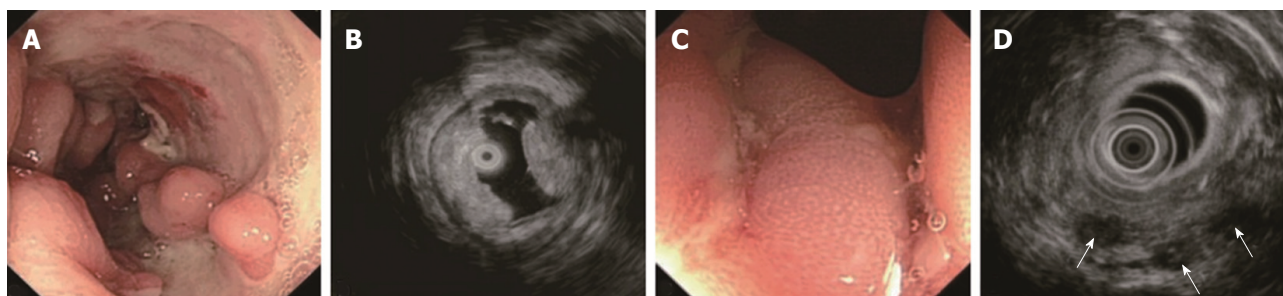


**Figure 2** A 21-year-old male with confirmed Crohn's disease. A: Multiple irregular ulcers with cobblestone appearance; B: EUS shows heterogeneous thickened bowel wall, thickened SM and absent M; C: Longitudinal ulcers within the swollen M; D: EUS shows irregular heterogeneous hypoechoic areas (arrows) which were considered to be abscesses. CD: Crohn's disease; EUS: Endoscopic ultrasound; M: Mucosa; SM: Submucosa.

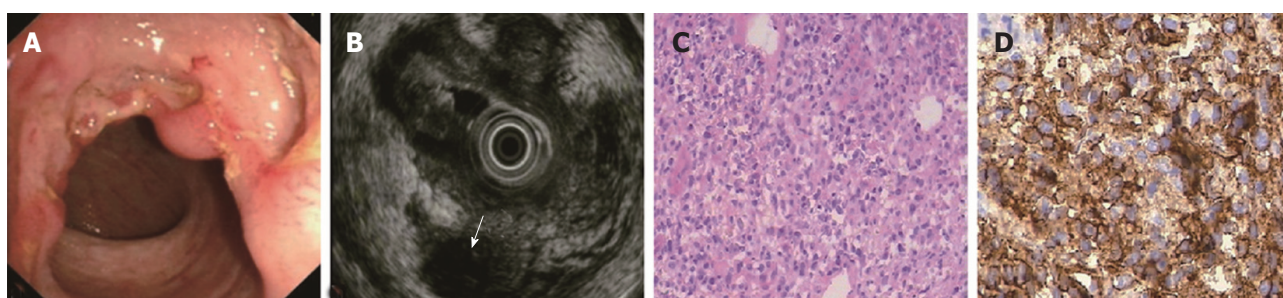


**Figure 3** A 58-year-old male with confirmed primary intestinal lymphoma. A: A circular ulcer with a nodular edge and smooth base; B: EUS shows disappearance of layers, instead of an irregular diffuse area with adjacent nodules (arrow); C, D: Diffuse large B-cell lymphoma confirmed by big-forceps deep biopsy and immunohistochemistry. EUS: Endoscopic ultrasound.

(110/119), 99.4% (165/166) and 86.1% (149/173), respectively.

## DISCUSSION

EUS can detect lesions which cannot be identified by white light endoscopy<sup>[16-20]</sup>, and allows observation of the bowel wall structure<sup>[21]</sup>. EUS is also used for the treatment of complications and follow-up studies<sup>[22-27]</sup>. This study investigated the differential diagnosis of CD, PIL and ITB using EUS. We created an EUS diagnostic classification method by reviewing and summarizing previous articles on pathology at low magnification and EUS data.

The EUS features of CD included thickened SM, visible layer borders, and the echo level of the SM ranging between hyperechoic and medium echoic<sup>[15,26]</sup>. Significantly thickened SM was closely associated with severe edema and lymphangiectasis<sup>[28]</sup>, which lowered the echo level of SM by increasing the sonolucency, and is always observed in resected CD bowels at low magnification. Invisible stratification is hardly seen, unless the illness is extremely severe. This sign was detected in only 4 cases in our study. We also found that the lesion was involved in the S and interrupted in 6 severe CD cases, which seemed impossible if CD was not complicated by malignancy. We suggest that severe fibrosis occurred in the bowels, making the S deformed, causing echo artifacts. Some studies have reported that vessels in the SM with a diameter > 2

mm were a specific EUS sign of CD<sup>[29-32]</sup>. This was not detected in the PIL and ITB cases in the training set; thus, the other specific signs of CD, such as fistulae, in this study were considered independent differentiation factors accordingly. In the test set, fistulae were found in only 2 cases. One was due to necrosis of lymphoma, and the other was due to anastomotic leakage.

The diagnostic sensitivity (77.9%) was not high. In total, 17 CD cases were misdiagnosed, 12 cases due to thickened M and 5 cases due to the collapse stratification or low-level echo caused by severe inflammation or infection. Five of these twelve cases with small TWT (< 5 mm) were in the early stage, resulting in incorrect recognition of thickened layers. The other 7 misdiagnosed cases were caused by two reasons which are commonly seen at the start of the disease - difficulty in scanning ulcers on the ileocecal valve and disturbance due to pseudopolyps.

The EUS features of PIL included invisible layer borders, thus layer thickening was impossible to identify; the lesions were diffusely hypoechoic. The lymphoma cells derived from M or SM were always densely packed<sup>[33,34]</sup> and tight with rare stromal cells, making the lesion echo diffusely hypoechoic and homogeneous. We found that several cases just had thickened M (5/30 = 16.7%) or SM (2/30 = 6.7%) with visible layer borders, which were quite different from the majority. These PIL cases were in the early stage, and the stratification had not yet been destroyed.

In the present study, low sensitivity (60.0%) was



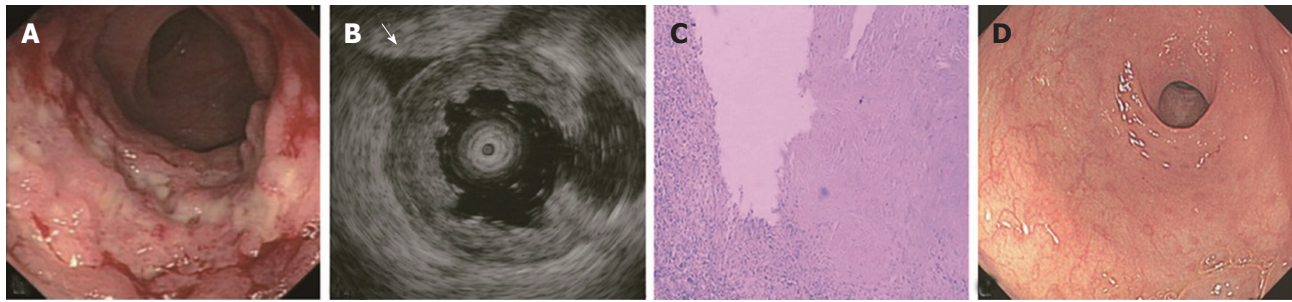


**Figure 4** A 49-year-old male with confirmed intestinal tuberculosis. A: Circular ulcers with a nodular base; B: EUS shows significantly thickened M, thinned obscure SM and extra-luminal fluid sonolucent areas (arrow); C: Biopsy shows caseous necrosis in M; D: Healed M after 4 mo of anti-TB therapy. EUS: Endoscopic ultrasound; M: Mucosa; SM: Submucosa; TB: Tuberculosis.

**Table 4** Special bowel wall signs and extra-luminal presentation of Crohn's disease, primary intestinal lymphoma and intestinal tuberculosis *n* (%)

	CD	PIL	ITB
Special bowel wall signs			
Cobblestone	18 (9.0)	0 (0)	0 (0)
Vasculature in SM	19 (9.5)	0 (0)	0 (0)
≤ 2 mm	11 (5.5)	0 (0)	0 (0)
> 2 mm	8 (4.0)	0 (0)	0 (0)
Extra-luminal presentations			
Abscesses	2 (1.0)	0 (0)	0 (0)
Sinus or fistulae	7 (3.5)	0 (0)	0 (0)
Ascites	7 (3.5)	2 (6.7)	2 (10.0)
Lymph nodes	36 (18.0)	19 (63.3)	5 (25.0)
Single	22 (11.0)	3 (10.0)	4 (20.0)
Multiple	14 (7.0)	16 (53.3)	1 (5.0)
Merged	2 (1.0)	4 (13.3)	0 (0)

CD: Crohn's disease; ITB: Intestinal tuberculosis; PIL: Primary intestinal lymphoma; SM: Submucosa.

observed before adjustment and these early cases were excluded. If a diffusely hypoechoic lesion was the only diagnostic consideration, 9 misdiagnosed PIL cases would have the correct diagnoses, increasing the sensitivity to 90% without a decrease in specificity. On the other hand, echo level in PIL is lower and more homogeneous than in cancer, which is a useful clue for differential diagnosis. We re-diagnosed several previously diagnosed PIL cases as cancer, further improving the specificity with little change in accuracy in the CD and ITB groups. We also followed these two principles (adjustments) in daily practice when faced with the same conditions.

The EUS features of ITB included M thickening, the echo level of M being hyperechoic or a little higher than medium level, and visible layer borders<sup>[35,36]</sup>. ITB is mainly caused by TB bacilli in the swallowed sputum, which likely invade the ileocecum where lymph tissues are located<sup>[37]</sup>. Thus, the M bears the brunt of invasion and subsequent inflammation, and then becomes thickened. In contrast, the SM does not thicken. Some studies have shown that SM is thin or sometimes interrupted due to inflammation and scarring<sup>[38,39]</sup>. This could be a differentiation factor for

CD and other forms of enteritis. However, we observed this sign in only 30% of ITB cases. Furthermore, we also found thinned SM in 3 cases with other diseases (radiation-induced bowel injury, solitary ulcer, ulcers after surgery). Similar to CD, the layer borders of the bowel in ITB were visible, except in the very few cases with severe inflammation. In addition, similar to CD, the S was interrupted in fewer ITB cases, possibly for the same reason. Several cases with non-smooth S were complicated by TB peritonitis.

A sensitivity of 78.3% showed that almost one-fourth of ITB cases were misdiagnosed using the classification method. This may be due to the small number of cases, which provided poor reliability of the summarized EUS features of ITB. Moreover, the possibility of confusion between ITB and common enteritis exists with this method which lacks specificity<sup>[39]</sup>. In total, 15 cases of nonspecific enteritis were misdiagnosed as ITB. Our confidence in diagnosing ITB using EUS in daily practice does not match the high diagnostic accuracy of ITB observed in this study. High diagnostic accuracies for CD and PIL greatly increased the specificity of ITB due to the few cases of ITB (approximately 12% of total cases).

In this study, we created a classification method based on univariate logistic regression analysis and the algorithm reported by Lee *et al.*<sup>[40]</sup> and Mao *et al.*<sup>[41]</sup>. In general, when  $P < 0.05$  is an option, the score increases if OR is  $> 1$  and decreases if OR is  $< 1$ ; when  $P \geq 0.05$ , the score did not change. When a pathological option was not statistically significant ( $P \geq 0.05$ ) but the proportion was greater than 50% and OR  $> 1$  in a disease (*i.e.* echo level 2 in ITB), one point should be added because this option is a clue in distinguishing a pathological state from a normal state, and still showed the tendency to the disease, although it was not powerful enough to differentiate the three diseases. In contrast, the score was zero even when a non-pathological option met the score-raising condition, because the option could not be used to identify whether the state was pathological.

The reasons for some of the rules used in the classification are as follows: (1) The cause of an infinitesimal OR and an unavailable  $P$  value was a zero



**Table 5** Univariate logistic regression analysis of endoscopic ultrasound parameters

Parameters	CD		PIL		ITB		Score		
	OR	P value	OR	P value	OR	P value	CD	PIL	ITB
Layer changed (discrete variable)									
M normal	67.81	< 0.001	0.02	< 0.001	0.04	< 0.001	0	-1	-1
M thickened	0.23	< 0.001	0.85	0.75	18.56	< 0.001	-1	0	1
SM normal	0.22	< 0.001	0.82	0.708	24.75	< 0.001	-1	0	0
SM thickened	92.38	< 0.001	0.02	< 0.001	0.02	< 0.001	1	-1	-1
MP normal	29.87	< 0.001	0.01	< 0.001	0.85	0.804	0	-1	0
S normal	53.08	< 0.001	0.01	< 0.001	0.75	0.668	0	-1	0
Layer disappeared	0.01	< 0.001	141.29	< 0.001	1.45	0.576	-1	1	0
Layer borders (discrete variable)									
M/SM clear	2.62	0.009	0.15	0.003	1.08	0.878	0	-1	0
M/SM unclear	3.55	< 0.001	0.13	< 0.001	0.82	0.668	1	-1	0
M/SM invisible	0.02	< 0.001	99.98	< 0.001	1.33	0.668	-1	1	0
SM/MP clear	8.52	< 0.001	0.03	< 0.001	0.66	0.379	0	-1	0
SM/MP invisible	0.01	< 0.001	141.29	< 0.001	1.45	0.576	-1	1	0
Echo level (discrete variable)									
1 (hyperechoic)	0.87	0.807	In	N/A	3.86	0.03	0	-1	1
2	15.46	< 0.001	In	N/A	0.58	0.253	1	-1	1
3 (medium)	0.18	0.026	6	0.023	1.96	0.541	-1	1	0
4	0.11	1.217	3.47	0.03	0.7	0.74	0	1	0
5 (hypoechoic)	0.03	< 0.001	72.87	< 0.001	0.8	0.775	-1	1	0
Echo homogeneity (discrete variable)									
Homogeneous	0.6	0.115	4.57	< 0.001	0.36	0.058	0	1	0
Heterogeneous	1.69	0.102	0.26	0.003	1.92	0.179	1	-1	1
Diffuse lesion	0.01	< 0.001	470.17	< 0.001	In	N/A	-1	1	-1
Serosa integrity (discrete variable)									
Smooth	9.62	< 0.001	0.08	< 0.001	0.45	0.148	0	-1	0
Non-smooth	0.35	0.055	1.14	0.87	4.98	0.012	0	0	1
Interrupted	0.07	< 0.001	26.62	< 0.001	0.55	0.573	-1	1	0
Lymph nodes (ordinal variable)									
Multiple	0.13	< 0.001	17.36	< 0.001	0.39	0.369	0	1	0
Emerged	0.12	0.015	16.77	0.003	In	N/A	-1	1	-1

The reference category of CD, PIL and ITB was non-CD (PIL & ITB), non-PIL (CD & ITB), and non-ITB (CD & PIL), respectively. The options with statistical insignificance in the three diseases are not given. The right section shows the scores of each option for each disease. CD: Crohn's disease; In: Infinitesimal; ITB: Intestinal tuberculosis; M: Mucosa; MP: Muscularis propria; N/A: Not available; PIL: Primary intestinal lymphoma; S: Serosa; SM: Submucosa.

**Table 6** Tendency scores of endoscopic ultrasound options in Crohn's disease, primary intestinal lymphoma and intestinal tuberculosis

	CD	PIL	ITB
+1	SM thickened M/SM unclear Echo level 2 Heterogeneous Lesion echo	Layer disappeared Echo level 3-5 Homogeneous and diffuse Lesion echo Interrupted S Multiple and emerged lymph nodes	M thickened Echo level 1 and 2 Heterogeneous Echo Non-smooth S
-1	M thickened SM normal Layer disappeared Echo level 3 and 5 Diffuse lesion echo Interrupted S Lymph nodes emerged	M, MP, S normal SM thickened Visible layer borders Echo level 1 and 2 Heterogeneous echo level Smooth S	M normal SM thickened Diffuse lesion Echo Lymph nodes emerged

Data are presented as *n* (%). CD: Crohn's disease; ITB: Intestinal tuberculosis; M: Mucosa; MP: Muscularis propria; PIL: Primary intestinal lymphoma; S: Serosa; SM: Submucosa.

case number, which is a strong clue for ruling out a disease; thus, the score was -1 when this condition was met; (2) The borders disappear with the layer disappearance; therefore, when the parameters "layers changed" and "layer borders" both met the option "disappeared", only one point should be added or

subtracted; (3) Special signs are the specific symbols of a disease. In general, special signs belong to different diseases and would not be seen in an independent case, such as in the three sets. If this occurs, such as an ITB case with a fistula, our classification mode would not be applicable. However, this situation is rare

in clinical practice; and (4) The highest score of < 2 suggests that the EUS pattern is not found in the three diseases. A non-unique highest score indicates a difficult case; thus, the diagnosis would be “other diseases”.

There were limitations to this study. There was an attempt to eliminate interference from the original written reports when dealing with the test set. The images were analyzed without written reports; therefore, it was difficult to determine the location of the lesion and to match the EUS images to white light endoscopic images. However, this problem can be solved easily in clinical practice, and the diagnostic accuracy may be even higher in the real situation.

## ARTICLE HIGHLIGHTS

### Research background

Some gastrointestinal diseases, including Crohn's disease (CD), primary intestinal lymphoma (PIL) and intestinal tuberculosis (ITB), can lead to colorectal ulcers, are difficult to differentiate, and usually require entirely different treatments. Their architecture on resection histology can be easily distinguished at low magnification. Endoscopic ultrasound (EUS) can demonstrate bowel wall structural changes, and identify lesions under the mucosa

### Research motivation

There are few reports available regarding the value of EUS in the differential diagnosis of these three diseases. The authors attempted to explore the EUS diagnostic accuracy of these diseases and to create a new reliable diagnostic method.

### Research objectives

The authors attempted to create an EUS diagnostic classification method which can be used for accurately differentiating CD, PIL, ITB and other colorectal ulcerative diseases.

### Research method

The authors searched the in-patient medical record database for confirmed cases of CD, PIL and ITB from 2008 to 2015 at our center, and collected data on EUS from randomly-chosen patients who formed the training set. All cases found to have colorectal ulcers using EUS were obtained from the endoscopy database and formed the test set. The authors then removed the cases which were easily diagnosed, and the remaining cases formed the perplexing test set. The authors conducted univariate logistic regression analysis on the training set to summarize EUS features of CD, PIL and ITB, and created a diagnostic classification method, rediagnosed the cases in the training set, test set and perplexing set using the classification method, and determined EUS diagnostic accuracies. The authors analyzed the origin of the problems, which were reflected from the diagnostic accuracy, adjusted the classification then repeated the rediagnosing and accuracy-calculating steps, obtaining a result which was closer to the facts.

### Research results

The EUS features of CD, PIL and ITB are different. The diagnostic classification method, as a new statistical method, is reliable in the differential diagnosis of colorectal ulcerative diseases. But, the case numbers of PIL and ITB were too small.

### Research conclusions

EUS is good for differentiating CD, PIL and ITB; An EUS classification system for differentiating CD, PIL and ITB; A new statistical method and an original scoring system.

## Research perspectives

The authors will increase the number of ITB and PIL to obtain a higher reliability of the classification method, and will perform a multicenter study.

## REFERENCES

- 1 **Kiesslich R**, Neurath MF. Advanced endoscopy imaging in inflammatory bowel diseases. *Gastrointest Endosc* 2017; **85**: 496-508 [PMID: 27816496 DOI: 10.1016/j.gie.2016.10.034]
- 2 **Tontini GE**, Wiedbrauck F, Cavallaro F, Koulaouzidis A, Marino R, Pastorelli L, Spina L, McAlindon ME, Leoni P, Vitagliano P, Cadoni S, Rondonotti E, Vecchi M. Small-bowel capsule endoscopy with panoramic view: results of the first multicenter, observational study (with videos). *Gastrointest Endosc* 2017; **85**:401-408 [PMID: 27515129 DOI: 10.1016/j.gie.2016.07.063]
- 3 **Sato S**, Yao K, Yao T, Schlemper RJ, Matsui T, Sakurai T, Iwashita A. Colonoscopy in the diagnosis of intestinal tuberculosis in asymptomatic patients. *Gastrointest Endosc* 2004; **59**: 362-368 [PMID: 27515129 DOI: 10.1016/S0016-5107(03)02716-0]
- 4 **Kucharski M**, Karczewski J, Mańkowska-Wierzbicka D, Karmelita-Katulska K, Kaczmarek E, Iwanik K, Rzymiski P, Grzymislawski M, Linke K, Dobrowolska A. Usefulness of Endoscopic Indices in Determination of Disease Activity in Patients with Crohn's Disease. *Gastroenterol Res Pract* 2016; **2016**: 7896478 [PMID: 26997952 DOI: 10.1155/2016/7896478]
- 5 **Ellrichmann M**, Wietzke-Braun P, Dhar S, Nikolaus S, Arlt A, Bethge J, Kuehbachner T, Wintermeyer L, Balschun K, Klapper W, Schreiber S, Fritscher-Ravens A. Endoscopic ultrasound of the colon for the differentiation of Crohn's disease and ulcerative colitis in comparison with healthy controls. *Aliment Pharmacol Ther* 2014; **39**: 823-833 [PMID: 24612000 DOI: 10.1111/apt.12671]
- 6 **Wu D**, Li JN, Qian JM. Endoscopic Diagnosis and Treatment of Precancerous Colorectal Lesions in Patients with Inflammatory Bowel Disease: How Does the Latest SCENIC International Consensus Intersect with Our Clinical Practice? *J Transl Int Med* 2017; **5**: 4-7 [PMID: 28680833 DOI: 10.1515/jtim-2017-0008]
- 7 **Miu YL**, Ouyang Q, Zhou ZF, Pu P, Chen DY. Histological pathologic study on Crohn's disease and intestinal tuberculosis (in Chinese). *Linchuang Neike Zazhi* 2002; **2**: 109-111
- 8 **Malmström ML**, Săftoiu A, Vilmann P, Klausen TW, Gögenur I. Endoscopic ultrasound for staging of colonic cancer proximal to the rectum: A systematic review and meta-analysis. *Endosc Ultrasound* 2016; **5**: 307-314 [PMID: 27803903 DOI: 10.4103/2303-9027.191610]
- 9 **Ustundag Y**, Fusaroli P. Are rigid probes sufficient to provide reliable data for rectal cancer staging? *Endosc Ultrasound* 2015; **4**: 270 [PMID: 26374591 DOI: 10.4103/2303-9027.163023]
- 10 **Ge N**, Sun S. Endoscopic ultrasound: An all in one technique vibrates virtually around the whole internal medical field. *J Transl Int Med* 2014; **2**:104-106 [DOI: 10.4103/2224-4018.141829]
- 11 **Okasha HH**, Amin M, Ezzat R, El-Nady M, Nagy A. Small bowel intussusception induced by a jejunal gastrointestinal stromal cell tumor diagnosed by endoscopic ultrasound. *Endosc Ultrasound* 2016; **5**: 346-347 [PMID: 27803910 DOI: 10.4103/2303-9027.191683]
- 12 **Bhutani MS**, Annangi S, Koduru P, Aggarwal A, Suzuki R. Diagnosis of cystic lymphangioma of the colon by endoscopic ultrasound: Biopsy is not needed! *Endosc Ultrasound* 2016; **5**: 335-338 [PMID: 27803907 DOI: 10.4103/2303-9027.191668]
- 13 **Leighton D**, Oudjhane K, Ben Mohammed H. The sternoclavicular joint in trauma: retrosternal dislocation versus epiphyseal fracture. *Pediatr Radiol* 1989; **20**: 126-127 [PMID: 2602005 DOI: 10.4103/2303-9027.156748]
- 14 **Makino T**, Kanmura S, Sasaki F, Nasu Y, Funakawa K, Tanaka A, Arima S, Nakazawa J, Taguchi H, Hashimoto S, Numata M, Uto H, Tsubouchi H, Ido A. Preoperative classification of submucosal

- fibrosis in colorectal laterally spreading tumors by endoscopic ultrasonography. *Endosc Int Open* 2015; **3**: E363-E367 [PMID: 26357682 DOI: 10.1055/s-0034-1391782]
- 15 **Gast P.** Endorectal ultrasound in infectious colitis may predict development of chronic colitis. *Endoscopy* 1999; **31**: 265-268 [PMID: 10344433 DOI: 10.1055/s-1999-13680]
- 16 **Seicean A,** Mosteanu O, Seicean R. Maximizing the endosonography: The role of contrast harmonics, elastography and confocal endomicroscopy. *World J Gastroenterol* 2017; **23**: 25-41 [PMID: 28104978 DOI: 10.3748/wjg.v23.i1.25]
- 17 **Roshdy MA,** Marzouk AS. The subgenus Persicargas (Ixodoidea: Argasidae: Argas). 36. structure and postembryonic development of the neurohemal organ in A. (P.) arboreus. *Z Parasitenkd* 1982; **66**: 345-351 [PMID: 7080615 DOI: 10.4103/2303-9027.180482]
- 18 **Mukae M,** Kobayashi K, Sada M, Yokoyama K, Koizumi W, Saegusa M. Diagnostic performance of EUS for evaluating the invasion depth of early colorectal cancers. *Gastrointest Endosc* 2015; **81**: 682-690 [PMID: 25708755 DOI: 10.1016/j.gie.2014.10.027]
- 19 **Thosani N,** Singh H, Kapadia A, Ochi N, Lee JH, Ajani J, Swisher SG, Hofstetter WL, Guha S, Bhutani MS. Diagnostic accuracy of EUS in differentiating mucosal versus submucosal invasion of superficial esophageal cancers: a systematic review and meta-analysis. *Gastrointest Endosc* 2012; **75**: 242-253 [PMID: 22115605 DOI: 10.1016/j.gie.2011.09.016]
- 20 **Choudhary NS,** Puri R, Lipi L, Saraf N. Eosinophilic gastroenteritis mimicking as a malignant gastric ulcer with lymphadenopathy as shown by computed tomography and endoscopic ultrasound. *Endosc Ultrasound* 2015; **4**: 78-79 [PMID: 25789292 DOI: 10.4103/2303-9027.151373]
- 21 **Arya N,** Sahai AV, Paquin SC. Credentialing for endoscopic ultrasound: A proposal for Canadian guidelines. *Endosc Ultrasound* 2016; **5**: 4-7 [PMID: 26879160 DOI: 10.4103/2303-9027.175875]
- 22 **Ratone JP,** Bertrand J, Godat S, Bernard JP, Heyries L. Transrectal drainage of pelvic collections: Experience of a single center. *Endosc Ultrasound* 2016; **5**: 108-110 [PMID: 27080609 DOI: 10.4103/2303-9027.180474]
- 23 **Luz LP,** Cote GA, Al-Haddad MA, McHenry L, LeBlanc JK, Sherman S, Moreira DM, El Hajj II, McGreevy K, DeWitt J. Utility of EUS following endoscopic polypectomy of high-risk rectosigmoid lesions. *Endosc Ultrasound* 2015; **4**: 137-144 [PMID: 26020049 DOI: 10.4103/2303-9027.156744]
- 24 **Sirtori C.** [The biology of gastric cancer]. *Minerva Med* 1970; **61**: 3575-3577 [PMID: 5506412 DOI: 10.1515/jtim-2017-0004]
- 25 **Spradlin NM,** Wise PE, Herline AJ, Muldoon RL, Rosen M, Schwartz DA. A randomized prospective trial of endoscopic ultrasound to guide combination medical and surgical treatment for Crohn's perianal fistulas. *Am J Gastroenterol* 2008; **103**: 2527-2535 [PMID: 18684178 DOI: 10.1111/j.1572-0241.2008.02063.x]
- 26 **Lew RJ,** Ginsberg GG. The role of endoscopic ultrasound in inflammatory bowel disease. *Gastrointest Endosc Clin N Am* 2002; **12**: 561-571 [PMID: 12486944 DOI: 10.1016/S1052-5157(02)00016-8]
- 27 **Wiese DM,** Beaulieu D, Slaughter JC, Horst S, Wagon J, Duley C, Annis K, Nohl A, Herline A, Muldoon R, Geiger T, Wise PE, Schwartz DA. Use of Endoscopic Ultrasound to Guide Adalimumab Treatment in Perianal Crohn's Disease Results in Faster Fistula Healing. *Inflamm Bowel Dis* 2015; **21**: 1594-1599 [PMID: 25985245 DOI: 10.1097/MIB.0000000000000409]
- 28 **Hu PJ,** Qian JM, Wu KC, Ran ZH. Consensus about diagnosis and treatment of inflammatory bowel disease in China. *Neike Lilun Shijian* 2013; **1**: 61-75
- 29 **Dağlı U,** Over H, Tezel A, Ulker A, Temuçin G. Transrectal ultrasound in the diagnosis and management of inflammatory bowel disease. *Endoscopy* 1999; **31**: 152-157 [PMID: 10223365 DOI: 10.1055/s-1999-13664]
- 30 **Gast P,** Belaïche J. Rectal endosonography in inflammatory bowel disease: differential diagnosis and prediction of remission. *Endoscopy* 1999; **31**: 158-166 [PMID: 10223366 DOI: 10.1055/s-1999-13665]
- 31 **Wakefield AJ,** Sankey EA, Dhillon AP, Sawyerr AM, More L, Sim R, Pittilo RM, Rowles PM, Hudson M, Lewis AA. Granulomatous vasculitis in Crohn's disease. *Gastroenterology* 1991; **100**: 1279-1287 [PMID: 2013373 DOI: 10.1016/0016-5085(91)90779-K]
- 32 **Cangir A,** Vietti TJ, Gehan EA, Burgert EO Jr, Thomas P, Tefft M, Nesbit ME, Kissane J, Pritchard D. Ewing's sarcoma metastatic at diagnosis. Results and comparisons of two intergroup Ewing's sarcoma studies. *Cancer* 1990; **66**: 887-893 [PMID: 2201433 DOI: 10.1186/1471-230x-11-113]
- 33 **El-Zahabi LM,** Jamali FR, El-Hajj II, Naja M, Salem Z, Shamseddine A, El-Saghir NS, Zaatari G, Geara F, Soweid AM. The value of EUS in predicting the response of gastric mucosa-associated lymphoid tissue lymphoma to Helicobacter pylori eradication. *Gastrointest Endosc* 2007; **65**: 89-96 [PMID: 17185085 DOI: 10.1016/j.gie.2006.05.009]
- 34 **Schizas D,** Ntanasis-Stathopoulos I, Tsilimigras DI, Sioulas AD, Moris D, Spartalis E, Scotiniotis I, Papanikolaou IS. The Role of Endoscopic Ultrasound in the Diagnosis and Management of Primary Gastric Lymphoma. *Gastroenterol Res Pract* 2017; **2017**: 2397430 [PMID: 28400819 DOI: 10.1155/2017/2397430]
- 35 **Rana SS,** Bhasin DK, Rao C, Srinivasan R, Singh K. Tuberculosis presenting as Dysphagia: clinical, endoscopic, radiological and endosonographic features. *Endosc Ultrasound* 2013; **2**: 92-95 [PMID: 24949371 DOI: 10.4103/2303-9027.117693]
- 36 **Han XM,** Yang JM, Xu LH, Nie LM, Zhao ZS. Endoscopic ultrasonography in esophageal tuberculosis. *Endoscopy* 2008; **40**: 701-702 [PMID: 18680081 DOI: 10.1055/s-2008-1077479]
- 37 **Rathi P,** Gambhire P. Abdominal Tuberculosis. *J Assoc Physicians India* 2016; **64**: 38-47 [PMID: 27730779]
- 38 **Shimizu S,** Tada M, Kawai K. Endoscopic ultrasonography in inflammatory bowel diseases. *Gastrointest Endosc Clin N Am* 1995; **5**: 851-859 [PMID: 8535634]
- 39 **Sharma V,** Rana SS, Chhabra P, Sharma R, Gupta N, Bhasin DK. Primary esophageal tuberculosis mimicking esophageal cancer with vascular involvement. *Endosc Ultrasound* 2016; **5**: 61-62 [PMID: 26879170 DOI: 10.4103/2303-9027.175924]
- 40 **Lee YJ,** Yang SK, Byeon JS, Myung SJ, Chang HS, Hong SS, Kim KJ, Lee GH, Jung HY, Hong WS, Kim JH, Min YI, Chang SJ, Yu CS. Analysis of colonoscopic findings in the differential diagnosis between intestinal tuberculosis and Crohn's disease. *Endoscopy* 2006; **38**: 592-597 [PMID: 16673312 DOI: 10.1055/s-2006-924996]
- 41 **Mao R,** Liao WD, He Y, Ouyang CH, Zhu ZH, Yu C, Long SH, Chen YJ, Li ZP, Wu XP, Lv NH, Hu P, Chen M. Computed tomographic enterography adds value to colonoscopy in differentiating Crohn's disease from intestinal tuberculosis: a potential diagnostic algorithm. *Endoscopy* 2015; **47**: 322-329 [PMID: 25675175 DOI: 10.1055/s-0034-1391230]

**P- Reviewer:** Chamberlain MC, Higuchi K, Okada S

**S- Editor:** Ma Y J **L- Editor:** Filipodia **E- Editor:** Ma YJ



## Clinical Trials Study

# Characteristics of fecal microbial communities in patients with non-anastomotic biliary strictures after liver transplantation

Jing Zhang, Feng-Gang Ren, Peng Liu, Hong-Ke Zhang, Hao-Yang Zhu, Zhe Feng, Xu-Feng Zhang, Bo Wang, Xue-Ming Liu, Xiao-Gang Zhang, Rong-Qian Wu, Yi Lv

Jing Zhang, Feng-Gang Ren, Peng Liu, Hong-Ke Zhang, Hao-Yang Zhu, Zhe Feng, Xu-Feng Zhang, Bo Wang, Xue-Ming Liu, Xiao-Gang Zhang, Yi Lv, Department of Hepatobiliary Surgery, First Affiliated Hospital of Xi'an Jiaotong University, Xi'an 710061, Shaanxi Province, China

Jing Zhang, Feng-Gang Ren, Peng Liu, Hong-Ke Zhang, Hao-Yang Zhu, Zhe Feng, Xu-Feng Zhang, Bo Wang, Xue-Ming Liu, Xiao-Gang Zhang, Rong-Qian Wu, Yi Lv, Institute of Advanced Surgical Technology and Engineering, First Affiliated Hospital of Xi'an Jiaotong University, Xi'an 710061, Shaanxi Province, China

Jing Zhang, Feng-Gang Ren, Peng Liu, Hong-Ke Zhang, Hao-Yang Zhu, Zhe Feng, Xu-Feng Zhang, Bo Wang, Xue-Ming Liu, Xiao-Gang Zhang, Rong-Qian Wu, Yi Lv, Shaanxi Provincial Center for Regenerative Medicine and Surgical Engineering, First Affiliated Hospital of Xi'an Jiaotong University, Xi'an 710061, Shaanxi Province, China

ORCID number: Jing Zhang (0000-0003-2248-5179); Feng-Gang Ren (0000-0002-5799-8516); Peng Liu (0000-0003-2370-7810); Hong-Ke Zhang (0000-0001-6786-2324); Hao-Yang Zhu (0000-0002-2491-0020); Zhe Feng (0000-0001-6360-3261); Xu-Feng Zhang (0000-0002-7908-1645); Bo Wang (0000-0001-5776-2944); Xue-Ming Liu (0000-0002-4489-9439); Xiao-Gang Zhang (0000-0002-6197-703X); Rong-Qian Wu (0000-0003-0993-4531); Yi Lv (0000-0002-7104-2414).

**Author contributions:** Zhang J, Lv Y, Wu RQ, Wang B, Liu XM and Zhang XG designed the study; Zhang J and Feng Z collected the samples; Zhang J, Liu P and Feng Z performed the DNA extraction; Zhang J, Ren FG, Zhu HY, Zhang XF and Lv Y performed the data analysis and interpretation; Zhang J, Ren FG, Liu P and Zhu HY drafted the manuscript; Lv Y and Wu RQ revised the manuscript critically; the funders had no role in study design, data collection and analysis, decision to publish, or preparation of the manuscript.

Supported by the National Natural Science Foundation of

China, No. 81470896.

**Institutional review board statement:** The study was reviewed and approved by The First Affiliated Hospital of Xi'an Jiaotong University Institutional Review Board.

**Informed consent statement:** All participants were totally informed of the related matters prior to entering in and signed the informed consent form.

**Conflict-of-interest statement:** The authors declare no competing financial interests.

**Data sharing statement:** No additional unpublished data are available.

**Open-Access:** This article is an open-access article which was selected by an in-house editor and fully peer-reviewed by external reviewers. It is distributed in accordance with the Creative Commons Attribution Non Commercial (CC BY-NC 4.0) license, which permits others to distribute, remix, adapt, build upon this work non-commercially, and license their derivative works on different terms, provided the original work is properly cited and the use is non-commercial. See: <http://creativecommons.org/licenses/by-nc/4.0/>

Manuscript source: Unsolicited manuscript

**Correspondence to:** Yi Lv, MD, PhD, Professor, Department of Hepatobiliary Surgery, The First Affiliated Hospital of Xi'an Jiaotong University, 277 West Yanta Road, Xi'an 710061, Shaanxi Province, China. [luyi169@126.com](mailto:luyi169@126.com)  
**Telephone:** +86-13991200581  
**Fax:** +86-29-82653903

**Received:** August 2, 2017  
**Peer-review started:** August 5, 2017  
**First decision:** August 30, 2017  
**Revised:** September 13, 2017  
**Accepted:** November 7, 2017  
**Article in press:** November 7, 2017  
**Published online:** December 14, 2017



## Abstract

### AIM

To explore the possible relationship between fecal microbial communities and non-anastomotic stricture (NAS) after liver transplantation (LT).

### METHODS

A total of 30 subjects including 10 patients with NAS, 10 patients with no complications after LT, and 10 non-LT healthy individuals were enrolled. Fecal microbial communities were assessed by the 16S rRNA gene sequencing technology.

### RESULTS

Different from the uncomplicated and healthy groups, unbalanced fecal bacterium ratio existed in patients with NAS after LT. The results showed that NAS patients were associated with a decrease of *Firmicutes* and *Bacteroidetes* and an increase of *Proteobacteria* at the phylum level, with the proportion-ratio imbalance between potential pathogenic families including *Enterococcaceae*, *Streptococcaceae*, *Enterobacteriaceae*, *Pseudomonadaceae* and dominant families including *Bacteroidaceae*.

### CONCLUSION

The compositional shifts of the increase of potential pathogenic bacteria as well as the decrease of dominant bacteria might contribute to the incidence of NAS.

**Key words:** Non-anastomotic stricture; Orthotopic liver transplantation; Fecal microbiota; Dysbacteriosis; Ischemia-reperfusion injury

© The Author(s) 2017. Published by Baishideng Publishing Group Inc. All rights reserved.

**Core tip:** This study is the first attempt to investigate the possible relationship between gut microbiota and post-liver transplantation (LT) biliary complication based on the 16S rRNA sequencing technology. Our results showed unbalanced ratio of pathogenic bacteria to dominant bacteria really existed in patients with non-anastomotic stricture after LT. The shifts of fecal microbial communities may be involved in or exacerbate the process of bile duct injury, which may contribute to the mechanism research and prevention in future.

Zhang J, Ren FG, Liu P, Zhang HK, Zhu HY, Feng Z, Zhang XF, Wang B, Liu XM, Zhang XG, Wu RQ, Lv Y. Characteristics of fecal microbial communities in patients with non-anastomotic biliary strictures after liver transplantation. *World J Gastroenterol* 2017; 23(46): 8217-8226 Available from: URL: <http://www.wjgnet.com/1007-9327/full/v23/i46/8217.htm> DOI: <http://dx.doi.org/10.3748/wjg.v23.i46.8217>

## INTRODUCTION

As Thomas Starzl performed the first human liver transplantation in 1963, orthotopic liver transplantation (OLT) has been regarded as the standard therapy for patients with end-stage liver diseases. In the past three decades, the postoperative complications of OLT decreased markedly due to the improvement of surgical techniques and immunosuppressive treatment<sup>[1,2]</sup>. However, the morbidity of biliary stricture after OLT is still high, ranging from 5% to 20%<sup>[3]</sup>. Non-anastomotic stricture (NAS), also known as ischemic type biliary stricture, is a lethal complication for recipients and severely affects their long-term prognosis<sup>[4]</sup>. Factors including poor liver graft, ABO-incompatibility, cytomegalovirus (CMV) infection may contribute to the development of NAS, and ischemic reperfusion related inflammatory injury is commonly regarded as an inducer of this pathologic process<sup>[5-8]</sup>. But up to date, the definite mechanisms of NAS remain unknown.

Gut microbiota is the general term for all microorganisms (mainly for bacteria) living in the human intestine, with a microbial density larger than  $10^{14}$  cells/g, containing 100 times more genes than human's<sup>[9,10]</sup>. Current studies have titled the gut bacteria as another human organ for its enormous influences on human metabolic activity, barrier function, and immunity development. However, endotoxemia caused by dysbacteriosis was also connected to obesity, diabetes, nonalcoholic fatty liver diseases (NAFLD), and autoimmune disorders<sup>[11,12]</sup>, and even played a key role in ischemic reperfusion injury<sup>[13]</sup>. While for patients who underwent liver transplantation, complex factors like portal vein blocking, ischemic reperfusion injury, antibiotics or immunosuppression use can seriously impair recipient's immune function, destroy the intestinal barrier, and finally increase the risk of dysbacteriosis. These changes of microbiota may directly injury host liver parenchyma through the "gut-liver" axis<sup>[14]</sup>. Actually, the relationship between dysbacteriosis and postoperative complications including acute rejection, early-stage infection, and graft loss is under investigation<sup>[15,16]</sup>. To account for all of these, we hypothesized that quantitative or qualitative alterations of gut microbiota may be involved in or exacerbate graft's ischemic reperfusion injury, which eventually leads to NAS. But so far, the detailed relationship between them has never been explored. Furthermore, whether the changes of gut microbiota contribute to the occurrence of NAS after OLT is still obscure.

In this study, we explored the potential relationship between gut microbiota and NAS by investigating the changes in microbial communities in patients diagnosed with NAS.

## MATERIALS AND METHODS

### Patient enrollment

All subjects in this study came from the First Affiliated Hospital of Xi'an Jiaotong University, with no history of the use of systemic antibiotics or probiotics within previous 3 mo. We excluded patients accompanied by other digestive comorbidities, autoimmune disorders, NAFLD, obesity, or diabetes mellitus, and those who suffered from diarrhea or constipation within 1 mo were not included either. Patients with NAS were defined as suffering from repeated cholangitis, and the magnetic resonance cholangio-pancreatography (MRCP) or endoscopic retrograde cholangio-pancreatography (ERCP) results suggesting multiple strictures located in the donor biliary system with/without anastomotic stricture. To eliminate arterial factors, those accompanied with hepatic artery thrombosis were not included. For patients in an uncomplicated group, they had no obvious complications after OLT, and the regular reexaminations (symptoms, physical examinations, B-ultrasound, CT scan, biochemical tests, and plasma concentration of immunosuppressive drugs) were normal. The healthy controls were those non-LT individuals who came to hospital for a routine health examination, with no digestive diseases or surgical history and their routine tests indexes were in normal ranges. Finally, a total of 30 patients meeting the inclusion criteria were enrolled, including 20 post-LT patients (10 in the NAS group and 10 in the uncomplicated group) and 10 healthy controls.

All participants were totally informed of the related matters prior to entering in and signed the informed consent form. This study was performed in accordance with the ethical guidelines of the 1975 Declaration of Helsinki and was approved by the institutional review board of the First Affiliated Hospital of Xi'an Jiaotong University.

### Surgical procedure

All post-LT patients underwent OLT at the First Affiliated Hospital of Xi'an Jiaotong University. Organ donation or transplantation in this study was strictly implemented under the regulation of the China Organ Donation Committee (CODC), Organ Transplant Committee (OTC), and the Declaration of Helsinki. Recipients were carefully evaluated before operation, while candidates diagnosed with hepatocellular carcinoma (HCC) totally accorded with the Milan criteria<sup>[17]</sup>. Operations were performed with an ABO-compatible liver graft by the same group of doctors. All grafts derived from donors of cardiac death (DCD) and preserved in University of Wisconsin solution at 4 °C before LT. During the operation, graft's common bile duct were bonded to recipient's by means of duct to duct anastomosis, interruptedly suturing for the anterior wall and continuously for the posterior wall with 6-0 absorbable strings. A T-tube was applied

just as necessarily required. After operation, they were given the triple regimen anti-rejection therapy consisting of tacrolimus, mycophenolate mofetil, and methylprednisone.

### Variables evaluated

We documented individual's basic characteristics, including age, gender, body mass index (BMI), current state of smoking or drinking, blood routine test, and liver function indexes within 48 h before sample collecting. For post-LT patients, graft related factors (warm and cold ischemic time) and perioperative characteristics (including Child-Pugh classification, total duration of operation, anhepatic phase, bleeding volume, T-tube inserted or not) were reviewed. The duration from LT to diagnosis and the duration from LT to sample collecting were also respectively recorded.

### Sample collection

All fecal samples were carefully collected to avoid the pollution by urine, accurately weighed, sub-packaged into a 2 mL micro-centrifuge tube (180-200 mg per tube), and immediately stored at -80 °C before analysis. All these stages were finished within 30 min.

### DNA extraction

The fecal DNA was extracted according to the manufacturer's instructions of a testing kit (QIAamp DNA Stool Mini Kit, Qiagen, Valencia, CA, United States). For one aliquot, a little bit of stool was scraped into a 2 mL microcentrifuge tube on ice, and 1.4 mL of buffer ASL (from the QIAamp DNA Stool Mini Kit) was added before the sample thawed. The tube was then vortexed continuously for 1 min until the sample was thoroughly homogenized. After incubation in a water bath for 5 min at 70 °C, the tube was vortexed for 15 s and centrifuged at 2000 *g* for 1 min. The sediment was then discarded, and 1.2 mL of the supernatant was pipetted into a new 2 mL microcentrifuge tube. An inhibitEX tablet (from the kit) was added and vortexed for 1 min until the tablet was completely suspended. After incubation of the suspension for 1 min at room temperature and centrifugation for 3 min, all the supernatant was pipetted into a new 1.5 mL microcentrifuge tube and centrifuged for 3 min. Above 200 µL supernatant was pipetted into a new 1.5 mL microcentrifuge tube which had already contained 15 µL proteinase K. Then, 200 µL of Buffer AL (from the kit) was added, and the tube was vortexed for 15 s and incubated at 70 °C for 10 min. Following the addition of 200 µL of anhydrous ethanol to the lysate, the tube was vortexed thoroughly. Subsequently, the lysate was carefully applied to the QIAamp spin column. After centrifugation for 1 min, the QIAamp spin column was transferred into a new 2 mL collection tube, and the tube containing filtrate was discarded. Then, 500 µL of Buffer AW1 (from the kit) was added. After centrifugation for 1 min and discarding

**Table 1** Characteristics of subjects *n* (%)

	Healthy, ( <i>n</i> = 10)	Post-LT	
		Uncomplicated, ( <i>n</i> = 10)	NAS, ( <i>n</i> = 10)
Age (yr)	38 ± 12	43 ± 11	42 ± 9
Male	9 (90.0)	8 (80.0)	8 (80.0)
BMI (kg/m <sup>2</sup> )	23.3 ± 2.5	22.1 ± 2.6	22.4 ± 2.7
Current smoking	3 (30.0)	2 (10.0)	0
Current drinking	2 (20.0)	0	0
Blood routine test			
HB (g/L)	122.5 ± 12.7	129.0 ± 20.0	127.4 ± 9.0
WBC (×10 <sup>9</sup> )	6.0 ± 1.7	5.1 ± 2.2	5.2 ± 2.5
Neu (%)	59.6 ± 14.8	66.4 ± 16.4	64.3 ± 20.0
Liver function			
AST (U/L)	21.3 (7.9-39.6)	41.0 (13.0-93.0)	57.1 (17.0-107.0) <sup>ac</sup>
ALT (U/L)	20.1 (14.6-34.4)	49.3 (12.0-89.1)	57.3 (18.0-111.0) <sup>ac</sup>
ALP (U/L)	77.3 ± 31.7	93.9 ± 17.2	332.8 ± 52.4 <sup>ac</sup>
GGT (U/L)	27.2 ± 8.2	53.3 ± 35.6	226.4 ± 83.4 <sup>ac</sup>
TB (μmol/L)	13.7 ± 6.7	27.4 ± 17.6	104.43 ± 47.8 <sup>ac</sup>
DB (μmol/L)	5.4 ± 3.1	12.5 ± 8.6	43.8 ± 6.8 <sup>ac</sup>
ALB (g/L)	41.1 ± 2.9	41.9 ± 5.3	34.1 ± 5.0 <sup>ac</sup>

Healthy: Healthy non-LT individuals, *n* = 10; NAS: Patients diagnosed with non-anastomotic biliary strictures after liver transplantation, *n* = 10; Uncomplicated: Patients with no complications after liver transplantation, *n* = 10. Blood routine tests and liver function indexes were obtained within 48 h before sample collecting. Data are presented as mean ± standard deviation, median (range), or percentage where appropriate. <sup>a</sup>*P* < 0.05 *vs* healthy control group; <sup>c</sup>*P* < 0.05 *vs* uncomplicated group. BMI: Body mass index; HGB: Hemoglobin; WBC: White blood cells; Neu%: Neutrophil ratio; AST: Aspartate aminotransferase; ALT: Alanine aminotransferase; ALP: Alkaline phosphatase; GGT: Gamma-glutamyltransferase; ALB: Albumin; TBIL: Total bilirubin; DBIL: Direct bilirubin; LT: Liver transplantation.

the filtrate, 500 μL of Buffer AW2 (from the kit) was added. Following centrifugation for 3 min, the spin column was placed into a new 2 mL collection tube and centrifuged for 1 min. The spin column was transferred into a new 1.5 mL tube, and 200 μL of Buffer AE was pipetted onto the QIAamp membrane. The tube was incubated at room temperature for 1 min and then centrifuged for 1 min to elute DNA. Finally, the filtrate (containing DNA) was stored at -20 °C.

### PCR and sequencing

The DNA isolated from fecal samples was used as the template for the amplification of the 16S rRNA V3-V4 region. The universal primers used were F (5'-NNNNNNN ACTCCTACGGGAGGCAGCA-3') and R (5'-NNNNNNN GGACTACVSGGGTATCTAAT-3'), with the NNNNNNN being unique seven-base barcode used to tag each PCR product. The PCR reaction was performed according to the touchdown protocol<sup>[18]</sup> in a system of 25 μL containing 5.0 μL 5 × reaction buffer (TaKaRa, Dalian, China), 5.0 μL 5 × high GC buffer (TaKaRa, Dalian, China), 0.5 μL dNTPs (10 mmol/L) mixture, 1.0 μL forward primer (10 μmol/L), 1.0 μL reverse primer (10 μmol/L), 0.25 μL Q5 high-fidelity DNA polymerase (5 U/μL, TaKaRa, Dalian, China), and 1 μL DNA template. Each PCR product was purified by 2% agarose gel electrophoresis. DNA was isolated

using the Axygen Axy Prep DNA Gel Extraction kit (Axygen, Shanghai, China). The sequencing was finished with the help of the Illumina Miseq System (Illumina).

### Bioinformatics analysis

The sequencing data of samples were analyzed using pyrosequencing pipeline tools at RDP 10 (<http://pyro.cme.msu.edu/>). Bacterial diversity was determined by sampling-based analysis of operational taxonomic units (OTUs),  $\alpha$ -diversity index (including rarefaction curves, Chao1 index, ACE index, Shannon index, and Simpson index, estimated at a distance of 5%), as well as principal component analysis (PCA). The OTU is an operational definition referring to those closely related individuals, in the system of biological classification, and it is defined based on a similarity threshold to classify microbial species into different taxonomic levels (97% similarity equal to the level of species)<sup>[19,20]</sup>. Species accumulation curve is applied to assess species richness based on the results of species and individual sampling. It can only be compared when the species richness has reached a clear asymptote<sup>[21]</sup>. PCA is mathematically defined as an orthogonal linear transformation which transforms the original data to a new system defined as principal component. Hence, the greatest variance by some projection of the data comes to lie on the corresponding principal component, which makes it easier to investigate the correlation between multiple variables<sup>[22]</sup>.

### Data analysis

Diversity indexes and the species accumulation curve were calculated by QIIME. PCA plots of the bacterial communities were created using *pcaMethods* (Stacklies *et al.*, 2007) in R (R Development Core Team, 2012). Differences of categorical variables among groups were analyzed by Chi-square or Fisher's exact test, and final results are expressed as percentage (%). For continuous variables, ANOVA test was used if data met the normal distribution or Mann-Whitney test if not, with corresponding results expressed as mean ± SD or median (range). Statistical analyses were performed with SPSS version 18.0 (SPSS Inc., Chicago, IL, United States). *P*-values < 0.05 were considered statistically significant.

## RESULTS

### Patient characteristics

As Table 1 shows, patients in the three groups shared the similar age distribution, gender proportion, and BMI (*P* > 0.05 for all). Results of blood routine tests were generally in normal ranges and showed no differences among the groups (*P* > 0.05, Table 1). While for liver function, all median or mean values were obviously abnormal for patients diagnosed with NAS, but no differences existed between the

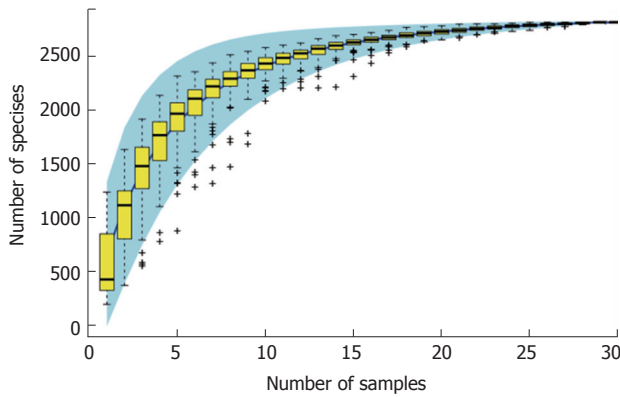


Figure 1 Species accumulation curve.

**Table 2** Operative characteristics of post-liver transplantation patients *n* (%)

	Uncomplicated, ( <i>n</i> = 10)	NAS, ( <i>n</i> = 10)	<i>P</i> value
Primary disease			
HBV cirrhosis	8 (80.0)	8 (80.0)	0.568
HBV SALF	0 (0.0)	1 (10.0)	
HCC	1 (10.0)	1 (10.0)	
DILI	1 (10.0)	0 (0.0)	
Child-Pugh classification			
A	1 (10.0)	1 (10.0)	0.834
B	4 (40.0)	4 (40.0)	
C	5 (50.0)	5 (50.0)	
WIT (min)	7 ± 2	8 ± 0	0.108
CIT (h)	7 ± 1	6 ± 1	0.291
Total operation duration (min)	366 ± 80	377 ± 62	0.893
Anhepatic phase (min)	46 ± 10	49 ± 7	0.513
Bleeding Volume (mL)	1760 ± 347	1311 ± 268	0.329
T-tube insertion	8 (80.00)	7 (70.00)	0.906
Median time from LT to NAS (m)	-	9 (5-13)	-
Median time from LT to SC (m)	15 (6-36)	21 (13-32)	0.129

<sup>a</sup>*P* < 0.05 *vs* healthy control group, <sup>c</sup>*P* < 0.05 *vs* uncomplicated group. SALF: Subacute liver failure; HCC: Hepatocellular carcinoma; DILI: Drug-induced liver injury; WIT: Warm ischemia time; CIT: Cold ischemia time; SC: Sample collecting; LT: Liver transplantation.

uncomplicated and healthy control groups. Notably, for patients with NAS, biliary tract associated indexes like ALP and GGT were elevated as nearly 4 times as healthy controls' (*P* < 0.05), while ALB level was seriously decreased with a mean value of 34.14 g/L (41.1 g/L for healthy and 41.9 g/L for uncomplicated, *P* < 0.05).

For all patients who underwent LT, the main inducers were HBV-related cirrhosis (80.00% *vs* 80.00%, *P* = 0.568, Table 2), and others including subacute liver failure (SALF), hepatocellular carcinoma (HCC), and drug-induced liver injury (DILI) were relatively few in this study. Distributions of preoperative Child-Pugh scores between two groups were similar also, with the percentage of patients having Child-Pugh A or B were 50% *vs* 50% (*P* = 0.834, Table 2). In addition, other factors such as liver grafts' ischemic time, the mean duration of anhepatic

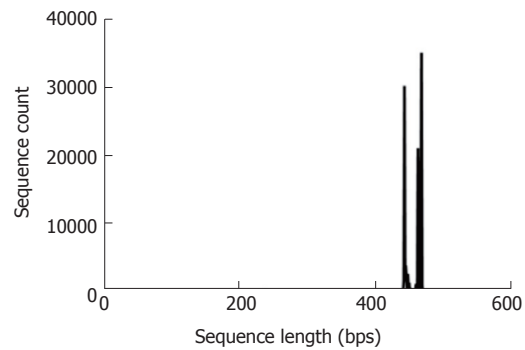


Figure 2 The distribution of sequence length of all patients.

phase, total operation duration, intraoperative bleeding volume, and the proportion of T-tube application were all equally distributed (*P* > 0.05 for all, Table 2). The median duration from LT to final diagnosis of NAS was 9 months, and those from LT to sample collecting in two post-LT groups were 21 and 15 months, respectively (*P* = 0.129).

### DNA sequencing results

According to the sample number and species OTUs, we calculated the species accumulation curve of all participants (Figure 1). In this study, the curve had reached a plateau, and the species had no more obvious increase as the sample number increased, which indicated that the sample volume in our study was relatively large enough to reflect the species richness.

### Microbiota diversity characteristics

To ensure the validity, we excluded those rare OTUs of which the richness was less than 0.001% of the total, and also took a flattening process to eliminate the bias of sequencing depth. Finally, we got a total of 1,494,713 valid sequences, with an average sequence length of 468 bps. For these three groups, the mean valid sequence numbers were 52222, 49947, and 47302, respectively (*P* > 0.05, Figures 2 and 3).

As for the microbial community diversity, the OTUs number at the phylum level in the healthy control group was 969 ± 43, while in the two post-LT groups, the numbers were 443 ± 75 and 568 ± 122, respectively, obviously smaller than that of healthy controls (*P* < 0.05 for both, Table 3). It seemed that there were more OTUs in the NAS group than in the uncomplicated group, but the difference was not significant. Similarly, these manifestations were also applicable to the OTUs distributions at the order/family/genus/species levels (Table 3). Meanwhile, both two post-LT groups showed smaller  $\alpha$ -diversity index (including Chao1, ACE, Simpson, and Shannon indexes) than the healthy controls (*P* < 0.01, Table 4). All of these indicated that patients who underwent LT had a lower gut microbiota diversity (including richness and species number) than healthy controls.



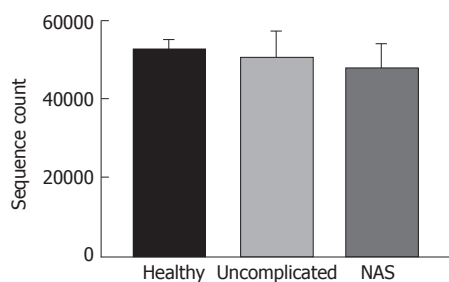


Figure 3 Sequence number in the three groups.

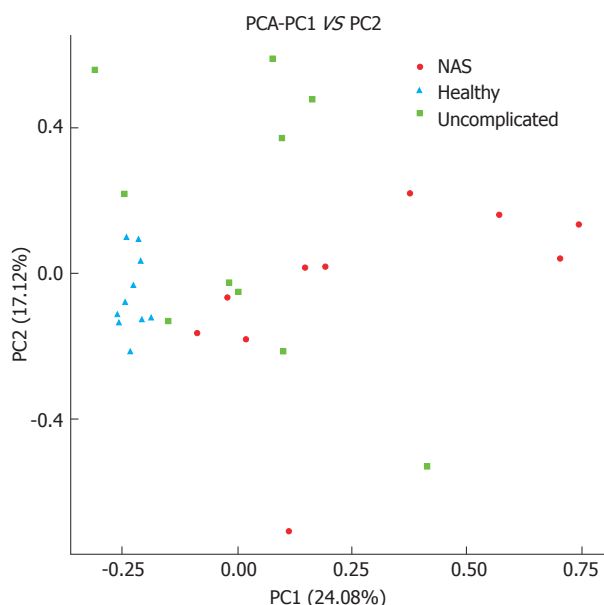


Figure 4 Principal component analysis.

Furthermore, despite no significant differences, gut microbiota of patients with NAS after LT was more diverse than that of the uncomplicated group. We surmise that it was mainly due to the increase of potentially pathogenic bacteria (details will be described later).

About the PCA of different groups, the healthy controls were shown to well aggregate and not overlap with the two post-LT groups. Post-LT individuals of the two groups were partially overlapped, but they still had their own trend to aggregate separately. Therefore, we can still distinguish the NAS cluster from the uncomplicated group (Figure 4). Collectively, we can conclude that the variation among groups was larger than that within groups, and clustering in our study was actually feasible (PC1 = 24.08%, PC2 = 17.12%).

### Distribution of gut bacteria

As shown in Figure 5, gut microbiota in this study was mainly composed of six phyla, including *Firmicutes*, *Bacteroidetes*, *Proteobacteria*, *Actinobacteria*, *Acidobacteria*, and *Verrucomicrobia*. *Firmicutes* and *Bacteroidetes*, as the main bacteria coexisting in human intestine, contributed to 92.32% of the

Table 3 OTUs distribution in the three groups at different levels

	Healthy (n = 10)	Post-LT	
		Uncomplicated (n = 10)	NAS (n = 10)
Phylum	969 ± 43	443 ± 75 <sup>a</sup>	568 ± 122 <sup>a</sup>
Class	969 ± 43	443 ± 75 <sup>a</sup>	568 ± 122 <sup>a</sup>
Order	969 ± 43	443 ± 75 <sup>a</sup>	567 ± 122 <sup>a</sup>
Family	889 ± 37	413 ± 68 <sup>a</sup>	525 ± 110 <sup>a</sup>
Genus	414 ± 14	254 ± 35 <sup>a</sup>	261 ± 44 <sup>a</sup>
Species	129 ± 7	88 ± 9 <sup>a</sup>	81 ± 11 <sup>a</sup>

<sup>a</sup>P < 0.05 vs healthy control group. LT: Liver transplantation.

Table 4 α-diversity indexes in the three groups

	Healthy (n = 10)	Post-LT	
		Uncomplicated (n = 10)	NAS (n = 10)
Chao1 Index	649.30 ± 34.76	269.70 ± 45.09 <sup>a</sup>	303.44 ± 76.86 <sup>a</sup>
ACE	834.03 ± 59.10	346.72 ± 67.73 <sup>a</sup>	413.30 ± 88.68 <sup>a</sup>
Simpson	0.91 ± 0.01	0.81 ± 0.02 <sup>a</sup>	0.75 ± 0.04 <sup>a</sup>
Shannon	5.71 ± 0.26	3.73 ± 0.33 <sup>a</sup>	3.65 ± 0.50 <sup>a</sup>

<sup>a</sup>P < 0.05 vs healthy control group. LT: Liver transplantation.

total microbiota in the healthy control group, while the proportions were 77.11% in the uncomplicated group and 57.40% in the NAS group, which were significantly smaller than that of healthy controls ( $P < 0.05$  for both). Specifically, the change of *Firmicutes* in post-LT patients was mostly due to the decrease of *Lachnospiraceae* and *Ruminococcaceae* at the family level, accompanied by the increase of *Enterococcaceae* and *Streptococcaceae* (all owned to *Bacilli* class, Table 5). Especially for the NAS group, the proportions of the latter two were significantly larger than those in the uncomplicated group (2.60% vs 1.20%, 8.60% vs 3.90%,  $P < 0.05$  for both, Table 5). For *Bacteroidetes*, uncomplicated patients after LT shared the similar proportion to the healthy group ( $P > 0.05$ ). While further analyzing, this phenomenon was caused by the increase of *Bacteroidaceae* and equivalent decrease of *Prevotellaceae* at the family level. However, phylum of *Bacteroidetes* was substantially decreased in the NAS group, with a constituent ratio of only 5.11%, nearly one fifth of that in the healthy group ( $P < 0.05$ , Table 5). The decrease of *Bacteroidaceae* and *Prevotellaceae* at the family level played the inducing role in this change, from the normal 11.60% and 11.60% to 2.70% and 0.70%, respectively ( $P < 0.05$  for both, Table 5). As for the phylum of *Proteobacteria*, it increased obviously in the two post-LT groups, especially for patients with NAS, in whom the proportion of *Proteobacteria* was up to nearly 30 times than that in the healthy group ( $32.44\% \pm 7.32\%$  vs  $1.99\% \pm 0.25\%$ ,  $P < 0.05$ , Figure 5). The proportions of family of *Enterobacteriaceae* in the three groups were 0.70%, 12.80%, and 27.60%, respectively, and those of *Pseudomonadaceae* were 0.00%, 0.00%

**Table 5** Main bacterial families contributing to the changes in microbial community

Phylum	Class	Family	Healthy (n = 10)	Post-LT	
				Uncomplicated (n = 10)	NAS (n = 10)
Bacteroidetes	Bacteroidia	<i>Bacteroidaceae</i>	11.60% ± 5.33%	16.20% ± 3.20%	2.70% ± 0.97% <sup>a,c</sup>
Firmicutes	Bacilli	<i>Prevotellaceae</i>	11.60% ± 4.56%	0.00% ± 0.00% <sup>a</sup>	0.70% ± 0.08% <sup>a</sup>
		<i>Enterococcaceae</i>	0.00% ± 0.00%	1.20% ± 0.45% <sup>a</sup>	2.60% ± 0.87% <sup>a,c</sup>
		<i>Leuconostocaceae</i>	0.00% ± 0.00%	0.70% ± 0.20%	0.40% ± 0.05%
		<i>Streptococcaceae</i>	0.30% ± 0.11%	3.90% ± 1.05% <sup>a</sup>	8.60% ± 4.10% <sup>a,c</sup>
		<i>Lachnospiraceae</i>	21.50% ± 6.78%	9.80% ± 2.45% <sup>a</sup>	10.50% ± 3.44% <sup>a</sup>
Proteobacteria	γ-proteobacteria	<i>Ruminococcaceae</i>	30.90% ± 6.78%	7.00% ± 3.16% <sup>a</sup>	11.20% ± 2.33% <sup>a</sup>
		<i>Enterobacteriaceae</i>	0.70% ± 0.35%	12.80% ± 2.56% <sup>a</sup>	27.60% ± 7.06% <sup>a,c</sup>
		<i>Pseudomonadaceae</i>	0.00% ± 0.00%	0.00% ± 0.00%	5.90% ± 3.16% <sup>a,c</sup>
Verrucomicrobia	Verrucomicrobiae	<i>Verrucomicrobiaceae</i>	0.10% ± 0.09%	0.40% ± 0.16% <sup>a</sup>	0.40% ± 0.05% <sup>a</sup>

<sup>a</sup>*P* < 0.05 vs healthy control group, <sup>c</sup>*P* < 0.05 vs uncomplicated group. LT: Liver transplantation.

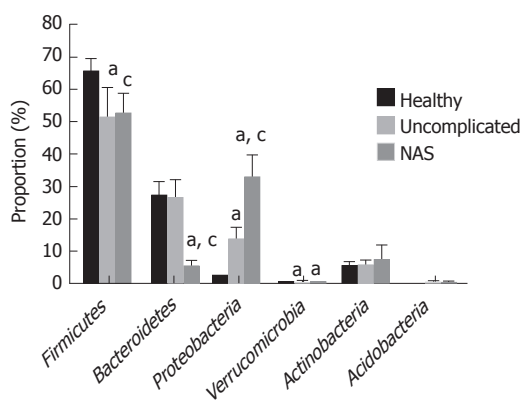


**Figure 5** Distribution of bacteria at different phyla. <sup>a</sup>*P* < 0.05 vs healthy controls group; <sup>c</sup>*P* < 0.05 vs uncomplicated group.

and 5.90%, respectively (*P* < 0.05 for all, Table 4). Similarly, phylum of *Verrucomicrobia* also increased in post-LT patients (*P* < 0.05, Figure 4). Besides these, the proportions of *Actinobacteria* and *Acidobacteria* were relatively balanced, and no significant differences existed among the three groups.

## DISCUSSION

Nowadays, more and more studies have suggested the potential relationship between gut microbiota and liver diseases. Bacterial overgrowth or dysbacteriosis has also been proved to contribute to recipient's post-LT complications<sup>[23]</sup>. In this study, we investigated the fecal microbial communities in patients diagnosed with NAS by pyrosequencing of the 16S rRNA V3-V4 region, taking the well-recovered recipients (uncomplicated) after OLT as negative controls and normal non-LT individuals as healthy controls, to explore the possible relationship between post-LT biliary complications and host's gut microbiota.

According to our results, a structural change of fecal microbial communities was observed in patients who underwent LT, especially for those diagnosed with NAS. As  $\alpha$ -diversity indexes reflected, post-LT patients presented with a significantly lower gut

microbial diversity than healthy individuals, with the decrease of *Firmicutes* and *Bacteroidetes* and increase of *Proteobacteria* and *Verrucomicrobia* at the phylum level. *Firmicutes* and *Bacteroidetes* were intestinal dominant bacteria, playing a key role in maintaining host's intestinal homeostasis. A decrease of these two bacteria always indicated the destruction of intestinal barrier function and increased risk of bacterial translocation<sup>[24]</sup>. In fact, the decrease of these two phyla was partially attributed to the increase of *Proteobacteria* and *Verrucomicrobia*, which usually contributed to a very small portion of human gut microbiota<sup>[25,26]</sup>. Similar changes had also been reported in cirrhotic patients waiting for OLT<sup>[27]</sup>. However, the shifts in our study were more obvious. At the family level, we found that the proportions of *Prevotellaceae*, *Bacteroidaceae*, *Lachnospiraceae*, and *Ruminococcaceae* were lower in post-LT patients, accompanied with an increase of *Enterococcaceae*, *Streptococcaceae*, *Enterobacteriaceae*, and *Pseudomonadaceae*. In previous studies, families of *Lachnospiraceae* and *Ruminococcaceae* were suggested to participate in the metabolism of short-chain fatty acids (SCFAs), while SCFAs have been regarded as a molecular link between the microbiota and inflammation by acting on their specific G protein-coupled receptors 43 (GPR 43). Exogenous supplement of SCFAs can inhibit oxidative stress and inflammatory response induced by high glucose and bacterial endotoxins (LPS)<sup>[28-30]</sup>. Therefore, loss of these potentially beneficial bacteria during the perioperative period may aggravate systemic inflammatory reaction and finally lead to liver injury<sup>[31]</sup>. Meanwhile, families of *Enterococcaceae*, *Streptococcaceae*, *Enterobacteriaceae*, and *Pseudomonadaceae* were commonly regarded as pathogenic bacteria, and their overgrowth has been found to participate in various kinds of human diseases, and even linearly correlated to patient's Child-Pugh score<sup>[27,32-34]</sup>. Moreover, bacterial translocation and elevation of LPS have been estimated in rats with liver ischemia-reperfusion injury or post-LT acute rejection<sup>[35-37]</sup>. Ren *et al.*<sup>[38]</sup> also found that liver ischemic preconditioning can improve intestinal barrier

function and promote the restorations of intestinal microbiota following OLT.

Compared with patients without complications after liver transplantation, patients diagnosed with NAS in our study showed a more significant decrease of *Bacteroidetes* and increase of *Proteobacteria* at the phylum level, with higher proportions of *Enterococcaceae*, *Streptococcaceae*, *Enterobacteriaceae*, and *Pseudomonadaceae*. This dramatic shift in the ratio between phyla or the expansion of *Proteobacteria* is often referred to as dysbacteriosis. Outgrowth of *Enterococcaceae*, *Streptococcaceae*, *Enterobacteriaceae*, and *Pseudomonadaceae* will lead to a large release of LPS and peptidoglycan. When recognized by human immune system via Toll-like receptors (TLRs) or nucleotide-binding oligomerization domain like receptors (NLRs), LPS and peptidoglycan would trigger the pro-inflammatory NF- $\kappa$ B cascade and directly stimulate hepatic stellate cells, which finally contributed to liver damage and liver disease progression<sup>[14,39,40]</sup>. For patients who underwent hepatic inflow occlusion and immunosuppressive treatment during or after OLT, these overgrown pathogenic bacteria may easily penetrate through the intestinal barrier and translocate in the bloodstream, finally aggravating the ischemic reperfusion injury. While bile ducts are susceptible to inflammatory damage, so serious gut dysbacteriosis may exacerbate the cholangiocyte apoptosis and eventually lead to bile duct strictures<sup>[41,42]</sup>. Whereas, the proportions of *Lachnospiraceae* and *Ruminococcaceae* were similar between the NAS group and uncomplicated group, indicating that the overgrowth of the former four pathogenic bacteria contributed more effect to the pathologic process. Nevertheless, the detailed relationship between bacterial shifts and NAS is not clear.

NAS is a serious and progressive complication after OLT. Since graft associated factors are commonly uncontrollable, seeking new breakthrough from recipients themselves is quite important for its prevention. Interestingly, adjustment of microbial structure has been recommended in the treatment of inflammatory bowel disease and metabolic diseases<sup>[43]</sup>. Inhibition of pathogenic bacteria with antibiotics or probiotics has also been proved to improve cirrhosis patient's prognosis, preventing the early-stage infection and acute rejection after OLT<sup>[44-46]</sup>. Therefore, targeted interventions to result in microbial compositional shift in NAS may contribute to its treatment in future.

As we know, this study is the first attempt to investigate the possible relationship between gut microbiota and post-LT biliary complication. With all possible influencing factors including preoperative characteristics and postoperative intervention equally distributed between all subjects, unbalanced ratio between pathogenic bacteria to dominant bacteria existed in patients with non-anastomotic biliary strictures after liver transplantation. This finding might indicate the shifts of fecal microbial communities participate in or exacerbate the process of bile duct injury. However, we

admitted that this is a small-volume study from a single-center experience, and gut microbial changes related to NAS remain obscure. To verify the possible mechanisms, larger-scale, multicenter studies are necessary in the future.

In conclusion, our findings show that fecal microbial composition of patients with non-anastomotic biliary stricture is distinct from that of patients with no complications after orthotopic liver transplantation. These compositional shifts of the increase of potential pathogenic bacteria (e.g., *Enterococcaceae*, *Streptococcaceae*, *Enterobacteriaceae*, and *Pseudomonadaceae*) as well as the decrease of dominant bacteria (e.g., *Bacteroidaceae*) might contribute to the incidence of NAS. However, the underlying mechanism warrants further investigation.

## ARTICLE HIGHLIGHTS

### Research background

Non-anastomotic biliary stricture (NAS) is a lethal disorder after liver transplantation (LT), but the mechanisms are still obscure. Gut microbiota has been shown to participate in the pathogenesis of some post-LT complications, while the characteristics of microbial communities in patients with NAS have never been investigated.

### Research motivation

The purpose of this study was to explore the possible relationship between fecal microbial communities and NAS after OLT.

### Research objectives

To perform possible mechanism research about NAS after LT to shed some light on its prevention in future.

### Research methods

A total of 30 subjects including 10 patients with NAS, 10 patients with no complications after LT, and 10 non-LT healthy individuals were enrolled. Fecal microbial communities were assessed by the 16S rRNA gene sequencing technology. Diversity indexes and the species accumulation curve were calculated by QIIME. PCA plots of the bacterial communities were created using *pcaMethods*. Other data analysis was finished by Chi-square or Fisher's exact test or ANOVA test using SPSS software.

### Research results

Different from the uncomplicated and healthy groups, unbalanced fecal bacterium ratio existed in patients with non-anastomotic biliary strictures after liver transplantation. The results showed that NAS patients were associated with a decrease of *Firmicutes* and *Bacteroidetes* and an increase of *Proteobacteria* at the phylum level, with the proportion-ratio imbalance between potentially pathogenic families including *Enterococcaceae*, *Streptococcaceae*, *Enterobacteriaceae*, and *Pseudomonadaceae* and dominant families including *Bacteroidaceae*.

### Research conclusions

The compositional shifts of the increase of potential pathogenic bacterium as well as the decrease of dominant bacterium might contribute to the incidence of NAS. Gut microbiota may participate in the pathological process of NAS. Factors including poor liver graft, ABO-incompatibility, cytomegalovirus (CMV) infection contribute to the development of NAS.

Dysbacteriosis may be another inducer contributing to the development of NAS. The shifts of fecal microbial communities may participate in or exacerbate the process of bile duct injury. Unbalanced ratio of pathogenic bacteria to dominant bacteria really existed in patients with NAS after liver transplantation.

What are the implications of this? Bacterial intervention may be a new therapy for preventing the occurrence of NAS.

### Research perspectives

According to our study, shifts of fecal microbial communities may participate in or exacerbate the process of bile duct inflammation. This might be helpful for NAS prevention. While the definite relationship was obscure, more mechanism research about how microbiota affects the pathological process should be carried out in the future. To learn more interaction relationship between microbiota and biliary inflammatory injury, technology based on functional genomics may be used for future research.

## REFERENCES

- Federle MP.** Milestones and future trends in solid organ transplantation. *Radiol Clin North Am* 1995; **33**: 417-434 [PMID: 7740103]
- Zitta S, Schaffellner S, Gutschi J, Meinitzer A, Kniepeiss D, Artinger K, Reibnegger G, Rosenkranz AR, Wagner D.** The Effect of Mammalian Target of Rapamycin Versus Calcineurin Inhibitor-based Immunosuppression on Measured Versus Estimated Glomerular Filtration Rate After Orthotopic Liver Transplantation. *Transplantation* 2015; **99**: 1250-1256 [PMID: 25606796 DOI: 10.1097/TP.0000000000000521]
- Gastaca M.** Biliary complications after orthotopic liver transplantation: a review of incidence and risk factors. *Transplant Proc* 2012; **44**: 1545-1549 [PMID: 22841209 DOI: 10.1016/j.transproceed.2012.05.008]
- Seehofer D, Eurich D, Veltzke-Schlieker W, Neuhaus P.** Biliary complications after liver transplantation: old problems and new challenges. *Am J Transplant* 2013; **13**: 253-265 [PMID: 23331505 DOI: 10.1111/ajt.12034]
- Buis CI, Verdonk RC, Van der Jagt EJ, van der Hilst CS, Slooff MJ, Haagsma EB, Porte RJ.** Nonanastomotic biliary strictures after liver transplantation, part I: Radiological features and risk factors for early vs. late presentation. *Liver Transpl* 2007; **13**: 708-718 [PMID: 17457932 DOI: 10.1002/lt.21166]
- Heidenhain C, Pratschke J, Puhl G, Neumann U, Pascher A, Veltzke-Schlieker W, Neuhaus P.** Incidence of and risk factors for ischemic-type biliary lesions following orthotopic liver transplantation. *Transpl Int* 2010; **23**: 14-22 [PMID: 19691661 DOI: 10.1111/j.1432-2277.2009.00947.x]
- Serrano MT, Garcia-Gil A, Arenas J, Ber Y, Cortes L, Valiente C, Araiz JJ.** Outcome of liver transplantation using donors older than 60 years of age. *Clin Transplant* 2010; **24**: 543-549 [PMID: 19925474 DOI: 10.1111/j.1399-0012.2009.01135.x]
- Sundaram V, Jones DT, Shah NH, de Vera ME, Fontes P, Marsh JW, Humar A, Ahmad J.** Posttransplant biliary complications in the pre- and post-model for end-stage liver disease era. *Liver Transpl* 2011; **17**: 428-435 [PMID: 21445926 DOI: 10.1002/lt.22251]
- Ley RE, Turnbaugh PJ, Klein S, Gordon JI.** Microbial ecology: human gut microbes associated with obesity. *Nature* 2006; **444**: 1022-1023 [PMID: 17183309 DOI: 10.1038/4441022a]
- Tremaroli V, Bäckhed F.** Functional interactions between the gut microbiota and host metabolism. *Nature* 2012; **489**: 242-249 [PMID: 22972297 DOI: 10.1038/nature11552]
- Shanahan F, Quigley EM.** Manipulation of the microbiota for treatment of IBS and IBD-challenges and controversies. *Gastroenterology* 2014; **146**: 1554-1563 [PMID: 24486051 DOI: 10.1053/j.gastro.2014.01.050]
- Canli PD.** Metabolism in 2013: The gut microbiota manages host metabolism. *Nat Rev Endocrinol* 2014; **10**: 74-76 [PMID: 24322652 DOI: 10.1038/nrendo.2013.240]
- Wang W, Xu S, Ren Z, Jiang J, Zheng S.** Gut microbiota and allogeneic transplantation. *J Transl Med* 2015; **13**: 275 [PMID: 26298517 DOI: 10.1186/s12967-015-0640-8]
- Chassaing B, Etienne-Mesmin L, Gewirtz AT.** Microbiota-liver axis in hepatic disease. *Hepatology* 2014; **59**: 328-339 [PMID: 23703735 DOI: 10.1002/hep.26494]
- Xie Y, Chen H, Zhu B, Qin N, Chen Y, Li Z, Deng M, Jiang H, Xu X, Yang J, Ruan B, Li L.** Effect of intestinal microbiota alteration on hepatic damage in rats with acute rejection after liver transplantation. *Microb Ecol* 2014; **68**: 871-880 [PMID: 25004996 DOI: 10.1007/s00248-014-0452-z]
- Xie YR, Liu SL, Liu X, Luo ZB, Zhu B, Li ZF, Li LJ, He Y, Jiang L, Li H, Ruan B.** Intestinal microbiota and innate immunity-related gene alteration in cirrhotic rats with liver transplantation. *Transplant Proc* 2011; **43**: 3973-3979 [PMID: 22172882 DOI: 10.1016/j.transproceed.2011.08.113]
- Mazzaferro V, Regalia E, Doci R, Andreola S, Pulvirenti A, Bozzetti F, Montalto F, Ammatuna M, Morabito A, Gennari L.** Liver transplantation for the treatment of small hepatocellular carcinomas in patients with cirrhosis. *N Engl J Med* 1996; **334**: 693-699 [PMID: 8594428 DOI: 10.1056/NEJM199603143341104]
- Muyzer G, de Waal EC, Uitterlinden AG.** Profiling of complex microbial populations by denaturing gradient gel electrophoresis analysis of polymerase chain reaction-amplified genes coding for 16S rRNA. *Appl Environ Microbiol* 1993; **59**: 695-700 [PMID: 7683183]
- Sokal RR.** Principles and Practice of Numerical Taxonomy. *Am J Bot* 1962; **49**: 678.
- Blaxter M, Mann J, Chapman T, Thomas F, Whitton C, Floyd R, Abebe E.** Defining operational taxonomic units using DNA barcode data. *Philos Trans R Soc Lond B Biol Sci* 2005; **360**: 1935-1943 [PMID: 16214751 DOI: 10.1098/rstb.2005.1725]
- Xu G, Zhong X, Wang Y, Xu H.** An approach to detecting species diversity of microfaunas in colonization surveys for marine bioassessment based on rarefaction curves. *Mar Pollut Bull* 2014; **88**: 268-274 [PMID: 25220312 DOI: 10.1016/j.marpolbul.2014.08.032]
- Jolliffe IT, Cadima J.** Principal component analysis: a review and recent developments. *Philos Trans A Math Phys Eng Sci* 2016; **374**: 20150202 [PMID: 26953178 DOI: 10.1098/rsta.2015.0202]
- Doycheva I, Leise MD, Watt KD.** The Intestinal Microbiome and the Liver Transplant Recipient: What We Know and What We Need to Know. *Transplantation* 2016; **100**: 61-68 [PMID: 26647107 DOI: 10.1097/TP.0000000000001008]
- Arumugam M, Raes J, Pelletier E, Le Paslier D, Yamada T, Mende DR, Fernandes GR, Tap J, Bruls T, Batto JM, Bertalan M, Borruel N, Casellas F, Fernandez L, Gautier L, Hansen T, Hattori M, Hayashi T, Kleerebezem M, Kurokawa K, Leclerc M, Levenez F, Manichanh C, Nielsen HB, Nielsen T, Pons N, Poulain J, Qin J, Sicheritz-Ponten T, Tims S, Torrents D, Ugarte E, Zoetendal EG, Wang J, Guarner F, Pedersen O, de Vos WM, Brunak S, Doré J; MetaHIT Consortium, Antolin M, Artiguenave F, Blottiere HM, Almeida M, Brechot C, Cara C, Chervaux C, Cultrone A, Delorme C, Denariac G, Dervyn R, Foerster KU, Friss C, van de Guchte M, Guedon E, Haimet F, Huber W, van Hylckama-Vlieg J, Jamet A, Juste C, Kaci G, Knol J, Lakhdari O, Layec S, Le Roux K, Maguin E, Mérieux A, Melo Minardi R, M'rimini C, Muller J, Oozeer R, Parkhill J, Renault P, Rescigno M, Sanchez N, Sunagawa S, Torrejon A, Turner K, Vandemeulebrouck G, Varela E, Winogradsky Y, Zeller G, Weissenbach J, Ehrlich SD, Bork P.** Enterotypes of the human gut microbiome. *Nature* 2011; **473**: 174-180 [PMID: 21508958 DOI: 10.1038/nature09944]
- Lupp C, Robertson ML, Wickham ME, Sekirov I, Champion OL, Gaynor EC, Finlay BB.** Host-mediated inflammation disrupts the intestinal microbiota and promotes the overgrowth of Enterobacteriaceae. *Cell Host Microbe* 2007; **2**: 204 [PMID: 18030708 DOI: 10.1016/j.chom.2007.08.002]
- Balzan S, de Almeida Quadros C, de Cleva R, Zilberstein B, Ceconello I.** Bacterial translocation: overview of mechanisms and clinical impact. *J Gastroenterol Hepatol* 2007; **22**: 464-471 [PMID: 17376034 DOI: 10.1111/j.1440-1746.2007.04933.x]
- Qin N, Yang F, Li A, Prifti E, Chen Y, Shao L, Guo J, Le Chatelier E, Yao J, Wu L, Zhou J, Ni S, Liu L, Pons N, Batto JM, Kennedy SP, Leonard P, Yuan C, Ding W, Chen Y, Hu X, Zheng B, Qian G, Xu W, Ehrlich SD, Zheng S, Li L.** Alterations of the human gut microbiome in liver cirrhosis. *Nature* 2014; **513**: 59-64 [PMID: 25079328 DOI: 10.1038/nature13568]



- 28 **Huang W**, Guo HL, Deng X, Zhu TT, Xiong JF, Xu YH, Xu Y. Short-Chain Fatty Acids Inhibit Oxidative Stress and Inflammation in Mesangial Cells Induced by High Glucose and Lipopolysaccharide. *Exp Clin Endocrinol Diabetes* 2017; **125**: 98-105 [PMID: 28049222 DOI: 10.1055/s-0042-121493]
- 29 **Lin MY**, de Zoete MR, van Putten JP, Strijbis K. Redirection of Epithelial Immune Responses by Short-Chain Fatty Acids through Inhibition of Histone Deacetylases. *Front Immunol* 2015; **6**: 554 [PMID: 26579129 DOI: 10.3389/fimmu.2015.00554]
- 30 **Kim CH**, Park J, Kim M. Gut microbiota-derived short-chain Fatty acids, T cells, and inflammation. *Immune Netw* 2014; **14**: 277-288 [PMID: 25550694 DOI: 10.4110/in.2014.14.6.277]
- 31 **Duncan SH**, Louis P, Flint HJ. Cultivable bacterial diversity from the human colon. *Lett Appl Microbiol* 2007; **44**: 343-350 [PMID: 17397470 DOI: 10.1111/j.1472-765X.2007.02129.x]
- 32 **Chen Y**, Yang F, Lu H, Wang B, Chen Y, Lei D, Wang Y, Zhu B, Li L. Characterization of fecal microbial communities in patients with liver cirrhosis. *Hepatology* 2011; **54**: 562-572 [PMID: 21574172 DOI: 10.1002/hep.24423]
- 33 **Riordan SM**, Williams R. The intestinal flora and bacterial infection in cirrhosis. *J Hepatol* 2006; **45**: 744-757 [PMID: 16979776 DOI: 10.1016/j.jhep.2006.08.001]
- 34 **Pande C**, Kumar A, Sarin SK. Small-intestinal bacterial overgrowth in cirrhosis is related to the severity of liver disease. *Aliment Pharmacol Ther* 2009; **29**: 1273-1281 [PMID: 19302262 DOI: 10.1111/j.1365-2036.2009.03994.x]
- 35 **Xie Y**, Luo Z, Li Z, Deng M, Liu H, Zhu B, Ruan B, Li L. Structural shifts of fecal microbial communities in rats with acute rejection after liver transplantation. *Microb Ecol* 2012; **64**: 546-554 [PMID: 22430504 DOI: 10.1007/s00248-012-0030-1]
- 36 **Xing HC**, Li LJ, Xu KJ, Shen T, Chen YB, Sheng JF, Yu YS, Chen YG. Intestinal microflora in rats with ischemia/reperfusion liver injury. *J Zhejiang Univ Sci B* 2005; **6**: 14-21 [PMID: 15593386 DOI: 10.1631/jzus.2005.B0014]
- 37 **Wu ZW**, Ling ZX, Lu HF, Zuo J, Sheng JF, Zheng SS, Li LJ. Changes of gut bacteria and immune parameters in liver transplant recipients. *Hepatobiliary Pancreat Dis Int* 2012; **11**: 40-50 [PMID: 22251469 DOI: 10.1016/S1499-3872(11)60124-0]
- 38 **Ren Z**, Cui G, Lu H, Chen X, Jiang J, Liu H, He Y, Ding S, Hu Z, Wang W, Zheng S. Liver ischemic preconditioning (IPC) improves intestinal microbiota following liver transplantation in rats through 16s rDNA-based analysis of microbial structure shift. *PLoS One* 2013; **8**: e75950 [PMID: 24098410 DOI: 10.1371/journal.pone.0075950]
- 39 **Fung TC**, Olson CA, Hsiao EY. Interactions between the microbiota, immune and nervous systems in health and disease. *Nat Neurosci* 2017; **20**: 145-155 [PMID: 28092661 DOI: 10.1038/nn.4476]
- 40 **Seki E**, De Minicis S, Osterreicher CH, Kluwe J, Osawa Y, Brenner DA, Schwabe RF. TLR4 enhances TGF-beta signaling and hepatic fibrosis. *Nat Med* 2007; **13**: 1324-1332 [PMID: 17952090 DOI: 10.1038/nml1663]
- 41 **Imamura H**, Brault A, Huet PM. Effects of extended cold preservation and transplantation on the rat liver microcirculation. *Hepatology* 1997; **25**: 664-671 [PMID: 9049216 DOI: 10.1002/hep.510250329]
- 42 **Moench C**, Moench K, Lohse AW, Thies J, Otto G. Prevention of ischemic-type biliary lesions by arterial back-table pressure perfusion. *Liver Transpl* 2003; **9**: 285-289 [PMID: 12619026 DOI: 10.1053/jlts.2003.50015]
- 43 **Yuan F**, Ni H, Asche CV, Kim M, Walayat S, Ren J. Efficacy of Bifidobacterium infantis 35624 in patients with irritable bowel syndrome: a meta-analysis. *Curr Med Res Opin* 2017; **33**: 1191-1197 [PMID: 28166427 DOI: 10.1080/03007795.2017.1292230]
- 44 **Liu Q**, Duan ZP, Ha DK, Bengmark S, Kurtovic J, Riordan SM. Synbiotic modulation of gut flora: effect on minimal hepatic encephalopathy in patients with cirrhosis. *Hepatology* 2004; **39**: 1441-1449 [PMID: 15122774 DOI: 10.1002/hep.20194]
- 45 **Safdar N**, Said A, Lucey MR. The role of selective digestive decontamination for reducing infection in patients undergoing liver transplantation: a systematic review and meta-analysis. *Liver Transpl* 2004; **10**: 817-827 [PMID: 15237363 DOI: 10.1002/lt.20108]
- 46 **Rayes N**, Seehofer D, Theruvath T, Schiller RA, Langrehr JM, Jonas S, Bengmark S, Neuhaus P. Supply of pre- and probiotics reduces bacterial infection rates after liver transplantation--a randomized, double-blind trial. *Am J Transplant* 2005; **5**: 125-130 [PMID: 15636620 DOI: 10.1111/j.1600-6143.2004.00649.x]

**P- Reviewer:** Kang KJ, Pompili M, Tsoulfas G **S- Editor:** Gong ZM  
**L- Editor:** Wang TQ **E- Editor:** Ma YJ



## Observational Study

# Balloon dilatation for treatment of hepatic venous outflow obstruction following pediatric liver transplantation

Zhi-Yuan Zhang, Long Jin, Guang Chen, Tian-Hao Su, Zhi-Jun Zhu, Li-Ying Sun, Zhen-Chang Wang, Guo-Wen Xiao

Zhi-Yuan Zhang, Long Jin, Guang Chen, Tian-Hao Su, Guo-Wen Xiao, Department of Interventional Radiology, Beijing Friendship Hospital, Capital Medical University, Beijing 100050, China

Zhi-Jun Zhu, Li-Ying Sun, Department of Transplantation Surgery, Beijing Friendship Hospital, Capital Medical University, Beijing 100050, China

Zhen-Chang Wang, Department of Radiology, Beijing Friendship Hospital, Capital Medical University, Beijing 100050, China

ORCID number: Zhi-Yuan Zhang (0000-0001-9947-9709); Long Jin (0000-0002-4742-6688); Guang Chen (0000-0003-1274-1677); Tian-Hao Su (0000-0002-5834-3669); Zhi-Jun Zhu (0000-0001-5719-5396); Li-Ying Sun (0000-0003-1101-7994); Zhen-Chang Wang (0000-0002-6748-0294); Guo-Wen Xiao (0000-0002-3679-8400).

**Author contributions:** Zhang ZY and Jin L contributed equally to this work; Zhang ZY, Jin L and Wang ZC designed the research; Zhang ZY, Jin L, Chen G, Su TH, Zhu ZJ, Sun LY and Xiao GW performed the research; Zhang ZY and Jin L analyzed the data; Zhang ZY and Jin L wrote the paper.

**Institutional review board statement:** This study was reviewed and approved by the Clinical Research Ethics Committee of the Affiliated Beijing Friendship Hospital of Capital Medical University.

**Informed consent statement:** Informed consent was not required for the study as the analysis used anonymous clinical data. Individuals cannot be identified based on the data presented.

**Conflict-of-interest statement:** The authors declare no conflicts of interests.

**Data sharing statement:** No additional data are available.

**Open-Access:** This article is an open-access article which was selected by an in-house editor and fully peer-reviewed by external reviewers. It is distributed in accordance with the Creative

Commons Attribution Non Commercial (CC BY-NC 4.0) license, which permits others to distribute, remix, adapt, build upon this work non-commercially, and license their derivative works on different terms, provided the original work is properly cited and the use is non-commercial. See: <http://creativecommons.org/licenses/by-nc/4.0/>

**Manuscript source:** Unsolicited manuscript

**Correspondence to:** Long Jin, MD, PhD, Chief Doctor, Professor, Department of Interventional Radiology, Beijing Friendship Hospital, Capital Medical University, No. 95, Yong'an Road, Xicheng District, Beijing 100050, China. [zhangzy@mail.ccmu.edu.cn](mailto:zhangzy@mail.ccmu.edu.cn).  
**Telephone:** +86-10-63138454  
**Fax:** +86-10-63138454

**Received:** October 20, 2017

**Peer-review started:** October 23, 2017

**First decision:** October 31, 2017

**Revised:** November 10, 2017

**Accepted:** November 22, 2017

**Article in press:** November 22, 2017

**Published online:** December 14, 2017

## Abstract

### AIM

To assess the efficacy and safety of balloon dilatation for the treatment of hepatic venous outflow obstruction (HVOO) following pediatric liver transplantation.

### METHODS

A total of 246 pediatric patients underwent liver transplantation at our hospital between June 2013 and September 2016. Among these patients, five were ultimately diagnosed with HVOO. Seven procedures (two patients underwent two balloon dilatation procedures) were included in this analysis. The demographic data,

types of donor and liver transplant, interventional examination and therapeutic outcomes of these five children were analyzed. The median interval time between pediatric liver transplantation and balloon dilatation procedures was 9.8 mo (range: 1-32).

## RESULTS

Five children with HVOO were successfully treated by balloon angioplasty without stent placement, with seven procedures performed for six stenotic lesions. All children underwent successful percutaneous intervention. Among these five patients, four were treated by single balloon angioplasty, and these patients did not develop recurrent stenosis. In seven episodes of balloon angioplasty across the stenosis, the pressure gradient was  $12.0 \pm 8.8$  mmHg before balloon dilatation and  $1.1 \pm 1.5$  mmHg after the procedures, which revealed a statistically significant reduction ( $P < 0.05$ ). The overall technical success rate among these seven procedures was 100% (7/7), and clinical success was achieved in all five patients (100%). The patients were followed for 4-33 mo (median: 15 mo). No significant procedural complications or procedure-related deaths occurred.

## CONCLUSION

Balloon dilatation is an effective and safe therapeutic option for HVOO in children undergoing pediatric liver transplantation. Venous angioplasty is also recommended in cases with recurrent HVOO.

**Key words:** Hepatic venous outflow obstruction; Pediatric liver transplantation; Percutaneous transluminal balloon dilatation; Pressure gradient; Recurrent

© **The Author(s) 2017.** Published by Baishideng Publishing Group Inc. All rights reserved.

**Core tip:** Hepatic venous outflow obstruction (HVOO) is a rare and severe complication following pediatric liver transplantation that leads to graft loss in the majority of patients. However, it remains controversial whether stent placement or balloon angioplasty is required for patients with HVOO. This study reported our experiences with using balloon dilatation as part of the treatment for HVOO in five children subjected to pediatric liver transplantation, providing valuable information for the successful treatment of such patients. Balloon dilatation is an effective and safe treatment for HVOO in pediatric patients following liver transplantation, and re-venoplasty is recommended even for patients with recurrent HVOO.

Zhang ZY, Jin L, Chen G, Su TH, Zhu ZJ, Sun LY, Wang ZC, Xiao GW. Balloon dilatation for treatment of hepatic venous outflow obstruction following pediatric liver transplantation. *World J Gastroenterol* 2017; 23(46): 8227-8234 Available from: URL: <http://www.wjgnet.com/1007-9327/full/v23/i46/8227.htm> DOI: <http://dx.doi.org/10.3748/wjg.v23.i46.8227>

## INTRODUCTION

Liver transplantation is the most effective treatment for end-stage liver disease. In recent years, significant progress has been achieved in surgical techniques, immunosuppressants and operative care, which has led to the optimization of post-transplant outcomes<sup>[1]</sup>. In an attempt to solve the shortage of donor organs and diminish the high mortality rate after re-transplantation, efforts have been made to develop liver transplantation techniques with reduced-size, split and living donor organs<sup>[2]</sup>. Nevertheless, vascular complications are still the most significant determinant factor for graft loss, especially for those undergoing partial liver transplantation with living donor grafts, during which the use of short vascular pedicles complicates the surgical procedure. In particular, hepatic venous outflow obstruction (HVOO) is a profound complication of pediatric liver transplantation; it has a high incidence (4%-9%) owing to the smaller anastomosis diameter and size mismatch of the hepatic vessels between the donor and recipient<sup>[3]</sup>. The treatments for HVOO in children after liver transplantation include surgical reconstruction, re-transplantation and endovascular angioplasty<sup>[4]</sup>. Endovascular angioplasty, either *via* balloon angioplasty or stent placement, is a less-invasive therapeutic option compared with surgical approaches for relieving HVOO and has become the first-line treatment of choice in pediatric transplant recipients<sup>[3,5]</sup>. However, it remains unclear whether stent placement or balloon angioplasty is required for patients with HVOO.

Therefore, this retrospective study was performed to evaluate data from pediatric patients undergoing endovascular angioplasty for HVOO after liver transplantation at our hospital from June 2013 to September 2016. This paper presents our successful treatment of HVOO in a series of five children using balloon angioplasty.

## MATERIALS AND METHODS

### Patients

Between June 2013 and September 2016, a total of 246 pediatric patients (< 18 years old) underwent liver transplantation at our hospital, including 149 living-donor and 97 deceased-donor transplants. Among these patients, five consecutive patients (four transplanted at our hospital and one transplanted at another hospital) underwent venography and manometric measurements due to suspicion of HVOO. Patients were suspected of having HVOO when they showed typical clinical signs or symptoms, including ascites, pleural effusion, or hepatomegaly. Enhanced computed tomography (CT) and/or Doppler ultrasound (US) were used to further detect hepatic venous outflow abnormalities. Abnormal Doppler US images included an undetectable flow signal, a persistent monophasic waveform, a slow flow of < 10 cm/s, or a reversed flow

**Table 1** Demographic data of the five pediatric patients

Case No.	Gender	Age	Original disease	Type of transplant	Graft type	Onset after transplantation (mo)
1	F	10 mo	Biliary atresia	LDLT	Left lateral lobe	4
2	F	3 yr	Biliary atresia	LDLT	Left lateral lobe	32
3	F	9 yr	OTCD	Cross-auxiliary double-domino donor liver transplantation	Right lobe	1
4	M	7 mo	Biliary atresia	LDLT	Left lateral lobe	9
5	F	10 mo	Biliary atresia	LDLT	Left lateral lobe	3

LDLT: Living-donor liver transplantation; OTCD: Ornithine transcarbamylase deficiency.

direction. Patients highly suspected of hepatic venous outflow abnormalities through Doppler US examination were subjected to a CT scan. The hepatic venous outflow abnormality was confirmed when the CT scan revealed non-opacification of the hepatic veins, greater than 70% focal luminal narrowing relative to the adjacent normal hepatic vessel in diameter, or a geographic area of low attenuation in the liver, along with clinical symptoms of hepatic congestion (ascites, pleural effusion, elevated liver enzymes, or abnormal findings) on the immediate postoperative Doppler US examination<sup>[3]</sup>. The hepatic venous outflow abnormality was further diagnosed by hepatic venography and through pressure measurements in the hepatic vein, inferior vena cava (IVC) and right atrium. Significant hepatic venous outflow stenosis was defined as a pressure gradient > 3 mmHg.

All five patients with hepatic venous outflow abnormalities underwent endovascular angioplasty. The median length of the period from the liver transplantation to the initial procedure was 9.8 mo (range: 1-32 mo). The baseline characteristics of these patients are summarized in Table 1.

### Procedures

Each patient or their legal guardian provided written informed consent. The present study was approved by our Institutional Ethics Committee (No. 2017-P2-029-01).

Three authors (Jin L, Chen G, and Su TH., with 22, 21 and 10 years of experience in interventional radiology, respectively) performed these procedures. Percutaneous interventions were performed under general anesthesia in all patients ( $n = 5$ ). Selective hepatic venography and balloon angioplasty were performed *via* the right internal jugular vein. A 0.035-inch hydrophilic guide wire (Terumo, Tokyo, Japan) and 5F cobra catheter (Cook, Bloomington, Indiana) were used to gain entry into the hepatic vein. After hepatic venography, the anastomotic pressure gradient was obtained. After the catheter passed through the desired site, the narrow pressure gradient (right atrium and left hepatic vein) was calculated by recording the intravenous pressure on both sides of the narrowing. Patients with a pressure gradient of > 3 mmHg were considered to have a significant outflow obstruction and were candidates for venoplasty,

in which a percutaneous transluminal angioplasty catheter (Powerflex Plus, Cordis) with a 6- to 8-mm-diameter and 20- to 40-mm-long balloon was utilized. The selection of the balloon was based on the contrast-enhanced CT and venography findings and was matched in size to the vein on the hepatic side of the stenosis. The balloon was laid across the stenosis and was inflated to widen the vein for 60 s at a pressure of 10 atm. Balloon dilation was performed three times, and the effectiveness of the venoplasty was examined by repeated venography and manometric measurements. Hemostasis was achieved by manual compression, without transhepatic track embolization. Patients did not receive heparinization during the whole procedure. Hence, the international normalized ratio was maintained between 1.5-2.0.

### Follow-up

The patients' vital signs were monitored in the intensive care unit or general ward every 4-8 h. US was performed one day after the procedure to examine the hepatic venous outflow and to detect post-procedural complications. CT was performed in selected patients within 1 wk after the procedure, according to the physician's need to investigate the hepatic vein and extrahepatic variceal flow and determine any post-procedural complications. Doppler US was performed bimonthly on an outpatient basis, and venography and manometry were performed when recurrent HVOO was suspected.

The following data were retrospectively collected: technical and clinical success, pre- and post-operative pressure gradients across the stenosis, major complications, and patency of the hepatic venous outflow. Technical success was defined as the achievement of a pressure gradient across a stenosis of < 3 mmHg on postprocedural manometry, or a stenosis of < 30% on postprocedural venography. Clinical success was defined as ameliorated signs and symptoms of HVOO, and an improvement in the preprocedural status evaluated by Doppler US<sup>[6]</sup>. The definition of a major complication was an event that required extended hospitalization or an advanced level of care<sup>[7]</sup>.

### Statistical analysis

Changes between pre- and post-procedural pressure gradients across the hepatic vein stenosis were



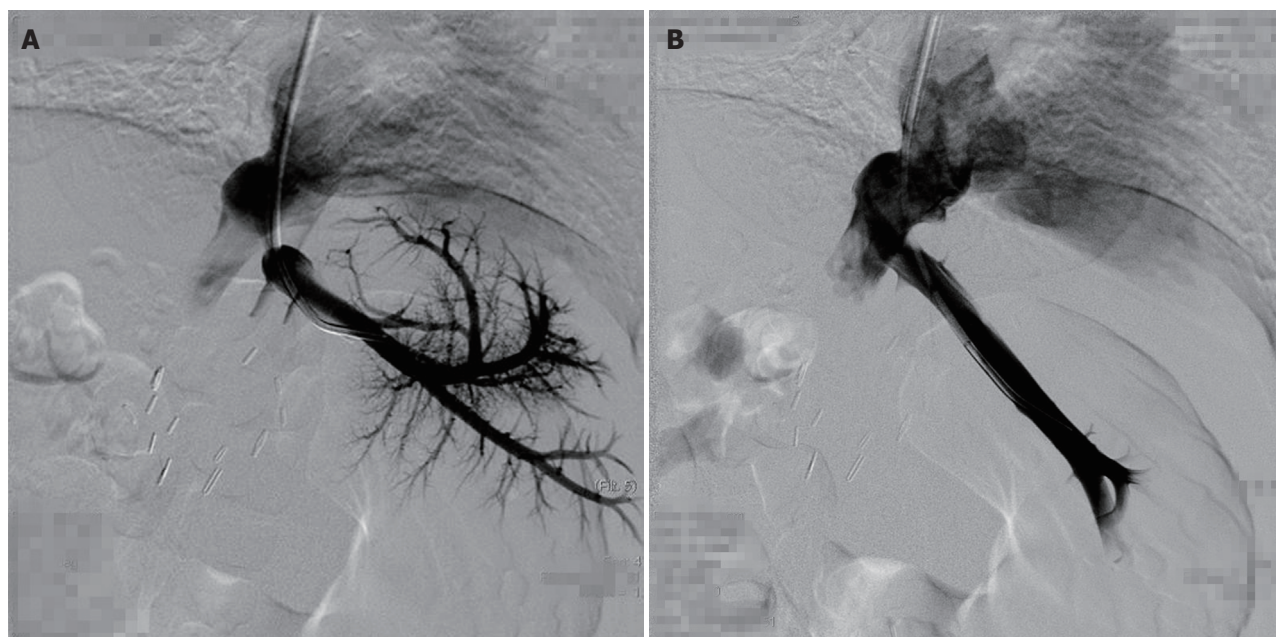


**Figure 1** Left lobe graft for biliary atresia in a 2-year-old boy. A: Hepatic venography shows severe blockage of the hepatic venous outflow. The pressure gradient between the right atrium and left vein was 13 mmHg. B: Hepatic venography after percutaneous transluminal venoplasty shows improved flow into the right atrium. The pressure gradient decreased to 3 mmHg.

**Table 2** Clinical outcomes following balloon dilatation

Case No.	Vessel	Procedure	Size	Pre-pressure (mmHg)	Post-pressure (mmHg)	Follow-up (mo)
1	HV	PTA	6 mm-4 cm	34/8	13/9	16
2	HV	PTA	8 mm-4 cm	29/7	18/18	16
3	RHV	PTA	8 mm-4 cm	17/10	10/10	1, recurrence
	RHV	PTA	8 mm-4 cm	22/14	15/15	10
4	HV	PTA	8 mm-4 cm	30/17	22/19	33
5	HV	PTA	6 mm-2 cm	17/13	17/15	4
	IVC	PTA	6 mm-2 cm	17/13	14/14	4

HV: Hepatic vein; RHV: Right hepatic vein; IVC: Inferior vena cava; PTA: Percutaneous transluminal angioplasty.

analyzed by paired Student's *t*-test. The analyses were performed using SPSS 21.0 statistical software (IBM, Chicago, IL, United States). A *P*-value < 0.05 was considered statistically significant.

## RESULTS

Four liver transplant recipients (one male and three females; age range: seven months to three years old) and one crossed-auxiliary double-domino donor liver transplantation patient (female, nine years old) were diagnosed with HVOO following liver transplantation in the present study (Table 1). The preliminary diagnosis of HVOO was initially assessed by Doppler US and confirmed by subsequent abdominal CT angiography and venography in all five patients. The hepatic vein stenosis rate was 1.62%. The onset of hepatic vein stenosis ranged from 1-32 mo (mean: 9.80 mo) after liver transplantation.

A total of seven procedures were performed for six stenotic lesions in five patients (there were two

anastomoses in one patient, Table 2). The overall technical success rate among these seven procedures was 100% (7/7). A patient with HVOO underwent a balloon angioplasty procedure twice at 15 d after liver transplantation and at one month after liver transplantation due to recurrence. The pressure gradient across the stenotic lesions at the anastomoses ( $n = 7$ ) was  $12.0 \pm 8.8$  mmHg (range: 4-26 mmHg) before balloon dilatation, and this value decreased significantly to  $1.1 \pm 1.5$  mmHg (range: 0-3 mmHg) immediately after the procedure ( $P < 0.05$ ).

Clinical success was achieved in all five patients (100%), as manifested by improved ascites and pleural effusion.

The patients were followed for 4-33 mo (median: 15 mo). The outcomes are shown in Table 2. Among these five patients, four patients were treated by single balloon angioplasty (Figures 1 and 2), and these patients did not develop recurrent stenosis. The patient who underwent two sessions of balloon angioplasty showed no recurrent HVOO for 10 mo during the

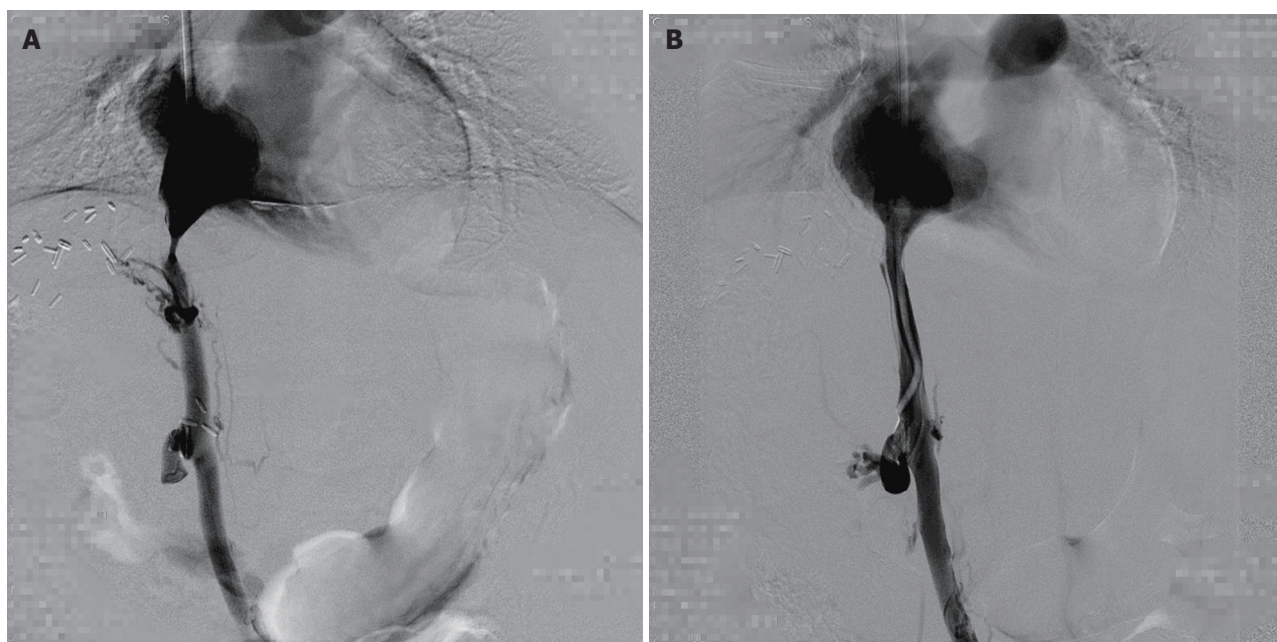


**Figure 2** Left lobe graft for biliary atresia in a 10-month-old girl. A: The inferior vena cava (IVC) image shows tight fibrotic stenosis at the superior anastomosis close to the right atrium. B: The IVC angiogram after angioplasty with a 6-20 mm balloon shows stricture resolution, no residual stenosis and free flow through the IVC into the right atrium.



**Figure 3** A 9-year-old male received cross-auxiliary double-domino donor liver transplantation. One month after the initial procedure, stenosis recurred. A: Hepatic venography shows a stricture at the piggyback hepatic vein anastomosis. B: Hepatic vein angiography after balloon dilatation shows the disappearance of the stricture and free flow through the anastomosis.

subsequent follow-up period (Figure 3). Furthermore, no major procedural complications during any of the seven balloon angioplasty procedures, procedure-related deaths or permanent adverse sequelae occurred.

## DISCUSSION

Few cases of HVOO have been reported in pediatric patients following liver transplantation; there have been fewer than ten cases within the past five years.



This study reported our experiences with using balloon dilatation as part of the treatment for HVOO in five children who underwent pediatric liver transplantation, providing valuable reference for the successful treatment of such patients.

HVOO is an infrequent but life-threatening complication following liver transplantation<sup>[8]</sup>. Living-donor or auxiliary liver transplantation has been accepted as an effective method to expand the pool of organ donors. At present, technical challenges remain, including HVOO<sup>[8,9]</sup>. In the present study, four cases who underwent transplantation at our hospital and one patient who underwent transplantation at another hospital were diagnosed with HVOO. In our center, the incidence of HVOO was 1.62% (4/246), which was lower than the incidences reported at other centers<sup>[10-12]</sup>. It has been reported that with the evolution and improvement of surgical techniques, the overall incidence of long-term hepatic vein stenosis has significantly decreased between the eras of 1988 to 1994 and 1995 to 2002<sup>[2]</sup>. In the present study, the time to onset of hepatic vein stenosis was 0.5-32 mo (mean: 9.70 mo) after liver transplantation, which was consistent with other studies<sup>[10-12]</sup>.

At our institution, patients with clinical signs and symptoms of HVOO routinely underwent some forms of noninvasive imaging. Color Doppler US was the most frequently used imaging technique in the present study, providing information on flow direction and velocity. Its results can be made immediately available without the use of ionizing radiation, and it can be conveniently performed at the bedside. Magnetic resonance (MR) venography and CT are excellent alternatives but require scanner availability and sedation in the pediatric population<sup>[13]</sup>. Although noninvasive evaluation can aid diagnosis, IVC venography with direct pressure gradient measurement across the suspected lesion is the gold standard for HVOO diagnosis<sup>[4]</sup>. In our cases, color Doppler US and enhanced CT findings were supported by the results of venography.

The quantification of the pressure gradient across the stenosis may help verify the significance of the lesion. At present, conflicting opinions exist for the deterministic diagnosis of HVOO through a pressure gradient across the stenotic region between the right atrium and hepatic vein of  $> 3$  mmHg or  $> 5$  mmHg. We recommend the consideration of the diagnosis of HVOO in pediatric recipients with clinical presentations of HVOO, even if their pressure gradients between the right atrium and hepatic vein are  $< 3$  mmHg. A pressure gradient that can sufficiently lead to clinical HVOO may be misleadingly reduced when the patient is ambulatory or lying in the supine position during an operation, leading to a missed or faulty diagnosis. In addition, pressure gradients are typically measured in children under general anesthesia, which affects hepatic and portal vein flow velocities, resulting in the misdiagnosis of HVOO<sup>[11]</sup>. In the present study, we recommend measuring the pressure gradient repeatedly

at the same location and as far as possible from the vessel wall. In addition, a diagnostic standard of  $> 3$  mmHg for the pressure gradient is recommended.

At present, endovascular treatment, including percutaneous balloon angioplasty and stent placement, is the preferred treatment for HVOO after liver transplantation<sup>[14]</sup>. However, it remains unclear whether balloon angioplasty or stent placement is preferable<sup>[10,11,15]</sup>. Kubo *et al.*<sup>[16]</sup> performed endovascular treatments in 20 patients with HVOO after liver transplantation. A technically successful balloon venoplasty procedure was initially achieved in all cases. However, 11 (55%) patients had recurrent obstruction, which is suggestive of a high rate of reintervention. Most patients ( $n = 10$ ) were treated by balloon angioplasty, and one patient was rescued by stent placement. The patency rate of the hepatic venous outflow was 1.00 during a follow-up period of 60 mo. Another study reported 10 pediatric patients with HVOO who were treated with stents; after 42 months of follow-up, all stent lumens remained patent. Moreover, the retained stents did not cause profound adverse effects that were harmful to the growth of blood vessels<sup>[12]</sup>. Ko *et al.*<sup>[17]</sup> performed primary stent placement for early post-transplant HVOO and achieved favorable long-term patency. Overall, the 1-, 3- and 5-year primary patency rates were 82.3%, 75.0% and 72.4%, respectively.

However, many centers hesitate to perform stent placement in children for several reasons<sup>[18]</sup>. First, stents are prone to the development of neointimal hyperplasia, leading to recurrent stenosis. Second, a stenotic lesion would be developed when the child matures, since the stent placed has a fixed diameter. Third, the location of the internal stent in children is technically problematic if re-transplantation is required. Finally, the long-term patency of stents remains unknown. The present study demonstrated excellent results for both technical and clinical success (100.0% and 100.0%, respectively) with a low recurrence rate (20%). During the follow-up period, severe complications such as dissection, vascular rupture, thrombosis or death did not occur. More importantly, repeated balloon dilation could achieve satisfactory or even curative outcomes, as shown by our results<sup>[11]</sup>. Therefore, we propose that repeated balloon angioplasty can be a primary treatment modality for HVOO in pediatric patients following liver transplantation, even for those with recurrent HVOO.

The individualized selection of balloons (type and size) as well as careful deployment is vital for achieving a desirable outcome. In the present study, the selection of the balloon was based on the experience and skill of the interventional radiologist. We used short balloons (diameter range: 6-8 mm; length:  $\leq 4$  cm) for all patients. Although the impact of the type and size of the balloon on long-term patency has not been clearly demonstrated, we speculate that a balloon with an appropriate diameter and a short length ensures better long-term patency for treating HVOO in pediatric liver

transplant recipients.

### Future directions

Although insufficient evidence has been obtained to support the benefits of stent placement for HVOO, novel stenting devices, such as drug-eluting and biodegradable stents, may be promising for the management of HVOO. Averin *et al.*<sup>[15]</sup> reported the use of a customized endovascular stent for the treatment of inferior vena cava obstruction following pediatric liver transplantation, in an attempt to relieve the risk of hepatic venous vein egress. However, the long-term efficacy of endovascular stent placement remains unproven.

### Limitation of study

In spite of the technical success and satisfactory clinical outcomes in these five children, the present study had certain limitations, including the retrospective nature of the study, a relatively small sample size, and a relatively short follow-up period. Further studies with a larger sample size that could identify relevant risk factors for HVOO development following transplantation and HVOO recurrence after balloon angioplasty are needed.

In conclusion, balloon dilatation is an effective and safe treatment for HVOO in pediatric patients following liver transplantation, and re-venoplasty is recommended even for patients with recurrent HVOO.

## ARTICLE HIGHLIGHTS

### Research background

Liver transplantation is the most effective treatment for end-stage liver disease. Hepatic venous outflow obstruction (HVOO) is a severe complication of pediatric liver transplantation, which has a high incidence of 4%-9% owing to the smaller anastomosis diameter and size mismatch of the hepatic vessels between the donor and recipient. Endovascular angioplasty is a less-invasive therapeutic option that has become the first-line treatment option in pediatric transplant recipients. However, it remains controversial whether stent placement or balloon angioplasty is required for patients with HVOO. Rare cases of HVOO have been reported in pediatric patients following liver transplantation. This study reported our experiences with using balloon dilatation as part of the treatment for HVOO in five children subjected to pediatric liver transplantation, providing valuable data for the successful treatment of such patients.

### Research motivation

HVOO is a rare and severe complication following pediatric liver transplantation that leads to graft loss in the majority of patients. However, it remains controversial whether stent placement or balloon angioplasty is required for patients with HVOO. This study reported our experiences with using balloon dilatation as part of the treatment for HVOO in five children subjected to pediatric liver transplantation, providing valuable information for the successful treatment of such patients. Balloon dilatation is an effective and safe treatment for HVOO in pediatric patients following liver transplantation, and re-venoplasty is recommended even for patients with recurrent HVOO.

### Research objectives

Balloon dilatation is an effective and safe treatment for HVOO in pediatric patients following liver transplantation, and re-venoplasty is recommended even for patients with recurrent HVOO.

### Research methods

The authors enrolled a total of 246 pediatric patients who underwent liver transplantation between June 2013 and September 2016. Among these patients, five were ultimately diagnosed with HVOO. Percutaneous interventions were performed under general anesthesia in all patients ( $n = 5$ ). The demographic data, types of donor and liver transplant, interventional examination and therapeutic outcomes of these five children were collected and analyzed with SPSS version 21.0 software. Changes between pre- and post-procedural pressure gradients across the hepatic vein stenosis were analyzed by paired Student's *t*-test.

### Research results

The authors found that balloon dilatation is an effective and safe treatment for HVOO in pediatric patients following liver transplantation. The hepatic vein stenosis rate was 1.62%. The time to onset of hepatic vein stenosis ranged from 1-32 mo (mean: 9.80 mo) after liver transplantation. The pressure gradient across the stenotic lesions at the anastomoses before balloon dilatation decreased significantly after the procedure ( $P < 0.05$ ). Sustained follow-up did not reveal significant procedural complications or procedure-related deaths. Further studies with a larger sample size that could identify relevant risk factors for HVOO development following transplantation and HVOO recurrence after balloon angioplasty are needed.

### Research conclusions

This study investigated the efficacy and safety of balloon dilatation for the treatment of hepatic venous outflow obstruction following pediatric liver transplantation. HVOO is a rare and severe complication following pediatric liver transplantation that leads to graft loss in the majority of patients. However, it remains unclear whether stent placement or balloon angioplasty is required for patients with HVOO. This study reported our experiences with using balloon dilatation as part of the treatment for HVOO in five children subjected to pediatric liver transplantation, providing valuable information regarding the successful treatment of such patients. Balloon dilatation is an effective and safe treatment for HVOO in pediatric patients following liver transplantation, and re-venoplasty is recommended even for patients with recurrent HVOO. In spite of the technical success and satisfactory clinical outcomes in these five children, the present study had certain limitations, including the retrospective nature of the study, a relatively small sample size, and a short follow-up period. Further studies with a large sample size that could identify risk factors for HVOO development following transplantation and HVOO recurrence after balloon angioplasty are needed.

### Research perspectives

This study reported our experiences with using balloon dilatation as part of the treatment for HVOO in five children subjected to pediatric liver transplantation, providing valuable information for the successful treatment of such patients. Balloon dilatation is an effective and safe treatment for HVOO in pediatric patients following liver transplantation, and re-venoplasty is recommended even for patients with recurrent HVOO. In spite of the technical success and satisfactory clinical outcomes in these five children, the present study had certain limitations, including the retrospective nature of the study, a relatively small sample size, and a short follow-up period. Further studies with a large sample size that could identify risk factors for HVOO development following transplantation and HVOO recurrence after balloon angioplasty are needed.

## REFERENCES

- 1 **Cheng YF**, Chen CL, Huang TL, Chen TY, Chen YS, Wang CC, Tsang LL, Sun PL, Chiu KW, Eng HL, Jawan B. Angioplasty treatment of hepatic vein stenosis in pediatric liver transplants: long-term results. *Transpl Int* 2005; **18**: 556-561 [PMID: 15819804 DOI: 10.1111/j.1432-2277.2005.00088.x]
- 2 **Buell JF**, Funaki B, Cronin DC, Yoshida A, Perlman MK, Lorenz J, Kelly S, Brady L, Leef JA, Millis JM. Long-term venous complications after full-size and segmental pediatric liver transplantation. *Ann Surg* 2002; **236**: 658-666 [PMID: 12409673]



- DOI: 10.1097/0000658-200211000-00017]
- 3 **Choi JW**, Jae HJ, Kim HC, Yi NJ, Lee KW, Suh KS, Chung JW. Long-term outcome of endovascular intervention in hepatic venous outflow obstruction following pediatric liver transplantation. *Liver Transpl* 2015; **21**: 1219-1226 [PMID: 26197765 DOI: 10.1002/lt.24215]
  - 4 **Lee BB**, Villavicencio L, Kim YW, Do YS, Koh KC, Lim HK, Lim JH, Ahn KW. Primary Budd-Chiari syndrome: outcome of endovascular management for suprahepatic venous obstruction. *J Vasc Surg* 2006; **43**: 101-108 [PMID: 16414396 DOI: 10.1016/j.jvs.2005.09.003]
  - 5 **Fujimori M**, Yamakado K, Takaki H, Nakatsuka A, Uraki J, Yamanaka T, Hasegawa T, Sugino Y, Nakajima K, Matsushita N, Mizuno S, Sakuma H, Isaji S. Long-Term Results of Stent Placement in Patients with Outflow Block After Living-Donor-Liver Transplantation. *Cardiovasc Intervent Radiol* 2016; **39**: 566-574 [PMID: 26464222 DOI: 10.1007/s00270-015-1210-4]
  - 6 **Ohm JY**, Ko GY, Sung KB, Gwon DI, Ko HK. Safety and efficacy of transhepatic and transsplenic access for endovascular management of portal vein complications after liver transplantation. *Liver Transpl* 2017; **23**: 1133-1142 [PMID: 28152572 DOI: 10.1002/lt.24737]
  - 7 **Omary RA**, Bettmann MA, Cardella JF, Bakal CW, Schwartzberg MS, Sacks D, Rholl KS, Meranze SG, Lewis CA. Quality improvement guidelines for the reporting and archiving of interventional radiology procedures. *J Vasc Interv Radiol* 2002; **13**: 879-881 [PMID: 12354820 DOI: 10.1016/S1051-0443(07)61769-2]
  - 8 **Chu HH**, Yi NJ, Kim HC, Lee KW, Suh KS, Jae HJ, Chung JW. Longterm outcomes of stent placement for hepatic venous outflow obstruction in adult liver transplantation recipients. *Liver Transpl* 2016; **22**: 1554-1561 [PMID: 27516340 DOI: 10.1002/lt.24598]
  - 9 **Qu W**, Zhu ZJ, Wei L, Sun LY, Liu Y, Zeng ZG. Reconstruction of the Outflow Tract in Cross-Auxiliary Double-Domino Donor Liver Transplantation. *Transplant Proc* 2016; **48**: 2738-2741 [PMID: 27788810 DOI: 10.1016/j.transproceed.2016.07.031]
  - 10 **Yabuta M**, Shibata T, Shibata T, Shinozuka K, Isoda H, Okamoto S, Uemoto S, Togashi K. Long-term outcome of percutaneous interventions for hepatic venous outflow obstruction after pediatric living donor liver transplantation: experience from a single institute. *J Vasc Interv Radiol* 2013; **24**: 1673-1681 [PMID: 24008112 DOI: 10.1016/j.jvir.2013.07.010]
  - 11 **Rao W**, Sun LY, Zhu ZJ, Chen G, Sun XY, Gao W, Shi R. Successful percutaneous transluminal balloon dilatation for hepatic venous outflow obstruction after pediatric liver transplantation: A series of cases. *Hepatol Res* 2013; **43**: 1321-1326 [PMID: 23489344 DOI: 10.1111/hepr.12086]
  - 12 **Carnevale FC**, Machado AT, Moreira AM, De Gregorio MA, Suzuki L, Tannuri U, Gibelli N, Maksoud JG, Cerri GG. Midterm and long-term results of percutaneous endovascular treatment of venous outflow obstruction after pediatric liver transplantation. *J Vasc Interv Radiol* 2008; **19**: 1439-1448 [PMID: 18760627 DOI: 10.1016/j.jvir.2008.06.012]
  - 13 **Lorenz JM**, Van Ha T, Funaki B, Millis M, Leef JA, Bennett A, Rosenblum J. Percutaneous treatment of venous outflow obstruction in pediatric liver transplants. *J Vasc Interv Radiol* 2006; **17**: 1753-1761 [PMID: 17142705 DOI: 10.1097/01.RVI.0000241540.31081.52]
  - 14 **Zhang ZY**, Jin L, Chen G, Su TH, Zhu ZJ, Wei L, Xiao GW. Endovascular interventional therapy of portal vein stenosis after pediatric liver transplantation. *Zhongguo Jieru Yingxiang Yu Zhilixiao* 2017; **14**: 210-213 [DOI: 10.13929/j.1672-8475.201612016]
  - 15 **Averin K**, Bucuvalas J, Alonso MH, Kohli R, Heubi JE, Johnson ND, Goldstein BH. Treatment of Inferior Vena Cava Obstruction Following Pediatric Liver Transplantation: Novel Use of a Customized Endovascular Stent. *J Pediatr* 2017; **180**: 256-260 [PMID: 27793336 DOI: 10.1016/j.jpeds.2016.09.051]
  - 16 **Kubo T**, Shibata T, Itoh K, Maetani Y, Isoda H, Hiraoka M, Egawa H, Tanaka K, Togashi K. Outcome of percutaneous transhepatic venoplasty for hepatic venous outflow obstruction after living donor liver transplantation. *Radiology* 2006; **239**: 285-290 [PMID: 16567488 DOI: 10.1148/radiol.2391050387]
  - 17 **Ko GY**, Sung KB, Yoon HK, Kim JH, Song HY, Seo TS, Lee SG. Endovascular treatment of hepatic venous outflow obstruction after living-donor liver transplantation. *J Vasc Interv Radiol* 2002; **13**: 591-599 [PMID: 12050299 DOI: 10.1016/S1051-0443(07)61652-2]
  - 18 **Sakamoto S**, Egawa H, Kanazawa H, Shibata T, Miyagawa-Hayashino A, Haga H, Ogura Y, Kasahara M, Tanaka K, Uemoto S. Hepatic venous outflow obstruction in pediatric living donor liver transplantation using left-sided lobe grafts: Kyoto University experience. *Liver Transpl* 2010; **16**: 1207-1214 [PMID: 20879019 DOI: 10.1002/lt.22135]

**P- Reviewer:** Al-Haggag M, Quak SH, Rolle U **S- Editor:** Gong ZM  
**L- Editor:** Wang TQ **E- Editor:** Ma YJ



## Prospective Study

# Efficacy of noninvasive evaluations in monitoring inflammatory bowel disease activity: A prospective study in China

Jin-Min Chen, Tao Liu, Shan Gao, Xu-Dong Tong, Fei-Hong Deng, Biao Nie

Jin-Min Chen, Shan Gao, Xu-Dong Tong, Department of Gastroenterology, Xiangyang Central Hospital, Hubei University of Arts and Science, Xiangyang 441021, Hubei Province, China

Tao Liu, Department of Gastroenterology, the Sixth Affiliated Hospital of Sun Yat-sen University, Guangzhou 510665, Guangdong Province, China

Fei-Hong Deng, Guangdong Provincial Key Laboratory of Gastroenterology, Department of Gastroenterology, Nanfang Hospital, Southern Medical University, Guangzhou 510515, Guangdong Province, China

Biao Nie, Department of Gastroenterology, the First Affiliated Hospital of Jinan University, Jinan University, Guangzhou 510630, Guangdong Province, China

ORCID number: Jin-Min Chen (0000-0002-1842-064X); Tao Liu (0000-0003-3336-7207); Shan Gao (0000-0002-8232-4134); Xu-Dong Tong (0000-0002-3136-1242); Fei-Hong Deng (0000-0001-7711-4880); Biao Nie (0000-0002-5702-3540).

**Author contributions:** Chen JM and Nie B designed the study and wrote the manuscript; Deng FH collected fecal and blood samples and completed patient case report; Liu T and Nie B performed all endoscopies and completed the endoscopic scoring sheet; Tong XD quantified fecal calprotectin; Gao S performed data analysis; all authors read and approved the final manuscript.

**Supported by** National Natural Science Foundation of China to Biao Nie, No. 81471080.

**Institutional review board statement:** The study was reviewed and approved by the institutional review board of Department of Gastroenterology in Nanfang Hospital (Guangzhou, China) and the Medical Ethnic Committee of Nanfang Hospital (NFEC-2014-065).

**Clinical trial registration statement:** The clinical trial was registered in Chinese Clinical Trial Registry (registration ID:

ChiCTR-DDT-14005066). Details can be found at <http://www.chictr.org.cn/showproj.aspx?proj=4509>.

**Informed consent statement:** All study participants provided written informed consent prior to study enrollment.

**Conflict-of-interest statement:** The authors of this manuscript have no conflicts of interest to disclose.

**Data sharing statement:** Technical appendix, statistical code, and dataset available from the corresponding author at email: niebiao2@163.com. Participants gave informed consent for data sharing.

**Open-Access:** This article is an open-access article which was selected by an in-house editor and fully peer-reviewed by external reviewers. It is distributed in accordance with the Creative Commons Attribution Non Commercial (CC BY-NC 4.0) license, which permits others to distribute, remix, adapt, build upon this work non-commercially, and license their derivative works on different terms, provided the original work is properly cited and the use is non-commercial. See: <http://creativecommons.org/licenses/by-nc/4.0/>

**Manuscript source:** Invited manuscript

**Correspondence to:** Biao Nie, MD, PhD, Professor, Associate Chief Physician, Department of Gastroenterology, the First Affiliated Hospital of Jinan University, Jinan University, No. 614, West Huangpu Avenue, Guangzhou 510630, Guangdong Province, China. niebiao2@163.com  
Telephone: +86-15101503392  
Fax: +86-20-38688025

**Received:** July 31, 2017

**Peer-review started:** August 1, 2017

**First decision:** September 6, 2017

**Revised:** September 28, 2017

**Accepted:** November 2, 2017

**Article in press:** November 2, 2017

**Published online:** December 14, 2017

## Abstract

### AIM

To optimize the efficacy of noninvasive evaluations in monitoring the endoscopic activity of inflammatory bowel disease (IBD).

### METHODS

Fecal calprotectin (FC), clinical activity index (CAI), C-reactive protein (CRP), erythrocyte sedimentation rate (ESR), and procalcitonin (PCT) were measured for 136 IBD patients. Also, FC was measured in 25 irritable bowel syndrome (IBS) patients that served as controls. Then, endoscopic activity was determined by other two endoscopists for colonic or ileo-colonic Crohn's disease (CICD) with the "simple endoscopic score for Crohn's disease" (SES-CD), CD-related surgery patients with the Rutgeerts score, and ulcerative colitis (UC) with the Mayo score. The efficacies of these evaluations to predict the endoscopic disease activity were assessed by Mann-Whitney test,  $\chi^2$  test, Spearman's correlation, and multiple linear regression analysis.

### RESULTS

The median FC levels in CD, UC, and IBS patients were 449.6 (IQR, 137.9-1344.8), 497.9 (IQR, 131.7-118.0), and 9.9 (IQR, 0-49.7)  $\mu\text{g/g}$ , respectively ( $P < 0.001$ ). For FC, CDAI or CAI, CRP, and ESR differed significantly between endoscopic active and remission in CICD and UC patients, but not in CD-related surgery patients. The SES-CD correlated closely with levels of FC ( $r = 0.802$ ), followed by CDAI ( $r = 0.734$ ), CRP ( $r = 0.658$ ), and ESR ( $r = 0.557$ ). The Mayo score also correlated significantly with FC ( $r = 0.837$ ), CAI ( $r = 0.776$ ), ESR ( $r = 0.644$ ), and CRP ( $r = 0.634$ ). For FC, a cut-off value of 250  $\mu\text{g/g}$  indicated endoscopic active inflammation with accuracies of 87.5%, 60%, and 91.1%, respectively, for CICD, CD-related surgery, and UC patients. Moreover, clinical FC activity (CFA) calculated as  $0.8 \times \text{FC} + 4.6 \times \text{CDAI}$  showed higher area under the curve (AUC) of 0.962 for CICD and CFA calculated as  $0.2 \times \text{FC} + 50 \times \text{CAI}$  showed higher AUC (0.980) for UC patients than the FC. Also, the diagnostic accuracy of FC in identifying patients with mucosal inflammation in clinical remission was reflected by an AUC of 0.91 for CICD and 0.96 for UC patients.

### CONCLUSION

FC is the most promising noninvasive evaluation for monitoring the endoscopic activity of CICD and UC. CFA might be more accurate for IBD activity evaluation.

**Key words:** Inflammatory bowel disease; Crohn's disease; Ulcerative colitis; Fecal calprotectin; Disease activity

© The Author(s) 2017. Published by Baishideng Publishing Group Inc. All rights reserved.

**Core tip:** This was a prospective study conducted in China to assess the efficacy of noninvasive markers, including fecal calprotectin, clinical activity index (CAI), CRP, ESR, and procalcitonin (PCT) for monitoring disease activity in colonic or ileo-colonic Crohn's disease (CICD), CD-related surgery patients, and UC patients and further to optimize the accuracy of those noninvasive biomarkers in detecting active residual mucosal inflammation in IBD patients in clinical remission.

Chen JM, Liu T, Gao S, Tong XD, Deng FH, Nie B. Efficacy of noninvasive evaluations in monitoring inflammatory bowel disease activity: A prospective study in China. *World J Gastroenterol* 2017; 23(46): 8235-8247 Available from: URL: <http://www.wjgnet.com/1007-9327/full/v23/i46/8235.htm> DOI: <http://dx.doi.org/10.3748/wjg.v23.i46.8235>

## INTRODUCTION

Inflammatory bowel disease (IBD) is a chronic, destructive inflammatory disease of the gastrointestinal tract with unknown etiology<sup>[1]</sup>. Generally, it occurs most commonly at a young age and most patients need life-long medicine treatment, thus causing work disabilities and imposing heavy social and economic burdens<sup>[2]</sup>. IBD is no more than a "Western disease"; according to a multicenter study, IBD in Asia might be as severe as or worse than in the West, and China has the highest incidence of IBD in Asia<sup>[3]</sup>. Two recent prospective population-based studies also demonstrated that IBD has a high incidence and wide geographical coverage in China<sup>[4,5]</sup>.

Because IBD has a chronic relapsing-remitting course, patients and clinicians need a monitoring technique to detect an imminent flare for timely tailoring therapy regimen. To date, most clinicians monitor IBD activity and guide therapeutic decisions based on clinical activity indexes<sup>[6]</sup>. However, emerging data showed that IBD patients with a clinically quiescent disease may still have residual mucosal inflammation and remission of symptoms may not be an available predictor of long-term favorable outcome in IBD patients<sup>[7,8]</sup>. Mucosal healing (MH) has been proven to be a strong predictor of disease-related outcomes and has become a new therapeutic goal in IBD<sup>[9-11]</sup>. An endoscopic procedure for IBD can determine the disease location and mucosal lesions precisely and is considered the gold standard for assessing disease activity. However, endoscopy is invasive, uncomfortable, expensive, and not well tolerated by patients; therefore, regular monitoring of disease activity using endoscopy is not feasible<sup>[12]</sup>. Furthermore, some patients are terrified by painful

endoscopy experiences and they are reluctant to visit clinicians until the disease manifests as rectal bleeding or obstruction, which affects the prognosis. A simple, acceptable, and specific evaluation is needed to play an adjunctive role in the assessment of disease activity, enabling the most cost-effective use of medical resources<sup>[13,14]</sup>.

Clinical assessment indexes correlate poorly with endoscopic activity and remission of symptoms may not indicate remission of IBD<sup>[11,15]</sup>. Also, for patients with clinically overt relapse, their recent history and symptoms will give sufficient reasons for further endoscopic exploration or intensification of treatment, and there is no need to wait for the results of inflammatory biomarkers. Therefore, finding an evaluation that can detect increased endoscopic disease activity earlier before any clinical symptoms have occurred is an unmet clinical need.

The aim of this study, therefore, was to assess the efficacy of noninvasive evaluations, including fecal calprotectin (FC), clinical activity index (CDAI or CAI), C-reactive protein (CRP), erythrocyte sedimentation rate (ESR), and procalcitonin (PCT) for monitoring disease activity in colonic or ileo-colonic Crohn's disease (CICD), CD-related surgery patients, and UC patients and further to optimize the accuracy of those noninvasive evaluations in detecting active residual mucosal inflammation in IBD patients in clinical remission.

## MATERIALS AND METHODS

### Participants

This study was approved by the Ethics Committee of Nanfang Hospital, Southern Medical University (NFEC-2014-065). In this prospective study, we consecutively recruited 136 adult outpatients and inpatients with previously confirmed diagnoses of IBD referred for colonoscopy at the Department of Gastroenterology of Nanfang Hospital. The diagnosis of IBD was based on clinical, ileocolonoscopy, histopathological, and radiological findings. A second cohort of 25 IBS patients, defined according to the Rome III criteria, served as controls. Of the 136 IBD patients, six had undergone colonoscopy twice to evaluate therapy efficiency, and the interval between the two endoscopies was longer than 2 mo. First, 35 IBD patients were excluded because we could not timely collect a fecal sample before bowel preparation ( $n = 10$ ), a full colonoscopy was not performed due to a stricture or without a properly prepared colon compatible with adequate endoscopic assessment ( $n = 7$ ), the age was  $< 18$  years ( $n = 4$ ), blood samples were missed ( $n = 5$ ), patients used non-steroidal anti-inflammatory drugs (NSAIDs) ( $n = 3$ ), patients had poor compliance with fecal sampling ( $n = 4$ ), or patients had concomitant colorectal cancer ( $n = 2$ ). Outpatients were provided with a fecal collection

tube when they attended the endoscopy center to make an appointment with the physician and were asked to return a fecal sample before the endoscopic examination. In inpatients, the fecal collection set was prepared by a trained nurse and then sent to the laboratory.

For IBD patients, the day before the endoscopy, blood samples were taken to measure CRP, ESR, and PCT in the IBD Unit at Nanfang Hospital. At the same time, the patients were asked to complete a case report to record their demographic data, symptoms, and current medication usage.

### Inclusion criteria

A firm diagnosis of IBD must have been made or confirmed based on clinical, ileocolonoscopy, histopathological, and radiological findings at our institution. Other inclusion criteria were complete colonoscopy (ileum or neo-terminal ileum was included), age between 18 and 85 years, and fecal samples delivered from 1 to 3 d before bowel preparation.

### Exclusion criteria

The exclusion criteria included terminal ileum or neo-terminal ileum not reached; history of extensive bowel resection unrelated to IBD; indeterminate colitis (IC); pregnancy; age  $< 18$  years or  $> 85$  years; other deceptive reasons for elevated CRP/EST/PCT, such as infection (within one month), malignancy (current), rheumaimmune systemic diseases not related to IBD, trauma or surgery (within one month); and use of NSAIDs within three months before colonoscopic examination.

### Endoscopic disease activity

The endoscopic activities of IBD patients were graded according to validated endoscopic score tools. Simple endoscopic score for Crohn's disease" (SES-CD) was used for the CICD patients<sup>[16]</sup>. For the SES-CD, the four endoscopic parameters selected were ulcers, proportion of the surface covered by ulcers, proportion of the surface with any other lesions, and stenosis. Each variable was scored from 0 to 3 in each segment (the ileum, the right, transverse, and left colon, and the rectum). The SES-CD activity levels were graded as follows: inactive (remission), 0-3; mild activity, 4-10; moderate activity, 11-19; and severe activity,  $\geq 20$ , according to Schoepfer *et al.*<sup>[17]</sup>. The Rutgeerts score is a well-established endoscopic scoring system for assessing the neo-terminal ileum for patients having prior CD-related surgery<sup>[18]</sup>: i0, no lesion; i1,  $< 5$  aphthous lesions; i2,  $> 5$  aphthous lesions with normal mucosa between lesions, or skip areas of larger lesions or lesions confined to the ileo-colonic anastomosis; i3, diffuse aphthous ileitis with diffusely inflamed mucosa; and i4, diffuse inflammation with larger ulcers, nodules, and/or narrowing (i0-i1: endoscopic remission;  $\geq i2$ : endoscopic recurrence).



**Table 1 Clinical and demographic characteristics of included patients *n* (%)**

	CD	UC	IBS
Number of patients, <i>n</i>	92	44	25
Male	54 (58.7)	26 (59.1)	11 (44)
Median age at test (range)	29.5 (18-62)	38 (19-70)	35 (21-52)
Age at diagnosis (yr)			NA
A1 (< 16)	7 (7.6)	2 (4.5)	
A2 (17-40)	69 (75.0)	27 (61.4)	
A3 (> 40)	16 (17.4)	15 (34.1)	
Disease location			NA
Ileum (L1)	22 (23.9)	NA	
Colonic (L2)	10 (10.9)	NA	
Ileum-Colonic (L3)	60 (65.2)	NA	
Upper GI (L4)	9 (9.8)	NA	
Rectum (E1)	NA	15 (34.1)	
Distal colitis (E2)	NA	14 (31.8)	
Extensive colitis (E3)	NA	15 (34.1)	
Concomitant medications <sup>1</sup>			NA
No medication	9 (9.8)	3 (6.8)	
5-ASA	28 (30.4)	37 (84.1)	
Corticosteroids	22 (23.9)	9 (20.5)	
Immunosuppressants	39 (42.4)	1 (2.31)	
Anti-TNF therapy	36 (39.1)	4 (9.1)	
Previous IBD-related surgery: no/yes	69/23	NA	NA

<sup>1</sup>Because therapy regimens overlapped, the total is not 100%. GI: Gastrointestinal; ASA: 5-aminosalicylic acid; TNF: Tumor necrosis factor; NA: Not applicable; IBS: Irritable bowel syndrome; CD: Crohn's disease; UC: Ulcerative colitis.

The disease severity of UC was evaluated according to the Mayo score scale (0-2: remission; 3-5: mild; 6-10: moderate; 11-12: severe)<sup>[19]</sup>.

All endoscopies were performed by two experienced gastroenterologists with at least 5 years of experience in performing colonoscopies. The endoscopists completed an endoscopic scoring sheet immediately after the colonoscopic examination. To minimize the subjective nature of the scoring tools, we recorded a video of the endoscopy procedure. The two endoscopists analyzed the videos together and disagreements were resolved by discussion to realize consistent scoring. To avoid bias, the endoscopists performing the endoscopies were unaware of the FC, clinical activity index, CRP, ESR, and PCT results.

## FC

Upon arrival of stool samples at the laboratory, we sampled from six sites in each stool sample and mixed the sample with a stirrer. One volume of feces was diluted with 49 volumes of extraction buffer. After homogenizing by vigorous shaking for 30 min, the sample was centrifuged at 3000 *g* for 10 min and the supernatant was stored at -20 °C until analysis. The Bühlmann Calprotectin ELISA kit (Bühlmann, Schönenbuch, Switzerland) was designed for the quantitative determination of FC in stool samples. The assay was performed according to the manufacturer's instructions. Briefly, after a short extraction procedure, we diluted the stool extracts 1:150 with incubation buffer. Then, the calprotectin antigen was measured

by sandwich ELISA; the ELISA plates were read at 450 nm using a Spectra mini-reader. All results were normalized to stool wet weight (in grams), and FC concentrations are expressed in µg/g. The researcher carrying out the analyses was blinded to the identity of the patients and their clinical or endoscopic findings.

## Clinical activity and serological biomarkers

For CD patients, clinical activity was assessed based on the "Crohn's disease activity index" (CDAI; ≤ 150: clinical remission; 150-220: mild clinical activity; 220-450: moderate clinical activity; ≥ 450: severe clinical activity)<sup>[20]</sup>. For UC patients, clinical activity was assessed by the "clinical colitis activity index" (CAI; ≤ 4: clinical remission; 5-10: mild clinical activity; 11-17: moderate clinical activity; ≥ 18: severe clinical activity) according to Rachmilewitz<sup>[21]</sup>. Serological biomarkers included CRP (upper limit of normal, 5 mg/L), ESR (upper limit of normal, 10 mm/h), and PCT (lower limit of range, 0.02 ng/mL; upper limit of normal, 0.05 ng/mL).

## Statistical analysis

Data were recorded in an Excel sheet (Microsoft Excel 2007) and analyzed using SPSS software (ver. 15.0 for Windows; SPSS, China). The normality of the distribution of data was tested using the Kolmogorov-Smirnov test. The Mann-Whitney test was used to assess differences between groups. Non-parametric data were presented as medians and interquartile ranges (IQR) or ranges. Non-parametric tests were used when data were not normally distributed. The  $\chi^2$  test was used to assess associations of categorical data in two independent groups. A Bonferroni adjustment was carried out in multiple testing of noninvasive parameters according to endoscopic activity grade (inactive/mild/moderate/severe) and correlations of parameters with disease location (L1/L2/L3 or E1/E2/E3) in CD and UC patients. Associations between endoscopic disease activity and laboratory parameters were assessed using Spearman's correlation. The true positive rate (sensitivity) was plotted as a function of the false positive rate (1-specificity) for various cut-off points to plot a receiver operating characteristic (ROC) curve. The area under the ROC curve (AUC) was used to measure the ability of parameters to predict endoscopic severity. Multiple linear regression analysis with stepwise deletion was performed based on FC, CDAI/CAI, CRP, ESR, and PCT in order to construct a combined score that best predicted the endoscopy activity.

## RESULTS

### Patients and their characteristics

In total, 136 consecutive IBD patients and 25 recruited IBS patients who met the inclusion and exclusion criteria were enrolled between August 2014 and January 2015.

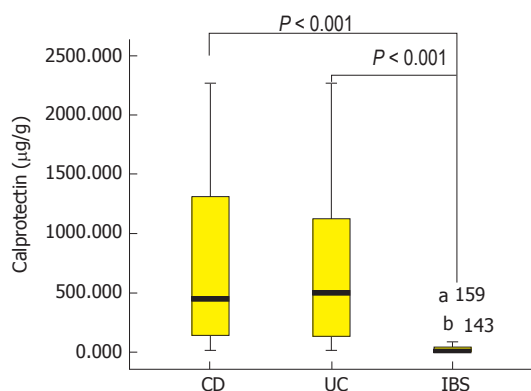


**Figure 1** Median fecal calprotectin levels in Crohn's disease, ulcerative colitis, and irritable bowel syndrome patients, illustrated by box plots. The box indicates the lower and upper quartiles, and the horizontal line in the middle of the box is the median. The 95% confidence interval is indicated by the whiskers, and values outside the whiskers are individual outliers. FC: Fecal calprotectin; IBD: Inflammatory bowel disease; CD: Crohn's disease; UC: Ulcerative colitis; a,b: the sample numbers of fecal calprotectin extreme values in box plot.

During the study period, six patients (three CIGD, two CD-related surgery, and one UC patients) underwent colonoscopy twice. Thus, a total of 142 endoscopies were performed in the 136 IBD patients. FC, CDAI/CAI, CRP and ESR were successfully measured in all included IBD patients. PCT was measured in 67 cases with CD, 18 cases with CD-related surgery, and 41 cases with UC. No adverse events happened when performing the ileo-colonoscopy. The demographic characteristics of the included patients are shown in Table 1.

Because the small bowel is not accessible in conventional colonoscopy, small-bowel CD patients are routinely determined to be endoscopically in remission according to SES-CD, but are shown to have active lesion by double-balloon or capsule endoscopy. We hypothesized that the evaluations could correlate more closely with the SES-CD in CIGD patients. Later in this article we performed the endoscopy disease activity analysis mainly in three subgroup patients: CIGD patients, CD-related surgery patients, and UC patients. Also, we included small bowel CD patients in the analysis of the correlation of non-invasive disease-activity parameters stratified according to disease location.

### Noninvasive parameters according to endoscopy-based inflammation categories

Baseline FC, clinical activity index (CAI or CDAI), and laboratory indexes (CRP, ESR, and PCT) according to endoscopy-based classification of active and inactive IBD patients and IBS patients are presented in Table 2. The median FC levels in CD, UC, and IBS patients were 449.6 (IQR, 137.9-1344.8), 497.9 (IQR, 131.7-118.0), and 9.9 (IQR, 0-49.7) µg/g, respectively (Figure 1). IBS patients had significantly lower FC levels than the three subgroups of endoscopically active IBD patients ( $P < 0.001$ ). Indeed, IBS patients also had

significantly lower levels of FC when compared with the three subgroups of IBD patients without endoscopic inflammation ( $P < 0.05$ , Table 2). After the IBD patients were grouped into CIGD, CD-related surgery, and UC subgroups, the median FC values were 695.0 (IQR, 147.1-1805.0), 188.5 (IQR, 72.06-559.7), and 497.9 (IQR, 131.7-1198.0) µg/g, respectively ( $P < 0.01$ ). Within each IBD subgroup, the evaluations were compared between the endoscopically active and inactive patients, and FC yielded a significant difference in the CIGD and UC subgroups. But in the CD-related surgery patients, FC values showed no difference based on Rutgeerts score-classified endoscopic inflammation. Also as shown in Table 2, differences in CDAI/CAI, CRP, and ESR according to endoscopy-based inflammation status were observed in CIGD patients and UC patients, but not in CD-related surgery patients. With regard to PCT, no significant difference was detected in the three groups of IBD patients.

Tables 3 and 4 summarize the median noninvasive parameter values for inactive, mild, moderate, and severe endoscopic grades in CIGD and UC patients. In the two subgroups of patients, FC had the clinical usage to distinguish inactive from mild and moderate from severe endoscopic activity; however, FC failed to distinguish mild from moderate endoscopic activity. For clinical activity index, CDAI not only could distinguish inactive from mild endoscopic activity, but also moderate from severe endoscopic activity in CIGD patients. For CAI, a significant difference could be detected between inactive vs mild and mild vs moderate endoscopic activity. CRP and ESR could only distinguish moderate from severe endoscopic activity in UC patients. Also, no Rutgeerts score-based endoscopic activity grade was individually distinguishable by noninvasive parameters. Median FC values according to endoscopic activity grade in three subgroups of IBD patients are vividly illustrated in Figure 2.

### Clinical activity and endoscopic activity

Base on CDAI/CAI, 34 CIGD, 19 CD-related surgery, and 25 UC patients were in clinical remission (CDAI  $\leq 150$ /CAI  $\leq 4$ ). Among the three subgroups of IBD patients in clinical remission, 14/34, 7/19, and 13/25 patients showed active endoscopic inflammation, respectively (SES-CD  $\geq 4$ /Rutgeerts  $\geq 2$ /Mayo  $\geq 3$ ). The noninvasive biomarker values in the three subgroups of IBD patients in clinical remission with and without evidence of endoscopic inflammation are shown in Supplementary Table 1. For CIGD and UC patients in clinical remission, FC, CRP, and ESR differed significantly between the endoscopically active and inactive patients, being higher in the group with endoscopic active disease. However, no noninvasive biomarker in the 19 CD-related surgery patients in clinical remission differed significantly between active and inactive disease at ileo-colonoscopy.

The sensitivities and specificities of FC at a cut-

**Table 2** Descriptive statistics of noninvasive evaluations for endoscopy-based classification of inflammation for inflammatory bowel disease and irritable bowel syndrome patients

	CICD		CD-related surgery		UC		IBS
	Inactive, <i>n</i> = 21	Active, <i>n</i> = 35	Inactive, <i>n</i> = 15	Active, <i>n</i> = 10	Inactive, <i>n</i> = 12	Active, <i>n</i> = 33	<i>n</i> = 25
FC ( $\mu\text{g/g}$ )							
Median	131.72 <sup>1,3</sup>	1795.8 <sup>1,2</sup>	142.97 <sup>3</sup>	229.27 <sup>2</sup>	45.31 <sup>1,3</sup>	690.6 <sup>1,2</sup>	9.9 <sup>2,3</sup>
Range	(0-658.71)	(264.64-2266.07)	(0.02-1805.0)	(0-1805.0)	(6.7-189.42)	(74.93-2266.01)	(0-385.4)
CDAI/CAI							NA
Median	63.12 <sup>1</sup>	168.45 <sup>1</sup>	81	135.64	1 <sup>1</sup>	6 <sup>1</sup>	
Range	(32.2-155.0)	(46.8-364.0)	(37.8-192.8)	(38.8-327.1)	(0-4)	(1-17)	
CRP (mg/L)							NA
Median	0.48 <sup>1</sup>	20.57 <sup>1</sup>	2.1	4.37	0.39 <sup>1</sup>	4 <sup>1</sup>	
Range	(0.10-12.88)	(0.2-79.8)	(0.13-134.6)	(0.10-41.20)	(0.04-2.1)	(0.08-65.40)	
ESR (mm/h)							NA
Median	8.0 <sup>1</sup>	30.0 <sup>1</sup>	9	17	4.3 <sup>1</sup>	14 <sup>1</sup>	
Range	(1.0-57.0)	(5.0-123.0)	(1.0-92.0)	(2.0-41.0)	(2.0-15.0)	(2.0-100.0)	
PCT (ng/mL)							NA
Median	0.037	0.043	0.028	0.025	0.028	0.025	
Range	(0-4.39)	(0-5.02)	(0-0.082)	(0-0.058)	(0-0.082)	(0-0.058)	

<sup>1</sup>Identical letters indicate significant differences between the three inactive and active IBD patient groups (Mann-Whitney *U*-tests,  $P < 0.001$  for all); <sup>2</sup>For all indices, IBS patients had significantly lower FC levels than the three groups of active IBD patients (Mann-Whitney *U*-tests,  $P < 0.001$  for all); <sup>3</sup>IBS patients had significantly lower FC levels than the three groups of endoscopic remission IBD patients (Mann-Whitney *U*-tests, for CICD and CD-related surgery patients,  $P < 0.001$ ; for UC patients,  $P < 0.05$ ). CICD: Colonic or ileo-colonic Crohn's disease; CD: Crohn's disease; UC: Ulcerative colitis; IBD: Inflammatory bowel disease; IBS: Irritable bowel syndrome; FC: Fecal calprotectin; CDAI/CAI: Clinical activity index; PCT: Procalcitonin; NA: Not applicable.

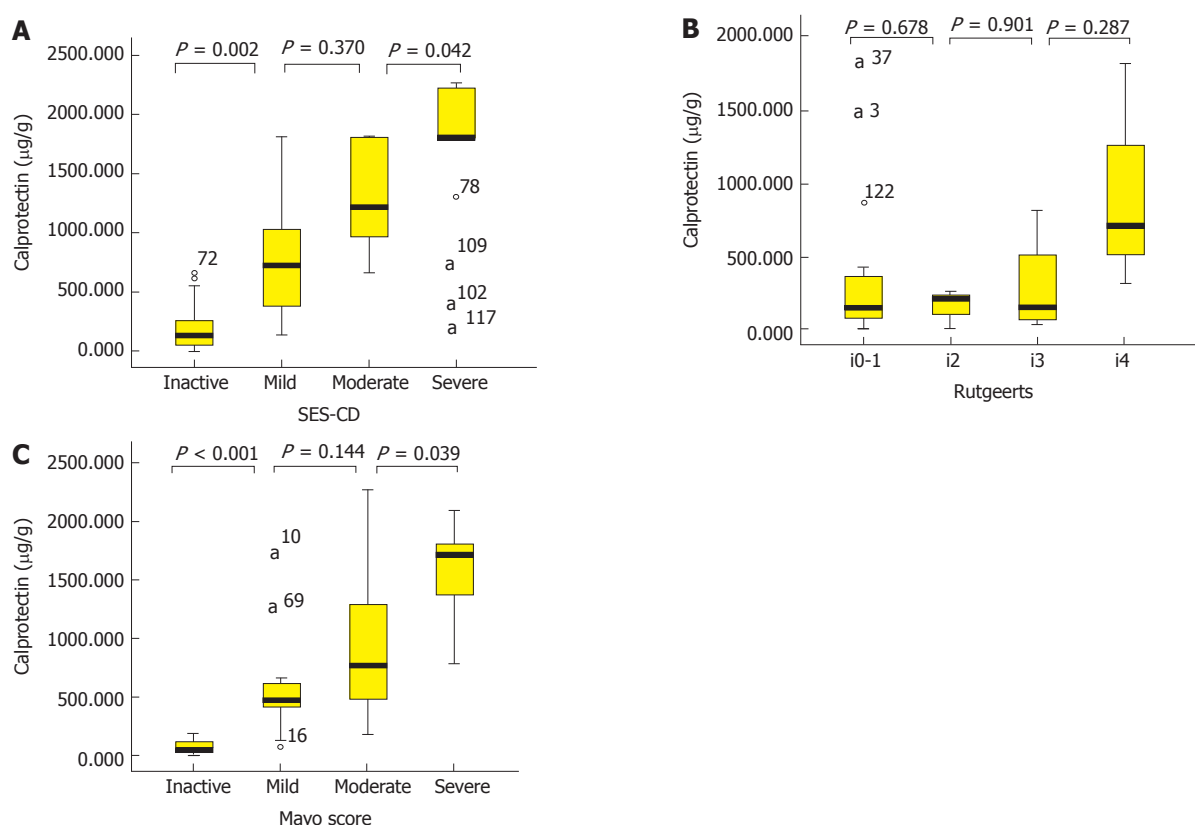


**Figure 2** Median fecal calprotectin levels according to endoscopic activity grade in three subgroups of inflammatory bowel disease patients, illustrated by box plots. A: The median FC levels in CICD patients grouped by SES-CD. B: The median FC levels in CD-related surgery patients grouped by Rutgeerts score. C: The median FC levels in UC patients grouped by Mayo score. a: the sample numbers of fecal calprotectin extreme values in box plots; FC: Fecal calprotectin; CD: Crohn's disease; UC: Ulcerative colitis; CICD: Colonic or ileo-colonic Crohn's disease; SES-CD: Simple endoscopic score for Crohn's disease.

off value of  $250 \mu\text{g/g}$ ,  $\text{CRP} \geq 5 \text{ mg/L}$ , and  $\text{ESR} \geq 10 \text{ mm/h}$  in discriminating patients with active disease at ileo-colonoscopy in CICD and UC patients in clinical

remission are shown in Table 5. AUCs for FC to detect active endoscopic inflammation were 0.91 and 0.96, for the two subgroups of IBD patients in clinical

**Table 3** Noninvasive parameters according to endoscopic activity grade in colonic or ileo-colonic Crohn's disease patients

	Inactive, $n_1 = 21$	Mild activity, $n_2 = 8$	Moderate activity, $n_3 = 9$	Severe activity, $n_4 = 18$
FC, median (range)	125.7(0-658.7)	717.8 (137.7-1805.0)	1211.8 (660.8-1805.0)	1805.0 (264.6-2266.1)
P value		< 0.05	NS	< 0.05
CDAI, median (range)	63.1 (32.2-155.0)	125.4 (46.8-157.8)	145.1 (75.0-234.9)	201.4 (64.7-364.0)
P value		< 0.05	NS	< 0.05
CRP, median (range)	0.48(0.1-12.9)	5.1 (0.20-48.1)	15.0 (0.6-70.8)	30.6 (1.1-79.8)
P value		NS	NS	< 0.05
ESR, median (range)	8.0(1.0-57.0)	22.0 (5.0-68.0)	28.0 (8.9-95.0)	37.0 (5.5-123.0)
P value		NS	NS	< 0.05
PCT, median (range)	0.037 (0-4.39)	0.038 (0.021-0.064)	0.038 (0-0.137)	0.049 (0.02-5.02)
P value		NS	NS	NS

FC: Fecal calprotectin; CDAI: Clinical activity index; PCT: Procalcitonin; NS: No significant.

**Table 4** Noninvasive parameters according to endoscopic activity grade in ulcerative colitis patients

	Inactive, $n_1 = 12$	Mild activity, $n_2 = 12$	Moderate activity, $n_3 = 16$	Severe activity, $n_4 = 5$
FC, median (range)	45.3 (6.7-189.42)	474.8 (74.9-1805.0)	769.9 (186.8-2266.1)	1704.6 (788.4-2092.4)
P value		< 0.001	NS	< 0.05
CAI, median (range)	1 (0-4)	2.5 (1-8)	6.5 (2-17)	9 (8-15)
P value		< 0.05	< 0.001	NS
CRP, median (range)	0.39 (0.04-2.10)	1.9 (0.26-65.40)	4.7 (0.08-28.19)	16.4 (7.1-53.2)
P value		NS	NS	< 0.05
ESR, median (range)	4.3 (2.0-15.0)	8.5 (2.0-40.0)	14.0 (2.0-88.0)	45.0 (24.0-100.0)
P value		NS	NS	< 0.05
PCT, median (range)	0.03 (0-0.041)	0.031 (0.023-0.127)	0.044 (0.021-0.538)	0.035 (0.026-0.085)
P value		NS	NS	NS

FC: Fecal calprotectin; CAI: Clinical activity index; PCT: Procalcitonin; UC: Ulcerative colitis; NS: No significant.

**Table 5** Sensitivity, specificity, positive predictive value, and negative predictive value of fecal calprotectin, CRP, and ESR in predicting endoscopic active disease in inflammatory bowel disease patients in clinical remission

	FC $\geq 250$ $\mu\text{g/g}$	CRP $\geq 5$ mg/L	ESR $\geq 10$ mm/h
Colonic or ileum-colonic CD (%)			
Sensitivity	93	46.2	61.5
Specificity	70	83.3	66.7
PPV	68.4	75.0	53.3
NPV	93.3	73.1	73.7
AUC	0.91	0.76	0.71
P value	< 0.001	0.011	0.042
UC			
Sensitivity	84.6	23.1	46.2
Specificity	100	100	83.3
PPV	100	100	75.0
NPV	85.7	54.5	58.8
AUC	0.96	0.84	0.76
P value	< 0.001	0.004	0.028

CD: Crohn's disease; UC: Ulcerative colitis; FC: Fecal calprotectin; PPV: Positive predictive value; NPV: Negative predictive value; AUC: Area under the ROC curve.

remission, respectively, suggesting that FC is the most accurate biomarker to predict preclinical active inflammation. In CIRD patients in clinical remission, FC at the cut-off value 250  $\mu\text{g/g}$  had the highest

sensitivity (93%) and a moderate specificity (70%) to predict active lesion, CRP had the highest specificity (83.3%) but lowest sensitivity (46.2%). ESR had a mild sensitivity and specificity of 61.5%, 66.7%, respectively. In UC patients in clinical remission, both FC and CRP had a 100% specificity to identify active disease, but the sensitivity of CRP was much lower (23.1%) compared with FC (84.6%). Also, all the noninvasive biomarkers were not useful as diagnostic tests for mucosal inflammation in CD-related surgery patients in clinical remission.

#### Correlation of noninvasive evaluations with endoscopic disease activity

Of 56 CIRD patients, the SES-CD correlated significantly with levels of FC (Spearman's rank correlation coefficient,  $r = 0.802$ ), CDAI ( $r = 0.734$ ), CRP ( $r = 0.658$ ), and ESR ( $r = 0.557$ ) ( $P < 0.01$  for all). However, PCT failed to significantly correlate with the SES-CD ( $r = 0.209$ ,  $P = 0.19$ ). In the 25 CD-related surgery patients, the median time between surgery and the endoscopic examination at entry was 432 (IQR, 266-755) d. There was no significant correlation between endoscopic score and the time from surgery to the endoscopic examination ( $P = 0.76$ ). Noninvasive evaluations had no significant correlation with Rutgeerts score. In 45 UC patients, the Mayo score correlated closely with



**Table 6** Sensitivity, specificity, positive predictive value, and negative predictive value of FC, CDAI/CAI, CRP, ESR, and CAF in predicting endoscopic active disease in three groups of inflammatory bowel disease patients

	FC $\geq 250$ $\mu\text{g/g}$	CDAI > 150/CAI > 4	CRP $\geq 5$ mg/L	ESR $\geq 10$ mm/h	CFA $\geq 850$ or $\geq 150$
Colonic or ileum-colonic CD (%)					
Sensitivity	97.1	60	71.4	82.8	91.4
Specificity	71.4	95.2	90.5	57.1	90.5
PPV	85	95.5	92.6	76.3	94.1
NPV	93.8	58.8	65.5	66.7	86.4
Accuracy	87.5	73.2	78.6	73.2	91.1
CD-related surgery (%)					
Sensitivity	50.0	40.0	50.0	60.0	NA
Specificity	66.7	73.3	73.3	53.3	NA
PPV	50	50.0	55.6	46.2	NA
NPV	66.7	64.7	68.8	66.7	NA
Accuracy	60	60.0	64.0	56.0	NA
UC					
Sensitivity	87.9	60.6	42.4	63.6	92.8
Specificity	100	100	100	83.3	91.7
PPV	100	100	100	91.3	96.8
NPV	75.0	48.0	38.7	45.5	78.6
Accuracy	91.1	71.1	57.8	68.89	91.1

CD: Crohn's disease; UC: Ulcerative colitis; FC: Fecal calprotectin; CDAI/CAI: Clinical activity index; CFA: Clinical FC activity; PPV: Positive predictive value; NPV: Negative predictive value.

FC ( $r = 0.837$ ), followed by CAI ( $r = 0.776$ ), ESR ( $r = 0.644$ ), and CRP ( $r = 0.634$ ) ( $P < 0.001$  for all).

### Correlations of noninvasive evaluations with disease location

Supplementary Table 2 describes the relationship between noninvasive evaluations and disease location in CD and UC patients. According to CD disease location, there were 22 (22.7%) cases with L1 (ileal) disease, 11 (11.3%) with L2 (colonic) disease, and 64 (66%) with L3 (ileo-colonic) disease. There was no significant difference between FC levels and disease location in CD patients ( $P = 0.361$ ). FC also did not differ between those with L2 or L3 disease vs those with L1 disease ( $P = 0.24$ ). In UC patients, extensive colitis UC (E3) was associated with significantly higher FC levels compared with distal colitis (E2;  $P = 0.001$ ) and left-sided colitis (E1;  $P < 0.001$ ) UC patients.

### Specificity, sensitivity, and diagnostic accuracy

The performance data of FC, clinical activity index (CDAI or CAI), CRP, ESR, and CAF in predicting the presence of endoscopic activity in the three categories of IBD patients are listed in Table 6. In CIRD patients, the ROC curves revealed that the AUCs were 0.93 and 0.85 for FC and CDAI, respectively, for the detection of endoscopic active disease, followed by elevated CRP (AUC = 0.81) and ESR (AUC = 0.77), as shown in Supplementary Figure 1A. We tested a FC threshold of 250  $\mu\text{g/g}$ , determined by our previous meta-analysis, to indicate endoscopic remission, with a 97.1% sensitivity and 71.4% specificity (PPV: 85.0%; NPV: 93.8%). As a non-invasive biomarker, FC had

the highest sensitivity, while CDAI had the highest specificity. We also constructed a Spearman's correlation based on the sums of differently emphasized FC, CDAI, CRP, ESR, and PCT. The scores based on the FC and CDAI proved consequently to be superior to other combinations of parameters or FC alone. The highest Spearman's correlation, 0.839, was obtained when using the following score:  $0.8 \times \text{FC} + 4.6 \times \text{CDAI}$ . The sensitivity for this score was 91.4% and the specificity was 90.5%, when using its resulting sum 850 as a cut-off value for endoscopic remission. The coefficients of multiple linear regression models to construct CFA are showed in Supplementary Table 3.

In UC, FC at a cutoff value of 250  $\mu\text{g/g}$  yielded a sensitivity, specificity, PPV, and NPV of 87.9%, 100%, 100%, and 75%, respectively. The ROC curves revealed that the AUCs were 0.96 for FC, 0.88 for CAI, 0.86 for CRP, and 0.81 for ESR, as shown in Supplementary Figure 1B. FC and CAI both had a 100% specificity to predict active mucosal lesion, but CAI had much lower sensitivity. For UC patients, we also constructed the score:  $0.2 \times \text{FC} + 50 \times \text{CAI}$  (Spearman's correlation  $r = 0.868$ ). With a cut-off value of 150, the sensitivity for this score was 92.8% and the specificity was 91.7%. Supplementary Table 3 describes the coefficients of multiple linear regression models to construct CFA.

However, FC, CDAI, CRP, ESR, and PCT were not useful as diagnostic tests for mucosal inflammation in CD-related surgery patients, with AUCs of 0.58 ( $P = 0.52$ ), 0.69 ( $P = 0.11$ ), 0.53 ( $P = 0.82$ ), 0.51 ( $P = 0.93$ ), and 0.49 ( $P = 1.00$ ), respectively. Table 6 shows the sensitivities and specificities of FC, CDAI, CRP, and ESR for the prediction of endoscopic recurrence.

## DISCUSSION

In this study, we found that FC was a more useful noninvasive marker of intestinal inflammation compared with the other evaluations in CIRD and UC patients. However, FC did not discriminate between endoscopic recurrent and remission in CD-related surgery patients, based on the Rutgeerts score. Our data confirmed the findings that IBD could be differentiated from IBS using FC. We also found that both FC and clinical activity index had a good correlation with SES-CD and Mayo score, and a combined score (CFA) of FC with the clinical activity index had better diagnostic accuracy to detect endoscopic active disease. In addition, we demonstrated that considerable IBD patients in clinical remission actually had active endoscopic inflammation, and FC had better diagnostic accuracy in detecting preclinical mucosal inflammation in CIRD and UC patients.

Why the FC was better than the others? Active lesion in IBD was associated with an acute inflammatory reaction and migration of leukocytes to the gut, resulting in considerable protective factors released to blood and stool<sup>[22]</sup>. For CRP in serum, its short half-life made it a valuable biomarker to detect disease activity in IBD, but the low sensitivity to detect active inflammation, especially in UC patients, limited its clinical usage<sup>[23]</sup>. ESR would take several days to respond or decrease when inflammation status was changed, so the ESR also appeared to be a less accurate measure to disease activity in IBD compared with CRP<sup>[22]</sup>. In this study, our results that elevated CRP and ESR had moderate efficiency to detect active endoscopic inflammation in IBD patients are consistent with previous studies. For PCT, to date only two studies, with small sample size, evaluated the correlation between PCT and endoscopic activity score, and controversial results were achieved<sup>[24,25]</sup>. We tested the PCT level and no significant difference was detected in patients with active endoscopic disease in comparison with the three subgroups of IBD patients with inactive disease. This result suggested that PCT is a more specific marker of bacterial infection, however, active IBD mainly involves the disorder of the immune system and defensive deficiency of the mucosa. FC is a surrogate marker of neutrophil turnover in the digestive tract and might become a better biomarker in measuring bowel inflammation for researchers and clinicians<sup>[26]</sup>. Unlike "traditional" serological biological markers, FC had higher specificity for the assessment of gastrointestinal inflammatory conditions. Indeed, IBS patients still had significantly lower levels of FC when compared with IBD patients in endoscopic remission. A high level of FC could be a reliable marker of persistent active microscopic inflammation. FC also had the advantage of showing excellent stability in feces at room temperature, for up to 3 d<sup>[27]</sup>. Those characteristics allowed patients themselves to retrieve samples in their homes and mail them to a hospital

where they were frozen, allowing for batching of samples.

In Western countries, it was reported that FC was a reliable marker of endoscopic activity in both CD and UC. Several prospective population-based studies showed that disease location and disease behavior differed between Western and Asian countries, especially for CD<sup>[3-5,28]</sup>. As CD is characterized by patchy and segmental inflammation, it is not reasonable to use SES-CD to quantify disease activity in small bowel CD and CD-related surgery patients. Schoepfer *et al.*<sup>[17]</sup>, Bjorksten *et al.*<sup>[29]</sup>, Sipponen *et al.*<sup>[30]</sup>, and Vieira *et al.*<sup>[31]</sup> used SES-CD or CDEIS to quantify CD-related surgery patients and ileal CD patients. All of these studies also demonstrated that FC showed a correlation with disease location, but using the SES-CD to quantify disease activity in isolated ileum disease was inappropriate because the small bowel was not accessible to routine endoscopic techniques. Sipponen *et al.* then made an improvement<sup>[32]</sup>: they used the terminal ileal SES-CD to assess the small bowel CD activity. As the terminal ileum was only the window of the small intestine, they failed to correlate FC with terminal ileal SES-CD. Thus, in this study, we assessed only CIRD disease activity using the SES-CD score. Similarly, in the current study, we found that when combining the CIRD patients with the small bowel CD patients, FC appeared to be a more sensitive biomarker in CIRD, with the correlation coefficient increased from 0.692 to 0.802. The cut-off point of FC at 250 µg/g was confirmed in our study by ROC curve analysis with a sensitivity of 97.1%, specificity of 71.4%, and accuracy of 87.5%. In clinical scenario, clinicians should note that 28.6% of endoscopic remission patients would be identified as false positives and receive excessive treatment. Meanwhile, treatment will be delayed in 2.9% of patients with active disease.

On the other hand, previous studies demonstrated that the correlation coefficients between endoscopic activity in UC patients and FC levels ranged from 0.49 to 0.83<sup>[31,33-35]</sup>, probably due to the different endoscopic scores used in those studies. In our study, the Mayo score correlated closely with FC ( $r = 0.837$ ). The accuracy rates of FC  $\geq 250$  µg/g and CAI  $> 4$  to detect endoscopic inflammation were 91.1% and 71.1%, respectively. Because the CAI scores underestimated endoscopic activity and depended almost exclusively on clinical features that were often subjective and non-specific, FC was a more promising marker of endoscopic inflammation in UC patients.

The introduction of immunosuppressive and biological therapies has led to a decline in the rate of IBD-related surgery<sup>[36-38]</sup>. However, the postoperative relapse rates have been reported to be rather high. Accurate monitoring of disease activity is necessary in postoperative IBD patients. Scarpa *et al.*<sup>[36]</sup>, Lamb *et al.*<sup>[37]</sup>, and Lasson *et al.*<sup>[38]</sup> failed to show a correlation between the FC and CD. However, Yamamoto *et al.*<sup>[39]</sup> and Sorrentino *et al.*<sup>[40]</sup> suggested that FC was

a promising marker in postoperative CD patients. Our results suggested that it was not appropriate to predict endoscopic activity using FC in CD-related surgery patients. These varying results might be explained by the different time intervals from the surgical resection and performance of different types of resection. For IBD-related surgery patients, surgeons would resect the severe macroscopic disease and retain the normal function bowel as much as possible. Therefore, considerable patients had no macroscopic anastomotic recurrence, but actually had microscopic inflammation, which would increase the FC concentration. Also, for patients with small bowel resection, the recurrence of disease would more likely involve proximal small bowel instead of anastomosis. Those conditions would result in higher FC level but lower endoscopic activity grade. Thus, we failed to correlate the FC with Rutgeerts score, but those patients with high FC level would easily experience worse prognosis.

Although clinical activity index was subjective in our study, we found that CDAI/CAI had moderate correlation with endoscopy score, which challenged previous observations of poor correlation between clinical activity index and endoscopic score. This might be explained by the fact that we separated the small bowel CD and CD-related surgery patients from CIBD patients. For assessing endoscopic activity, FC had the highest sensitivity, while CDAI had the highest specificity in CIBD patients. Meanwhile, FC and CAI both had a 100% specificity to predict active mucosal lesion in UC patients, but CAI had much lower sensitivity. Clearly, no one parameter clearly outperformed the other. Thus, it is of interest to consider a comprehensive index which may allow clinicians to more reliably assess the ileo-colonoscopy inflammation. We developed a combined score (CFA) based on FC and CDAI/CAI in CIBD and UC patients. The sensitivity for CFA was 91.4% and the specificity was 90.5%, when using its resulting sum 850 as a cut-off value for endoscopic remission in CIBD patients. With a cut-off value of 150, the sensitivity for this score was 92.8% and the specificity was 91.7% in UC patients. In both groups, CFA had higher accuracy to identify endoscopic active disease than the FC and CDAI/CAI separately. Clinicians could identify endoscopic active disease more accurately with CFA through a short inquiry and a FC test.

Emerging data show that remission of symptoms in IBD patients may not indicate remission of mucosal inflammation at endoscopy<sup>[41,42]</sup>. In our cohort, in the three subgroups of IBD patients in clinical remission, 41% of CIBD patients, 36.8% of CD-related surgery patients, and 52% of UC patients had active endoscopic inflammation. The sensitivities of CDAI > 150 and CAI > 4 were 60.0% and 60.6%, respectively, to detect active endoscopic inflammation. Thus, the clinical activity index underestimated the endoscopic inflammation. However, current ECCO guidelines

emphasize that routine endoscopy for IBD patients in clinical remission is unnecessary, unless it is likely to change patient management<sup>[12]</sup>. In this setting, defining IBD disease activity using FC might discriminate between those who have preclinical relapse and those with quiescent IBD, or to protect those who dissimulate against themselves. One previous study investigated FC as a marker of inflammation in 48 IBD patients in clinical remission<sup>[43]</sup>. FC levels above a cut-off of 30 µg/g indicated endoscopic inflammation with a 93.7% sensitivity and 50% specificity. We separately analyzed the CD and UC patients with an acknowledged cut-off value of 250 µg/g, and found that FC was higher in patients with active disease (93% sensitivity/70% specificity for SES-CD ≥ 4 and 86.4% sensitivity/100% specificity for Mayo score ≥ 3), confirming the value of FC in IBD patients in clinical remission. As a screening tool in IBD patients in clinical remission, FC could be measured frequently to detect preclinical mucosal inflammation and guide clinicians timely change their clinical regimen.

Our study had several limitations. First, to more accurately reflect the efficacy of FC, we categorized IBD patients into three subgroups, resulting in a relatively small number of patients in each subgroup. Second, because of the design of the study, we did not analyze small bowel CD patients' mucosal inflammation activity; thus, our results could not be extrapolated to small bowel CD patients. Also, the number of patients with purely ileal disease and colonic CD was limited, and we failed to detect a difference in FC levels according to disease location in CD patients, which thus needs to be further explored. Finally, the cut-off values for FC needs to be further explored. The difference between manufacture assays, heterogeneous operating conditions, no consensus definitions of endoscopic remission, and different patient spectrum could be accounted for when trying to define the optimal cut point. The optimal cut point may be different depending on if you are using this as a triage tool or as the final assessment for active disease. Thus, it may not be possible to set "an optimal cut point" for all scenarios and clinicians should form their own optimal cut-off value when implementing FC in clinical activity.

In conclusion, FC is the most promising noninvasive marker than the others for assessing mucosal inflammation in CIBD and UC patients, but not in CD-related surgery patients. Furthermore, CFA calculated as  $0.8 \times FC + 4.6 \times CDAI$  for colonic (ileo-colonic) CD or  $0.2 \times FC + 50 \times CAI$  for UC patients might be more accurate for IBD activity evaluation. FC also has the ability to detect active residual mucosal inflammation in IBD patients in clinical remission to guide clinicians to timely change their clinical regimen. With the increasing recognition of the clinical value of biomarkers, the next step is implementation of marker-guided treatment in patients with IBD. To achieve this, we should attempt to

improve the standardization of pre-analytical procedures and further clinical trials are warranted to demonstrate its value in clinical practice.

## ARTICLE HIGHLIGHTS

### Research background

Inflammatory bowel disease (IBD) is characterized by periods of relapsing-remitting. At present, most clinicians monitor IBD activity and guide therapeutic decisions based on clinical activity indexes. However, emerging data show that clinical assessment indexes correlate poorly with endoscopic activity and IBD patients with clinically quiescent disease may still have residual mucosal inflammation. An endoscopic procedure is considered the gold standard for assessing disease activity. However, the endoscopy is invasive, uncomfortable, and expensive.

### Research motivation

A simple, acceptable, and specific evaluation is needed to play an adjunctive role in the assessment of IBD activity. The specific and noninvasive evaluation could instruct clinicians to timely choose reasonable therapy regimen and predict prognosis. Furthermore, a new evaluation that can detect increased disease activity earlier before any clinical symptoms have occurred could change disease course, enabling the most cost-effective use of medical resources.

### Research objectives

The main objective of this study was to assess the efficacy of noninvasive evaluations for the disease activity in colonic or ileo-colonic Crohn's disease (CICD), CD-related surgery, and ulcerative colitis (UC) patients and further to optimize the accuracy of those noninvasive evaluations in detecting active residual mucosal inflammation in IBD patients in clinical remission. In our study we confirmed the efficacy of fecal calprotectin (FC) and the new clinical FC activity (CFA) in assessing disease activity in CICD and UC patients. In future, clinicians and researchers could use FC to recognize an imminent endoscopic flare. What's more, FC could be measured frequently as a clinical activity index to detect preclinical mucosal inflammation in clinical remission patients.

### Research methods

In total, 136 consecutive IBD patients and 25 recruited IBS patients were enrolled. For all IBD patients, the day before the endoscopy, fecal and blood samples were collected to measure FC, CRP, ESR, and PCT. At the same time, the patients were asked to complete a case report to calculate their clinical activity index (CDAI/CAI). Then, endoscopic activity was determined for CICD patients with the "simple endoscopic score for Crohn's disease" (SES-CD), CD-related surgery patients with the Rutgeerts score, and UC patients with the Mayo score. The efficacies of these evaluations to predict the endoscopic activity were assessed by Mann-Whitney test,  $\chi^2$  test, Spearman's correlation, and multiple linear regression analysis. In our study, multiple linear regression analysis with stepwise deletion was performed based on FC, CDAI/CAI, CRP, ESR, and PCT to construct a combined score, clinical FC activity (CFA), which could best predict the endoscopy activity. In clinical scenario, clinicians could identify endoscopic active disease more accurately with CFA through a short inquiry and a FC test.

### Research results

We found that FC and clinical FC activity (CFA) are useful, non-invasive, and sensitive stool markers for gut inflammation in both CICD and UC patients. However, the standard collection of fecal sample and best cutoff to predict endoscopic activity are needed to be solved.

### Research conclusions

This was the first study performed in China for disease activity analysis in the three groups of IBD patients separately. We also constructed a clinical FC activity (CFA) index to more accurately assess disease activity. Moreover, we found that FC had ability to detect active residual mucosal inflammation in IBD patients in clinical remission. Indeed, we also found that IBD patients in endoscopic remission still had significantly higher levels of FC when compared

with IBS patients. A high level of FC could be a reliable marker of persistent active microscopic inflammation. Then FC remission may indicate deep remission at histopathology level, which was proven to be a strong predictor of favorable prognosis in IBD. In future, the next step is to use FC to guide the clinicians to adjust the treatment regimen. We can schedule regular FC measurement and compare the change from baseline level to reflect the degree of response to treatment.

### Research perspectives

In our study, we confirmed the efficacy of FC in assessing disease activity in IBD patients. In future, we recommend periodic FC measurements instead of a single measurement in monitoring disease activity and deciding the treatment regimen. The clinical remission and biomarker healing could be the new therapeutic goals in IBD patients. To achieve those goals, multicenter, large-sample, randomized clinical trials are warranted to prove their value in clinical practice.

## REFERENCES

- 1 **Xavier RJ**, Podolsky DK. Unravelling the pathogenesis of inflammatory bowel disease. *Nature* 2007; **448**: 427-434 [PMID: 17653185 DOI: 10.1038/nature06005]
- 2 **Ananthakrishnan AN**, Weber LR, Knox JF, Skaros S, Emmons J, Lundeen S, Issa M, Otterson MF, Binion DG. Permanent work disability in Crohn's disease. *Am J Gastroenterol* 2008; **103**: 154-161 [PMID: 18076736 DOI: 10.1111/j.1572-0241.2007.01561.x]
- 3 **Ng SC**, Tang W, Ching JY, Wong M, Chow CM, Hui AJ, Wong TC, Leung VK, Tsang SW, Yu HH, Li MF, Ng KK, Kamm MA, Studd C, Bell S, Leong R, de Silva HJ, Kasturiratne A, Mufeen MN, Ling KL, Ooi CJ, Tan PS, Ong D, Goh KL, Hilmi I, Pisespong P, Manatsathit S, Rerknimitr R, Aniwang S, Wang YF, Ouyang Q, Zeng Z, Zhu Z, Chen MH, Hu PJ, Wu K, Wang X, Simadibrata M, Abdullah M, Wu JC, Sung JJ, Chan FK; Asia-Pacific Crohn's and Colitis Epidemiologic Study (ACCESS) Study Group. Incidence and phenotype of inflammatory bowel disease based on results from the Asia-Pacific Crohn's and colitis epidemiology study. *Gastroenterology* 2013; **145**: 158-165.e2 [PMID: 23583432 DOI: 10.1053/j.gastro.2013.04.007]
- 4 **Zhao J**, Ng SC, Lei Y, Yi F, Li J, Yu L, Zou K, Dan Z, Dai M, Ding Y, Song M, Mei Q, Fang X, Liu H, Shi Z, Zhou R, Xia M, Wu Q, Xiong Z, Zhu W, Deng L, Kamm MA, Xia B. First prospective, population-based inflammatory bowel disease incidence study in mainland of China: the emergence of "western" disease. *Inflamm Bowel Dis* 2013; **19**: 1839-1845 [PMID: 23669403 DOI: 10.1097/MIB.0b013e31828a6551]
- 5 **Zeng Z**, Zhu Z, Yang Y, Ruan W, Peng X, Su Y, Peng L, Chen J, Yin Q, Zhao C, Zhou H, Yuan S, Hao Y, Qian J, Ng SC, Chen M, Hu P. Incidence and clinical characteristics of inflammatory bowel disease in a developed region of Guangdong Province, China: a prospective population-based study. *J Gastroenterol Hepatol* 2013; **28**: 1148-1153 [PMID: 23432198 DOI: 10.1111/jgh.12164]
- 6 **Schoepfer AM**, Vavricka S, Zahnd-Straumann N, Straumann A, Beglinger C. Monitoring inflammatory bowel disease activity: clinical activity is judged to be more relevant than endoscopic severity or biomarkers. *J Crohns Colitis* 2012; **6**: 412-418 [PMID: 22398068 DOI: 10.1016/j.crohns.2011.09.008]
- 7 **Baars JE**, Nuij VJ, Oldenburg B, Kuipers EJ, van der Woude CJ. Majority of patients with inflammatory bowel disease in clinical remission have mucosal inflammation. *Inflamm Bowel Dis* 2012; **18**: 1634-1640 [PMID: 22069022 DOI: 10.1002/ibd.21925]
- 8 **Berrill JW**, Green JT, Hood K, Campbell AK. Symptoms of irritable bowel syndrome in patients with inflammatory bowel disease: examining the role of sub-clinical inflammation and the impact on clinical assessment of disease activity. *Aliment Pharmacol Ther* 2013; **38**: 44-51 [PMID: 23668698 DOI: 10.1111/apt.12335]
- 9 **af Björkstén CG**, Nieminen U, Sipponen T, Turunen U, Arkkila P, Färkkilä M. Mucosal healing at 3 months predicts long-term



- endoscopic remission in anti-TNF-treated luminal Crohn's disease. *Scand J Gastroenterol* 2013; **48**: 543-551 [PMID: 23477356 DOI: 10.3109/00365521.2013.772230]
- 10 **Frøslie KF**, Jahnsen J, Moum BA, Vatn MH; IBSEN Group. Mucosal healing in inflammatory bowel disease: results from a Norwegian population-based cohort. *Gastroenterology* 2007; **133**: 412-422 [PMID: 17681162 DOI: 10.1053/j.gastro.2007.05.051]
  - 11 **Meucci G**, Fasoli R, Saibeni S, Valpiani D, Gullotta R, Colombo E, D'Inca R, Terpin M, Lombardi G; IG-IBD. Prognostic significance of endoscopic remission in patients with active ulcerative colitis treated with oral and topical mesalazine: a prospective, multicenter study. *Inflamm Bowel Dis* 2012; **18**: 1006-1010 [PMID: 21830282 DOI: 10.1002/ibd.21838]
  - 12 **Annese V**, Daperno M, Rutter MD, Amiot A, Bossuyt P, East J, Ferrante M, Götz M, Katsanos KH, Kiebllich R, Ordás I, Repici A, Rosa B, Sebastian S, Kucharzik T, Eliakim R; European Crohn's and Colitis Organisation. European evidence based consensus for endoscopy in inflammatory bowel disease. *J Crohns Colitis* 2013; **7**: 982-1018 [PMID: 24184171 DOI: 10.1016/j.crohns.2013.09.016]
  - 13 **van Deen WK**, van Oijen MG, Myers KD, Centeno A, Howard W, Choi JM, Roth BE, McLaughlin EM, Hollander D, Wong-Swanson B, Sack J, Ong MK, Ha CY, Esrailian E, Hommes DW. A nationwide 2010-2012 analysis of U.S. health care utilization in inflammatory bowel diseases. *Inflamm Bowel Dis* 2014; **20**: 1747-1753 [PMID: 25137415 DOI: 10.1097/MIB.0000000000000139]
  - 14 **Gauss A**, Geib T, Hinz U, Schaefer R, Zwickel P, Zawierucha A, Stremmel W, Klute L. Quality of Life Is Related to Fecal Calprotectin Concentrations in Colonic Crohn Disease and Ulcerative Colitis, but not in Ileal Crohn Disease. *Medicine (Baltimore)* 2016; **95**: e3477 [PMID: 27100452 DOI: 10.1097/MD.0000000000000347]
  - 15 **Bodelier AG**, Jonkers D, van den Heuvel T, de Boer E, Hameeteman W, Masclee AA, Pierik MJ. High Percentage of IBD Patients with Indefinite Fecal Calprotectin Levels: Additional Value of a Combination Score. *Dig Dis Sci* 2017; **62**: 465-472 [PMID: 27933473 DOI: 10.1007/s10620-016-4397-6]
  - 16 **Daperno M**, D'Haens G, Van Assche G, Baert F, Bulois P, Maunoury V, Sostegni R, Rocca R, Pera A, Gevers A, Mary JY, Colombel JF, Rutgeerts P. Development and validation of a new, simplified endoscopic activity score for Crohn's disease: the SES-CD. *Gastrointest Endosc* 2004; **60**: 505-512 [PMID: 15472670 DOI: 10.1016/S0016-5107(04)01878-4]
  - 17 **Schoepfer AM**, Beglinger C, Straumann A, Trummel M, Vavricka SR, Bruegger LE, Seibold F. Fecal calprotectin correlates more closely with the Simple Endoscopic Score for Crohn's disease (SES-CD) than CRP, blood leukocytes, and the CDAI. *Am J Gastroenterol* 2010; **105**: 162-169 [PMID: 19755969 DOI: 10.1038/ajg.2009.545]
  - 18 **Rutgeerts P**, Geboes K, Vantrappen G, Beyls J, Kerremans R, Hiele M. Predictability of the postoperative course of Crohn's disease. *Gastroenterology* 1990; **99**: 956-963 [PMID: 2394349 DOI: 10.1016/0016-5085(90)90613-6]
  - 19 **Schroeder KW**, Tremaine WJ, Ilstrup DM. Coated oral 5-aminosalicylic acid therapy for mildly to moderately active ulcerative colitis. A randomized study. *N Engl J Med* 1987; **317**: 1625-1629 [PMID: 3317057 DOI: 10.1056/NEJM198712243172603]
  - 20 **Best WR**, Beckett JM, Singleton JW, Kern F Jr. Development of a Crohn's disease activity index. National Cooperative Crohn's Disease Study. *Gastroenterology* 1976; **70**: 439-444 [PMID: 1248701]
  - 21 **Rachmilewitz D**. Coated mesalazine (5-aminosalicylic acid) versus sulphasalazine in the treatment of active ulcerative colitis: a randomised trial. *BMJ* 1989; **298**: 82-86 [PMID: 2563951 DOI: 10.1136/bmj.298.6666.82]
  - 22 **Vermeire S**, Van Assche G, Rutgeerts P. Laboratory markers in IBD: useful, magic, or unnecessary toys? *Gut* 2006; **55**: 426-431 [PMID: 16474109 DOI: 10.1136/gut.2005.069476]
  - 23 **Saverymutter SH**, Hodgson HJ, Chadwick VS, Pepys MB. Differing acute phase responses in Crohn's disease and ulcerative colitis. *Gut* 1986; **27**: 809-813 [PMID: 3732890 DOI: 10.1136/gut.27.7.809]
  - 24 **Oussalah A**, Laurent V, Bruot O, Guéant JL, Régent D, Bigard MA, Peyrin-Biroulet L. Additional benefit of procalcitonin to C-reactive protein to assess disease activity and severity in Crohn's disease. *Aliment Pharmacol Ther* 2010; **32**: 1135-1144 [PMID: 21039675 DOI: 10.1111/j.1365-2036.2010.04459.x]
  - 25 **Koido S**, Ohkusa T, Takakura K, Odahara S, Tsukinaga S, Yukawa T, Mitobe J, Kajihara M, Uchiyama K, Arakawa H, Tajiri H. Clinical significance of serum procalcitonin in patients with ulcerative colitis. *World J Gastroenterol* 2013; **19**: 8335-8341 [PMID: 24363525 DOI: 10.3748/wjg.v19.i45.8335]
  - 26 **Summerton CB**, Longlands MG, Wiener K, Shreeve DR. Faecal calprotectin: a marker of inflammation throughout the intestinal tract. *Eur J Gastroenterol Hepatol* 2002; **14**: 841-845 [PMID: 12172403 DOI: 10.1097/00042737-200208000-00005]
  - 27 **Burri E**, Beglinger C. IBD: Faecal calprotectin testing--the need for better standardization. *Nat Rev Gastroenterol Hepatol* 2014; **11**: 583-584 [PMID: 25201042 DOI: 10.1038/nrgastro.2014.154]
  - 28 **Vester-Andersen MK**, Prosberg MV, Jess T, Andersson M, Bengtsson BG, Blixt T, Munkholm P, Bendtsen F, Vind I. Disease course and surgery rates in inflammatory bowel disease: a population-based, 7-year follow-up study in the era of immunomodulating therapy. *Am J Gastroenterol* 2014; **109**: 705-714 [PMID: 24642581 DOI: 10.1038/ajg.2014.45]
  - 29 **af Björkstén CG**, Nieminen U, Turunen U, Arkkila P, Sipponen T, Färkkilä M. Surrogate markers and clinical indices, alone or combined, as indicators for endoscopic remission in anti-TNF-treated luminal Crohn's disease. *Scand J Gastroenterol* 2012; **47**: 528-537 [PMID: 22356594 DOI: 10.3109/00365521.2012.660542]
  - 30 **Sipponen T**, Savilahti E, Kolho KL, Nuutinen H, Turunen U, Färkkilä M. Crohn's disease activity assessed by fecal calprotectin and lactoferrin: correlation with Crohn's disease activity index and endoscopic findings. *Inflamm Bowel Dis* 2008; **14**: 40-46 [PMID: 18022866 DOI: 10.1002/ibd.20312]
  - 31 **Vieira A**, Fang CB, Rolim EG, Klug WA, Steinwurz F, Rossini LG, Candelária PA. Inflammatory bowel disease activity assessed by fecal calprotectin and lactoferrin: correlation with laboratory parameters, clinical, endoscopic and histological indexes. *BMC Res Notes* 2009; **2**: 221 [PMID: 19874614 DOI: 10.1186/1756-0500-2-221]
  - 32 **Sipponen T**, Kärkkäinen P, Savilahti E, Kolho KL, Nuutinen H, Turunen U, Färkkilä M. Correlation of faecal calprotectin and lactoferrin with an endoscopic score for Crohn's disease and histological findings. *Aliment Pharmacol Ther* 2008; **28**: 1221-1229 [PMID: 18752630 DOI: 10.1111/j.1365-2036.2008.03835.x]
  - 33 **Schoepfer AM**, Beglinger C, Straumann A, Trummel M, Renzulli P, Seibold F. Ulcerative colitis: correlation of the Rachmilewitz endoscopic activity index with fecal calprotectin, clinical activity, C-reactive protein, and blood leukocytes. *Inflamm Bowel Dis* 2009; **15**: 1851-1858 [PMID: 19462421 DOI: 10.1002/ibd.20986]
  - 34 **Schoepfer AM**, Beglinger C, Straumann A, Safroneeva E, Romero Y, Armstrong D, Schmidt C, Trummel M, Pittet V, Vavricka SR. Fecal calprotectin more accurately reflects endoscopic activity of ulcerative colitis than the Lichtiger Index, C-reactive protein, platelets, hemoglobin, and blood leukocytes. *Inflamm Bowel Dis* 2013; **19**: 332-341 [PMID: 23328771 DOI: 10.1097/MIB.0b013e3182810066]
  - 35 **Önal İK**, Beyazit Y, Şener B, Savuk B, Özer Etik D, Sayilir A, Öztaş E, Torun S, Özderin Özün Y, Tunç Demirel B, Ülker A, Dağlı Ü. The value of fecal calprotectin as a marker of intestinal inflammation in patients with ulcerative colitis. *Turk J Gastroenterol* 2012; **23**: 509-514 [PMID: 23161295 DOI: 10.4318/tjg.2012.0421]
  - 36 **Scarpa M**, D'Inca R, Basso D, Ruffolo C, Polese L, Bertin E, Luise A, Frego M, Plebani M, Sturmiolo GC, D'Amico DF, Angriman I. Fecal lactoferrin and calprotectin after ileocolonic resection for Crohn's disease. *Dis Colon Rectum* 2007; **50**: 861-869 [PMID: 17473939 DOI: 10.1007/s10350-007-0225-6]

- 37 **Lamb CA**, Mohiuddin MK, Gicquel J, Neely D, Bergin FG, Hanson JM, Mansfield JC. Faecal calprotectin or lactoferrin can identify postoperative recurrence in Crohn's disease. *Br J Surg* 2009; **96**: 663-674 [PMID: 19384912 DOI: 10.1002/bjs.6593]
  - 38 **Lasson A**, Strid H, Ohman L, Isaksson S, Olsson M, Rydström B, Ung KA, Stotzer PO. Fecal calprotectin one year after ileocaecal resection for Crohn's disease--a comparison with findings at ileocolonoscopy. *J Crohns Colitis* 2014; **8**: 789-795 [PMID: 24418661 DOI: 10.1016/j.crohns.2013.12.015]
  - 39 **Yamamoto T**, Shiraki M, Bamba T, Umegae S, Matsumoto K. Faecal calprotectin and lactoferrin as markers for monitoring disease activity and predicting clinical recurrence in patients with Crohn's disease after ileocolonic resection: A prospective pilot study. *United European Gastroenterol J* 2013; **1**: 368-374 [PMID: 24917985 DOI: 10.1177/2050640613501818]
  - 40 **Sorrentino D**, Paviotti A, Terrosu G, Avellini C, Geraci M, Zarifi D. Low-dose maintenance therapy with infliximab prevents postsurgical recurrence of Crohn's disease. *Clin Gastroenterol Hepatol* 2010; **8**: 591-599.e1; quiz e78-79 [PMID: 20139033 DOI: 10.1016/j.cgh.2010.01.016]
  - 41 **Ferreiro-Iglesias R**, Barreiro-de Acosta M, Lorenzo-Gonzalez A, Dominguez-Muñoz JE. Accuracy of Consecutive Fecal Calprotectin Measurements to Predict Relapse in Inflammatory Bowel Disease Patients Under Maintenance With Anti-TNF Therapy: A Prospective Longitudinal Cohort Study. *J Clin Gastroenterol* 2016; Epub ahead of print [PMID: 27984399 DOI: 10.1097/MCG.0000000000000774]
  - 42 **Assa A**, Bronsky J, Kolho KL, Zarubova K, de Meij T, Ledder O, Sladek M, van Biervliet S, Strisciuglio C, Shamir R. Anti-TNF $\alpha$  Treatment After Surgical Resection for Crohn's Disease Is Effective Despite Previous Pharmacodynamic Failure. *Inflamm Bowel Dis* 2017; **23**: 791-797 [PMID: 28426458 DOI: 10.1097/MIB.0000000000001050]
  - 43 **Voiosu T**, Benguş A, Dinu R, Voiosu AM, Bălănescu P, Băicuş C, Diculescu M, Voiosu R, Mateescu B. Rapid fecal calprotectin level assessment and the SIBDQ score can accurately detect active mucosal inflammation in IBD patients in clinical remission: a prospective study. *J Gastrointest Liver Dis* 2014; **23**: 273-278 [PMID: 25267955]
- P- Reviewer:** Jadallah KA, Manguso F, Sergi CM    **S- Editor:** Gong ZM    **L- Editor:** Wang TQ    **E- Editor:** Ma YJ



## Are liver nested stromal epithelial tumors always low aggressive?

Tania Meletani, Luca Cantini, Andrea Lanese, Daniele Nicolini, Alessia Cimagamore, Andrea Agostini, Giulia Ricci, Stefania Antognoli, Alessandra Mandolesi, Maria Guido, Rita Alaggio, Gian Marco Giuseppetti, Marina Scarpelli, Marco Vivarelli, Rossana Berardi

Tania Meletani, Luca Cantini, Andrea Lanese, Giulia Ricci, Stefania Antognoli, Rossana Berardi, Medical Oncology, University Hospital and Polytechnic University Ancona, 60126 Marche, Italy

Daniele Nicolini, Marco Vivarelli, Hepatobiliary and Transplantation Surgery, Department of Clinical and Experimental Medicine, University Hospital and Polytechnic University Ancona, 60126 Marche, Italy

Alessia Cimagamore, Alessandra Mandolesi, Marina Scarpelli, Section of Pathological Anatomy, Department of Biomedical Sciences and Public Health, University Hospital and Polytechnic University Ancona, 60126 Marche, Italy

Andrea Agostini, Gian Marco Giuseppetti, Department of Radiology, University Hospital and Polytechnic University Ancona, 60126 Marche, Italy

Maria Guido, Rita Alaggio, Pathology Department, Padova University, 35121 Padova, Italy

ORCID number: Tania Meletani (0000-0002-2641-0417); Luca Cantini (0000-0002-6294-4758); Andrea Lanese (0000-0002-3790-7031); Daniele Nicolini (0000-0002-5477-3346); Alessia Cimagamore (0000-0001-5981-3514); Andrea Agostini (0000-0002-0693-8257); Giulia Ricci (0000-0002-7262-7481); Stefania Antognoli (0000-0001-5234-9544); Alessandra Mandolesi (0000-0002-5297-3061); Maria Guido (0000-0002-8558-0723); Rita Alaggio (0000-0003-3915-3816); Gian Marco Giuseppetti (0000-0001-9373-5134); Marina Scarpelli (0000-0002-8815-1844); Marco Vivarelli (0000-0001-8982-2163); Rossana Berardi (0000-0002-9529-2960).

**Author contributions:** Meletani T, Cantini L, Lanese A, Giuseppetti GM, Vivarelli M and Berardi R designed the report; Cimagamore A, Mandolesi A, Guido M, Alaggio R and Scarpelli M performed the pathological analyses; Ricci G and Antognoli S collected the patient's clinical data; Meletani T, Cantini L, Lanese A, Nicolini D, Cimagamore A and Agostini A analyzed the data

and wrote the paper.

**Institutional review board statement:** The study was reviewed and approved by the local Ethical Committee.

**Informed consent statement:** The patient involved in this study gave verbal informed consent authorizing the use and disclosure of his protected health information.

**Conflict-of-interest statement:** All authors declare having no conflicting interest.

**Open-Access:** This article is an open-access article which was selected by an in-house editor and fully peer-reviewed by external reviewers. It is distributed in accordance with the Creative Commons Attribution Non Commercial (CC BY-NC 4.0) license, which permits others to distribute, remix, adapt, build upon this work non-commercially, and license their derivative works on different terms, provided the original work is properly cited and the use is non-commercial. See: <http://creativecommons.org/licenses/by-nc/4.0/>

**Manuscript source:** Unsolicited manuscript

**Correspondence to:** Rossana Berardi, MD, Head of Department of Medical Oncology, Director of the Postgraduate School of Medical Oncology, Director of "Genetic Cancer" Center, Deputy Director of Department of Clinical and Molecular Science, University Hospital Ospedali Riuniti Umberto I - GM Lancisi - G Salesi and Polytechnic University Ancona, via conca 71, 60126 Marche, Italy. [r.berardi@univpm.it](mailto:r.berardi@univpm.it)  
Telephone: +39-71-5964169  
Fax: +39-71-65964192

**Received:** June 20, 2017

**Peer-review started:** June 22, 2017

**First decision:** July 13, 2017

**Revised:** July 27, 2017

**Accepted:** August 25, 2017

**Article in press:** August 25, 2017

**Published online:** December 14, 2017

## Abstract

Nested stromal-epithelial tumor (NSET) is a non-hepatocytic and non-biliary tumor of the liver consisting of nests of epithelial and spindled cells with associated myofibroblastic stroma and variable intra-lesional calcification and ossification, which represents a very rare and challenging disease. Most of the reported cases have been treated with surgery, obtaining a long survival outcome. Here, we report the case of a 31-year-old Caucasian man who underwent surgery at our institution for a large, lobulated, multinodular mass of the right hemi-liver. The histological exam confirmed the diagnosis of NSET. After 6 mo from surgery, a liver recurrence was described and a chemo-embolization was performed. After a further disease progression, based on the correlation between the histological features of the disease and those of the hepatoblastoma, a similar chemotherapy regimen (with cisplatin and ifosfamide/mesna chemotherapy, omitting doxorubicin due to liver impairment) was administered. However, infection of the biliary catheter required a dose modification of the treatment. No benefit was noted and a progression of disease was radiologically assessed after only four cycles. The worsening of the clinical status prevented further treatments, and the patient died a few months later. This case report documents how the NSET might have an aggressive and non-preventable behavior. No chemotherapy schedules with a proved efficacy are available, and new data are needed to shed light on this rare neoplasm.

**Key words:** Nested stromal epithelial tumor; Liver; Rare; Chemotherapy; Aggressive; Metastatic

© The Author(s) 2017. Published by Baishideng Publishing Group Inc. All rights reserved.

**Core tip:** Nested stromal-epithelial tumor (NSET) of the liver is a very rare type of cancer, few cases have been reported in the world. Most of the literature described a low tendency of relapse, the majority of the reported cases have been treated with surgery, obtaining a long survival outcome. Our patient developed a more aggressive disease, which relapsed soon after surgery, and progressed after first line chemotherapy. We aimed to update the literature about NEST, especially in patients with either metastatic or recurrent disease, for whom no standard treatment is currently available.

Meletani T, Cantini L, Lanese A, Nicolini D, Cimadamore A, Agostini A, Ricci G, Antognoli S, Mandolesi A, Guido M, Alaggio R, Giuseppetti GM, Scarpelli M, Vivarelli M, Berardi R. Are liver nested stromal epithelial tumors always low aggressive? *World J Gastroenterol* 2017; 23(46): 8248-8255 Available from: URL: <http://www.wjgnet.com/1007-9327/full/v23/i46/8248.htm> DOI: <http://dx.doi.org/10.3748/wjg.v23.i46.8248>

## INTRODUCTION

Nested stromal-epithelial tumor (NSET) of the liver is a very rare type of cancer<sup>[1]</sup>, with few cases diagnosed worldwide. It usually affects young people with age range from 1 to 34 years<sup>[2]</sup> and no sex preference. Cushing syndrome is often the presenting symptom of this neoplasm<sup>[2-4]</sup>.

The right liver lobe is mostly involved, with a well-circumscribed, large mass characterized by calcification at the computer tomography (CT) scan imaging<sup>[1]</sup>. Histological features include circumscribed nests and islands of bland-appearing spindled to focally epithelioid cells, surrounded by a cellular desmoplastic stroma, with non-hepatocytic and non-biliary duct characteristics<sup>[5]</sup>.

Here, we present a clinical case of a patient with NSET, with the aim of sharing our experience.

## CASE REPORT

### Diagnosis and surgery

In March 2015, a 31-year-old Caucasian man presented at the Surgery Department complaining of weight loss (approximately 5% of body weight during the previous 2 mo) and abdominal pain. His father underwent liver resection for unspecified liver neoplasm 12 years before but no other significant family history of illness or tumor emerged. The patient had no history of alcohol abuse or hepatitis; he had been followed for arterial hypertension and treated with ramipril and nebivolol.

Physical examination revealed a palpable large abdominal mass in the right upper quadrant, with no evidence of ascites or splenomegaly. Laboratory findings revealed a high level of gamma-glutamyl transferase (349 U/L) and a mild leukocytosis ( $13.8 \times 10^3$  cells/mm<sup>3</sup>); serology findings for hepatitis B and C, autoimmune hepatitis and human immunodeficiency virus were negative. Serum findings for alpha-fetoprotein (AFP), carcinoembryonic antigen (CEA) and carbohydrate antigen (CA) 19-9 were within normal range.

The CT scan showed a large, lobulated, multinodular mass (22 cm × 13 cm × 25 cm), with few round calcifications mainly in the central part, involving entirely the right hemi-liver, partially the Couinaud's segment 4, and the caudate lobe. After administration of iodinated contrast material, the tumor showed non-homogeneous, early enhancement in the arterial phase, with subsequent washout in the portal and delayed phases. The CT images also demonstrated an extensive infiltration of the right portal branch and of the right and middle hepatic veins, with a consequent spontaneous hypertrophy of the left lobe (Figure 1).

The surgical procedure, consisting of a virtual



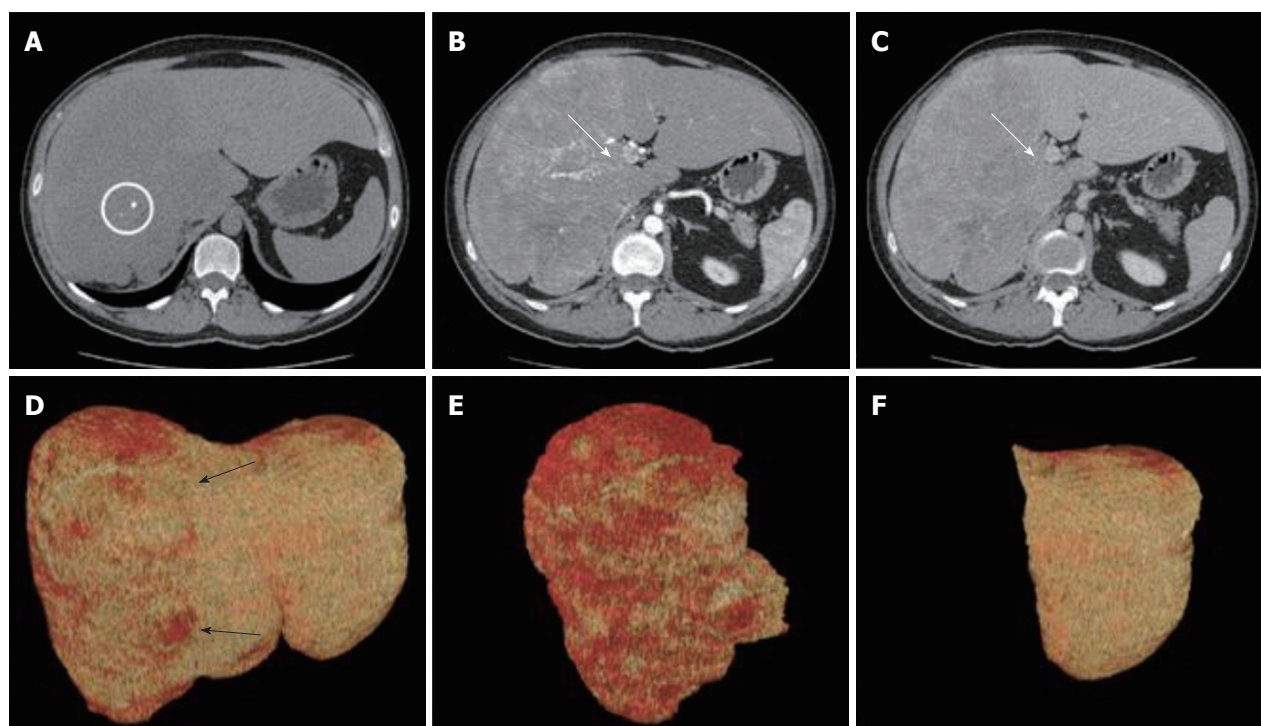


**Figure 1** Computer tomography examination and virtual resection. A: Pre-contrast acquisition, axial image cranial to the hilar plane showing a large, hypo-attenuating lobulated lesion involving the right hemi-liver and part of the segment 4 (white circle: calcification within the neoplastic lesion); B and C: Axial images across the hilar plane during arterial (B) and portal (C) phase. Then neoplastic, lobulated lesion shows early arterial enhancement resulting in hypo-attenuation during the portal phase. The right portal branch is not visible due to neoplastic infiltration (white arrows); D-F: Virtual resection, volume renderings of CT images; D: Total liver volume; the non-homogenous red color of the right hemi-liver corresponds to the lesion (black arrows); E: Tumor lesion; F: Future remnant liver corresponding to segments 2 and 3.

resection, was planned<sup>[6]</sup>. The quantitative analysis of CT images showed a total liver volume of 5797 cm<sup>3</sup> and a tumor volume of 3879 cm<sup>3</sup> with a hypertrophic remnant left liver lobe (Couinaud's segments II and III) of 1329 cm<sup>3</sup>. The future liver remnant, thus, was 69%, markedly over the safe cut-off<sup>[6]</sup>. Based on these radiological findings, a right trisectionectomy extending to the caudate lobe was proposed.

On laparotomy, careful exploration of the abdominal cavity ruled out no extra-hepatic manifestations; intraoperative ultrasound revealed another 2 cm nodule in segment II. The remaining left lobe did not show any histological alterations at intraoperative biopsy. Hepatoduodenal ligament was dissected to isolate and ligate the right hepatic artery, portal vein and bile duct as well as the biliary and vascular elements for segments IV and I (Figure 2). After transection of the right portal vein, that appeared infiltrated by the tumor, the hepatic parenchyma was dissected between segments II/III and segment IV by using Cavitron ultrasonic surgical aspirator and argon diathermy. Afterwards, the nodule at the hepatic segment II was treated by radiofrequency ablation.

Postoperative course was uneventful, except for a 4.5 cm fluid collection on the cut surface of the liver that was successfully treated by percutaneous

drainage. The patient was discharged on postoperative day 21 with a completely preserved liver function.

### Pathological features

**Gross appearance:** The right hepatic lobe was almost entirely occupied by a multinodular mass with homogeneous whitish cut surface, partial necrosis and calcifications. The lesion had a greatest diameter of 19 cm and was 0.5 mm far from the surgical margin (Figure 3).

### Microscopic and immunohistochemical features:

Histologically, the neoplasm showed an organoid arranged tumor of well-defined nests of epithelioid and spindle cells with focal necrosis, surrounded by hypercellular stroma with areas of osseous metaplasia and calcifications. The cellular nests were oval, elongated, and irregular with rounded edges. The epithelioid part of the tumor was composed of monomorphous polygonal and spindle-shaped cells, round to oval nuclei with finely stippled chromatin and no appearance of nucleoli. The cytoplasm was eosinophilic in most areas, with few cells containing clear cytoplasm (Figure 4). The cellular nests showed positive staining for markers of epithelial differentiation (CAM 5.2, AE1/AE3, EMA (focal),  $\beta$ -catenin (both



Figure 2 Intra-operative images and tumoral tissue.

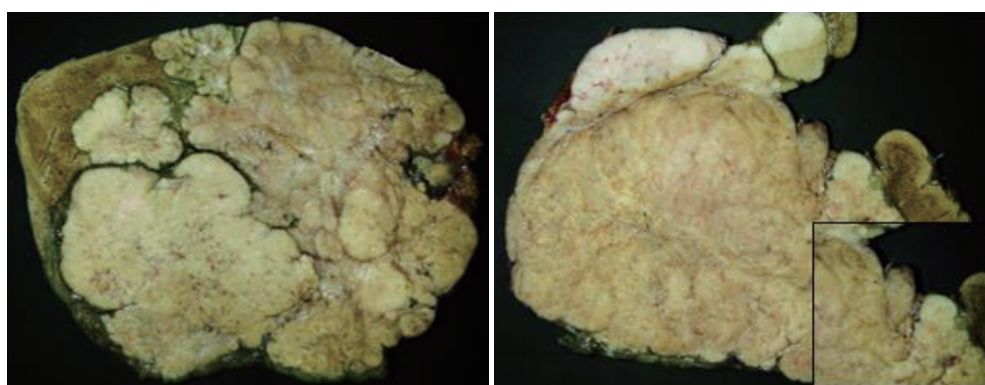


Figure 3 Grossly, right hepatic lobe was almost entirely occupied by a well-circumscribed multinodular mass with homogeneous, whitish cut surface and with calcification areas. In detail, macroscopic neoplastic vascular invasion of a portal vein branch.

membrane and nuclear), WT1 (both membrane and cytoplasmatic), GPC3 (focally cytoplasmatic) and CD56 (diffuse) and negative staining for hepatocyte antigen EpPar1 (hepatocyte paraffin 1), CK7, CK19, CD34, CD99, chromogranin and desmin.

The calcifications were most commonly within or adjacent to cellular nests. The mitotic index was 10 mitoses/10 high power field (40 × objective). The stroma surrounding the cellular nests showed a myofibroblastic nature, with spindled cells with long tapered cytoplasmic processes, positive staining for smooth muscle actin and negative staining for cytokeratins and EpPar1. Bile ducts entrapped in the fibrous stroma were normal and were highlighted by CK7 and CK19 immunohistochemical stains (Figure 5). The neoplastic cells infiltrated the surrounding hepatic

parenchyma and peri-hepatic soft tissue. Vascular invasion of a portal vein branch was demonstrated.

**Differential diagnosis:** The differential diagnosis of a biphasic tumor, with a spindled and epithelioid component, variable calcifications and osseous metaplasia includes in the first instance synovial sarcoma, mixed epithelial and mesenchymal hepatoblastoma and calcifying NSET. Desmoplastic small round cell tumor (DSRCT) is also a diagnostic consideration in a young patient. In addition, the possibility of sarcomatous variants of hepatocellular carcinoma or cholangiocarcinoma should be considered. However, these tumors lack the nested, organoid architecture of NSET, typically showing a greater cytological atypia.

Areas predominantly composed of epithelioid nests



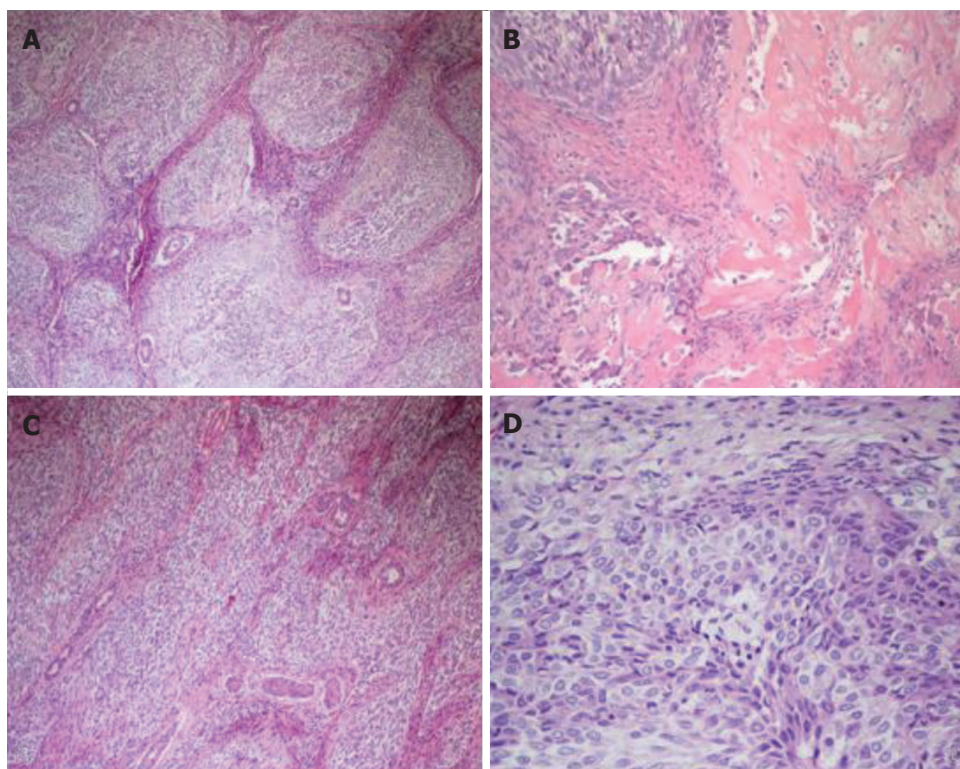


**Figure 4** Tumor showing organoid appearance with well-demarcated nests in a myofibroblastic stroma (A). B: Areas of osseous metaplasia and calcifications; C: Epithelioid and spindle cellular nests with bile ducts entrapped in fibrous stroma; D: Epithelioid and spindle-shape cells with eosinophilic and clear cytoplasm.

may resemble islands of fetal hepatoblastoma cells. However, the neoplasm in this report lacked the fetal and/or embryonic hepatoid features of the epithelial component of mixed hepatoblastoma, and neither the spindled nor the epithelioid lesional cells stained with the hepatocyte-specific tissue stain EpPar1.

The overall histology and immunohistochemical features supported the diagnosis of NSET, a very rare tumor defined as a non-hepatocytic and non-biliary tumor of the liver consisting of nests of epithelial and spindled cells with associated myofibroblastic stroma and variable intralesional calcification and ossification<sup>[4,7,8]</sup>.

For a comprehensive report, molecular analysis was performed. Reverse transcriptase-polymerase chain reactions for SYT-SSX and EWS-WT1 were negative in our case. Such findings, combined with the histological appearance, allowed us to rule out the hypothesis of synovial sarcoma and DSRCT, respectively.

### Relapse

In September 2015, the patient underwent a CT scan, which showed several liver lesions (maximum diameter of 17 mm), and also a positron emission tomography (PET) that documented a pre-sacral nodule (SUV = 5). After discussion within the Multidisciplinary Tumor Board (MTB), since surgery was judged not feasible, a liver chemo-embolization (DCBeads + doxorubin) was performed. Although the arteriography showed a higher number of the lesions, only five nodules

were treated with the chemoembolization. Due to an increase in the gamma-glutamyl transferase level (944 U/L), no further treatment was practicable.

In November 2015, a re-assessment with a CT scan showed a local progression and an increased number of abdominal lymphadenopathies. Hyperbilirubinemia (10.2 mg/dL) was also observed with a dilatation of the intrahepatic biliary duct. Therefore, a trans-cutaneous biliary catheter was positioned, with consequent improvement of the hepatic and biliary function. The patient was re-evaluated within the MTB and we hypothesized a regimen with ifosfamide/mesna, platin and anthracycline according to ifosfamide/cisplatin/pirarubicine (commonly known as the IPA) schedule. Due to the correlation of the histological features of the disease with the hepatoblastoma, as described in literature<sup>[9-12]</sup>, four courses of cisplatin (100 mg/m<sup>2</sup>) and ifosfamide/mesna (3 g/mq) were administered, omitting doxorubicin because of the liver impairment.

Anyway, infections of the biliary catheter, with fever and abdominal pain, affected the treatment, and required both antibiotics and a dose modification of the chemotherapy schedule. In fact, cisplatin alone was administered in the second course and ifosfamide/mesna was added again from the third course, reducing by 50% of its total dose. The patient received a total of four cycles of chemotherapy.

In April 2016, a restaging CT scan showed a progressive disease, represented by an increase of the hepatic lesion (5 cm vs 2.4 cm) and of the pre-

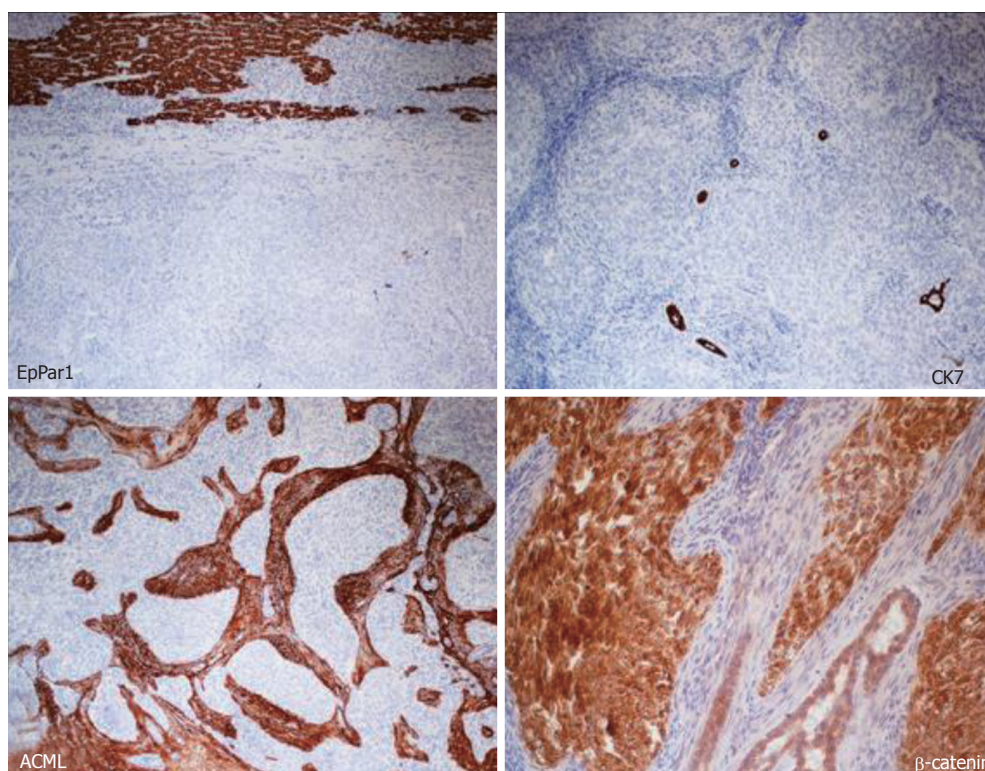


**Figure 5** Immunohistochemical stains showing neoplasm negativity for hepatocyte paraffin 1 (EpPar1) (counterstained normal liver parenchyma), negativity for CK7 (highlighted entrapped bile ducts between the tumor cell), stromal positivity for ACML and positivity for  $\beta$ -catenin (both membrane and nuclear).

sacral nodule (2.6 cm vs 1.7 cm). Ascites was also documented (Figure 6). Unfortunately, the worsening of the clinical status, the rise in total bilirubin up to 27.4 mg/dL and alterations of sodium and potassium prevented further administration of chemotherapy and the patient died in June 2016.

## DISCUSSION

NSETs are a very rare type of cancer, and few data about their treatment are available. As far as we know, there are no predisposing factors increasing the risk of occurrence of this rare type of tumor. In the literature a few cases of NSET associated with Cushing syndrome at diagnosis have been described. In these cases, after excision of the tumors, the Cushing syndrome was abated, but the correlation remained unknown<sup>[2-4]</sup>.

Considering the low tendency of relapse, the majority of the reported cases have been treated with surgery, obtaining a long survival outcome (up to a complete response) in most<sup>[2,12]</sup>. Liver transplantation is a further treatment that should be taken in account in patients with unresectable and not extra-hepatic disease, although not as a first choice<sup>[1,13]</sup>. Hommann *et al.*<sup>[13]</sup> treated a 19-year-old patient who underwent liver surgery for a NSET and developed liver metastasis a few years later, with liver transplantation achieving 37 mo of overall survival (OS).

Our patient relapsed within 6 mo after surgery,

with several focal lesions in the residual liver, showing an aggressive and unusual behavior of the disease. Necrosis, high mitotic rate, invasion of the surrounding parenchyma and vascular invasion are the features that might explain the malignant potential and the aggressive behavior of this rare neoplasm. Furthermore, a liver transplantation was not performed because of the presence of the extra-hepatic pre-sacral nodule. Consequently, chemotherapy seemed to be the only feasible therapeutic approach, although no guidelines, nor prognostic or predictive factors are currently known to choose the most appropriate treatment.

The analogies between NSET tumors and hepatoblastoma led us to use a hepatoblastoma chemotherapy protocol to treat our patient. This decision was also supported by the literature. In fact cases of both recurrent and metastatic disease have been treated with a good outcome<sup>[12]</sup>. Among the others, a 3-year-old child was treated both before and after resection, achieving a minimal shrinkage of the tumor<sup>[4]</sup>. The other two patients, of about 14-years-old and 2-years-old, were treated after surgery with the same chemotherapy protocol, with a disease-free survival of 90 mo and 84 mo, respectively<sup>[1]</sup>. It should be noted that all these cases were younger than our patient.

Nevertheless, our patient developed a more aggressive disease with a worse prognosis compared to the other case reports, and also several issues



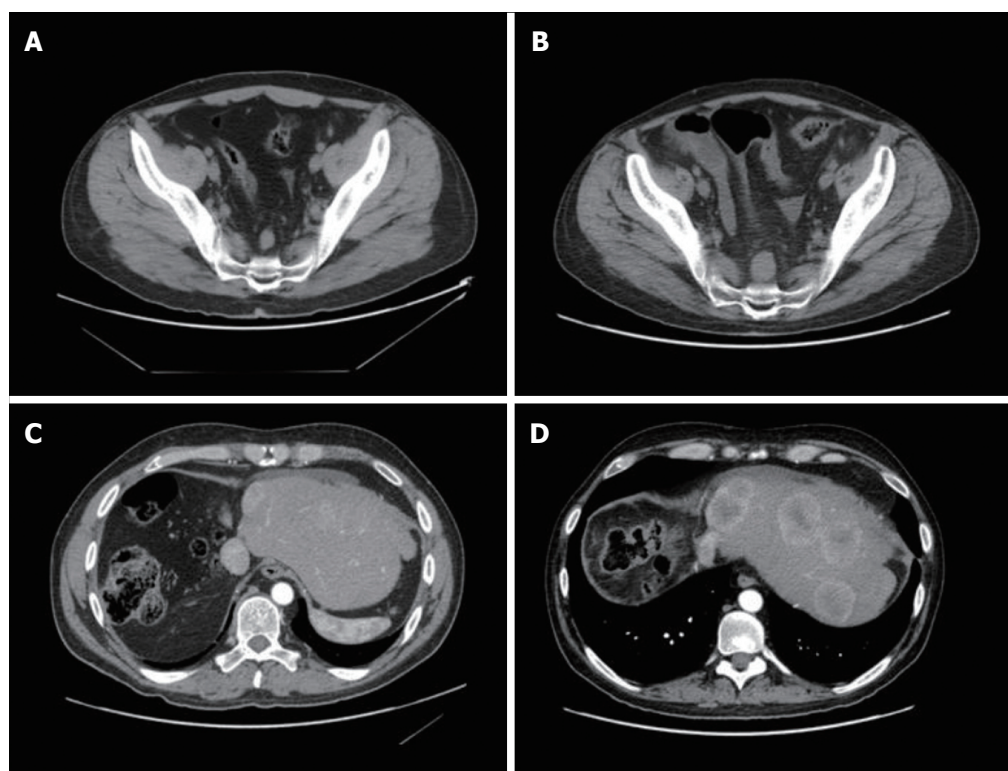


**Figure 6 Computer tomography scan.** A: CT scan performed in November 2015 showing the sacral lesion; B: CT scan performed in April 2016 showing increase of the sacral lesion; C: CT scan performed in November 2015 showing liver lesions; D: CT scan performed in April 2016 showing increase of liver lesions. CT: Computer tomography.

prevented a good compliance to the treatment. No tumor shrinkage was noted, but a progression of the disease in both liver and pre-sacral sites was observed. Other cases in the literature had a poor prognosis<sup>[1,14]</sup>, with OS around 37 mo to 40 mo, which was better than our patient outcome (OS of 15 mo), probably because they underwent liver transplantation.

In conclusion, in sharing our experience, we aimed to enhance the knowledge of NSET in the literature, especially for patients with either metastatic or recurrent disease, when a chemotherapeutic rather than a surgical approach is requested and where prognostic and predictive factors are not still available.

## COMMENTS

### Case characteristics

A 31-year-old Caucasian man presented at our institution for a large, lobulated, multinodular mass of the right hemi-liver.

### Clinical diagnosis

Distended abdomen with diffuse tenderness, palpable large abdominal mass in the right upper quadrant, with no evidence of ascites or splenomegaly.

### Differential diagnosis

Hepatocellular carcinoma, metastatic adenocarcinoma, cirrhosis, hepatoblastoma.

### Laboratory diagnosis

Increased gamma-glutamyl transferase (349 U/L) and a mild leukocytosis ( $13.8 \times 10^3$  cells/mm<sup>3</sup>). Negative serology for hepatitis B and C, autoimmune hepatitis

and human immunodeficiency virus. Serum alpha-fetoprotein, carcinoembryonic antigen and CA 19-9 within normal range.

### Imaging diagnosis

The computed tomography (CT) scan showed a large, lobulated, multinodular mass (22 cm × 13 cm × 25 cm) with few round calcifications, mainly in the central part and involving the right hemi-liver entirely, and partially involving the Couinaud's segment 4 and the caudate lobe. The CT images also demonstrated an extensive infiltration of the right portal branch and of the right and middle hepatic veins, with a consequent spontaneous hypertrophy of the left lobe.

### Pathological diagnosis

The histological exam confirmed the diagnosis of nested stromal-epithelial tumor (NSET).

### Treatment

The first approach was surgery. After relapse, four courses of cisplatin (100 mg/m<sup>2</sup>) and ifosfamide/mesna (3 g/mq) were administered, omitting doxorubicin because of the liver impairment.

### Related reports

NSET of the liver is a very rare type of cancer, that affects young people without sex preference. Cushing syndrome is often the presenting symptom of this neoplasm.

### Term explanation

NSET is usually a large hepatic lesion, partially necrotic and with calcifications. Upon histological analysis, it appears as well-defined nests of epithelioid and spindle cells with focal necrosis, surrounded by hypercellular stroma.

### Experiences and lessons

This entity is usually associated with a good prognosis after surgery. Nevertheless, our patient's prognosis was poor, and the disease showed

an aggressive behavior. No standard therapy is approved for the metastatic disease.

### Peer-review

This case report showed the uncommon situation of a patient with a metastatic NSET, and the chemotherapy administered which had provided no benefit. The authors present very precisely the case of very rare type of liver cancer which had a very aggressive form and progressed after surgery and first-line chemotherapy.

## REFERENCES

- 1 **Schaffer LR**, Shehata BM, Yin J, Schemankewitz E, Alazraki A. Calcifying nested stromal-epithelial tumor (CNSET) of the liver: a newly recognized entity to be considered in the radiologist's differential diagnosis. *Clin Imaging* 2016; **40**: 137-139 [PMID: 26589005 DOI: 10.1016/j.clinimag.2015.10.003]
- 2 **Makhlouf HR**, Abdul-Al HM, Wang G, Goodman ZD. Calcifying nested stromal-epithelial tumors of the liver: a clinicopathologic, immunohistochemical, and molecular genetic study of 9 cases with a long-term follow-up. *Am J Surg Pathol* 2009; **33**: 976-983 [PMID: 19363442 DOI: 10.1097/PAS.0b013e31819c1ab3]
- 3 **Weeda VB**, de Reuver PR, Bras H, Zsíros J, Lamers WH, Aronson DC. Cushing syndrome as presenting symptom of calcifying nested stromal-epithelial tumor of the liver in an adolescent boy: a case report. *J Med Case Rep* 2016; **10**: 160 [PMID: 27306557 DOI: 10.1186/s13256-016-0951-2]
- 4 **Heerema-McKenney A**, Leuschner I, Smith N, Sennesh J, Finegold MJ. Nested stromal epithelial tumor of the liver: six cases of a distinctive pediatric neoplasm with frequent calcifications and association with cushing syndrome. *Am J Surg Pathol* 2005; **29**: 10-20 [PMID: 15613852]
- 5 **Grazi GL**, Vetrone G, d'Errico A, Caprara G, Ercolani G, Cescon M, Ravaioli M, Del Gaudio M, Vivarelli M, Zanello M, Pinna AD. Nested stromal-epithelial tumor (NSET) of the liver: a case report of an extremely rare tumor. *Pathol Res Pract* 2010; **206**: 282-286 [PMID: 19487085 DOI: 10.1016/j.prp.2009.04.012]
- 6 **Schindl MJ**, Redhead DN, Fearon KC, Garden OJ, Wigmore SJ; Edinburgh Liver Surgery and Transplantation Experimental Research Group (eLISTER). The value of residual liver volume as a predictor of hepatic dysfunction and infection after major liver resection. *Gut* 2005; **54**: 289-296 [PMID: 15647196 DOI: 10.1136/gut.2004.046524]
- 7 **Heywood G**, Burgart LJ, Nagorney DM. Ossifying malignant mixed epithelial and stromal tumor of the liver: a case report of a previously undescribed tumor. *Cancer* 2002; **94**: 1018-1022 [PMID: 11920471 DOI: 10.1002/cncr.10345]
- 8 **Hill DA**, Swanson PE, Anderson K, Covinsky MH, Finn LS, Ruchelli ED, Nascimento AG, Langer JC, Minkes RK, McAlister W, Dehner LP. Desmoplastic nested spindle cell tumor of liver: report of four cases of a proposed new entity. *Am J Surg Pathol* 2005; **29**: 1-9 [PMID: 15613851 DOI: 10.1097/00000478-200501000-00001]
- 9 **Assmann G**, Kappler R, Zeindl-Eberhart E, Schmid I, Häberle B, Graeb C, Jung A, Müller-Höcker J.  $\beta$ -Catenin mutations in 2 nested stromal epithelial tumors of the liver--a neoplasia with defective mesenchymal-epithelial transition. *Hum Pathol* 2012; **43**: 1815-1827 [PMID: 22749188 DOI: 10.1016/j.humpath.2012.03.018]
- 10 **Häberle B**, Bode U, von Schweinitz D. [Differentiated treatment protocols for high- and standard-risk hepatoblastoma--an interim report of the German Liver Tumor Study HB99]. *Klin Padiatr* 2003; **215**: 159-165 [PMID: 12778356 DOI: 10.1055/s-2003-39375]
- 11 **Procopio F**, Di Tommaso L, Armenia S, Quagliuolo V, Roncalli M, Torzilli G. Nested stromal-epithelial tumour of the liver: An unusual liver entity. *World J Hepatol* 2014; **6**: 155-159 [PMID: 24672646 DOI: 10.4254/wjh.v6.i3.155]
- 12 **Brodsky SV**, Sandoval C, Sharma N, Yusuf Y, Facciuto ME, Humphrey M, Yeh YA, Braun A, Melamed M, Finegold MJ. Recurrent nested stromal epithelial tumor of the liver with extrahepatic metastasis: case report and review of literature. *Pediatr Dev Pathol* 2008; **11**: 469-473 [PMID: 18338937 DOI: 10.2350/07-12-0391.1]
- 13 **Hommann M**, Kaemmerer D, Daffner W, Prasad V, Baum RP, Petrovitch A, Sauerbrey A, Katenkamp K, Kaufmann R, Settmacher U. Nested stromal epithelial tumor of the liver--liver transplantation and follow-up. *J Gastrointest Cancer* 2011; **42**: 292-295 [PMID: 21221846 DOI: 10.1007/s12029-010-9248-7]
- 14 **Misra S**, Bihari C. Desmoplastic nested spindle cell tumours and nested stromal epithelial tumours of the liver. *APMIS* 2016; **124**: 245-251 [PMID: 26994733 DOI: 10.1111/apm.12502]

**P- Reviewer:** Inoue K, Vorobjova T **S- Editor:** Gong ZM  
**L- Editor:** Filipodia **E- Editor:** Huang Y



## Combined thoracoscopic and endoscopic surgery for a large esophageal schwannoma

Yu Onodera, Toru Nakano, Daisuke Takeyama, Shota Maruyama, Yusuke Taniyama, Tadashi Sakurai, Takahiro Heishi, Chiaki Sato, Takuro Kumagai, Takashi Kamei

Yu Onodera, Shota Maruyama, Yusuke Taniyama, Tadashi Sakurai, Takahiro Heishi, Takuro Kumagai, Chiaki Sato and Takashi Kamei, Division of Advanced Surgical Science and Technology, Tohoku University Graduate School of Medicine, Aoba-ku, Sendai Miyagi 980-8574, Japan

Toru Nakano, Daisuke Takeyama, Division of Gastroenterological and Hepatobiliarypancreatic Surgery, Tohoku Medical and Pharmaceutical University, Miyagino-ku, Sendai Miyagi 983-8560, Japan

ORCID number: Yu Onodera (0000-0002-0298-3819); Toru Nakano (0000-0003-1824-9122); Daisuke Takeyama (0000-0001-7497-9037); Shota Maruyama (0000-0002-8067-4333); Yusuke Taniyama (0000-0003-2563-247X); Tadashi Sakurai (0000-0002-1451-6177); Takahiro Heishi (0000-0003-0331-1106); Chiaki Sato (0000-0003-1449-2053); Takuro Kumagai (0000-0001-8712-6527); Takashi Kamei (0000-0003-1282-0463).

**Author contributions:** Onodera Y is the first author and Nakano T is the correspondence author; Nakano T designed the study and planned the managements; Nakano T, Takeyama D and Kumagai T were operators of the thocoscopic procedure; Mruyama S was the operator of the endoscopic procedure; Onodera Y, Takeyama D, Taniyama Y, Sakurai T, Heishi T, Kumagai T and Kamei T were attending doctors and provided all treatment including the surgical operation; all authors agree with the content of the manuscript and the roles that are specifically attributed to them.

**Supported by** (partially) JSPS KAKENHI, No. JP15K15487.

**Informed consent statement:** Written informed consent was obtained from the patient.

**Conflict-of-interest statement:** All authors have no conflict-of-interest.

**Open-Access:** This article is an open-access article which was selected by an in-house editor and fully peer-reviewed by external reviewers. It is distributed in accordance with the Creative Commons Attribution Non Commercial (CC BY-NC 4.0) license, which permits others to distribute, remix, adapt, build upon this work non-commercially, and license their derivative works on different terms, provided the original work is properly cited and

the use is non-commercial. See: <http://creativecommons.org/licenses/by-nc/4.0/>

**Manuscript source:** Unsolicited manuscript

**Correspondence to:** Toru Nakano, MD, PhD, Associate professor, Division of Gastroenterological and Hepatobiliarypancreatic Surgery, Tohoku Medical and Pharmaceutical University, 1-12-1 Fumuro, Miyagino-ku, Sendai Miyagi 983-8560, Japan. [torun@med.tohoku.ac.jp](mailto:torun@med.tohoku.ac.jp)  
Telephone: +81-22-2591221  
Fax: +81-22-2591231

**Received:** June 25, 2017

**Peer-review started:** June 28, 2017

**First decision:** July 13, 2017

**Revised:** August 23, 2017

**Accepted:** September 13, 2017

**Article in press:** September 13, 2017

**Published online:** December 14, 2017

### Abstract

A 47-year-old woman presented to our hospital with complaints of dysphagia. Esophagogastroduodenoscopy identified a submucosal tumor in the left wall of the esophagus that was diagnosed as a benign schwannoma on biopsy. Computed tomography revealed a tumor of length 60 mm in the thoracic esophagus, with its cranial edge at the level of the aortic arch. On endoscopy, a submucosal tunnel was created 40 mm proximal to the cranial edge of the tumor, and its oral end was dissected from the mucosal and muscular layers. This was followed by the resection of the entire tumor by left-sided thoracoscopy. The esophageal defect was closed in layer by continuous suture from the thoracic side. Endoscopic closure was achieved by using clips. No postoperative complications were observed. Oral diet was resumed from postoperative day 7 and the patient was discharged on

postoperative day 9. This combined approach has not been described for similar tumors. Our experience demonstrated that large esophageal tumors can be safely excised with minimally invasive surgery by using a combination of thoracoscopy and endoscopy.

**Key words:** Esophagus; Thoracoscopy; Endoscopy; Schwannoma; Submucosal tumor

© The Author(s) 2017. Published by Baishideng Publishing Group Inc. All rights reserved.

**Core tip:** A 47-year-old woman was diagnosed with a benign schwannoma of length 60 mm in the thoracic esophagus. On endoscopy, a submucosal tunnel was created 40 mm proximal to the cranial edge of the tumor, and its only oral end was dissected from the mucosal and muscular layers. This was followed by the resection of the entire tumor by left-sided thoracoscopic procedure. Endoscopic closure was achieved by using clips. No postoperative complications were observed. Our experience demonstrated that large esophageal tumors can be safely excised with minimally invasive surgery by using a combination of thoracoscopy and endoscopy.

Onodera Y, Nakano T, Takeyama D, Maruyama S, Taniyama Y, Sakurai T, Heishi T, Sato C, Kumagai T, Kamei T. Combined thoracoscopic and endoscopic surgery for a large esophageal schwannoma. *World J Gastroenterol* 2017; 23(46): 8256-8260 Available from: URL: <http://www.wjgnet.com/1007-9327/full/v23/i46/8256.htm> DOI: <http://dx.doi.org/10.3748/wjg.v23.i46.8256>

## INTRODUCTION

Esophageal schwannoma is a relatively rare benign esophageal submucosal tumor (SMT). Enucleation is the treatment of choice, and minimally invasive surgery using thoracoscopy has been the usual approach<sup>[1-4]</sup>. The left thoracic approach, although considered better for tumors involving the left esophageal wall, is limited by the presence of the aortic arch and the trachea. In addition, the choice between thoracoscopy or thoracotomy is made depending on the size and/or location of the tumor<sup>[1,5,6]</sup>. Submucosal endoscopic tumor resection (SET) for esophageal SMT, was recently reported by Inoue *et al.*<sup>[7]</sup>, using the technique of submucosal tunnel described for peroral endoscopic myotomy (POEM) for esophageal achalasia<sup>[8]</sup>. Laparoscopic and endoscopic cooperative surgery (LECS) has been performed for gastric SMT or duodenal tumor recently<sup>[9-12]</sup>, while the treatment method combined thoracoscopy and endoscopy has not been established in esophageal SMT. In the present case report, we describe a combined technique of submucosal endoscopic resection and thoracoscopic

surgery in successfully resecting a large benign schwannoma.

## CASE REPORT

A 47-year-old woman presented to the Tohoku University Hospital with complaints of dysphagia. Esophagogastroduodenoscopy identified a smooth elevated lesion located about 27-33 cm from her incisors (Figure 1). Endoscopic ultrasonography (EUS) demonstrated a large tumor mass in the esophageal wall that was hypoechoic and appeared to originate from either the submucosal or the muscular layer. Enhanced computed tomography (CT) confirmed this to be a 60-mm-long tumor, with its cranial edge identified at the level of the aortic arch (Figure 2). Ultrasound-guided fine-needle aspiration biopsy (Liner echoendoscope [GF-UC240P-AL5], Olympus Corporation, Tokyo, Japan; Aspiration needle [Expect], Boston Scientific, MA, United States) demonstrated spindle-shaped cells without abnormal mitosis. Immunohistochemical staining was positive for S-100 protein and the expression level of Ki-67 was 2%-3%. These findings were strongly suggestive of a benign esophageal schwannoma. In view of the large tumor size, recent increase in size, and the patient's symptoms, resection of the tumor by a combined endoscopic and thoracoscopic approach was planned.

General anesthesia was administered using single-lumen endotracheal intubation for bilateral lung ventilation. The endoscopic procedure was performed in the supine position. We created a submucosal tunnel 40 mm proximal to the oral edge of the tumor and dissected its cranial end from the mucosal and muscular layers (Figure 3). We used two kinds of electrocautery knives [triangle-tip knife (KD-640L), and insulated-tip knife (KD-611L), Olympus Corporation, Tokyo, Japan] combined with an electrosurgical unit (ERBE VIO 300D, ERBE Corporation, Tuebingen, Germany). Endoscopic dissection was limited to about 30 mm of the tumor and could not proceed further owing to the limited mobility of the tumor within the submucosal tunnel. Thereafter, the patient was placed in the prone position, and a left thoracoscopic access was achieved under 8 mmHg of artificial pneumothorax. The following ports were placed: 5-mm ports at the mid-axillary line in the 3<sup>rd</sup> intercostal space (ICS), and the posterior axillary line in the 5<sup>th</sup> ICS, respectively, for the assistant; a 5-mm port at the mid-axillary line in the 8<sup>th</sup> ICS for grasping forceps; a 12-mm operating port at the posterior axillary line in the 7<sup>th</sup> ICS; and a 12-mm optical port at the posterior axillary line in the 9<sup>th</sup> ICS.

The surface of the tumor was easily identified on incising the esophageal muscular layer and dissection was performed along the tumor surface to enable its enucleation (Figure 4). The resected tumor was delivered out through the 12-mm operating port (7<sup>th</sup> ICS). We repaired the mucosal layer away from the



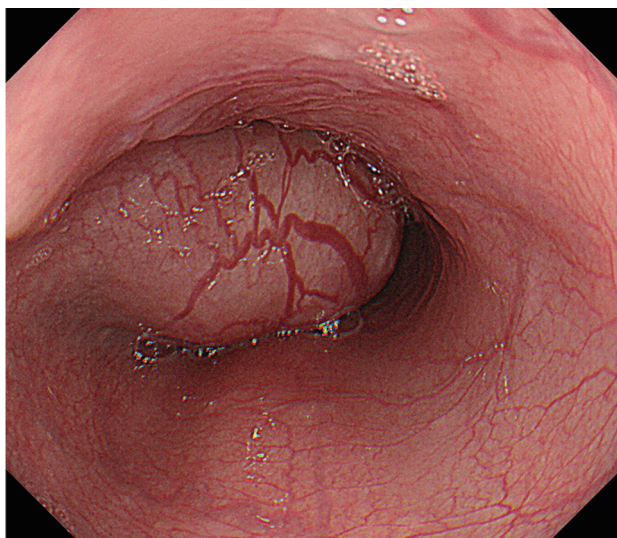


**Figure 1 Endoscopic findings.** The submucosal tumor is observed at 27-33 cm from the incisors. The endoscope could be passed beyond the tumor.

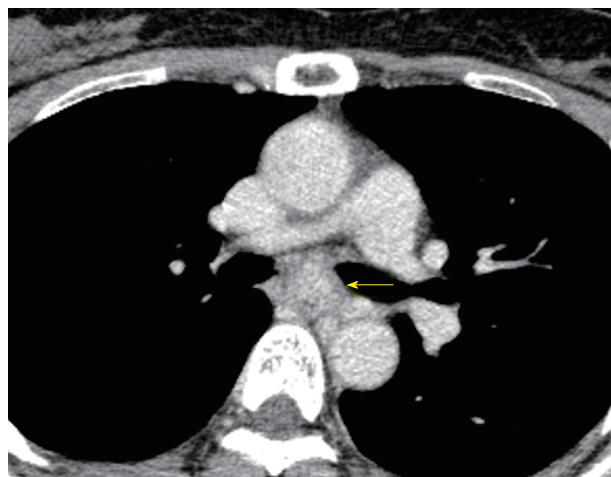


**Figure 2 Computed tomography images.** Computed tomography reveals a well demarcated, heterogeneous, esophageal tumor in the mid-thoracic esophagus (arrow). The longitudinal diameter of the tumor was 60 mm.

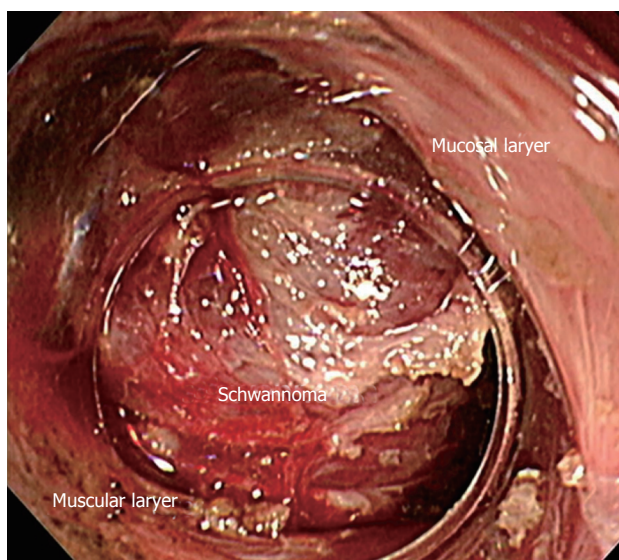


**Figure 3 Endoscopic procedure.** The esophageal schwannoma is visible through the submucosal tunnel created proximal to its cranial edge. The mucosal and muscular layers are dissected free of the tumor.

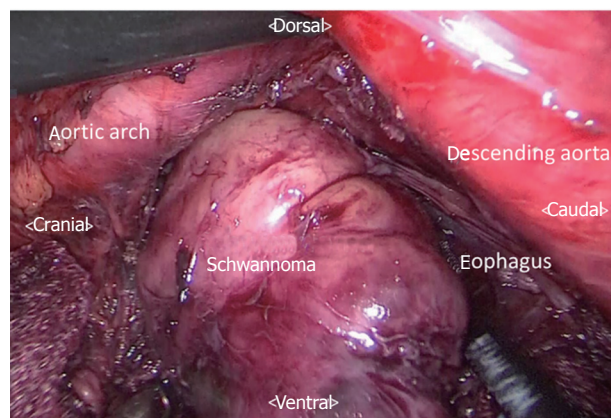


**Figure 4 Thoracoscopic procedure in the prone position, with access via the left thoracic cavity.** The cranial aspect of the tumor was already dissected free of the adjacent structures by endoscopic procedure. The part of the esophageal schwannoma that was not dissected endoscopically is removed from the submucosal space after incising the muscular layer of the esophagus, thoracoscopic method.

site of mucosal entry since it was damaged partially during the thoracoscopic procedure. The muscular layer of the esophagus was sutured separately by using a continuous barbed absorbable suture (V-Loc180, Medtronic, United States). The endoscopic defect, created for gaining mucosal entry for tunneling, was closed by using endoscopic clips. The total operation time was 498 min (thoracoscopic procedure: 317 min) and the total blood loss was 40 g. The post-operative course of the patient was uneventful. Oral diet was resumed from postoperative day 7 and the patient was discharged on postoperative day 9.

## DISCUSSION

Esophageal SMTs constitute less than 1% of all esophageal tumors. The most common among them

are leiomyomas, with esophageal schwannomas accounting for 2%-3.4% of all esophageal SMTs<sup>[5,13]</sup>. Enucleation is considered as the treatment of choice for benign tumors that are symptomatic or rapidly increasing in size<sup>[1]</sup>. Video-assisted thoracoscopic surgery including thoracoscopic enucleation is described as a minimally invasive surgical procedure for esophageal SMT<sup>[5]</sup>. Performing thoracoscopic enucleation in the prone position, as compared with thoracotomy or thoracoscopic surgery in the decubitus position, has the advantages of adequate working area, minimal blood loss, and short postoperative stay<sup>[2,3]</sup>. However, the possibility of thoracoscopic enucleation may be limited by the tumor location and size. Sato *et al.* reported that cases with tumor size of 50 mm or more, and tumor location at the upper esophagus, usually required thoracotomy<sup>[1]</sup>. Watanabe *et al.*<sup>[6]</sup> reported the need to convert from thoracoscopic enucleation to thoracoscopic subtotal esophagectomy owing to the

location of an esophageal schwannoma at the upper thoracic esophagus, and its size being in excess of 50 mm. Therefore, thoracotomy or esophagectomy would be usually chosen for tumors that are 50 mm or more in size or located in the upper and middle thirds of the thoracic esophagus. The laterality of the tumor may determine the side of thoracic access. Esophageal surgery, especially for esophagectomy, is usually performed through the right thoracic cavity. Although, the left thoracic approach may provide direct access to a tumor on the left esophageal wall, the aortic arch and the trachea may restrict this access, especially for tumors located in the upper and middle thoracic esophagus. The left thoracic approach is usually applied for tumors located in the lower thoracic esophagus or at the esophagogastric junction<sup>[13,14]</sup>.

SET is a recently developed technique for the treatment of esophageal SMT and was described by Inoue *et al.*<sup>[7]</sup>. This technique allows for a complete endoscopic tumor resection, and is associated with earlier onset of per-oral intake, shorter hospital stay, and minimal short-term complications. On the other hand, SET is only recommended for tumors up to 40 mm in size owing to the limited submucosal space available.

In the present case, the tumor originated in the left wall of the mid-thoracic esophagus and had a maximal diameter of 60 mm. Since the aortic arch and the main bronchus restricted left-sided thoracoscopic access, and SET alone was not applicable owing to the tumor size, we combined the two procedures to overcome their respective limitations. To avoid the aortic arch and the left bronchus in the thoracoscopic approach, we attempted to remove the cranial side of the tumor to the maximum extent possible by endoscopic dissection.

To our knowledge, this combined approach has not been reported for tumors involving the upper and middle thoracic esophagus. Kanetaka *et al.* applied a similar approach for a large esophageal leiomyoma that originated from the lower thoracic esophagus. However, lower mediastinal tumors may be relatively easily resected by thoracoscopy alone. In our case, endoscopic tunneling was required since the tumor was located in the middle thoracic esophagus, and complete tumor resection by the thoracoscopic approach was considered difficult. Indications for such a combined procedure may be further expanded to avoid unnecessary esophagectomy or thoracotomy.

Recently, the submucosal tunneling endoscopic resection (STER) technique has been used for the resection of esophageal GISTs<sup>[7]</sup>. The combined approach can aid in the removal of GISTs without disrupting the tumor capsule. However, further studies are necessary to evaluate whether this procedure is applicable for malignant tumors such as GISTs<sup>[7]</sup>.

In conclusion, this case report describes the successful resection of a large esophageal schwannoma by a combined method of endoscopic and thoracoscopic surgery. This method may be a possible minimally

invasive treatment option for large esophageal SMT.

## COMMENTS

### Case characteristics

A 47-year-old woman with no significant medical history presented with dysphagia.

### Clinical diagnosis

Esophageal submucosal tumor located in the middle thoracic esophagus.

### Differential diagnosis

Leiomyoma, gastrointestinal stromal tumor, schwannoma, or other submucosal tumor.

### Laboratory diagnosis

All laboratory results were within normal limits.

### Imaging diagnosis

Computed tomography imaging demonstrated a 60-mm-long tumor located in the middle thoracic esophagus, adjacent to the aortic arch.

### Pathological diagnosis

Benign esophageal schwannoma.

### Treatment

Combined thoracoscopic and endoscopic tumor resection.

### Term explanation

Esophageal schwannoma is a relatively rare esophageal submucosal tumor. Large esophageal schwannomas usually require thoracotomy or esophagectomy for their successful resection.

### Experiences and lessons

Combined thoracoscopic and endoscopic tumor resection can facilitate the resection of large esophageal submucosal tumors located in the upper or middle thoracic esophagus by minimally invasive surgery.

### Peer-review

The paper is well written.

## REFERENCES

- 1 **Sato S**, Takagi M, Watanabe M, Nagai E, Kyoden Y, Ohata K, Oba N, Suzuki M, Fukuchi K, Iseki J. A case report of benign esophageal schwannoma with FDG uptake on PET-CT and literature review of 42 cases in Japan. *Esophagus* 2012; **9**: 165-171 [DOI:10.1007/s10388-012-0311-2]
- 2 **Claus CM**, Cury Filho AM, Boscardim PC, Andriguetto PC, Loureiro MP, Bonin EA. Thoracoscopic enucleation of esophageal leiomyoma in prone position and single lumen endotracheal intubation. *Surg Endosc* 2013; **27**: 3364-3369 [PMID: 23549763 DOI: 10.1007/s00464-013-2918-3]
- 3 **Palanivelu C**, Rangarajan M, Senthilkumar R, Annapoorni S, Jategaonkar PA. Thoracoscopic management of benign tumors of the mid-esophagus: a retrospective study. *Int J Surg* 2007; **5**: 328-331 [PMID: 17638600 DOI: 10.1016/j.ijsu.2007.04.011]
- 4 **Palanivelu C**, Prakash A, Senthilkumar R, Senthilnathan P, Parthasarathi R, Rajan PS, Venkatachlam S. Minimally invasive esophagectomy: thoracoscopic mobilization of the esophagus and mediastinal lymphadenectomy in prone position--experience of 130 patients. *J Am Coll Surg* 2006; **203**: 7-16 [PMID: 16798482 DOI: 10.1016/j.jamcollsurg.2006.03.016]

- 5 **Shin S**, Choi YS, Shim YM, Kim HK, Kim K, Kim J. Enucleation of esophageal submucosal tumors: a single institution's experience. *Ann Thorac Surg* 2014; **97**: 454-459 [PMID: 24360088 DOI: 10.1016/j.athoracsur.2013.10.030]
- 6 **Watanabe T**, Miyazaki T, Saito H, Yoshida T, Kumakura Y, Honjo H, Yokobori T, Sakai M, Sohda M, Kuwano H. Resection of an esophageal schwannoma with thoracoscopic surgery: a case report. *Surg Case Rep* 2016; **2**: 127 [PMID: 27822873 DOI: 10.1186/s40792-016-0256-0]
- 7 **Inoue H**, Ikeda H, Hosoya T, Onimaru M, Yoshida A, Eleftheriadis N, Maselli R, Kudo S. Submucosal endoscopic tumor resection for subepithelial tumors in the esophagus and cardia. *Endoscopy* 2012; **44**: 225-230 [PMID: 22354822 DOI: 10.1055/s-0031-1291659]
- 8 **Inoue H**, Minami H, Kobayashi Y, Sato Y, Kaga M, Suzuki M, Satodate H, Odaka N, Itoh H, Kudo S. Peroral endoscopic myotomy (POEM) for esophageal achalasia. *Endoscopy* 2010; **42**: 265-271 [PMID: 20354937 DOI: 10.1055/s-0029-1244080]
- 9 **Hiki N**, Yamamoto Y, Fukunaga T, Yamaguchi T, Nunobe S, Tokunaga M, Miki A, Ohyama S, Seto Y. Laparoscopic and endoscopic cooperative surgery for gastrointestinal stromal tumor dissection. *Surg Endosc* 2008; **22**: 1729-1735 [PMID: 18074180 DOI: 10.1007/s00464-007-9696-8]
- 10 **Ntourakis D**, Mavrogenis G. Cooperative laparoscopic endoscopic and hybrid laparoscopic surgery for upper gastrointestinal tumors: Current status. *World J Gastroenterol* 2015; **21**: 12482-12497 [PMID: 26604655 DOI: 10.3748/wjg.v21.i43.12482]
- 11 **Irino T**, Nunobe S, Hiki N, Yamamoto Y, Hirasawa T, Ohashi M, Fujisaki J, Sano T, Yamaguchi T. Laparoscopic-endoscopic cooperative surgery for duodenal tumors: a unique procedure that helps ensure the safety of endoscopic submucosal dissection. *Endoscopy* 2015; **47**: 349-351 [PMID: 25479560 DOI: 10.1055/s-0034-1390909]
- 12 **Ichikawa D**, Komatsu S, Dohi O, Naito Y, Kosuga T, Kamada K, Okamoto K, Itoh Y, Otsuji E. Laparoscopic and endoscopic cooperative surgery for non-ampullary duodenal tumors. *World J Gastroenterol* 2016; **22**: 10424-10431 [PMID: 28058023 DOI: 10.3748/wjg.v22.i47.10424]
- 13 **Kang SK**, Yun JS, Kim SH, Song SY, Jung Y, Na KJ. Retrospective analysis of thoracoscopic surgery for esophageal submucosal tumors. *Korean J Thorac Cardiovasc Surg* 2015; **48**: 40-45 [PMID: 25705596 DOI: 10.5090/kjtc.2015.48.1.40]
- 14 **Shichinohe T**, Kato K, Ebihara Y, Kurashima Y, Tsuchikawa T, Matsumoto J, Nakamura T, Tanaka E, Hirano S. Thoracoscopic enucleation of esophageal submucosal tumor by prone position under artificial pneumothorax by CO2 insufflation. *Surg Laparosc Endosc Percutan Tech* 2014; **24**: e55-e58 [PMID: 24686363 DOI: 10.1097/SLE.0b013e31828f71e3]

**P- Reviewer:** Gupta V, Tsolakis AV **S- Editor:** Gong ZM **L- Editor:** A **E- Editor:** Ma YJ





## Extended pelvic side wall excision for locally advanced rectal cancers

Irshad A Shaikh, John T Jenkins

Irshad A Shaikh, Department of Surgery, Norfolk and Norwich University Hospital, Norwich NR47UY, United Kingdom

John T Jenkins, St Mark's Hospital, Harrow, London HA13UJ, United Kingdom

ORCID number: Irshad A Shaikh (0000-0002-1467-815X); John T Jenkins (0000-0002-3240-8305).

**Author contributions:** Shaikh IA drafted the manuscript and submission; Jenkins JT critical appraisal of the manuscript and correction.

**Conflict-of-interest statement:** All authors have no conflict of interest on this paper.

**Open-Access:** This article is an open-access article which was selected by an in-house editor and fully peer-reviewed by external reviewers. It is distributed in accordance with the Creative Commons Attribution Non Commercial (CC BY-NC 4.0) license, which permits others to distribute, remix, adapt, build upon this work non-commercially, and license their derivative works on different terms, provided the original work is properly cited and the use is non-commercial. See: <http://creativecommons.org/licenses/by-nc/4.0/>

**Manuscript source:** Unsolicited manuscript

**Correspondence to:** Irshad A Shaikh, FRCS (Gen Surg), Surgeon, Department of Surgery, Norfolk and Norwich University Hospital, Colney Lane, Norwich NR47UY, United Kingdom. [i.shaikh@nhs.net](mailto:i.shaikh@nhs.net)  
Telephone: +44-1603-286286  
Fax: +44-1603-287211

Received: September 6, 2017

Peer-review started: September 6, 2017

First decision: September 20, 2017

Revised: September 28, 2017

Accepted: November 2, 2017

Article in press: November 2, 2017

Published online: December 14, 2017

### Abstract

Extended pelvic side wall excision is a useful technique for treatment of recurrent or advanced rectal cancer involving sciatic notch and does not compromise the dissection of major pelvic vessels and vascular control.

**Key words:** Recurrent rectal cancers; Extended pelvic side wall excision; Pelvic side wall excision; Advanced rectal cancers

© **The Author(s) 2017.** Published by Baishideng Publishing Group Inc. All rights reserved.

**Core tip:** Extended pelvic side wall excision technique does not compromise the dissection of major pelvic vessels and vascular control during pelvic side wall clearance for recurrent/advanced rectal cancer.

Shaikh IA, Jenkins JT. Extended pelvic side wall excision for locally advanced rectal cancers. *World J Gastroenterol* 2017; 23(46): 8261-8262 Available from: URL: <http://www.wjgnet.com/1007-9327/full/v23/i46/8261.htm> DOI: <http://dx.doi.org/10.3748/wjg.v23.i46.8261>

### TO THE EDITOR

We read with interest the manuscript published by Lee *et al*<sup>[1]</sup>, titled "Advances in surgical management for locally recurrent rectal cancer: How far have we come?" published in *World Journal of gastroenterology*. The authors have attempted to appraise the current evidence for the management of locally advanced recurrent rectal cancer. We congratulate them for the exhaustive summary of various techniques employed to achieve R0 resection in these technically challenging



recurrent cancers.

We agree with authors review of the literature on the complexity of managing pelvic recurrence particularly on the side wall involving sciatic nerves, pelvic sidewalls or extending through the sciatic notch. The authors have referenced our report on the novel technique called extended lateral side wall excision (ELSiE) described at St Mark's Hospital<sup>[2]</sup>. This particular technique was described to increase R0 resection rate for the rectal cancers involving sciatic nerve, piriformis muscle or the tumours extending through the sciatic notch. In their review authors mention that with this technique it is not possible to control the iliac vessels. We wish to clarify the author's misinterpretation of our reported technique.

ELSiE technique has two stages: (1) Dissection in prone position; and (2) completion of the excision in supine position. The procedure starts in the prone position to dissect piriformis muscle and excise the ischial spine and isolate/excise the sciatic nerve as required. In our experience, this approach gives excellent views of sciatic notch, sacrospinous ligaments, and outer pelvic sidewall<sup>[3]</sup>. We believe that this approach also gives better control of the vessels around the sciatic notch and piriformis muscle which are otherwise potentially difficult to control from the abdomino-pelvic approach. The subsequent dissection

of the pelvic side wall *via* abdominal approach remains as described by Austin *et al*<sup>[4]</sup>, and referenced in the review. By starting in prone position, it does not make any difference to abdominal iliac vascular dissection. Since our original description of the technique, we are in the process of reporting our long term results of more than 50 such procedure and dissection in the prone position has not jeopardised subsequent iliac vascular dissection. We believe this technique offers an additional approach to manage the complex scenario where cancer involves the pelvic sidewall.

## REFERENCES

- 1 **Lee DJ**, Sagar PM, Sadacharam G, Tan KY. Advances in surgical management for locally recurrent rectal cancer: How far have we come? *World J Gastroenterol* 2017; **23**: 4170-4180 [PMID: 28694657 DOI: 10.3748/wjg.v23.i23.4170]
- 2 **Shaikh I**, Aston W, Hellawell G, Ross D, Littler S, Burling D, Marshall M, Northover JM, Antoniou A, Jenkins JT. Extended lateral pelvic sidewall excision (ELSiE): an approach to optimize complete resection rates in locally advanced or recurrent anorectal cancer involving the pelvic sidewall. *Tech Coloproctol* 2014; **18**: 1161-1168 [PMID: 25380742 DOI: 10.1007/s10151-014-1234-9]
- 3 ELSiE @ St Mark's Complex Cancer Clinic. Available from: URL: <https://www.youtube.com/watch?v=eobEeMDNw0Q>.
- 4 **Austin KK**, Solomon MJ. Pelvic exenteration with en bloc iliac vessel resection for lateral pelvic wall involvement. *Dis Colon Rectum* 2009; **52**: 1223-1233 [PMID: 19571697 DOI: 10.1007/DCR.0b013e3181a73f48]

**P- Reviewer:** Hidaka E, Lohsiriwat V, Stocchi L, Tsimogiannis KE

**S- Editor:** Ma YJ **L- Editor:** A **E- Editor:** Lu YJ





Published by **Baishideng Publishing Group Inc**  
7901 Stoneridge Drive, Suite 501, Pleasanton, CA 94588, USA  
Telephone: +1-925-223-8242  
Fax: +1-925-223-8243  
E-mail: [bpgoffice@wjgnet.com](mailto:bpgoffice@wjgnet.com)  
Help Desk: <http://www.f6publishing.com/helpdesk>  
<http://www.wjgnet.com>



ISSN 1007-9327

